Iterative Methods and Preconditioners for Systems of Linear Equations

Fundamentals *of* Algorithms

Editor-in-Chief: Nicholas J. Higham, University of Manchester

The SIAM series on Fundamentals of Algorithms is a collection of short user-oriented books on state-of-the-art numerical methods. Written by experts, the books provide readers with sufficient knowledge to choose an appropriate method for an application and to understand the method's strengths and limitations. The books cover a range of topics drawn from numerical analysis and scientific computing. The intended audiences are researchers and practitioners using the methods and upper level undergraduates in mathematics, engineering, and computational science.

Books in this series not only provide the mathematical background for a method or class of methods used in solving a specific problem but also explain how the method can be developed into an algorithm and translated into software. The books describe the range of applicability of a method and give guidance on troubleshooting solvers and interpreting results. The theory is presented at a level accessible to the practitioner. MATLAB® software is the preferred language for codes presented since it can be used across a wide variety of platforms and is an excellent environment for prototyping, testing, and problem solving.

The series is intended to provide guides to numerical algorithms that are readily accessible, contain practical advice not easily found elsewhere, and include understandable codes that implement the algorithms.

Series Volumes

Ciaramella, Gabriele and Gander, Martin J., *Iterative Methods and Preconditioners for Systems of Linear Equations*

Hansen, Per Christian, Jørgensen, Jakob Sauer, and Lionheart, William R. B., eds., *Computed Tomography: Algorithms, Insight, and Just Enough Theory*

Toledo, Sivan, *Location Estimation from the Ground Up*

Ketcheson, David I., LeVeque, Randall J., and del Razo, Mauricio J., *Riemann Problems and Jupyter Solutions*

Eldén, L., *Matrix Methods in Data Mining and Pattern Recognition, Second Edition*

Huang, T.-M., Li, R.-C., and Lin, W.-W., *Structure-Preserving Doubling Algorithms for Nonlinear Matrix Equations*

Aurentz, J. L., Mach, T., Robol, L., Vandebril, R., and Watkins, D. S., *Core-Chasing Algorithms for the Eigenvalue Problem*

Gander, M. J. and Kwok, F., *Numerical Analysis of Partial Differential Equations Using Maple and MATLAB*

Asch, M., Bocquet M., and Nodet, M., *Data Assimilation: Methods, Algorithms, and Applications*

Birgin, E. G. and Martínez, J. M., *Practical Augmented Lagrangian Methods for Constrained Optimization*

Bini, D. A., Iannazzo, B., and Meini, B., *Numerical Solution of Algebraic Riccati Equations*

Escalante, R. and Raydan, M., *Alternating Projection Methods*

Hansen, P. C., *Discrete Inverse Problems: Insight and Algorithms*

Modersitzki, J., *FAIR: Flexible Algorithms for Image Registration*

Chan, R. H.-F. and Jin, X.-Q., *An Introduction to Iterative Toeplitz Solvers*

Eldén, L., *Matrix Methods in Data Mining and Pattern Recognition*

Hansen, P. C., Nagy, J. G., and O'Leary, D. P., *Deblurring Images: Matrices, Spectra, and Filtering*

Davis, T. A., *Direct Methods for Sparse Linear Systems*

Kelley, C. T., *Solving Nonlinear Equations with Newton's Method*

Gabriele Ciaramella
Politecnico di Milano
Milan, Italy

Martin J. Gander
University of Geneva
Geneva, Switzerland

Iterative Methods and Preconditioners for Systems of Linear Equations

siam | Society for Industrial and Applied Mathematics

10 9 8 7 6 5 4 3 2 1

Publications Director	Kivmars H. Bowling
Executive Editor	Elizabeth Greenspan
Developmental Editor	Mellisa Pascale
Managing Editor	Kelly Thomas
Production Editor	Louis R. Primus
Copy Editor	Susan Fleshman
Production Manager	Donna Witzleben
Production Coordinator	Cally A. Shrader
Compositor	Cheryl Hufnagle
Graphic Designer	Doug Smock

Library of Congress Cataloging-in-Publication Data
Names: Ciaramella, G. (Gabriele), author. | Gander, Martin J., author.
Title: Iterative methods and preconditioners for systems of linear equations / Gabriele Ciaramella, Martin J. Gander.
Description: Philadelphia : Society for Industrial and Applied Mathematics, [2022] | Includes bibliographical references and index. | Summary: "This book gives an introduction to iterative methods and preconditioning for solving discretized elliptic partial differential equations (PDEs) and optimal control problems governed by elliptic PDEs, for which the use of matrix-free procedures is crucial"-- Provided by publisher.
Identifiers: LCCN 2021045671 (print) | LCCN 2021045672 (ebook) | ISBN 9781611976892 (paperback) | ISBN 9781611976908 (ebook)
Subjects: LCSH: Iterative methods (Mathematics) | Differential equations, Elliptic--Numerical solutions. | Control theory. | Mathematical optimization.
Classification: LCC QA297.8 .C424 2022 (print) | LCC QA297.8 (ebook) | DDC 518/.26--dc23/eng/20211108
LC record available at *https://lccn.loc.gov/2021045671*
LC ebook record available at *https://lccn.loc.gov/2021045672*

To Ivana and Mariagiovanna, our beloved companions in the journey of life.

Contents

Preface

This book gives an introduction to iterative methods and preconditioning for solving discretized elliptic partial differential equations (PDEs) and optimal control problems governed by elliptic PDEs, for which the use of matrix-free procedures is crucial. It grew out of a set of lecture notes going back to the Ph.D. days of the second author at Stanford, prepared for CS137. The lecture notes evolved through lectures given at McGill University and the University of Geneva by the second author, where the topic became a specialized advanced undergraduate/early graduate course. In 2017, when the first author was a teaching assistant in Geneva, the lecture notes were restructured, expanded, and enriched into an earlier form of the book, without optimal control yet. After that, the same subject was taught again (and in several different forms) by the second author at the University of Geneva and the first author as professor at the University of Konstanz. These last years allowed the authors to further improve the manuscript, further enrich it with several examples, and add new insights, new sections, and the new chapter about optimal control problems.

During this long period of studying and teaching this subject, a clear focus for the teaching methodology emerged:

- All methods are explained and analyzed starting from the historical ideas of the inventors, which are often quoted from their seminal works.

- The methods are illustrated immediately on the same PDE model problem, namely the Laplace equation, and the corresponding MATLAB codes are provided (available from https://bookstore.siam.org/fa19/bonus). An advection-reaction-diffusion problem is also introduced as a prototype of a nonsymmetric problem and used in the exercises to learn about similarities and differences with the Laplace problem.

- Stationary iterative methods and preconditioners for Krylov methods are intimately related, and we follow the principle to study and test all preconditioners first as stationary iterative solvers. This avoids the complication of mixing properties of the preconditioner and the Krylov method that makes their understanding difficult. We advocate, however, to always use Krylov acceleration at the end in practice.

- We emphasize that having a convergent stationary iterative method at the continuous level is a fundamental tool to obtain mesh size–independent convergence when the method is then discretized, and the same applies when the method is used as a preconditioner for a Krylov method.

- Once a clear and global picture about iterative methods for the solution of discretized PDEs is established, it is natural to move the focus to optimal control problems governed by PDEs. This class of constrained optimization problems represents a very important

application oriented benchmark for stationary and nonstationary iterative methods. The optimality (KKT) systems arising from these problems are generally saddle-point problems, and thus symmetric and indefinite, which completes the picture together with the symmetric Laplace problem and the nonsymmetric advection-reaction-diffusion problem.

The material is suitable for a one-semester course with four hours per week given to students from mathematics, computational science, and engineering. It is also possible to give selected topics in a two-hour semester course; we tested, for example, a more classical course on stationary iterative methods and basic Krylov methods, or a more modern course on Krylov methods and preconditioning, with just a brief review of the stationary iterative methods of Jacobi, Gauss–Seidel, and Richardson at the beginning, or a more advanced course about Krylov methods, preconditioners, and optimal control problems.

The book focuses on both analysis and numerical experiments, and it allows the material to be taught with very little preparation, since all the arguments are self-contained. It is therefore also possible to study the material independently and individually, without taking a course.

We are very thankful to (in chronological order) Kévin Santugini, who prepared many of the exercises as assistant when the second author taught the course for the first time in 2005; Yves Courvoisier, who was assistant in 2010 and proofread an earlier draft of the lecture notes; Stefan Banholzer, who was assistant in the course taught in Konstanz in 2018 and read an earlier version of this book; Conor McCoid, who was assistant in the course taught in Geneva in 2020 and read the manuscript while it was being put into final form; Michal Outrata, who read the Krylov and preconditioning chapters during the same time; and Stefan Volkwein, Luca Mechelli, and Tommaso Vanzan, who read the last chapter about optimal control problems and gave us several useful comments. All of them helped very much with their suggestions to improve the manuscript.

We are also thankful to three anonymous referees, who gave us interesting suggestions to improve this book.

Gabriele Ciaramella and Martin J. Gander
Milan and Geneva, June 2021

Chapter 1
Introduction

Now, three-dimensional models are commonplace and iterative methods are almost mandatory. The memory and the computational requirements for solving three-dimensional Partial Differential Equations, or two-dimensional ones involving many degrees of freedom per point, may seriously challenge the most efficient direct solvers available today. Also, iterative methods are gaining ground because they are easier to implement efficiently on high-performance computers than direct methods.

Yousef Saad, *Iterative Methods for Sparse Linear Systems*, 2003

There has been tremendous development in iterative methods and preconditioning over the past few decades, and research in this area is more active than ever, with many conference series dedicated entirely to this subject, like the international conference on domain decomposition methods, the Copper Mountain multigrid and iterative methods conferences, the preconditioning conference series, and the European multigrid conferences. Iterative methods and preconditioning also form an important part of almost all conferences on numerical analysis these days. This is due to the tremendously increased computing power and the advent of massively parallel computers, and multicore processors even in devices used in our daily lives, which permit simulations of unprecedented quality on such systems.

There are many excellent books and monographs on iterative methods for linear systems of equations, from which we benefited tremendously in our research and preparing the courses we taught on this subject. An invaluable source is the reference text by *Yousef Saad* [163], who has himself made many seminal contributions to modern iterative methods, and whom we quote frequently in this book. An outstanding reference for Krylov methods is the book by *Jörg Liesen* and *Zdeněk Strakoš* [124], with a focus on understanding the deep mathematics of the approximation properties of these methods. The book of *Anne Greenbaum* [94] has also been of great help in preparing and understanding material for our lectures. We would finally also like to mention the templates book [5], which motivated us to give implementations of all the algorithms we discuss, in our case directly runnable in MATLAB.

Our book is an introduction to the historical development of iterative methods methods, up to the state of the art today, and it includes convergence analyses of all the methods we discuss. The material is based on the authors' own experience and research with these methods and permits a rapid entry into this exciting field of research. To limit the scope, the focus is entirely on iterative methods for the solution of linear systems, with the approximate solution of discretized partial differential equations (PDEs) in mind.

1.1 ▪ Motivation

We move from direct methods, a classical topic that is rather thoroughly understood, to the relatively untamed territory of iterative methods. These are the methods that seem likely to dominate the large-scale computations of the future.

Lloyd N. Trefethen and David Bau, *Numerical Linear Algebra*, Lecture 32, 1997.

With the advent of modern computers, the fundamental difficulty of problems in mathematics has changed dramatically, because of algorithms that compute solutions iteratively. Let us consider two simple examples:

1. For a linear system of equations

$$A\boldsymbol{u} = \boldsymbol{f}, \quad \text{with } A \in \mathbb{R}^{n\times n} \text{ and } \boldsymbol{f} \in \mathbb{R}^n \text{ given},$$

we want to compute the solution $\boldsymbol{u} \in \mathbb{R}^n$. The classical approach is to use *Gaussian elimination*, named after *Carl Friedrich Gauss* from 1798,[1] which systematically eliminates the first unknown in the second to last equation, and then the second unknown in the third to last equation, and so on. This leads to the LU *factorization* of the matrix A (see, for example, [86, Chapter 3]), which was also discovered by Gauss in 1820.[2] Instead of solving the linear system, one can then solve in two steps $LU\boldsymbol{u} = \boldsymbol{f}$ (see also [86, Chapter 3]): setting $\boldsymbol{v} := U\boldsymbol{u}$, one first solves using *forward substitution* the triangular system

$$L\boldsymbol{v} = \boldsymbol{f}$$

for $\boldsymbol{v}$, followed by solving by *backward substitution*

$$U\boldsymbol{u} = \boldsymbol{v},$$

two triangular solves. For a matrix of size $n\times n$, the cost of computing the LU factorization is $O(n^3)$, and the forward and backward substitutions cost $O(n^2)$ floating point operations. This method gives in principle the exact solution (up to round-off error) to the linear system of equations in a finite number of steps; one could not imagine a more simple problem in mathematics.

2. Let us now consider the problem of finding the *eigenvalues* $\lambda_j \in \mathbb{C}$ and *eigenvectors* $\boldsymbol{\phi}_j \in \mathbb{C}^n$ of a given matrix $A \in \mathbb{R}^{n\times n}$,

$$A\boldsymbol{\phi}_j = \lambda_j \boldsymbol{\phi}_j, \quad j = 1, 2, \ldots, n.$$

Here there is no algorithm which can give us the exact solution after a finite number of steps, since the eigenvalues are the roots of the *characteristic polynomial* $p(\lambda) := \det(A - \lambda I)$, I the identity matrix, and it is well known by Galois theory that there exists no closed formula to express the roots of a polynomial of degree $n > 4$. Nevertheless, one can obtain the eigenvalues and eigenvectors to arbitrary accuracy in $O(n^3)$ operations using an iterative method, namely the *QR algorithm*; see, for example, [86, Chapter 7].

So while from a pure mathematical standpoint, solving a system of linear equations is trivial, and obtaining the eigenvalues of a matrix is impossible in closed form, there is little difference in obtaining the actual solution. We compare in Figure 1.1 the cost in MATLAB to compute the solution of random linear systems and the eigenvalues of the associated matrix. The figure was obtained with the MATLAB script

[1] Gaussian elimination was already known to Chinese mathematicians as early as 179 CE and can be found in Newton's notes from 1670 and in Lagrange's work on Lagrange multipliers from 1788.

[2] Note that it took Gauss more than twenty years to realize this important and nontrivial interpretation!

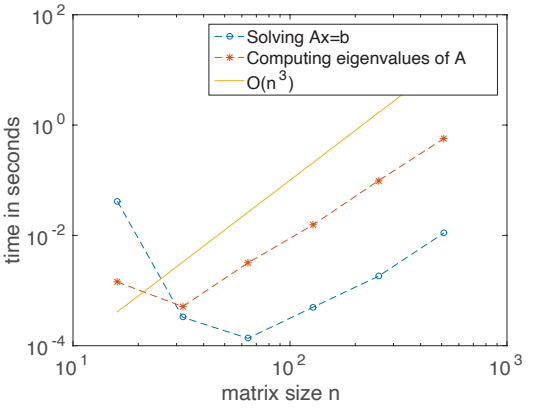

Figure 1.1. *Comparison of computing times for solving linear systems and obtaining the eigenvalues of the associated matrix, as a function of the matrix size.*

```
n=2.^(4:9);                                          % matrix sizes
T1=zeros(1,length(n)); T2=zeros(1,length(n));        % for storing times
for j=1:10                                           % do 10 experiments
  for i=1:length(n)                                  % to average times
    A=rand(n(i));
    t0=clock; B=lu(A); t1(i)=etime(clock,t0);        % compute LU
    t0=clock; E=eig(A); t2(i)=etime(clock,t0);       % compute eigenvalues
  end
  T1=T1+t1; T2=T2+t2;                                % sum times
end
loglog(n,T1/10,'--o',n,T2/10,'--*',n,n.^3/10000000,'-');
legend('Solving Ax=b','Computing eigenvalues of A','O(n^3)',...
       'location','NorthEast');
xlabel('matrix size n');
ylabel('time in seconds');
set(gca,'fontsize',20);                              % bigger font size
```

We see that indeed both problems have the same computational complexity $O(n^3)$; the eigenvalue problem just has a larger constant.

1.2 ▪ Gauss and Jacobi

Schwerlich werden Sie je wieder direct eliminieren, wenigstens nicht, wenn Sie mehr als 2 Unbekannte haben. Das indirecte Verfahren lässt sich halb im Schlafe ausführen, oder man kann während desselben an andere Dinge denken.

Carl F. Gauss, in a letter to his friend Christian L. Gerling, 1823.[a]

Die Beschwerlichkeit der strengen Auflösung einer grösseren Zahl linärer Gleichungen, auf welche in vielen Fällen die Methode der kleinsten Quadrate führt, hat an die Anwendung von Näherungsmethoden denken lassen.

Carl G. J. Jacobi, *Über eine neue Auflösungsart der bei der Methode der kleinsten Quadrate vorkommenden lineären Gleichungen*, 1845.

[a] For English translations of quotes, see p. 257.

Iterative methods for linear systems of equations have a long history. An overview of selected key events is shown in Figure 1.2, and we start with the first main inventions by *Carl Friedrich Gauss* and *Carl Gustav Jacob Jacobi*.

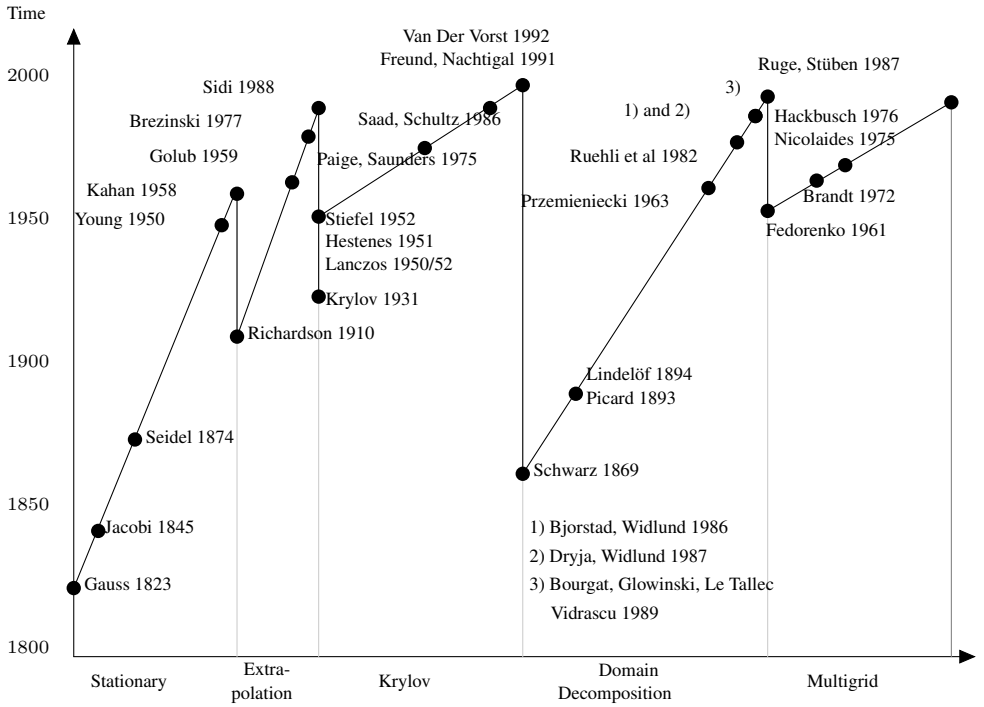

Figure 1.2. *An overview of key events in the historical development of iterative methods for linear systems of equations, and how they will appear throughout the text.*

On December 26, 1823, Gauss sent a letter to his friend Gerling [87] to explain how he computed an approximate *least squares* solution based on angle measurements between the locations Berger Warte, Johannisberg, Taufstein, and Milseburg. The system is symmetric (see Figure 1.3); it comes from the normal equations, and Gauss explains (translation by *Forsythe* [65]):

> In order to eliminate indirectly, I note that, if 3 of the quantities a, b, c, d are set to 0, the fourth gets the largest value when d is chosen as the fourth. Naturally, every quantity must be determined from its own equation, and hence d from the fourth. I therefore set $d = -201$ and substitute this value. The absolute terms then become: $+5232$, -6352, $+1074$, $+46$; the other terms remain the same.

In this first step, Gauss sets as approximation $a = b = c = 0$ and then uses the fourth equation to compute an approximation to d,

$$d = -\frac{22156}{110} \approx -201.$$

Assuming that $d = -201$ now, he can compute an updated right-hand side which he calls "absolute terms,"

$$\begin{aligned} 6 - 26d &\approx 5232, \\ -7558 - 6d &\approx -6352, \\ -14604 - 78d &\approx 1074, \\ 22156 + 110d &\approx 46, \end{aligned}$$

and we see that also the last equation does not have a right-hand-side zero; it is not necessary to compute d exactly. Gauss now continues as described in Figure 1.4. With the system with the new

Die Bedingungsgleichungen sind also:

$$\begin{aligned}
0 &= +\ 6 + 67a - 13b - 28c - 26d \\
0 &= -\ 7558 - 13a + 69b - 50c - 6d \\
0 &= -\ 14604 - 28a - 50b + 156c - 78d \\
0 &= +\ 22156 - 26a - 6b - 78c + 110d; \\
&\text{Summe} = 0.
\end{aligned}$$

Um nun indirect zu eliminiren, bemerke ich, dass, wenn 3 der Grössen a, b, c, d gleich 0 gesetzt werden, die vierte den grössten Werth bekommt, wenn d dafür gewählt wird. Natürlich muss jede Grösse aus ihrer eigenen Gleichung, also d aus der vierten, bestimmt werden. Ich setze also $d = -201$ und substituire diesen Werth. Die absoluten Theile werden dann: $+5232$, -6352, $+1074$, $+46$; das Übrige bleibt dasselbe.

Figure 1.3. *Letter of Gauss from 1823 explaining the first step of his new method to solve linear equations by the indirect method.*

Jetzt lasse ich b an die Reihe kommen, finde $b = +92$, substituire und finde die absoluten Theile: $+4036$, -4, -3526, -506. So fahre ich fort, bis nichts mehr zu corrigiren ist. Von dieser ganzen Rechnung schreibe ich aber in der Wirklichkeit bloss folgendes Schema:

	$d = -201$	$b = +92$	$a = -60$	$c = +12$	$a = +5$	$b = -2$	$a = -1$
$+6$	$+5232$	$+4036$	$+16$	-320	$+15$	$+41$	-26
-7558	-6352	-4	$+776$	$+176$	$+111$	-27	-14
-14604	$+1074$	-3526	-1846	$+26$	-114	-14	$+14$
$+22156$	$+46$	-506	$+1054$	$+118$	-12	0	$+26.$

Insofern ich die Rechnung nur auf das nächste 2000^{tel} [der] Secunde führe, sehe ich, dass jetzt nichts mehr zu corrigiren ist. Ich sammle daher

$a = -60$	$b = +92$	$c = +12$	$d = -201$
$+5$	-2		
-1			
-56	$+90$	$+12$	-201

Figure 1.4. *Continuation of the letter of Gauss from 1823 to his friend Gerling.*

right-hand side, he searches again for the variable with the biggest contribution when setting the other ones to zero and finds that it is b in this case, which leads to $b = \frac{6352}{69} \approx 92$. He computes again a new right-hand side and continues the procedure, saying that of all these computations he keeps only the table in Figure 1.4. He stops computing corrections with $a \approx -1$, and then sums for each variable all correction steps, which gives as approximate solution $a \approx -56$, $b \approx 90$, $c \approx 12$, $d \approx -201$. We can check these computations using the MATLAB script

```
A=[67 -13 -28 -26                % example of Gauss
   -13 69 -50 -6
```

```
   -28 -50 156 -78
   -26 -6 -78 110];
f=-[6                              % original right-hand side
  -7558
  -14604
   22156];
id=[4 2 1 3 1 2 1];                % sequence of variables used
D=diag(A);
fn=f;
u=zeros(4,1);                      % to sum corrections
F=[];
for i=1:length(id)                 % compute correction steps
  d=zeros(4,1);
  d(id(i))=round(fn(id(i))/D(id(i)))
  u(id(i))=u(id(i))+d(id(i));      % add correction
  fn=fn-A*d;                       % update the right-hand side
  F=[F -fn]                        % collect updated right-hand sides
  pause
end
u                                  % approximate solution of Gauss
uexact=A\f                         % compare with Matlab solution
[A*u-f A*uexact-f]                 % Gauss and Matlab solution residual
fm=f-u(4)*A(:,4);                  % compute Matlab solution with same 4th
uc=A(1:3,:)'\fm;                   % component as Gauss's solution
uc(4)=u(4);
[u uc]                             % compare again
```

The solution computed with a backslash in MATLAB, however, gives the warning

```
Warning: Matrix is close to singular or badly scaled. Results may be
inaccurate. RCOND = 1.744962e-17.
> In exampleGauss (line 23)
uexact =
 -234.6661
  -88.7902
 -167.0551
 -380.1850
```

and it is quite different from the solution computed by Gauss. So what happened here? We so far have not paid attention to an important comment of Gauss in Figure 1.3, namely "Summe=0," which means that summing all equations we obtain zero, the system is *singular*, but consistent, and thus has many solutions. The MATLAB script above also computes the solution with the same last component as the one Gauss found, and we see then that the solution of Gauss is very accurate from the MATLAB output

```
ans =
  -56.0000  -55.4810
   90.0000   90.3949
   12.0000   12.1300
 -201.0000 -201.0000
```

Gauss concludes his letter with the statement in Figure 1.5 (translation by Forsythe [65]):

> Almost every evening I make a new edition of the tableau, wherever there is easy improvement. Against the monotony of the surveying business, this is always a pleasant entertainment; one can also see immediately whether anything doubtful has crept in, what still remains

> Fast jeden Abend mache ich eine neue Auflage des Tableaus, wo immer leicht nachzuhelfen ist. Bei der Einförmigkeit des Messungsgeschäfts gibt dies immer eine angenehme Unterhaltung; man sieht dann auch immer gleich, ob etwas zweifelhaftes eingeschlichen ist, was noch wünschenswerth bleibt, etc. Ich empfehle Ihnen diesen Modus zur Nachahmung. Schwerlich werden Sie je wieder direct elimininiren, wenigstens nicht, wenn Sie mehr als 2 Unbekannte haben. Das indirecte Verfahren lässt sich halb im Schlafe ausführen, oder man kann während desselben an andere Dinge denken.

Figure 1.5. *Gauss explains how relaxing these relaxations are.*

> to be desired, etc. I recommend this method to you for imitation. You will hardly ever again eliminate directly, at least not when you have more than 2 unknowns. The indirect procedure can be done while half asleep, or while thinking about other things.

So instead of watching TV or surfing on the Internet, it would be better for all of us to do some relaxing relaxations in the evening to find approximate solutions to linear systems of equations![3]

The following MATLAB function attempts to solve a general linear system of equations precisely using the method described by Gauss, i.e., always choosing the most promising variable to do an update.

```
function u=Gauss(A,f,maxiter,tol,Rnd)
% GAUSS original iterative method by Gauss
%   u=Gauss(A,f,iter,tol,Rnd) attempts to solve the linear
%   system A*u=f using the iterative method originally proposed by
%   Gauss. The parameter maxiter limits the maximum number of
%   iterations, if the norm of the right-hand side obtained compared
%   to the original one does not go below the parameter tol before.
%   Rnd is a flag to turn the rounding Gauss used on (Rnd=1) or off
%   (Rnd=0).

m=length(f);
D=diag(A);
fn=f;                              % keep original right hand side
u=zeros(m,1);                      % to sum corrections
i=1;
while norm(fn)/norm(f)>tol && i<=maxiter
  [du,id]=max(abs(fn./D));         % find biggest contribution
  d=zeros(m,1);
  d(id)=fn(id)/D(id);
  if Rnd, d(id)=round(d(id)); end  % round if desired
  u=u+d;                           % add correction
  fn=fn-A*d;                       % update the right-hand side
  i=i+1;
end
```

This function allows us to reproduce the example of Gauss, and also to test the method for arbitrary linear problems $A\boldsymbol{u} = \boldsymbol{f}$. To reproduce the Gauss example, we can now simply call `Gauss(A,f,7,1e-6,1)` with the original matrix A and right-hand-side vector $\boldsymbol{f}$

[3] The first author, assistant for the course "Méthodes Itératives" in Geneva, in an email to the second author, two weeks into the course: "Following the suggestion 'do some relaxation calculus to relax in the evening,' :-) I computed the iteration matrix of the alternating Schwarz method for three holes, or in another picture the iteration matrix of a modified method of reflections."

from the Gauss example, to find the same result. If we try more iterations, for example, `Gauss(A,f,10,1e-6,1)`, the result, however, does not become more accurate, because we reached the level of accuracy one can obtain using rounding, and the method *stagnates*. Turning rounding off, `Gauss(A,f,10,1e-6,0)`, we obtain

```
ans =
  -56.0383
   89.8419
   11.5599
 -201.5456
```

and we can indeed reach a more and more accurate solution by reducing the tolerance and increasing the maximum number of iterations, e.g.,

```
u=Gauss(A,f,10,1e-12,0);
norm(f-A*u)
u=Gauss(A,f,20,1e-12,0);
norm(f-A*u)
u=Gauss(A,f,40,1e-12,0);
norm(f-A*u)
```

which leads to the residual norms `3.9411, 0.0080, 4.8106e-08`. As a further example, we consider the symmetric positive definite matrix

$$A = \begin{bmatrix} 4 & -1 & 0 & 0 \\ -1 & 4 & -1 & 0 \\ 0 & -1 & 4 & -1 \\ 0 & 0 & -1 & 4 \end{bmatrix} \quad \text{and} \quad \boldsymbol{f} = \begin{bmatrix} 1 \\ 1 \\ 1 \\ 1 \end{bmatrix}.$$

Using the MATLAB commands

```
A=[4 -1 0 0;
   -1 4 -1 0;
   0 -1 4 -1;
   0 0 -1 4];
f=ones(4,1);
Gauss(A,f,30,1e-6,0)
A\f
```

we see that the method works very well. Trying, however, random matrices,

```
A=rand(5);
f=ones(5,1);
u=Gauss(A,f,100,1e-12,0)
u-A\f
```

the method almost always fails. The difference between the computed `u` and the exact solution `A\f` is very large. If we try, however, symmetric positive definite matrices, which we can construct from random matrices by multiplying by their transpose, the method seems to always work, provided we do enough iterations,

```
A=rand(5);
A=A'*A;
f=ones(5,1);
u=Gauss(A,f,10000,1e-12,0)
u-A\f
```

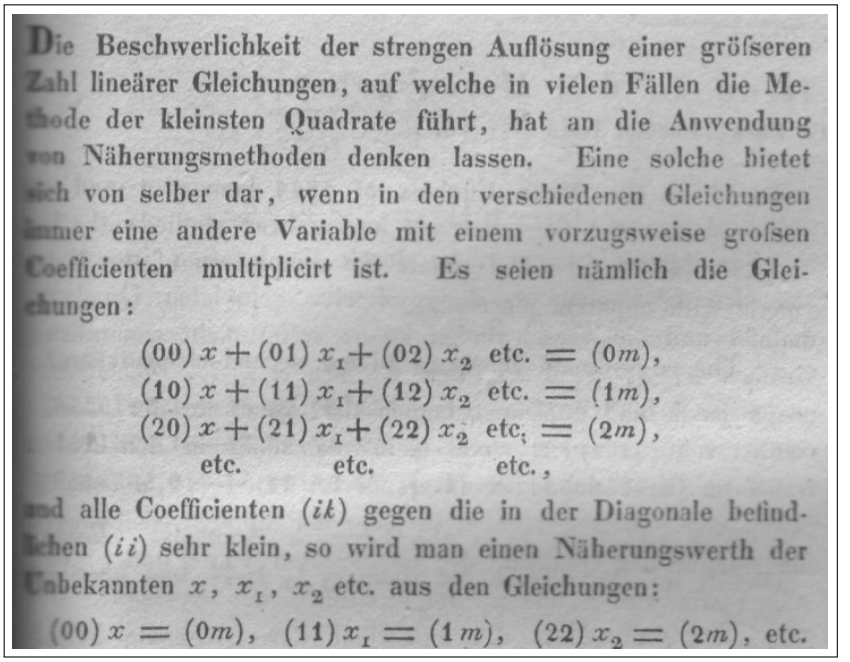

Die Beschwerlichkeit der strengen Auflösung einer gröfseren Zahl lineärer Gleichungen, auf welche in vielen Fällen die Methode der kleinsten Quadrate führt, hat an die Anwendung von Näherungsmethoden denken lassen. Eine solche bietet sich von selber dar, wenn in den verschiedenen Gleichungen immer eine andere Variable mit einem vorzugsweise grofsen Coefficienten multiplicirt ist. Es seien nämlich die Gleichungen:

$$\begin{aligned}(00)\,x + (01)\,x_1 + (02)\,x_2 \text{ etc.} &= (0m),\\ (10)\,x + (11)\,x_1 + (12)\,x_2 \text{ etc.} &= (1m),\\ (20)\,x + (21)\,x_1 + (22)\,x_2 \text{ etc.} &= (2m),\\ \text{etc.} \quad \text{etc.} \quad \text{etc.},&\end{aligned}$$

und alle Coefficienten (ik) gegen die in der Diagonale befindlichen (ii) sehr klein, so wird man einen Näherungswerth der Unbekannten x, x_1, x_2 etc. aus den Gleichungen:

$$(00)\,x = (0m),\quad (11)\,x_1 = (1m),\quad (22)\,x_2 = (2m),\ \text{etc.}$$

Figure 1.6. *Main idea of Jacobi inventing a different iterative method to solve linear systems of equations.*

About half a century after Gauss, in 1874, a general description of this iterative method was given for the normal equations by *Ludwig von Seidel* [169], who also proved convergence of the method in this case,[4] and proposed to do the relaxations cyclically, instead of always choosing the equation that gives the largest contribution. Seidel finally even suggested distributing the computations to two computers (humans) to do parallel computing.[5] We will study the convergence properties of the Gauss method in Section 2.7.

Before Seidel's general description of the method of Gauss, however, *Jacobi* presented in 1845 a variant of the Gauss method now known as the Jacobi method [112].[6] We show in Figure 1.6 how Jacobi imagined the first iteration step of the method. Note how modern the notation already is: matrix entries we denote today by a_{ij} are denoted by (ij), and the vector of unknowns is $\boldsymbol{x} = (x, x_1, x_2, \ldots)$, where we now use $\boldsymbol{x} = (x_1, x_2, x_3, \ldots)$. Also the right-hand side is using vector notation, $\boldsymbol{b} = (0m, 1m, 2m, \ldots)$, where we nowadays use $\boldsymbol{b} = (b_1, b_2, b_3, \ldots)$. So in modern notation, the system in Figure 1.6 reads

$$\begin{aligned} a_{11}x_1 + a_{12}x_2 + a_{13}x_3 + \cdots &= b_1,\\ a_{21}x_1 + a_{22}x_2 + a_{23}x_3 + \cdots &= b_2,\\ a_{31}x_1 + a_{32}x_2 + a_{33}x_3 + \cdots &= b_3,\\ &\vdots \end{aligned}$$

[4] . . . and considered this to be the end of research needed on iterative methods, because all systems can be transformed into a system of normal equations: "Wohl aber kann man auch jedes beliebige System linearer Gleichungen mit gleich vielen Unbekannten in die Normalform (B) bringen, genau nach der auf die Gleichungen (A) angewendeten Vorschrift, und aus dieser Form ist es nach unserer Methode ganz ebenso auflösbar, wie die aus Beobachtungen abgeleiteten Normalgleichungen."

[5] "sich unter zwei Rechner so vertheilen lässt."

[6] Seidel was a student of Jacobi, and Jacobi thanks him for computations he had performed for him: "Man wird dort aus den von einem meiner gelehrten Freunde, Herrn Dr. Seidl in München, mit grosser Sorgfalt geführten Rechnungen ersehen."

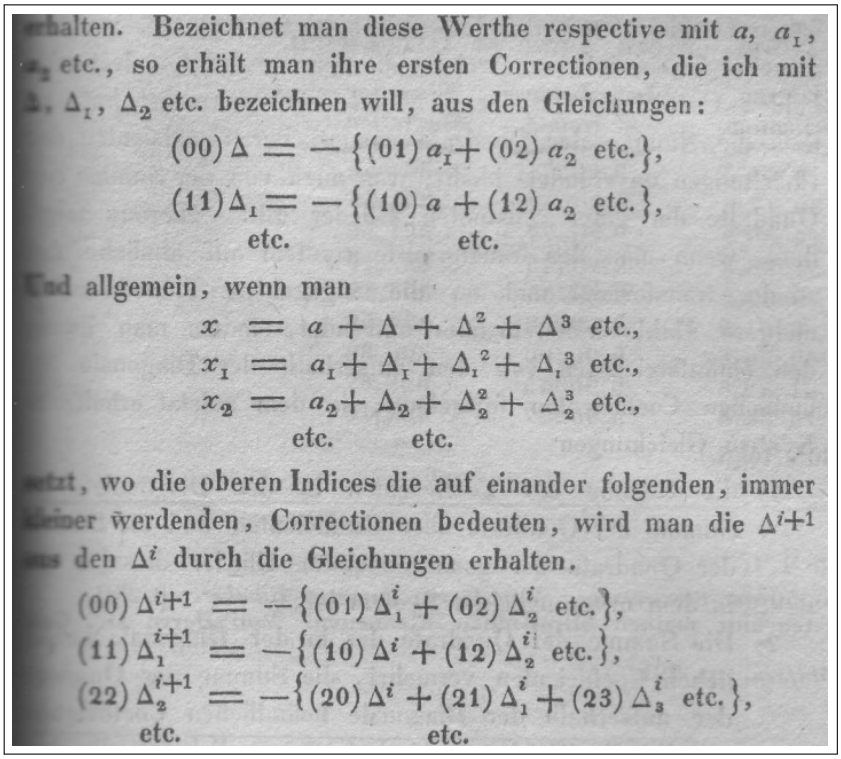

erhalten. Bezeichnet man diese Werthe respective mit a, a_1, a_2 etc., so erhält man ihre ersten Correctionen, die ich mit Δ, Δ_1, Δ_2 etc. bezeichnen will, aus den Gleichungen:

$$(00)\,\Delta = -\{(01)\,a_1 + (02)\,a_2 \text{ etc.}\},$$
$$(11)\,\Delta_1 = -\{(10)\,a + (12)\,a_2 \text{ etc.}\},$$
etc. etc.

Und allgemein, wenn man

$$x = a + \Delta + \Delta^2 + \Delta^3 \text{ etc.},$$
$$x_1 = a_1 + \Delta_1 + \Delta_1^2 + \Delta_1^3 \text{ etc.},$$
$$x_2 = a_2 + \Delta_2 + \Delta_2^2 + \Delta_2^3 \text{ etc.},$$
etc. etc.

setzt, wo die oberen Indices die auf einander folgenden, immer kleiner werdenden, Correctionen bedeuten, wird man die Δ^{i+1} aus den Δ^i durch die Gleichungen erhalten.

$$(00)\,\Delta^{i+1} = -\{(01)\,\Delta_1^i + (02)\,\Delta_2^i \text{ etc.}\},$$
$$(11)\,\Delta_1^{i+1} = -\{(10)\,\Delta^i + (12)\,\Delta_2^i \text{ etc.}\},$$
$$(22)\,\Delta_2^{i+1} = -\{(20)\,\Delta^i + (21)\,\Delta_1^i + (23)\,\Delta_3^i \text{ etc.}\},$$
etc. etc.

Figure 1.7. *Jacobi writing the method directly as a modern iterative method with iteration index i.*

Jacobi then says right below the linear system in Figure 1.6 that if the off-diagonal coefficients a_{ik} are all small compared to the a_{ii} on the diagonal, then a good approximation to the solution of the linear system can already be obtained by just solving the diagonal system, i.e.,

$$x_1 \approx \frac{b_1}{a_{11}},\ x_2 \approx \frac{b_2}{a_{22}},\ x_3 \approx \frac{b_3}{a_{33}},\ \dots\ .$$

If these approximations are not good enough, Jacobi then explains (see Figure 1.7) how one can obtain the first corrections to improve the approximations, by computing

$$\begin{aligned}\Delta_1 &= \tfrac{1}{a_{11}}(-a_{12}x_2 - a_{13}x_3 - \cdots),\\ \Delta_2 &= \tfrac{1}{a_{22}}(-a_{21}x_1 - a_{23}x_3 - \cdots),\\ &\vdots\end{aligned}$$

and in general better and better approximations can be obtained by setting

$$\begin{aligned}x_1 &\approx \tfrac{b_1}{a_{11}} + \Delta_1 + \Delta_1^2 + \Delta_1^3 + \cdots,\\ x_2 &\approx \tfrac{b_2}{a_{22}} + \Delta_2 + \Delta_2^2 + \Delta_2^3 + \cdots,\\ x_3 &\approx \tfrac{b_3}{a_{33}} + \Delta_3 + \Delta_3^2 + \Delta_3^3 + \cdots,\\ &\vdots\end{aligned}$$

See again Figure 1.7, where now the corrections Δ_j^i are computed by the iteration[7]

$$\begin{aligned}
\Delta_1^{i+1} &= -\tfrac{1}{a_{11}}(a_{12}\Delta_2^i + a_{13}\Delta_3^i - \cdots),\\
\Delta_2^{i+1} &= -\tfrac{1}{a_{22}}(a_{21}\Delta_1^i + a_{23}\Delta_3^i - \cdots),\\
\Delta_3^{i+1} &= -\tfrac{1}{a_{33}}(a_{31}\Delta_1^i + a_{32}\Delta_2^i - \cdots),\\
&\vdots
\end{aligned}$$

Note in Figure 1.7 how Jacobi used groundbreaking modern notation, writing a general iterative method with iteration index i for the corrections.

Even though Gauss said that one will hardly ever use direct elimination for systems bigger than two by two, nowadays direct elimination is commonly used for linear systems with many thousands of unknowns. Linear systems which really benefit from iterative methods are systems where the size is such that it is an approximation to infinity, and we present now a typical example of such a system.

1.3 ▪ Laplace's equation as a typical example

> *The title of this book, Matrix Iterative Analysis, suggests that we might consider here all matrix numerical methods which are iterative in nature. However, such an ambitious goal is in fact replaced by the more practical one where we seek to consider in some detail that smaller branch of numerical analysis concerned with the efficient solution, by means of iteration, of matrix equations arising from discrete approximations to partial differential equations.*
>
> Richard S. Varga, *Matrix Iterative Analysis*, 1962

The solution of PDEs by *discretization* often leads to large and *sparse linear systems* of equations, and these are ideally suited for iterative methods, as Varga already emphasized in his seminal book [181]; see also the quote above. A first example is shown in Figure 1.8, from [68]. In the top panel, we see a two-dimensional cross section of Apartment 208 at 3421 Durocher, Montreal, where the Ganders were living. The floorplan is shown with a finite-element discretization (see, e.g., [76] for more on the finite-element method) and a decomposition into the different rooms (see Section 4.6 for more on domain decomposition): on the left is the living room, connected to the kitchen and with a long hallway to the bathroom and bedroom on the right. Insulated walls are shown in blue, the windows on top are shown in black, where we assume -20 degrees Celsius for a regular Montreal winter day, and the doors at the bottom and on the right are also shown in black. They lead to a heated public hallway, at about 15 degrees Celsius. In the bottom panel, we show the solution of the corresponding steady state heat equation we will introduce shortly, representing the temperature distribution: one can see that while the heaters in the living room on the left and the bedroom on the right are well placed to block the cold from the windows, the heater on the left wall in the bathroom is not effective to keep the room warm, a fact the Ganders strongly felt in winter. Also, the kitchen is not heated and stays cold, except when cooking and baking.

A second example, trying to cook a chicken in a microwave oven [56], is show in Figure 1.9. From the magnetic field intensity computed on the right by solving *Maxwell's equations* in three dimensions, one can see why a turntable is so important in a microwave oven: there are hot spots, where the intensity of the standing wave is high in the chicken, and other areas where there is very little heating happening, because the electric field is close to zero. Using a turntable

[7] Notice that Jacobi stated his algorithm in a difference form: the iterations are defined in terms of Δ_j^k that can be computed as $\Delta_j^k = x_j^k - x_j^{k-1}$, where the approximation of the solution at the iteration k is $x_j^k = \frac{b_j}{a_{jj}} + \sum_{\ell=1}^{k} \Delta_j^\ell$. The difference form of an iterative method is discussed in Section 2.1.

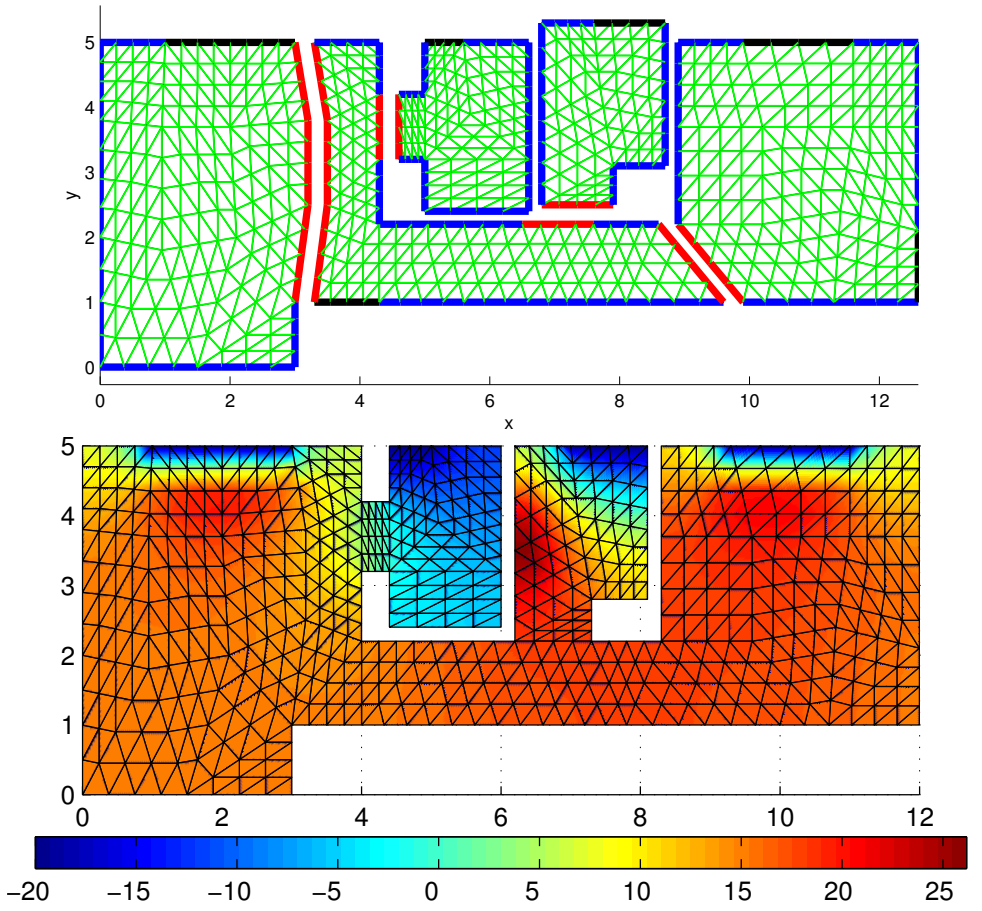

Figure 1.8. *Top: Discretization of Apartment 208 at 3421 Durocher, Montreal, with the rooms slightly separated. Bottom: Temperature distribution on a cold winter day.*

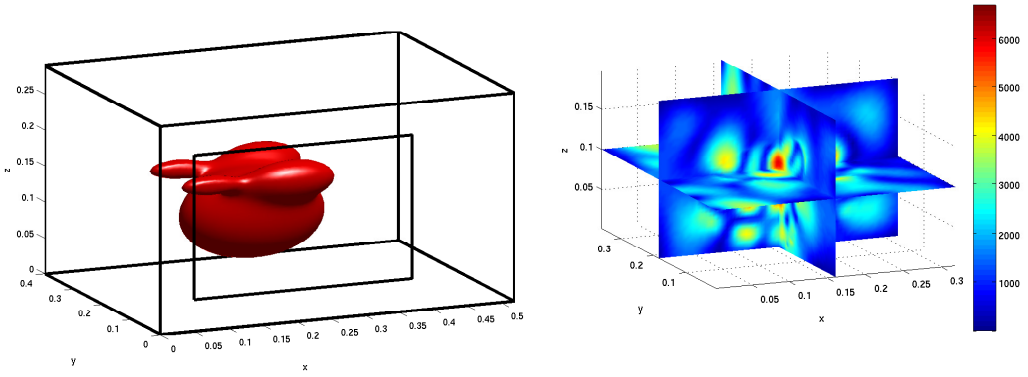

Figure 1.9. *Heating a chicken in our Whirlpool Talent Combi 4 microwave oven from our times in Paris. Left: The geometry of the microwave and the chicken. Right: The electric field intensity in the chicken.*

which turns the food steadily can avoid hot spots and lead to an approximately even heating of the chicken. Another possibility in modern microwave ovens is to change the frequency of the source periodically, which also moves the hot spots around.

Let us now get back to the *heat equation* of the first example, and let us consider the propagation of heat in an enclosed space, e.g., a room in a building. The temperature is a function of time t and space $\boldsymbol{x}$, which we denote by $u(t, \boldsymbol{x})$. Now how does the total amount of heat in a given volume V evolve? The *Fourier law of heat transfer*, which was discovered experimentally by *Jean-Baptiste Joseph Fourier* in 1822 and was known to Jean-Baptiste Biot mathematically already in 1804, says that the heat flux $\boldsymbol{F}$ is proportional to the gradient of the temperature, $\boldsymbol{F} = -\nu\nabla u$ for some constant ν we will assume for simplicity to equal one, $\nu = 1$, and the minus sign is because heat always moves from warm to cold, not the other way around. If in the volume V there is no heat source or sink, then the total amount of heat in the volume can only be increased or diminished by the heat which flows through its boundary ∂V, and we thus must have

$$\frac{\partial}{\partial t}\int_V u(\boldsymbol{x},t)d\boldsymbol{x} = -\int_{\partial V}\boldsymbol{F}(\boldsymbol{x},t)\cdot\boldsymbol{n}\,ds = \int_{\partial V}\nabla u(\boldsymbol{x},t)\cdot\boldsymbol{n}\,ds, \tag{1.1}$$

where $\boldsymbol{n}$ is the unit outward normal on the boundary ∂V of the volume V, and $d\boldsymbol{s}$ denotes a surface element for the integration on ∂V. Using now the *Divergence Theorem of Gauss* from 1813 to transform the surface integral on the right into a volume integral, we get

$$\frac{\partial}{\partial t}\int_V u(\boldsymbol{x},t)d\boldsymbol{x} = \int_V \nabla\cdot\nabla u(\boldsymbol{x},t)d\boldsymbol{x}, \tag{1.2}$$

and noticing that the divergence of the gradient is the *Laplacian*[8]

$$\nabla\cdot\nabla = \begin{bmatrix}\partial_x\\ \partial_y\\ \partial_z\end{bmatrix}\cdot\begin{bmatrix}\partial_x\\ \partial_y\\ \partial_z\end{bmatrix} = \partial_x^2+\partial_y^2+\partial_z^2 = \Delta,$$

and exchanging time differentiation and integration, we obtain

$$\int_V \frac{\partial}{\partial t}u(\boldsymbol{x},t) - \Delta u(\boldsymbol{x},t)d\boldsymbol{x} = 0. \tag{1.3}$$

Equation (1.3) must hold for any arbitrary volume V, and thus the term under the integral sign must vanish identically, which leads to the *heat equation*

$$u_t = \Delta u. \tag{1.4}$$

This is the equation which describes the evolution of temperature in a domain Ω, and to solve it, one needs to know what the initial temperature is, $u(\boldsymbol{x}, 0) = u^0(\boldsymbol{x})$, and also the temperature on the boundary of the domain, $u(\boldsymbol{x}, t) = g(\boldsymbol{x}, t)$ for $\boldsymbol{x} \in \partial\Omega$. If we are only interested in the stationary equilibrium, then for $t \to \infty$ we have $u_t = 0$ and the equation simplifies to[9]

$$\begin{aligned} -\Delta u &= 0 \qquad \text{in } \Omega,\\ u &= g \qquad \text{on } \partial\Omega. \end{aligned} \tag{1.5}$$

Equation (1.5) is called *Laplace's equation*, and we derived it considering heat transfer like Fourier in 1822. Laplace, however, discovered this equation in 1785, considering the attraction

[8] We use for partial derivatives interchangeably $\frac{\partial}{\partial x}u = \partial_x u = u_x$.

[9] We use the minus sign throughout to have a positive operator $-\Delta$, which is also natural if we had considered a source term in the heat equation, $u_t = \Delta u + f$, which for $t \to \infty$ gives $u_t = 0$, and the stationary *Poisson equation* $-\Delta u = f$, again with the minus sign.

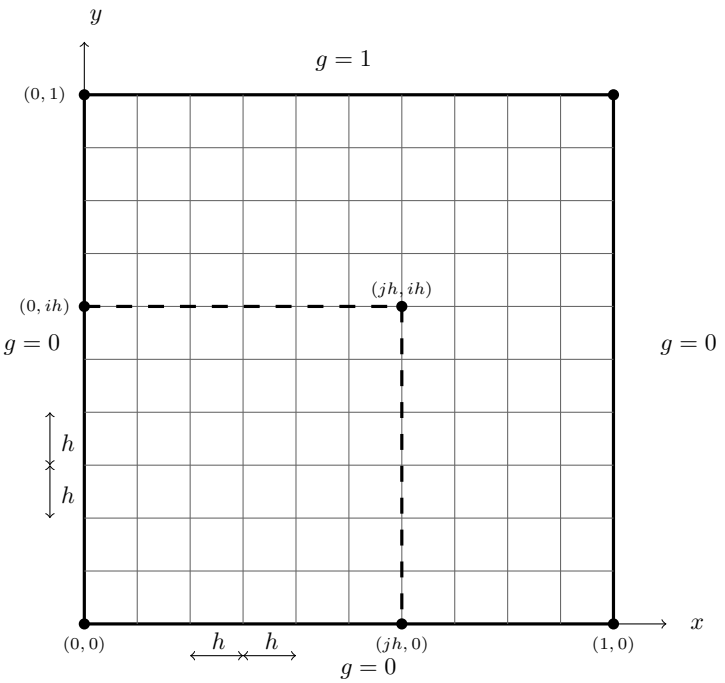

Figure 1.10. *Discretization grid used to approximate the Laplace equation* (1.5)*. Notice that the domain is discretized with $m + 2$ points in both x and y directions. The grid size is $h = \frac{1}{m+1}$ and each point of the grid is of the form $(x_j, y_i) = (jh, ih)$ for $j, i = 0, 1, \ldots, m, m + 1$. The function g defined on the boundary $\partial\Omega$ represents the boundary function that we use as a Dirichlet boundary condition.*

of celestial bodies, when he generalized Newton's inverse square law from 1687 for point masses to objects having nonzero volume. Laplace's equation turns out to be fundamental in many areas of physics and mathematics:

- theory of *the attraction of celestial bodies* (Laplace, 1785);
- theory of *stationary heat transfer* (Fourier, 1822);
- theory of *magnetism* (Gauss and Weber in Göttingen, 1839);
- theory of *electric fields* (W. Thomson, later Lord Kelvin, 1847, and Liouville, 1847);
- *conformal mappings* (Gauss, 1825);
- irrotational *fluid motion* in two dimensions (Helmholtz, 1858);
- in *complex analysis* (Cauchy, 1825, Riemann thesis, 1851).

To solve Laplace's equation (1.5), one needs to find a function such that it equals g on the boundary $\partial\Omega$, and when one computes the second partial derivatives with respect to each spatial variable and sums them, one obtains zero. It is very difficult to find such a function, and in general one can only obtain an approximation. To do so, let us consider a simple two-dimensional example, where the domain Ω is the unit square, the stationary heat distribution is a function of two variables, $u(x, y)$, and the boundary function g is as given in Figure 1.10. To obtain an approximate solution, we introduce a grid with grid size $h = \frac{1}{m+1}$, for $m \in \mathbb{N}^+$, and search

for an approximation u_{ij} of $u(x, y)$ only at the gridpoints. Since it is natural to think in column vectors when solving linear systems, we order the unknowns columnwise, so $u_{ij} \approx u(jh, ih)$. The solution stored in the matrix u_{ij} can be pictured like shown in Figure 1.10; one only has to remember that the first element in the top left corner of the matrix u_{ij} is in the bottom left corner of the figure, and the y coordinate is increasing from bottom to top, like one is used to. This ordering is also used in MATLAB for its plotting and meshing commands like `mesh`, `surf`, `reshape`, and `numgrid` and will greatly simplify its use. The *Laplace operator* in two dimensions,

$$\Delta u = \frac{\partial^2 u}{\partial x^2} + \frac{\partial^2 u}{\partial y^2},$$

is discretized using finite differences (see Problem 1),

$$\frac{\partial^2 u}{\partial x^2}(x, y) \approx \frac{u(x + h, y) - 2u(x, y) + u(x - h, y)}{h^2},$$

and similarly

$$\frac{\partial^2 u}{\partial y^2}(x, y) \approx \frac{u(x, y + h) - 2u(x, y) + u(x, y - h)}{h^2}.$$

Introducing these approximations into (1.5) and multiplying by the common factor h^2, we obtain for the approximation at point (jh, ih) the equation

$$-(u_{i,j-1} + u_{i-1,j} - 4u_{i,j} + u_{i+1,j} + u_{i,j+1}) = 0. \tag{1.6}$$

This equation reveals an interesting property of the approximate solution: at each point of the grid, it is precisely the average of the values at its four neighboring points,

$$u_{i,j} = \frac{1}{4}\big(u_{i,j-1} + u_{i-1,j} + u_{i+1,j} + u_{i,j+1}\big), \tag{1.7}$$

a very remarkable fact of the discrete Laplacian in (1.6). This implies, for example, that the approximation inside the domain Ω can have neither a local maximum nor a local minimum, since otherwise it could not be the average of its neighbors. This is known as the *discrete maximum principle* for this so-called five-point finite-difference discretization of the Laplace equation. We now introduce the vectors

$$\boldsymbol{u}_j = \begin{bmatrix} u_{1,j} \\ \vdots \\ u_{m,j} \end{bmatrix}, \quad j = 1, 2, \ldots, m,$$

which contain the values $u_{i,j}$, for $i = 1, \ldots, m$, on a vertical column corresponding to j in Figure 1.10. Writing the equation (1.6) for each point i in the column, we obtain

$$\begin{aligned}
4u_{1,j} - u_{2,j} - u_{1,j-1} - u_{1,j+1} &= 0, & i &= 1, \\
-u_{1,j} + 4u_{2,j} - u_{3,j} - u_{2,j-1} - u_{2,j+1} &= 0, & i &= 2, \\
&\vdots & &\vdots \\
-u_{m-2,j} + 4u_{m-1,j} - u_{m,j} - u_{m-1,j-1} - u_{m-1,j+1} &= 0, & i &= m-1, \\
-u_{m-1,j} + 4u_{m,j} - u_{m,j-1} - u_{m,j+1} &= u_{m+1,j}, & i &= m,
\end{aligned}$$

where we put the value $u_{m+1,j}$ into the right-hand side, because its value is known to equal 1 from the boundary condition imposed at the top. Writing this for $j = 1, \ldots, m$ as a vector equation, we get

$$-\boldsymbol{u}_{j-1} + T\boldsymbol{u}_j - \boldsymbol{u}_{j+1} = \boldsymbol{e}_m, \tag{1.8}$$

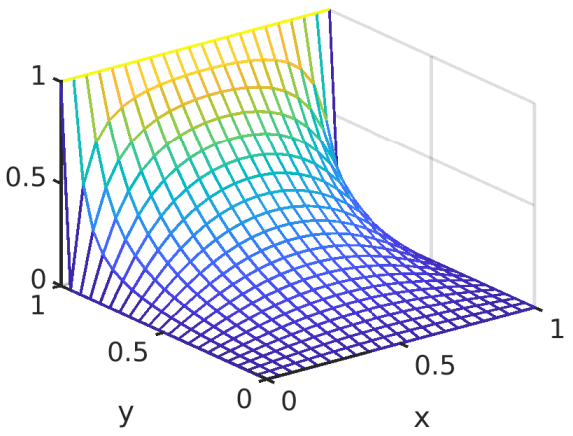

Figure 1.11. *Approximate solution of Laplace's equation with Dirichlet boundary condition equal to 1 at the top and 0 on the other boundaries.*

where the unit vector $\boldsymbol{e}_m = \begin{bmatrix} 0, \ldots, 0, 1 \end{bmatrix}^\top$ appears because of the top boundary condition, where $u = 1$, and the tridiagonal matrix T is given by

$$T = \begin{bmatrix} 4 & -1 & & \\ -1 & 4 & \ddots & \\ & \ddots & \ddots & -1 \\ & & -1 & 4 \end{bmatrix}. \tag{1.9}$$

If we now introduce the vector of all unknowns

$$\boldsymbol{u} = \begin{bmatrix} \boldsymbol{u}_1 \\ \vdots \\ \boldsymbol{u}_m \end{bmatrix}$$

and write the equations (1.8) all stacked on top of one another, then we obtain a large *sparse linear system* of equations with $n = m^2$ equations for n unknowns,

$$A\boldsymbol{u} = \boldsymbol{f}, \tag{1.10}$$

with the block-tridiagonal matrix

$$A = \begin{bmatrix} T & -I & & \\ -I & T & \ddots & \\ & \ddots & \ddots & -I \\ & & -I & T \end{bmatrix}, \tag{1.11}$$

and the right-hand-side vector $\boldsymbol{f}$ containing the boundary conditions. We show in Figure 1.11 the solution we obtain using the MATLAB script

```
m=20;                          % number of gridpoints
A=Laplacian(m,2);              % five-point Laplacian
```

```
f=zeros(m*m,1);                    % construct right-hand side
f(m:m:end)=1;
u=A\f;                             % solve by sparse Gaussian elimination
U=zeros(m+2);                      % fill solution into 2d
U(2:m+1,2:m+1)=reshape(u,m,m);     % fills matrix columnwise
U(end,1:m+2)=1;                    % add boundary condition
x=0:1/(m+1):1; y=x;                % mesh point vectors
mesh(x,y,U);
xlabel('x'); ylabel('y');          % labeling
```

in which we use the following function `Laplacian` that needs to be placed in the file `Laplacian.m`,

```
function A=Laplacian(m,d)
% LAPLACIAN computes a negative finite difference Laplacian.
%   A=Laplacian(m,d) computes a negative finite difference Laplacian on
%   an interval/square/cube (d=1,2,3) using m interior points.
%   Notice that the mesh size is not included in A.

if d==2
  G=numgrid('S',m+2); A=delsq(G); % Matlab way to construct 2D Laplacian
else
  error('not implemented yet, see Problem 2')
end
```

and which generates the finite-difference matrix from our construction. This function will be completed in Problem 2 to also include discrete Laplacians in other spatial dimensions. We see in Figure 1.10 how nicely smooth the approximate temperature distribution links the boundary temperature 1 to the boundary temperature 0. Note also that the `reshape` command in MATLAB automatically puts the long solution vector `u` in the correct ordering into the matrix `U` in the form u_{ij} as we designed it, and the `mesh` command plots it in the orientation of the plot in Figure 1.11 we are used to seeing. Every other choice of ordering would make this reshape and plotting very cumbersome.

The matrix A is sparse, with only five nonzero elements per row, and has a regular structure. If we assume that $m = 100$, then we have $n = 10{,}000$ unknowns and 100 million matrix entries, of which only $50{,}000$ (0.05%) are nonzero. This is precisely such a system where the size n is basically an approximation to infinity, an infinitely fine grid. We show in Figure 1.12 a comparison of the solution cost of such systems using *Gaussian elimination*, a sparse variant thereof, and the best currently known iterative method for such problems, called *multigrid*. We see that as soon as the problem becomes large, the iterative multigrid algorithm is faster, and we also observe that asymptotically the growth of the iterative method cost is much slower than the growth for the direct methods based on Gaussian elimination.

Multigrid is based on a very simple iterative method and a fundamental observation we can already show now: from the fact we observed in (1.7) that the approximation at each point is the average of its neighbors, a simple iterative method is to start with an arbitrary initial guess for the solution, and then at each point to replace the value by the average of its neighbors, i.e., starting with some $u^0_{i,j}$, we compute for all points simultaneously at each iteration $k = 1, 2, \ldots$

$$u^k_{i,j} = \frac{1}{4}\big(u^{k-1}_{i,j-1} + u^{k-1}_{i-1,j} + u^{k-1}_{i+1,j} + u^{k-1}_{i,j+1}\big), \tag{1.12}$$

which is in fact precisely the method Jacobi had proposed. We show in Figure 1.13 the first four iterations for grid sizes $m = 2, 4, 8, 16$. These results were obtained with the simple MATLAB script

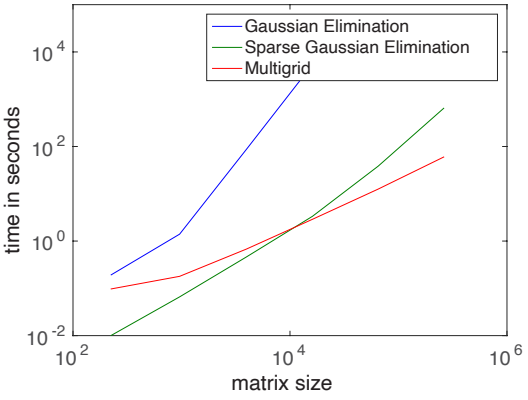

Figure 1.12. *Solving Laplace's equation discretized by finite differences using Gaussian elimination, a sparse variant of Gaussian elimination, and multigrid.*

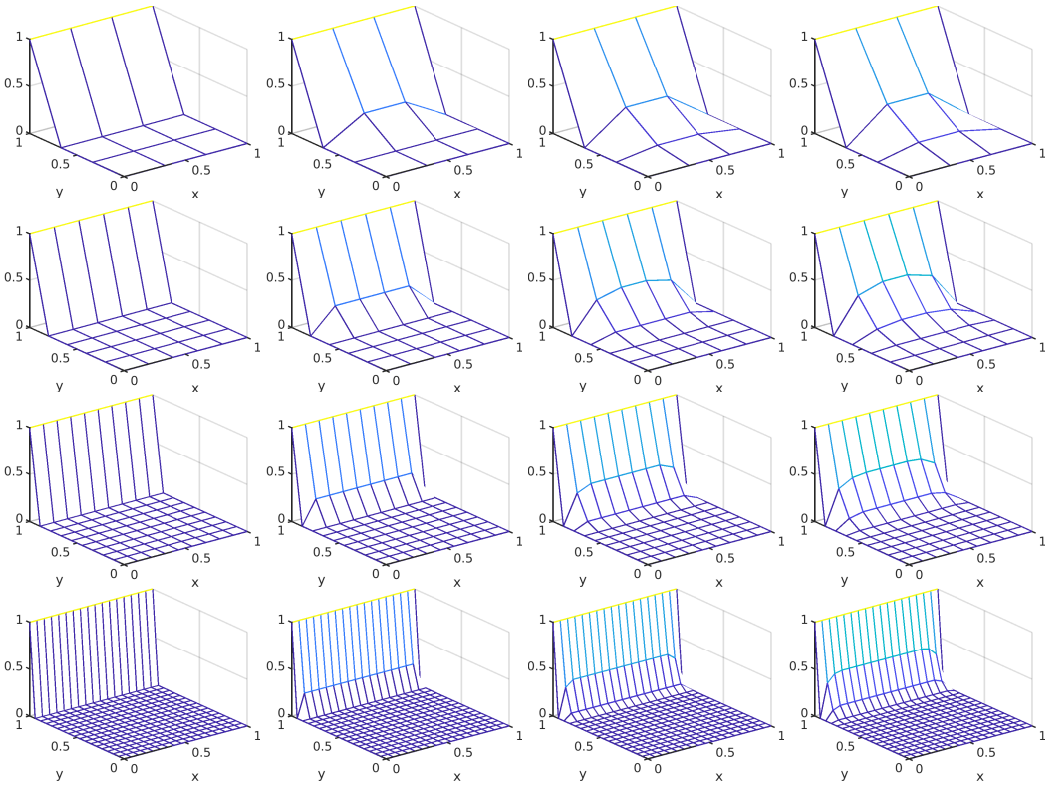

Figure 1.13. *Initial guess and first three iterations of Jacobi's method for Laplace's equation for increasing mesh resolution.*

```
m=2; A=Laplacian(m,2);              % setup Laplace equation as before
f=zeros(m*m,1); f(m:m:end)=1;
x=0:1/(m+1):1;
u=zeros(size(f)); U=zeros(m+2);
U(end,1:m+2)=1;
for k=1:4                           % do four Jacobi steps
  U(2:m+1,2:m+1)=reshape(u,m,m);
  mesh(x,x,U);                      % plot current approximation
  xlabel('x');ylabel('y');
  u=u+(f-A*u)./diag(A);             % perform one Jacobi step
  pause
end
```

We see that for a few gridpoints, $m = 2$, after just a few steps the approximate solution has the correct shape, as the high-resolution approximation in Figure 1.11. When m becomes larger, however, it seems to take more and more steps of the Jacobi iteration to produce a good approximation of the solution, and for $m = 16$, after three steps one still has the approximate solution zero in most of the domain. This is not surprising, since starting with a zero initial guess $u^0_{i,j} = 0$ at all points, the average of the neighboring points will remain zero as long as a point does not touch the boundary where the solution equals 1. The key idea of the multigrid method is to use a very coarse grid, e.g., $m = 2$, to get very quickly a good first approximation, and to then use this as an initial guess on a finer grid, e.g., $m = 4$, to do a few corrections, and so on. Doing this leads to the very fast iterative method tested in Figure 1.12.

1.4 ▪ An advection-reaction-diffusion problem as a typical nonsymmetric example

Differential equations (DE) provide the baseline of many mathematical models for real life applications. Seldom, these equations can be solved in "closed" form: the exact solution can rarely be characterized through explicit mathematical formulae that are easily computable. Almost invariably, one has to resort to appropriate numerical methods whose scope is the approximation (or discretization) of the exact differential model and, henceforth, of the exact solution.

Alfio M. Quarteroni, *Numerical Models for Differential Problems*, 2009

The Laplace problem presented in Section 1.3 leads to the linear system (1.10) characterized by a symmetric positive definite matrix of coefficients. However, nonsymmetric problems are also common in practical applications and their numerical treatment requires generally different numerical methods. A typical example of a nonsymmetric problem is the (stationary) *advection-reaction-diffusion problem*

$$\begin{aligned} -\nu\Delta u + \boldsymbol{b}^\top \nabla u + cu &= f \qquad \text{in } \Omega, \\ u &= g \qquad \text{on } \partial\Omega, \end{aligned} \tag{1.13}$$

where $\nu > 0$ is the viscosity, $c \geq 0$ is the reaction strength, and $\boldsymbol{b}$ is the advection velocity field. The PDE is a combination of the diffusion and advection equations, includes a reaction term, and models the state of physical systems where particles, energy, or other physical quantities are transported/modified in the domain Ω due to three processes: diffusion, advection, and reaction. The first term on the left-hand side of (1.13), namely $-\nu\Delta u$, describes the diffusion, the second term $\boldsymbol{b}^\top \nabla u$ represents the advection (or transport), while the third term, that is, cu, models the reaction. The functions f and g are assumed to be sufficiently regular.

The advection-reaction-diffusion equation (1.13) encloses several physical models. This becomes visible if one considers a general stationary equation written in divergence form, namely

$$\nabla \cdot (-\nu\nabla u + \boldsymbol{b}u) = f,$$

expands the divergence (assuming ν to be constant)

$$-\nu\Delta u + \boldsymbol{b}^\top \nabla u + (\nabla \cdot \boldsymbol{b})u = f,$$

and defines $c := \nabla \cdot \boldsymbol{b}$. If the flow field $\boldsymbol{b}$ is divergence free, meaning that $c = \nabla \cdot \boldsymbol{b} = 0$, then (1.13) is an advection-diffusion (divergence-free) equation.

Moreover, if in (1.13) $\boldsymbol{b} = 0$ and the sign of c is negative, that is, $c = -\omega^2$, one gets the celebrated *Helmholtz equation*, where ω represents the wave frequency.

As in Section 1.3, one can discretize (1.13) using the finite-difference method. The diffusion term $-\Delta u$ can be discretized using the five-point discretization given in, e.g., (1.6) and discussed in Problem 1. The advection term $\boldsymbol{b}^\top \nabla u = b_1 \partial_x u + b_2 \partial_y u$ can be discretized using the centered finite-difference formula:

$$\partial_x u(x_j, y_i) \approx \frac{u(x_{j+1}, y_i) - u(x_{j-1}, y_i)}{2h}, \; \partial_y u(x_j, y_i) \approx \frac{u(x_j, y_{i+1}) - u(x_j, y_{i-1})}{2h}.$$

If we do so, we obtain a system of the type $A\boldsymbol{u} = \boldsymbol{f}$ characterized by a nonsymmetric matrix A.

The centered finite-difference formula will lead to nonphysical oscillations in the solution if the advection $\boldsymbol{b}$ is large compared to the diffusion ν and the mesh is not fine enough (see, e.g., [152, 76]). This can be regarded as a feature, since these oscillations indicate that the mesh is not fine enough, and they disappear when the mesh is fine enough. If such fine meshes are not feasible, one often uses an upwind discretization which never oscillates [76]; see also Problem 4.

We use the Laplace problem of Section 1.3 as the main model problem to test our iterative methods throughout the book. The advection-reaction-diffusion problem is used in the exercises. The reader is asked to consider (whenever possible) problem (1.13) and reproduce the tests and results obtained for the Laplace problem. This allows the reader to follow the main path of the book traced using the fundamental (symmetric) Laplace problem and, at the same time, to maintain a more general perspective that includes nonsymmetric and possibly indefinite problems in the Helmholtz case.

1.5 ▪ Problems

Problem 1. *Consider a uniform grid Ω_h in $\mathbb{R}^2$ with mesh size h such that $(x_j, y_i) \in \Omega_h$ with $x_{j+1} = x_j + h$ and $y_{i+1} = y_i + h$. Using Taylor series, show that the scheme of finite differences for the discrete Laplacian defined on Ω_h given by*

$$\frac{u(x_{j+1}, y_i) + u(x_j, y_{i+1}) - 4u(x_j, y_i) + u(x_{j-1}, y_i) + u(x_j, y_{i-1})}{h^2}$$

is a second-order approximation of the Laplace operator.

Problem 2. *Write a MATLAB function that takes as input the dimension of the grid and the spatial dimension of the domain and returns the matrix corresponding to the discrete Laplacian. Use the interface and header*

```
function A=Laplacian(m,d)
% LAPLACIAN computes a negative finite difference Laplacian.
%   A=Laplacian(m,d) computes a negative finite difference Laplacian on
%   an interval/square/cube (d=1,2,3) using m interior points.
%   Notice that the mesh size is not included in A.
```

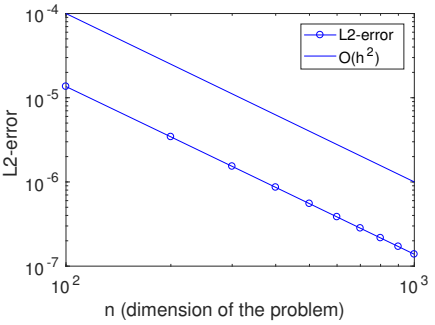

Figure 1.14. *Convergence of the finite-difference scheme in the discrete L^2-norm.*

Note that for two spatial dimensions, you could use the solution shown already in this chapter, but it is better to develop a solution using the Kronecker product and the MATLAB function `kron`*, because then the generalization to higher dimensions is very easy.*

Problem 3. *Consider the Laplace equation*

$$\begin{aligned} -\Delta u &= 0 \ \text{ in } \Omega = (0,1) \times (0,1), \\ u &= g \ \text{ on } \partial\Omega, \end{aligned}$$

where $g(0,y) = \sin(\pi y)$, $g(x,0) = 0$, $g(x,1) = 0$, $g(1,y) = 0$.

- *Prove that the solution to this problem is* $u(x,y) = \sin(\pi y)\frac{e^{-\pi x} - e^{\pi(x-2)}}{1-e^{-2\pi}}$.
- *Discretize the above Laplace problem using finite differences.*
- *Write a MATLAB code to solve the obtained discrete Laplace problem.*
- *Solve the discrete Laplace problem for several* h *and plot the* L^2*-error to obtain Figure 1.14.*

Problem 4. *Consider the advection-reaction-diffusion problem* (1.13)

$$\begin{aligned} -\nu\Delta u + \boldsymbol{b}^\top \nabla u + cu &= f \qquad \text{in } \Omega, \\ u &= 0 \qquad \text{on } \partial\Omega, \end{aligned}$$

where Ω *is the unit square and* $f = 1$.

- *Discretize the problem using the finite-difference method.*
- *Write a MATLAB function (like the one of Problem 2) that takes as input the dimension of the grid, a (constant) velocity vector* $\boldsymbol{b}$*, and the (constant) reaction and diffusion coefficients* c *and* ν *and returns the corresponding finite-difference matrix* A*. Use the interface header*

```
function A=AdvectionReactionDiffusion(m,b,c,nu)
% ADVECTIONREACTIONDIFFUSION finite difference advection-reaction-diffusion
%   A=AdvectionReactionDiffusion(m,b,c) computes a finite difference
%   advection-reaction-diffusion matrix on the unit square using m interior
%   points in each direction. Here, b is the (constant) velocity field and
%   c is the (constant) reaction coefficient, and nu is the (constant)
%   diffusion coefficient.
```

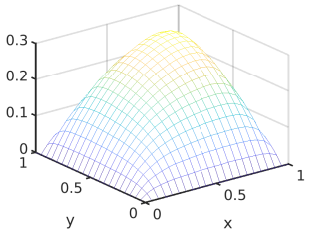

Figure 1.15. *Solution to the advection-reaction-diffusion problem for* $f = 1$ $m = 10$, $c = 1$, $\boldsymbol{b} = [\,1\,,\,1\,]^\top$, *and* $\nu = 0.1$.

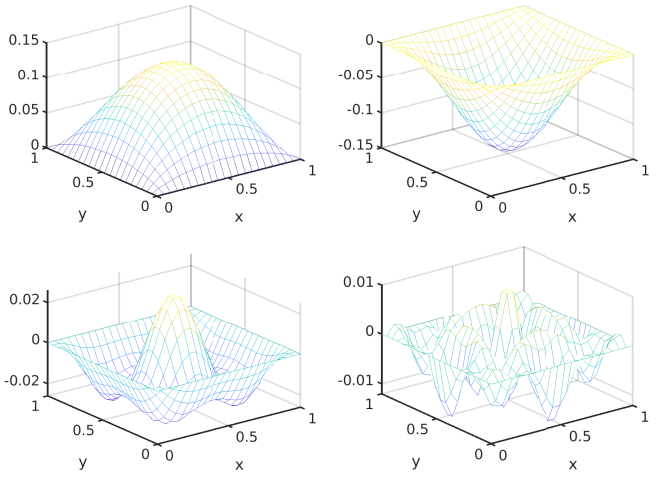

Figure 1.16. *Solution to the advection-reaction-diffusion problem for* $f = 1$ $m = 10$, $\boldsymbol{b} = 0$, $\nu = 1$, *and* $\omega = 2$ *(top left),* $\omega = 4$ *(top right),* $\omega = 8$ *(bottom left), and* $\omega = 16$ *(bottom right).*

- *Solve the advection-reaction-diffusion problem for* $c = 1$ *and* $\boldsymbol{b} = [\,1\,,\,1\,]^\top$ *with different values of* ν *(e.g.,* $\nu = 10, 1, 0.1, 0.01$*). Comment on the results that you obtain. What do you observe for* $\nu = 0.01$ *and* $m = 15$*? Repeat the experiment using a finer mesh and comment on the result that you obtain. See, e.g., Figures 1.15 and 1.16.*

- *Consider* $m = 20$, $\nu = 1$, $\boldsymbol{b} = 0$, *and* $c = -\omega^2$ *with* $\omega = 2, 4, 8, 16, \ldots$. *Comment on the results that you obtain.*

- *Consider* $m = 20$, $\nu = 1$, $\boldsymbol{b} = 0$, *and* $c = \omega^2$ *and* $c = -\omega^2$ *with*

$$\omega = \omega_{j,\ell} := \frac{1}{h}\sqrt{4 + 2\cos\Big(\frac{j\pi}{m+1}\Big) + 2\cos\Big(\frac{\ell\pi}{m+1}\Big)},$$

and $j, \ell = 1, 2, 3, \ldots$. *Compute the eigenvalues of* A, *compare them with* $\omega_{j,\ell}$, *and comment on the results that you obtain.*

Chapter 2

Stationary Iterative Methods

> *Let us pass on to methods which have this property in common: that starting from a table of numbers, correct at the boundary, but otherwise merely as near as one can guess, one proceeds by definite methods to modify this table and thereby to cause it to approach without limit towards the true finite-difference integral.*
>
> Lewis F. Richardson, *The Approximate Arithmetical Solution by Finite Differences of Physical Problems Involving Differential Equations, with an Application to the Stresses in a Masonry Dam*, 1911

Richardson describes above how he imagined iterative methods for a discretized PDE to function: they start with some given approximation, and then proceed by applying precisely prescribed rules to improve this approximation until a good enough approximation is achieved. A very general way to describe such an iterative method for solving the linear system of equations

$$A\boldsymbol{u} = \boldsymbol{f}, \quad A \in \mathbb{R}^{n\times n},\ \boldsymbol{f} \in \mathbb{R}^n,$$

is to *split the matrix* into $A = M - N$. If M is invertible, this splitting induces the *stationary iteration*

$$M\boldsymbol{u}_{k+1} = N\boldsymbol{u}_k + \boldsymbol{f}, \quad k = 0, 1, 2, \ldots, \tag{2.1}$$

where an initial guess $\boldsymbol{u}_0 \in \mathbb{R}^n$ is needed to start the iteration. The method is called stationary, because neither M nor N depends on the iteration count k.

To obtain an efficient method, the *matrix splitting* must be such that solving linear systems with the matrix M is cheap, and the iteration (2.1) converges fast. These are unfortunately in general conflicting requirements, as one can see from the extreme case where we chose $M = A$, and thus $N = 0$, and we converge in one iteration to the solution, but this iteration is as expensive as solving the underlying system.

2.1 ▪ Error, residual, and difference of iterates

> *To each of the three iterative methods described, we can associate error vectors $\boldsymbol{e}^{(m)}$ defined by ...*
>
> Richard S. Varga, *Matrix Iterative Analysis*, 1962

Using the matrix splitting $A = M - N$, the *standard form* of the stationary iteration is

$$M\boldsymbol{u}_{k+1} = N\boldsymbol{u}_k + \boldsymbol{f} \iff \boldsymbol{u}_{k+1} = M^{-1}N\boldsymbol{u}_k + M^{-1}\boldsymbol{f}. \tag{2.2}$$

Since the right-hand side in (2.2) satisfies

$$M^{-1}N\boldsymbol{u}_k + M^{-1}\boldsymbol{f} = M^{-1}(M - A)\boldsymbol{u}_k + M^{-1}\boldsymbol{f} = \boldsymbol{u}_k + M^{-1}(\boldsymbol{f} - A\boldsymbol{u}_k),$$

we can write the stationary iteration also in the so-called correction form,

$$\boldsymbol{u}_{k+1} = \boldsymbol{u}_k + M^{-1}\boldsymbol{r}_k, \tag{2.3}$$

where we introduced the *residual* $\boldsymbol{r}_k := \boldsymbol{f} - A\boldsymbol{u}_k$, which is a measure of how good the approximation $\boldsymbol{u}_k$ is. The matrix M is called a *preconditioner*, since by iterating with (2.3), if $\boldsymbol{u}_k$ converges to $\boldsymbol{u}_\infty$, then $\boldsymbol{u}_\infty$ is a solution of the *preconditioned system*

$$M^{-1}A\boldsymbol{u} = M^{-1}\boldsymbol{f}.$$

If we subtract the iteration from the split system, we get

$$\left.\begin{array}{ll} M\boldsymbol{u} & = N\boldsymbol{u} + \boldsymbol{f} \\ M\boldsymbol{u}_{k+1} & = N\boldsymbol{u}_k + \boldsymbol{f} \end{array}\right\} \Rightarrow M(\boldsymbol{u} - \boldsymbol{u}_{k+1}) = N(\boldsymbol{u} - \boldsymbol{u}_k).$$

Introducing the *error* $\boldsymbol{e}_k := \boldsymbol{u} - \boldsymbol{u}_k$, we obtain an *iteration for the error*,

$$M\boldsymbol{e}_{k+1} = N\boldsymbol{e}_k \iff \boldsymbol{e}_{k+1} = M^{-1}N\boldsymbol{e}_k. \tag{2.4}$$

Multiplying the correction form (2.3) with A and subtracting the result from the right-hand side $\boldsymbol{f}$, we obtain

$$\underbrace{\boldsymbol{f} - A\boldsymbol{u}_{k+1}}_{\boldsymbol{r}_{k+1}} = \underbrace{\boldsymbol{f} - A\boldsymbol{u}_k}_{\boldsymbol{r}_k} - AM^{-1}\boldsymbol{r}_k$$

and an *iteration for the residual vectors*,

$$\boldsymbol{r}_{k+1} = (I - AM^{-1})\boldsymbol{r}_k = (I - AM^{-1})^k\boldsymbol{r}_0. \tag{2.5}$$

Therefore, recalling that $A = M - N$, we obtain

$$I - AM^{-1} = NM^{-1} = M(M^{-1}N)M^{-1},$$

which shows that the iteration matrices $I - AM^{-1}$ in (2.5) and $M^{-1}N$ in (2.4) are similar and hence must have the same eigenvalues.

We now introduce also the *difference of consecutive iterates*,

$$\boldsymbol{d}_k := \boldsymbol{u}_{k+1} - \boldsymbol{u}_k.$$

Using the standard form of the stationary iteration (2.2), we get the *iteration for the differences*

$$\begin{aligned} \boldsymbol{d}_k &= \boldsymbol{u}_{k+1} - \boldsymbol{u}_k = M^{-1}N\boldsymbol{u}_k + M^{-1}\boldsymbol{f} - M^{-1}N\boldsymbol{u}_{k-1} - M^{-1}\boldsymbol{f} \\ &= M^{-1}N(\boldsymbol{u}_k - \boldsymbol{u}_{k-1}) \\ &= M^{-1}N\boldsymbol{d}_{k-1}. \end{aligned}$$

Hence the differences of consecutive iterates satisfy the same iteration as the error. Notice that an example of an iterative method written in *difference form* is the method proposed by Jacobi in 1845 and shown in Figures 1.6 and 1.7. Furthermore, from

$$\begin{aligned} \boldsymbol{d}_k &= M^{-1}N(\boldsymbol{u}_k - \boldsymbol{u} + \boldsymbol{u} - \boldsymbol{u}_{k-1}) \\ &= M^{-1}N(-\boldsymbol{e}_k + \boldsymbol{e}_{k-1}) = -M^{-1}N\boldsymbol{e}_k + \boldsymbol{e}_k \\ &= (I - M^{-1}N)\boldsymbol{e}_k \end{aligned}$$

we obtain a relation between the difference of consecutive iterates and the error:

$$\boldsymbol{d}_k = M^{-1}A\boldsymbol{e}_k.$$

Finally, from the stationary iteration in correction form (2.3) we have $M\boldsymbol{d}_k = \boldsymbol{r}_k$, which relates the difference of consecutive iterates to the residual. We have thus proved the following.

Theorem 2.1 (Error, residual, and difference recurrences). *For an invertible matrix $A \in \mathbb{R}^{n\times n}$ and $\boldsymbol{f} \in \mathbb{R}^n$, let $\boldsymbol{u} \in \mathbb{R}^n$ be the solution of $A\boldsymbol{u} = \boldsymbol{f}$, and let $A = M - N$ be a splitting with M invertible. Choose $\boldsymbol{u}_0 \in \mathbb{R}^n$ and consider the sequence of iterates $\boldsymbol{u}_{k+1} = M^{-1}N\boldsymbol{u}_k + M^{-1}\boldsymbol{f}$. Let $\boldsymbol{e}_k := \boldsymbol{u} - \boldsymbol{u}_k$ be the error and $\boldsymbol{r}_k := \boldsymbol{f} - A\boldsymbol{u}_k$ be the residual at step k, and let $\boldsymbol{d}_k := \boldsymbol{u}_{k+1} - \boldsymbol{u}_k$ be the difference of two consecutive iterates. Then these vectors can be computed by the recurrences*

$$\boldsymbol{e}_{k+1} = M^{-1}N\boldsymbol{e}_k, \tag{2.6}$$
$$\boldsymbol{d}_{k+1} = M^{-1}N\boldsymbol{d}_k, \tag{2.7}$$
$$\boldsymbol{r}_{k+1} = (I - AM^{-1})\boldsymbol{r}_k = NM^{-1}\boldsymbol{r}_k, \tag{2.8}$$

where $(I - AM^{-1})$ and $M^{-1}N$ are similar matrices. Moreover, we have the relation

$$M\boldsymbol{d}_k = \boldsymbol{r}_k = A\boldsymbol{e}_k. \tag{2.9}$$

The last relation (2.9) in Theorem 2.1 has a nice interpretation: the solution of the linear system $A\boldsymbol{u} = \boldsymbol{f}$ can be obtained by solving the correction equation $A\boldsymbol{e}_k = \boldsymbol{r}_k$ and then adding the correction $\boldsymbol{u} = \boldsymbol{u}_k + \boldsymbol{e}_k$. However, we cannot afford to solve systems with the matrix A because the matrix A is in general too large to be stored and factored. Therefore we replace the original problem by an easier one and solve instead $M\boldsymbol{d}_k = \boldsymbol{r}_k$, and then we iterate $\boldsymbol{u}_{k+1} = \boldsymbol{u}_k + \boldsymbol{d}_k$.

It is clear from (2.6)-(2.7)-(2.8) that the behavior of a stationary method is related to the matrix $M^{-1}N$. For this reason we have the following definition.

Definition 2.2 (Iteration matrix). *For any matrix splitting $A = M - N$ with M invertible, the matrix $G := M^{-1}N$ is called the* iteration matrix.

In the next section we show that the convergence behavior of a stationary iteration based on the splitting $A = M - N$ is governed by the spectrum of the iteration matrix G.

2.2 ▪ Convergence analysis

> *The convergence of these methods is rarely guaranteed for all matrices, but a large body of theory exists for the case where the coefficient matrix arises from the finite difference discretization of elliptic partial differential equations.*
>
> Yousef Saad, *Iterative Methods for Sparse Linear Systems*, 2003.

We now study under which conditions a stationary iteration of the form (2.2) or (2.3) converges. We assume that the linear system $A\boldsymbol{u} = \boldsymbol{f}$ has a unique solution and consider the matrix splitting $A = M - N$ with an invertible matrix M. A first convergence result is obtained by using any vector norm $\|\cdot\| : \mathbb{R}^n \to \mathbb{R}^+$ and the corresponding *induced matrix norm* $\|A\| := \sup_{\|\boldsymbol{u}\|=1} \|A\boldsymbol{u}\|$: taking norms on both sides of the iteration for the error (2.4), we obtain

$$\|\boldsymbol{e}_{k+1}\| \le \|M^{-1}N\|\,\|\boldsymbol{e}_k\| \le \cdots \le \|M^{-1}N\|^{k+1}\|\boldsymbol{e}_0\|.$$

We therefore have convergence if $\|M^{-1}N\| < 1$ for the chosen norm. This is, however, a sufficient but not a necessary condition for convergence: as a counterexample, consider a triangular

matrix R with zero diagonal. This matrix can have a norm $\|R\| > 1$, but since R is nilpotent, we have $R^k \to 0$ for $k \to \infty$. Therefore we need another quantity that describes convergence more accurately.

Definition 2.3 (Spectral radius). *The* spectral radius *of a matrix $A \in \mathbb{R}^{n\times n}$ is*

$$\rho(A) := \max_{j=1,\ldots,n} |\lambda_j(A)|,$$

where $\lambda_j(A)$ denotes the jth eigenvalue of A.

One can wonder whether there is a relation between the spectral radius and the norm of a matrix. We have the following results.

Lemma 2.4 (Norm and spectral radius). *For all induced matrix norms, $\rho(A) \leq \|A\|$ holds.*

Proof. Let $\lambda, \boldsymbol{v}$ be an eigenpair of A. From the eigenvector-eigenvalue relation $A\boldsymbol{v} = \lambda\boldsymbol{v}$, we obtain that

$$|\lambda|\|\boldsymbol{v}\| = \|\lambda\boldsymbol{v}\| = \|A\boldsymbol{v}\| \leq \|A\|\,\|\boldsymbol{v}\|.$$

Now since $\|\boldsymbol{v}\| \neq 0$, we obtain $|\lambda| \leq \|A\|$, and since this holds for any eigenvalue λ, we also get $\rho(A) = \max_{j=1,\ldots,n} |\lambda_j(A)| \leq \|A\|$. ∎

For symmetric matrices, the two concepts of norm and spectral radius are definitely related.

Lemma 2.5 (Norm and spectral radius for symmetric matrices). *For symmetric matrices $A \in \mathbb{R}^{n\times n}$, the spectral radius equals the 2-norm, $\rho(A) = \|A\|_2$.*

Proof. Using the definition of the 2-norm, we obtain

$$\|A\|_2^2 = \lambda_{\max}(A^\top A) = \lambda_{\max}(A^2) = \max|\lambda(A)|^2 = \rho(A)^2. \qquad ∎$$

However, the spectral radius is not a norm in general. For norms, $\|A\| = 0$ implies that $A = 0$, which does not hold for the spectral radius: for an upper triangular matrix R with zero diagonal (thus all eigenvalues are zero) we have $\rho(R) = 0$ but $R \neq 0$. Furthermore, the triangle inequality

$$\rho(A + B) \leq \rho(A) + \rho(B)$$

also does not hold in general: take for example

$$A = \begin{bmatrix} 0 & 1 \\ 0 & 0 \end{bmatrix} \text{ and } B = \begin{bmatrix} 0 & 0 \\ 1 & 0 \end{bmatrix}.$$

Then $\rho(A + B) = 1$, but $\rho(A) = \rho(B) = 0$. Nonetheless, the following result holds.

Theorem 2.6 (Norm and spectral radius). *Let $A \in \mathbb{R}^{n\times n}$. Then for any given $\epsilon > 0$, there exists a norm $\|\cdot\|$, which depends on A and ϵ, such that*

$$\rho(A) \leq \|A\| \leq \rho(A) + \varepsilon.$$

Proof. See Problem 7. ∎

We are now ready to prove convergence of stationary iterative methods based on the matrix splitting $A = M - N$.

Theorem 2.7 (Convergence of stationary methods). *Let $A \in \mathbb{R}^{n\times n}$ be invertible, let $A = M - N$ with M invertible, and let $\boldsymbol{f} \in \mathbb{R}^n$. The stationary iterative method*

$$M\boldsymbol{u}_{k+1} = N\boldsymbol{u}_k + \boldsymbol{f}$$

converges for any initial vector $\boldsymbol{u}_0 \in \mathbb{R}^n$ to the solution $\boldsymbol{u}$ of the linear system $A\boldsymbol{u} = \boldsymbol{f}$ if and only if $\rho(M^{-1}N) < 1$.

Proof. We start by showing the "only if" part with a proof by contraposition: assume that $|\lambda_m| = \rho(M^{-1}N) \geq 1$. Choosing $\boldsymbol{u}_0$ such that $\boldsymbol{e}_0 = \boldsymbol{u} - \boldsymbol{u}_0$ is a corresponding eigenvector, and applying the error recurrence (2.4), we get

$$\boldsymbol{e}_{k+1} = M^{-1}N\boldsymbol{e}_k = \cdots = (M^{-1}N)^{k+1}\boldsymbol{e}_0 = \lambda_m^{k+1}\boldsymbol{e}_0.$$

Thus, if $|\lambda_m| > 1$, then $|\lambda_m^{k+1}| \to \infty$, so the error cannot converge to zero. If $|\lambda_m| = 1$, then we also have no convergence since the error does not decrease.

For the "if" part, we assume that $\rho(M^{-1}N) < 1$. We then consider the *Jordan decomposition* (see, e.g., [91])

$$M^{-1}N = VJV^{-1} \quad \text{with } V, J \in \mathbb{C}^{n\times n} \text{ and } V \text{ nonsingular.}$$

The matrix J is block-diagonal,

$$J = \begin{bmatrix} J_{m_1}(\lambda_1) & 0 & 0 & \cdots & 0 \\ 0 & J_{m_2}(\lambda_2) & 0 & \cdots & 0 \\ \vdots & \ddots & \ddots & \ddots & \vdots \\ 0 & \cdots & 0 & J_{m_{s-1}}(\lambda_{s-1}) & 0 \\ 0 & \cdots & \cdots & 0 & J_{m_s}(\lambda_s) \end{bmatrix}$$

with

$$J_{m_i}(\lambda_i) = \begin{bmatrix} \lambda_i & 1 & 0 & \cdots & 0 \\ 0 & \lambda_i & 1 & \cdots & 0 \\ \vdots & \vdots & \ddots & \ddots & \vdots \\ 0 & 0 & \cdots & \lambda_i & 1 \\ 0 & 0 & \cdots & 0 & \lambda_i \end{bmatrix} \in \mathbb{C}^{m_i\times m_i}, \quad i = 1, \ldots, s,$$

where s is the number of Jordan blocks, λ_i are the eigenvalues of $M^{-1}N$, and m_i is the dimension of the ith block. Now notice that the matrix $J_{m_i}(\lambda_i)$ can be written as the sum of a diagonal matrix and a nilpotent matrix,

$$J_{m_i}(\lambda_i) = \big(\lambda_i I + \widetilde{J}\big),$$

where I is the $m_i \times m_i$ identity and

$$\widetilde{J} = \begin{bmatrix} 0 & 1 & 0 & \cdots & 0 \\ 0 & 0 & 1 & \cdots & 0 \\ \vdots & \vdots & \ddots & \ddots & \vdots \\ 0 & 0 & \cdots & 0 & 1 \\ 0 & 0 & \cdots & 0 & 0 \end{bmatrix}.$$

Now, since $\lambda_i I$ and $\widetilde{J}$ commute, we can use the *binomial theorem for matrices*[10] [183, Section 21, Theorem 21.1] to deduce that

$$\big(J_{m_i}(\lambda_i)\big)^k = \big(\lambda_i I + \widetilde{J}\big)^k = \sum_{r=0}^{k} \binom{k}{r} \lambda_i^{k-r} \widetilde{J}^r = \sum_{r=0}^{\min(k,m_i-1)} \binom{k}{r} \lambda_i^{k-r} \widetilde{J}^r, \tag{2.10}$$

where we used that

$$\widetilde{J}^2 = \begin{bmatrix} 0 & 0 & 1 & \cdots & 0 & 0 \\ 0 & 0 & 0 & \cdots & 0 & 0 \\ \vdots & \vdots & \ddots & \ddots & \ddots & \vdots \\ 0 & 0 & \cdots & 0 & 0 & 1 \\ 0 & 0 & \cdots & 0 & 0 & 0 \\ 0 & 0 & \cdots & 0 & 0 & 0 \end{bmatrix}, \quad \ldots, \quad \widetilde{J}^{m_i-1} = \begin{bmatrix} 0 & 0 & 0 & \cdots & 0 & 1 \\ 0 & 0 & 0 & \cdots & 0 & 0 \\ \vdots & \vdots & \ddots & \ddots & \ddots & \vdots \\ 0 & 0 & \cdots & 0 & 0 & 0 \\ 0 & 0 & \cdots & 0 & 0 & 0 \\ 0 & 0 & \cdots & 0 & 0 & 0 \end{bmatrix}.$$

Notice that $(M^{-1}N)^k = VJ^kV^{-1}$, and since J is block-diagonal, we get

$$J^k = \begin{bmatrix} (J_{m_1}(\lambda_1))^k & 0 & 0 & \cdots & 0 \\ 0 & (J_{m_2}(\lambda_2))^k & 0 & \cdots & 0 \\ \vdots & \ddots & \ddots & \ddots & \vdots \\ 0 & \cdots & 0 & (J_{m_{s-1}}(\lambda_{s-1}))^k & 0 \\ 0 & \cdots & \cdots & 0 & (J_{m_s}(\lambda_s))^k \end{bmatrix}.$$

Using (2.10) we obtain the well-known expression for the powers of a *Jordan block*

$$J_{m_i}^k(\lambda_i) = \begin{bmatrix} \lambda_i^k & \binom{k}{1}\lambda_i^{k-1} & \binom{k}{2}\lambda_i^{k-2} & \cdots & \binom{k}{m_i-1}\lambda_i^{k-m_i+1} \\ 0 & \lambda_i^k & \binom{k}{1}\lambda_i^{k-1} & \cdots & \binom{k}{m_i-2}\lambda_i^{k-m_i+2} \\ \vdots & \vdots & \ddots & \ddots & \vdots \\ 0 & 0 & \cdots & \lambda_i^k & \binom{k}{1}\lambda_i^{k-1} \\ 0 & 0 & \cdots & 0 & \lambda_i^k \end{bmatrix}.$$

Therefore, if $\rho(M^{-1}N) < 1$, then $|\lambda_i| < 1$ for all i, so that (recall Problem 9)

$$\lim_{k\to\infty} J_{m_i}^k(\lambda_i) = 0$$

for all Jordan blocks. It follows that $\lim_{k\to\infty} J^k = 0$. This implies that

$$\lim_{k\to\infty} (M^{-1}N)^k = \lim_{k\to\infty} VJ^kV^{-1} = V\big(\lim_{k\to\infty} J^k\big)V^{-1} = 0. \qquad \square$$

[10] The binomial theorem for matrices states: Let A and B be two commuting matrices, then $(A+B)^k = \sum_{r=0}^{k} \binom{k}{r} A^r B^{k-r}$.

2.3 ▪ Convergence factor and convergence rate

> *The convergence rate is the (natural) logarithm of the inverse of the convergence factor.*
>
> Yousef Saad, *Iterative Methods for Sparse Linear Systems*, 2003.

If the second author had carefully read Saad's book, in particular the quote above, he would not have created such a confusion in his early publications, until a careful reviewer finally straightened things out between the two notions of convergence factor and convergence rate. In order to understand the convergence behavior, we take the iteration for the error (2.4) and obtain by induction

$$\boldsymbol{e}_k = (M^{-1}N)^k \boldsymbol{e}_0.$$

Taking norms on both sides gives a bound for the error reduction over k iteration steps,

$$\frac{\|\boldsymbol{e}_k\|}{\|\boldsymbol{e}_0\|} \leq \|(M^{-1}N)^k\|.$$

If we want to know how many iterations are needed for the error measured in this norm to be reduced to a given tolerance ε, it suffices to impose

$$\frac{\|\boldsymbol{e}_k\|}{\|\boldsymbol{e}_0\|} \leq \|(M^{-1}N)^k\| < \varepsilon.$$

Rewriting the right-hand side in the form

$$\|(M^{-1}N)^k\| = \left(\left\|(M^{-1}N)^k\right\|^{\frac{1}{k}}\right)^k < \varepsilon$$

and taking the logarithm, we get

$$k > \frac{\ln(\varepsilon)}{\ln\left(\left\|(M^{-1}N)^k\right\|^{\frac{1}{k}}\right)}. \tag{2.11}$$

Since the number of necessary iterations k also appears on the right-hand side, (2.11) does not seem very useful at first glance to determine the number of iterations to take. However, for large k we can get a good estimate using the following lemma.

Lemma 2.8 (Gelfand's formula). *For any matrix $G \in \mathbb{R}^{n\times n}$ with spectral radius $\rho(G)$ and any induced matrix norm $\|\cdot\|$, we have*

$$\lim_{k\to\infty} \|G^k\|^{\frac{1}{k}} = \rho(G).$$

Proof. See Problem 8. □

Definition 2.9 (Convergence factor). *The* mean convergence factor *of an iteration matrix G is the number*

$$\rho_k(G) = \|G^k\|^{\frac{1}{k}}. \tag{2.12}$$

The asymptotic convergence factor *is the spectral radius*

$$\rho(G) = \lim_{k\to\infty} \rho_k(G). \tag{2.13}$$

Definition 2.10 (Convergence rate). *The* mean convergence rate *of an iteration matrix G is the number*

$$R_k(G) = -\ln\left(\|G^k\|^{\frac{1}{k}}\right) = -\ln(\rho_k(G)). \tag{2.14}$$

The asymptotic convergence rate *is*

$$R_\infty(G) = -\ln(\rho(G)). \tag{2.15}$$

We can now say how many iteration steps k are necessary until the error reduction reaches a given tolerance ε, or until the error decreases by a factor δ, with $\varepsilon = 1/\delta$, namely

$$k \approx -\frac{\ln \varepsilon}{R_\infty(M^{-1}N)} = \frac{\ln \delta}{R_\infty(M^{-1}N)}.$$

Example 2.11. Consider the matrix

$$A = \begin{bmatrix} 4 & -1 & 0 \\ -1 & 4 & -1 \\ 0 & -1 & 4 \end{bmatrix}$$

and the splitting $A = M - N$, where

$$M = \begin{bmatrix} 4 & 0 & 0 \\ 0 & 4 & 0 \\ 0 & 0 & 4 \end{bmatrix} \quad \text{and} \quad N = \begin{bmatrix} 0 & 1 & 0 \\ 1 & 0 & 1 \\ 0 & 1 & 0 \end{bmatrix}.$$

The iteration matrix is given by $G = M^{-1}N$. The spectral radius of G (computed by the next MATLAB script) is $\rho(M^{-1}N) \approx 0.35$. Consider a vector $\boldsymbol{e}_0 = [1\,1\,1]^\top$. Then we can estimate the number of iterations needed to obtain a reduction of the error of a factor of $\delta = 1000$ ($\varepsilon = 1/\delta$):

$$K = \frac{\ln \varepsilon}{-\ln \rho(M^{-1}N)} \approx 6.64.$$

Thus, we need about seven iterations. The following MATLAB script performs seven iterations of the type $\boldsymbol{e}_{k+1} = G\boldsymbol{e}_k$.

```
A=[4 -1 0; -1 4 -1; 0 -1 4];
M=diag(diag(A));                    % decomposition A=M-N
N=M-A;
G=M\N;                              % iteration matrix
rho=max(abs(eig(G)))                % spectral radius of G
R_inf=-log(rho)                     % asymptoric convergence rate
delta=1000;                         % reduction factor
epsi=1/delta;                       % tolerance
K=-log(epsi)/R_inf                  % estimate of the iterations "k"
e=ones(3,1);                        % initial error
nor(1)=norm(e,2);
for j=1:round(K)                    % approximate K by the closest integer
  e=G*e;                            % iteration step
  nor(j+1)=norm(e,2)/nor(1);
  disp(['j=' num2str(j) ' | norm=' num2str(nor(j+1))]);
end
v=0:round(K);
semilogy(v,nor,'ob-',v,10*rho.^v,'b');
```

```
legend('error','asymptotic convergence');
xlabel('iteration');
ylabel('error');
set(gca,'fontsize',16);                    % bigger font size
```

The results we obtain are

```
rho = 0.35355
R_inf = 1.0397
K = 6.6439
j=1 | norm=0.35355
j=2 | norm=0.125
j=3 | norm=0.044194
j=4 | norm=0.015625
j=5 | norm=0.0055243
j=6 | norm=0.0019531
j=7 | norm=0.00069053
```

and we can see that after seven iterations the reduction of the error in the norm $\|\cdot\|_\infty$ is about 10^{-3} as expected. Moreover, the convergence behavior is shown in Figure 2.1, where the error $\frac{\|e_k\|_2}{\|e_0\|_2}$ is compared with the asymptotic convergence rate. ∎

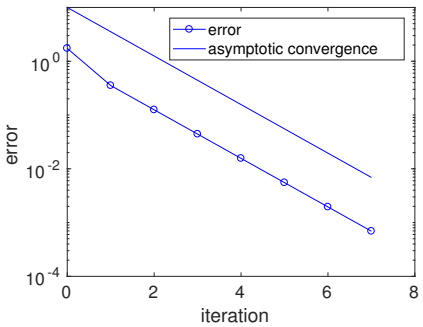

Figure 2.1. *Error* $\frac{\|e_k\|_2}{\|e_0\|_2}$ *and asymptotic convergence rate.*

Notice that the convergence rate $R_\infty(G)$ represents the slope that the convergence curve of the norm of the error sequence should have asymptotically (for k sufficiently large). One may wonder whether the convergence of the error sequence is monotone for all k and whether it becomes asymptotically a straight line (as shown in Figure 2.1). The answer is negative in both cases, and we show in the following example that one can construct a matrix G that gives rise to a convergence curve that is not monotonically decreasing for k "small" and that is not a straight line even for "large" values of k.

Example 2.12. Consider the iteration matrix

$$G = \begin{bmatrix} a & 0 & 0 \\ 1 & 0 & 0 \\ 1 & 1 & \frac{1}{2} \end{bmatrix},$$

where $a, b \in (0,1)$. It holds that $\rho(G) = \max(a, \frac{1}{2})$ and $R_\infty(G) = -\ln(\max(a, \frac{1}{2}))$. If we set $a = \frac{1.9}{2}$ and an initial vector $e^0 = \begin{bmatrix} 1 & 1 & 1 \end{bmatrix}^\top$ and evaluate the infinity norm of the

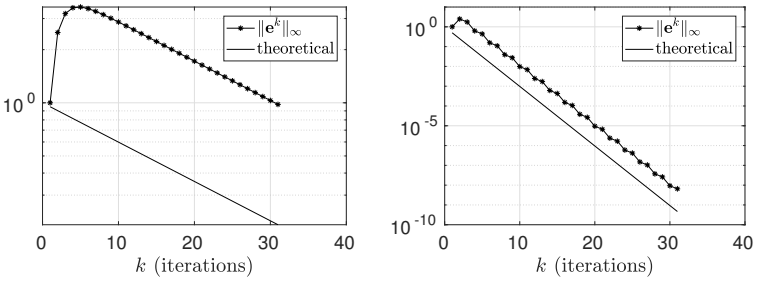

Figure 2.2. *Convergence behavior discussed in Example 2.12.*

sequence $\boldsymbol{e}_{k+1} := G\boldsymbol{e}_k$ for $k = 0, 1, 2 \ldots$, we obtain that $\|\boldsymbol{e}_k\|_\infty \geq \|\boldsymbol{e}_{k-1}\|_\infty$ for $k = 1, 2, 3, 4$. Therefore, the error in the infinity norm increases in the first iterations and then starts to decay. This behavior is clearly shown in Figure 2.2 (left), where we observe a significant growth of the quantity $\|\boldsymbol{e}_k\|_\infty$ in the first iteration. For k large the error decays with the expected asymptotic rate $R_\infty(G)$.

Next, we consider $a = -\frac{1}{2}$. This means that the iteration matrix G has two eigenvalues with the same modulus and opposite signs. In this case we observe the behavior shown in Figure 2.2 (right), where the convergence curve decays monotonically with an averaged slope equal to $R_\infty(G)$. However, the convergence curve is not a straight line. This is due to the two eigenvalues of G with opposite sign, which are $\frac{1}{2}$ and $-\frac{1}{2}$. ∎

2.4 ▪ Regular splittings and M-matrices

> *Interestingly enough, the basis for the analysis of such modern cyclic iterative methods can be traced back to fundamental research by Perron and Frobenius on non-negative matrices, and our first aim is more nearly to survey the basic results on cyclic iterative methods, using the Perron-Frobenius theory as a basis.*
>
> Richard S. Varga, *Matrix Iterative Analysis*, 1962

When computers started to become more and more available, stationary iterations became an attractive alternative to direct solvers for linear systems, and it was important to find general criteria for matrices and associated splittings that lead to convergent stationary iterations. We follow in this subsection the pioneering work of Varga [181], which led to many interesting results on properties of matrices in general and sparked the more important later research field of how to design rapidly converging stationary iterations and preconditioners.

Definition 2.13 (Nonnegative matrix). *A matrix $A \in \mathbb{R}^{n\times n}$ is said to be* nonnegative *(*nonpositive*) if $a_{ij} \geq 0$ (respectively, $a_{ij} \leq 0$) for $i, j = 1, \ldots, n$. To denote a nonnegative (nonpositive) matrix we use the symbol $A \geq 0$ (respectively, $A \leq 0$).*[11]

Perron and Frobenius discovered an interesting property of nonnegative matrices.

Theorem 2.14 (Perron–Frobenius, 1907/1912). *Let $A \in \mathbb{R}^{n\times n}$ be a nonnegative matrix. Then A has a nonnegative real eigenvalue λ which equals the spectral radius of A, $\lambda = \rho(A)$, and a corresponding eigenvector which is nonnegative.*

[11] The notation $A \geq 0$ is also used in functional analysis to denote a positive semidefinite operator; see, e.g., [119, Section 9.3]. However, we do not adopt such notation in the present book.

Proof. See, e.g., [94, Theorem 10.2.4] and [181, Theorem 2.7]. □

The original result of Perron and Frobenius is slightly stronger: it requires also that the matrix A be *irreducible* (i.e., there exists no permutation matrix P such that $P^\top AP$ is block upper triangular), and then "nonnegative" can be replaced by "positive" in Theorem 2.14.

We now introduce a particular class of splittings for matrices, for which one can obtain very general convergence results.

Definition 2.15 (Regular splitting). *A splitting $A = M - N$ is said to be* regular *if M is invertible and if both M^{-1} and N are nonnegative.*

Theorem 2.16 (Convergence of regular splitting stationary methods). *Let $A \in \mathbb{R}^{n\times n}$ be a given matrix and $A = M - N$ be a regular splitting. Then*

$$\rho(M^{-1}N) < 1 \quad \Longleftrightarrow \quad A \text{ is invertible and } A^{-1} \text{ nonnegative}.$$

Proof. If $\rho(M^{-1}N) < 1$, then 1 is not an eigenvalue of $M^{-1}N$. Hence, the determinant of $(I - M^{-1}N)$ is nonzero, which means that $(I - M^{-1}N)$ is invertible. Therefore, we recall that M is invertible and write $A = M - N = M(I - M^{-1}N)$ to deduce that A is invertible as well. Furthermore, using the Neumann series (see Problem 10), we obtain

$$A^{-1} = (I - M^{-1}N)^{-1}M^{-1} = \sum_{j=0}^{\infty}(M^{-1}N)^j M^{-1},$$

which shows that A^{-1} is nonnegative since products and sums of nonnegative matrices are nonnegative matrices as well.

On the other hand, suppose A is invertible and A^{-1} is nonnegative. Since M is invertible, we obtain from $A = M - N = M(I - M^{-1}N)$ that also $(I - M^{-1}N)$ is invertible. Thus

$$A^{-1}N = (M(I - M^{-1}N))^{-1}N = (I - M^{-1}N)^{-1}M^{-1}N. \tag{2.16}$$

By assumption, both matrices M^{-1} and N are nonnegative, and thus their product is also nonnegative. Using Theorem 2.14, there exists a nonnegative vector $\boldsymbol{v}$ such that

$$M^{-1}N\boldsymbol{v} = \lambda\boldsymbol{v}, \quad \lambda = \rho(M^{-1}N).$$

Using (2.16), we obtain

$$A^{-1}N\boldsymbol{v} = (I - M^{-1}N)^{-1}M^{-1}N\boldsymbol{v} = \rho(M^{-1}N)(I - M^{-1}N)^{-1}\boldsymbol{v}. \tag{2.17}$$

Now, since $(I - M^{-1}N)$ is invertible, 1 is not an eigenvalue of $M^{-1}N$. Moreover, since the eigenvalue λ that corresponds to $\rho(M^{-1}N)$ is real and nonnegative, we have that $\rho(M^{-1}N) \neq 1$. Therefore, we can write that

$$(I - M^{-1}N)\boldsymbol{v} = (1 - \rho(M^{-1}N))\boldsymbol{v} \;\Leftrightarrow\; (I - M^{-1}N)^{-1}\boldsymbol{v} = \frac{1}{1 - \rho(M^{-1}N)}\boldsymbol{v}.$$

Replacing this equation into (2.17), we obtain

$$A^{-1}N\boldsymbol{v} = \frac{\rho(M^{-1}N)}{1 - \rho(M^{-1}N)}\boldsymbol{v}.$$

Now since A^{-1}, N, and $\boldsymbol{v}$ are nonnegative, we get

$$\frac{\rho(M^{-1}N)}{1-\rho(M^{-1}N)} \geq 0 \quad \Longrightarrow \quad 1-\rho(M^{-1}N) \geq 0 \quad \Longrightarrow \quad 0 \leq \rho(M^{-1}N) \leq 1.$$

We have already seen that the invertibility of $I - M^{-1}N$ and Theorem 2.14 ensures that $\rho(M^{-1}N) \neq 1$. Hence, we must have $\rho(M^{-1}N) < 1$. □

An example of a regular splitting is given by the matrices A, M, and N in Example 2.11. However, a regular splitting of an arbitrary matrix does not necessary exist, as we show in the next example.

Example 2.17. Take any matrix $A \in \mathbb{R}^{2\times 2}$ such that $a_{j,k} > 0$ for all $j, k = 1, 2$. We write that $A > 0$, where this inequality is understood in a componentwise manner. Assume that a regular splitting $A = M - N$ exists. Since $A > 0$ and $N \geq 0$, we get $M = A + N \geq A > 0$. Therefore, all the entries of M must be positive, that is, $m_{j,k} > 0$ for all $j, k = 1, 2$. Since the splitting is regular, the matrix M must be invertible, which means that its determinant is nonzero, that is, $m_{1,1}m_{2,2} - m_{2,1}m_{1,2} \neq 0$, and we get $M^{-1} = \frac{1}{m_{1,1}m_{2,2}-m_{2,1}m_{2,2}} \begin{bmatrix} m_{2,2} & -m_{1,2} \\ -m_{2,1} & m_{1,1} \end{bmatrix}$. However, this matrix is not nonnegative, because all of its entries are nonzero and some of them must be necessarily negative. This contradicts our hypothesis. ∎

We now introduce the notion of M-matrix and provide a corresponding example.

Definition 2.18 (M-matrix). *A matrix $A \in \mathbb{R}^{n\times n}$ is an* M-matrix *if*

1. $a_{ii} > 0$ *for* $i = 1, \ldots, n$;
2. $a_{ij} \leq 0$ *for* $i \neq j$, $i, j = 1, \ldots, n$;
3. A *is invertible;*
4. $A^{-1} \geq 0$.

Example 2.19. Consider the boundary value problem

$$-u''(x) = f(x) \text{ for } x \in (0,1), \quad u(0) = u(1) = 0.$$

After discretizing with step-size $h = 1/(n+1)$, $x_j = jh$, $u_j \approx u(x_j)$ and approximating

$$u''(x_j) \approx \frac{u_{j-1} - 2u_j + u_{j+1}}{h^2},$$

we obtain the linear system

$$\begin{bmatrix} 2 & -1 & & \\ -1 & 2 & \ddots & \\ & \ddots & \ddots & -1 \\ & & -1 & 2 \end{bmatrix} \begin{bmatrix} u_1 \\ u_2 \\ \vdots \\ u_n \end{bmatrix} = h^2 \begin{bmatrix} f_1 \\ f_2 \\ \vdots \\ f_n \end{bmatrix}.$$

Since the matrix of the system A has the nonnegative inverse $B = A^{-1}$ where B is computed explicitly with the MATLAB statements (see Problem 24)

```
L=tril(ones(n)); v=ones(n,1);
B=L'*(eye(n)-1/(n+1)*(v*v'))*L;
```

we conclude that A is an M-matrix. This can also be proved analytically, see Problem 11. ∎

As a consequence of Theorem 2.16 we obtain the following general convergence result.

Corollary 2.20. *Let $A \in \mathbb{R}^{n\times n}$ be an M-matrix and $A = M - N$ be a regular splitting. Then the stationary iteration $M\boldsymbol{u}_{k+1} = N\boldsymbol{u}_k + \boldsymbol{f}$ converges to the solution of $A\boldsymbol{u} = \boldsymbol{f}$.*

A further result, which is attributed to Householder [110] and John [113], is the following theorem (see also [16]).

Theorem 2.21 (Householder–John, 1955/1956). *Let $A \in \mathbb{R}^{n\times n}$ be symmetric and invertible. Let $A = M - N$ be a splitting with a real, invertible matrix M and assume that $N + M^\top$ is symmetric positive definite. Then*

$$\rho(M^{-1}N) < 1 \iff A \text{ is positive definite.}$$

Proof. We prove first that if A is positive definite, then $\rho(M^{-1}N) < 1$. Let $(\lambda, \boldsymbol{v})$ be a possibly complex eigenpair of the matrix $M^{-1}N$, $M^{-1}N\boldsymbol{v} = \lambda\boldsymbol{v}$. Then it holds that

$$A = M(I - M^{-1}N) \quad \Longrightarrow \quad A\boldsymbol{v} = (1-\lambda)M\boldsymbol{v},$$

and multiplying from the left with $\boldsymbol{v}^*$ we obtain

$$\boldsymbol{v}^*A\boldsymbol{v} = (1-\lambda)\boldsymbol{v}^*M\boldsymbol{v}, \tag{2.18}$$

which shows that $\lambda \neq 1$, since A is positive definite. If we take the conjugate transpose of the last equation, we get

$$(1-\bar{\lambda})\boldsymbol{v}^*M^*\boldsymbol{v} = (\boldsymbol{v}^*A\boldsymbol{v})^* = \boldsymbol{v}^*A^*\boldsymbol{v} = \boldsymbol{v}^*A\boldsymbol{v}. \tag{2.19}$$

Since M is real we have $M^* = M^\top$. Let $Q = N + M^\top = M + M^\top - A$, which is by assumption positive definite. Dividing (2.18) and (2.19), respectively, by $(1-\lambda)$ and $(1-\bar{\lambda})$ (which cannot vanish, since we have seen $\lambda \neq 1$) and adding them, we get

$$\underbrace{\left(\frac{1}{1-\lambda} + \frac{1}{1-\bar{\lambda}}\right)}_{2\,\mathrm{Re}\,\frac{1}{1-\lambda}} \boldsymbol{v}^*A\boldsymbol{v} = \boldsymbol{v}^*(\underbrace{M + M^\top}_{Q+A})\boldsymbol{v}.$$

This implies that

$$2\,\mathrm{Re}\,\frac{1}{1-\lambda} = \frac{\boldsymbol{v}^*Q\boldsymbol{v} + \boldsymbol{v}^*A\boldsymbol{v}}{\boldsymbol{v}^*A\boldsymbol{v}} = 1 + \frac{\boldsymbol{v}^*Q\boldsymbol{v}}{\boldsymbol{v}^*A\boldsymbol{v}} > 1$$

since both Q and A are positive definite. We therefore have

$$2\,\mathrm{Re}\,\frac{1}{1-\lambda} > 1,$$

which, using $\lambda = \alpha + i\beta$ with $\alpha, \beta \in \mathbb{R}$, gives

$$2\,\mathrm{Re}\,\frac{1}{1-\lambda} = \frac{2(1-\alpha)}{(1-\alpha)^2 + \beta^2} > 1 \iff |\lambda|^2 = \alpha^2 + \beta^2 < 1 \implies \rho(M^{-1}N) < 1.$$

We have then obtained that if A is positive definite, then $\rho(M^{-1}N) < 1$.

To prove the other direction, namely that if $\rho(M^{-1}N) < 1$, then A is positive definite, we first need the following lemma.

Lemma 2.22. *Under the same conditions as in Theorem 2.21, the following identity holds:*

$$A - (M^{-1}N)^\top A(M^{-1}N) = (I - M^{-1}N)^\top (M^\top + N)(I - M^{-1}N). \tag{2.20}$$

Proof. To prove this lemma, we replace $A = M - N$, expand the left- and right-hand sides of (2.20), and show that they are equal. The expansion of the right-hand side gives

$$\begin{aligned} &(I - M^{-1}N)^\top (M^\top + N)(I - M^{-1}N) \\ &= (M^\top + N - N^\top - N^\top M^{-\top} N)(I - M^{-1}N). \end{aligned}$$

Because of the symmetry $A^\top = A \iff M^\top - N^\top = M - N$ we get

$$\begin{aligned} &(I - M^{-1}N)^\top (M^\top + N)(I - M^{-1}N) \\ &= (M - N^\top M^{-\top} N)(I - M^{-1}N) \\ &= M - N^\top M^{-\top} N - N + N^\top M^{-\top} N M^{-1} N. \end{aligned}$$

Expanding the left-hand side, we obtain

$$\begin{aligned} &A - (M^{-1}N)^\top A(M^{-1}N) \\ &= M - N - N^\top M^{-\top}(M - N)M^{-1}N \\ &= M - N - (N^\top M^{-\top} M - N^\top M^{-\top} N)M^{-1}N \\ &= M - N - (N^\top M^{-\top} N - N^\top M^{-\top} N M^{-1} N) \\ &= M - N^\top M^{-\top} N - N + N^\top M^{-\top} N M^{-1} N, \end{aligned}$$

the same expression as for the right-hand side, which concludes this proof. □

Continuing with the proof of Theorem 2.21, we now prove the second part by contraposition. We suppose that A is not positive definite and show that this implies $\rho(M^{-1}N) \geq 1$. Let $\boldsymbol{e}_0 \in \mathbb{R}^n$ be given. We consider the sequence of vectors

$$\boldsymbol{e}_{k+1} = M^{-1}N\boldsymbol{e}_k.$$

Applying the lemma, we obtain

$$A\boldsymbol{e}_k - (M^{-1}N)^\top A \underbrace{(M^{-1}N)\boldsymbol{e}_k}_{\boldsymbol{e}_{k+1}} = (I - M^{-1}N)^\top \underbrace{(M^\top + N)}_{Q} \underbrace{(I - M^{-1}N)\boldsymbol{e}_k}_{\boldsymbol{e}_k - \boldsymbol{e}_{k+1}}.$$

Multiplying the last equation from the left with $\boldsymbol{e}_k^\top$ yields

$$\boldsymbol{e}_k^\top A\boldsymbol{e}_k - \boldsymbol{e}_{k+1}^\top A\boldsymbol{e}_{k+1} = (\boldsymbol{e}_k - \boldsymbol{e}_{k+1})^\top Q(\boldsymbol{e}_k - \boldsymbol{e}_{k+1}) \geq 0,$$

since Q is positive definite. Therefore the sequence $\boldsymbol{e}_k^\top A\boldsymbol{e}_k$ satisfies

$$\boldsymbol{e}_k^\top A\boldsymbol{e}_k \geq \boldsymbol{e}_{k+1}^\top A\boldsymbol{e}_{k+1}$$

and is thus nonincreasing. Since A is assumed to be invertible but not positive definite, we can find an initial vector $\boldsymbol{e}_0$ such that

$$0 > \boldsymbol{e}_0^\top A\boldsymbol{e}_0 \geq \boldsymbol{e}_1^\top A\boldsymbol{e}_1 \geq \cdots.$$

This means that $\boldsymbol{e}_k$ is not convergent to 0. Thus $\rho(M^{-1}N) \geq 1$. □

We will now get back to the classical, historical stationary iterations of Jacobi, Gauss, and Seidel we have seen in Chapter 1. These methods can be written by splitting the matrix A into the strictly lower triangular part L, the diagonal part $D = \mathrm{diag}(A)$, and the strictly upper triangular part U,

$$A = L + D + U.$$

2.5 ▪ Jacobi

> *Eine solche [Näherungsmethode] bietet sich von selber dar, wenn in den verschiedenen Gleichungen immer eine andere Variable mit einem vorzugsweise grossen Coefficienten multiplicirt ist.*
>
> Carl G. J. Jacobi, *Über eine neue Auflösungsart der bei der Methode der kleinsten Quadrate vorkommenden lineären Gleichungen*, 1845.

The *Jacobi method* is based on solving for every variable locally, with the other variables frozen at their old values, as we have seen in Section 1.2. This corresponds to the iteration

$$(\boldsymbol{u}_{k+1})_i = \frac{1}{a_{ii}}\Big[\boldsymbol{f}_i - \sum_{j=1, j\neq i}^{n} a_{ij}(\boldsymbol{u}_k)_j\Big], \tag{2.21}$$

which can be performed in parallel for all i. This iteration can be written as a matrix splitting $A = M - N$, with

$$M = D, \quad N = -L - U \quad \Longrightarrow \quad D\boldsymbol{u}_{k+1} = -(L+U)\boldsymbol{u}_k + \boldsymbol{f}. \tag{2.22}$$

With the following MATLAB program one can test the Jacobi method on our Laplace model problem from Section 1.3:

```
m=15;                           % number of gridpoints
A=Laplacian(m,2);               % five-point Laplacian
f=zeros(m*m,1); f(m:m:end)=1;   % put bc into the rhs
u=A\f;                          % solve by sparse Gaussian elimination
x=0:1/(m+1):1; y=x;             % mesh point vectors
uj=zeros(size(f));              % initial guess
U=zeros(m+2); U(end,1:m+2)=1;   % for plotting
for k=0:10                      % do 10 Jacobi steps
  err(k+1)=max(max(abs(u-uj))); % compute error
  U(2:m+1,2:m+1)=reshape(uj,m,m);
  mesh(x,y,U);                  % plot current approximation
  xlabel('x');ylabel('y');
  uj=uj+(f-A*uj)./diag(A);      % perform one Jacobi step
  pause
end
```

We show in Figure 2.3 the first few approximations computed by the Jacobi method starting with a zero initial guess. Comparing with the shape of the solution shown in Figure 1.11, we see that the method apparently converges, but rather slowly. A classical convergence result for the Jacobi method, which motivated Jacobi to actually consider the method—see the quote above—is given in the following theorem.

Theorem 2.23 (Convergence of Jacobi's method for diagonally dominant matrices). *If the matrix $A \in \mathbb{R}^{n\times n}$ is strictly diagonally dominant, i.e.,*

$$|a_{ii}| > \sum_{j\neq i} |a_{ij}| \quad \textit{for } i = 1, \ldots, n, \tag{2.23}$$

then the Jacobi iteration (2.22) *converges.*

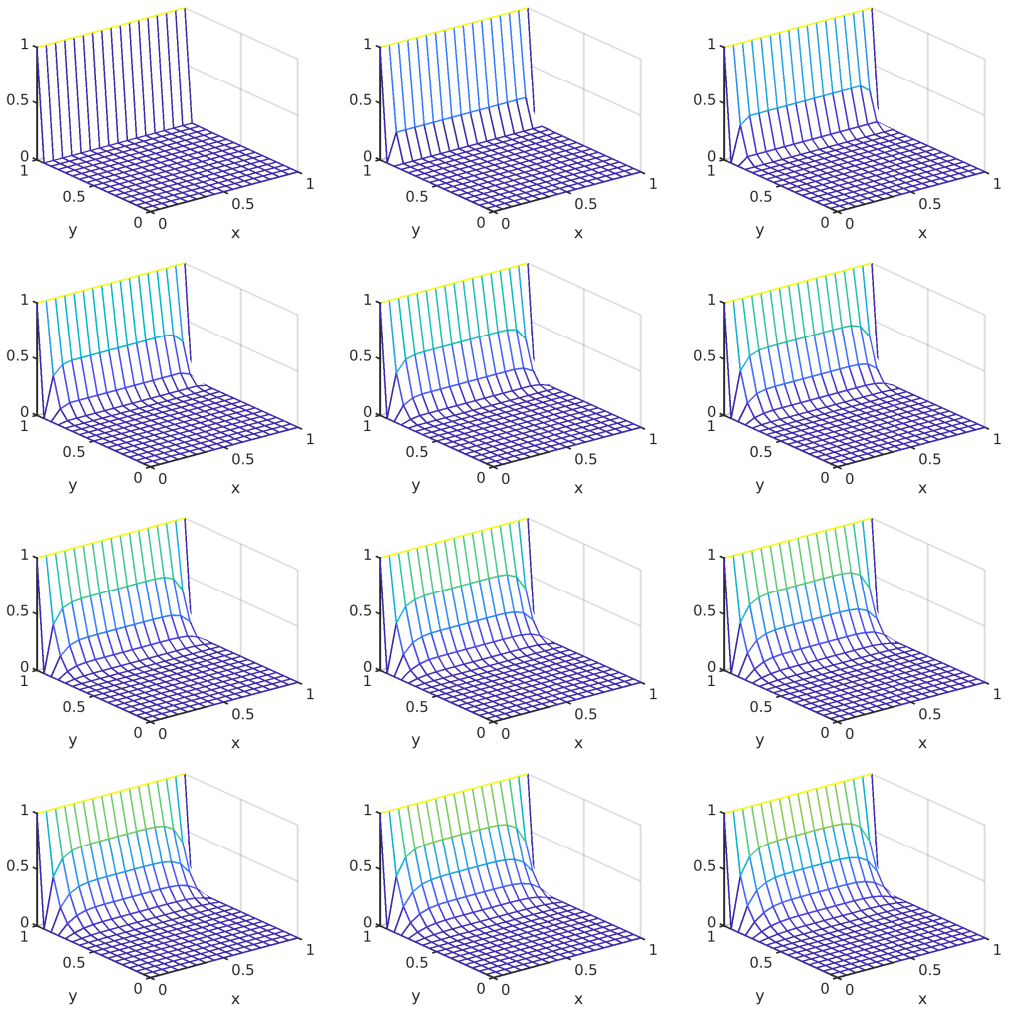

Figure 2.3. *Initial guess and first iterations of the Jacobi method* (2.22) *applied to our Laplace model problem from Section 1.3.*

Proof. The iteration matrix of the Jacobi method is $G_{\mathrm{J}} = -D^{-1}(L+U)$. The condition (2.23) allows us to estimate that

$$\|G_{\mathrm{J}}\|_\infty = \max_{i\in\{1,\dots,n\}} \frac{1}{|a_{ii}|} \sum_{j\neq i} |a_{ij}| < 1.$$

Using Lemma 2.4, we obtain

$$\rho_{G_{\mathrm{J}}} \leq \|G_{\mathrm{J}}\|_\infty < 1,$$

which together with Theorem 2.7 concludes the proof. □

We now apply Theorem 2.21 to the method of Jacobi.

Theorem 2.24 (Convergence of Jacobi for symmetric matrices). *Let $A \in \mathbb{R}^{n\times n}$ be symmetric and invertible and consider the splitting $A = D + L + L^\top$ with L strictly lower triangular and D diagonal and positive definite, $D_{ii} > 0$ for $i = 1, \ldots, n$. Then the Jacobi iteration converges if and only if A and $2D - A$ are positive definite.*

Proof. If A and $Q := 2D-A$ are positive definite, then according to Theorem 2.21 (Householder–John) Jacobi converges. In fact, it suffices to set $M = D$ and $N = -(L + L^\top)$, which implies that $N + M^\top = 2D - A$.

For the reverse, we assume now that Jacobi is convergent, and we want to show that A and Q are positive definite. Consider an eigenpair $(\lambda, \boldsymbol{v})$ of the iteration matrix $G_{\mathrm{J}} := -D^{-1}(L^\top + L)$,

$$M^{-1}N\boldsymbol{v} = \underbrace{-D^{-1}(L + L^\top)}_{G_{\mathrm{J}}}\boldsymbol{v} = \lambda\boldsymbol{v}. \tag{2.24}$$

Since D is positive definite, we can take its square root, $D = D^{\frac{1}{2}}D^{\frac{1}{2}}$. The matrix G_{J} is then similar to the symmetric matrix

$$D^{\frac{1}{2}}G_{\mathrm{J}}D^{-\frac{1}{2}} = -D^{-\frac{1}{2}}(L^\top + L)D^{-\frac{1}{2}},$$

therefore the eigenvalues of the iteration matrix are real, and since we suppose that Jacobi is convergent, we have $|\lambda| < 1$ (see Theorem 2.7). Furthermore, from the eigenvalue equation (2.24), we have

$$(L + L^\top)\boldsymbol{v} = -\lambda D\boldsymbol{v}, \tag{2.25}$$

and adding on both sides $D\boldsymbol{v}$ gives

$$\begin{aligned} & A\boldsymbol{v} = (1-\lambda)D\boldsymbol{v} \\ \iff & \underbrace{D^{-\frac{1}{2}}AD^{-\frac{1}{2}}}_{\widetilde{A}}\underbrace{D^{\frac{1}{2}}\boldsymbol{v}}_{\boldsymbol{y}} = (1-\lambda)\underbrace{D^{\frac{1}{2}}\boldsymbol{v}}_{\boldsymbol{y}}. \end{aligned}$$

This means that $1 - \lambda > 0$ is an eigenvalue of $\widetilde{A}$ with the corresponding eigenvector $\boldsymbol{y}$. Thus $\widetilde{A}$ is positive definite, which means that $0 < \boldsymbol{y}^\top\widetilde{A}\boldsymbol{y} = \boldsymbol{v}^\top A\boldsymbol{v}$ for all $\boldsymbol{y} \neq 0$ and therefore also for all $\boldsymbol{v} = D^{-\frac{1}{2}}\boldsymbol{y} \neq 0$. Therefore also A is positive definite.

A similar argument holds for Q. Multiplying (2.25) by -1 and adding $D\boldsymbol{v}$ on both sides yields

$$\underbrace{(D - (L + L^\top))}_{Q}\boldsymbol{v} = (1+\lambda)D\boldsymbol{v}.$$

As before

$$D^{-\frac{1}{2}}QD^{-\frac{1}{2}}\boldsymbol{y} = (1+\lambda)\boldsymbol{y},$$

and since $1 + \lambda > 0$ we conclude that Q is also positive definite. ∎

Using Theorem 2.24, one can show that Jacobi's method applied to the discrete Laplace problem converges; see Problem 14.

Proving convergence was the dominant task early on when studying iterative methods, but when using such methods to solve practical problems, one is really interested in the convergence speed. In particular, when solving discretized PDEs, one would like to solve problems with finer and finer mesh sizes to get more and more accurate solutions, and thus one is interested in how convergence depends on the mesh size. We show in Figure 2.4 how the error decreases as the iterations progress when Jacobi is used to solve our Laplace model problem from Section 1.3 for the

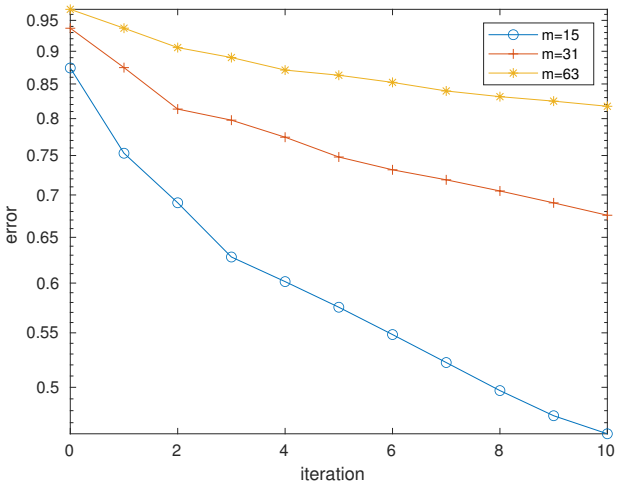

Figure 2.4. *Convergence of the Jacobi method for different mesh sizes* $h = \frac{1}{m+1}$.

mesh we used for Figure 2.3 with $m = 15$ interior mesh points, and also on two refined meshes with $m = 31$ and $m = 63$ interior mesh points. We see that convergence strongly depends on the mesh parameter h and deteriorates when the mesh is refined, a very undesirable property. In this particular case where A is equal to the (negative) two-dimensional finite-difference Laplacian, it is possible to characterize precisely the deterioration of the Jacobi method with respect to the grid size h. A well-known fact is that the eigenvalues of A are given by (see Problem 11 and the corresponding hints)

$$\lambda_{j,k}(A) = 4 + 2\cos\Big(\frac{k\pi}{m+1}\Big) + 2\cos\Big(\frac{j\pi}{m+1}\Big) \tag{2.26}$$

for $j, k = 1, \ldots, m$. Since the Jacobi iteration matrix is $G_{\mathrm{J}} = -D^{-1}(L + L^\top) = I - \frac{1}{4}A$, the corresponding eigenvalues are

$$\lambda_{j,k}(G_{\mathrm{J}}) = 1 - \frac{1}{4}\lambda_{j,k}(A).$$

Hence, the spectral radius of G_{J} (as a function of the mesh size h) is

$$\begin{aligned} \rho_{G_{\mathrm{J}}}(h) &= \max_{k,j}\Big|1 - \frac{1}{4}\lambda_{k,j}(A)\Big| \\ &= \frac{1}{2}\max_{k,j}\Big|\cos\Big(\frac{k\pi}{m+1}\Big) + \cos\Big(\frac{j\pi}{m+1}\Big)\Big| = \cos\big(h\pi\big), \end{aligned} \tag{2.27}$$

where we used that $h = \frac{1}{m+1}$. A Taylor expansion of $\rho_{G_{\mathrm{J}}}(h)$ around zero leads to

$$\rho_{G_{\mathrm{J}}}(h) = 1 - \frac{\pi^2}{2}h^2 + O(h^4), \tag{2.28}$$

which shows precisely the deterioration of $\rho_{G_{\mathrm{J}}}(h)$ as $h \to 0$. This deterioration is related to the fact that Jacobi only treats neighboring mesh points in each iteration, and as Figure 2.3 indicates, for finer and finer meshes, approximations will take longer and longer to reach gridpoints with small y coordinate.

A similar convergence result as in Theorem 2.24 can be proved in the case that the decomposition is obtained by block matrices. For example, consider the block-tridiagonal matrix A given in the introduction in (1.11),

$$A = \begin{bmatrix} T & -I & & \\ -I & T & \ddots & \\ & \ddots & \ddots & -I \\ & & -I & T \end{bmatrix}.$$

It is natural to use a block splitting $A = D + L + L^\top$, where

$$D = \begin{bmatrix} T & & & \\ & T & & \\ & & \ddots & \\ & & & T \end{bmatrix} \quad \text{and} \quad L = \begin{bmatrix} 0 & & & \\ -I & 0 & & \\ & \ddots & \ddots & \\ & & -I & 0 \end{bmatrix}.$$

We then get a *block-Jacobi iteration*.

Theorem 2.25 (Convergence of the block-Jacobi method). *Let $A \in \mathbb{R}^{n\times n}$ be symmetric and invertible and consider the splitting $A = D + L + L^\top$, where*

$$D = \begin{bmatrix} \ddots & & \\ & D_{jj} & \\ & & \ddots \end{bmatrix} \tag{2.29}$$

with the blocks D_{jj} positive definite, and L is strictly lower block-triangular. Then the Jacobi iteration converges if and only if A and $2D - A$ are positive definite.

Proof. The proof is identical to the proof of Theorem 2.24: we only need to note that since the blocks D_{jj} are positive definite, D is positive definite as well. Hence, we have the decomposition $D = D^{\frac{1}{2}} D^{\frac{1}{2}}$. □

This slight modification of Theorem 2.24 can be used to show that block-Jacobi converges for the matrix A given in (1.11). We know that A is a positive definite matrix; see Problem 11. According to Theorem 2.25, it suffices to show that

$$2D - A = \begin{bmatrix} T & I & & \\ I & T & \ddots & \\ & \ddots & \ddots & I \\ & & I & T \end{bmatrix}$$

is also positive definite; see Problem 17. Finally, we wish to remark that block Jacobi is very much related to domain decomposition methods. In particular, it is equivalent to a discrete parallel Schwarz method with minimal overlap; see Chapter 4 and Problem 56.

2.6 ▪ Gauss–Seidel

Wenn man also, von irgend welchem Systeme von Anfangswerthen ausgehend, und in irgend welcher Aufeinanderfolge der Unbekannten (wobei es nicht nöthig ist, den ganzen Cyklus derselben durchzugehen, ehe man wieder auf eine schon verbesserte zurückkommt), successive Correctionen an den Unbekannten anbringt, indem man Sorge trägt, die jedesmalige Verbesserung einer jeden immer so zu bestimmen, dass durch dieselbe diejenige Normalgleichung erfüllt wird, in der die betreffende Unbekannte die ausgezeichnete Stellung in der Diagonale einnimmt, so verringert man Schritt für Schritt die Summe der Fehlerquadrate, solange an ihr noch etwas zu verringern ist.

Ludwig von Seidel, *Über ein Verfahren, die Gleichungen, auf welche die Methode der kleinsten Quadrate führt, sowie lineäre Gleichungen überhaupt, durch successive Annäherung aufzulösen*, 1874.

Today, the *Gauss–Seidel method* is the original Gauss method we have seen in Section 1.2 and more generally described by Seidel (see the quote above), but simply cycling through all the variables sequentially, i.e.,

$$(\boldsymbol{u}_{k+1})_i = \frac{1}{a_{ii}} \left[\boldsymbol{f}_i - \sum_{j=1}^{i-1} a_{ij} (\boldsymbol{u}_{k+1})_j - \sum_{j=i+1}^{n} a_{ij} (\boldsymbol{u}_k)_j \right]. \tag{2.30}$$

This corresponds to the matrix splitting

$$M = D + L, \quad N = -U \quad \Rightarrow \quad (D + L)\boldsymbol{u}_{k+1} = -U\boldsymbol{u}_k + \boldsymbol{f}. \tag{2.31}$$

With the following MATLAB program one can test the Gauss–Seidel method on our Laplace model problem from Section 1.3:

```
m=15;                              % number of gridpoints
A=Laplacian(m,2);                  % five-point Laplacian
f=zeros(m*m,1); f(m:m:end)=1;      % put bc into the rhs
u=A\f;                             % solve by sparse Gaussian elimination
x=0:1/(m+1):1; y=x;                % mesh point vectors
ugs=zeros(size(f));                % initial guess
U=zeros(m+2); U(end,1:m+2)=1;      % for plotting
LD=tril(A);                        % L+D
for k=0:10                         % do 10 Gauss-Seidel steps
  err(k+1)=max(max(abs(u-ugs)));   % compute error
  U(2:m+1,2:m+1)=reshape(ugs,m,m);
  mesh(x,y,U);                     % plot current approximation
  xlabel('x');ylabel('y');
  ugs=ugs+LD\(f-A*ugs);            % perform one Gauss-Seidel step
  pause
end
```

We show in Figure 2.5 the first few approximations computed by the Gauss–Seidel method starting with a zero initial guess. Comparing with the iterates of the Jacobi method in Figure 2.3, we see that Gauss–Seidel converges a bit faster; see also Figure 2.9 later, which shows error curves. This seems to be natural, since Gauss–Seidel uses the updated values as soon as they are available. Faster convergence is often the case, e.g., for our Laplace model problem $\Delta u = 0$, for which one can show that only half of the iteration steps are needed for the same accuracy;

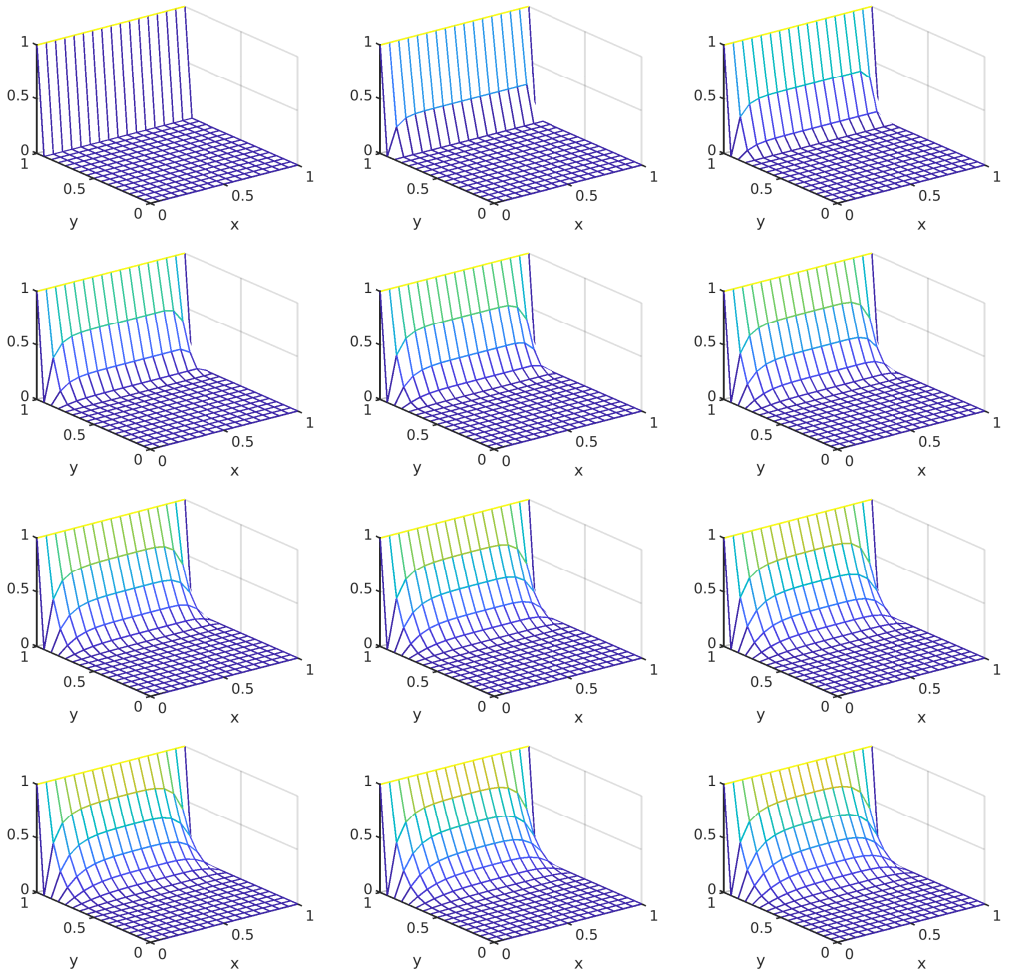

Figure 2.5. *Initial guess and first iterations of the Gauss–Seidel method* (2.31) *applied to our Laplace model problem from Section 1.3.*

see, e.g., Problem 19. However, here is an example where Jacobi converges and Gauss–Seidel does not.

Example 2.26. Consider the matrix

$$A = \begin{bmatrix} -1 & 0 & -1 \\ -1 & 1 & 0 \\ 1 & 2 & -3 \end{bmatrix}.$$

The Jacobi iteration matrix is

$$G_{\text{J}} = -D^{-1}(L+U) = \begin{bmatrix} 0 & 0 & -1 \\ 1 & 0 & 0 \\ \frac{1}{3} & \frac{2}{3} & 0 \end{bmatrix},$$

whose eigenvalues are approximately $0.373 \pm i0.867$ and -0.747. Thus $\rho_{G_{\text{J}}} \approx 0.944 < 1$ and

the iteration converges. On the other hand, the iteration matrix of Gauss–Seidel is

$$G_{\mathrm{GS}} = -(D+L)^{-1}U = \begin{bmatrix} 0 & 0 & -1 \\ 0 & 0 & -1 \\ 0 & 0 & -1 \end{bmatrix},$$

which has the eigenvalues 0, 0, -1 with $\rho_{G_{\mathrm{GS}}} = 1$. The iteration therefore does not converge in general. ∎

In the next example, we show a case where the Gauss–Seidel method converges, while the Jacobi method can diverge.

Example 2.27. Consider the matrix

$$A = \begin{bmatrix} 1 & t & t \\ t & 1 & t \\ t & t & 1 \end{bmatrix},$$

where t is a positive arbitrary parameter in $(0, 1)$. The Gauss–Seidel and Jacobi iteration matrices are

$$G_{\mathrm{GS}} = \begin{bmatrix} 0 & -t & -t \\ 0 & t^2 & t^2 - t \\ 0 & t^2 - t^3 & 2t^2 - t^3 \end{bmatrix} \quad \text{and} \quad G_{\mathrm{J}} = \begin{bmatrix} 0 & -t & -t \\ -t & 0 & -t \\ -t & -t & 0 \end{bmatrix}.$$

The eigenvalues of these matrices are in absolute value given by

$$|\lambda(G_{\mathrm{GS}})| = \left\{ \frac{|t^3 + \sqrt{t^2 - 4t}(t^2 - t) - 3t^2|}{2}, \frac{|t^3 - \sqrt{t^2 - 4t}(t^2 - t) - 3t^2|}{2}, 0 \right\}$$

and

$$|\lambda(G_{\mathrm{J}})| = \{2|t|, |t|, |t|\}.$$

If we plot $\rho_{G_{\mathrm{GS}}}$ as a function of t, we obtain Figure 2.6, where it is clear that $\rho_{G_{\mathrm{GS}}} < 1$ for any $t \in (0, 1)$. On the other hand, it is obvious that $\rho_{G_{\mathrm{J}}} = 2|t|$. Hence, $\rho_{G_{\mathrm{J}}} > 1$ for all $t > \frac{1}{2}$. ∎

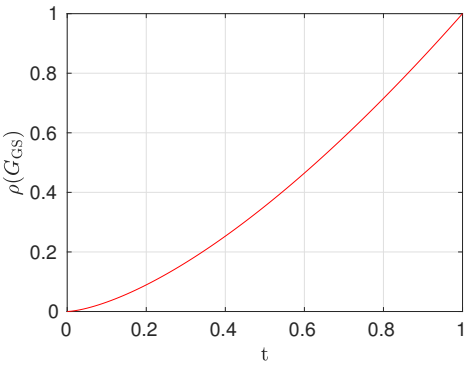

Figure 2.6. $\rho_{G_{\mathrm{GS}}}$ *as function of* t *for* $t \in [0, 1]$.

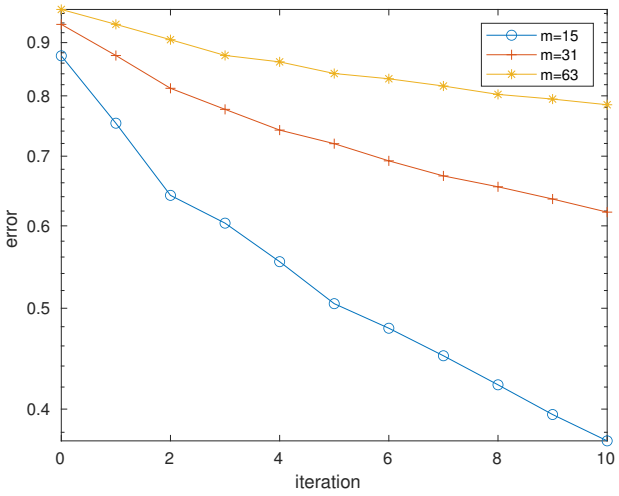

Figure 2.7. *Convergence of the Gauss–Seidel method for different mesh sizes* $h = \frac{1}{m+1}$.

Like Jacobi, Gauss–Seidel also only works on neighboring mesh points when solving discretized PDEs, and one can expect that convergence also deteriorates when the mesh is refined. We show in Figure 2.7 how the error decreases as the iterations progress when Gauss–Seidel is used to solve our Laplace model problem from Section 1.3 for the mesh we used for Figure 2.5 with $m = 15$ interior mesh points, and also on two refined meshes with $m = 31$ and $m = 63$ interior mesh points. We see that like for Jacobi, convergence strongly depends on the mesh parameter h and deteriorates when the mesh is refined. So even though Gauss–Seidel is a bit faster than Jacobi (note the different scale in Figure 2.7 compared to Figure 2.4), Gauss–Seidel has the same problems as Jacobi to solve discretized PDEs: for finer and finer meshes, approximations will take longer and longer to travel across the grid. In particular, similarly as for Jacobi one can prove that

$$\rho_{G_{\mathrm{GS}}}(h) = 1 - \pi^2 h^2 + O(h^4),$$

which clearly shows the deterioration of the convergence factor of Gauss–Seidel for $h \to 0$. To obtain this result, a convergence analysis is required. However, instead of analyzing the convergence of the Gauss–Seidel method, we now show an important generalization, with improved convergence behavior. The convergence analysis of the generalization then also contains Gauss–Seidel as a special case.

2.7 ▪ Successive overrelaxation: SOR

One can use a fixed relaxation factor, and, if this single factor is suitably chosen, a large gain in the rate of convergence is possible.

David Young, Ph.D. Thesis, 1950.

The *successive overrelaxation method* (SOR) is derived from the Gauss–Seidel method by introducing a relaxation parameter ω and was the core subject of the Ph.D. thesis of *David Young* [186], who managed to determine the optimal choice of the parameter for a large class of problems (see the quote above). This was the first attempt to design a rapidly converging stationary iteration, not just to obtain a convergent one, and the ideas of David Young still influence research on stationary iterations and preconditioning today, as we will see in Section 4.6 on domain decomposition methods. In SOR, the component $(\boldsymbol{u}_{k+1})_i$ is computed as for Gauss–Seidel but

then averaged with its value from the previous iteration,

$$(\boldsymbol{u}_{k+1})_i = (1-\omega)(\boldsymbol{u}_k)_i + \frac{\omega}{a_{ii}}\left[\boldsymbol{f}_i - \sum_{j=1}^{i-1} a_{ij}(\boldsymbol{u}_{k+1})_j - \sum_{j=i+1}^{n} a_{ij}(\boldsymbol{u}_k)_j\right]. \tag{2.32}$$

One can clearly see that $\omega = 1$ leads to the Gauss–Seidel method (2.30). In fact, SOR can also be derived by considering the Gauss–Seidel iteration form

$$(D+L)\boldsymbol{u} = -U\boldsymbol{u} + \boldsymbol{f}. \tag{2.33}$$

Multiplying (2.33) by ω and adding on both sides the expression $(1-\omega)D\boldsymbol{u}$, we obtain the SOR iteration

$$(D+\omega L)\boldsymbol{u}_{k+1} = (-\omega U + (1-\omega)D)\boldsymbol{u}_k + \omega\boldsymbol{f}. \tag{2.34}$$

SOR is therefore based on the splitting

$$A = M - N \text{ with } M = \frac{1}{\omega}D + L \text{ and } N = -U + \left(\frac{1}{\omega} - 1\right)D, \tag{2.35}$$

where we divided (2.34) by ω in order to remove the factor ω in front of the right-hand-side term $\boldsymbol{f}$ and obtain the stationary iterative method in standard form (2.2). We can again clearly see that for $\omega = 1$ we get as special case the Gauss–Seidel method.

It is very easy to adapt the Gauss–Seidel MATLAB program from Section 2.6 to perform SOR iterations. Testing the convergence with a suitable choice of the parameter ω that we will see later, we obtain the first iterates shown in Figure 2.8. Comparing with the Gauss–Seidel iterates in Figure 2.5, we see that SOR is substantially faster. How much faster the convergence truly is is illustrated in Figure 2.9, which shows the errors measured: SOR is much faster than Jacobi or Gauss–Seidel. Using an optimized relaxation parameter makes all the difference!

To start our investigation of SOR, we now show that one cannot choose the relaxation parameter arbitrarily if one wants to obtain a convergent method. This general, very elegant result is due to William Kahan from his Ph.D. thesis [115].

Theorem 2.28 (Kahan, 1958). *Let $A \in \mathbb{R}^{n\times n}$ and $A = L + D + U$ with D diagonal and invertible, and L and U strictly lower and upper triangular. If*

$$G_{\mathrm{SOR}} = (D+\omega L)^{-1}(-\omega U + (1-\omega)D) \tag{2.36}$$

is the SOR iteration matrix, then

$$\rho_{G_{\mathrm{SOR}}} \geq |\omega - 1| \ \forall \omega \in \mathbb{R}. \tag{2.37}$$

Proof. The key idea is to insert DD^{-1} between the factors of G_{SOR},

$$\begin{aligned} G_{\mathrm{SOR}} &= (D+\omega L)^{-1}DD^{-1}(-\omega U + (1-\omega)D) \\ &= (I+\omega D^{-1}L)^{-1}(-\omega D^{-1}U + (1-\omega)I). \end{aligned}$$

Now the determinant of $(I+\omega D^{-1}L)$ equals 1, since this matrix is lower triangular with unit diagonal, which implies that the determinant of its inverse also equals 1. Therefore

$$\det(G_{\mathrm{SOR}}) = \det(-\omega D^{-1}U + (1-\omega)I) = (1-\omega)^n,$$

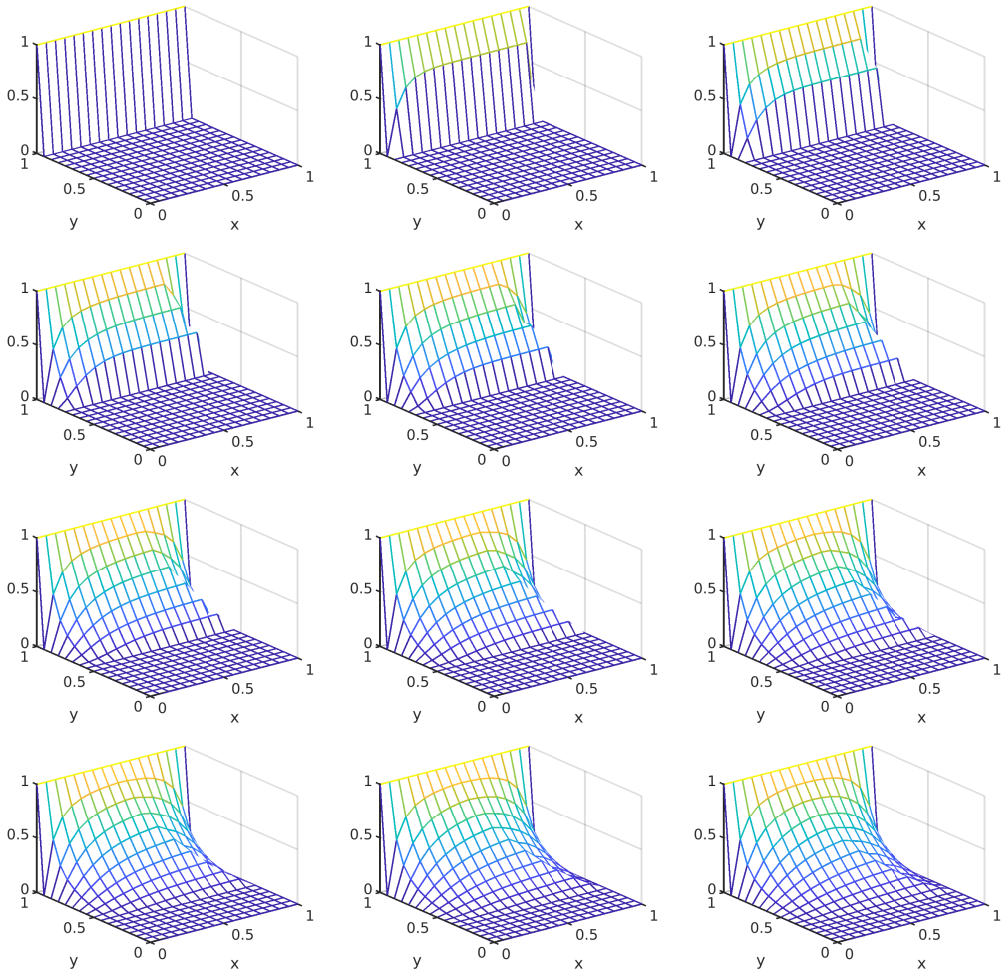

Figure 2.8. *Initial guess and first iterations of the SOR method* (2.34) *applied to our Laplace model problem from Section 1.3.*

since this second factor is upper triangular with $1-\omega$ on the diagonal. The determinant of a matrix is equal to the product of its eigenvalues, which in our case yields

$$\prod_{j=1}^{n} \lambda_j(G_{\mathrm{SOR}}) = (1-\omega)^n \quad \Longrightarrow \quad |1-\omega|^n \leq \left(\max_j |\lambda_j(G_{\mathrm{SOR}})| \right)^n = \rho_{G_{\mathrm{SOR}}}^n,$$

and thus implies the result after taking the nth root. ∎

From this elegant result, we can conclude that

$$\rho_{G_{\mathrm{SOR}}} < 1 \quad \Longrightarrow \quad 0 < \omega < 2,$$

and thus for convergence of SOR it is necessary to choose $0 < \omega < 2$.

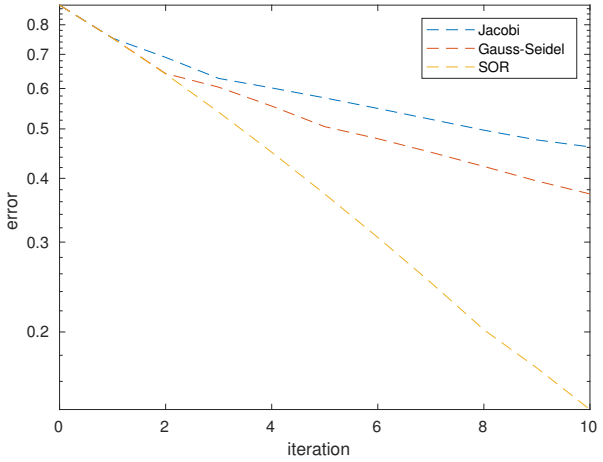

Figure 2.9. *Errors measured for the iterates shown for Jacobi in Figure 2.3, Gauss–Seidel in Figure 2.5, and SOR in Figure 2.8.*

The next result is a general convergence result for SOR, due to Ostrowski and Reich.[12] It is for a restricted class of matrices and does not answer the question yet on how to choose ω in order to obtain a fast method.

Theorem 2.29 (Ostrowski–Reich). *Let $A \in \mathbb{R}^{n\times n}$ be symmetric and invertible. Consider the usual splitting $A = D+L+L^\top$ with D diagonal and positive definite, $D_{jj} > 0$ for $j = 1, \ldots, n$. Then SOR converges for all $0 < \omega < 2$ if and only if A is positive definite.*

Proof. Since A is symmetric, recalling (2.35) the SOR iteration is

$$\underbrace{\left(\frac{1}{\omega}D + L\right)}_{M}\boldsymbol{u}_{k+1} = \underbrace{\left(\frac{1-\omega}{\omega}D - L^\top\right)}_{N}\boldsymbol{u}_k + \boldsymbol{f}.$$

M is invertible, since $D_{jj} > 0$. Consider

$$Q = N + M^\top = \frac{2-\omega}{\omega}D.$$

Q is positive definite because $D_{jj} > 0$ and $0 < \omega < 2$. Now we can apply Theorem 2.21 (Householder–John) to conclude the proof. ∎

Theorem 2.29 implies that Gauss–Seidel and SOR applied to the discrete Laplace problem converge, as we observed already in Figures 2.8 and 2.9.

An important question, which has remained unanswered so far, is how to choose the parameter ω in SOR in order to obtain a fast method. The pioneer in this area was David Young, who answered this question for a large class of matrices in his Ph.D. thesis [186].[13]

[12] Reich established this result for Gauss–Seidel in [156] and Ostrowski for the general SOR case in [140].

[13] An electronic version is available at http://www.ma.utexas.edu/CNA/DMY/.

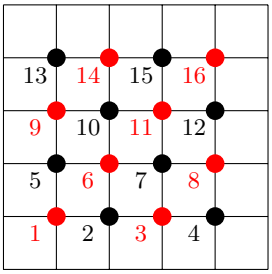

Figure 2.10. *Discretization grid and chessboard used to define the red-black ordering.*

Definition 2.30 (Property A). *A matrix $A \in \mathbb{R}^{n\times n}$ has Property A if there exists a permutation matrix P such that*

$$P^\top AP = \begin{bmatrix} D_1 & F \\ E & D_2 \end{bmatrix} \text{ with } D_1 \text{ and } D_2 \text{ diagonal.} \tag{2.38}$$

Example 2.31. If we discretize the one-dimensional (negative) Laplacian $-\frac{\partial^2}{\partial x^2}$ by finite differences on a regular grid, the discrete operator becomes

$$A = \frac{1}{h^2}\begin{bmatrix} 2 & -1 & & & \\ -1 & 2 & -1 & & \\ & -1 & \ddots & \ddots & \\ & & \ddots & \ddots & -1 \\ & & & -1 & 2 \end{bmatrix} \in \mathbb{R}^{n\times n}.$$

If n is even, then A can be permuted as required for Property A,

$$P^\top AP = \frac{1}{h^2}\left[\begin{array}{cccc|cccc} 2 & & & & -1 & & & \\ & \ddots & & & -1 & \ddots & & \\ & & \ddots & & & \ddots & \ddots & \\ & & & 2 & & & -1 & -1 \\ \hline -1 & -1 & & & 2 & & & \\ & \ddots & \ddots & & & \ddots & & \\ & & \ddots & -1 & & & \ddots & \\ & & & -1 & & & & 2 \end{array}\right],$$

with P constructed by ordering first the odd canonical vectors $\boldsymbol{e}_j$ and then the even ones as follows:

$$P = \begin{bmatrix} \boldsymbol{e}_1 & \boldsymbol{e}_3 & \boldsymbol{e}_5 & \cdots & \boldsymbol{e}_{n-1} & \boldsymbol{e}_2 & \boldsymbol{e}_4 & \boldsymbol{e}_6 & \cdots & \boldsymbol{e}_n \end{bmatrix}.$$

To see Property A for the two-dimensional discrete Laplace it is possible to use the so-called red-black ordering. To do so, we consider a grid of m interior points in each direction to approximate the domain Ω (see Figure 1.10) and then assign a red or black color to each interior node of the grid in a chessboard fashion; see Figure 2.10. The red-black ordering consists in collecting in a vector first the red elements and then the black ones. For example, for the red-black chessboard given in Figure 2.10 we have

$$\boldsymbol{u}_{\mathrm{RB}} = \begin{bmatrix} u_1 & u_3 & u_6 & \cdots & u_{16} & u_2 & u_4 & u_5 & \cdots & u_{15} \end{bmatrix}.$$

To obtain the vector $\boldsymbol{u}_{\mathrm{RB}}$, one can consider the permutation matrix

$$P = \begin{bmatrix} \boldsymbol{e}_1 & \boldsymbol{e}_3 & \boldsymbol{e}_6 & \cdots & \boldsymbol{e}_{16} & \boldsymbol{e}_2 & \boldsymbol{e}_4 & \boldsymbol{e}_5 & \cdots & \boldsymbol{e}_{15} \end{bmatrix}.$$

This matrix allows us to obtain $\boldsymbol{u}_{\mathrm{RB}} = P^\top \boldsymbol{u}$ and a matrix $P^\top AP$ having the same structure as in (2.38). ∎

For matrices with Property A, a useful relation exists between the eigenvalues of the associated Jacobi and SOR iteration matrices. We first need the next lemma.

Lemma 2.32. *Let B be a matrix having a zero diagonal and the block structure*

$$B = \begin{bmatrix} 0 & F \\ E & 0 \end{bmatrix} = L + U,$$

where L and U are the strictly lower and upper triangular parts. If μ is an eigenvalue of B, then so is $-\mu$. Furthermore, B and $\alpha L + \frac{1}{\alpha} U$ are similar and thus have the same eigenvalues for all $\alpha \neq 0$.

Proof. Consider the diagonal matrix

$$S = \begin{bmatrix} I & 0 \\ 0 & \alpha I \end{bmatrix} \quad \Longrightarrow \quad SBS^{-1} = \begin{bmatrix} 0 & \frac{1}{\alpha} F \\ \alpha E & 0 \end{bmatrix} = \alpha L + \frac{1}{\alpha} U.$$

Furthermore, if $\begin{bmatrix} \boldsymbol{u} \\ \boldsymbol{v} \end{bmatrix}$ is an eigenvector of B,

$$B \begin{bmatrix} \boldsymbol{u} \\ \boldsymbol{v} \end{bmatrix} = \mu \begin{bmatrix} \boldsymbol{u} \\ \boldsymbol{v} \end{bmatrix} \;\Rightarrow\; \begin{bmatrix} F\boldsymbol{v} \\ E\boldsymbol{u} \end{bmatrix} = \begin{bmatrix} \mu \boldsymbol{u} \\ \mu \boldsymbol{v} \end{bmatrix},$$

then $\begin{bmatrix} \boldsymbol{u} \\ -\boldsymbol{v} \end{bmatrix}$ is an eigenvector with eigenvalue $-\mu$, because

$$B \begin{bmatrix} \boldsymbol{u} \\ -\boldsymbol{v} \end{bmatrix} = \begin{bmatrix} -F\boldsymbol{v} \\ E\boldsymbol{u} \end{bmatrix} = \begin{bmatrix} -\mu \boldsymbol{u} \\ \mu \boldsymbol{v} \end{bmatrix} = -\mu \begin{bmatrix} \boldsymbol{u} \\ -\boldsymbol{v} \end{bmatrix}. \qquad \square$$

Theorem 2.33 (Relation between eigenvalues of G_{SOR} and G_{J}). *Let $A \in \mathbb{R}^{n \times n}$ have Property A, and let*

$$\widetilde{A} = P^\top AP = \begin{bmatrix} D_1 & F \\ E & D_2 \end{bmatrix} = L + D + U$$

with all diagonal elements of D_1 and D_2 nonzero. Let

$$G_{\mathrm{SOR}} = (D + \omega L)^{-1}(-\omega U + (1 - \omega) D)$$

be the SOR iteration matrix for $\widetilde{A}$ and

$$G_{\mathrm{J}} = -D^{-1}(L + U)$$

the Jacobi iteration matrix. Assume that $\omega \neq 0$ and take a $\lambda \neq 0$. Then we have that λ is an eigenvalue of G_{SOR} if and only if μ, solution of

$$(\lambda + \omega - 1)^2 = \lambda \omega^2 \mu^2,$$

is an eigenvalue of G_{J}.

Proof. As before, we have

$$\begin{aligned} G_{\mathrm{SOR}} &= (D+\omega L)^{-1}DD^{-1}(-\omega U+(1-\omega)D) \\ &= (I+\omega D^{-1}L)^{-1}(-\omega D^{-1}U+(1-\omega)I), \end{aligned}$$

and therefore λ is an eigenvalue if and only if

$$\begin{aligned} &\det((I+\omega D^{-1}L)^{-1}(-\omega D^{-1}U+(1-\omega)I)-\lambda I)=0 \\ \iff &\det(-\omega D^{-1}U+(1-\omega)I-\lambda(I+\omega D^{-1}L))=0 \\ \iff &\det\big((\lambda+\omega-1)I+\omega D^{-1}(\lambda L+U)\big)=0. \end{aligned} \tag{2.39}$$

Now factoring out $\omega\sqrt{\lambda}$ (which is nonzero by assumption) in the determinant, we get

$$(2.39) \iff \det\left(\frac{\lambda+\omega-1}{\omega\sqrt{\lambda}}I+D^{-1}(\sqrt{\lambda}L+\frac{1}{\sqrt{\lambda}}U)\right)=0. \tag{2.40}$$

This equation means that $\frac{\lambda+\omega-1}{\omega\sqrt{\lambda}}$ is an eigenvalue of $-D^{-1}(\sqrt{\lambda}L+\frac{1}{\sqrt{\lambda}}U)$. Using Lemma 2.32, we obtain

$$-D^{-1}\left(\sqrt{\lambda}L+\frac{1}{\sqrt{\lambda}}U\right)=-\left(\sqrt{\lambda}D^{-1}L+\frac{1}{\sqrt{\lambda}}D^{-1}U\right) \text{ is similar to } G_{\mathrm{J}}=-D^{-1}(L+U),$$

therefore they have the same eigenvalues. Since μ and $-\mu$ are eigenvalues of G_{J}, we get

$$\pm\,\mu=\frac{\lambda+\omega-1}{\omega\sqrt{\lambda}} \quad\iff\quad (\lambda+\omega-1)^2=\lambda\omega^2\mu^2. \qquad \square \tag{2.41}$$

We are now ready to prove the most important result for SOR methods: the optimal choice of the relaxation parameter ω, that is, the $\omega\in(0,2)$ that minimizes $\rho_{G_{\mathrm{SOR}}}(\omega)$, given by Young in his thesis [186].

Theorem 2.34 (Optimal choice of ω—David Young, 1950). *Let A, $\widetilde{A}$, and G_{J} be defined as in Theorem 2.33. If the eigenvalues $\mu(G_{\mathrm{J}})$ are real and $\rho_{G_{\mathrm{J}}}<1$, then the optimal SOR parameter ω for $\widetilde{A}$ is*

$$\omega^*=\frac{2}{1+\sqrt{1-\rho_{G_{\mathrm{J}}}^2}}.$$

Proof. Considering the SOR iteration matrix G_{SOR} of $\widetilde{A}$ as in Theorem 2.33, our goal is to solve the problem

$$\min_{\omega\in(0,2)}\rho_{G_{\mathrm{SOR}}}(\omega).$$

From (2.41), we obtain

$$\pm\,\mu\sqrt{\lambda}=\frac{\lambda+\omega-1}{\omega}. \tag{2.42}$$

For μ fixed, the left-hand side of (2.42) is the equation of a parabola, whereas the right-hand side is that of a straight line passing through the point (1,1) with slope $1/\omega$. Figure 2.11 shows the roots of this equation. We see that the roots can be real or complex, depending on ω. If the roots are real, λ_1 is always bigger in modulus than λ_2, and λ_1 is increasing in μ and decreasing in ω. Solving for λ, we obtain the quadratic equation

$$\lambda^2+(2(\omega-1)-\omega^2\mu^2)\lambda+(\omega-1)^2=0 \tag{2.43}$$

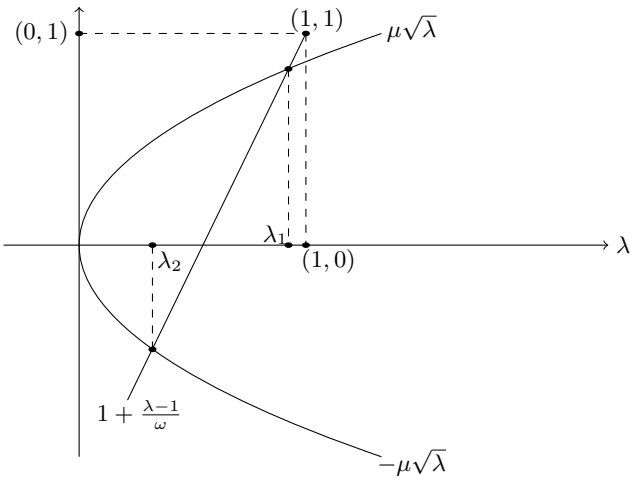

Figure 2.11. *Relation between the roots of Jacobi and SOR. Assuming that $\lambda \in \mathbb{R}$, the straight line $\lambda \mapsto 1 + \frac{\lambda-1}{\omega}$ intersects the parabola $\pm\mu\sqrt{\lambda}$ in two points corresponding to λ_1 and λ_2.*

with the solutions

$$\lambda_{1,2} = \frac{1}{2}\left(\omega^2\mu^2 - 2(\omega-1) \pm \sqrt{\omega^2\mu^2(\omega^2\mu^2 - 4(\omega-1))}\right).$$

With the discriminant $d(\omega,\mu) := \omega^2\mu^2 - 4(\omega-1)$, we have that $d(0,\mu) = 4$ and $d(2,\mu) = -4 + 4\mu^2 < 0$, and d becomes zero if

$$4 - 4\omega + \omega^2\mu^2 = 0 \iff \omega_{1,2} = \frac{2 \pm 2\sqrt{1-\mu^2}}{\mu^2}.$$

Of the two possible values for ω, we have to consider only the smaller one,

$$\omega_1(\mu) = \frac{2 - 2\sqrt{1-\mu^2}}{\mu^2} = \frac{2}{1+\sqrt{1-\mu^2}},$$

since the second value $\omega_2 > 2$ cannot lead to a convergent method; see Theorem 2.28. Thus for $\omega \in (0,\omega_1)$, the eigenvalues are real and λ_1 is the bigger one in a modulus.

For larger values $\omega \in (\omega_1, 2)$, the discriminant is negative and $\lambda_{1,2}$ are complex conjugates (hence $|\lambda_1| = |\lambda_2|$). From (2.43), we see that[14] $\lambda_1\lambda_2 = (\omega-1)^2$, so that in the complex case we have $|\lambda_1| = |\omega-1|$. We thus obtain for each eigenvalue μ of the Jacobi method the corresponding curve shown in Figure 2.12, and since in the real case λ_1 is increasing with μ, we obtain

$$\rho_{G_{\mathrm{SOR}}} = \begin{cases} \frac{1}{2}\left(\omega^2\rho_{G_{\mathrm{J}}}^2 - 2(\omega-1) + \sqrt{\omega^2\rho_{G_{\mathrm{J}}}^2(\omega^2\rho_{G_{\mathrm{J}}}^2 - 4(\omega-1))}\right) \\ \qquad\qquad \text{for } \omega \in (0,\omega_1), \text{ decreasing}, \\ |\omega-1| \qquad \text{for } \omega \in (\omega_1, 2), \text{ linearly increasing}. \end{cases}$$

The minimum of $\rho_{G_{\mathrm{SOR}}}(\omega)$ is thus reached for $\omega^* = \omega_1(\rho_{G_{\mathrm{J}}})$. □

[14] To see this, notice that $\lambda_1+\lambda_2 = \omega^2\mu^2 - 2(\omega-1)$. Hence, from (2.43) we have $\lambda_1^2 + -(\lambda_1+\lambda_2)\lambda_1 + (\omega-1)^2 = 0$, which implies that $\lambda_1\lambda_2 = (\omega-1)^2$.

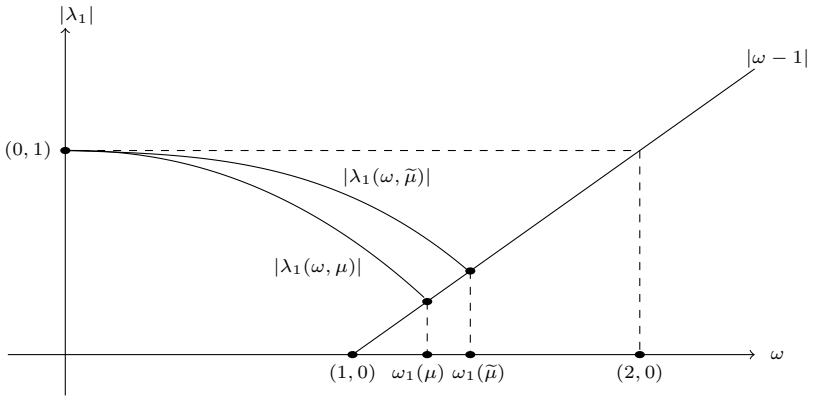

Figure 2.12. *Value of $|\lambda_1|$ as functions of ω. The two curves correspond to different values μ and $\widetilde{\mu}$ such that $\mu < \widetilde{\mu}$.*

For ω^*, the optimized convergence factor of SOR becomes

$$\rho^*_{G_{\mathrm{SOR}}} = \omega^* - 1 = \frac{1 - \sqrt{1 - \rho^2_{G_{\mathrm{J}}}}}{1 + \sqrt{1 - \rho^2_{G_{\mathrm{J}}}}} = \left(\frac{\rho_{G_{\mathrm{J}}}}{1 + \sqrt{1 - \rho^2_{G_{\mathrm{J}}}}} \right)^2 . \tag{2.44}$$

In general, we do not know in advance the spectral radius $\rho_{G_{\mathrm{J}}}$. So we cannot compute ω^* for SOR and have to rely on estimates. The rule of thumb is to try to overestimate ω, because of the steeper slope on the left; see Figure 2.13. To illustrate this, we consider the MATLAB function

```
function r=Rho(omega,mu)
% Rho computes spectral radius for SOR
%   r=Rho(omega,mu) computes the spectral radius of the iteration
%   matrix for SOR, given the spectral radius mu of the Jacobi
%   iteration matrix and the relaxation parameter omega

if omega<2/(1+sqrt(1-mu^2))
  r=((omega*mu)^2-2*(omega-1)+sqrt((omega*mu)^2*...
    ((omega*mu)^2-4*(omega-1))))/2;
else
  r=abs(omega-1);
end
```

and plot it for various values of μ using the commands

```
axis([0,2,0,1])
hold on
xx=[0:0.01:2];
for mu=0.1:0.1:0.9
  yy=[];
  for x=xx
    yy=[yy Rho(x,mu)];
  end
  plot(xx,yy,'b')
end
```

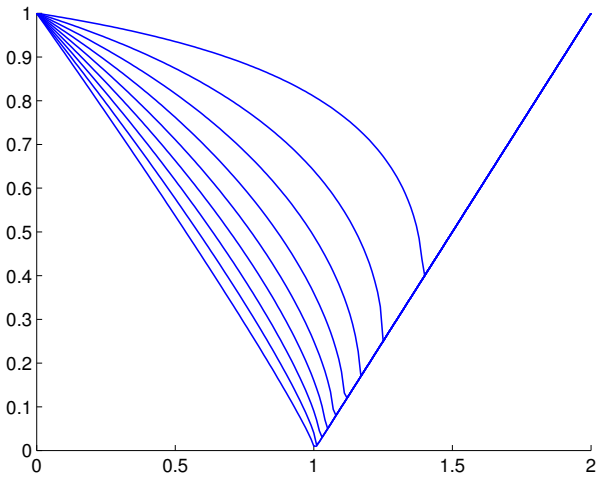

Figure 2.13. $\rho_{G_{\rm SOR}}$ *as function of* ω *for* $\mu = 0.1, 0.2, \ldots, 0.9$. *Notice that* $\rho_{G_{\rm SOR}}$ *increases with* μ.

We can see in Figure 2.13 that for $\mu = 0.9$, the choice of $\omega \approx 1.4$ yields a convergence factor of about 0.4. This is a drastic improvement over Jacobi, leading to about 8 to 9 times fewer iterations, since $\mu^{8.5} \approx 0.4$.

The optimal choice of the relaxation parameter ω also improves the convergence factor asymptotically: one gains a square root, as one can see when setting $\rho_{G_{\rm J}} = 1 - \varepsilon$, and then expanding the corresponding optimized $\rho(G_{SOR})$ for small ε. Using the Maple commands

```
rho:=mu^2/(1+sqrt(1-mu^2))^2;
mu:=1-epsilon;
series(rho,epsilon,1);
```

we obtain $\rho(G_{SOR}) = 1 - 2\sqrt{2\varepsilon} + O(\varepsilon)$, which shows that indeed the improvement is a square root.

Notice that Theorem 2.34 allows us to compute (or estimate) the optimal parameter ω^* that minimizes the spectral radius of the iteration matrix $\widetilde{G}_{\rm SOR}(\omega)$ corresponding to the matrix $\widetilde{A} := P^\top AP$, and not to A. Consider the splittings $\widetilde{A} = \widetilde{D} + \widetilde{L} + \widetilde{U}$ and $A = D + L + U$, where $\widetilde{D}$ and D are diagonal, L and $\widetilde{L}$ strictly lower triangular, and U and $\widetilde{U}$ strictly upper triangular. The Jacobi and SOR iteration matrices corresponding to $\widetilde{A}$ are

$$\widetilde{G}_{\rm J} = -\widetilde{D}^{-1}(\widetilde{L} + \widetilde{U}) \quad \text{and} \quad \widetilde{G}_{\rm SOR}(\omega) = (\widetilde{D} + \omega\widetilde{L})^{-1}(-\omega\widetilde{U} + (1-\omega)\widetilde{D}).$$

On the other hand, the Jacobi and SOR iteration matrices corresponding to A are

$$G_{\rm J} = -D^{-1}(L + U) \quad \text{and} \quad G_{\rm SOR}(\omega) = (D + \omega L)^{-1}(-\omega U + (1-\omega)D).$$

Now notice that the relations $\widetilde{D} = P^\top DP$ and $\widetilde{L} + \widetilde{U} = P^\top(L + U)P$ hold. Hence, one can show that

$$\widetilde{G}_{\rm J} = -\widetilde{D}^{-1}(\widetilde{L} + \widetilde{U}) = -P^\top D^{-1} PP^\top (L + U)P = P^\top G_{\rm J} P,$$

which means that $G_{\rm J}$ and $\widetilde{G}_{\rm J}$ are similar. However, the same similarity does not hold in general for $G_{\rm SOR}(\omega)$ and $\widetilde{G}_{\rm SOR}(\omega)$, as the following example shows.

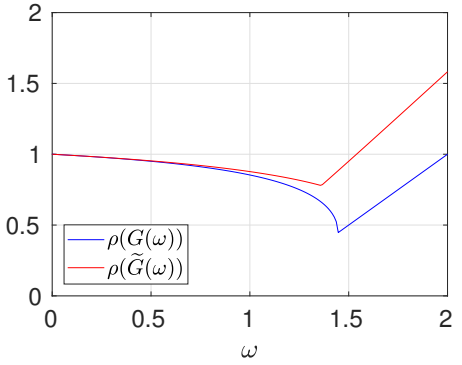

Figure 2.14. *Spectral radii $\rho(G(\omega))$ and $\rho(\widetilde{G}(\omega))$ corresponding to the SOR iteration matrices constructed in Example 2.35.*

Example 2.35. Consider the matrix

$$A = \begin{bmatrix} 1 & 0 & 1 & 1 \\ 0 & 1 & \frac{1}{2} & 1 \\ \frac{1}{2} & 0 & 1 & 0 \\ 0 & \frac{1}{2} & 0 & 1 \end{bmatrix}$$

and the matrix

$$\widetilde{A} := P_{14} A P_{14}^{\top} = \begin{bmatrix} 1 & \frac{1}{2} & 0 & 0 \\ 1 & 1 & \frac{1}{2} & 0 \\ 0 & 0 & 1 & \frac{1}{2} \\ 1 & 0 & 1 & 1 \end{bmatrix}, \text{ where } P_{14} = \begin{bmatrix} 0 & 0 & 0 & 1 \\ 0 & 1 & 0 & 0 \\ 0 & 0 & 1 & 0 \\ 1 & 0 & 0 & 0 \end{bmatrix}.$$

Consider the splittings $A = D + L + U$ and $\widetilde{A} = \widetilde{D} + \widetilde{L} + \widetilde{U}$, where D and $\widetilde{D}$ are diagonal, L and $\widetilde{L}$ are strictly lower triangular, and U and $\widetilde{U}$ are strictly upper triangular. The corresponding SOR iteration matrices are $G_{\mathrm{SOR}}(\omega) = (D+\omega L)^{-1}(-\omega U + (1-\omega)D)$ and $\widetilde{G}_{\mathrm{SOR}}(\omega) = (\widetilde{D} + \omega\widetilde{L})^{-1}(-\omega\widetilde{U}+(1-\omega)\widetilde{D})$. Their spectral radii are shown in Figure 2.14 as functions of $\omega \in [0, 2]$. It is clear that $\rho(G(\omega))$ and $\rho(\widetilde{G}(\omega))$ do not coincide, most notably for $\omega > 1$. Therefore the two matrices $G(\omega)$ and $\widetilde{G}(\omega)$ are not similar. Notice also that $\rho(G(\omega))$ and $\rho(\widetilde{G}(\omega))$ attain their minima at different ω. ∎

Example 2.35 shows that $G_{\mathrm{SOR}}(\omega)$ and $\widetilde{G}_{\mathrm{SOR}}(\omega)$ are not in general similar. Therefore, the optimal parameter ω^* for $\widetilde{G}_{\mathrm{SOR}}(\omega)$ does not necessarily coincide with the optimal parameter for $G_{\mathrm{SOR}}(\omega)$. However, if A is the discrete Laplace operator obtained by a finite-difference discretization, ω^* for $\widetilde{G}_{\mathrm{SOR}}(\omega)$ coincides with the optimal parameter for $G_{\mathrm{SOR}}(\omega)$. To see it, we need to introduce the following property.

Definition 2.36 (Property B). *A matrix $A \in \mathbb{R}^{n\times n}$ is said to have Property B (or the "Banholzer Property")*[15] *if*

$$\det\left(\alpha D + \beta L + \beta^{-1} U\right) = \det\left(\alpha D + L + U\right)$$

for the usual splitting $A = D + L + U$ and all $\alpha, \beta \in \mathbb{R} \setminus \{0\}$.

[15] This property has already been discussed in the literature; see, e.g., [94, 111, 185]. However, the term "Property B" was invented by Stefan Banholzer, assistant for the course in Konstanz. His idea was to mimic the very neutral name "Property A" introduced by David Young. Poor Stefan didn't realize that the "B" could stand for "Banholzer"! Hence, we also called it the "Banholzer Property" and wish him all the best!

The next theorem shows that Property A and Property B are related; see [94, Theorem 10.1.5] and [111, Lemma 10.6].

Theorem 2.37 (Property A and Property B). *If a matrix A has Property A, then there exists a permutation matrix P such that $P^\top AP$ has Property B.*

Proof. The proof can be found in [111, Lemma 10.6]. □

Theorem 2.38 (Eigenvalues of G_{SOR} and G_{J}). *Assume that the matrix $A \in \mathbb{R}^{n\times n}$ has Property B with all diagonal elements of D being nonzero and let G_{J} and $G_{\mathrm{SOR}}(\omega)$ be the iteration matrices of Jacobi and SOR for the matrix A. Assume that $\omega \neq 0$ holds and take a $\lambda \neq 0$. Then λ is an eigenvalue of $G_{\mathrm{SOR}}(\omega)$ if and only if the solution μ of*

$$(\lambda + \omega - 1)^2 = \lambda\omega^2\mu^2 \tag{2.45}$$

is an eigenvalue of G_{J}.

Proof. Following exactly the lines of the proof of Theorem 2.33 one gets that λ is an eigenvalue of $G_{\mathrm{SOR}}(\omega)$ if and only if (compare (2.40))

$$\det\left(\frac{\lambda+\omega-1}{\omega\sqrt{\lambda}}I + D^{-1}\left(\sqrt{\lambda}L + \frac{1}{\sqrt{\lambda}}U\right)\right) = 0. \tag{2.46}$$

Since the diagonal matrix D is invertible by assumption, we have $\det(D) \neq 0$, and hence (2.46) is equivalent to

$$\det\left(\frac{\lambda+\omega-1}{\omega\sqrt{\lambda}}D + \sqrt{\lambda}L + \frac{1}{\sqrt{\lambda}}U\right) = 0. \tag{2.47}$$

Using Property B yields

$$(2.47) \iff \det\left(\frac{\lambda+\omega-1}{\omega\sqrt{\lambda}}D + L + U\right) = 0. \tag{2.48}$$

Finally, since $\det(D^{-1}) \neq 0$ we can conclude that

$$(2.48) \iff \det\left(\frac{\lambda+\omega-1}{\omega\sqrt{\lambda}}I - G_{\mathrm{J}}\right) = 0, \tag{2.49}$$

which is equivalent to $\mu = \frac{\lambda+\omega-1}{\omega\sqrt{\lambda}}$ being an eigenvalue of the matrix G_{J}. □

With this result we can reformulate Theorem 13 to show the optimal choice of the parameter ω for the SOR iteration matrix of the matrix A.

Theorem 2.39 (Optimal choice of ω for matrices having Property B). *Assume that the matrix $A \in \mathbb{R}^{n\times n}$ has Property B with all diagonal elements of D being nonzero and let G_{J} and $G_{\mathrm{SOR}}(\omega)$ be the iteration matrices of Jacobi and SOR for the matrix A. If all eigenvalues $\mu(G_{\mathrm{J}})$ are real and $\rho_{G_{\mathrm{J}}} < 1$, then the optimal SOR parameter ω for $G_{\mathrm{SOR}}(\omega)$ is*

$$\omega^* = \frac{2}{1 + \sqrt{1 - \rho_{G_{\mathrm{J}}}^2}}.$$

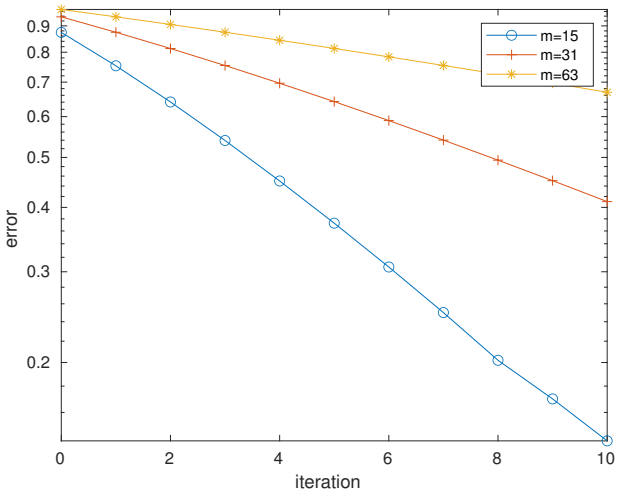

Figure 2.15. *Convergence of the SOR method for different mesh sizes* $h = \frac{1}{m+1}$.

Proof. The proof is exactly the same as the one of Theorem 2.34, since we only use formula (2.45), which relates the eigenvalues of G_{J} with the eigenvalues of $G_{\mathrm{SOR}}(\omega)$. □

Theorems 2.34 and 2.39 imply that if a matrix A has both Property A and Property B, then the optimal parameters for the SOR iterations matrices corresponding to A and $\widetilde{A}$ coincide. This is exactly the case of the discrete Laplace operator.

Theorem 2.40 (Property B of the discrete Laplace operator). *Let A be the discrete (negative) Laplace operator in any dimension $d \in \mathbb{N}^+$ obtained by the second-order finite-difference scheme. Then A has Property B.*

Proof. A proof is given in [185, Lemma 1]. □

So can the optimized parameter in SOR remove the dependence on the mesh size of the convergence when solving discretized PDEs? We show in Figure 2.15 how the error decreases as the iterations progress when SOR is used to solve our Laplace model problem from Section 1.3 for the mesh we used for Figure 2.8 with $m = 15$ interior mesh points, and also on two refined meshes with $m = 31$ and $m = 63$ interior mesh points. We see that like for Jacobi and Gauss–Seidel, although SOR is substantially faster, convergence still depends on the mesh parameter h, also when the optimized overrelaxation parameter is used. Like Jacobi and Gauss–Seidel, for finer and finer meshes, approximations will take longer and longer to travel across the grid. This can be seen very clearly if one replaces the expression (2.27), that is, $\rho_{G_{\mathrm{J}}}(h) = \cos(\pi h)$, into formula (2.44) and computes the Taylor expansion:

$$\rho_{G_{\mathrm{SOR}}}(h) = \frac{1 - \sqrt{1 - \rho_{G_{\mathrm{J}}}(h)^2}}{1 + \sqrt{1 - \rho_{G_{\mathrm{J}}}(h)^2}} = \frac{1 - \sin(\pi h)}{1 + \sin(\pi h)} = 1 - 2\pi h + O(h^2).$$

This expansion shows that, on the one hand, the convergence of SOR deteriorates for $h \to 0$, but on the other hand the deterioration is slower compared to Jacobi and Gauss–Seidel. Therefore, the optimization of the parameter ω leads to a substantial improvement: not only is SOR faster, but its convergence factor deteriorates significantly more slowly than the ones of Jacobi and Gauss–Seidel.

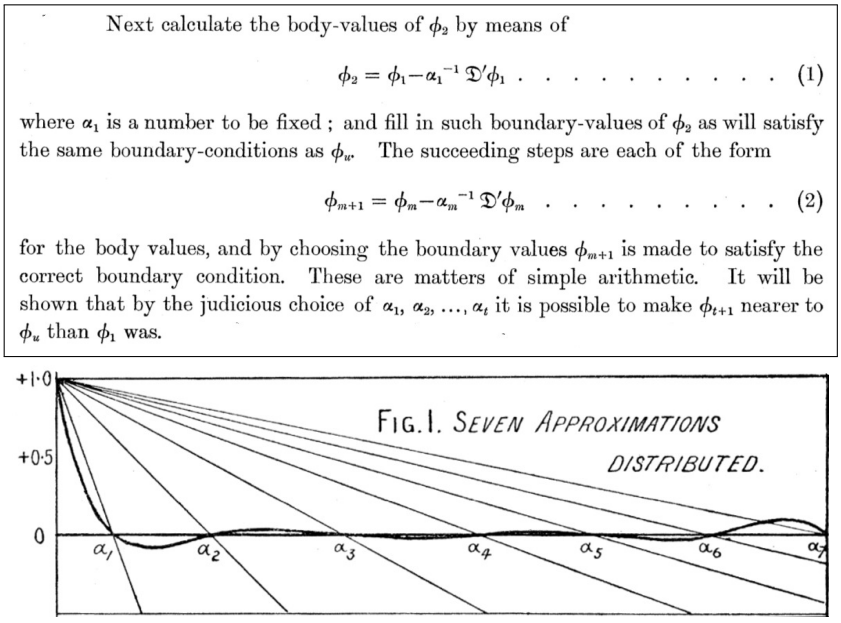

Next calculate the body-values of ϕ_2 by means of

$$\phi_2 = \phi_1 - \alpha_1^{-1}\mathfrak{D}'\phi_1 \quad . \quad . \quad . \quad . \quad . \quad . \quad . \quad . \quad . \quad . \quad (1)$$

where α_1 is a number to be fixed ; and fill in such boundary-values of ϕ_2 as will satisfy the same boundary-conditions as ϕ_u. The succeeding steps are each of the form

$$\phi_{m+1} = \phi_m - \alpha_m^{-1}\mathfrak{D}'\phi_m \quad . \quad . \quad . \quad . \quad . \quad . \quad . \quad . \quad . \quad (2)$$

for the body values, and by choosing the boundary values ϕ_{m+1} is made to satisfy the correct boundary condition. These are matters of simple arithmetic. It will be shown that by the judicious choice of $\alpha_1, \alpha_2, \ldots, \alpha_t$ it is possible to make ϕ_{t+1} nearer to ϕ_u than ϕ_1 was.

Figure 2.16. *The true Richardson iterative method with a relaxation parameter which depends on the iteration, $\alpha = \alpha_k$, and a manually optimized choice by Richardson himself trying to minimize the* residual polynomial *without using Chebyshev theory. Republished with permission of the Royal Society of London, from [157]; permission conveyed through Copyright Clearance Center, Inc.*

2.8 ▪ Richardson

> *It follows that by judiciously spacing the α's along the horizontal axis and by taking a sufficient number of such points (that is of approximations) the successive maxima and minima can be made all less, in absolute value, than any finite quantity ϵ however small.*
>
> Lewis F. Richardson, *The Approximate Arithmetical Solution by Finite Differences of Physical Problems Involving Differential Equations, with an Application to the Stresses in a Masonry Dam*, 1911

In order to explain the Richardson iteration, we consider the correction form (2.3) of the stationary iterative method,

$$\boldsymbol{u}_{k+1} = \boldsymbol{u}_k + M^{-1}\boldsymbol{r}_k.$$

If we choose $M^{-1} = \alpha I$, which corresponds to the splitting $M = \frac{1}{\alpha}I$ and $N = \frac{1}{\alpha}I - A$, we obtain what is often called the *Method of Richardson*,

$$\boldsymbol{u}_{k+1} = \boldsymbol{u}_k + \alpha(\boldsymbol{f} - A\boldsymbol{u}_k) = (I - \alpha A)\boldsymbol{u}_k + \alpha\boldsymbol{f}. \tag{2.50}$$

Lewis Fry Richardson, however, considered a much more interesting method, namely

$$\boldsymbol{u}_{k+1} = \boldsymbol{u}_k + \alpha_k(\boldsymbol{f} - A\boldsymbol{u}_k), \tag{2.51}$$

as one can see from the quote above and in Figure 2.16 from his original publication [157].[16] This is, however, a nonstationary method, and we will get back to such methods in Chapter 3. For the

[16] This is a masterpiece of a scientific publication in the field of numerical analysis: it contains discretization techniques for PDEs, the invention of Richardson extrapolation to decrease the truncation error, a groundbreaking new iterative method with a polynomial approximation optimized in the sense of Chebyshev without knowing Chebyshev theory, and the application of all these inventions to simulate a masonry dam!

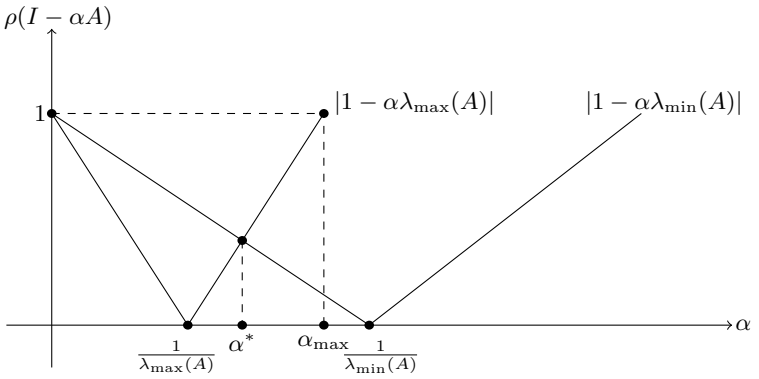

Figure 2.17. *Determining an optimal α for the Richardson iteration.*

simple, stationary form of Richardson's method in (2.50), we have the following convergence theorem.

Theorem 2.41 (Convergence of Richardson's method). *Let $A \in \mathbb{R}^{n\times n}$ be symmetric and positive definite. Then*

(a) *Richardson converges if and only if $0 < \alpha < \frac{2}{\rho(A)}$.*

(b) *The convergence is optimal for $\alpha^* = \frac{2}{\lambda_{\max}(A)+\lambda_{\min}(A)}$.*

(c) *The convergence factor is $\rho(I-\alpha^* A) = \frac{\kappa(A)-1}{\kappa(A)+1}$ with $\kappa(A) := \frac{\lambda_{\max}(A)}{\lambda_{\min}(A)}$.*

Proof. Since A is positive definite, we have

$$0 < \lambda_{\min}(A) \le \lambda_j(A) \le \lambda_{\max}(A) = \rho(A)$$

for $j = 1, \ldots, n$. The iteration matrix $M^{-1}N = I - \alpha A$ has the eigenvalues $1 - \alpha\lambda_j(A)$, hence

$$\rho(I-\alpha A) < 1 \quad \iff \quad 1-\alpha\lambda_{\min}(A) < 1 \text{ and } 1-\alpha\lambda_{\max}(A) > -1.$$

Thus we have convergence for

$$0 < \alpha < \frac{2}{\lambda_{\max}(A)}.$$

To minimize $\rho(I-\alpha A)$, we consider Figure 2.17, which shows the curves $|1-\alpha\lambda_{\max}|$ and $|1-\alpha\lambda_{\min}|$. We see that the optimal α is determined by the intersection point between the two lines, since the curves $|1-\alpha\lambda_j(A)|$ for other j lie in between these two lines. This means

$$\alpha\lambda_{\max}(A) - 1 = 1 - \alpha\lambda_{\min}(A) \quad \implies \quad \alpha^* = \frac{2}{\lambda_{\max}(A)+\lambda_{\min}(A)}.$$

For the optimal α, we get

$$\rho_{\text{opt}} = \rho(I-\alpha^* A) = \frac{\lambda_{\max}(A)-\lambda_{\min}(A)}{\lambda_{\max}(A)+\lambda_{\min}(A)} = \frac{\kappa(A)-1}{\kappa(A)+1} \tag{2.52}$$

with $\kappa(A) = \frac{\lambda_{\max}(A)}{\lambda_{\min}(A)}$. □

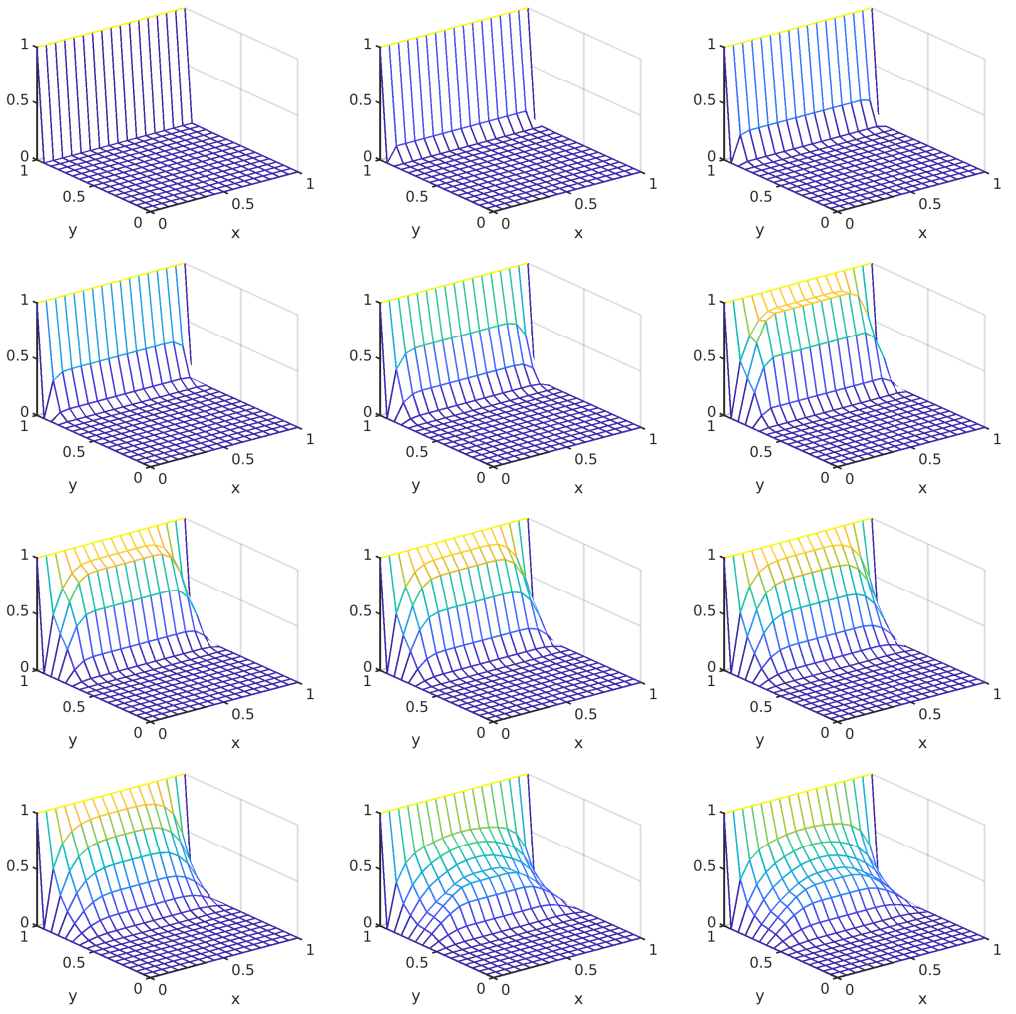

Figure 2.18. *Initial guess and first iterations of the true Richardson method* (2.51) *with optimized* α_k *for five precomputed choices applied to our Laplace model problem from Section 1.3*

For our Laplace model problem, the simplified Richardson iteration with the optimized relaxation parameter is equivalent to Jacobi's method, since the diagonal is simply a constant in this case; see Problem 22. We show in Figure 2.18 the first iterations of the true Richardson method using five different relaxation parameters α_k determined as the roots of appropriate Chebyshev polynomials; see Problem 23. We see a very interesting convergence behavior: depending on which range of frequencies the parameter α_k addresses, the approximation converges with different components in the solution. In Figure 2.19 we show the errors measured for simplified Richardson with one optimized parameter α, compared to the true method of Richardson with variable α_k optimized for 5 or 10 precomputed values. We see that the true Richardson method is much faster, and convergence looks superlinear in intervals corresponding to the length of the number of optimized α_k values. The Krylov methods in the next chapter will also achieve this, and surprisingly in an automated fashion, so no tuning of parameters will be needed!

So can an optimized sequence of parameters in the true Richardson method remove the dependence on the mesh size of the convergence when solving discretized PDEs? We show in

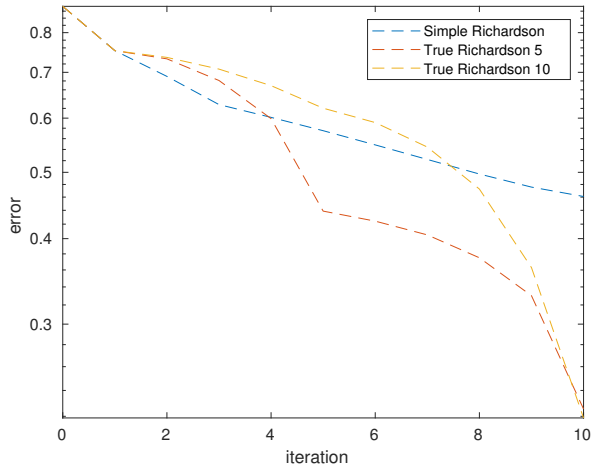

Figure 2.19. *Errors measured for the simplified Richardson iteration with one optimized parameter compared to the true Richardson method* (2.51) *with optimized* α_k *for 5 and 10 precomputed choices applied to our Laplace model problem from Section 1.3.*

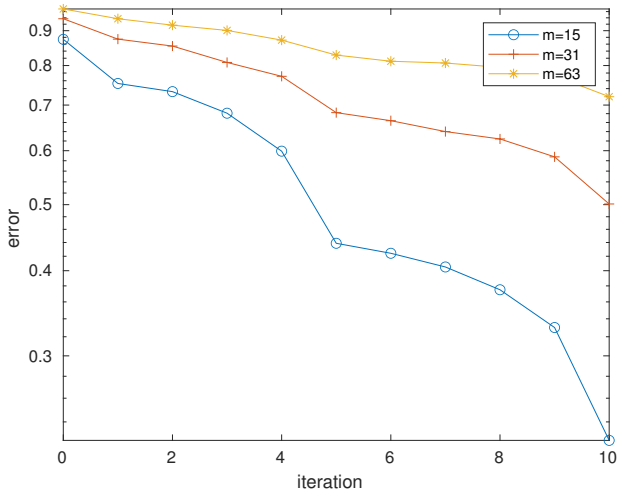

Figure 2.20. *Convergence of the true Richardson method for different mesh sizes* $h = \frac{1}{m+1}$.

Figure 2.20 how the error decreases as the iterations progress when Richardson is used to solve our Laplace model problem from Section 1.3 for $m = 15$, 31, and 63 interior mesh points, and we see that convergence still depends on the mesh parameter h. Like for the other stationary iterative methods, for finer and finer meshes, approximations will take longer and longer to travel across the grid.

2.9 ▪ Problems

Problem 5. *For* $\boldsymbol{x} \in \mathbb{C}^m$ *and* $1 \leq p < \infty$, *the p-norms and the* ∞*-norm are defined by*

$$\|\boldsymbol{x}\|_p = \left(\sum_{i=1}^{m} |x_i|^p \right)^{\frac{1}{p}}, \quad \|\boldsymbol{x}\|_\infty = \max_{1 \leq i \leq m} \{|x_i|\}.$$

For a matrix $A \in \mathbb{C}^{n\times m}$, the corresponding induced matrix norms are

$$\|A\|_{pq} = \sup_{\boldsymbol{x}\neq 0} \frac{\|A\boldsymbol{x}\|_p}{\|\boldsymbol{x}\|_q} \quad \textit{for } 1 \le p, q \le \infty.$$

In the particular case $p = q$, we consider the notation $\|\cdot\|_{pp} = \|\cdot\|_p$. A further common matrix norm is the Frobenius norm,

$$\|A\|_F^2 = \sum_{i=1}^{n}\sum_{j=1}^{m} |a_{ij}|^2.$$

Prove the following four equalities, where $\rho(A) := \max\{|\lambda_i|\}$ is the spectral radius and λ_i are the eigenvalues of A.

$$\|A\|_1 = \max_{1\le j\le m}\sum_{i=1}^{n}|a_{ij}|, \quad \|A\|_\infty = \max_{1\le i\le n}\sum_{j=1}^{m}|a_{ij}|,$$
$$\|A\|_2 = (\rho(A^*A))^{\frac{1}{2}}, \qquad \|A\|_F = (\mathrm{trace}(A^*A))^{\frac{1}{2}} = (\mathrm{trace}(AA^*))^{\frac{1}{2}}.$$

Problem 6. *Prove that the Frobenius norm satisfies the submultiplicative property*

$$\|AB\|_F \le \|A\|_F \|B\|_F.$$

Is the Frobenius norm an induced norm? Why?

Problem 7. *Let $A \in \mathbb{C}^{n\times n}$. Then for any given $\varepsilon > 0$, there exists a (vector) norm for $\mathbb{C}^n$ such that the induced matrix norm $\|\cdot\|$, which depends on A and ε, satisfies*

$$\rho(A) \le \|A\| \le \rho(A) + \varepsilon.$$

Problem 8. *For any matrix $G \in \mathbb{R}^{n\times n}$ with spectral radius $\rho(G)$ and any induced matrix norm, we have*

$$\lim_{k\to\infty} \|G^k\|^{\frac{1}{k}} = \rho(G).$$

Problem 9. *Prove that for a given positive integer p,*

$$\lim_{k\to\infty} \binom{k}{p}^{\frac{1}{k}} = 1,$$

and for $0 < \rho < 1$,

$$\lim_{k\to\infty} \binom{k}{p}\rho^k = 0.$$

Problem 10. *Let $B \in \mathbb{C}^{n\times n}$ be a square matrix with a spectral radius $\rho(B) < 1$. Prove that $I - B$ is invertible and that*

$$(I - B)^{-1} = \sum_{j=0}^{\infty} B^j.$$

This series is a particular case of the Neumann series.

Problem 11. *Show that the matrix A representing the discrete negative Laplacian obtained by the standard second-order finite-difference discretization in dimensions 1 and 2 is an M-matrix. Hint in one dimension: Consider a (regular) splitting $A = M - N$, show that $\rho(M^{-1}N) < 1$, and use Theorem 2.16. Notice that for a tridiagonal matrix $A \in \mathbb{R}^{n\times n}$ with Toeplitz structure*

$$A = \begin{bmatrix} a & c & & & \\ b & a & c & & \\ & b & a & c & \\ & & \ddots & \ddots & \ddots \end{bmatrix},$$

the eigenvalues are given by $\lambda_k(A) = a + 2\sqrt{bc}\cos\left(\frac{k\pi}{n+1}\right)$ for $k = 1, \ldots, n$.
Hint in two dimensions:

- *Let A_x and A_y be the discrete matrices corresponding to $-\frac{d^2}{dx^2}$ and $-\frac{d^2}{dy^2}$. Then the matrix A can be obtained as $A = A_x \otimes I_y + I_x \otimes A_y$, where $\otimes$ denotes the Kronecker product and I_x and I_y are the identity matrices in directions x and y.*

- *Let $(\lambda_x, \boldsymbol{v}_x)$ and $(\lambda_y, \boldsymbol{v}_y)$ be the eigenpairs of A_x and A_y. Prove that the eigenvalues of A are given by $\lambda = \lambda_x + \lambda_y$. To show this property, consider the vector $\boldsymbol{w} := \boldsymbol{v}_x \otimes \boldsymbol{v}_y$ and the product $A\boldsymbol{w} = \big(A_x \otimes I_y + I_x \otimes A_y\big)\big(\boldsymbol{v}_x \otimes \boldsymbol{v}_y\big)$ using the formula $(A \otimes B)(C \otimes D) = (AC) \otimes (BD)$.*

- *Consider a splitting $A = M - N$, show that $\rho(M^{-1}N) < 1$, and use Theorem 2.16.*

Problem 12. *Write the iterative methods Jacobi, Gauss–Seidel, and SOR in their standard, correction, residual, and differences forms.*

Problem 13. *Write a MATLAB script for the solution of the Laplace equation*

$$\begin{aligned} -\Delta u &= f \ \text{ in } \Omega = (0,1) \times (0,1), \\ u &= g \ \text{ on } \partial\Omega, \end{aligned}$$

by using the methods of Jacobi, Gauss–Seidel, and SOR. The three iterative solvers have to be implemented in three independent functions, so they can be reused for arbitrary linear systems of equations.

Problem 14. *Use Theorem 2.24 to prove that Jacobi applied to the discrete Laplace problem converges.*

Problem 15. *Find an example of a matrix A such that Gauss–Seidel does not converge.*

Problem 16. *Consider the iteration matrix $G = \begin{bmatrix} \frac{5}{2} & -1 \\ 1 & 0 \end{bmatrix}$. Consider the initial vector $\boldsymbol{v}_0 = \begin{bmatrix} 1 \\ 2 \end{bmatrix}$, and compute the iterations $\boldsymbol{v}_1 = G\boldsymbol{v}_0$, $\boldsymbol{v}_2 = G\boldsymbol{v}_1$ and their norms. What do you observe? Repeat the experiment for the initial vector $\boldsymbol{w}_0 = \begin{bmatrix} 2 \\ 1 \end{bmatrix}$. Do you observe the same behavior? Why?*
Hint: Compute eigenvalues and eigenvectors of G and recall Theorem 3.

Problem 17. *Let A be the standard discrete five-point (negative) Laplace matrix in dimension 2,*

$$A = \begin{bmatrix} T & -I & & \\ -I & T & \ddots & \\ & \ddots & \ddots & -I \\ & & -I & T \end{bmatrix} \quad \textit{with} \quad T = \begin{bmatrix} 4 & -1 & & \\ -1 & 4 & \ddots & \\ & \ddots & \ddots & -1 \\ & & -1 & 4 \end{bmatrix}.$$

Consider the block-Jacobi splitting $A = D + L + L^\top = M - N$ with

$$M = D = \begin{bmatrix} T & & & \\ & T & & \\ & & \ddots & \\ & & & T \end{bmatrix} \quad \textit{and} \quad N = -\big(L + L^\top\big) = \begin{bmatrix} 0 & I & & \\ I & 0 & \ddots & \\ & \ddots & \ddots & I \\ & & I & 0 \end{bmatrix}.$$

Using Theorem 2.25, prove that the block-Jacobi method converges.
Hint: Prove that T, A, and $2D - A$ are positive definite.

Problem 18. *Compute the optimal parameter of the SOR method for the discrete negative Laplacian in dimension 2. Do the same for the Richardson method.*

Problem 19. *Consider a matrix A having Property A. Prove that Gauss–Seidel converges twice as fast as Jacobi in this case.*
Hint: Use Theorem 2.33 and the formula $(\lambda + \omega - 1)^2 = \lambda\omega^2\mu^2$, where λ is an eigenvalue of the SOR iteration matrix, μ is an eigenvalue of the Jacobi iteration matrix, and ω is the relaxation parameter SOR.

Problem 20. *Recall that the SOR iteration matrix is*

$$G_{\mathrm{SOR}} = \big(D + \omega L\big)^{-1}\Big(-\omega U + (1-\omega)D\Big).$$

If $\lambda = 0$ is an eigenvalue of G_{SOR}, what is the value of ω?

Problem 21. *Write a function in MATLAB that solves a linear system $A\boldsymbol{u} = \boldsymbol{f}$ by means of the SOR method. Test this function solving the problem*

$$\begin{aligned} -\Delta u &= 1 \ \textit{ in } \Omega = (0,1) \times (0,1), \\ u &= 0 \ \textit{ on } \partial\Omega. \end{aligned}$$

Moreover, using also the methods of Jacobi and Gauss–Seidel (see Problem 13) plot the convergence curves (residuals or errors) corresponding to these methods.

Problem 22. *Consider A the discrete matrix of $-\Delta$ in dimension 2. Show that Jacobi and Richardson (with the optimal parameter α_{opt} computed in Problem 18) have the same convergence behavior.*

Problem 23. *Implement the true Richardson method with a variable relaxation parameter α_k and a general symmetric and positive definite matrix. Experiment with different choices of α_k. Can you determine, for a fixed number of different relaxation parameters, an optimized choice of their values using Chebyshev polynomials, in the same spirit Richardson did this by hand for seven parameters in Figure 2.16?*

Problem 24. *Consider the one-dimensional (negative) Laplacian matrix $A \in \mathbb{R}^{n\times n}$ given, e.g., in Example 2.19. Using the Sherman–Morrison formula, prove that*

$$A^{-1} = L^\top \Big(I - \frac{1}{n+1} (\boldsymbol{v}\boldsymbol{v}^\top) \Big) L,$$

where $\boldsymbol{v}^\top = \begin{bmatrix} 1 & \cdots & 1 \end{bmatrix}$ *and*

$$L = \begin{bmatrix} 1 & & & \\ 1 & 1 & & \\ \vdots & & \ddots & \\ 1 & & \cdots & 1 \end{bmatrix}.$$

Problem 25. *Write two functions in MATLAB that solve a linear system $A\boldsymbol{u} = \boldsymbol{f}$ by means of Jacobi and Gauss–Seidel/SOR (see Problem 13). Test these functions solving the advection-reaction-diffusion problem*

$$\begin{aligned} -\nu \Delta u + \boldsymbol{b}^\top \nabla u + cu &= f \qquad \text{in } \Omega, \\ u &= 0 \qquad \text{on } \partial\Omega, \end{aligned} \tag{2.53}$$

where Ω is the unit square, $f = 1$, $c = 1$, $\nu = 0.1$, and $\boldsymbol{b} = [\,1\,,\,1\,]^\top$. Use a random initial guess and plot the first iterations of the two methods and the corresponding convergence curves (residuals or errors). Comment on the results that you obtain.

Problem 26. *Modify the codes obtained for Problem 25 to obtain the results of Figures 2.3, 2.5, and 2.8 for the advection-reaction-diffusion problem*

$$\begin{aligned} -\nu \Delta u + \boldsymbol{b}^\top \nabla u + cu &= 0 \qquad \text{in } \Omega, \\ u &= g \qquad \text{on } \partial\Omega \end{aligned}$$

for $c = 1$, $\nu = 0.1$, and $\boldsymbol{b} = [\,1\,,\,1\,]^\top$ and the boundary function g defined as in (1.5) *and Figure 1.10.*

Problem 27. *Consider the matrix A representing the discrete advection-reaction-diffusion operator $-\nu\Delta + \boldsymbol{b}^\top \nabla + cI$ defined on a domain Ω in dimensions 1 (Ω is an interval) and 2 (Ω is a rectangle) and obtained by the standard second-order finite-difference discretization for the Laplace operator and by the centered finite-difference formula for the gradient operator. Assume that $\boldsymbol{b} = 1$ in dimension 1 and $\boldsymbol{b} = [\,1\,,\,1\,]^\top$ in dimension 2. For which values of $\nu > 0$ and $c \geq 0$ is the matrix A an M-matrix?*
Hint in one dimension: Since the matrix A is tridiagonal, one can consider the same hint given for Problem 11.
Hint in two dimensions: In addition to the hints given for Problem 11, consider that if D_x and D_y denote the discrete matrices corresponding to $\frac{d}{dx}$ and $\frac{d}{dy}$, then the matrix corresponding to $\boldsymbol{b}^\top \nabla$ can be obtained as $D_x \otimes I_y + I_x \otimes D_y$, where $\otimes$ denotes the Kronecker product and I_x and I_y are identity matrices in x and y.

Problem 28. *Consider the advection-reaction-diffusion problem* (2.53) *and the Jacobi method. Compute (analytically) the spectral radius of Jacobi (see also Problem 27) and its Taylor expansion with respect to the mesh size h (similar to, e.g.,* (2.28)*). Verify numerically your results and give a short comment about them.*

Problem 29. *Consider the advection-reaction-diffusion problem* (2.53) *(recall Problems 25 and 28) and the SOR method. Is it possible to use the results of Theorem 2.34? If yes, compute the optimal SOR parameter and test your results by direct numerical experiments.*

Problem 30. *Consider the matrix A representing the discrete advection-reaction-diffusion operator $-\nu\Delta + \boldsymbol{b}^\top \nabla + cI$ as in Problem 27. Is it possible to use in this case the result proved in Theorem 2.41? Motivate your answer.*

Problem 31. *Consider the advection-reaction-diffusion problem* (2.53)*. Solve this problem numerically using Jacobi, Gauss–Seidel, SOR, and Richardson and study the convergence of these methods with respect to the mesh size h.*

Chapter 3
Krylov Methods

Because of their overwhelming success in applications, Krylov subspace methods are counted among the "Top 10 Algorithms" of the 20th century.

Jörg Liesen and Zdeněk Strakoš, *Krylov Subspace Methods, Principles and Analysis*, 2013.

We have seen that, in his original method, Richardson used a different parameter at each iteration, namely

$$\boldsymbol{u}_{k+1} = \boldsymbol{u}_k + \alpha_k(\boldsymbol{f} - A\boldsymbol{u}_k), \tag{3.1}$$

and he tried to find a good sequence of parameters $\{\alpha_k\}_k$ to speed up the convergence; see Figure 2.16. This is an excellent idea, but it is much harder than the one parameter α we optimized resulting in Theorem 2.41. Richardson's dream was realized when *Gene Golub* invented the Chebyshev semi-iterative method in his Ph.D. thesis in 1959 [90]. Using the roots of the Chebyshev polynomials, which are the smallest polynomials in a given interval in the $\|\cdot\|_{L^\infty}$-norm, and their recurrence relation, Golub managed to derive a method where the optimal α_k for a symmetric positive definite matrix with a given spectral interval estimate are derived on the fly using the recurrence relation of the Chebyshev polynomials. A precise description of this invention can be found in [86, Section 11.5]. There is, however, an even better approach, which does not require the estimate of the spectral interval of the matrix, which leads to the so-called Krylov methods that we study in this chapter, and which were selected among the top 10 algorithms of the 20th century; see the quote above.

We follow in the beginning the groundbreaking work of Eduard Stiefel in [172], where he describes for the first time the algorithm of conjugate gradients, the first Krylov method dating from 1951. These methods are called Krylov methods because they involve what is called a Krylov space; they also appear in a paper by *Nikolay Mitrofanovich Krylov* from 1931, who studied vibration phenomena arising in linear systems of second-order ordinary differential equations [120]. As one can see from the quotes in Section 3.2, Stiefel had already emphasized that the method of conjugate gradients gives both successive approximations to the solution as well as the solution after a finite number of steps. In the publication with Hestenes then the finite number of steps were more emphasized. This was misleading for the algorithm, which in finite-precision arithmetic rarely converges in a finite number of steps, and so it took almost a generation of numerical analysts to expand research into more general Krylov methods like GMRES [165], which we will also see in this chapter. We start first, however, with a simple idea coming from optimization.

3.1 ▪ Steepest Descent

Étant donné un système d'équations simultanées qu'il s'agit de résoudre, on commence ordinairement par les réduire à une seule, à l'aide d'éliminations successives, sauf à résoudre définitivement, s'il se peut, l'équation résultante. Mais il est important d'observer: 1° que, dans un grand nombre de cas, l'élimination ne peut s'effectuer en aucune manière; 2° que l'équation résultante est généralement très compliquée, lors même les équations données sont assez simples. Pour ces deux motifs, on concoit qu'il serait très utile de connaitre une méthode générale qui pût servir à résoudre directement un système d'équations simultanées. Telle est celle que j'ai obtenue, et dont je vais dire ici quelques mots.

Augustin-Luis Cauchy, *Méthode générale pour la résolution des systèmes d'équations simultanées*, 1847.

Es handelt sich hier im Grunde genommen um eine Anwendung des Ritzschen Gedankens, ein Minimum angenähert dadurch zu bestimmen, dass man die Konkurrenz auf eine leicht zu handhabende lineare Schar beschränkt.

Eduard Stiefel, *Über einige Methoden der Relaxationsrechnung*, 1952.

The invention of the Steepest Descent method can be traced back to the work *Méthode générale pour la résolution des systemes d'équations simultanées* that Augustin-Luis Cauchy wrote in 1847 [31] (see also [29] for an English translation). As explained in the quote above, Cauchy developed his method for the solution of general systems of nonlinear equations. His crucial idea was to consider a Taylor expansion of a (nonnegative) function of which he wanted to calculate the roots. The splendid work of Cauchy leads to the definition of Steepest Descent for a general (nonlinear) optimization problem. However, given our interest in solving linear systems, we proceed with the definition of Steepest Descent by directly considering a quadratic problem. The interested reader will surely find some interesting relations with Cauchy's original work.

If the matrix A is symmetric and positive definite, then instead of solving the linear system of equations $A\boldsymbol{u} = \boldsymbol{f}$, we can minimize $F(\boldsymbol{u}) := \frac{1}{2}\boldsymbol{u}^\top A\boldsymbol{u} - \boldsymbol{u}^\top \boldsymbol{f}$ to find the solution. To see that, note that for a minimum of the function $F(\boldsymbol{u})$ we need that the gradient $\nabla F(\boldsymbol{u})$ is zero and the second derivative is positive. Now the gradient is, using that $A^\top = A$,

$$\nabla F(\boldsymbol{u}) = \frac{1}{2}A\boldsymbol{u} + \frac{1}{2}A^\top \boldsymbol{u} - \boldsymbol{f} = A\boldsymbol{u} - \boldsymbol{f}.$$

Setting the gradient to zero, we see that the minimizer solves the linear system of equations $A\boldsymbol{u} = \boldsymbol{f}$. Since the Hessian matrix $\nabla^2 F(\boldsymbol{u}) = A$ and A is by assumption positive definite, we have indeed a minimum of $F(\boldsymbol{u})$ as the solution of $A\boldsymbol{u} = \boldsymbol{f}$.[17] Figure 3.1 shows a two-dimensional example of such a function $F(\boldsymbol{u})$.

To find the minimum of $F(\boldsymbol{u})$, one can start at some initial guess $\boldsymbol{u}_0$ and then compute for $k = 0, 1, 2, \ldots$

$$\boldsymbol{u}_{k+1} = \boldsymbol{u}_k + \alpha_k \boldsymbol{p}_k.$$

The question is how to choose the search directions $\boldsymbol{p}_k$ and the distance to go in that search direction, α_k.

Since we want to find a minimum, we could intuitively go into the direction where the function $F(\boldsymbol{u})$ decreases most, which is a reasonable tactic.[18] This would be in the opposite direction

[17] Since the Hessian of F coincides with A, which is positive definite, the Hessian is positive definite and thus F is strictly convex. Hence a necessary and sufficient condition for $\boldsymbol{u}$ to be the unique global minimum is $\nabla F(\boldsymbol{u}) = 0$; see, e.g., [25].

[18] Stiefel was a colonel in the Swiss army and carefully distinguished between a tactic, which is locally best, and a strategy to win globally.

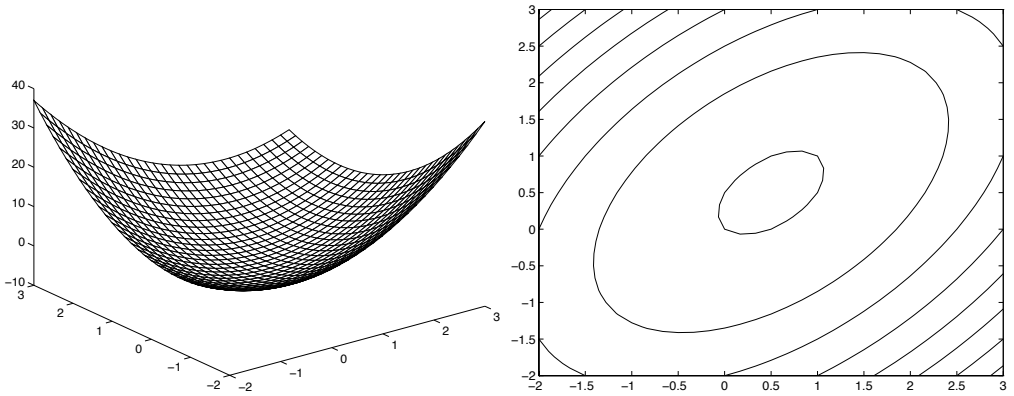

Figure 3.1. *Example of a function* $F(\boldsymbol{u}) = \frac{1}{2}\boldsymbol{u}^\top A\boldsymbol{u} - \boldsymbol{u}^\top \boldsymbol{f}$ *which is minimized to find a solution to the linear system* $A\boldsymbol{u} = \boldsymbol{f}$.

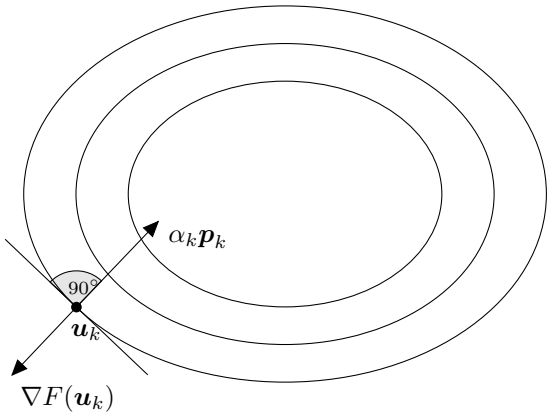

Figure 3.2. *The method of Steepest Descent: the black curves are the level sets of* F*; the black dot represents the approximate solution* $\boldsymbol{u}_k$ *at the* k*th iterate; the two vectors represent the gradient of* F *at* $\boldsymbol{u}_k$ *and the new search direction* $\boldsymbol{p}_k$ *multiplied by the step-length* α_k.

of the gradient of $F(\boldsymbol{u})$, as shown in Figure 3.2. The direction opposite to the gradient of $F(\boldsymbol{u}_k)$ is

$$-\nabla F(\boldsymbol{u}_k) = -(A\boldsymbol{u}_k - \boldsymbol{f}) = \boldsymbol{f} - A\boldsymbol{u}_k = \boldsymbol{r}_k,$$

and hence the search direction $\boldsymbol{p}_k$ equals the residual at step k, $\boldsymbol{r}_k$. Doing this, we find surprisingly again the method of Richardson (3.1)! But now, to determine how far we want to go in that direction, we can employ the tactic of going as long as it goes down, since we want to find a minimum, which is precisely the "Ritzscher Gedanke" in the quote above. This is equivalent to minimizing the function $F(\boldsymbol{u}_k + \alpha_k \boldsymbol{r}_k)$ with respect to the parameter α_k to find the new iterate $\boldsymbol{u}_{k+1}$. Performing this minimization we obtain

$$\frac{d}{d\alpha_k} F(\boldsymbol{u}_{k+1}) = \frac{d}{d\alpha_k} F(\boldsymbol{u}_k + \alpha_k \boldsymbol{r}_k) = (\nabla F(\boldsymbol{u}_{k+1}))^\top \boldsymbol{r}_k = 0,$$

which means that we have to choose $\boldsymbol{u}_{k+1}$ such that $\nabla F(\boldsymbol{u}_{k+1})$ is orthogonal to the current

residual $\boldsymbol{r}_k$. But $\nabla F(\boldsymbol{u}_{k+1}) \equiv -\boldsymbol{r}_{k+1}$ and thus we can compute the parameter α_k as

$$\begin{aligned} 0 &= \boldsymbol{r}_{k+1}^\top \boldsymbol{r}_k \\ &= (\boldsymbol{f} - A\boldsymbol{u}_{k+1})^\top \boldsymbol{r}_k \\ &= (\boldsymbol{f} - A(\boldsymbol{u}_k + \alpha_k \boldsymbol{r}_k))^\top \boldsymbol{r}_k \\ &= (\boldsymbol{f} - A\boldsymbol{u}_k - \alpha_k A\boldsymbol{r}_k)^\top \boldsymbol{r}_k \\ &= (\boldsymbol{r}_k - \alpha_k A\boldsymbol{r}_k)^\top \boldsymbol{r}_k \\ &= \boldsymbol{r}_k^\top \boldsymbol{r}_k - \alpha_k \boldsymbol{r}_k^\top A\boldsymbol{r}_k \end{aligned}$$

and hence, solving for α_k, we get

$$\alpha_k = \frac{\boldsymbol{r}_k^\top \boldsymbol{r}_k}{\boldsymbol{r}_k^\top A\boldsymbol{r}_k}. \tag{3.2}$$

So the algorithm of Steepest Descent for the linear system $A\boldsymbol{u} = \boldsymbol{f}$, where A is symmetric and positive definite, is given in MATLAB as follows:

```
function [u,uk,res]=SteepestDescent(A,f,u0,tol,m)
% STEEPESTDESCENT solves Au=f using the steepest descent method
%   [u,uk,res]=SteepestDescent(A,f,u0,tol,m); solves Au=f using steepest
%   descent starting at the initial guess u0 up to a tolerance tol using
%   at most m iterations. A has to be symmetric positive definite.
%   SteepestDescent returns in the matrix uk the iterates, in u the
%   solution computed, and in res the history of the norm of the residuals.

if nargin<5, m=100; end          % default values
if nargin<4, tol=1e-6; end
r=f-A*u0;
res(1)=norm(r);
uk(:,1)=u0;
k=0;
while res(k+1)/norm(f)>tol && k<=m
  k=k+1;
  al=r'*r/(r'*A*r);
  uk(:,k+1)=uk(:,k)+al*r;
  r=f-A*uk(:,k+1);
  res(k+1)=norm(r);
end
u=uk(:,k+1);
```

Applying Steepest Descent to our Laplace model problem from Section 1.3,[19] we obtain for the first iterates the approximations shown in Figure 3.3. We see that the method converges, comparable to the convergence of Jacobi in Figure 2.3. We next prove that Steepest Descent is converging for such problems, and we give a convergence estimate.

Theorem 3.1 (Convergence of Steepest Descent). *Let $A \in \mathbb{R}^{n\times n}$ be symmetric and positive definite. Then Steepest Descent converges, and the errors satisfy the convergence estimate*

$$\|\boldsymbol{e}_k\|_A \leq \left(\frac{\kappa(A)-1}{\kappa(A)+1}\right)^k \|\boldsymbol{e}_0\|_A, \tag{3.3}$$

where $\kappa(A) := \frac{\lambda_{\max}(A)}{\lambda_{\min}(A)}$ is the spectral condition number *of A, and $\|\boldsymbol{v}\|_A := \sqrt{\boldsymbol{v}^\top A\boldsymbol{v}}$.*

[19] Notice that if A is not symmetric and positive definite, then the problem of minimizing $F(\boldsymbol{u})$ is not necessarily well posed and one cannot use Steepest Descent. However, an idea to still use Steepest Descent to solve a linear system $A\boldsymbol{u} = \boldsymbol{f}$ for a nonsymmetric matrix is given in Problem 35.

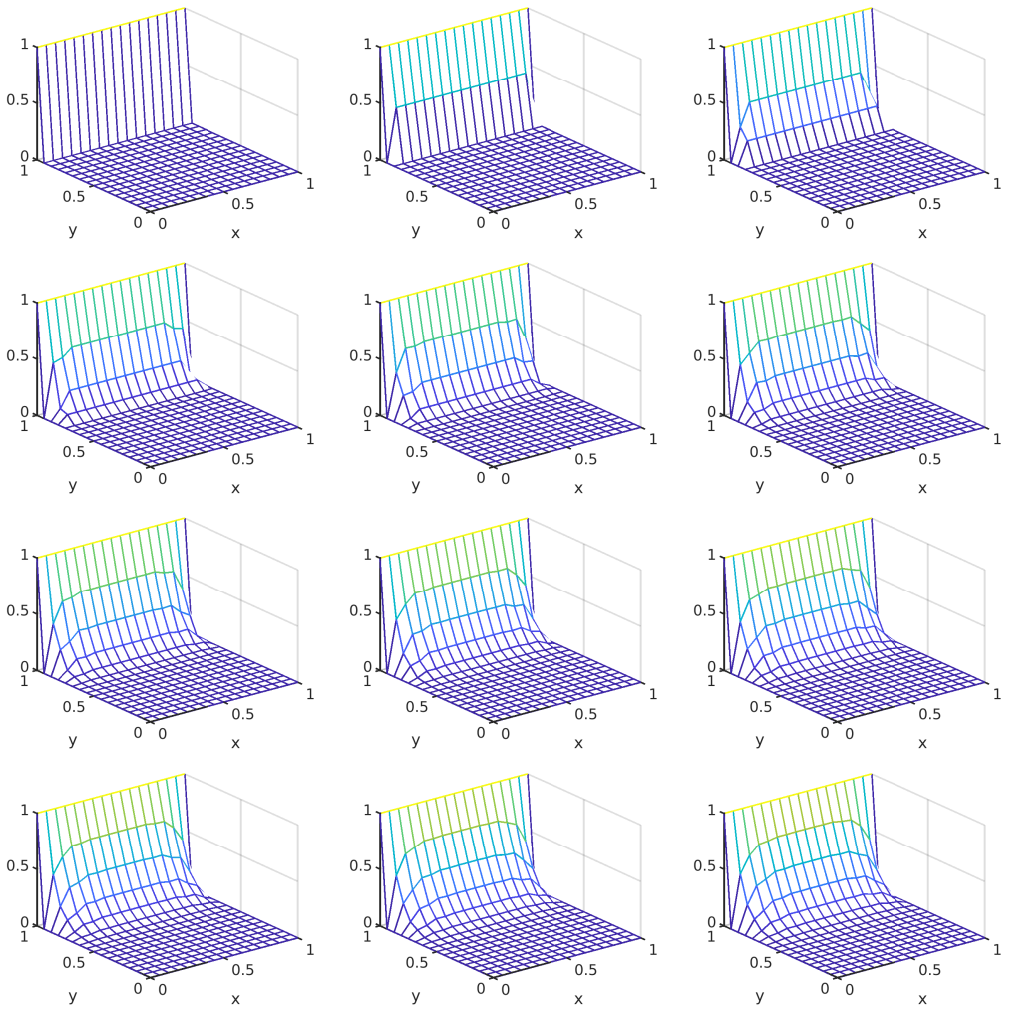

Figure 3.3. *Initial guess and first iterations of Steepest Descent* (2.51) *applied to our Laplace model problem from Section 1.3.*

Proof. To study if the sequence $\|\boldsymbol{e}_k\|_A$ converges to zero as k goes to infinity, recall that

$$\boldsymbol{e}_{k+1} = \boldsymbol{u} - \boldsymbol{u}_{k+1} = \boldsymbol{u} - \boldsymbol{u}_k - \alpha_k \boldsymbol{r}_k = \boldsymbol{e}_k - \alpha_k \boldsymbol{r}_k,$$

and, using that $A = A^\top$, compute

$$\begin{aligned}\|\boldsymbol{e}_{k+1}\|_A^2 &= \boldsymbol{e}_{k+1}^\top A \boldsymbol{e}_{k+1} \\ &= (\boldsymbol{e}_k - \alpha_k \boldsymbol{r}_k)^\top A (\boldsymbol{e}_k - \alpha_k \boldsymbol{r}_k) \\ &= \boldsymbol{e}_k^\top A \boldsymbol{e}_k - 2\alpha_k \boldsymbol{r}_k^\top A \boldsymbol{e}_k + \alpha_k^2 \boldsymbol{r}_k^\top A \boldsymbol{r}_k.\end{aligned}$$

Since $A\boldsymbol{e}_k = A\boldsymbol{u} - A\boldsymbol{u}_k = \boldsymbol{f} - A\boldsymbol{u}_k = \boldsymbol{r}_k$, we obtain that

$$\begin{aligned}\|\boldsymbol{e}_{k+1}\|_A^2 &= \boldsymbol{e}_k^\top A \boldsymbol{e}_k - 2\alpha_k \boldsymbol{r}_k^\top \boldsymbol{r}_k + \alpha_k^2 \boldsymbol{r}_k^\top A \boldsymbol{r}_k \\ &= \|\boldsymbol{e}_k\|_A^2 - 2\alpha_k \|\boldsymbol{r}_k\|_2^2 + \alpha_k^2 \|\boldsymbol{r}_k\|_A^2 \\ &= \|\boldsymbol{e}_k\|_A^2 - \alpha_k \|\boldsymbol{r}_k\|_2^2,\end{aligned}$$

where we used (3.2). Inserting again the value of α_k given by (3.2) and dividing by $\|\boldsymbol{e}_k\|_A^2$, we get

$$\frac{\|\boldsymbol{e}_{k+1}\|_A^2}{\|\boldsymbol{e}_k\|_A^2} = 1 - \frac{\|\boldsymbol{r}_k\|_2^4}{(\boldsymbol{r}_k^\top A\boldsymbol{r}_k)(\boldsymbol{e}_k^\top A\boldsymbol{e}_k)} = 1 - \frac{\|\boldsymbol{r}_k\|_2^4}{(\boldsymbol{r}_k^\top A\boldsymbol{r}_k)(\boldsymbol{r}_k^\top A^{-1}\boldsymbol{r}_k)},$$

where we used that $A\boldsymbol{e}_k = \boldsymbol{r}_k$ and $\boldsymbol{e}_k^\top = (A^{-1}\boldsymbol{r}_k)^\top = \boldsymbol{r}_k^\top A^{-1}$, since A is symmetric. By the Kantorovich inequality (see Theorem 3.2 below), the right-hand side can be bounded using $\kappa := \kappa(A)$, the condition number of A, and we obtain

$$\frac{\|\boldsymbol{e}_{k+1}\|_A^2}{\|\boldsymbol{e}_k\|_A^2} \le 1 - \frac{4}{(\sqrt{\kappa} + \frac{1}{\sqrt{\kappa}})^2} = \left(\frac{\kappa - 1}{\kappa + 1}\right)^2 < 1,$$

which concludes the proof using induction. ∎

Note that since

$$\begin{aligned}\|\boldsymbol{r}_k\|_{A^{-1}}^2 &= (\boldsymbol{f} - A\boldsymbol{u}_k)^\top A^{-1}(\boldsymbol{f} - A\boldsymbol{u}_k)\\ &= (A^{-1}(\boldsymbol{f} - A\boldsymbol{u}_k))^\top A(A^{-1}(\boldsymbol{f} - A\boldsymbol{u}_k))\\ &= (\boldsymbol{u} - \boldsymbol{u}_k)^\top A(\boldsymbol{u} - \boldsymbol{u}_k)\\ &= \|\boldsymbol{u} - \boldsymbol{u}_k\|_A^2,\end{aligned}$$

Theorem 3.1 also gives immediately an estimate for the residual $\boldsymbol{r}_k$ in the norm $\|\boldsymbol{v}\|_{A^{-1}} = \sqrt{\boldsymbol{v}^\top A^{-1}\boldsymbol{v}}$.

Theorem 3.2 (Kantorovich inequality). *Let $A \in \mathbb{R}^{n\times n}$ be symmetric and positive definite. Then for all $\boldsymbol{v} \in \mathbb{R}^n$, $\boldsymbol{v} \neq 0$, we have*

$$1 \le \frac{(\boldsymbol{v}^\top A\boldsymbol{v})(\boldsymbol{v}^\top A^{-1}\boldsymbol{v})}{(\boldsymbol{v}^\top\boldsymbol{v})^2} \le \frac{\left(\sqrt{\kappa(A)} + \left(\sqrt{\kappa(A)}\right)^{-1}\right)^2}{4}, \tag{3.4}$$

where $\kappa(A) := \frac{\lambda_{\max}(A)}{\lambda_{\min}(A)}$ is the spectral condition number *of A.*

Proof. Let $A = Q\Lambda Q^\top$ be the eigendecomposition of A, with Q orthogonal and $\Lambda = \operatorname{diag}(\lambda_1, \dots, \lambda_n)$, where $0 < \lambda_1 \le \cdots \le \lambda_n$ because A is positive definite. Then defining $\Lambda^{1/2} = \operatorname{diag}(\sqrt{\lambda_1}, \dots, \sqrt{\lambda_n})$, we can write

$$\begin{aligned}\boldsymbol{v}^\top\boldsymbol{v} &= \boldsymbol{v}^\top QQ^\top\boldsymbol{v} && (Q \text{ is orthogonal})\\ &= \boldsymbol{v}^\top Q\Lambda^{1/2}\Lambda^{-1/2}Q^\top\boldsymbol{v}\\ &\le \|\Lambda^{1/2}Q^\top\boldsymbol{v}\|_2\|\Lambda^{-1/2}Q^\top\boldsymbol{v}\|_2 && (\text{Cauchy–Schwarz})\\ &= (\boldsymbol{v}^\top Q\Lambda Q^\top\boldsymbol{v})^{1/2}(\boldsymbol{v}^\top Q\Lambda^{-1}Q^\top\boldsymbol{v})^{1/2}\\ &= (\boldsymbol{v}^\top A\boldsymbol{v})^{1/2}(\boldsymbol{v}^\top A^{-1}\boldsymbol{v})^{1/2}.\end{aligned}$$

Squaring and dividing by $(\boldsymbol{v}^\top\boldsymbol{v})^2$ then yields the first inequality.

For the second inequality, let $c > 0$ be a constant (to be chosen later) and let $\widetilde{A} := cA$. Then

$$\begin{aligned}(\boldsymbol{v}^\top A\boldsymbol{v})^{1/2}(\boldsymbol{v}^\top A^{-1}\boldsymbol{v})^{1/2} &= (\boldsymbol{v}^\top(cA)\boldsymbol{v})^{1/2}(\boldsymbol{v}^\top(cA)^{-1}\boldsymbol{v})^{1/2}\\ &\le \frac{1}{2}(\boldsymbol{v}^\top\widetilde{A}\boldsymbol{v} + \boldsymbol{v}^\top\widetilde{A}^{-1}\boldsymbol{v})\\ &= \frac{1}{2}\boldsymbol{v}^\top Q(\widetilde{\Lambda} + \widetilde{\Lambda}^{-1})Q^\top\boldsymbol{v},\end{aligned}$$

where we have used the arithmetic-geometric mean inequality $\sqrt{ab} \leq \frac{1}{2}(a+b)$ for $a, b \geq 0$. If we now define the function $f(\lambda) := \lambda + \lambda^{-1}$, then the inequality above becomes

$$\begin{aligned}(\boldsymbol{v}^\top A\boldsymbol{v})^{1/2}(\boldsymbol{v}^\top A^{-1}\boldsymbol{v})^{1/2} &\leq \frac{1}{2}(Q^\top \boldsymbol{v})^\top f(\widetilde{\Lambda})(Q^\top \boldsymbol{v}) \\ &\leq \frac{1}{2}\|f(\widetilde{\Lambda})\|_2 \|Q^\top \boldsymbol{v}\|_2^2 = \frac{1}{2}\max_j |f(\widetilde{\lambda}_j)| \boldsymbol{v}^\top \boldsymbol{v}.\end{aligned}$$

But $f(\lambda) > 0$ and $f''(\lambda) = 2\lambda^{-3} > 0$ for $\lambda > 0$, so f is a positive convex function over the interval $\left[\widetilde{\lambda}_1, \widetilde{\lambda}_n\right]$ (where $\widetilde{\lambda}_j = c\lambda_j$). Thus, we have

$$\max_j |f(\widetilde{\lambda}_j)| = \max\{f(\widetilde{\lambda}_1), f(\widetilde{\lambda}_n)\},$$

so picking $c = 1/\sqrt{\lambda_1 \lambda_n}$ gives

$$\widetilde{\lambda}_1 = \sqrt{\frac{\lambda_1}{\lambda_n}}, \qquad \widetilde{\lambda}_n = \sqrt{\frac{\lambda_n}{\lambda_1}},$$

which in turn yields

$$\max_j |f(\widetilde{\lambda}_j)| = f(\widetilde{\lambda}_1) = f(\widetilde{\lambda}_n) = \sqrt{\frac{\lambda_1}{\lambda_n}} + \sqrt{\frac{\lambda_n}{\lambda_1}}.$$

Finally, noting that $\kappa(A) = \lambda_n/\lambda_1$, we obtain

$$(\boldsymbol{v}^\top A\boldsymbol{v})^{1/2}(\boldsymbol{v}^\top A^{-1}\boldsymbol{v})^{1/2} \leq \frac{1}{2}\left(\sqrt{\kappa(A)} + \frac{1}{\sqrt{\kappa(A)}}\right)\boldsymbol{v}^\top \boldsymbol{v},$$

which, upon squaring and dividing by $(\boldsymbol{v}^\top \boldsymbol{v})^2$, gives the second inequality. □

Theorem 3.1 shows that Steepest Descent always converges, but the convergence may be very slow. To see why, consider the situation where the function $F(\boldsymbol{u})$ represents a narrow valley, like shown in Figure 3.4 on the right. Steepest Descent is in that case zigzagging through the valley and therefore approaching the minimum very slowly.

Let us now study the convergence of Steepest Descent for decreasing values of the grid size h, as we did for all the methods of Chapter 2. We show in Figure 3.5 how the error decreases as the iterations progress when Steepest Descent is used to solve our Laplace model problem (see Section 1.3) for different values of interior gridpoints: $m = 15$, $m = 31$, and $m = 63$. We observe that the convergence strongly depends on the grid size and deteriorates quite fast for decreasing h. This behavior can also be seen by studying the theoretical convergence bound of Theorem 3.1 as a function of h and expanding it around zero. This expansion leads to

$$\frac{\kappa(A) - 1}{\kappa(A) + 1} = 1 - \frac{\pi^2 h^2}{2} + O(h^4),$$

which is similar to the results obtained for Jacobi and Gauss–Seidel. Moreover, all the depicted convergence curves decay faster at the first iterations, but then the convergence becomes slower. This corresponds to the highly zigzagging behavior shown in Figure 3.4 (right). Such behavior was already recognized by Stiefel in [172].[20]

[20] Stiefel writes, "Das Auftreten von Käfigen ist eine allgemeine Erscheinung bei Relaxationsverfahren und sehr unerwünscht. Es bewirkt, dass die Relaxation am Anfang flott vorwärtsgeht, aber dann immer weniger ausgiebig wird"; see Figure 3.5.

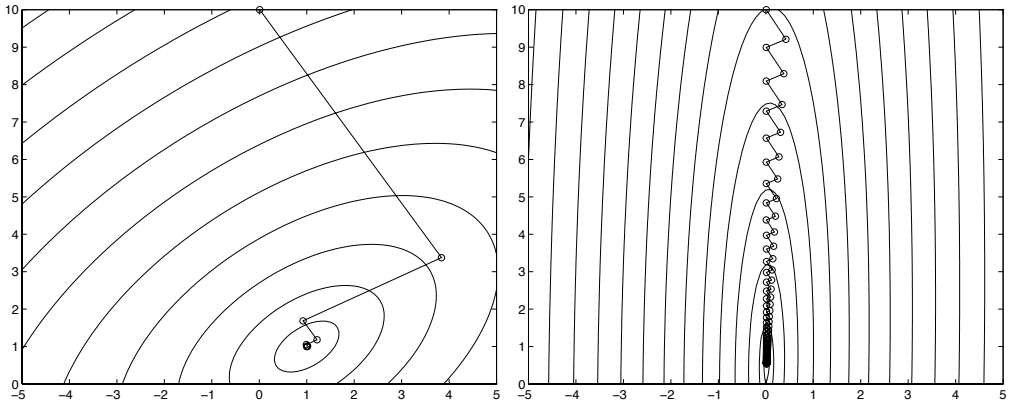

Figure 3.4. *Good convergence of Steepest Descent on the left, and a steep valley which slows down the convergence dramatically on the right.*

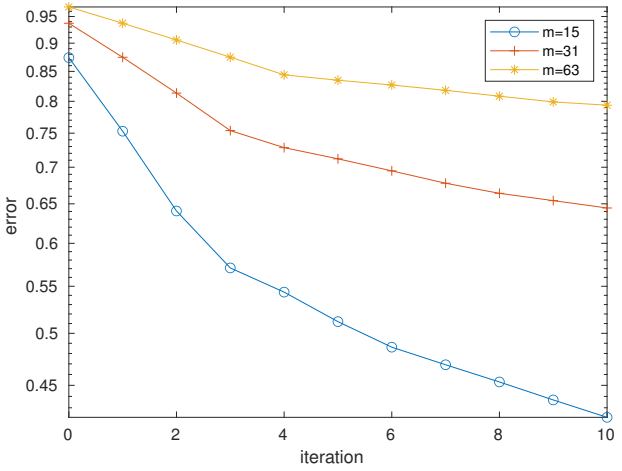

Figure 3.5. *Convergence of the Steepest Descent method for different mesh sizes* $h = \frac{1}{m+1}$.

3.2 ▪ The conjugate gradient method

> *Nach dem bekannten Verfahren des stärksten Abstiegs und der Iteration in Gesamtschritten wird in Abschnitt 5 ein 'n-Schritt-Verfahren' angegeben, welches sowohl eine sukzessive Approximation an die Lösung, als auch deren exakte Bestimmung in endlich vielen Schritten liefert.*
>
> Eduard Stiefel, *Über einige Methoden der Relaxationsrechnung*, 1952.

> *An iterative algorithm is given for solving a system* $A\boldsymbol{x} = \boldsymbol{k}$ *of* n *linear equations in* n *unknowns. The solution is given in* n *steps.*
>
> Magnus R. Hestenes and Eduard Stiefel, *Methods of Conjugate Gradients for Solving Linear Systems*, 1952.

The problem of Steepest Descent is that the same search directions are used over and over again. A better idea is to use each search direction only once and go far enough so that one never has to go in that direction again. If we do this in a two-dimensional problem, there are only two

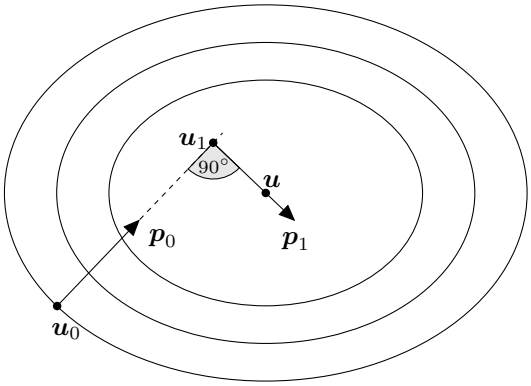

Figure 3.6. *Optimal method: $\boldsymbol{u}$ is the minimum of F; the black curves are the level sets of F; the search directions $\boldsymbol{p}_0$ and $\boldsymbol{p}_1$ are orthogonal and lead to an optimal method that converges in two steps starting from $\boldsymbol{u}_0$ and passing through the first approximation $\boldsymbol{u}_1$.*

independent directions, so the algorithm must converge in two steps, and more generally for n-dimensional problems in n steps; see the quotes above. But how can this be achieved? Consider the example given in Figure 3.6. The two independent search directions are given by $\boldsymbol{p}_0$ and $\boldsymbol{p}_1$. First we go in the direction $\boldsymbol{p}_0$. How far do we have to go if we never want to go again into this direction? We have to go until the search direction is orthogonal to the direction where the solution lies, i.e., $\boldsymbol{p}_k$ is orthogonal to the new error vector $\boldsymbol{e}_{k+1}$ at the next step,

$$\boldsymbol{p}_k^\top \boldsymbol{e}_{k+1} = 0.$$

From this equation we can derive the parameter α_k by

$$\begin{aligned}
\boldsymbol{p}_k^\top \boldsymbol{e}_{k+1} &= 0,\\
\boldsymbol{p}_k^\top (\boldsymbol{u} - \boldsymbol{u}_{k+1}) &= 0,\\
\boldsymbol{p}_k^\top (\boldsymbol{u} - \boldsymbol{u}_k - \alpha_k \boldsymbol{p}_k) &= 0,\\
\boldsymbol{p}_k^\top \boldsymbol{e}_k - \alpha_k \boldsymbol{p}_k^\top \boldsymbol{p}_k &= 0
\end{aligned}$$

and thus

$$\alpha_k = \frac{\boldsymbol{p}_k^\top \boldsymbol{e}_k}{\boldsymbol{p}_k^\top \boldsymbol{p}_k}.$$

Hence given n orthogonal search directions $\boldsymbol{p}_k$ this algorithm finds the solution to $A\boldsymbol{u} = \boldsymbol{f}$ in at most n steps for A symmetric positive definite. To see this, consider any initial guess $\boldsymbol{u}_0 \in \mathbb{R}^n$ and the corresponding error $\boldsymbol{e}_0 = \boldsymbol{u} - \boldsymbol{u}_0$. Since the n search directions are linearly independent they form a basis in $\mathbb{R}^n$ and we can expand the error $\boldsymbol{e}_0$ as $\boldsymbol{e}_0 = \sum_{j=0}^{n-1} c_j \boldsymbol{p}_j$ for some coefficients c_j. Now, recalling that $\boldsymbol{u}_{k+1} = \boldsymbol{u}_k + \alpha_k \boldsymbol{p}_k$ and working recursively we get

$$\begin{aligned}
\boldsymbol{e}_{k+1} &= \boldsymbol{u} - \boldsymbol{u}_{k+1} = \boldsymbol{u} - \boldsymbol{u}_k - \alpha_k \boldsymbol{p}_k\\
&= \boldsymbol{e}_k - \alpha_k \boldsymbol{p}_k = \boldsymbol{e}_{k-1} - \alpha_{k-1}\boldsymbol{p}_{k-1} - \alpha_k \boldsymbol{p}_k\\
&= \cdots = \boldsymbol{e}_0 - \sum_{j=0}^{k} \alpha_j \boldsymbol{p}_j = \sum_{j=0}^{n-1} c_j \boldsymbol{p}_j - \sum_{j=0}^{k} \alpha_j \boldsymbol{p}_j.
\end{aligned}$$

Using the orthogonality condition $\boldsymbol{p}_k^\top \boldsymbol{e}_{k+1} = 0$ together with the orthogonality of the $\boldsymbol{p}_j$'s, the previous equality allows us to compute

$$0 = \boldsymbol{p}_k^\top \boldsymbol{e}_{k+1} = (c_k - \alpha_k)\|\boldsymbol{p}_k\|_2^2,$$

which implies that $\alpha_k = c_k$ for $k = 0, \ldots, n-1$. Therefore, we have that

$$\begin{aligned}\boldsymbol{e}_n &= \boldsymbol{e}_{n-1} - \alpha_{n-1}\boldsymbol{p}_{n-1} = \boldsymbol{e}_{n-2} - \alpha_{n-2}\boldsymbol{p}_{n-2} - \alpha_{n-1}\boldsymbol{p}_{n-1} \\ &= \cdots = \boldsymbol{e}_0 - \sum_{j=0}^{n-1} \alpha_j \boldsymbol{p}_j = \sum_{j=0}^{n-1} (c_j - \alpha_j)\boldsymbol{p}_j = 0.\end{aligned}$$

This shows that this algorithm converges theoretically in at most n steps. However, there is a big problem in practice: to compute how far we have to go along a search direction, we need to know already where the solution is, since we have to enforce $\boldsymbol{p}_k^\top \boldsymbol{e}_{k+1} = 0$, and to compute the error vector $\boldsymbol{e}_{k+1}$ we need to know $\boldsymbol{u}$, since $\boldsymbol{e}_{k+1} = \boldsymbol{u} - \boldsymbol{u}_{k+1}$. So in this form the algorithm is not practical.

The key idea now is to note that even without knowing $\boldsymbol{e}_{k+1}$ we know the value of $A\boldsymbol{e}_{k+1}$ because

$$A\boldsymbol{e}_{k+1} = A\boldsymbol{u} - A\boldsymbol{u}_{k+1} = \boldsymbol{f} - A\boldsymbol{u}_{k+1} = \boldsymbol{r}_{k+1},$$

the residual at step $k+1$. This suggests using a different inner product to enforce orthogonality in. Instead of using the Euclidean inner product of two vectors $\boldsymbol{u}^\top \boldsymbol{v}$ we will use the weighted inner product $\boldsymbol{u}^\top A\boldsymbol{v}$. Suppose we have a set of search directions $\boldsymbol{p}_k$ which is A-orthogonal, namely $\boldsymbol{p}_j^\top A\boldsymbol{p}_k = 0$ for $j \neq k$. Then we perform the same iteration as before,

$$\boldsymbol{u}_{k+1} = \boldsymbol{u}_k + \alpha_k \boldsymbol{p}_k,$$

but instead of choosing α_k so that the new error is orthogonal to the current search direction $\boldsymbol{p}_k$, we move into that direction until the new error is A-orthogonal to the current search direction, namely

$$\boldsymbol{p}_k^\top A\boldsymbol{e}_{k+1} = 0.$$

Note that now we can determine the parameter α_k without knowing the exact solution by using

$$\begin{aligned}0 &= \boldsymbol{p}_k^\top A\boldsymbol{e}_{k+1} \\ &= \boldsymbol{p}_k^\top A(\boldsymbol{u} - \boldsymbol{u}_{k+1}) \\ &= \boldsymbol{p}_k^\top A(\boldsymbol{u} - \boldsymbol{u}_k - \alpha_k \boldsymbol{p}_k) \\ &= \boldsymbol{p}_k^\top A\boldsymbol{e}_k - \alpha_k \boldsymbol{p}_k^\top A\boldsymbol{p}_k \\ &= \boldsymbol{p}_k^\top \boldsymbol{r}_k - \alpha_k \boldsymbol{p}_k^\top A\boldsymbol{p}_k.\end{aligned}$$

Hence the optimal choice is

$$\alpha_k = \frac{\boldsymbol{p}_k^\top \boldsymbol{r}_k}{\boldsymbol{p}_k^\top A\boldsymbol{p}_k}, \tag{3.5}$$

which is explicitly known since the residual $\boldsymbol{r}_k$ is given by $\boldsymbol{r}_k = \boldsymbol{f} - A\boldsymbol{u}_k$. Thus given a set of n A-orthogonal search directions $\boldsymbol{p}_k$, such an algorithm finds the solution to $A\boldsymbol{u} = \boldsymbol{f}$ in n steps for A symmetric and positive definite.

One could in principle construct an A-orthogonal basis of search directions in advance and make this algorithm practical, but as we will see now, this is not necessary, because it is possible to construct such A-orthogonal search directions on the fly. This leads to the famous *conjugate gradient method (CG)* invented independently by Stiefel [172] and Forsythe, Hestenes, and

Rosser [66] and that led to the famous joint paper of Hestenes and Stiefel on the method [106]. In fact, Rosser and Stiefel attended the same symposium held at INA in August 1951, and both presented the same algorithm.

So how is it possible to generate A-orthogonal search directions on the fly? Consider as initial search direction the residual as in Steepest Descent,

$$\boldsymbol{p}_0 := \boldsymbol{r}_0 = \boldsymbol{f} - A\boldsymbol{u}_0. \tag{3.6}$$

Then we obtain for the distance to go along that direction according to (3.5),

$$\alpha_0 := \frac{\boldsymbol{r}_0^\top \boldsymbol{p}_0}{\boldsymbol{p}_0^\top A\boldsymbol{p}_0}, \tag{3.7}$$

and the new approximation is

$$\boldsymbol{u}_1 = \boldsymbol{u}_0 + \alpha_0\boldsymbol{p}_0 = \boldsymbol{u}_0 + \frac{\boldsymbol{r}_0^\top \boldsymbol{p}_0}{\boldsymbol{p}_0^\top A\boldsymbol{p}_0}\boldsymbol{p}_0. \tag{3.8}$$

Now the new residual

$$\boldsymbol{r}_1 = \boldsymbol{f} - A\boldsymbol{u}_1 = \boldsymbol{f} - A\boldsymbol{u}_0 - \alpha_0 A\boldsymbol{p}_0 = \boldsymbol{r}_0 - \alpha_0 A\boldsymbol{p}_0$$

satisfies

$$\boldsymbol{p}_0^\top \boldsymbol{r}_1 = \boldsymbol{p}_0^\top(\boldsymbol{r}_0 - \alpha_0 A\boldsymbol{p}_0) = \boldsymbol{p}_0^\top \boldsymbol{r}_0 - \frac{\boldsymbol{r}_0^\top \boldsymbol{p}_0}{\boldsymbol{p}_0^\top A\boldsymbol{p}_0}\boldsymbol{p}_0^\top A\boldsymbol{p}_0 = 0, \tag{3.9}$$

which means it is orthogonal to the first search direction $\boldsymbol{p}_0$ and thus a good candidate for the new search direction $\boldsymbol{p}_1$ if we want to avoid searching in the same direction again. We just need to A-orthogonalize it with respect to the previous search direction $\boldsymbol{p}_0$ to obtain a method of conjugate search directions. This is achieved by choosing a scalar β_0 such that $\boldsymbol{p}_1 = \boldsymbol{r}_1 + \beta_0\boldsymbol{p}_0$ is A-orthogonal to $\boldsymbol{p}_0$, i.e.,

$$0 = \boldsymbol{p}_0^\top A\boldsymbol{p}_1 = \boldsymbol{p}_0^\top A(\boldsymbol{r}_1 + \beta_0\boldsymbol{p}_0) = \boldsymbol{p}_0^\top A\boldsymbol{r}_1 + \beta_0\boldsymbol{p}_0^\top A\boldsymbol{p}_0, \tag{3.10}$$

which implies

$$\beta_0 = -\frac{\boldsymbol{p}_0^\top A\boldsymbol{r}_1}{\boldsymbol{p}_0^\top A\boldsymbol{p}_0}. \tag{3.11}$$

The amazing discovery of Stiefel and Hestenes is that this step is also sufficient for the following iterations.

Theorem 3.3 (The conjugate gradient method, Hestenes and Stiefel, 1952). *For a given linear system $A\boldsymbol{u} = \boldsymbol{f}$ with symmetric positive definite matrix $A \in \mathbb{R}^{n\times n}$, and initial approximation $\boldsymbol{u}_0 \in \mathbb{R}^n$, we set $\boldsymbol{p}_0 := \boldsymbol{r}_0 = \boldsymbol{f} - A\boldsymbol{u}_0$ and compute for $k = 0, 1, 2, \ldots$ the approximate solutions*

$$\boldsymbol{u}_{k+1} := \boldsymbol{u}_k + \alpha_k\boldsymbol{p}_k, \quad \alpha_k = \frac{\boldsymbol{r}_k^\top \boldsymbol{p}_k}{\boldsymbol{p}_k^\top A\boldsymbol{p}_k}, \tag{3.12}$$

and search directions

$$\boldsymbol{p}_{k+1} := \boldsymbol{r}_{k+1} + \beta_k\boldsymbol{p}_k, \quad \beta_k = -\frac{\boldsymbol{p}_k^\top A\boldsymbol{r}_{k+1}}{\boldsymbol{p}_k^\top A\boldsymbol{p}_k}. \tag{3.13}$$

Then the residuals $\boldsymbol{r}_j := \boldsymbol{f} - A\boldsymbol{u}_j$ are orthogonal,

$$\boldsymbol{r}_{k+1}^\top \boldsymbol{r}_j = 0, \quad j = 0, 1, \ldots, k, \tag{3.14}$$

the residuals are orthogonal to the search directions,

$$\boldsymbol{r}_{k+1}^\top \boldsymbol{p}_j = 0, \quad j = 0, 1, \ldots, k, \tag{3.15}$$

and the search directions are A-orthogonal,

$$\boldsymbol{p}_{k+1}^\top A\boldsymbol{p}_j = 0, \quad j = 0, 1, \ldots, k. \tag{3.16}$$

Proof. The proof is by induction. We have already seen that the result holds for $k = 0$; see (3.9), and (3.10) with (3.11). So we assume that the result holds for k and show that it then still must hold for $k + 1$. For the orthogonality of the residuals, we compute

$$\begin{aligned}
\boldsymbol{r}_{k+1}^\top \boldsymbol{r}_j &= \boldsymbol{r}_j^\top \boldsymbol{r}_{k+1} \\
&= \boldsymbol{r}_j^\top (\boldsymbol{f} - A\boldsymbol{u}_{k+1}) \\
&= \boldsymbol{r}_j^\top \big(\boldsymbol{f} - A(\boldsymbol{u}_k + \alpha_k \boldsymbol{p}_k)\big) \\
&= \boldsymbol{r}_j^\top \boldsymbol{r}_k - \alpha_k \boldsymbol{r}_j^\top A\boldsymbol{p}_k,
\end{aligned}$$

and using from the first equation in (3.13) that $\boldsymbol{r}_j = \boldsymbol{p}_j - \beta_{j-1}\boldsymbol{p}_{j-1}$ to replace the second occurrence of $\boldsymbol{r}_j$ on the right leads to

$$\boldsymbol{r}_{k+1}^\top \boldsymbol{r}_j = \boldsymbol{r}_j^\top \boldsymbol{r}_k - \alpha_k(\boldsymbol{p}_j^\top A\boldsymbol{p}_k - \beta_{j-1}\boldsymbol{p}_{j-1}^\top A\boldsymbol{p}_k) = \boldsymbol{r}_j^\top \boldsymbol{r}_k - \alpha_k \boldsymbol{p}_j^\top A\boldsymbol{p}_k \tag{3.17}$$

since $\boldsymbol{p}_{j-1}^\top A\boldsymbol{p}_k = 0$ for $j \leq k$ by the induction hypothesis. Now we distinguish two cases, $j = k$ and $j < k$: if $j < k$, then also $\boldsymbol{r}_j^\top \boldsymbol{r}_k = 0$ and $\boldsymbol{p}_j^\top A\boldsymbol{p}_k = 0$ by the induction hypothesis, and thus $\boldsymbol{r}_{k+1}^\top \boldsymbol{r}_j = 0$ for $j < k$. Now for $j = k$, we obtain from (3.17) using the definition of α_k in (3.12) that

$$\begin{aligned}
\boldsymbol{r}_{k+1}^\top \boldsymbol{r}_k &= \boldsymbol{r}_k^\top \boldsymbol{r}_k - \frac{\boldsymbol{r}_k^\top \boldsymbol{p}_k}{\boldsymbol{p}_k^\top A\boldsymbol{p}_k} \boldsymbol{p}_k^\top A\boldsymbol{p}_k \\
&= \boldsymbol{r}_k^\top \boldsymbol{r}_k - \boldsymbol{r}_k^\top \boldsymbol{p}_k \\
&= \boldsymbol{r}_k^\top \boldsymbol{r}_k - \boldsymbol{r}_k^\top (\boldsymbol{r}_k + \beta_{k-1}\boldsymbol{p}_{k-1}) \\
&= -\beta_{k-1} \boldsymbol{r}_k^\top \boldsymbol{p}_{k-1},
\end{aligned}$$

where we used $\boldsymbol{p}_k = \boldsymbol{r}_k + \beta_{k-1}\boldsymbol{p}_{k-1}$ from the first equation in (3.13). By the induction hypothesis we have that $\boldsymbol{r}_k^\top \boldsymbol{p}_{k-1} = 0$, which concludes the proof of orthogonality of the residuals in (3.14).

Next, we prove the orthogonality relation (3.15). To do so, we consider the product $\boldsymbol{r}_{k+1}^\top \boldsymbol{p}_j$ and notice that

$$\boldsymbol{r}_{k+1} = \boldsymbol{f} - A\boldsymbol{u}_{k+1} = \boldsymbol{f} - A(\boldsymbol{u}_k + \alpha_k \boldsymbol{p}_k) = \boldsymbol{r}_k - \alpha_k A\boldsymbol{p}_k.$$

Hence, we compute

$$\boldsymbol{r}_{k+1}^\top \boldsymbol{p}_j = \boldsymbol{r}_k^\top \boldsymbol{p}_j - \alpha_k \boldsymbol{p}_k^\top A\boldsymbol{p}_j,$$

where we used that $A = A^\top$. Now we again distinguish two cases, $j < k$ and $j = k$: if $j < k$, then $\boldsymbol{r}_k^\top \boldsymbol{p}_j = 0$ and $\boldsymbol{p}_k^\top A\boldsymbol{p}_j = 0$ by the induction hypothesis. If $j = k$, then using (3.12) we have

$$\boldsymbol{r}_{k+1}^\top \boldsymbol{p}_k = \boldsymbol{r}_k^\top \boldsymbol{p}_k - \alpha_k \boldsymbol{p}_k^\top A\boldsymbol{p}_k = \boldsymbol{r}_k^\top \boldsymbol{p}_k - \frac{\boldsymbol{r}_k^\top \boldsymbol{p}_k}{\boldsymbol{p}_k^\top A\boldsymbol{p}_k} \boldsymbol{p}_k^\top A\boldsymbol{p}_k = 0,$$

which concludes the proof of (3.15).

To prove the A-orthogonality of the search directions, $\boldsymbol{p}_{k+1}^\top A\boldsymbol{p}_j = 0$ for $j = 0, 1, \ldots, k$, we first note that by construction this holds already for $j = k$ by the definition of β_k. For $j < k$, we first compute

$$\boldsymbol{r}_{j+1} = \boldsymbol{f} - A\boldsymbol{u}_{j+1} = \boldsymbol{f} - A(\boldsymbol{u}_j + \alpha_j\boldsymbol{p}_j) = \boldsymbol{r}_j - \alpha_j A\boldsymbol{p}_j$$

from which we obtain that

$$A\boldsymbol{p}_j = \frac{1}{\alpha_j}(\boldsymbol{r}_j - \boldsymbol{r}_{j+1}). \tag{3.18}$$

Now using again $\boldsymbol{p}_{k+1} = \boldsymbol{r}_{k+1} + \beta_k\boldsymbol{p}_k$ from (3.13), and then inserting (3.18), we get

$$\boldsymbol{p}_{k+1}^\top A\boldsymbol{p}_j = (\boldsymbol{r}_{k+1} + \beta_k\boldsymbol{p}_k)^\top A\boldsymbol{p}_j = \frac{1}{\alpha_j}\boldsymbol{r}_{k+1}^\top(\boldsymbol{r}_j - \boldsymbol{r}_{j+1}) + \beta_k\boldsymbol{p}_k^\top A\boldsymbol{p}_j = 0,$$

since we proved already that $\boldsymbol{r}_{k+1}^\top\boldsymbol{r}_j = 0$ and $\boldsymbol{r}_{k+1}^\top\boldsymbol{r}_{j+1} = 0$ for $j < k$, and by the induction hypothesis also $\boldsymbol{p}_k^\top A\boldsymbol{p}_j = 0$ for $j < k$. □

It appears at first sight that one iteration of the CG algorithm in Theorem 3.3 requires three matrix-vector products: $A\boldsymbol{p}_k$ in (3.12) is used to compute $\alpha_k = \frac{\boldsymbol{r}_k^\top\boldsymbol{p}_k}{\boldsymbol{p}_k^\top A\boldsymbol{p}_k}$, $A\boldsymbol{r}_{k+1}$ in (3.13) is used to compute $\beta_k = -\frac{\boldsymbol{p}_k^\top A\boldsymbol{r}_{k+1}}{\boldsymbol{p}_k^\top A\boldsymbol{p}_k}$, and then the residual $\boldsymbol{r}_{k+1} = \boldsymbol{f} - A\boldsymbol{u}_{k+1}$ also needs to be computed. This can, however, be reduced to the single matrix-vector product $A\boldsymbol{p}_k$ as follows: for the residual, we can compute

$$\boldsymbol{r}_{k+1} = \boldsymbol{f} - A\boldsymbol{u}_{k+1} = \boldsymbol{f} - A(\boldsymbol{u}_k + \alpha_k\boldsymbol{p}_k) = \boldsymbol{r}_k - \alpha_k A\boldsymbol{p}_k \tag{3.19}$$

and thus only $A\boldsymbol{p}_k$ is needed. To compute β_k, we first compute

$$\boldsymbol{r}_{k+1}^\top\boldsymbol{p}_{k+1} = (\boldsymbol{r}_k - \alpha_k A\boldsymbol{p}_k)^\top\boldsymbol{p}_{k+1} = \boldsymbol{r}_k^\top\boldsymbol{p}_{k+1} = \boldsymbol{r}_k^\top(\boldsymbol{r}_{k+1} + \beta_k\boldsymbol{p}_k) = \beta_k\boldsymbol{r}_k^\top\boldsymbol{p}_k,$$

where we used the A-orthogonality of the search directions $\boldsymbol{p}_k$ and orthogonality of the residuals $\boldsymbol{r}_k$. Solving for β_k, and using again that the residuals are orthogonal to the search directions, we get

$$\beta_k = \frac{\boldsymbol{r}_{k+1}^\top\boldsymbol{p}_{k+1}}{\boldsymbol{r}_k^\top\boldsymbol{p}_k} = \frac{\boldsymbol{r}_{k+1}^\top(\boldsymbol{r}_{k+1} + \beta_k\boldsymbol{p}_k)}{\boldsymbol{r}_k^\top(\boldsymbol{r}_k + \beta_{k-1}\boldsymbol{p}_{k-1})} = \frac{\|\boldsymbol{r}_{k+1}\|_2^2}{\|\boldsymbol{r}_k\|_2^2}.$$

Because of $\boldsymbol{r}_k^\top\boldsymbol{p}_k = \|\boldsymbol{r}_k\|_2^2$, the computation of α_k simplifies also to

$$\alpha_k = \frac{\|\boldsymbol{r}_k\|_2^2}{\boldsymbol{p}_k^\top A\boldsymbol{p}_k}. \tag{3.20}$$

With these observations, we obtain a version of CG which uses only one matrix-vector multiplication per iteration step:

```
function [u,uk,res]=CG(A,f,u0,tol,m)
% CG conjugate gradient method
%   [u,uk,res]=CG(A,f,u0,tol,m) solves Au=f using the conjugate gradient
%   method starting at the initial guess u0 up to a tolerance tol using
%   at most m iterations. The matrix A has to be symmetric positive
%   definite. CG returns in the matrix uk the iterates, in u the solution
%   computed, and in res the history of the norm of the residuals.

if nargin<5, m=100; end              % default values
if nargin<4, tol=1e-6; end
```

```
uk(:,1)=u0;
r=f-A*uk(:,1);
p=r;
oldrho=r'*r;
res(1)=sqrt(oldrho);
k=0;
while sqrt(oldrho)/norm(f)>tol && k<=m
  k=k+1;
  Ap=A*p;
  alpha=oldrho/(p'*Ap);
  uk(:,k+1)=uk(:,k)+alpha*p;
  r=r-alpha*Ap;
  rho=r'*r;
  beta=rho/oldrho; oldrho=rho;
  res(k+1)=sqrt(oldrho);
  p=r+beta*p;
end
u=uk(:,k+1);
```

Applying CG to our Laplace model problem from Section 1.3, we obtain for the first iterates the approximations shown in Figure 3.7. We see that the method converges rather quickly, comparable to SOR in Figure 2.8 and the true Richardson's method in Figure 2.18. We have seen by construction that CG converges in exact arithmetic after at most n iterations for a problem with n unknowns,[21] and this was emphasized in the early days as one of the main features of CG. Figure 3.7 indicates, however, that CG has an even more important convergence property: one often needs many fewer iterations to obtain very good approximations to the solution. To see this, we now introduce the Krylov space that appears in the work of Krylov from 1931 when he studied the solution of second-order linear systems of ordinary differential equation [120]. Krylov spaces play a major role in the CG method and its generalizations, as we will see later.

Definition 3.4 (Krylov space). *For given $A \in \mathbb{R}^{n\times n}$ and $\boldsymbol{v} \in \mathbb{R}^n$ the* Krylov space *(of order k) is defined as*

$$\mathcal{K}_k(A, \boldsymbol{v}) := \operatorname{span}\{\boldsymbol{v}, A\boldsymbol{v}, \ldots, A^{k-1}\boldsymbol{v}\}. \tag{3.21}$$

For our purposes, we consider the Krylov space associated with a linear system of equations $A\boldsymbol{u} = \boldsymbol{f}$ with $A \in \mathbb{R}^{n\times n}$, $\boldsymbol{u}, \boldsymbol{f} \in \mathbb{R}^n$, and initial guess $\boldsymbol{u}_0 \in \mathbb{R}^n$, that is,

$$\mathcal{K}_k(A, \boldsymbol{r}_0) = \operatorname{span}\{\boldsymbol{r}_0, A\boldsymbol{r}_0, \ldots, A^{k-1}\boldsymbol{r}_0\},$$

where $\boldsymbol{r}_0 := \boldsymbol{f} - A\boldsymbol{u}_0$ denotes the residual of the initial guess.

Before we relate the Krylov space $\mathcal{K}_k(A, \boldsymbol{r}_0)$ with the residuals $\boldsymbol{r}_k$ and the search directions $\boldsymbol{p}_k$ of CG, we study some properties of $\mathcal{K}_k(A, \boldsymbol{r}_0)$. To do so, we recall the definition of the minimal polynomial of a given matrix A; see, e.g., [160, Section 6.1].

Definition 3.5 (Minimal polynomial). *The minimal polynomial of a matrix $A \in \mathbb{R}^{n\times n}$ is the nonzero monic polynomial $p_{\min}$ of lowest degree such that $p_{\min}(A) = 0$. Moreover, we define the minimal polynomial of a pair $(A, \boldsymbol{v}) \in \mathbb{R}^{n\times n} \times \mathbb{R}^n$ as the nonzero monic polynomial $p^{\boldsymbol{v}}_{\min}$ of lowest degree such that $p^{\boldsymbol{v}}_{\min}(A)\boldsymbol{v} = 0$, and it is clear that $\deg(p^{\boldsymbol{v}}_{\min}) \le \deg(p_{\min})$.*

We recall a few important properties of the minimal polynomial in the following lemma.

[21] Convergence in floating point arithmetic is more delicate but has been well understood since the seminal work of Chris Paige [141]; see also [124].

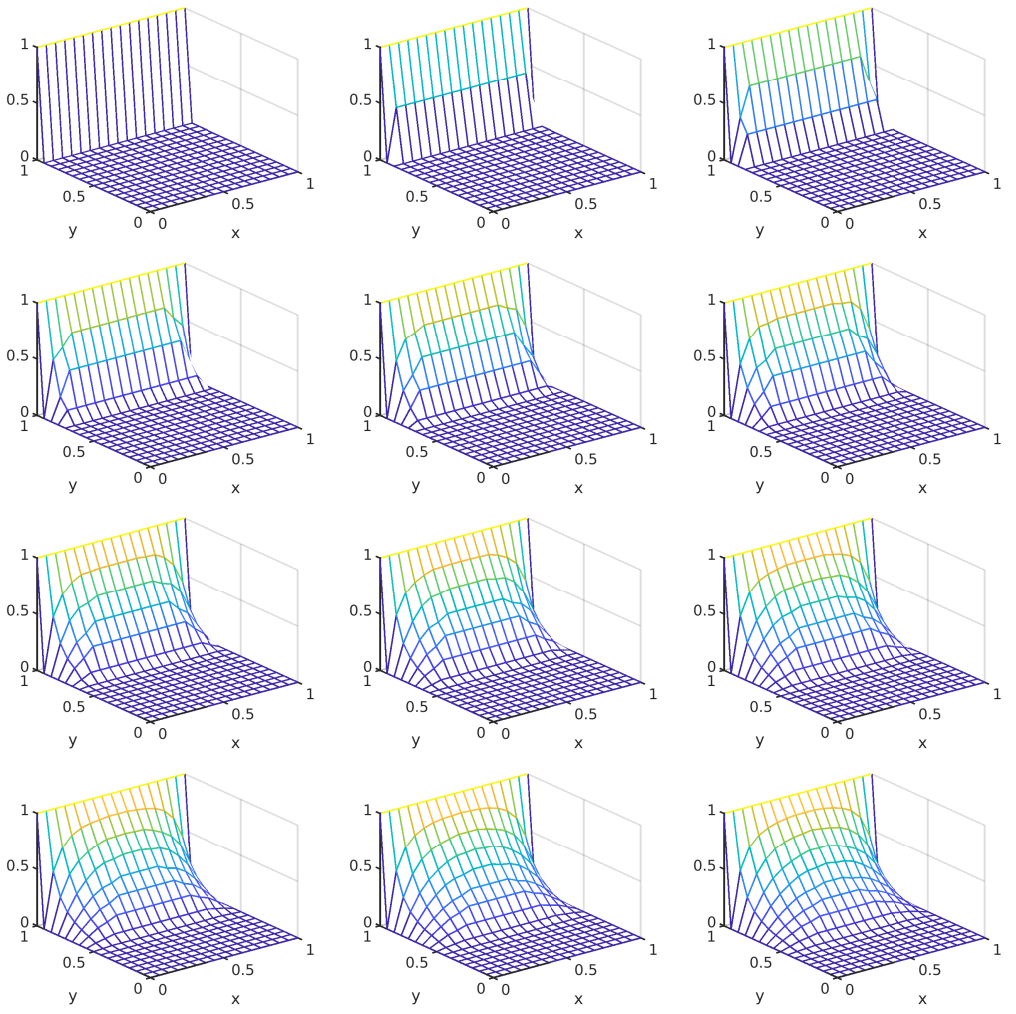

Figure 3.7. *Initial guess and first iterations of CG applied to our Laplace model problem from Section 1.3.*

Lemma 3.6 (Properties of the minimal polynomial). *Let $p_{\min}$ be the minimal polynomial of a matrix A of size $n \times n$. Then*

(a) *$p_{\min}$ is unique;*

(b) *if A is diagonalizable and has $m \leq n$ distinct eigenvalues, then $p_{\min}$ has degree m;*

(c) *if A is invertible, then the constant coefficient of $p_{\min}$ is necessarily nonzero;*

(d) *a scalar $\lambda \in \mathbb{C}$ is an eigenvalue of A if and only if $p_{\min}(\lambda) = 0$.*

Proof. To prove (a), take any polynomial p such that $p(A) = 0$. According to the standard Euclidean division of polynomials, if we divide p by $p_{\min}$, we get $p = qp_{\min} + r$, where q and r are the quotient and the remainder with $\deg(r) < \deg(p_{\min})$. Hence, either $r = 0$ or $r \neq 0$ with degree smaller than $p_{\min}$. Now, we have $0 = p(A) = q(A)p_{\min}(A) + r(A) = r(A)$. Therefore p

and r represent two possible candidates to be (or to construct by dividing them by their highest-degree coefficient) a minimal polynomial. If $r = 0$, then $p(x) = q(x)p_{\min}(x)$ and hence p has degree higher than or equal to the degree of $p_{\min}$, and if p and $p_{\min}$ have the same degree, then $q(x) = q$ is constant and $p(x)/q = p_{\min}(x)$. Now if $r \neq 0$, then $\deg(r) < \deg(p)$. So it is sufficient to study r. Denote by γ the highest-degree coefficient of r and notice that $\widetilde{r} := \frac{r}{\gamma}$ is a monic polynomial of the same degree of r and $\widetilde{r}(A) = 0$. Therefore, $\widetilde{r}$ is a possible candidate to be a minimal polynomial, but since $\deg(\widetilde{r}) < \deg(p_{\min})$, we get a contradiction to the fact that $p_{\min}$ has minimal degree among the monic polynomials that are zero in A.

Now, we prove (b). To do so, we recall that the minimal polynomial of a diagonalizable matrix is the product of distinct monic factors [108, Corollary 3.3.8]. Hence, since A has m distinct eigenvalues its minimal polynomial has degree m.

Let us now prove (c). Assume that A is invertible and $p_{\min}$ has degree n, and denote its coefficients by γ_j for $j = 0, \ldots, n$. Seeking a contradiction, assume that $\gamma_0 = 0$. Therefore, we have that $p_{\min}(A) = A^n + \gamma_{n-1}A^{n-1} + \cdots + \gamma_1 A$. Since A is invertible, we can define the monic polynomial $\widetilde{p}(A) := A^{-1}p_{\min}(A)$. Notice that $\widetilde{p}(A) = A^{n-1} + \gamma_{n-1}A^{n-2} + \cdots + \gamma_1$ and $\widetilde{p}(A) = 0$, which contradicts the fact that $p_{\min}$ has minimal degree.

Finally, we prove (d). Assume that λ is an eigenvalue of A, that is, $A\boldsymbol{v} = \lambda\boldsymbol{v}$ with $\boldsymbol{v} \neq 0$. Then $0 = p_{\min}(A)\boldsymbol{v} = p_{\min}(\lambda)\boldsymbol{v}$, which implies that $p_{\min}(\lambda) = 0$ since $\boldsymbol{v} \neq 0$. Now, assume that $p_{\min}(\lambda) = 0$ and denote by χ the characteristic polynomial of A. By the *Cayley–Hamilton theorem* we have that $\chi(A) = 0$; see, e.g., [108, Theorem 2.4.3.2]. Now, the minimal polynomial $p_{\min}$ divides χ, that is, there exists a polynomial h such that $\chi = hp_{\min} + r$ with $r = 0$ (otherwise one would get a contradiction as in point (a)); see, e.g., [108, Theorem 3.3.1]. This means that $\chi(\lambda) = h(\lambda)p_{\min}(\lambda) = 0$, which implies that λ is a root of the characteristic polynomial χ and thus an eigenvalue of A. □

The minimal polynomial of A allows us to characterize the Krylov space; see, e.g., [160].

Theorem 3.7 (Invariance of a Krylov space). *Consider a matrix $A \in \mathbb{R}^{n\times n}$ and a vector $\boldsymbol{v} \in \mathbb{R}^n$. Let $p^{\boldsymbol{v}}_{\min}$ be the minimal polynomial of $(A, \boldsymbol{v})$ and assume that $p^{\boldsymbol{v}}_{\min}$ has degree k. Then the Krylov space $\mathcal{K}_k(A, \boldsymbol{v})$ is invariant under A, that is, for any $\boldsymbol{w} \in \mathcal{K}_k(A, \boldsymbol{v})$ it holds that $A\boldsymbol{w} \in \mathcal{K}_k(A, \boldsymbol{v})$. Similarly, if the minimal polynomial $p_{\min}$ of A has degree k, then $\mathcal{K}_k(A, \boldsymbol{v})$ is invariant under A for any vector $\boldsymbol{v}$.*

Proof. Consider any vector $\boldsymbol{w} \in \mathcal{K}_k(A, \boldsymbol{v})$. Then $\boldsymbol{w} = \sum_{j=0}^{k-1} \gamma_j A^j \boldsymbol{v}$ for some coefficients γ_j. Now, assume that $\gamma_{k-1} = 0$; then $A\boldsymbol{w} \in \mathcal{K}_k(A, \boldsymbol{v})$. In the case $\gamma_{k-1} \neq 0$, we have to show that $A(A^{k-1}\boldsymbol{v}) = A^k\boldsymbol{v} \in \mathcal{K}_k(A, \boldsymbol{v})$ as well. To do so, consider the minimal polynomial $p^{\boldsymbol{v}}_{\min}(x) = x^k + c_{k-1}x^{k-1} + \cdots + c_0$. Since $p^{\boldsymbol{v}}_{\min}(A)\boldsymbol{v} = 0$, we get

$$0 = p^{\boldsymbol{v}}_{\min}(A)\boldsymbol{v} = A^k\boldsymbol{v} + c_{k-1}A^{k-1}\boldsymbol{v} + \cdots + c_1 A\boldsymbol{v} + c_0\boldsymbol{v},$$

which implies that

$$A^k\boldsymbol{v} = -[c_{k-1}A^{k-1}\boldsymbol{v} + \cdots + c_1 A\boldsymbol{v} + c_0\boldsymbol{v}] \in \mathcal{K}_k(A, \boldsymbol{v}).$$

Hence, it holds that $A\boldsymbol{w} \in \mathcal{K}_k(A, \boldsymbol{v})$. The second statement follows from similar arguments and our proof is complete. □

Theorem 3.8 (Dimension of a Krylov space). *Consider a nonsingular matrix $A \in \mathbb{R}^{n\times n}$ and a nonzero vector $\boldsymbol{v} \in \mathbb{R}^n$. The Krylov space $\mathcal{K}_k(A, \boldsymbol{v})$ is of dimension k if and only if the degree of the minimal polynomial $p^{\boldsymbol{v}}_{\min}$ of the pair $(A, \boldsymbol{v})$ is larger than $k - 1$, that is, $\deg(p^{\boldsymbol{v}}_{\min}) \geq k$.*

Proof. Since A is invertible, its kernel is $\ker(A) = \{0\}$, and recalling that $\boldsymbol{v}$ is nonzero, it holds that $A^j\boldsymbol{v}$ is nonzero for any positive integer $j < \infty$. Now, the nonzero vectors $\boldsymbol{v}, A\boldsymbol{v}, \ldots, A^{k-1}\boldsymbol{v}$ form a basis of $\mathcal{K}_k(A, \boldsymbol{v})$ if and only if for any complex k-tuple γ_j for $j = 0, \ldots, k-1$, where at least one γ_j is nonzero, the linear combination $\sum_{j=0}^{k-1} \gamma_j A^j\boldsymbol{v}$ is nonzero. This condition is equivalent to the condition that there is no nonzero polynomial p of degree lower than or equal to $k-1$ such that $p(A)\boldsymbol{v} = 0$. □

It is clear from Theorem 3.8 that the vector $\boldsymbol{v}$ influences the dimension of $\mathcal{K}_k(A, \boldsymbol{v})$; see also the following example.

Example 3.9. Consider the matrix

$$A = \begin{bmatrix} 2 & -1 & 0 \\ -1 & 2 & -1 \\ 0 & -1 & 2 \end{bmatrix}$$

and the three canonical vectors $\boldsymbol{e}_1$, $\boldsymbol{e}_2$, and $\boldsymbol{e}_3$. The corresponding Krylov spaces are

$$\mathcal{K}_3(A, \boldsymbol{e}_1) = \operatorname{span}\left\{ \begin{bmatrix} 1 \\ 0 \\ 0 \end{bmatrix}, \begin{bmatrix} 2 \\ -1 \\ 0 \end{bmatrix}, \begin{bmatrix} 5 \\ -4 \\ 1 \end{bmatrix} \right\} \quad \text{with } \dim \mathcal{K}_3(A, \boldsymbol{e}_1) = 3,$$

$$\mathcal{K}_3(A, \boldsymbol{e}_2) = \operatorname{span}\left\{ \begin{bmatrix} 0 \\ 1 \\ 0 \end{bmatrix}, \begin{bmatrix} -1 \\ 2 \\ -1 \end{bmatrix}, \begin{bmatrix} -4 \\ 6 \\ -4 \end{bmatrix} \right\} \quad \text{with } \dim \mathcal{K}_3(A, \boldsymbol{e}_2) = 2,$$

$$\mathcal{K}_3(A, \boldsymbol{e}_3) = \operatorname{span}\left\{ \begin{bmatrix} 0 \\ 0 \\ 1 \end{bmatrix}, \begin{bmatrix} 0 \\ -1 \\ 2 \end{bmatrix}, \begin{bmatrix} 1 \\ -4 \\ 5 \end{bmatrix} \right\} \quad \text{with } \dim \mathcal{K}_3(A, \boldsymbol{e}_3) = 3.$$

It is clear that the choice of the vector $\boldsymbol{v}$ influences the dimension of $\mathcal{K}_3(A, \boldsymbol{v})$. Notice also that the minimal polynomial of A is $p_{\min}(x) = x^3 - 6x^2 + 10x - 4$, while the minimal polynomial of the pair $(A, \boldsymbol{e}_2)$ is $p^{\boldsymbol{e}_2}_{\min}(x) = x^2 - 4x + 2$. ■

An interesting property of the Krylov space $\mathcal{K}_k(A, \boldsymbol{f})$ associated to the system $A\boldsymbol{u} = \boldsymbol{f}$ is given by the following theorem.

Theorem 3.10 (Krylov space and solution of $A\boldsymbol{u} = \boldsymbol{f}$). *If the minimal polynomial $p_{\min}$ of the invertible matrix A has degree m, then the solution to $A\boldsymbol{u} = \boldsymbol{f}$ belongs to the space $\mathcal{K}_m(A, \boldsymbol{f})$. Moreover, let $\boldsymbol{u}_0 \in \mathbb{R}^n$ be a given vector and $\boldsymbol{r}_0 = \boldsymbol{f} - A\boldsymbol{u}_0$. Then $\boldsymbol{u}$ belongs to the* affine Krylov space $\boldsymbol{u}_0 + \mathcal{K}_m(A, \boldsymbol{r}_0)$.

Proof. Since the minimal polynomial has degree m, it holds that

$$0 = p_{\min}(A) = \gamma_0 \left(I + \sum_{j=1}^{m} \frac{\gamma_j}{\gamma_0} A^j \right),$$

where $\gamma_0 \neq 0$ because A is invertible (Lemma 3.6). This implies that

$$A^{-1} = -\sum_{j=0}^{m-1} \frac{\gamma_{j+1}}{\gamma_0} A^j,$$

and we conclude by noticing that

$$\boldsymbol{u} = A^{-1}\boldsymbol{f} = -\sum_{j=0}^{m-1} \frac{\gamma_{j+1}}{\gamma_0} A^j \boldsymbol{f}$$

and

$$\boldsymbol{u} = A^{-1}\boldsymbol{f} = A^{-1}(\boldsymbol{f} - A\boldsymbol{u}_0) + \boldsymbol{u}_0 = \boldsymbol{u}_0 + A^{-1}\boldsymbol{r}_0 = \boldsymbol{u}_0 - \sum_{j=0}^{m-1} \frac{\gamma_{j+1}}{\gamma_0} A^j \boldsymbol{r}_0. \qquad \square$$

Notice also that, in general, the Krylov space $\mathcal{K}_m(A, \boldsymbol{f})$ and its affine counterpart $\boldsymbol{u}_0 + \mathcal{K}_m(A, \boldsymbol{r}_0)$ do not coincide. Consider as an example the first two canonical vectors $\boldsymbol{e}_1$ and $\boldsymbol{e}_2$ of $\mathbb{R}^3$, the matrix A of Example 3.9, the vector $\boldsymbol{f} = \boldsymbol{e}_1$, the vector $\boldsymbol{u}_0 = \frac{1}{8}[5\ -2\ 1]^\top$ (which gives $\boldsymbol{r}_0 = \boldsymbol{f} - A\boldsymbol{u}_0 = \boldsymbol{e}_2$), and the spaces $\mathcal{K}_3(A, \boldsymbol{e}_1)$ and $\boldsymbol{u}_0 + \mathcal{K}_3(A, \boldsymbol{e}_2)$. A simple argument allows one to see that $\frac{1}{8}\boldsymbol{e}_1 \in \mathcal{K}_3(A, \boldsymbol{e}_1)$ but $\frac{1}{8}\boldsymbol{e}_1 \notin \boldsymbol{u}_0 + \mathcal{K}_3(A, \boldsymbol{e}_2)$.

Theorem 3.10 anticipates an important feature of Krylov methods that we will see in this chapter: if $\boldsymbol{u}_0$ is the initialization vector, Krylov methods construct the solution $\boldsymbol{u}$ to $A\boldsymbol{u} = \boldsymbol{f}$, exploiting the structure of affine Krylov spaces $\boldsymbol{u}_0 + \mathcal{K}_k(A, \boldsymbol{r}_0)$, where k is the iteration count. Indeed, different Krylov methods exploit these spaces in different manners, as we will see in Section 3.6.

Let us now continue with the analysis of CG by relating its residuals and search directions to the Krylov space.

Lemma 3.11 (Residuals, search directions, and Krylov space – 1). *The residual vectors $\boldsymbol{r}_k$ and the search directions $\boldsymbol{p}_k$ generated by the CG algorithm are contained in the Krylov space,*

$$\boldsymbol{r}_k, \boldsymbol{p}_k \in \mathcal{K}_{k+1}(A, \boldsymbol{r}_0). \tag{3.22}$$

Proof. The proof is by induction. The result clearly holds initially for $k = 0$, because by definition $\boldsymbol{r}_0 = \boldsymbol{p}_0 \in \mathcal{K}_1(A, \boldsymbol{r}_0) = \operatorname{span}\{\boldsymbol{r}_0\}$. So we assume that (3.22) holds for k, and we show that then the same also holds for $k + 1$. Recalling (3.19), that is,

$$\boldsymbol{r}_{k+1} = \boldsymbol{r}_k - \alpha_k A\boldsymbol{p}_k,$$

and using the induction hypothesis $\boldsymbol{r}_k \in \mathcal{K}_{k+1}(A, \boldsymbol{r}_0) \subseteq \mathcal{K}_{k+2}(A, \boldsymbol{r}_0)$, and $\boldsymbol{p}_k \in \mathcal{K}_{k+1}(A, \boldsymbol{r}_0)$, which implies that $A\boldsymbol{p}_k \in \mathcal{K}_{k+2}(A, \boldsymbol{r}_0)$, we obtain the first claim.

Now for the search directions, using (3.13) and the induction hypothesis on $\boldsymbol{p}_k$, we obtain that

$$\boldsymbol{p}_{k+1} = \boldsymbol{r}_{k+1} + \beta_k \boldsymbol{p}_k \in \mathcal{K}_{k+2}(A, \boldsymbol{r}_0),$$

because we have already shown that $\boldsymbol{r}_{k+1} \in \mathcal{K}_{k+2}(A, \boldsymbol{r}_0)$. This concludes the proof. $\square$

Note that the previous result implies that $\boldsymbol{r}_{j-1} \in \mathcal{K}_j(A, \boldsymbol{r}_0) \subseteq \mathcal{K}_k(A, \boldsymbol{r}_0)$ for $j = 1, \ldots, k$. Therefore, we have that

$$\operatorname{span}\{\boldsymbol{r}_0, \ldots, \boldsymbol{r}_{k-1}\} \subset \mathcal{K}_k(A, \boldsymbol{r}_0) \tag{3.23}$$

and

$$\operatorname{span}\{\boldsymbol{p}_0, \ldots, \boldsymbol{p}_{k-1}\} \subset \mathcal{K}_k(A, \boldsymbol{r}_0). \tag{3.24}$$

However, equality holds in both cases. To see this, it is sufficient to notice that, according to Theorem 3.3, residuals and search directions generated by the CG algorithm are linearly independent, hence

$$\dim(\operatorname{span}\{\boldsymbol{r}_0, \ldots, \boldsymbol{r}_{k-1}\}) = k \text{ and } \dim(\operatorname{span}\{\boldsymbol{p}_0, \ldots, \boldsymbol{p}_{k-1}\}) = k.$$

Hence equality in (3.23) and (3.24) follows by noticing that $\dim(\mathcal{K}_k(A, \boldsymbol{r}_0)) \leq k$ (see also Theorem 3.8). We prove this property, independently of Theorem 3.3, in the next lemma; see, e.g., [138].

Lemma 3.12 (Residuals, search directions, and Krylov space – 2). *Consider the vectors $\boldsymbol{r}_j$ and $\boldsymbol{p}_j$ for $j = 0, \ldots, k-1$ generated by the CG iterations till the kth iterate. We have*

$$\operatorname{span}\{\boldsymbol{r}_0, \ldots, \boldsymbol{r}_{k-1}\} = \mathcal{K}_k(A, \boldsymbol{r}_0) \tag{3.25}$$

and

$$\operatorname{span}\{\boldsymbol{p}_0, \ldots, \boldsymbol{p}_{k-1}\} = \mathcal{K}_k(A, \boldsymbol{r}_0). \tag{3.26}$$

Proof. We proceed by induction. The equalities (3.25) and (3.26) are trivially satisfied for $k = 1$. We assume by induction that they are satisfied for some k and we prove that they hold for $k+1$. By Lemma 3.11 we have that $\boldsymbol{r}_k, \boldsymbol{p}_k \in \mathcal{K}_{k+1}(A, \boldsymbol{r}_0)$ for any k, and since $\boldsymbol{r}_{j-1}, \boldsymbol{p}_{j-1} \in \mathcal{K}_j(A, \boldsymbol{r}_0) \subset \mathcal{K}_{k+1}(A, \boldsymbol{r}_0)$ for $j = 1, \ldots, k+1$ we obtain that (3.23) and (3.24) hold for $k+1$. Hence we need to show that the reverse inclusions hold as well. To do so, we first notice that by the induction hypothesis (3.26) we have

$$A^k \boldsymbol{r}_0 = A(A^{k-1}\boldsymbol{r}_0) \in \operatorname{span}\{A\boldsymbol{p}_0, A\boldsymbol{p}_1, \ldots, A\boldsymbol{p}_{k-1}\}. \tag{3.27}$$

Now, since by (3.18) it holds that $A\boldsymbol{p}_j = \frac{1}{\alpha_j}(\boldsymbol{r}_j - \boldsymbol{r}_{j+1})$ for $j = 0, \ldots, k-1$, we obtain from (3.27) that

$$A^k \boldsymbol{r}_0 \in \operatorname{span}\{\boldsymbol{r}_0, \boldsymbol{r}_1, \ldots, \boldsymbol{r}_{k-1}, \boldsymbol{r}_k\}. \tag{3.28}$$

By combining (3.28) with the induction hypothesis (3.25), we get

$$\mathcal{K}_{k+1}(A, \boldsymbol{r}_0) = \operatorname{span}\{\boldsymbol{r}_0, A\boldsymbol{r}_0, \ldots, A^{k-1}\boldsymbol{r}_0, A^k\boldsymbol{r}_0\} \subset \operatorname{span}\{\boldsymbol{r}_0, \boldsymbol{r}_1, \ldots, \boldsymbol{r}_{k-1}, \boldsymbol{r}_k\}.$$

Therefore, (3.25) holds also for $k+1$. Next, we show that (3.26) continues to hold when k is replaced by $k+1$. Indeed,

$$\begin{aligned}
&\operatorname{span}\{\boldsymbol{p}_0, \boldsymbol{p}_1, \ldots, \boldsymbol{p}_{k-1}, \boldsymbol{p}_k\} \\
&\quad = \operatorname{span}\{\boldsymbol{p}_0, \boldsymbol{p}_1, \ldots, \boldsymbol{p}_{k-1}, \boldsymbol{r}_k\} && \text{(by (3.13))} \\
&\quad = \operatorname{span}\{\boldsymbol{r}_0, A\boldsymbol{r}_0, \ldots, A^{k-1}\boldsymbol{r}_0, \boldsymbol{r}_k\} && \text{(by the induction hypothesis (3.26))} \\
&\quad = \operatorname{span}\{\boldsymbol{r}_0, \boldsymbol{r}_1, \ldots, \boldsymbol{r}_{k-1}, \boldsymbol{r}_k\} && \text{(by (3.25) for } k\text{)} \\
&\quad = \operatorname{span}\{\boldsymbol{r}_0, A\boldsymbol{r}_0, \ldots, A^{k-1}\boldsymbol{r}_0, A^k\boldsymbol{r}_0\} && \text{(by (3.25) for } k+1\text{),}
\end{aligned}$$

which is (3.26) for $k+1$. ∎

Remark 1. *Note that recalling $\boldsymbol{r}_k \perp \boldsymbol{r}_j$ for $j = 0, 1, \ldots, k-1$, and* (3.25)*, that is $\mathcal{K}_k(A, \boldsymbol{r}_0) = \operatorname{span}\{\boldsymbol{r}_0, \ldots, \boldsymbol{r}_{k-1}\}$, we have that*

$$\boldsymbol{r}_k \perp \mathcal{K}_k(A, \boldsymbol{r}_0).$$

We next show that the CG algorithm finds at iteration k the best approximation of the unknown solution $\boldsymbol{u}$ of the linear system $A\boldsymbol{u} = \boldsymbol{f}$ in the *affine Krylov space* $\boldsymbol{u}_0 + \mathcal{K}_k(A, \boldsymbol{r}_0)$ (recall also Theorem 3.10) in the energy norm $\|\boldsymbol{v}\|_A := \sqrt{\boldsymbol{v}^\top A \boldsymbol{v}}$, also called the A-norm.

Lemma 3.13 (Best approximation property of CG). *Let $\boldsymbol{u}$ be the solution of $A\boldsymbol{u} = \boldsymbol{f}$, with $A \in \mathbb{R}^{n \times n}$ symmetric and positive definite. Then, at iteration k, the approximation $\boldsymbol{u}_k$ computed by CG minimizes the A-norm of the error,*

$$\boldsymbol{u}_k = \underset{\widetilde{\boldsymbol{u}} \in \boldsymbol{u}_0 + \mathcal{K}_k(A, \boldsymbol{r}_0)}{\arg\min} \|\boldsymbol{u} - \widetilde{\boldsymbol{u}}\|_A. \tag{3.29}$$

Proof. We first show that $\boldsymbol{u}_k \in \boldsymbol{u}_0 + \mathcal{K}_k(A, \boldsymbol{r}_0)$,

$$\boldsymbol{u}_k = \boldsymbol{u}_{k-1} + \alpha_{k-1}\boldsymbol{p}_{k-1} = \boldsymbol{u}_{k-2} + \alpha_{k-2}\boldsymbol{p}_{k-2} + \alpha_{k-1}\boldsymbol{p}_{k-1} = \cdots = \boldsymbol{u}_0 + \sum_{j=0}^{k-1} \alpha_j \boldsymbol{p}_j,$$

and $\boldsymbol{p}_{j-1} \in \mathcal{K}_j(A, \boldsymbol{r}_0) \subseteq \mathcal{K}_k(A, \boldsymbol{r}_0)$ for $j = 1, 2, \ldots, k$ (see Lemma 3.11), and hence

$$\boldsymbol{u}_k \in \boldsymbol{u}_0 + \mathcal{K}_k(A, \boldsymbol{r}_0).$$

Now let $\widetilde{\boldsymbol{u}} := \boldsymbol{u}_k + \delta\boldsymbol{u}$ for some $\delta\boldsymbol{u} \in \mathcal{K}_k(A, \boldsymbol{r}_0)$. This implies that $\widetilde{\boldsymbol{u}} \in \boldsymbol{u}_0 + \mathcal{K}_k(A, \boldsymbol{r}_0)$, and we obtain

$$\begin{aligned}
\|\boldsymbol{u} - \widetilde{\boldsymbol{u}}\|_A^2 &= (\boldsymbol{u} - \widetilde{\boldsymbol{u}})^\top A(\boldsymbol{u} - \widetilde{\boldsymbol{u}}) \\
&= (\boldsymbol{u} - \boldsymbol{u}_k - \delta\boldsymbol{u})^\top A(\boldsymbol{u} - \boldsymbol{u}_k - \delta\boldsymbol{u}) \\
&= (\boldsymbol{u} - \boldsymbol{u}_k)^\top A(\boldsymbol{u} - \boldsymbol{u}_k) - \delta\boldsymbol{u}^\top A(\boldsymbol{u} - \boldsymbol{u}_k) \\
&\quad -(\boldsymbol{u} - \boldsymbol{u}_k)^\top A\delta\boldsymbol{u} + \delta\boldsymbol{u}^\top A\delta\boldsymbol{u} \\
&= \|\boldsymbol{u} - \boldsymbol{u}_k\|_A^2 - 2\delta\boldsymbol{u}^\top A(\boldsymbol{u} - \boldsymbol{u}_k) + \|\delta\boldsymbol{u}\|_A^2 \\
&= \|\boldsymbol{u} - \boldsymbol{u}_k\|_A^2 + \|\delta\boldsymbol{u}\|_A^2,
\end{aligned}$$

where we used that $A^\top = A$ for the second to last line, and for the last line the orthogonality of the residuals to the Krylov space from Remark 1,

$$A(\boldsymbol{u} - \boldsymbol{u}_k) = \boldsymbol{f} - A\boldsymbol{u}_k = \boldsymbol{r}_k \perp \mathcal{K}_k(A, \boldsymbol{r}_0),$$

which implies that the mixed term $2\delta\boldsymbol{u}^\top A(\boldsymbol{u} - \boldsymbol{u}_{k+1}) = 0$, since $\delta\boldsymbol{u} \in \mathcal{K}_k(A, \boldsymbol{r}_0)$. Therefore $\|\boldsymbol{u} - \widetilde{\boldsymbol{u}}\|_A^2$ is minimal if $\delta\boldsymbol{u} = 0$, which means that $\boldsymbol{u}_k = \widetilde{\boldsymbol{u}}$, the solution of the best approximation problem (3.29). □

We next show that the best approximation problem can be interpreted as a polynomial approximation problem.

Lemma 3.14 (Polynomial best approximation property of CG). *Under the same hypotheses as in Lemma 3.13, we have*

$$\|\boldsymbol{u} - \boldsymbol{u}_k\|_A = \min_{\substack{p \in \mathcal{P}_k \\ p(0)=1}} \|p(A)(\boldsymbol{u} - \boldsymbol{u}_0)\|_A,$$

where $\mathcal{P}_k$ denotes the set of polynomials[22] of degree lower than or equal to k and $\boldsymbol{u}_0$ is a given initial guess.

Proof. Recalling Definition 3.4, we have

$$\boldsymbol{u}_k \in \boldsymbol{u}_0 + \mathcal{K}_k(A, \boldsymbol{r}_0) = \boldsymbol{u}_0 + \text{span}\{\boldsymbol{r}_0, A\boldsymbol{r}_0, \ldots, A^{k-1}\boldsymbol{r}_0\},$$

which implies that there exist coefficients γ_j such that

$$\boldsymbol{u}_k = \boldsymbol{u}_0 + \sum_{j=0}^{k-1} \gamma_j A^j \boldsymbol{r}_0 = \boldsymbol{u}_0 + q_{k-1}(A)\boldsymbol{r}_0$$

[22] With the condition $p(0) = 1$ these are called residual polynomials.

for the polynomial $q_{k-1}(x) := \sum_{j=0}^{k-1} \gamma_j x^j$ with $q_{k-1} \in \mathcal{P}_{k-1}$. Similarly, for any $\widetilde{\boldsymbol{u}} \in \boldsymbol{u}_0 + \mathcal{K}_k(A, \boldsymbol{r}_0)$ we have that $\widetilde{\boldsymbol{u}} = \boldsymbol{u}_0 + \widetilde{q}(A)\boldsymbol{r}_0$ for some polynomial $\widetilde{q} \in \mathcal{P}_{k-1}$. Now from Lemma 3.13, we know that $\boldsymbol{u}_k$ minimizes the error in the A-norm,

$$\begin{aligned}
\|\boldsymbol{u} - \boldsymbol{u}_k\|_A &= \min_{\widetilde{\boldsymbol{u}} \in \boldsymbol{u}_0 + \mathcal{K}_k(A, \boldsymbol{r}_0)} \|\boldsymbol{u} - \widetilde{\boldsymbol{u}}\|_A \\
&= \min_{\widetilde{q} \in \mathcal{P}_{k-1}} \|\boldsymbol{u} - (\boldsymbol{u}_0 + \widetilde{q}(A)\boldsymbol{r}_0)\|_A \\
&= \min_{\widetilde{q} \in \mathcal{P}_{k-1}} \|\boldsymbol{u} - (\boldsymbol{u}_0 + \widetilde{q}(A)(\boldsymbol{f} - A\boldsymbol{u}_0))\|_A \\
&= \min_{\widetilde{q} \in \mathcal{P}_{k-1}} \|\boldsymbol{u} - (\boldsymbol{u}_0 + \widetilde{q}(A)A(\boldsymbol{u} - \boldsymbol{u}_0))\|_A \\
&= \min_{\substack{p \in \mathcal{P}_k \\ p(0)=1}} \|p(A)(\boldsymbol{u} - \boldsymbol{u}_0)\|_A,
\end{aligned}$$

where on the last line the new polynomial $p(x) = 1 - \widetilde{q}(x)x$ is in $\mathcal{P}_k$ since $\widetilde{q}(x)$ is in $\mathcal{P}_{k-1}$, and $p(0) = 1$. ∎

Corollary 3.15 (Convergence of CG in finite number of iterations). *If the (symmetric positive definite) matrix A has $m \leq n$ distinct eigenvalues, then CG converges in at most m steps.*

Proof. Since A is diagonalizable and has m distinct eigenvalues, Lemma 3.6(b) implies that the minimal polynomial $p_{\min}$ of A has degree m. Moreover, since A is invertible, Lemma 3.6 ensures that the constant coefficient c_0 of the minimal polynomial $p_{\min}$ is nonzero. Hence we can define the polynomial $p^*_{\min} := p_{\min}/c_0$ that satisfies $p^*_{\min}(0) = 1$ and $p^*_{\min}(A) = 0$ and has degree m. Therefore, by Lemma 3.14 at the mth iterate we have

$$\|\boldsymbol{u} - \boldsymbol{u}_m\|_A = \min_{\substack{p \in \mathcal{P}_m \\ p(0)=1}} \|p(A)(\boldsymbol{u} - \boldsymbol{u}_0)\|_A \leq \|p^*_{\min}(A)(\boldsymbol{u} - \boldsymbol{u}_0)\|_A = 0,$$

which implies the claim. ∎

In order to obtain a convergence estimate for CG, we need the *Chebyshev polynomials*, which go back to the work by Chebyshev on minimizing the wear and tear of the transmission used in steam engines from the cylinder to the wheels [34].

Definition 3.16 (Chebyshev polynomials). *The* Chebyshev polynomials $T_k(t)$ *are defined by*

$$T_k(t) := \cos(k \arccos t), \quad -1 \leq t \leq 1, \quad k = 0, 1, 2, \ldots. \tag{3.30}$$

We show in Figure 3.8 the first seven Chebyshev polynomials, which we plotted using the Maple commands

```
> with(orthopoly);
> plot([seq(T(i,t),i=0..6)],t=-1..1);
```

The definition of T_k does not readily reveal that it is a polynomial, but when evaluating the first ones, we find

$$\begin{aligned}
T_0(t) &= \cos(0 \arccos t) = \cos(0) = 1, \\
T_1(t) &= \cos(1 \arccos t) = t, \\
T_2(t) &= \cos(2 \arccos t) = \cos(\arccos t)^2 - \sin(\arccos t)^2 = t^2 - (1 - t^2) = 2t^2 - 1,
\end{aligned}$$

where we used on the last line the trigonometric identities $\cos(a + b) = \cos a \cos b - \sin a \sin b$ and $\sin^2 x + \cos^2 x = 1$. It is not convenient, however, to continue in this fashion. A better

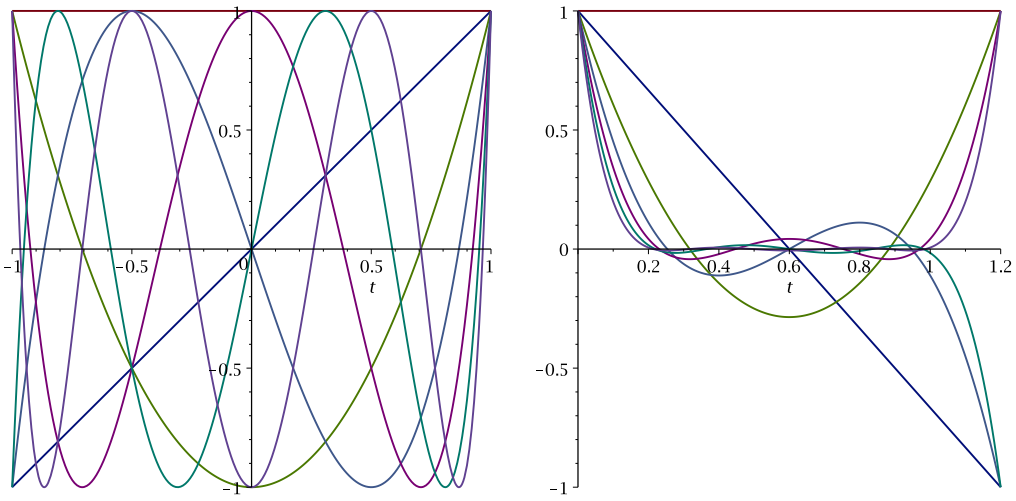

Figure 3.8. *The first seven Chebyshev polynomials on the left, and the shifted scaled ones on the right.*

approach is to sum the trigonometric identities

$$\cos((k+1)\alpha) = \cos(k\alpha + \alpha) = \cos(k\alpha)\cos\alpha - \sin(k\alpha)\sin\alpha$$

and

$$\cos((k-1)\alpha) = \cos(k\alpha - \alpha) = \cos(k\alpha)\cos\alpha + \sin(k\alpha)\sin\alpha,$$

leading to

$$\cos((k+1)\alpha) + \cos((k-1)\alpha) = 2\cos(k\alpha)\cos\alpha,$$

which translates by inserting $\alpha = \arccos t$ into the well-known *three-term recurrence relation* for Chebyshev polynomials,

$$T_0(t) = 1, \quad T_1(t) = t, \quad T_{k+1}(t) = 2tT_k(t) - T_{k-1}(t), \quad k = 1, 2, \ldots. \tag{3.31}$$

From this recurrence relation, we can clearly see now that the $T_k(t)$ are polynomials of degree k.

For k even, T_k is an even function, i.e., $T_k(t) = T_k(-t)$ for all t. This can be proved by induction from the recurrence relation. Similarly, for k odd, we have $T_k(t) = -T_k(-t)$. These properties can also be observed in Figure 3.8.

The important result related to Chebyshev polynomials we will need for the convergence analysis is that the polynomial which solves the min-max problem

$$\widetilde{p} = \arg\min_{\substack{p\in\mathcal{P}_k \\ p(0)=1}} \max_{\substack{t\in[\alpha,\beta] \\ 0\notin[\alpha,\beta]}} |p(t)|, \tag{3.32}$$

i.e., the smallest polynomial on the interval $[\alpha, \beta]$ which equals one at zero, is the following shifted and scaled Chebyshev polynomial (see, e.g., [160, Section 6.11]):

$$\widetilde{p}(t) = \frac{T_k(1 - 2\frac{\beta - t}{\beta - \alpha})}{T_k(1 - 2\frac{\beta}{\beta - \alpha})}. \tag{3.33}$$

The first few such polynomials are shown in Figure 3.8 on the right, plotted with the Maple commands

```
> with(orthopoly);
> a:=0.2;b:=1;
> plot([seq(T(i,1-2*(b-t)/(b-a))/T(i,1-2*b/(b-a)),i=0..6)],t=0..1.2);
```

We can clearly see how they become small very rapidly in the interval $[\alpha, \beta]$ as the degree increases and how they equioscillate around the maximum on the interval $[\alpha, \beta]$ and grow rapidly outside the interval. These would have been the polynomials Richardson could have used in the true Richardson's method (3.1); see also Figure 2.16, where he tried by trial and error to find a good such polynomial. Before we show that CG converges at least as fast as such an optimized true Richardson's method, which was realized by the Chebyshev semi-iterative method of *Gene Golub* [90], we need a final property of the Chebyshev polynomials, which appears naturally when we generalize the argument $t \in \mathbb{R}$ to a complex argument $z \in \mathbb{C}$.

Lemma 3.17 (Complex representation of Chebyshev polynomials). *The Chebyshev polynomials can also be expressed as*

$$T_k(z) = \frac{w^k + w^{-k}}{2}, \quad z = (w + w^{-1})/2, \quad \textit{with } w, z \in \mathbb{C}. \tag{3.34}$$

Proof. We verify by induction that the quantities $T_k(z)$ defined by (3.34) obey the three-term recurrence relation (3.31). For $k = 0$ we have $T_0(z) = (w^0 + w^{-0})/2 = 1$, and it is clear that $T_1(z) = (w + w^{-1})/2 = z$. So we assume now that (3.34) holds for $j \le k$. Then

$$\begin{aligned} T_{k+1}(z) &= 2zT_k(z) - T_{k-1}(z) \\ &= (w + w^{-1})\frac{w^k + w^{-k}}{2} - \frac{w^{k-1} + w^{-(k-1)}}{2} \\ &= \frac{w^{k+1} + w^{-k+1} + w^{k-1} + w^{-k-1} - w^{k-1} - w^{-(k-1)}}{2} \\ &= \frac{w^{k+1} + w^{-(k+1)}}{2}, \end{aligned}$$

which concludes the proof. □

Note that if we solve the equation

$$z = (w + w^{-1})/2 \quad \Longleftrightarrow \quad w^2 - 2zw + 1 = 0$$

for w, we get the two solutions

$$w_1 = z + \sqrt{z^2 - 1}, \quad w_2 = z - \sqrt{z^2 - 1} = \frac{1}{w_1}.$$

Hence, we have $w_1 = \frac{1}{w_2}$. Thus $T_k(z)$ does not depend on which root is chosen, and we find in either case

$$T_k(z) = \frac{\left(z + \sqrt{z^2 - 1}\right)^k + \left(z - \sqrt{z^2 - 1}\right)^k}{2}. \tag{3.35}$$

We are now ready to prove a convergence estimate for CG.

Theorem 3.18 (Convergence estimate for CG). *Let $\boldsymbol{u} \in \mathbb{R}^n$ be the solution of $A\boldsymbol{u} = \boldsymbol{f}$, with $A \in \mathbb{R}^{n\times n}$ symmetric and positive definite with $\lambda_{\max} > \lambda_{\min}$, and $\boldsymbol{f} \in \mathbb{R}^n$ with a given initial guess $\boldsymbol{u}_0 \in \mathbb{R}^n$. Then the approximation $\boldsymbol{u}_k$ computed by CG satisfies the estimate*

$$\|\boldsymbol{u} - \boldsymbol{u}_k\|_A \le 2\left(\frac{\sqrt{\kappa(A)} - 1}{\sqrt{\kappa(A)} + 1}\right)^k \|\boldsymbol{u} - \boldsymbol{u}_0\|_A, \tag{3.36}$$

where $\kappa(A) = \frac{\lambda_{\max}(A)}{\lambda_{\min}(A)}$ is the condition number of the matrix A.

Proof. From Lemma 3.14 we have that

$$\|\boldsymbol{u} - \boldsymbol{u}_k\|_A = \min_{\substack{p \in \mathcal{P}_k \\ p(0)=1}} \|p(A)(\boldsymbol{u} - \boldsymbol{u}_0)\|_A. \tag{3.37}$$

Since A is symmetric, its Schur decomposition is $A = Q\Lambda Q^\top$, with

$$Q = \begin{bmatrix} \boldsymbol{q}_1, \boldsymbol{q}_2, \ldots, \boldsymbol{q}_n \end{bmatrix} \quad \text{and} \quad \Lambda = \begin{bmatrix} \lambda_1 & & & \\ & \lambda_2 & & \\ & & \ddots & \\ & & & \lambda_n \end{bmatrix},$$

where Q is orthogonal and $\boldsymbol{q}_j$ and λ_j are the eigenvectors and the eigenvalues of A. Recall that since $A \in \mathbb{R}^{n\times n}$ is symmetric positive definite, its eigenvectors form a basis for $\mathbb{R}^n$. Therefore, we can decompose $\boldsymbol{u} - \boldsymbol{u}_0$ into eigenvectors of A and obtain

$$\boldsymbol{u} - \boldsymbol{u}_0 = \sum_{j=1}^{n} \gamma_j \boldsymbol{q}_j$$

for appropriate scalars γ_j. This implies that

$$p(A)(\boldsymbol{u} - \boldsymbol{u}_0) = \sum_{j=1}^{n} \gamma_j p(A)\boldsymbol{q}_j = \sum_{j=1}^{n} \gamma_j p(\lambda_j)\boldsymbol{q}_j, \tag{3.38}$$

where we used that $\boldsymbol{q}_j$ are eigenvectors of A. Moreover, using that $Q^\top(\boldsymbol{u}-\boldsymbol{u}_0) = Q^\top \sum_{j=1}^n \gamma_j \boldsymbol{q}_j$ $= \sum_{j=1}^n \gamma_j \boldsymbol{e}_j$, where $\boldsymbol{e}_j$ denotes the jth canonical vector, we get

$$\begin{aligned} \|\boldsymbol{u} - \boldsymbol{u}_0\|_A^2 &= (\boldsymbol{u} - \boldsymbol{u}_0)^\top A(\boldsymbol{u} - \boldsymbol{u}_0) \\ &= (\boldsymbol{u} - \boldsymbol{u}_0)^\top Q\Lambda Q^\top(\boldsymbol{u} - \boldsymbol{u}_0) \\ &= (Q^\top(\boldsymbol{u} - \boldsymbol{u}_0))^\top \Lambda (Q^\top(\boldsymbol{u} - \boldsymbol{u}_0)) \\ &= \sum_{j=1}^{n} \gamma_j^2 \lambda_j. \end{aligned} \tag{3.39}$$

Using (3.38) and (3.39), we obtain

$$\begin{aligned} \|p(A)(\boldsymbol{u} - \boldsymbol{u}_0)\|_A^2 &= \Big(p(A)(\boldsymbol{u} - \boldsymbol{u}_0)\Big)^\top A\Big(p(A)(\boldsymbol{u} - \boldsymbol{u}_0)\Big) \\ &= \left(\sum_{j=1}^{n} \gamma_j p(\lambda_j)\boldsymbol{q}_j\right)^\top Q\Lambda Q^\top \left(\sum_{j=1}^{n} \gamma_j p(\lambda_j)\boldsymbol{q}_j\right) \\ &= \sum_{j=1}^{n} (p(\lambda_j))^2 \gamma_j^2 \lambda_j \le \Big(\max_{j=1,2,\ldots} |p(\lambda_j)|^2\Big) \sum_{j=1}^{n} \gamma_j^2 \lambda_j \\ &= \Big(\max_{j=1,2,\ldots} |p(\lambda_j)|^2\Big) \|\boldsymbol{u} - \boldsymbol{u}_0\|_A^2. \end{aligned}$$

Next, we denote by $\lambda_{\max}$ and $\lambda_{\min}$ the maximum and minimum eigenvalues of A. By taking the square root, and estimating over the entire interval that contains the positive eigenvalues of A instead of the discrete set, we get

$$\|p(A)(\boldsymbol{u} - \boldsymbol{u}_0)\|_A \le \max_{\lambda \in [\lambda_{\min}, \lambda_{\max}]} |p(\lambda)| \|\boldsymbol{u} - \boldsymbol{u}_0\|_A. \tag{3.40}$$

Replacing (3.40) into (3.37) leads to

$$\|\boldsymbol{u}-\boldsymbol{u}_k\|_A \leq \min_{\substack{p\in\mathcal{P}_k\\ p(0)=1}} \max_{\lambda\in[\lambda_{\min},\lambda_{\max}]} |p(\lambda)|\|\boldsymbol{u}-\boldsymbol{u}_0\|_A. \tag{3.41}$$

Now, the polynomial that solves the min-max problem on the right-hand side of (3.41), that is, the smallest on the interval $[\lambda_{\min},\lambda_{\max}]$ with $p(0)=1$, is the real, scaled, and shifted Chebyshev polynomial

$$\widetilde{p}(\lambda) := \frac{T_k\Big(1-2\frac{\lambda_{\max}-\lambda}{\lambda_{\max}-\lambda_{\min}}\Big)}{T_k\Big(1-2\frac{\lambda_{\max}}{\lambda_{\max}-\lambda_{\min}}\Big)},$$

where T_k is the Chebyshev polynomial defined on the interval $[-1,1]$. Recall that $\lambda_{\max}>\lambda_{\min}$. We have

$$\begin{aligned}\max_{\lambda\in[\lambda_{\min},\lambda_{\max}]} |\widetilde{p}(\lambda)| &= \frac{1}{\Big|T_k\Big(1-2\frac{\lambda_{\max}}{\lambda_{\max}-\lambda_{\min}}\Big)\Big|} = \frac{1}{\Big|T_k\Big(\frac{\lambda_{\max}-\lambda_{\min}-2\lambda_{\max}}{\lambda_{\max}-\lambda_{\min}}\Big)\Big|}\\ &= \frac{1}{\Big|T_k\Big(\frac{\lambda_{\max}+\lambda_{\min}}{\lambda_{\max}-\lambda_{\min}}\Big)\Big|},\end{aligned}$$

where we used the properties of T_k; see Figure 3.8. Recalling that $\kappa(A)=\frac{\lambda_{\max}}{\lambda_{\min}}$, we obtain

$$\max_{\lambda\in[\lambda_{\min},\lambda_{\max}]} |\widetilde{p}(\lambda)| = \frac{1}{\Big|T_k\Big(\frac{\kappa(A)+1}{\kappa(A)-1}\Big)\Big|}. \tag{3.42}$$

Using the complex representation (3.34) given in Lemma 3.17, that is,

$$T_k(z)=\frac{w^k+w^{-k}}{2}, \quad z=\frac{w+w^{-1}}{2}, \quad \text{with } w,z\in\mathbb{C},$$

we find (for $z=\frac{\kappa(A)+1}{\kappa(A)-1}$) that

$$w^2-2zw+1 = w^2-2\frac{\kappa(A)+1}{\kappa(A)-1}w+1=0,$$

which is solved by

$$\begin{aligned} w &= \frac{\kappa(A)+1}{\kappa(A)-1}+\sqrt{\Big(\frac{\kappa(A)+1}{\kappa(A)-1}\Big)^2-1}\\ &= \frac{\kappa(A)+1+\sqrt{(\kappa(A)+1)^2-(\kappa(A)-1)^2}}{\kappa(A)-1}\\ &= \frac{\kappa(A)+1+\sqrt{4\kappa(A)}}{\kappa(A)-1}\\ &= \frac{(\sqrt{\kappa(A)}+1)^2}{(\sqrt{\kappa(A)}+1)(\sqrt{\kappa(A)}-1)}\\ &= \frac{\sqrt{\kappa(A)}+1}{\sqrt{\kappa(A)}-1}.\end{aligned}$$

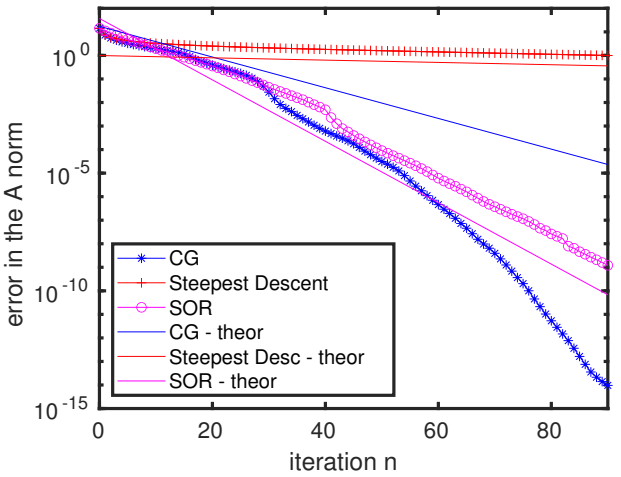

Figure 3.9. *Decay of the error when using Steepest Descent, SOR with optimized parameter, and CG, together with the theoretical convergence estimates.*

Therefore, we have that

$$T_k(z) = \frac{1}{2}\left[\left(\frac{\sqrt{\kappa(A)}+1}{\sqrt{\kappa(A)}-1}\right)^k + \left(\frac{\sqrt{\kappa(A)}+1}{\sqrt{\kappa(A)}-1}\right)^{-k}\right]. \tag{3.43}$$

Finally, by combining (3.41), (3.42), and (3.43), we obtain

$$\begin{aligned}\|\boldsymbol{u}-\boldsymbol{u}_k\|_A &\le \frac{2}{\left(\frac{\sqrt{\kappa(A)}+1}{\sqrt{\kappa(A)}-1}\right)^k + \left(\frac{\sqrt{\kappa(A)}+1}{\sqrt{\kappa(A)}-1}\right)^{-k}}\|\boldsymbol{u}-\boldsymbol{u}_0\|_A \\ &= \frac{2\left(\frac{\sqrt{\kappa(A)}-1}{\sqrt{\kappa(A)}+1}\right)^k}{1+\left(\frac{\sqrt{\kappa(A)}-1}{\sqrt{\kappa(A)}+1}\right)^{2k}}\|\boldsymbol{u}-\boldsymbol{u}_0\|_A \\ &\le 2\left(\frac{\sqrt{\kappa(A)}-1}{\sqrt{\kappa(A)}+1}\right)^k\|\boldsymbol{u}-\boldsymbol{u}_0\|_A,\end{aligned}$$

which is our claim. □

Note that in the last step of the proof, we neglected the additional term in the denominator, which becomes small when the iteration number k becomes large, so the estimate remains sharp for k large. For k small, however, especially if the condition number $\kappa(A)$ is large, this term compensates for almost the additional factor 2 in the estimate. Notice that, using (3.36), a similar estimate can be obtained in the norm $\|\cdot\|_2$; see Problem 39.

We show in Figure 3.9 a comparison of the convergence of Steepest Descent, SOR with the optimally chosen parameter, and the CG algorithm applied to the discretized Laplace problem on the unit square with 16 gridpoints, whose solution was shown in Figure 1.11. We measured the error in the A-norm and also plot the convergence estimate we proved in Theorem 3.1 for

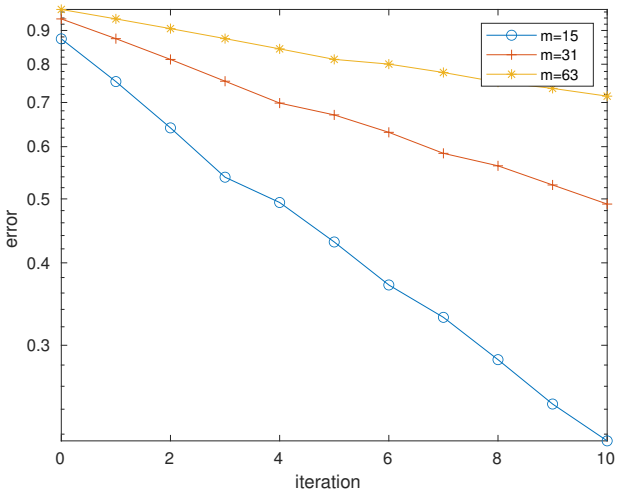

Figure 3.10. *Convergence of CG for different mesh sizes* $h = \frac{1}{m+1}$.

Steepest Descent, the asymptotic contraction factor of SOR from (2.44), and the convergence estimate from Theorem 3.18 for CG. We see that Steepest Descent is clearly the slowest method, a good local tactic is not necessarily good for an efficient global strategy, and the convergence estimate we proved is accurate. The CG method on the other hand is by far the fastest asymptotically. It only initially follows the pessimistic convergence estimate from Theorem 3.18, and then speeds up after about 30 iterations. SOR with optimized parameter is initially as fast as CG, but is then beaten after about 30 iterations in this example. This shows that well-tuned stationary iterative methods can still be interesting, and we will see in Chapter 4 that it is precisely such methods that lead to the best preconditioners when they are used combined with Krylov acceleration.

Preconditioners are necessary, since CG, and Krylov methods in general, cannot remove the mesh dependence of their convergence, since they still use only local connections between the gridpoints in the discretization matrix when performing the matrix vector products, even though an optimal polynomial combination is then used to approximate the solution. This we can see already in Figure 3.7, where still unknowns with small y coordinate are not improving their approximation and remain at zero. We illustrate this in Figure 3.10, where we see how the error decreases as the iterations progress when CG is used to solve our Laplace model problem from Section 1.3 for the mesh we used for Figure 3.7 with $m = 15$ interior mesh points, and two refined meshes with $m = 31$ and $m = 63$ interior mesh points. The convergence deterioration of CG can be also seen by studying the convergence factor estimated in Theorem 3.18 as a function of the grid size h. The expansion of this convergence factor around zero leads to

$$\frac{\sqrt{\kappa(A)} - 1}{\sqrt{\kappa(A)} + 1} = 1 - \pi h + O(h^2),$$

which is similar to the result obtained for SOR (with optimal parameter) and shows clearly that CG behaves better than Jacobi, Gauss–Seidel, and Steepest Descent. Moreover, notice that asymptotically CG converges faster than the predicted theoretical upper bound (see also Figure 3.9) because its optimized residual polynomial becomes better and better adapted to the concrete spectrum of the system matrix, not just the interval containing the spectrum.

3.3 ▪ The Arnoldi iteration

> *An interpretation of Dr. Cornelius Lanczos' iteration method, which he has named "minimized iterations", is discussed in this article, expounding the method as applied to the solution of the characteristic matrix equations both in homogeneous and non-homogeneous form. This interpretation leads to a variation of the Lanczos procedure which may frequently be advantageous by virtue of reducing the volume of numerical work in practical applications. Both methods employ essentially the same algorithm, requiring the generation of a series of orthogonal functions through which a simple matrix equation of reduced order is established.*
>
> Walter E. Arnoldi, *The Principle of Minimized Iterations in the Solution of the Matrix Eigenvalue Problem*, 1951.

The *Arnoldi iteration* was invented by *Walter E. Arnoldi* in 1951 [1] following the invention of the Lanczos algorithm by *Cornelius Lanczos* in 1950 [121] (see the quote above), but we start here with the Arnoldi iteration, because then the Lanczos process treated in the next section becomes just a special case for symmetric positive definite matrices.

Each matrix $A \in \mathbb{R}^{n\times n}$ can be transformed by an orthogonal matrix $Q \in \mathbb{R}^{n\times n}$ into an upper Hessenberg matrix $H \in \mathbb{R}^{n\times n}$,

$$H = Q^\top AQ \quad (\Longleftrightarrow\ A = QHQ^\top), \tag{3.44}$$

where the upper Hessenberg matrix has only zero entries in the lower triangular part except for next to the diagonal, i.e., $H_{i,j} = 0$ for $i > j+1$. This can be achieved for example using Givens rotations or Householder reflections; see [86, Section 7.5]. Arnoldi first considered only the first k columns of the matrix Q,

$$Q_k := [\boldsymbol{q}_1, \boldsymbol{q}_2, \ldots, \boldsymbol{q}_k]\,.$$

From (3.44), we have

$$AQ = QH,$$

and if we only consider the first k columns, we get

$$A\,[\boldsymbol{q}_1, \boldsymbol{q}_2, \ldots, \boldsymbol{q}_k] = \big[\boldsymbol{q}_1, \boldsymbol{q}_2, \ldots, \boldsymbol{q}_{k+1}\big] \begin{bmatrix} h_{11} & h_{12} & \cdots & h_{1k} \\ h_{21} & h_{22} & \cdots & h_{2k} \\ & \ddots & \ddots & \vdots \\ & & \ddots & h_{k,k} \\ & & & h_{k+1,k} \end{bmatrix}$$

or

$$AQ_k = Q_{k+1}H_k.$$

The kth column in this matrix identity states

$$A\boldsymbol{q}_k = \sum_{j=1}^{k+1} h_{jk}\boldsymbol{q}_j \quad \Longleftrightarrow \quad h_{k+1,k}\boldsymbol{q}_{k+1} = A\boldsymbol{q}_k - \sum_{j=1}^{k} h_{jk}\boldsymbol{q}_j. \tag{3.45}$$

Hence, if we know the first k vectors $\boldsymbol{q}_1$, $\boldsymbol{q}_1$, …, $\boldsymbol{q}_k$, we can compute $\boldsymbol{q}_{k+1}$. In fact, (3.45) is just an orthogonalization of a new vector $A\boldsymbol{q}_k$ with respect to the already known vectors $\boldsymbol{q}_j$, $j = 1, 2, \ldots, k$. If one uses the (modified) Gram–Schmidt orthogonalization process to do this, we obtain, starting with an arbitrary vector $\boldsymbol{b}$, the Arnoldi iteration

```
function [H,Q,v]=Arnoldi(A,b,k)
% ARNOLDI Arnoldi iteration
```

```
%   [H,Q,v]=Arnoldi(A,b,k) applies k<=n steps of the Arnoldi iteration to
%   the matrix A starting with the vector b. Computes Q orthogonal and
%   H upper Hessenberg such that AQ=QH+ve_k^T, with Q(:,1)=b/norm(b).

Q(:,1)=b/norm(b);
for j=1:k
  v=A*Q(:,j);
  for i=1:j
    H(i,j)=Q(:,i)'*v;
    v=v-H(i,j)*Q(:,i);
  end
  if j<k
    H(j+1,j)=norm(v);
    if H(j+1,j)<1e-15, disp('lucky breakdown'); break; end
    Q(:,j+1)=v/H(j+1,j);
  end
end
```

Notice that in the previous algorithm the vector v given as an output is $\mathtt{v} = A\boldsymbol{q}_k - \sum_{j=1}^{k} h_{jk}\boldsymbol{q}_j$. The output matrices of the algorithm are $\mathtt{Q} = Q_k \in \mathbb{R}^{n\times k}$ and $\mathtt{H} \in \mathbb{R}^{k\times k}$, and observe that

$$\begin{aligned} AQ_k = Q_{k+1}H_k &= \begin{bmatrix} Q_k & \boldsymbol{q}_{k+1} \end{bmatrix} \begin{bmatrix} \mathtt{H} \\ h_{k+1,k}\boldsymbol{e}_k^\top \end{bmatrix} = Q_k\mathtt{H} + h_{k+1,k}\boldsymbol{q}_{k+1}\boldsymbol{e}_k^\top \\ &= Q_k\mathtt{H} + \Big(A\boldsymbol{q}_k - \sum_{j=1}^{k} h_{jk}\boldsymbol{q}_j\Big)\boldsymbol{e}_k^\top = \mathtt{QH} + \mathtt{v}\boldsymbol{e}_k^\top, \end{aligned} \tag{3.46}$$

where $\boldsymbol{e}_k$ denotes the kth canonical vector and we used (3.45). Notice that $\mathtt{H}\in \mathbb{R}^{k\times k}$ is the matrix $H_k \in \mathbb{R}^{k+1\times k}$ without the last row.

Moreover, we remark that $h_{j+1,j}$ is posed to be equal to $\|\mathtt{v}\|_2$. This can be explained by noticing that $\mathtt{v} = A\boldsymbol{q}_k - \sum_{j=1}^{k} h_{jk}\boldsymbol{q}_j = h_{k+1,k}\boldsymbol{q}_{k+1}$ (by (3.45)). Hence, we have that $\boldsymbol{q}_{k+1} = \frac{1}{h_{k+1,k}}\mathtt{v}$. Since $\boldsymbol{q}_{j+1}$ has to be normalized, if follows that $h_{j+1,j} = \|\mathtt{v}\|_2$.

The following lemma shows that the vectors $\boldsymbol{q}_j$ generated by the Arnoldi iterations form a basis of the Krylov space $\mathcal{K}_k(A, \boldsymbol{q}_1)$; see, e.g., [160].

Lemma 3.19 (Arnoldi as span of Krylov spaces). *Assume that the Arnoldi procedure generates the vectors $\boldsymbol{q}_1, \dots, \boldsymbol{q}_k$ with $h_{j+1,j} \neq 0$ for $j = 1, \dots, k$. Then the vectors $\boldsymbol{q}_1, \dots, \boldsymbol{q}_k$ form an orthonormal basis of the Krylov space*

$$\mathcal{K}_k(A, \boldsymbol{q}_1) = \operatorname{span}\{\boldsymbol{q}_1, A\boldsymbol{q}_1, \dots, A^{k-1}\boldsymbol{q}_1\}.$$

Proof. The orthonormality of $\boldsymbol{q}_1, \dots, \boldsymbol{q}_k$ follows by their construction in the Arnoldi procedure.

We want to show that each vector $\boldsymbol{q}_j$ can be written as $q_{j-1}(A)\boldsymbol{q}_1$, where q_{j-1} is a polynomial of degree $j-1$. This is obtained by induction. The result trivially holds for $j = 1$ because $\boldsymbol{q}_1 = q_0(A)\boldsymbol{q}_1$ with $q_0(x) := 1$. Now, we assume that $\boldsymbol{q}_\ell = q_{\ell-1}(A)\boldsymbol{q}_1$ for $\ell = 1, \dots, j$, and we want to show that the same holds for $\ell = j+1$. Recalling (3.45) and using the induction hypothesis, we obtain

$$h_{j+1,j}\boldsymbol{q}_{j+1} = A\boldsymbol{q}_j - \sum_{\ell=1}^{j} h_{\ell,j}\boldsymbol{q}_\ell = Aq_{j-1}(A)\boldsymbol{q}_1 - \sum_{\ell=1}^{j} h_{\ell,j}q_{\ell-1}(A)\boldsymbol{q}_1,$$

which means that $\boldsymbol{q}_{j+1}$ can be written as $q_j(A)\boldsymbol{q}_1$, where q_j is a polynomial of degree j.

Since each $\boldsymbol{q}_j$ has the form of $q_{j-1}(A)\boldsymbol{q}_1$, it holds that

$$\operatorname{span}\{\boldsymbol{q}_1, \boldsymbol{q}_2, \ldots, \boldsymbol{q}_k\} \subset \mathcal{K}_k(A, \boldsymbol{q}_1).$$

The claim follows recalling the orthonormality of $\boldsymbol{q}_1, \ldots, \boldsymbol{q}_k$ and the fact that $\dim \mathcal{K}_k(A, \boldsymbol{q}_1) \leq k$. □

The following lemma explains an early termination of the Arnoldi method, also known as the *lucky breakdown* of the Arnoldi algorithm presented above.

Lemma 3.20 (Arnoldi early termination (lucky breakdown)). *Let A be invertible. Arnoldi's method stops at step j, that is, $h_{j+1,j} = 0$, if and only if the minimal polynomial $p_{\min}^{\boldsymbol{q}_1}$ of the pair $(A, \boldsymbol{q}_1)$ is of degree j. In this case, the space $\mathcal{K}_j(A, \boldsymbol{q}_1)$ is invariant under A.*

Proof. First we show that if $\deg(p_{\min}^{\boldsymbol{q}_1}) = j$, then $h_{j+1,j} = 0$. Assume by contradiction that $h_{j+1,j} \neq 0$; then $\boldsymbol{q}_{k+1}$ can be defined by (3.45). By Lemma 3.19 the Krylov space $\mathcal{K}_{j+1}(A, \boldsymbol{q}_1)$ would be of dimension $j+1$. Since $\deg(p_{\min}^{\boldsymbol{q}_1}) = j < j+1$, we get a contradiction to Theorem 3.8. Hence $h_{j+1,j} = 0$.

To show the reverse, assume that $h_{j+1,j} = 0$, that is, $\boldsymbol{q}_{j+1} = 0$. Then Lemma 3.19 (together with the orthogonality of the $\boldsymbol{q}_j$) implies that $\dim \mathcal{K}_j(A, \boldsymbol{q}_1) = j$. Therefore, Theorem 3.8 ensures that $\deg(p_{\min}^{\boldsymbol{q}_1}) \geq j$. Moreover, since $\boldsymbol{q}_{j+1} = 0$ we have $\dim \mathcal{K}_{j+1}(A, \boldsymbol{q}_1) < j+1$; otherwise there would be a contradiction to Lemma 3.19. Since $\dim \mathcal{K}_{j+1}(A, \boldsymbol{q}_1) < j+1$ we cannot have that $\deg(p_{\min}^{\boldsymbol{q}_1}) > j$ according to Theorem 3.8. Therefore we obtain that $\deg(p_{\min}^{\boldsymbol{q}_1}) = j$.

The fact that $\mathcal{K}_j(A, \boldsymbol{q}_1)$ is invariant under A follows then from Theorem 3.7. □

Remark 2. *The eigenvalues of the matrix H_k without the last line (that is, the matrix $\mathtt{H}$ in the above algorithm) are good approximations to the extremal eigenvalues of A, which was the main motivation of Arnoldi for this iteration. This is suggested by the formula* (3.46)*. In fact, by multiplying by $Q_k^\top$, we get $Q_k^\top A Q_k = \mathtt{H}$. We refer the reader to [176, Lecture 34].*

Remark 3. *Notice that the previous algorithm uses the modified Gram–Schmidt orthogonalization procedure. However, there are other, more efficient practical implementations of the Arnoldi procedure based, e.g., on Householder reflections; see, e.g., [160, Section 6.3.2].*

3.4 ▪ The Lanczos algorithm

> *Moreover, the method leads to a well convergent successive approximation procedure by which the solution of integral equations of the Fredholm type and the solution of the eigenvalue problem of linear differential and integral operators may be accomplished.*
>
> Cornelius Lanczos, *An Iteration Method for the Solution of the Eigenvalue Problem of Linear Differential and Integral Operators*, 1950.

If we apply the Arnoldi iteration to a symmetric matrix, $A = A^\top$, then the decomposition (3.44) can be simplified. Since

$$QHQ^\top = A = A^\top = (QHQ^\top)^\top = QH^\top Q^\top,$$

the Hessenberg matrix must also be symmetric, $H^\top = H$, and we obtain a tridiagonal matrix $T := H = H^\top$. This also simplifies the recurrence relation (3.45), namely

$$t_{k+1,k}\boldsymbol{q}_{k+1} = A\boldsymbol{q}_k - \sum_{j=k-1}^{k} t_{jk}\boldsymbol{q}_j,$$

because all the remaining terms are zero, or

$$\beta_k\boldsymbol{q}_{k+1} = A\boldsymbol{q}_k - \beta_{k-1}\boldsymbol{q}_{k-1} - \alpha_k\boldsymbol{q}_k, \tag{3.47}$$

if the tridiagonal matrix entries are named as

$$T_k = \begin{bmatrix} \alpha_1 & \beta_1 & & \\ \beta_1 & \alpha_2 & \ddots & \\ & \ddots & \ddots & \beta_{k-1} \\ & & \beta_{k-1} & \alpha_k \end{bmatrix}.$$

We thus obtain the Lanczos algorithm

```
function [alpha,beta,Q,v]=Lanczos(A,b,k)
% LANCZOS Lanczos algorithm
%   [alpha,beta,Q,v]=Lanczos(A,b,k) applies k<=n steps of the Lanczos
%   algorithm to the symmetric matrix A starting with the vector b.
%   Computes Q (theoretically) orthogonal and a symmetric tridiagonal
%   matrix given by the diagonal in the vector alpha, and the super- and
%   subdiagonal in the vector beta.

Q(:,1)=b/norm(b);
if k==1, beta=[]; end
for j=1:k
  v=A*Q(:,j);
  alpha(j)=Q(:,j)'*v;
  v=v-alpha(j)*Q(:,j);
  if j>1
    v=v-beta(j-1)*Q(:,j-1);
  end
  if j<k
    beta(j)=norm(v);
    Q(:,j+1)=v/beta(j);
  end
end
```

The choice of naming the entries α_j and β_j in the tridiagonal matrix T is not a coincidence; the Lanczos algorithm is the same process as the one used by the CG algorithm (see Theorem 3.3)—there is just a scaling difference (see Problem 40). Since the Lanczos algorithm is the underlying method for the CG method to solve symmetric linear systems, one could use the Arnoldi iteration to obtain a Krylov method for a general, nonsymmetric matrix (recall the advection-reaction-diffusion problem introduced in Section 1.4). GMRES is precisely realizing this idea but in a different way, as we show next.

3.5 ▪ Generalized minimal residual: GMRES

We present an iterative method for solving linear systems, which has the property of minimizing at every step the norm of the residual vector over a Krylov subspace. The algorithm is derived from the Arnoldi process for constructing an l_2-orthogonal basis of Krylov subspaces. It can be considered as a generalization of Paige and Saunders' MINRES *algorithm and is theoretically equivalent to the* Generalized Conjugate Residual *(*GCR*) method and to* ORTHODIR.

Yousef Saad and Martin H. Schultz, *GMRES: A Generalized Minimal Residual Algorithm for Solving Nonsymmetric Linear Systems*, 1986.

The *generalized minimal residual method* (GMRES),[23] proposed by Saad and Schultz [165], constructs at iteration k an approximation $\boldsymbol{u}_k$ in the affine Krylov space $\boldsymbol{u}_0 + \mathcal{K}_k(A, \boldsymbol{r}_0)$ not by making the new residual orthogonal to the current Krylov subspace like in CG, but by making the new residual norm $\|\boldsymbol{r}_k\|_2 = \|\boldsymbol{f} - A\boldsymbol{u}_k\|_2$ as small as possible; see the quote above. To simplify the notation, but without loss of generality, we will assume in the following that we start the iteration with $\boldsymbol{u}_0 = 0$. Then $\boldsymbol{r}_0 = \boldsymbol{f}$ and $\boldsymbol{u}_k \in \mathcal{K}_k(A, \boldsymbol{f})$.

Theorem 3.21 (Foundation of GMRES). *Let $A \in \mathbb{R}^{n\times n}$, $\boldsymbol{f} \in \mathbb{R}^n$ and let $AQ_k = Q_{k+1}H_k$ be the decomposition computed by the Arnoldi (initialized by $\boldsymbol{r}_0 = \boldsymbol{f}$) iteration at step k. Then the minimizer*

$$\boldsymbol{u}_k = \operatorname*{arg\,min}_{\widetilde{\boldsymbol{u}} \in \mathcal{K}_k(A,\boldsymbol{f})} \|\boldsymbol{f} - A\widetilde{\boldsymbol{u}}\|_2$$

is given by $\boldsymbol{u}_k = Q_k\boldsymbol{v}$, where $\boldsymbol{v} \in \mathbb{R}^k$ is the solution of the least squares problem

$$\boldsymbol{v} = \operatorname*{arg\,min}_{\boldsymbol{w}\in\mathbb{R}^k} \big\| \|\boldsymbol{f}\|_2 \boldsymbol{e}_1 - H_k\boldsymbol{w} \big\|_2. \tag{3.48}$$

Proof. According to Lemma 3.19, Q_k from the Arnoldi iteration contains in its columns an orthonormal basis of the Krylov space $\mathcal{K}_k(A, \boldsymbol{f})$. Hence one can express $\widetilde{\boldsymbol{u}} \in \mathcal{K}_k(A, \boldsymbol{f})$ as $\widetilde{\boldsymbol{u}} = Q_k\boldsymbol{v}$ for some appropriate vector $\boldsymbol{v} \in \mathbb{R}^k$. Using also from the Arnoldi iteration that $AQ_k = Q_{k+1}H_k$, we thus get

$$\begin{aligned}\min_{\widetilde{\boldsymbol{u}} \in \mathcal{K}_k(A,\boldsymbol{f})} \|\boldsymbol{f} - A\widetilde{\boldsymbol{u}}\|_2 &= \min_{\boldsymbol{v}\in\mathbb{R}^k} \|\boldsymbol{f} - AQ_k\boldsymbol{v}\|_2 \\ &= \min_{\boldsymbol{v}\in\mathbb{R}^k} \|\boldsymbol{f} - Q_{k+1}H_k\boldsymbol{v}\|_2.\end{aligned}$$

Now since $\boldsymbol{q}_1 = \boldsymbol{f}/\|\boldsymbol{f}\|_2$ from the Arnoldi process,

$$\boldsymbol{f} = \|\boldsymbol{f}\|_2 Q_{k+1}\boldsymbol{e}_1,$$

with $\boldsymbol{e}_1 = [1, 0, \ldots, 0]^\top \in \mathbb{R}^{k+1}$, and since for any vector $\boldsymbol{w}$ we have by the orthogonality of the columns of Q_{k+1} that

$$\|Q_{k+1}\boldsymbol{w}\|_2^2 = \boldsymbol{w}^\top Q_{k+1}^\top Q_{k+1}\boldsymbol{w} = \boldsymbol{w}^\top\boldsymbol{w} = \|\boldsymbol{w}\|_2^2,$$

we obtain

$$\begin{aligned}\min_{\widetilde{\boldsymbol{u}} \in \mathcal{K}_k(A,\boldsymbol{f})} \|\boldsymbol{f} - A\widetilde{\boldsymbol{u}}\|_2 &= \min_{\boldsymbol{v}\in\mathbb{R}^k} \big\| Q_{k+1}(\|\boldsymbol{f}\|_2\boldsymbol{e}_1 - H_k\boldsymbol{v}) \big\|_2 \\ &= \min_{\boldsymbol{v}\in\mathbb{R}^k} \big\| \|\boldsymbol{f}\|_2\boldsymbol{e}_1 - H_k\boldsymbol{v} \big\|_2,\end{aligned}$$

which concludes the proof. □

[23] For a chronological and more complete description of Krylov methods we refer the reader to Section 3.6.

Remark 4 (Foundation of GMRES for $\boldsymbol{u_0 \neq 0}$). *Notice that Theorem 3.21 can be easily generalized for $\boldsymbol{u}_0 \neq 0$. In this case, we write*

$$\begin{aligned}\boldsymbol{u}_k &= \underset{\widetilde{\boldsymbol{u}} \in \boldsymbol{u}_0 + \mathcal{K}_k(A, \boldsymbol{r}_0)}{\arg\min} \|\boldsymbol{f} - A\widetilde{\boldsymbol{u}}\|_2 = \boldsymbol{u}_0 + \underset{\widetilde{\boldsymbol{u}} \in \mathcal{K}_k(A, \boldsymbol{r}_0)}{\arg\min} \|\boldsymbol{f} - A\boldsymbol{u}_0 - A\widetilde{\boldsymbol{u}}\|_2 \\ &= \boldsymbol{u}_0 + \underset{\widetilde{\boldsymbol{u}} \in \mathcal{K}_k(A, \boldsymbol{r}_0)}{\arg\min} \|\boldsymbol{r}_0 - A\widetilde{\boldsymbol{u}}\|_2.\end{aligned}$$

Therefore, using Theorem 3.21 for the problem $\arg\min_{\widetilde{\boldsymbol{u}} \in \mathcal{K}_k(A, \boldsymbol{r}_0)} \|\boldsymbol{r}_0 - A\widetilde{\boldsymbol{u}}\|_2$ *we get that* $\boldsymbol{u}_k = \boldsymbol{u}_0 + Q_k \boldsymbol{v}$*, where*

$$\boldsymbol{v} = \underset{\boldsymbol{w} \in \mathbb{R}^k}{\arg\min} \big\| \|\boldsymbol{r}_0\|_2 \boldsymbol{e}_1 - H_k \boldsymbol{w} \big\|_2,$$

and one clearly has that

$$\|\boldsymbol{r}_k\|_2 = \min_{\widetilde{\boldsymbol{u}} \in \mathcal{K}_k(A, \boldsymbol{r}_0)} \|\boldsymbol{r}_0 - A\widetilde{u}\|_2 = \min_{\boldsymbol{w} \in \mathbb{R}^k} \big\| \|\boldsymbol{r}_0\|_2 \boldsymbol{e}_1 - H_k \boldsymbol{w} \big\|_2.$$

The least squares problem (3.48) has a special structure: the matrix H_k is upper Hessenberg and there are $k+1$ equations and k unknowns. Such problems are best solved by applying k Givens rotations to reduce the system to an equivalent system with an upper triangular matrix; see Problem 43.

GMRES solves implicitly a polynomial approximation problem. Since $\boldsymbol{u}_k \in \mathcal{K}_k(A, \boldsymbol{f})$, it is a linear combination of the basis vectors $A^j \boldsymbol{f}$, $j = 0, \ldots, k-1$,

$$\boldsymbol{u}_k = \sum_{j=0}^{k-1} \gamma_j A^j \boldsymbol{f}$$

for some coefficients γ_j. For the residual $\boldsymbol{r}_k = \boldsymbol{f} - A\boldsymbol{u}_k$, we get

$$\boldsymbol{r}_k = \boldsymbol{f} - \sum_{j=0}^{k-1} \gamma_j A^{j+1} \boldsymbol{f} = \sum_{j=0}^{k} \zeta_j A^j \boldsymbol{f}, \quad \zeta_0 = 1,\ \zeta_j = -\gamma_{j-1}.$$

With the *residual polynomial*

$$p_k(A) = \sum_{j=0}^{k} \zeta_j A^j, \quad p_k(0) = 1,$$

and denoting the set of all polynomials of degree lower than or equal to k by $\mathcal{P}_k$, the minimization problem becomes

$$\min_{\widetilde{\boldsymbol{u}} \in \mathcal{K}_k(A, \boldsymbol{f})} \|\boldsymbol{f} - A\widetilde{\boldsymbol{u}}\|_2 = \min_{\widetilde{\zeta}_1, \ldots, \widetilde{\zeta}_{k-1}} \|\boldsymbol{f} + \sum_{j=1}^{k} \widetilde{\zeta}_j A^j \boldsymbol{f}\|_2 = \min_{\substack{p \in \mathcal{P}_k \\ p(0)=1}} \|p(A)\boldsymbol{f}\|_2. \tag{3.49}$$

Notice that the polynomial approximation problem (3.49) seems similar to the one that we obtained in Lemma 3.14 for CG. However, there is a big difference between these two problems. It is possible to prove (see Problem 38) that at each iteration CG, for A symmetric and positive definite, minimizes the residual in the A^{-1}-norm ($\|\boldsymbol{z}\|_{A^{-1}} = \sqrt{\boldsymbol{z}^\top A^{-1} \boldsymbol{z}}$) in the sense that

$$\|\boldsymbol{r}_k\|_{A^{-1}} = \min_{\substack{p \in \mathcal{P}_k \\ p(0)=1}} \|p(A)\boldsymbol{r}_0\|_{A^{-1}}. \tag{3.50}$$

Recalling that $\boldsymbol{u}_0 = 0$ and hence $\boldsymbol{r}_0 = \boldsymbol{f}$, the GMRES polynomial approximation problem gives

$$\|\boldsymbol{r}_k\|_2 = \min_{\substack{p\in\mathcal{P}_k \\ p(0)=1}} \|p(A)\boldsymbol{r}_0\|_2, \tag{3.51}$$

and we clearly see that while GMRES minimizes the residual in the 2-norm, CG minimizes the residual in the A^{-1}-norm.

The polynomial approximation problem (3.49) is crucial for the convergence analysis of GMRES: it allows one to obtain different convergence bounds.

The first bound is based on the spectrum of the matrix A, which is assumed to be diagonalizable, and on the condition number of the corresponding eigenvector matrix. This result is derived in Theorem 3.22 and leads to the famous convergence estimate given in Theorem 3.26, where the eigenvalues of A are assumed to lie in an ellipse that does not contain the origin.

A second class of convergence estimates is based on the so-called *numerical range* of the matrix A (see Definition 3.27), which leads to different convergence bounds that do not require A to be diagonalizable.

Finally, a recent third class of convergence estimates is based on the pseudospectrum of the matrix A; see, e.g., [94, page 57], [177], and [61].

Theorem 3.22 (Convergence bound for GMRES). *Let $A \in \mathbb{R}^{n\times n}$ be diagonalizable, $A = S\Lambda S^{-1}$, with the diagonal matrix $\Lambda = \operatorname{diag}(\lambda_1, \ldots, \lambda_n)$ and $\boldsymbol{f} \in \mathbb{R}^n$. Then at the kth step of the GMRES iteration, we have*

$$\frac{\|\boldsymbol{f} - A\boldsymbol{u}_k\|_2}{\|\boldsymbol{f}\|_2} \le \kappa(S) \min_{\substack{p\in\mathcal{P}_k \\ p(0)=1}} \max_{\lambda\in\{\lambda_1,\ldots,\lambda_n\}} |p(\lambda)|,$$

where $\kappa(S) := \|S\|_2\|S^{-1}\|_2$ is the condition number of the matrix S.

Proof. The approximation problem (3.49) is

$$\begin{aligned}
\min_{\widetilde{\boldsymbol{u}}\in\mathcal{K}_k(A,\boldsymbol{f})} \|\boldsymbol{f} - A\widetilde{\boldsymbol{u}}\|_2 &= \min_{\substack{p\in\mathcal{P}_k \\ p(0)=1}} \|p(A)\boldsymbol{f}\|_2 = \min_{\substack{p\in\mathcal{P}_k \\ p(0)=1}} \|p(S\Lambda S^{-1})\boldsymbol{f}\|_2 \\
&= \min_{\substack{p\in\mathcal{P}_k \\ p(0)=1}} \|S\,p(\Lambda)\,S^{-1}\boldsymbol{f}\|_2 \\
&\le \underbrace{\|S\|_2\|S^{-1}\|_2}_{\kappa(S)} \|\boldsymbol{f}\|_2 \min_{\substack{p\in\mathcal{P}_k \\ p(0)=1}} \max_{\lambda\in\{\lambda_1,\ldots,\lambda_n\}} |p(\lambda)|. \qquad \square
\end{aligned}$$

Since A is not assumed to be symmetric, its eigenvectors S and eigenvalues λ_j may be complex. Therefore, in order to estimate the convergence rate of GMRES, we need to find polynomials that are small on a given set of complex numbers. The following lemma will be helpful in finding such polynomials.

Lemma 3.23. *Let $C(0, r)$ denote the circle of radius r centered at the origin. Let $\gamma \in \mathbb{C}$ with $|\gamma| > r$. Then*

$$\min_{\substack{p\in\mathcal{P}_k \\ p(\gamma)=1}} \max_{z\in C(0,r)} |p(z)| = \left(\frac{r}{|\gamma|}\right)^k, \tag{3.52}$$

and the minimum is attained for $\widehat{p}(z) = \left(\frac{z}{\gamma}\right)^k$.

Proof. The polynomial $\widehat{p}(z) = \left(\frac{z}{\gamma}\right)^k$ satisfies $\widehat{p}(\gamma) = 1$. Moreover, since any $z \in C(0,r)$ is of the form $re^{i\vartheta}$, it holds that

$$|\widehat{p}(z)| = \left(\frac{r}{|\gamma|}\right)^k \quad \forall z \in C(0,r), \tag{3.53}$$

and hence

$$\max_{z\in C(0,r)} |\widehat{p}(z)| = \left(\frac{r}{|\gamma|}\right)^k. \tag{3.54}$$

Thus it is sufficient to show that no polynomial with the same normalization is smaller. To do so, consider any polynomial p_k of degree k and its normalized version,

$$g_k(z) = \frac{p_k(z)}{p_k(\gamma)}.$$

Seeking a contradiction, we assume that

$$|g_k(z)| = \left|\frac{p_k(z)}{p_k(\gamma)}\right| < |\widehat{p}(z)| = \left|\frac{r}{\gamma}\right|^k \qquad \forall z \in C(0,r) \tag{3.55}$$

holds, and notice that if we contradict (3.55), then recalling (3.53) and (3.54) we obtain that

$$|g_k(z)| \geq |\widehat{p}(z)| = \left(\frac{r}{|\gamma|}\right)^k = \max_{\widetilde{z}\in C(0,r)} |\widehat{p}(\widetilde{z})|$$

for any $z \in C(0,r)$, which implies that $\widehat{p}$ solves (3.52).

By the *Rouché theorem*[24] (see, e.g., [171, Chapter 3, Theorem 4.3] and [174, Theorem 3.42]), if for two analytic functions f, g we have $|g(z)| < |f(z)|$ for all $z \in C(0,r)$, then f and $f-g$ have the same number of zeros inside $C(0,r)$. Now $(\frac{z}{\gamma})^k$ has a zero of multiplicity k at 0, and the difference $(\frac{z}{\gamma})^k - \frac{p_k(z)}{p_k(\gamma)}$ vanishes at $z = \gamma$, which implies that

$$\left(\frac{z}{\gamma}\right)^k - \frac{p_k(z)}{p_k(\gamma)} = (z-\gamma)q_{k-1}(z)$$

with some polynomial q_{k-1} of degree lower than or equal to $k-1$ with at most $k-1$ zeros inside $C(0,r)$. Since γ is a root of $(\frac{z}{\gamma})^k - \frac{p_k(z)}{p_k(\gamma)}$ outside of $C(0,r)$, we have a contradiction to the Rouché theorem, and therefore no such polynomial exists. ∎

Note that with a change of variables $\widetilde{z} = z + c$, Lemma 3.23 can be applied to a circle centered at c. We have

$$\min_{\substack{p\in\mathcal{P}_k \\ p(\gamma)=1}} \max_{\widetilde{z}\in C(c,r)} |p(\widetilde{z})| = \min_{\substack{p\in\mathcal{P}_k \\ p(\gamma-c)=1}} \max_{z\in C(0,r)} |p(z)| = \left(\frac{r}{|\gamma-c|}\right)^k,$$

where the second equality follows by Lemma 3.23.

As a next ingredient in our search for small polynomials, we will need the conformal mapping

$$J(w) = \frac{w + w^{-1}}{2},$$

[24] Rouché's theorem: Consider any two functions $f, g : \Omega \to \mathbb{C}$ that are analytic in a bounded, open, and simply connected domain $\Omega \subset \mathbb{C}$ whose boundary $\partial\Omega$ is a closed contour. If $|g(z)| < |f(z)|$ for any $z \in \partial\Omega$, then $f(z)$ and $f(z) + g(z)$ have the same number of zeros in Ω. Notice that the function g in this statement is the function $-g$ in our proof; in fact a direct inspection of the proof of the Rouché theorem reveals that the sign of g does not affect the result; see, e.g., [171, Chapter 3, Theorems 4.1 and 4.3].

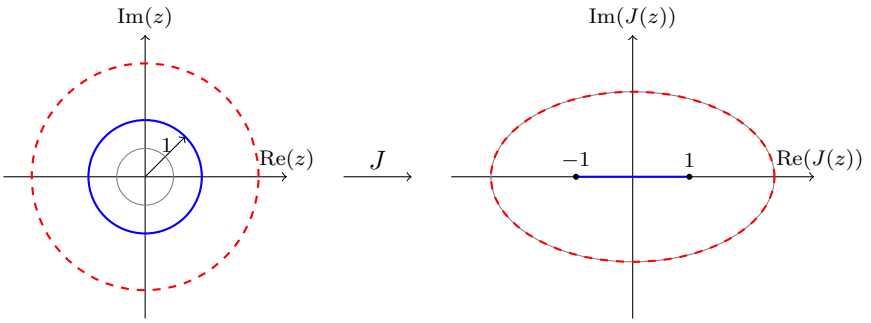

Figure 3.11. *The Joukowski transformation J. Left: Three circles of radius $r = 1$ (blue), $r = 2$ (red-dashed), and $r = \frac{1}{2}$ (gray). Right: The three ellipses obtained by the Joukowski transformation J applied to the three circles. The blue line is the (degenerate) ellipsis that corresponds to the (blue) circle of radius $r = 1$. The two ellipses (gray and red-dashed) are obtained transforming the gray and dashed red circles (notice that these two ellipses coincide). The two points are the foci of the gray and red-dashed ellipses.*

which is called the *Joukowski transformation*. It maps the circle $C(0, r)$ defined by $w = re^{i\vartheta}$ to

$$\begin{aligned} z &= \frac{1}{2}\left(re^{i\vartheta} + \frac{1}{r}e^{-i\vartheta}\right) = \frac{1}{2}\left(r\cos\vartheta + ir\sin\vartheta + \frac{1}{r}\cos\vartheta - \frac{i}{r}\sin\vartheta\right) \\ &= \frac{1}{2}\left(\left(r + \frac{1}{r}\right)\cos\vartheta + i\left(r - \frac{1}{r}\right)\sin\vartheta\right), \end{aligned}$$

an ellipse with foci at -1 and 1 and principal axes $a = \left(r + \frac{1}{r}\right)/2$ and $b = \left(r - \frac{1}{r}\right)/2$. Without loss of generality, we may assume $r > 1$, since r and $1/r$ produce the same ellipse. For $r = 1$ the ellipse is degenerate: the circle is mapped to the real interval $[-1, 1]$. See Figure 3.11.

The Joukowski transformation can be used for expressing the Chebyshev polynomials defined by the recursion (3.31), as we have already seen in Lemma 3.17, which led to the representation formula (3.35) for the Chebyshev polynomials.

Lemma 3.24. *Let E_J denote the ellipse obtained from the circle $C(0, r)$ using the Joukowski transformation $J(w)$, and let γ be a point outside E_J. Let w_γ be the solution with larger modulus of $J(w) = \gamma$. Then*

$$\frac{r^k}{|w_\gamma|^k} \le \min_{\substack{p\in\mathcal{P}_k \\ p(\gamma)=1}} \max_{z\in E_J} |p(z)| \le \frac{r^k + r^{-k}}{|w_\gamma^k + w_\gamma^{-k}|}. \tag{3.56}$$

Proof. Every polynomial $p \in \mathcal{P}_k$ with $p(\gamma) = 1$ can be written as

$$p(z) = \frac{\sum_{j=0}^k \zeta_j z^j}{\sum_{j=0}^k \zeta_j \gamma^j}.$$

Using the Joukowski transformation $z = J(w)$, this becomes

$$p(z) = \frac{\sum_{j=0}^k \widetilde{\zeta}_j (w^j + w^{-j})}{\sum_{j=0}^k \widetilde{\zeta}_j (w_\gamma^j + w_\gamma^{-j})}. \tag{3.57}$$

In particular, for $\widetilde{\zeta}_k = 1$ and $\widetilde{\zeta}_j = 0$, $j = 0, 1, \ldots, k-1$, we obtain a normalized Chebyshev polynomial,

$$p^*(z) = \frac{w^k + w^{-k}}{w_\gamma^k + w_\gamma^{-k}} = \frac{T_k(z)}{T_k(\gamma)}.$$

Letting $w = re^{i\vartheta}$, we get

$$\left| r^k e^{ik\vartheta} + \frac{1}{r^k} e^{-ik\vartheta} \right| \leq \left| r^k e^{ik\vartheta} \right| + \left| \frac{1}{r^k} e^{-ik\vartheta} \right| = r^k + \frac{1}{r^k},$$

and the maximum of $p^*(z)$ on $J(C(0,r)) = E_{\mathrm{J}}$ is attained for $\vartheta = 0$. Therefore, we have found that

$$\max_{z \in E_{\mathrm{J}}} |p^*(z)| = \frac{r^k + r^{-k}}{|w_\gamma^k + w_\gamma^{-k}|},$$

which implies

$$\min_{\substack{p \in \mathcal{P}_k \\ p(\gamma)=1}} \max_{z \in E_{\mathrm{J}}} |p(z)| \leq \max_{z \in E_{\mathrm{J}}} |p^*(z)| = \frac{r^k + r^{-k}}{|w_\gamma^k + w_\gamma^{-k}|}.$$

Thus the upper bound in (3.56) is proved.

In order to prove the lower bound, we rewrite (3.57) as

$$p(z) = \frac{w^{-k}}{w_\gamma^{-k}} \frac{\sum_{j=0}^k \widetilde{\zeta}_j (w^{k+j} + w^{k-j})}{\sum_{j=0}^k \widetilde{\zeta}_j (w_\gamma^{k+j} + w_\gamma^{k-j})}.$$

The absolute value becomes

$$|p(z)| = \frac{r^{-k}}{|w_\gamma|^{-k}} |q_{2k}(w)|,$$

where q_{2k} is a polynomial of degree lower than or equal to $2k$ with $q_{2k}(w_\gamma) = 1$. By Lemma 3.23, we have

$$|q_{2k}(w)| \geq \frac{r^{2k}}{|w_\gamma|^{2k}} \quad \Longrightarrow \quad \max_{z \in E_{\mathrm{J}}} |p(z)| \geq \frac{r^{-k}}{|w_\gamma|^{-k}} \frac{r^{2k}}{|w_\gamma|^{2k}} = \frac{r^k}{|w_\gamma|^k},$$

which is the lower bound. □

Corollary 3.25. *The upper bound estimate* (3.56) *in Lemma 3.24 also holds in the interior of the ellipse.*

Proof. This follows directly from an application of the maximum principle for the modulus of analytic (holomorphic) functions (see, e.g., [174, Chapter 5] and [93, Chapter 6]), which says that functions that are analytic in a bounded and simply connected domain $\Omega \subset \mathbb{C}$ attain their maximum in modulus on the boundary $\partial\Omega$. □

Since the difference between the two expressions

$$\frac{r^k}{|w_\gamma|^k} \quad \text{and} \quad \frac{r^k + r^{-k}}{|w_\gamma^k + w_\gamma^{-k}|}$$

converges to zero for $k \to \infty$, we conclude that for large k the complex Chebyshev polynomial

$$p^*(z) = \frac{w^k + w^{-k}}{w_\gamma^k + w_\gamma^{-k}} = \frac{T_k(z)}{T_k(\gamma)}$$

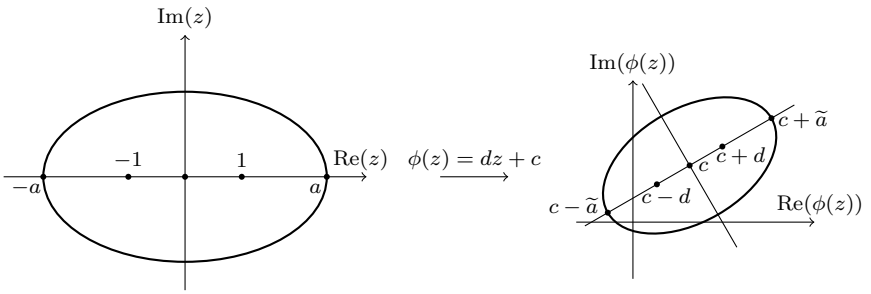

Figure 3.12. *Joukowski ellipse $E_J = J(C(0,r))$ (left) and its transformation $\phi(E_J)$ (right).*

is optimal. But $p^*(z)$ is only optimal asymptotically for k large, which is different from the real case, where the Chebyshev polynomials are optimal for all k.

Lemma 3.24 can be generalized to any ellipse in the complex plane. To do so, consider the transformation $z \mapsto \phi(z) := dz + c$. If we write $d = |d|e^{i\theta}$, then c, $|d|$, and θ are translation, scaling, and rotation parameters and we define $\widetilde{a} = ad$. So we denote by $E(c,d,\widetilde{a})$ the ellipse $\phi(E_J)$ (see Figure 3.12), where c, $c \pm d$, and $c \pm \widetilde{a}$ are the positions of the center, the focal points, and the extrema shown in Figure 3.12. Notice that $\frac{\widetilde{a}}{d} = \frac{ad}{d} = a > 1$. As before, we denote by $\mathrm{int}E(c,d,\widetilde{a})$ the set of points inside $E(c,d,\widetilde{a})$, and we define $\overline{E(c,d,\widetilde{a})} := \mathrm{int}E(c,d,\widetilde{a}) \cup E(c,d,\widetilde{a})$. Now, recalling the proof of Lemma 3.24, we have that (with $\widetilde{z} = \phi(z)$)

$$\min_{\substack{p\in\mathcal{P}_k \\ p\left(\frac{\gamma-c}{d}\right)=1}} \max_{z\in\overline{E_J}} |p(z)| = \min_{\substack{p\in\mathcal{P}_k \\ p(\gamma)=1}} \max_{\widetilde{z}\in\overline{E(c,d,\widetilde{a})}} |p(\widetilde{z})|$$

$$\leq \max_{\widetilde{z}\in\overline{E(c,d,\widetilde{a})}} |p^*(\widetilde{z})| = \max_{\widetilde{z}\in\overline{E(c,d,\widetilde{a})}} |\widehat{T}_k(\widetilde{z})|,$$

where $\widehat{T}_k(\widetilde{z}) = \frac{T_k\left(\frac{\widetilde{z}-c}{d}\right)}{T_k\left(\frac{\gamma-c}{d}\right)}$. The maximum is attained at $\widetilde{z} = c + \widetilde{a}$, as we have seen in the proof of Lemma 3.24, and hence

$$\max_{\widetilde{z}\in\overline{E(c,d,\widetilde{a})}} |\widehat{T}_k(\widetilde{z})| = \left| \frac{T_k\left(\frac{\widetilde{a}}{d}\right)}{T_k\left(\frac{\gamma-c}{d}\right)} \right| = \frac{T_k\left(\frac{\widetilde{a}}{d}\right)}{|T_k\left(\frac{\gamma-c}{d}\right)|},$$

where we removed the modulus in the numerator, since $\frac{\widetilde{a}}{d} > 1$, which means $T_k(\frac{\widetilde{a}}{d}) > 0$.

Theorem 3.26 (Convergence estimate for GMRES). *Let $A \in \mathbb{R}^{n\times n}$ be diagonalizable, $A = S\Lambda S^{-1}$ with $\Lambda = \mathrm{diag}(\lambda_1,\ldots,\lambda_n)$, and assume that all $\lambda_j \in \overline{E(c,d,\widetilde{a})}$ and that the origin is not contained in the ellipse. Then at the kth iteration of GMRES, we have*

$$\frac{\|\boldsymbol{f} - A\boldsymbol{u}_k\|_2}{\|\boldsymbol{f}\|_2} \leq \kappa(S) \frac{T_k\left(\frac{\widetilde{a}}{d}\right)}{|T_k\left(\frac{c}{d}\right)|}.$$

Proof. From Theorem 3.22 we know that

$$\frac{\|\boldsymbol{f} - A\boldsymbol{u}_k\|_2}{\|\boldsymbol{f}\|_2} \leq \kappa(S) \min_{\substack{p\in\mathcal{P}_k \\ p(0)=1}} \max_i |p(\lambda_i)|.$$

Now, we recall that $\{\lambda_1,\ldots,\lambda_n\} \subset \overline{E(c,d,\widetilde{a})}$. Then Lemma 3.24, the change of variables, and

setting $\gamma = 0$ show that

$$\min_{\substack{p\in\mathcal{P}_k\\ p(0)=1}} \max_{\widetilde{z}\in E(c,d,\widetilde{a})} |p(\widetilde{z})| \le \frac{T_k\left(\frac{\widetilde{a}}{d}\right)}{|T_k\left(-\frac{c}{d}\right)|} = \frac{T_k\left(\frac{\widetilde{a}}{d}\right)}{|T_k\left(\frac{c}{d}\right)|},$$

since $|T_k(-z)| = |T_k(z)|$. □

If $a, c, d \in \mathbb{R}$, then for $c > \widetilde{a} > d$, we get

$$\begin{aligned}\frac{T_k\left(\frac{\widetilde{a}}{d}\right)}{|T_k\left(\frac{c}{d}\right)|} &= \frac{\left(\frac{\widetilde{a}}{d}+\sqrt{\left(\frac{\widetilde{a}}{d}\right)^2-1}\right)^k + \left(\frac{\widetilde{a}}{d}+\sqrt{\left(\frac{\widetilde{a}}{d}\right)^2-1}\right)^{-k}}{\left|\left(\frac{c}{d}+\sqrt{\left(\frac{c}{d}\right)^2-1}\right)^k + \left(\frac{c}{d}+\sqrt{\left(\frac{c}{d}\right)^2-1}\right)^{-k}\right|} \\ &\approx \left(\frac{\frac{\widetilde{a}}{d}+\sqrt{\left(\frac{\widetilde{a}}{d}\right)^2-1}}{\frac{c}{d}+\sqrt{\left(\frac{c}{d}\right)^2-1}}\right)^k = \left(\frac{\widetilde{a}+\sqrt{\widetilde{a}^2-d^2}}{c+\sqrt{c^2-d^2}}\right)^k\end{aligned} \tag{3.58}$$

for k sufficiently large.

If the spectrum of GMRES does not lie in an ellipse excluding the origin, or if the matrix is not diagonalizable, different techniques need to be used to study the convergence of GMRES, and this is still an active area of research; see, e.g., the monograph [124, Section 5.7] and references therein. If the matrix A is nonnormal, but its eigenvector matrix S is well conditioned, then the convergence bounds obtained in Theorems 3.22 and 3.26 give reasonable estimates of the norm of the residual, even if they are not necessarily sharp. The distribution of the eigenvalues of the matrix A is then essentially sufficient to describe the GMRES behavior [94]. In general, however, the behavior of GMRES cannot be determined from the eigenvalues alone. To overcome this problem, the numerical range of the matrix A is important.

Definition 3.27 (Numerical range and numerical radius). *Consider a matrix $A \in \mathbb{C}^{n\times n}$. The set*

$$\mathcal{F}(A) := \{\boldsymbol{y}^* A\boldsymbol{y} \,:\, \boldsymbol{y} \in \mathbb{C}^n, \boldsymbol{y}^*\boldsymbol{y} = 1\}$$

is called the numerical range *of A. The value*

$$\nu(A) := \max\{|z| \,:\, z \in \mathcal{F}(A)\}$$

is called the numerical radius *of A.*

In the literature, the numerical range is also often called the *field of values*, *range of values*, *Hausdorff domain*, and *Wertvorrat*; see, e.g., [151]. Some of the main properties of the numerical range and the numerical radius are summarized in the following theorem. Other properties can be found in, e.g., [109, 102, 151].

Theorem 3.28 (Properties of $\mathcal{F}(A)$ and $\nu(A)$). *For any $A, B \in \mathbb{C}^{n\times n}$ and any $\alpha, \beta \in \mathbb{C}$ the following holds:*

(a) *$\mathcal{F}(A)$ is a compact subset of $\mathbb{C}$.*

(b) *$\mathcal{F}(\alpha A + \beta I) = \alpha\mathcal{F}(A) + \beta$ (I is the identity matrix).*

(c) *$\mathcal{F}(A)$ is convex.*

(d) *The spectrum of A is contained in $\mathcal{F}(A)$ and $\rho(A) \leq \nu(A)$.*

(e) $\nu(A+B) \leq \nu(A) + \nu(B)$.

(f) $\nu(\alpha A) = |\alpha|\nu(A)$.

(g) $\frac{1}{2}\|A\|_2 \leq \nu(A) \leq \|A\|_2$.

(h) $\nu(A^m) \leq [\nu(A)]^m$ *for* $m = 1, 2, \ldots$.

Proof. Property (a) clearly holds, since $\mathcal{F}(A)$ is the image of the unit sphere (a compact set) under the continuous map $\boldsymbol{y} \mapsto \boldsymbol{y}^* A\boldsymbol{y}$. Statement (c) is the famous Toeplitz–Hausdorff theorem; we refer the reader to [151] for a proof. The proofs of statements (b), (d), (e), and (f) are not difficult and just use the definitions of $\mathcal{F}(A)$ and $\nu(A)$; they are left as an exercises to the reader (see Problem 44). More interesting are the proofs of (g) and (h), which we now give, adapted from [94] and [143].

Let us begin with (g). For any $\boldsymbol{y} \in \mathbb{C}^n$ such that $\|\boldsymbol{y}\|_2 = 1$, we use the Cauchy–Schwarz inequality to write

$$|\boldsymbol{y}^* A\boldsymbol{y}| \leq \|\boldsymbol{y}\|_2 \|A\boldsymbol{y}\|_2 \leq \|A\|_2,$$

since $\boldsymbol{y}$ is normalized, which implies the right inequality of (g), that is, $\nu(A) \leq \|A\|_2$. To prove the left inequality, we use the standard decomposition $A = S + H$, where $H = \frac{1}{2}(A + A^*)$ is the Hermitian part of A and $S = \frac{1}{2}(A - A^*)$ is the skew-Hermitian part of A. Since H and S are normal matrices, one can show that $\rho(H) = \|H\|_2 = \nu(H)$ and $\rho(S) = \|S\|_2 = \nu(S)$ (see Problem 45). Using these relations, the triangle inequality, and the fact that $\nu(A) = \nu(A^*)$, we obtain

$$\begin{aligned}
\|A\|_2 &\leq \|H\|_2 + \|S\|_2 = \nu(H) + \nu(S) \\
&= \frac{1}{2}\Big[\max_{\|\boldsymbol{y}\|_2^2=1} |\boldsymbol{y}^*(A + A^*)\boldsymbol{y}| + \max_{\|\boldsymbol{y}\|_2^2=1} |\boldsymbol{y}^*(A - A^*)\boldsymbol{y}|\Big] \\
&\leq \frac{1}{2}\Big[2 \max_{\|\boldsymbol{y}\|_2^2=1} |\boldsymbol{y}^* A\boldsymbol{y}| + 2 \max_{\|\boldsymbol{y}\|_2^2=1} |\boldsymbol{y}^* A^*\boldsymbol{y}|\Big] \\
&\leq 2\nu(A),
\end{aligned}$$

which implies $\frac{1}{2}\|A\|_2 \leq \nu(A)$.

Let us now prove (h). To do so, we make use of the two polynomial identities

$$1 - z^m = \prod_{k=1}^{m} (1 - w^k z) \tag{3.59}$$

and

$$1 = \sum_{k=1}^{m} \frac{1}{m} \prod_{\ell=1, \ell\neq k}^{m} (1 - w^\ell z), \tag{3.60}$$

where $w = \exp(\frac{2\pi i}{m})$, i is the imaginary unit, and m is an arbitrary positive integer. The polynomial identities (3.59) and (3.60) are proved in Theorem 6.4 in the appendix. Now, consider any matrix $C \in \mathbb{C}^{n\times n}$ and any vector $\boldsymbol{x} \in \mathbb{C}^n$ such that $\|\boldsymbol{x}\|_2 = 1$, and define the vectors

$$\boldsymbol{x}_k := \prod_{\ell=1, \ell\neq k}^{m} [I - w^\ell C]\boldsymbol{x} \tag{3.61}$$

for $k = 1, \ldots, m$. Using the notation $\langle \boldsymbol{y}, \boldsymbol{x} \rangle := \boldsymbol{x}^* \boldsymbol{y}$, we write

$$\begin{aligned}
1 - \langle C^m \boldsymbol{x}, \boldsymbol{x} \rangle &= \langle [I - C^m] \boldsymbol{x}, \boldsymbol{x} \rangle \\
&= \left\langle [I - C^m] \boldsymbol{x}, \sum_{k=1}^{m} \frac{1}{m} \prod_{\ell=1, \ell \neq k}^{m} (1 - w^\ell C) \boldsymbol{x} \right\rangle && \text{(using (3.60))} \\
&= \frac{1}{m} \sum_{k=1}^{m} \langle [I - C^m] \boldsymbol{x}, \boldsymbol{x}_k \rangle && \text{(using (3.61))} \\
&= \frac{1}{m} \sum_{k=1}^{m} \left\langle \prod_{\ell=1}^{m} (I - w^\ell C) \boldsymbol{x}, \boldsymbol{x}_k \right\rangle && \text{(using (3.59))} \\
&= \frac{1}{m} \sum_{k=1}^{m} \langle (I - w^k C) \boldsymbol{x}_k, \boldsymbol{x}_k \rangle && \text{(using (3.61))} \\
&= \frac{1}{m} \sum_{k=1}^{m} \|\boldsymbol{x}_k\|_2^2 \left[1 - w^k \left\langle C \frac{\boldsymbol{x}_k}{\|\boldsymbol{x}_k\|_2}, \frac{\boldsymbol{x}_k}{\|\boldsymbol{x}_k\|_2} \right\rangle \right],
\end{aligned}$$

which gives us the relation

$$1 - \langle C^m \boldsymbol{x}, \boldsymbol{x} \rangle = \frac{1}{m} \sum_{k=1}^{m} \|\boldsymbol{x}_k\|_2^2 \left[1 - w^k \left\langle C \frac{\boldsymbol{x}_k}{\|\boldsymbol{x}_k\|_2}, \frac{\boldsymbol{x}_k}{\|\boldsymbol{x}_k\|_2} \right\rangle \right] \tag{3.62}$$

for any normalized $\boldsymbol{x}$ and any matrix C. If we choose $C = \exp(i\vartheta)B$, for an arbitrary matrix $B \in \mathbb{C}^{n \times n}$ and $\vartheta \in \mathbb{R}$, and replace it in (3.62), we get

$$1 - \exp(im\vartheta) \langle B^m \boldsymbol{x}, \boldsymbol{x} \rangle = \frac{1}{m} \sum_{k=1}^{m} \|\boldsymbol{x}_k\|_2^2 \left[1 - w^k \exp(i\vartheta) \left\langle B \frac{\boldsymbol{x}_k}{\|\boldsymbol{x}_k\|_2}, \frac{\boldsymbol{x}_k}{\|\boldsymbol{x}_k\|_2} \right\rangle \right]. \tag{3.63}$$

If $\nu(B) \leq 1$ holds, then the term $1 - w^k \exp(i\vartheta) \langle B \frac{\boldsymbol{x}_k}{\|\boldsymbol{x}_k\|_2}, \frac{\boldsymbol{x}_k}{\|\boldsymbol{x}_k\|_2} \rangle$ has nonnegative real part for any $\vartheta \in \mathbb{R}$:

$$\operatorname{Re} \left[1 - w^k \exp(i\vartheta) \left\langle B \frac{\boldsymbol{x}_k}{\|\boldsymbol{x}_k\|_2}, \frac{\boldsymbol{x}_k}{\|\boldsymbol{x}_k\|_2} \right\rangle \right] \geq 0 \quad \forall \vartheta \in \mathbb{R}$$

for $k = 1, \ldots, m$. Therefore, the left-hand side of (3.63) also has nonnegative real part. This implies that

$$\operatorname{Re} \Big[\exp(im\vartheta) \langle B^m \boldsymbol{x}, \boldsymbol{x} \rangle \Big] \leq 1 \quad \forall \vartheta \in \mathbb{R},$$

which then gives us the relation $|\langle B^m \boldsymbol{x}, \boldsymbol{x} \rangle| \leq 1$ for any normalized vector $\boldsymbol{x}$.[25] Therefore, we obtain

$$\nu(B^m) \leq 1. \tag{3.64}$$

Hence, if $\nu(B) \leq 1$ holds, then $\nu(B^m) \leq 1$.

Now, let us consider any nonzero matrix $A \in \mathbb{C}^{n \times n}$. We define $B := \frac{1}{\nu(A)} A$ and, using (f), compute

$$\nu(B) = \nu \Big(\frac{1}{\nu(A)} A \Big) = \frac{1}{\nu(A)} \nu(A) = 1.$$

[25] To see this, one can write $1 \geq \operatorname{Re} \big(e^{im\vartheta} \langle B^m \boldsymbol{x}, \boldsymbol{x} \rangle \big) = \operatorname{Re} \big(e^{i(m\vartheta + \delta))} |\langle B^m \boldsymbol{x}, \boldsymbol{x} \rangle| \big)$ and then choose $\theta = -\delta/m$.

Therefore (3.64) holds and we get

$$1 \geq \nu(B^m) = \nu\Big(\frac{1}{\nu(A)^m} A^m\Big) = \frac{1}{\nu(A)^m}\nu(A^m),$$

which implies that $\nu(A)^m \geq \nu(A^m)$. In the special case $A = 0$, we obviously have that $\nu(A) = 0$ and $\nu(A^m) = 0$. Hence the result follows. ∎

We can now prove the following convergence estimate. Recall that we assumed in our analysis that $\boldsymbol{u}_0 = 0$, i.e., $\boldsymbol{r}_0 = \boldsymbol{f}$.

Theorem 3.29 (Convergence bound for GMRES). *Consider a matrix $A \in \mathbb{R}^{n\times n}$, a vector $\boldsymbol{f} \in \mathbb{R}^n$, and an initial guess $\boldsymbol{u}_0 = 0$. Suppose that the numerical range of A is contained in a disk of radius $s \in \mathbb{R}$ and center $c \in \mathbb{C}$ that does not contain the origin (hence $s/|c| < 1$):*

$$0 \notin \{z \in \mathbb{C} : |z - c| \leq s\} \supset \mathcal{F}(A).$$

Then the residual $\boldsymbol{r}_k$ of GMRES is bounded for any k by

$$\|\boldsymbol{r}_k\|_2 \leq 2\Big(\frac{s}{|c|}\Big)^k \|\boldsymbol{f}\|_2. \tag{3.65}$$

Proof. Using (3.49) we get

$$\|\boldsymbol{r}_k\|_2 = \min_{\substack{p\in\mathcal{P}_k \\ p(0)=1}} \|p(A)\boldsymbol{f}\|_2 \leq \|\widetilde{p}_k(A)\boldsymbol{f}\|_2 \tag{3.66}$$

with $\widetilde{p}_k(z) = (1 - z/c)^k$. Theorem 3.28 allows us to obtain

$$\begin{aligned}
\|\widetilde{p}_k(A)\boldsymbol{f}\|_2 \leq \|\widetilde{p}_k(A)\|_2\|\boldsymbol{f}\|_2 &= \Big\|\Big(I - \frac{1}{c}A\Big)^k\Big\|_2\|\boldsymbol{f}\|_2 \\
&\leq 2\nu\Big(\Big(I - \frac{1}{c}A\Big)^k\Big)\|\boldsymbol{f}\|_2 && \text{(by Theorem 3.28(g))} \\
&\leq 2\Big[\nu\Big(I - \frac{1}{c}A\Big)\Big]^k\|\boldsymbol{f}\|_2 && \text{(by Theorem 3.28(h)).}
\end{aligned}$$

Moreover, using Theorem 3.28(b) we get[26]

$$\mathcal{F}\Big(I - \frac{1}{c}A\Big) = 1 - \frac{1}{c}\mathcal{F}(A) \subset \Big\{z \in \mathbb{C} : |z| \leq \frac{s}{|c|}\Big\},$$

which implies that $\nu\big(I - \frac{1}{c}A\big) \leq \frac{s}{|c|}$. Hence the claim follows. ∎

The result obtained in Theorem 3.29 is quantitative and requires the numerical range to lie in a disk bounded away from the origin. However, by exploiting further properties of the numerical range it is possible to obtain a general residual bound for GMRES. This is a very intriguing research area, which is still very active and whose charm is heightened by the famous *Crouzeix's conjecture*. This fascinating story began with the work [55] of Bernard and François Delyon, who proved in 1999 that, given a smooth, bounded, and convex domain $\Omega \subset \mathbb{C}$ that contains the (closure of the) numerical range $\mathcal{F}(A)$, there exists a best constant $C_\Omega > 0$ such that

$$\|f(A)\|_2 \leq C_\Omega \sup_{z\in\Omega} |f(z)| \tag{3.67}$$

[26] Notice that $1 - \frac{1}{c}\mathcal{F}(A)$ is a simple transformation that scales, translates, and rotates $\mathcal{F}(A)$. If one applies the same transformation to the circle containing $\mathcal{F}(A)$, then this circle is mapped into another circle of radius $s/|c|$, centered in the origin, and containing $1 - \frac{1}{c}\mathcal{F}(A)$.

for any rational function f.[27] This work inspired *Michel Crouzeix*, who in 2004 stated the following conjecture [49].

Conjecture 1 (Crouzeix's conjecture, 2004). *Let* $\mathcal{Q} := \sup_{\Omega} C_{\Omega}$*; then* $\mathcal{Q} = 2$.

This conjecture is still unsolved. Crouzeix proved a few years later in [50] that $2 \leq \mathcal{Q} \leq 11.81$. Very recently, in 2017 in the manuscript [52], Crouzeix and Palencia strongly improved his bound to $2 \leq \mathcal{Q} \leq 1 + \sqrt{2}$, which is very close to the conjectured bound! This result was generalized in 2019 by Crouzeix and Greenbaum for more general regions in the complex plane [51].

Moreover, it is known that the conjecture holds for tridiagonal 3×3 matrices with elliptic field of values centered at an eigenvalue [89] and for general $n \times n$ matrices that are nearly Jordan blocks [36]. Furthermore, Greenbaum and Overton provided numerical support for Crouzeix's conjecture [95]. Despite all these very recent improvements, the conjecture is still unsolved in the general case.

Let us return to the convergence bound for GMRES. As shown in [52] (and recalling that $\mathcal{F}(A)$ is compact; see Theorem 3.28), it holds that

$$\|f(A)\|_2 \leq \widetilde{\mathcal{Q}} \max_{z \in \mathcal{F}(A)} |f(z)|, \tag{3.68}$$

where $\widetilde{\mathcal{Q}} = 1 + \sqrt{2}$ (and $\widetilde{\mathcal{Q}} = 2$ if Crouzeix's conjecture holds); using the relation (3.49) one can get the famous convergence bound

$$\|\boldsymbol{r}_k\|_2 \leq \widetilde{\mathcal{Q}} \min_{\substack{p \in \mathcal{P}_k \\ p(0)=1}} \max_{z \in \mathcal{F}(A)} |p(z)| \, \|\boldsymbol{f}\|_2,$$

i.e., one has to find residual polynomials that are small on the numerical range of A.

Let us now briefly discuss a third approach that permits us to get a convergence bound for GMRES using the notion of the ϵ-pseudospectrum of A. This bound is based on an idea presented in [177]; see also [94, page 57] and [61] for more details. The ϵ-pseudospectrum of A is defined as

$$\Lambda_\epsilon := \{z \in \mathbb{C} : \|(zI - A)^{-1}\|_2 \geq \epsilon^{-1}\},$$

where $\epsilon < 0$, and we denote by Γ_ϵ the boundary of Λ_ϵ. For any polynomial p we can use the Cauchy integral to write

$$p(A) = \frac{1}{2\pi i} \int_{\Gamma} p(z)(zI - A)^{-1} dz,$$

where Γ is any simple closed curve (or the union of simple closed curves) in $\mathbb{C}$ containing the spectrum of A. We denote by $L(\Gamma)$ the length of this curve. If one chooses $\Gamma = \Gamma_\epsilon$ (which clearly contains the spectrum of A) and uses the previous equality, we can obtain the bound

$$\|p(A)\|_2 \leq \frac{L(\Gamma_\epsilon)}{2\pi} \max_{z \in \Gamma_\epsilon} \|p(z)(zI - A)^{-1}\|_2 \leq \frac{L(\Gamma_\epsilon)}{2\pi\epsilon} \max_{z \in \Gamma_\epsilon} |p(z)|. \tag{3.69}$$

Now, using the bound (3.49) and the estimate (3.69) we obtain

$$\|\boldsymbol{r}_k\|_2 \leq \frac{L(\Gamma_\epsilon)}{2\pi\epsilon} \max_{z \in \Gamma_\epsilon} |p(z)| \|\boldsymbol{f}\|_2. \tag{3.70}$$

The accuracy of the estimate (3.5) strongly depends on the choice of the parameter ϵ, which is unfortunately often not so easy in practice.

[27] Notice that this result is proved in a general Hilbert space setting [55].

In general, as we have seen, the convergence analysis of GMRES is not an easy task. All the bounds obtained above are in some cases far from being sharp; see, e.g., [94, 61]. Greenbaum, Pták, and Strakoš [96, 97] have shown that any nonincreasing curve represents a plot of residual norm versus iteration number for GMRES applied to some problem, and this for an arbitrary set of chosen eigenvalues. Hence, for example, eigenvalues tightly clustered around 1 are not necessarily leading to good convergence of Krylov methods when the matrix is highly nonnormal. To see this, consider a matrix A of the form [94]

$$A = \begin{bmatrix} 0 & \times & 0 & 0 & \cdots & 0 \\ 0 & \times & \times & 0 & \cdots & 0 \\ \vdots & \vdots & \vdots & \ddots & \ddots & \vdots \\ 0 & \times & \times & \cdots & \times & 0 \\ 0 & \times & \times & \cdots & \times & \times \\ \times & \times & \times & \cdots & \times & \times \end{bmatrix}. \tag{3.71}$$

Recalling our assumption $\boldsymbol{u}_0 = 0$, if $\boldsymbol{r}_0 = \boldsymbol{f}$ is a multiple of the first canonical vector $\boldsymbol{e}_1$, then $A\boldsymbol{f}$ is a multiple of $\boldsymbol{e}_n$, $A^2\boldsymbol{f}$ is a linear combination of $\boldsymbol{e}_n$, and $\boldsymbol{e}_{n-1}$, $A^3\boldsymbol{f}$ is a linear combination of $\boldsymbol{e}_n$, $\boldsymbol{e}_{n-1}$, and $\boldsymbol{e}_{n-2}$, etc.[28] This means that $\boldsymbol{r}_0 = \boldsymbol{f}$ is orthogonal to the set $\mathrm{span}\{A\boldsymbol{f}, \ldots, A^{n-1}\boldsymbol{f}\}$, and hence

$$\boldsymbol{u}_k = \underset{\widetilde{\boldsymbol{u}} \in \mathcal{K}_k(A, \boldsymbol{f})}{\arg\min} \|\boldsymbol{f} - A\widetilde{\boldsymbol{u}}\|_2 = 0$$

for $k = 1, \ldots, n-1$. This means that GMRES makes no progress until step n! Now, the class of matrices of the form (3.71) includes all $n \times n$ companion matrices

$$A = \begin{bmatrix} 0 & 1 & 0 & 0 & \cdots & 0 \\ 0 & 0 & 1 & 0 & \cdots & 0 \\ \vdots & \vdots & \vdots & \ddots & \ddots & \vdots \\ 0 & 0 & 0 & \cdots & 1 & 0 \\ 0 & 0 & 0 & \cdots & 0 & 1 \\ c_0 & c_1 & c_2 & \cdots & c_{n-2} & c_{n-1} \end{bmatrix},$$

whose eigenvalues are the roots of the (characteristic and minimal) polynomial $p(z) = z^n - \sum_{j=0}^{n-1} c_j z^j$, and the coefficients $c_0, \ldots, c_{n-1}$ can be chosen to make this matrix have any desired eigenvalues! Let us consider two examples.

Example 3.30 (Companion matrix with eigenvalues equal to 1). Consider the polynomial $p(z) = (z-1)^3$ and the corresponding companion matrix

$$A = \begin{bmatrix} 0 & 1 & 0 \\ 0 & 0 & 1 \\ 1 & -3 & 3 \end{bmatrix},$$

which has all eigenvalues equal to 1. However, if we consider $\boldsymbol{u}_0 = 0$ and $\boldsymbol{f} = \boldsymbol{e}_1$, the first canonical vector in $\mathbb{R}^3$, then GMRES will produce approximations $\boldsymbol{u}_k$ such that $\|\boldsymbol{r}_k\|_2 = 1$ for $k = 0, 1, 2$, and only at the third iteration one gets $\|\boldsymbol{r}_3\|_2 = 0$, as illustrated by the MATLAB script

[28] This information propagation mechanism is similar to the one we observed in all the methods we tested so far for Laplace's equation: because of the local connectivity only in the discrete Laplace matrix, the approximation computed by all the methods remained zero in the part of the domain where y is small, for both stationary and Krylov methods. The main goal of preconditioners in Chapter 4 is to change this!

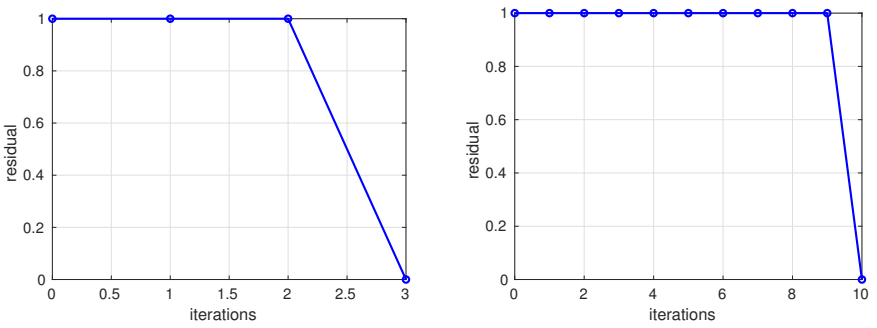

Figure 3.13. *GMRES iterations corresponding to Example 3.30 (left) and Example 3.31 (right).*

```
A = [ 0 1 0 ; 0 0 1 ; 1 -3 3 ];     % companion matrix, with minimal
                                    % polynomial p(z)=(z-1)^3=z^3-3z^2+3z-1
f=zeros(3,1); f(1)=1;               % right-hand side vector equal to e1
u0=zeros(3,1);                      % initial guess for gmres
[u,uk,res]=GMRES(A,f,u0,1e-16,3);   % solve using gmres
plot(0:3,res,'o-b','Linewidth',2);  % plot gmres residuals
grid on;                            % switch grid on
xlabel('iterations');
ylabel('residual');
set(gca,'fontsize',14);             % enlarge the size of the text
```

which produces the graph shown in Figure 3.13 (left). This example clearly shows that even though all the eigenvalues of A are equal to 1, the GMRES residual remains constant for the first two iterations.[29] ∎

Example 3.31 (Companion matrix with random eigenvalues). In this example, we construct a companion matrix A in $\mathbb{R}^{n\times n}$ corresponding to a minimal polynomial with randomly chosen roots, and then solve the problem $A\boldsymbol{u} = \boldsymbol{f}$, with $\boldsymbol{f} = \boldsymbol{e}_1$, the first canonical vector in $\mathbb{R}^n$ starting from an initial guess $\boldsymbol{u}_0 = 0$. This is done by the MATLAB script

```
n=10;                               % dimension of the problem
rootp=1-2*rand(n,1);                % generate a random vector of roots
coeff=poly(rootp);                  % find the corresponding coefficients
coeff=coeff./coeff(1);              % make the polynomial monic
coeff=fliplr(coeff);                % flip the vector of coefficients
A=diag(ones(n-1,1),1);              % construct companion matrix
A(end,:)=-coeff(1:end-1);
u0=zeros(n,1);                      % initial guess for gmres
f=zeros(n,1); f(1)=1;               % right-hand side vector equal to e1
[u,uk,res]=GMRES(A,f,u0,1e-16,n);
plot(0:n,res,'o-b','Linewidth',2);  % plot gmres residuals
grid on;
xlabel('iterations');
ylabel('residual');
set(gca,'fontsize',14);             % enlarge the size of the text
```

[29] Notice also that if $\boldsymbol{e}_1$ denotes the first canonical vector in $\mathbb{R}^3$, then $\boldsymbol{e}_1^\top A\boldsymbol{e}_1 = 0$ (with $\boldsymbol{e}_1^\top \boldsymbol{e} = 1$). Hence, it holds that $0 \in \mathcal{F}(A)$ and Theorem 3.29 is not valid in this case.

which produces the graph shown in Figure 3.13 (right). It is clear from this graph that the GMRES residuals are equal to 1 for all $k = 1, \ldots, n-1$ and only at the last iteration the residual drops to zero. ∎

These examples are not in contradiction with the convergence estimate for GMRES in Theorem 3.26, since the condition number $\kappa(S)$ of the corresponding eigenvector matrix that appears in the estimate is quite large here (just try `[S,E]=eig(A); cond(S)`), so the theoretical estimate is not useful anymore. One probably would not use GMRES to solve a linear system with the sparsity pattern in (3.71), but the same holds for any matrix that is unitarily similar to one of the form (3.71). Note also that (3.71) is simply a permuted triangular matrix. Every matrix is similar to a lower triangular matrix (recall the Schur decomposition), but fortunately most matrices are not unitarily similar to one of the form (3.71).

In exact arithmetic, we can make another statement about the convergence of GMRES. To do so, we make use of the minimal polynomial introduced in Definition 3.5 and characterized in Lemma 3.6. We have the next theorem.

Theorem 3.32 (Convergence of GMRES in a finite number of iterations). *Let $A \in \mathbb{R}^{n\times n}$ be invertible, $\boldsymbol{f} \in \mathbb{R}^n$, and assume that the minimal polynomial $p_{\min}$ of A has degree m. Then GMRES applied to the linear system $A\boldsymbol{u} = \boldsymbol{f}$ converges to the exact solution in at most m iterations.*[30]

Proof. Since A is invertible, the minimal polynomial $p_{\min}(A)$ has the constant coefficient $\alpha_0 \neq 0$. Thus the polynomial

$$p^*(A) = \frac{1}{\alpha_0} p_{\min}(A)$$

satisfies $p^*(0) = 1$ and $p^*(A) = 0$. GMRES minimizes the residual, which is equivalent to the polynomial approximation problem

$$\min_{\boldsymbol{u}_k \in \mathcal{K}_k(A,\boldsymbol{f})} \|\boldsymbol{f} - A\boldsymbol{u}_k\|_2 = \min_{\substack{p\in\mathcal{P}_k \\ p(0)=1}} \|p(A)\boldsymbol{f}\|_2 \leq \|p^*(A)\boldsymbol{f}\|_2 = 0 \quad \text{when } k = m. \qquad \square$$

```
function [u,uk,res]=GMRES(A,f,u0,tol,m)
% GMRES Generalized Minimal Residual
%   [u,uk,res]=GMRES(A,f,u0,tol,m) solves Au=f using the GMRES
%   method starting at the initial guess u0 up to a tolerance tol using
%   at most m iterations. It computes u in the affine Krylov space
%   u0+(r0,Ar0...,A^(k-1)r0) by minimizing the norm ||f-A*u||_2 where k is
%   the smallest integer such that ||f-A*u||_2<tol.
%   GMRES returns in the matrix uk the iterates, in u the solution
%   computed, and in res the history of the norm of the residuals.

if nargin<5, m=100; end            % default values
if nargin<4, tol=1e-6; end
k=1;                               % Initialize the iteration index
uk(:,1)=u0;
r0=f-A*u0;                         % Compute the initial residual
res=norm(r0);                      % Initialize the vercor of residuals
rhs=res;                           % Initialize the right-hand side
Q(:,1)=r0/res;                     % First column of Q
while res(end)/norm(f)>tol && k<=m % GMRES iterations
```

[30] Notice that the assumption that $p_{\min}$ has degree m is satisfied for a matrix A that is diagonalizable and that has m distinct eigenvalues; see Lemma 3.6.

```
  Q(:,k+1)=A*Q(:,k);              % PART 1: Arnoldi: (A Q_k = Q_{k+1} H_k)
  for j=1:k                       % modified Gram-Schmidt on v=A*Q(:,k)
    H(j,k)=Q(:,k+1)'*Q(:,j);
    Q(:,k+1)=Q(:,k+1)-H(j,k)*Q(:,j);
  end
  H(k+1,k)=norm(Q(:,k+1));        % Lower-diagonal element
  Q(:,k+1)=Q(:,k+1)/H(k+1,k);     % Compute the vector Q(:,k+1)
  R(k+1,k)=0;                     % PART 2: QR by Givens rotations
  R(:,k)=H(:,k);                  % New column of R
  for j=1:k-1                     % Former Givens rotations on last column
    Rk=c(j)*R(j,k)+s(j)*R(j+1,k);
    R(j+1,k)=-s(j)*R(j,k)+c(j)*R(j+1,k);
    R(j,k)=Rk;
  end                             % Next apply the new Givens rotation
  c(k)=R(k,k)/sqrt(R(k,k)^2+R(k+1,k)^2);
  s(k)=R(k+1,k)/sqrt(R(k,k)^2+R(k+1,k)^2);
  R(k,k)=c(k)*R(k,k)+s(k)*R(k+1,k);
  R(k+1,k)=0;
  rhs(k+1)=-s(k)*rhs(k);           % PART 3: Update rhs and residuals
  rhs(k)=c(k)*rhs(k);              % New Givens rotation on rhs
  res(k+1)=abs(rhs(k+1));          % Compute the new norm of the residual
  k=k+1;                           % Update iteration index
  if nargout>1
    y=R\rhs';                      % Compute the coefficients y_j
    uk(:,k)=u0+Q(:,1:end-1)*y;     % Compute u as sum_j y_j q_j
  end
end
y=R\rhs';                          % Compute the coefficients y_j
u=u0+Q(:,1:end-1)*y;               % Compute u as u0+sum_j y_j q_j
```

Next, we explain some details of this implementation. At each iteration k, the GMRES loop is given by three main parts:

- Part 1: One step of the Arnoldi method is performed to compute the new column $\boldsymbol{q}_{k+1}$ of Q_{k+1} and the kth columns of $H_k \in \mathbb{R}^{k+1\times k}$. This is obtained by a modified Gram–Schmidt orthogonalization process applied to the vector $\boldsymbol{v} = A\boldsymbol{q}_k$. Notice that Q_{k+1} has size $n \times k+1$, where n is the length of $\boldsymbol{f}$.

- Part 2: The matrix H_k is QR-factorized as $H_k = \widetilde{Q}R_k$ using Givens rotations. In particular, $\widetilde{Q} \in \mathbb{R}^{k+1\times k+1}$ is an orthogonal matrix obtained as the product $\widetilde{Q} = (G_k G_{k-1} \cdots G_1)^\top$, where each Givens matrix G_j has the form

$$G_j = \begin{bmatrix} I_{j-1} & & \\ & \begin{bmatrix} c_j & s_j \\ -s_j & c_j \end{bmatrix} & \\ & & I_{k-j-1} \end{bmatrix},$$

  with I_{j-1} and I_{k-j-1} identities of dimension $j-1$ and $k-j-1$. The scalars c_k and s_k are computed to obtain that

$$[G_k(G_{k-1} \cdots G_1 H_k)]_{j+1,j} = 0.$$

  Notice that the matrices G_j are not explicitly constructed. At the iteration k, first the matrix $(G_{k-1} \cdots G_1 H_k)$ is assembled, and then the action of G_k on $(G_{k-1} \cdots G_1 H_k)$ is computed. Using the structure of the matrices G_j, this is achieved in $O(n)$ operations; see Problem 43 for more details.

- Part 3: The Givens matrix G_k is applied to the vector

$$\texttt{rhs} = G_{k-1} \cdots G_1(\|\boldsymbol{r}_0\|_2 \boldsymbol{e}_1) = \|\boldsymbol{r}_0\|_2 \widetilde{Q}^\top \boldsymbol{e}_1 =: \boldsymbol{w}_{k-1}.$$

This is necessary to solve the least squares problem (3.48). To see this, recall the QR factorization of H_k (Part 2) and observe that

$$\boldsymbol{w}_k = G_k G_{k-1} \cdots G_1(\|\boldsymbol{r}_0\|_2 \boldsymbol{e}_1) = G_k \boldsymbol{w}_{k-1}.$$

Hence, at iteration k, the vector $\boldsymbol{w}_k$ is obtained by applying G_k to $\boldsymbol{w}_{k-1}$, constructed at the previous iteration. Now, we denote $\boldsymbol{w}_k = \begin{bmatrix} \boldsymbol{w} \\ w_{k+1,k} \end{bmatrix}$ and $R_k = \begin{bmatrix} R \\ 0 \end{bmatrix}$, where $R \in \mathbb{R}^{k \times k}$ is upper triangular, and write

$$\begin{aligned} \left\| \|\boldsymbol{r}_0\|_2 \boldsymbol{e}_1 - H_k \boldsymbol{y} \right\|_2 &= \left\| \|\boldsymbol{r}_0\|_2 \boldsymbol{e}_1 - \widetilde{Q} R_k \boldsymbol{y} \right\|_2 = \left\| \widetilde{Q}(\|\boldsymbol{r}_0\|_2 \widetilde{Q}^\top \boldsymbol{e}_1 - R_k \boldsymbol{y}) \right\|_2 \\ &= \left\| \|\boldsymbol{r}_0\|_2 \widetilde{Q}^\top \boldsymbol{e}_1 - R_k \boldsymbol{y} \right\|_2 = \left\| \boldsymbol{w}_k - R_k \boldsymbol{y} \right\|_2 \\ &= \sqrt{\left\| \boldsymbol{w} - R\boldsymbol{y} \right\|_2^2 + |w_{k+1,k}|^2}. \end{aligned}$$

Since we assume that $\boldsymbol{y} = R^{-1}\boldsymbol{w}$, Theorem 3.21 (together with Remark 4) allows us to compute the norm of the residual as follows:

$$\begin{aligned} \|\boldsymbol{r}_k\|_2 = \|\boldsymbol{f} - A\boldsymbol{u}_k\|_2 &= \left\| \|\boldsymbol{r}_0\|_2 \boldsymbol{e}_1 - H_k \boldsymbol{y} \right\|_2 \\ &= \sqrt{\left\| \boldsymbol{w} - R\boldsymbol{y} \right\|_2^2 + |w_{k+1,k}|^2} \\ &= |w_{k+1,k}|. \end{aligned}$$

Even though GMRES is for general linear systems, and does too much work for symmetric positive definite problems, we now test it on our Laplace model problem from Section 1.3 using the analogous MATLAB script we have shown already for testing the more suitable CG algorithm for the Laplace model problem in Section 3.2.[31] The first iterates we obtain from GMRES are shown in Figure 3.14. We see that GMRES converges rather quickly, comparable to CG in Figure 3.7. Since GMRES minimized the residual, and CG the A-norm of the error, we plot these quantities for comparison for GMRES and CG in Figure 3.15, together with the l^2-norm of the error. We clearly see that the A-norm of the error is smaller for CG than for GMRES, and also the l^2-norm of the error, but the residual is smaller for GMRES than for CG. Since the problem is symmetric, one should have used *MINRES* for these computations, which gives the same result as GMRES, but for much lower computational cost, comparable to CG; see also Section 3.6. Finally, we test the behavior of GMRES for different values of the mesh size h. If we solve our Laplace test problem for different values of the mesh size, we obtain the result depicted in Figure 3.16, which shows the deterioration of the convergence properties of GMRES for decreasing h (compare with Figure 3.10).

Remark 5 (Restarted GMRES). *Each GMRES iteration generates a new vector $\boldsymbol{q}_k$, which has to be stored in memory. For large (but sparse) matrices, this can quickly use up the available memory and lead to problems. Therefore, one often uses GMRES with restarts: after m iterations, the vectors $\boldsymbol{q}_1, \boldsymbol{q}_2, \ldots, \boldsymbol{q}_m$ are discarded, the best approximation $\boldsymbol{u}_m$ found so far is retained, and GMRES is restarted in order to solve for the corrections $\widetilde{\boldsymbol{u}}$ the system*

$$A\widetilde{\boldsymbol{u}} = \boldsymbol{f} - A\boldsymbol{u}_m = \boldsymbol{r}_m.$$

[31] The reader is asked, in the problems at the end of this chapter, to test GMRES on the nonsymmetric advection-reaction-diffusion problem of Section 1.4.

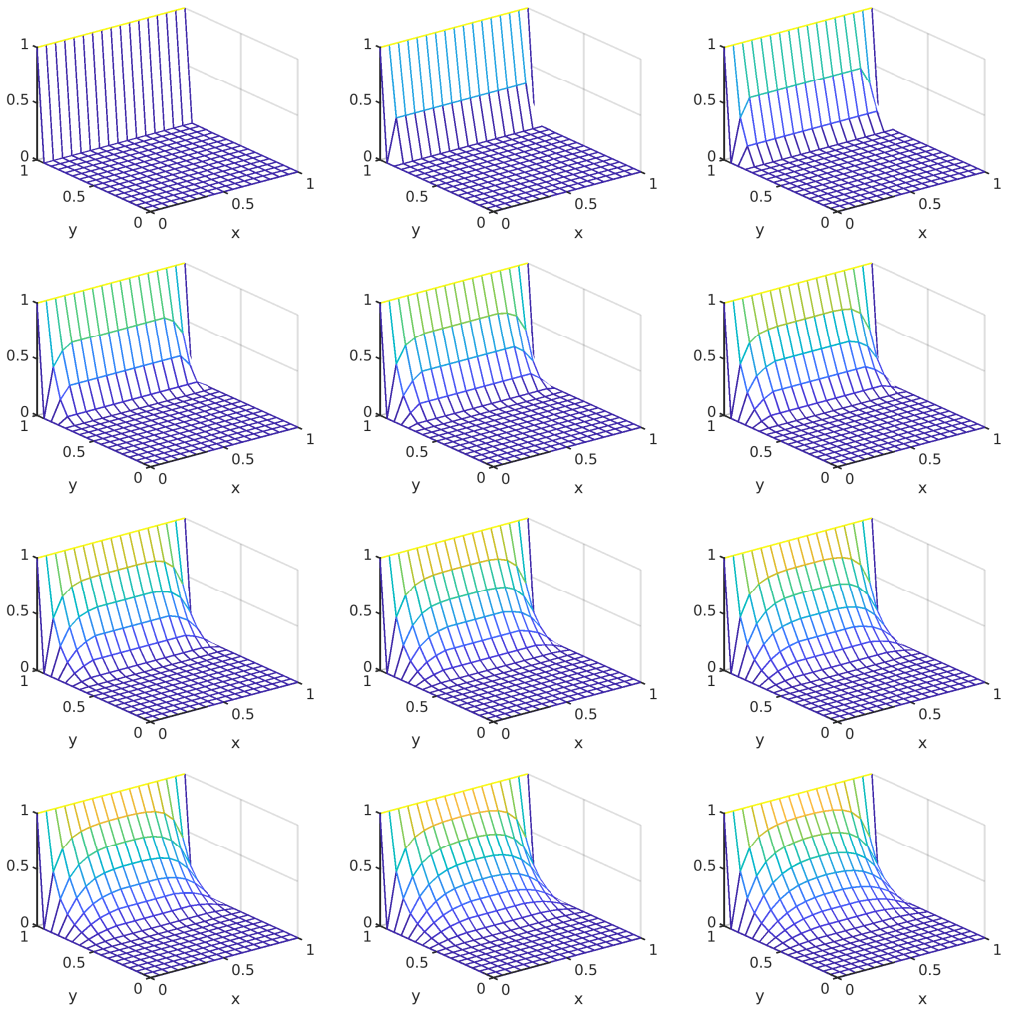

Figure 3.14. *Initial guess and first iterations of GMRES applied to our Laplace model problem from Section 1.3.*

Remark 6 (Early termination (lucky breakdown) of GMRES). *If it happens that $h_{k+1,k} = 0$, then the GMRES iteration breaks down. This early termination of GMRES is also known as a lucky breakdown, since if $h_{k+1,k} = 0$ holds, then the approximation $\boldsymbol{u}_k$ computed by GMRES at the kth iteration coincides with the exact solution $\boldsymbol{u}$. To see this, we recall the relation* (3.46) *and denote by $\widetilde{H}_k$ the $k \times k$ matrix obtained from H_k by deleting the last row. Since $h_{k+1,k} = 0$, we have that $Q_k \widetilde{H}_k = AQ_k$. Therefore, the invertibility of A and the fact that $\operatorname{rank}(Q_k) = k$ allow us to write*

$$k \geq \operatorname{rank}(\widetilde{H}_k) = \operatorname{rank}(Q_k \widetilde{H}_k) = \operatorname{rank}(AQ_k) = \operatorname{rank}(Q_k) = k,$$

which means that $\widetilde{H}_k$ (and hence also H_k) has full rank. Hence, using Theorem 3.21 and Remark 4 the residual norm $\|\boldsymbol{f} - A\widetilde{\boldsymbol{u}}\|_2 = \left\| \|\boldsymbol{r}_0\|_2 \boldsymbol{e}_1 - \widetilde{H}_k \boldsymbol{w} \right\|_2$ is minimized by $\boldsymbol{w} = \widetilde{H}_k^{-1}(\|\boldsymbol{r}_0\|_2 \boldsymbol{e}_1)$, which obviously gives residual zero. This means that a breakdown of GMRES occurs if the exact solution has been found.

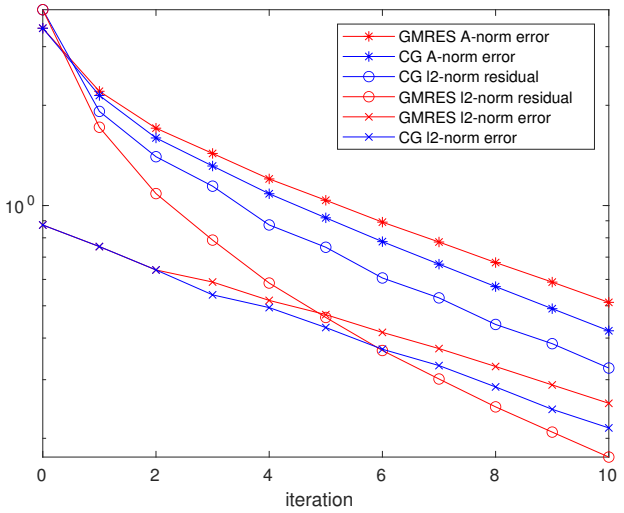

Figure 3.15. *Comparison of CG and GMRES applied to our Laplace model problem from Section 1.3.*

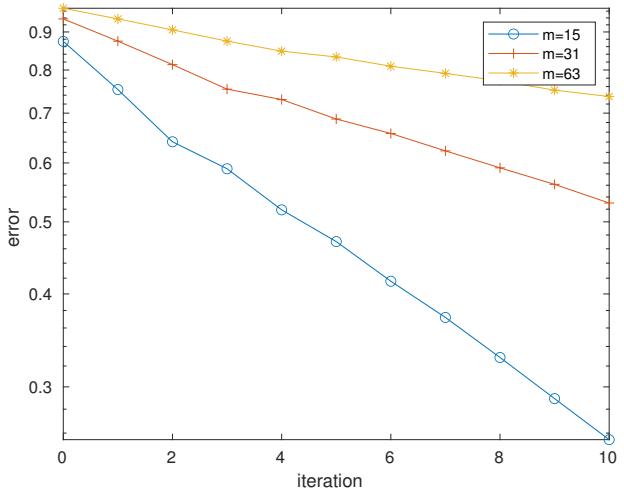

Figure 3.16. *Convergence of GMRES for different grid sizes* $h = \frac{1}{m+1}$.

Notice that this situation coincides with the breakdown of the Arnoldi procedure, which we discussed in Lemma 3.20. This lemma can be used together with Theorem 3.32 to obtain that the breakdown condition $h_{k+1,k} = 0$ *implies that GMRES converged to the exact solution.*

Remark 7 (Modified Gram–Schmidt and Householder Arnoldi). *In Remark 3 we briefly mentioned that while the original Arnoldi algorithm uses the modified Gram–Schmidt orthogonalization procedure, there exist more efficient implementations that cure the possible loss of orthogonality that characterizes the numerical behavior of modified Gram–Schmidt. One of these implementations is based on a Householder Arnoldi process, which guarantees more robust numerical orthogonalization. Similarly, the GMRES implementation can be changed by using a Householder Arnoldi process; see, e.g., [160] and the MATLAB implementation* `gmres`.

However, Liesen and Strakoš clarify in [124] that

> *In conclusion, unless the matrix A is close to singular, MGS GMRES provides, despite the (gradual) loss of orthogonality among the computed MGS Arnoldi vectors, an approximate solution with normwise relative backward error comparable to the Householder Arnoldi GMRES.*

3.6 ▪ Two families of Krylov methods

> *The following theorem gives the mathematical description of several important Krylov subspace methods in terms of the search and constraints spaces, and it shows the corresponding optimality properties.*
>
> Jörg Liesen and Zdeněk Strakoš, *Krylov Subspace Methods, Principles and Analysis*, 2013.

We have seen two main ideas to find an approximate solution of a given linear system $A\boldsymbol{u} = \boldsymbol{f}$ in the affine Krylov space $\boldsymbol{u}_0 + \mathcal{K}_k(A, \boldsymbol{r}_0)$:

1. Methods based on orthogonalization of the residual with respect to the Krylov space $\mathcal{K}_k(A, \boldsymbol{r}_0)$. These methods find an approximate solution $\boldsymbol{u}_k \in \boldsymbol{u}_0 + \mathcal{K}_k(A, \boldsymbol{r}_0)$ such that
$$\boldsymbol{r}_k = \boldsymbol{f} - A\boldsymbol{u}_k \perp \mathcal{K}_k(A, \boldsymbol{r}_0).$$
Methods in this class are the following:
   - CG, the conjugate gradient method, for symmetric positive definite matrices A, which was the first method of this type, invented independently by *David Hestenes* and *Eduard Stiefel* in 1952; see their joint paper [106].
   - SymmLQ, for symmetric but indefinite matrices A, invented by *Chris Paige* and *Michael Saunders* in 1975. This method is based on the Lanczos process and an LQ factorization of the obtained tridiagonal matrix and thus has a short recurrence with low storage requirements similar to CG; see [142]. The LQ factorization is the analogue of the QR factorization, but with a lower triangular matrix L instead of the upper triangular matrix R. For a discussion about the relations between SymmLQ and CG see [142, Section 8] and also [124, Section 2.5.4]. For symmetric positive definite problems CG and SymmLQ give essentially the same results at convergence, but CG is computationally more efficient.
   - FOM, the full orthogonalization method, which works for arbitrary matrices A and was invented by *Yousef Saad* in 1981. The method uses Arnoldi and thus requires substantially more storage, like GMRES; see [159].
   - BiCGStab, the biconjugate gradient method with stabilization, which is also a method for general matrices A, invented by *Henk A. van der Vorst* in 1992. The method constructs two biorthogonal sequences of vectors, one based on A and one based on $A^\top$; see [179]. The method uses short recurrences requiring therefore less storage than FOM, but it does not fully solve the problem of orthogonalization like in FOM.
2. Methods based on minimization of the residual norm:
   - MINRES, the minimum residual method, for symmetric but possibly indefinite matrices A. This method was also invented by Paige and Saunders in 1975, in the same paper as SymmLQ (see [142]), and uses a short recurrence based on the Lanczos process with storage requirements similar to CG.

- GMRES, the generalized minimum residual method, for arbitrary matrices A, invented by Saad and Schultz in 1986, based on the Arnoldi process; see [165]. Even though this method needs a lot of storage, it is very popular for testing preconditioners, since it really minimizes the residual.
- QMR, the quasi-minimum residual method, also for general matrices A, and using a short recurrence based on the *unsymmetric Lanczos process* (see, e.g., [86, Section 11.7.7]) with storage requirements similar to CG. This method was invented by *Roland W. Freund* and *Noël M. Nachtigal* in 1991 and only approximately solves the minimization problem; see [67].

Krylov methods are still a very active area of research, see the recent monograph [124] and references therein, and their convergence properties are far from being completely understood, even without taking into account round-off error. For normal matrices A, however, i.e., matrices such that $AA^\top = A^\top A$, all these methods have a good convergence behavior if their spectrum $\{\lambda_j(A)\}$ is close to 1 in the complex plane. For most matrices coming from applications, however, this is unfortunately not the case, especially for discretizations of PDEs, and the system first needs to be transformed into a new system which has a more favorable spectrum. This process is called preconditioning and is the subject of the next chapter.

3.7 ▪ Problems

Problem 32. *Consider a function $f : \mathbb{R}^n \to \mathbb{R}$ and denote by $\nabla f(\boldsymbol{v})$ the gradient of f in $\boldsymbol{v} \in \mathbb{R}^n$ obtained by the usual scalar product for $\mathbb{R}^n$. Prove that $\nabla f(\boldsymbol{v})$ is orthogonal to the level set of f in $\boldsymbol{v}$ and that $-\nabla f(\boldsymbol{v})$ defines the direction of Steepest Descent of f in $\boldsymbol{v}$.*

Problem 33. *Implement the Steepest Descent method to solve a linear system $A\boldsymbol{u} = \boldsymbol{f}$. Test your codes to solve the Laplace equation.*

Problem 34. *In this exercise we prove the Kantorovich inequality using the Wielandt inequality [108]. Consider a Hermitian positive definite matrix $A \in \mathbb{C}^{n\times n}$ having eigenvalues $0 < \lambda_1 \leq \lambda_2 \leq \cdots \leq \lambda_n$. The Wielandt inequality is*

$$|\boldsymbol{u}^* A\boldsymbol{v}|^2 \leq \left(\frac{\lambda_1 - \lambda_n}{\lambda_1 + \lambda_n}\right)^2 (\boldsymbol{u}^* A\boldsymbol{u})(\boldsymbol{v}^* A\boldsymbol{v}) \quad \forall \text{ orthogonal } \boldsymbol{u}, \boldsymbol{v} \in \mathbb{C}^n, \tag{3.72}$$

and the Kantorovich inequality is

$$(\boldsymbol{u}^* A\boldsymbol{u})(\boldsymbol{u}^* A^{-1}\boldsymbol{u}) \leq \frac{(\lambda_1 + \lambda_n)^2}{4\lambda_1\lambda_n} \|\boldsymbol{u}\|_2^4 \quad \forall \boldsymbol{u} \in \mathbb{C}^n. \tag{3.73}$$

The Kantorovich inequality can be obtained by the Wielandt inequality following the next steps.

(a) *Show that* (3.72) *and* (3.73) *are both satisfied if $\boldsymbol{u} \in \mathbb{C}^n$ is an eigenvector of A. Hint: Use the arithmetic-geometric mean inequality $\sqrt{ab} \leq \frac{1}{2}(a + b)$ for any $a, b > 0$.*

(b) *Show that if $\boldsymbol{u} \in \mathbb{C}^n$ is not an eigenvector of A, then $A^{-1}x - (\boldsymbol{u}^* A^{-1}\boldsymbol{u})\boldsymbol{u} \neq 0$ and $x - (\boldsymbol{u}^* A^{-1}\boldsymbol{u})A\boldsymbol{u} \neq 0$.*

(c) *Show that if $\boldsymbol{u} \in \mathbb{C}^n$ is a unit vector, that is, $\|\boldsymbol{u}\|_2 = 1$, then $(\boldsymbol{u}^* A\boldsymbol{u})(\boldsymbol{u}^* A^{-1}\boldsymbol{u}) \geq 1$, with strict inequality if $\boldsymbol{u}$ is not an eigenvector of A. Hint: Begin with $1 = (\boldsymbol{u}^*\boldsymbol{u})^2 = (\boldsymbol{u}^* A^{1/2} A^{-1/2}\boldsymbol{u})^2$ and use the Cauchy–Schwarz inequality.*

(d) *Consider a unit vector* $\boldsymbol{u} \in \mathbb{C}^n$ *which is not an eigenvector of* A. *Define* $\boldsymbol{v} := A^{-1}\boldsymbol{u} - (\boldsymbol{u}^* A^{-1}\boldsymbol{u})\boldsymbol{u}$. *Show that*

1. $\boldsymbol{v}^*\boldsymbol{u} = 0$,
2. $A\boldsymbol{v} \neq 0$,
3. $\boldsymbol{u}^* A\boldsymbol{v} = 1 - (\boldsymbol{u}^* A\boldsymbol{u})(\boldsymbol{u}^* A^{-1}\boldsymbol{u}) < 0$,
4. $\boldsymbol{v}^* A\boldsymbol{v} = -(\boldsymbol{u}^* A^{-1}\boldsymbol{u})(\boldsymbol{v}^* A\boldsymbol{u})$.

Hint: Use the results proved in (b) and (c).

(e) Use the Wielandt inequality (3.72) *and the results proved above to obtain the Kantorovich inequality* (3.73).

Problem 35. *Recall Problem 25 and consider the advection-reaction-diffusion problem* (2.53) *in the finite-differences discrete form* $A\boldsymbol{u} = \boldsymbol{f}$.

- *Prove that problem* $A\boldsymbol{u} = \boldsymbol{f}$ *is equivalent to*

$$\min_{\boldsymbol{u}} F(\boldsymbol{u}),$$

where $F(\boldsymbol{u}) := \frac{1}{2}\|A\boldsymbol{u} - \boldsymbol{f}\|_2^2$.

- *Rewrite* $F(\boldsymbol{u})$ *in the form* $\frac{1}{2}\boldsymbol{u}^\top \widetilde{A}\boldsymbol{u} - \boldsymbol{u}^\top \widetilde{\boldsymbol{f}} + c$ *for some matrix* $\widetilde{A}$, *vector* $\widetilde{\boldsymbol{f}}$ *and scalar* c.

- *Solve the problem* $\min_{\boldsymbol{u}} \frac{1}{2}\boldsymbol{u}^\top \widetilde{A}\boldsymbol{u} - \boldsymbol{u}^\top \widetilde{\boldsymbol{f}} + c$ *using Steepest Descent.*

- *Study the convergence of the method and comment on the results you obtain in light of Theorem 3.1.*

- *What happens if one uses Steepest Descent to solve directly the original problem* $A\boldsymbol{u} = \boldsymbol{f}$? *Test the Steepest Descent algorithm and comment on the results that you obtain.*

Problem 36. *Implement the CG method to solve a linear system* $A\boldsymbol{u} = \boldsymbol{f}$. *Test your codes to solve the Laplace equation.*

Problem 37. *Show that the step-length* $\alpha_k = \frac{\boldsymbol{r}_k^\top \boldsymbol{p}_k}{\boldsymbol{p}_k^\top A \boldsymbol{p}_k}$ *is optimal in the sense that it minimizes the function*

$$\alpha \mapsto \phi(\alpha) := \frac{1}{2}(\boldsymbol{u}_k + \alpha\boldsymbol{p}_k)^\top A(\boldsymbol{u}_k + \alpha\boldsymbol{p}_k) - \boldsymbol{f}^\top(\boldsymbol{u}_k + \alpha\boldsymbol{p}_k).$$

Show that α_k *is also a minimizer for*

$$\alpha \mapsto \varphi(\alpha) := \|\boldsymbol{u}_k + \alpha\boldsymbol{p}_k - \boldsymbol{u}\|_A^2.$$

Problem 38. *Using Lemma 3.14, prove that CG minimizes at each iteration the residual in the* A^{-1}*-norm (*$\|\boldsymbol{z}\|_{A^{-1}} = \sqrt{\boldsymbol{z}^\top A^{-1}\boldsymbol{z}}$*), that is,*

$$\|\boldsymbol{r}_k\|_{A^{-1}} = \min_{\substack{p \in \mathcal{P}_k \\ p(0)=1}} \|p(A)\boldsymbol{r}_0\|_{A^{-1}}.$$

Problem 39. *Let A be a symmetric and positive definite matrix. Using the estimate* (3.36)*, prove that*

$$\|\boldsymbol{u}-\boldsymbol{u}_k\|_2 \leq 2\sqrt{\kappa(A)}\left(\frac{\sqrt{\kappa(A)}-1}{\sqrt{\kappa(A)}+1}\right)^k \|\boldsymbol{u}-\boldsymbol{u}_0\|_2.$$

Hint: First show that $\lambda_{\min}(A)\|\boldsymbol{x}\|_2^2 \leq \|\boldsymbol{x}\|_A^2 \leq \lambda_{\max}(A)\|\boldsymbol{x}\|_2^2$ for any vector $\boldsymbol{x}$, and then use (3.36)*.*

Problem 40. *In this exercise you will derive the CG method, for the solution of $A\boldsymbol{u}=\boldsymbol{f}$ ($A\in\mathbb{R}^{n\times n}$ symmetric positive definite), from the Lanczos method. To do so, consider the following steps.*

1. *Recall the decomposition $AQ_k = Q_{k+1}H_k$, where $Q_k = \begin{bmatrix}\boldsymbol{q}_1 & \cdots & \boldsymbol{q}_k\end{bmatrix}\in\mathbb{R}^{n\times k}$ and assume that $\boldsymbol{q}_1 = \frac{1}{\|\boldsymbol{f}\|_2}\boldsymbol{f}$. The matrix H_k has the form $H_k = \begin{bmatrix}T_k\\ \boldsymbol{v}\end{bmatrix}$, where*

$$T_k = \begin{bmatrix}\alpha_1 & \beta_1 & & & \\ \beta_1 & \alpha_2 & \beta_2 & & \\ & & \ddots & & \\ & & & \beta_{k-1} & \alpha_k\end{bmatrix},$$

and $\boldsymbol{v} = \begin{bmatrix}0 & \cdots & 0 & \beta_k\end{bmatrix}$.

   (a) *Show that $Q_k^\top A Q_k = T_k$.*

   (b) *Show that*

$$\boldsymbol{u}_k := \underset{\boldsymbol{x}_k\in\operatorname{span}\{\boldsymbol{q}_1\cdots\boldsymbol{q}_k\}}{\arg\min}\ \frac{1}{2}\boldsymbol{x}_k^\top A\boldsymbol{x}_k - \boldsymbol{x}_k^\top\boldsymbol{f} = Q_k T_k^{-1}\big(\|\boldsymbol{f}\|_2\boldsymbol{e}_1\big).$$

   Hint: Introduce a vector $\boldsymbol{y}\in\mathbb{R}^k$ such that $\boldsymbol{x}_k = Q_k\boldsymbol{y}$ and prove that $\boldsymbol{y} = T_k^{-1}Q_k^\top\boldsymbol{f}$.

2. *Consider the LU-decomposition of T_k, that is, $T_k = L_kU_k$, where*

$$L_k = \begin{bmatrix}1 & & & \\ \gamma_1 & 1 & & \\ & \ddots & \ddots & \\ & & \gamma_{k-1} & 1\end{bmatrix} \quad\text{and}\quad U_k = \begin{bmatrix}\eta_1 & \beta_1 & & \\ & \eta_2 & \beta_2 & \\ & & \ddots & \\ & & & \eta_k\end{bmatrix}.$$

   (a) *Show that $\gamma_{k-1} = \frac{\beta_{k-1}}{\eta_{k-1}}$ and $\eta_k = \alpha_k - \gamma_{k-1}\beta_{k-1}$.*

   (b) *Define $P_k := Q_kU_k^{-1}$ and show that the columns $\boldsymbol{p}_j$ of P_k satisfy $\boldsymbol{p}_j = \frac{1}{\eta_j}\big(\boldsymbol{q}_j - \beta_{j-1}\boldsymbol{p}_{j-1}\big)$ for $j=1,\dots,k-1$ and $\boldsymbol{p}_k = \frac{1}{\eta_k}\boldsymbol{q}_k$.*

   (c) *Show that $\boldsymbol{u}_k = \boldsymbol{u}_{k-1}+\zeta_k\boldsymbol{p}_k$ for a $\zeta_k\in\mathbb{R}$. Hint: Begin with $\boldsymbol{u}_k = Q_kT_k^{-1}\big(\|\boldsymbol{f}\|_2\boldsymbol{e}_1\big)$ and use the LU decomposition of T_k.*

3. *Prove that*

   - *the vectors $\boldsymbol{p}_k$ are A-orthogonal;*
   - *$\boldsymbol{r}_k = \sigma_k\boldsymbol{q}_{k+1}$ for some $\sigma_k\in\mathbb{R}$, where $\boldsymbol{r}_k = \boldsymbol{f} - A\boldsymbol{u}_k$ is the residual;*
   - *$\boldsymbol{r}_k\perp\boldsymbol{q}_j$ for $j=1,\dots,k-1$ and that $\boldsymbol{r}_k\perp\boldsymbol{r}_{k-1}$.*

4. *Take a vector $\widetilde{\boldsymbol{p}}_{k-1}$ parallel to $\boldsymbol{p}_k$; then we can rewrite $\boldsymbol{u}_k = \boldsymbol{u}_{k-1} + \zeta_k \boldsymbol{p}_k$ 2(c) as $\boldsymbol{u}_k = \boldsymbol{u}_{k-1} + \widetilde{\alpha}_{k-1}\widetilde{\boldsymbol{p}}_{k-1}$ for some α_{k-1}.*
   - *Show that $\widetilde{\boldsymbol{p}}_k = \boldsymbol{r}_k + \widetilde{\beta}_k \widetilde{\boldsymbol{p}}_{k-1}$ for some $\widetilde{\beta}_k \in \mathbb{R}$.*
   - *Compute $\widetilde{\alpha}_k$ by using the orthogonality $\boldsymbol{r}_k \perp \boldsymbol{r}_{k-1}$.*
   - *Compute $\widetilde{\beta}_k$ by using the A-orthogonality of the vectors $\widetilde{p}_k$. Hint: You should obtain that $\widetilde{\alpha}_k = \frac{\|\boldsymbol{r}_k\|_2^2}{\widetilde{\boldsymbol{p}}_k^\top A \widetilde{\boldsymbol{p}}_k}$ and $\widetilde{\beta}_k = \frac{\|\boldsymbol{r}_k\|_2^2}{\|\boldsymbol{r}_{k-1}\|_2^2}$.*
5. *Summarize the obtained results and compare them with the CG algorithm.*

Problem 41. *Write a MATLAB script to solve the one-dimensional Laplace problem*

$$\begin{aligned} -u'' &= 0 \text{ in } (0,1), \\ u(0) &= 1, \\ u(1) &= 0 \end{aligned}$$

using CG. Use for the tolerance of the norm of the residual 10^{-10} and an initial vector $\boldsymbol{u}_0 = 0$. How many iterations does CG need to converge? Plot the approximation $\boldsymbol{u}_k$ at each iteration. What do you observe? Discuss the relations between this convergence behavior and the Krylov space generated by the CG method.

Problem 42. *Consider the same tasks of Problem 35 using CG instead of Steepest Descent.*

Problem 43. *Construct an algorithm that computes in $O(n^2)$ operations the QR decomposition of a Hessenberg matrix H of size $n \times n$ using Givens rotations. Next, suppose that the QR decomposition is already known for the matrix that corresponds to the first $n-1$ columns of H. Show how this information can be used to compute the QR decomposition in $O(n)$ operations.*

Problem 44. *Prove the statements (b), (d), (e), and (f) of Theorem 3.28.*

Problem 45. *Let $H \in \mathbb{C}^{n\times n}$ and $S \in \mathbb{C}^{n\times n}$ be Hermitian and skew-Hermitian, respectively. Prove that $\rho(H) = \|H\|_2 = \nu(H)$ and $\rho(S) = \|S\|_2 = \nu(S)$, where $\nu(H)$ and $\nu(S)$ are the numerical radii of H and S.*

Problem 46. *Consider the GMRES algorithm for the solution of $A\boldsymbol{u} = \boldsymbol{f}$, with the matrix $A \in \mathbb{R}^{2n\times 2n}$ given by*

$$A = \begin{bmatrix} I & B \\ 0 & I \end{bmatrix},$$

where I is the $n \times n$ identity and $B \in \mathbb{R}^{n\times n}$ is an arbitrary matrix. How many iterations are at most performed (for an arbitrary choice of $\boldsymbol{f} \in \mathbb{R}^n$ and $\boldsymbol{u}_0 \in \mathbb{R}^n$) by GMRES to converge?

Problem 47. *Consider Theorem 3.22.*

- *Assume that A is the discrete finite-difference negative Laplace matrix (see Section 1.3). Which properties does the matrix S of Theorem 3.22 have? Can one compute explicitly $\kappa(S)$?*
- *Assume that A is the discrete finite-difference advection-reaction-diffusion matrix corresponding, e.g., to Problem 4. Recalling Problems 11 and 27, compute explicitly the matrix S. What can one say about $\kappa(S)$?*

Hint: Notice that the eigenvectors $\boldsymbol{v}_k$, $k = 1, \dots, n$, of a tridiagonal matrix $A \in \mathbb{R}^{n\times n}$ with Toeplitz structure

$$A = \begin{bmatrix} a & c & & & \\ b & a & c & & \\ & b & a & c & \\ & & \ddots & \ddots & \ddots \end{bmatrix}$$

are given by $\boldsymbol{v}_{k,j} = \left[\left(\frac{b}{c}\right)^{1/2} \sin\left(\frac{1\pi k}{n+1}\right) \quad \cdots \quad \left(\frac{b}{c}\right)^{n/2} \sin\left(\frac{n\pi k}{n+1}\right) \right]^\top$.

Problem 48. *Test GMRES for the solution to the advection-reaction-diffusion problem* (2.53)*. In particular, consider a random initialization and*

- *plot the first iterations of the method;*
- *plot the convergence curve (errors and residuals); and*
- *repeat the experiments for different h and study the convergence of the method.*

Problem 49. *Modify the codes obtained for Problem 48 to obtain the results of Figure 3.14 for the advection-reaction-diffusion problem*

$$\begin{aligned} -\nu\Delta u + \boldsymbol{b}^\top \nabla u + cu = 0 \qquad & \text{in } \Omega, \\ u = g \qquad & \text{on } \partial\Omega \end{aligned}$$

for $c = 1$, $\nu = 0.1$, and $\boldsymbol{b} = [\,1\,,\,1\,]^\top$ and the boundary function g defined as in (1.5) *and Figure 1.10.*

Problem 50. *Consider the matrix $A \in \mathbb{R}^{n\times n}$ corresponding to the PDE of Problem 48 for $c = 1$, $\nu = 0.01$, and $\boldsymbol{b} = [\,1\,,\,1\,]^\top$. Use MATLAB to compute the eigenvalues of A and find an ellipse (parametrized as in Theorem 3.26) that contains all the eigenvalues but not the origin. Test the convergence bound of Theorem 3.26.*

Chapter 4
Preconditioning

Es werden in der Regel doch mehrere der ausserhalb der Diagonale befindlichen Coefficienten so bedeutende Werthe annehmen, dass der Erfolg der soeben angegebenenen Näherungsmethode dadurch vereitelt wird. Man kann aber, wie ich im Folgenden zeigen will, durch Wiederholung einer leichten Rechnung die Gleichungen in andere umformen, in welchen der erwähnte Uebelstand immer weniger hervortritt, so dass zuletzt die Gleichungen eine Form erhalten, welche die Anwendung der obigen Näherungsmethode verstattet.

Jacobi, *Über eine neue Auflösungsart der bei der Methode der kleinsten Quadrate vorkommenden lineären Gleichungen*, 1845.

We have seen that Krylov methods are based on an optimality principle, minimizing for example the error or the residual for a given number of matrix vector multiplications, and it seems therefore that one cannot do better than these methods. Nevertheless in practice, often the convergence of Krylov methods is slow, and one has to first transform the linear system into a new one, such that the Krylov method converges better when applied to the transformed system. This process of transforming the original system into a new one is called *preconditioning*. The first traces we know about preconditioning go back to the original paper of Jacobi [112], where he invented the Jacobi method, and the preconditioning step he uses makes the Jacobi method converge faster; see the quote above. With the advent of Krylov methods, preconditioning became a main research area, and intensive efforts are ongoing today.

4.1 ▪ Stationary iterative methods and preconditioning

Thus, any iterative technique can be used as a preconditioner: block-SOR, SSOR, ADI, Multi-grid, etc. More interestingly, iterative procedures such as GMRES, CGNR, or CGS can also be used as preconditioners.

Yousef Saad, *Iterative Methods for Sparse Linear Systems*, 2003.

There is an important relation between stationary iterative methods and preconditioning, as Saad emphasized in the quote above. To explain this, we first have to introduce the idea of preconditioning: we consider a linear system $A\boldsymbol{u} = \boldsymbol{f}$ with $A \in \mathbb{R}^{n\times n}$, $\boldsymbol{u}, \boldsymbol{f} \in \mathbb{R}^n$. The Krylov methods discussed in Chapter 3 converge well if the spectrum of A is very close to 1, that is, if A is close to the identity.[32] Most matrices A from applications are, however, far from the identity, and Krylov methods are converging very slowly; a typical example is the discretized Laplacian

[32] This statement rigorously holds only for normal matrices. For nonnormal matrices, convergence can still be very bad (see [124, Section 5.7.2]) because the bounds based on spectral information contain the condition number of the eigenvectors which can make them useless for understanding convergence of the Krylov method. See also the example given in Section 3.5 after Theorem 3.29.

we have used as our guiding example in this book. One should then transform the system $A\boldsymbol{u} = \boldsymbol{f}$ in order to make it easier to solve with a Krylov method. To do so, let $M \in \mathbb{R}^{n\times n}$ be an invertible matrix, called a preconditioner; the transformed (or preconditioned) system is then given by

$$M^{-1}A\boldsymbol{u} = M^{-1}\boldsymbol{f}. \tag{4.1}$$

From (4.1), we can see that

1. $M = A$ would be the best possible preconditioner, since the system (4.1) becomes

   $$I\boldsymbol{u} = A^{-1}\boldsymbol{f}$$

   with all eigenvalues equal to 1, not just close to one, and a Krylov method will converge in one step, since the solution lies in the initial affine Krylov space $\boldsymbol{u}_0 + \mathcal{K}_0(M^{-1}A, \boldsymbol{r}_0) = \boldsymbol{u}_0 + \text{span}\{A^{-1}\boldsymbol{f} - \boldsymbol{u}_0\}$;

2. the computation of M^{-1}, i.e., solving linear systems with system matrix M, should, however, be much less expensive than solving systems with the original matrix A, since otherwise one would better solve the system $A\boldsymbol{u} = \boldsymbol{f}$ directly.

In preconditioning one must therefore find a compromise: an M that is reasonably close to A, but easy and cheap to invert. The preconditioning in (4.1) is called *left preconditioning*, since the preconditioner M acts on the left of A. *Right preconditioning* is also possible: in this case one would solve

$$AM^{-1}\boldsymbol{v} = \boldsymbol{f} \quad \text{with} \quad \boldsymbol{u} = M^{-1}\boldsymbol{v}. \tag{4.2}$$

If M is symmetric and positive definite, then one can *precondition symmetrically*,

$$L^{-1}AL^{-\top}\boldsymbol{v} = L^{-1}\boldsymbol{f} \quad \text{with} \quad \boldsymbol{u} = L^{-\top}\boldsymbol{v}, \tag{4.3}$$

where $M = LL^{\top}$. The matrix L could be, for example, the lower triangular Cholesky factor of M. Preconditioners can be based purely on algebraic information, i.e., the matrix (see the early contribution quoted above from [134]), or on the underlying physical problem, which is done with the domain decomposition methods quoted above from [184], and multigrid methods.

In Chapter 2 we have studied stationary iterative methods based on the splitting $A = M - N$, and the conditions for obtaining a good method, i.e., a good matrix M, were that

1. the spectral radius of the iteration matrix $I - M^{-1}A$ should be small, close to zero, for fast convergence of the stationary iterative method;

2. the computation of M^{-1} should be cheap, like with the diagonal M for Jacobi, or the triangular M for Gauss–Seidel.

Comparing these two conditions to the conditions for a good preconditioner for a Krylov method earlier, we see that they are very much related, and it is not a coincidence that these matrices are called M in both cases: the condition of easy invertibility of M is identical, and the condition that the spectral radius of the iteration matrix $I - M^{-1}A$ should be small implies that the eigenvalues of $M^{-1}A$ should be close to 1. Rewriting the stationary iteration (2.1), i.e.,

$$M\boldsymbol{u}_{k+1} = N\boldsymbol{u}_k + \boldsymbol{f}, \tag{4.4}$$

in the form

$$\boldsymbol{u}_{k+1} = M^{-1}N\boldsymbol{u}_k + M^{-1}\boldsymbol{f} = (I - M^{-1}A)\boldsymbol{u}_k + M^{-1}\boldsymbol{f}, \tag{4.5}$$

we see that at convergence of the stationary iterative method, we obtain the system

$$\boldsymbol{u} = (I - M^{-1}A)\boldsymbol{u} + M^{-1}\boldsymbol{f} \quad \Longleftrightarrow \quad M^{-1}A\boldsymbol{u} = M^{-1}\boldsymbol{f},$$

which is precisely the preconditioned system (4.1). So one can solve the preconditioned system (4.1) using either the associated stationary iterative method (4.4) or a Krylov method. The following theorem indicates that one should always use a Krylov method!

Theorem 4.1 (Preconditioned Krylov methods versus stationary iterative methods). *Consider a splitting $A = M - N$ with M invertible and the corresponding stationary method* (4.5) *and a Krylov method minimizing the residual applied to the preconditioned system* (4.1) *(both initialized by the same vector $\boldsymbol{u}_0$). Define the corresponding preconditioned residuals as $\boldsymbol{r}_k^{\mathrm{stat}} := M^{-1}\boldsymbol{f} - M^{-1}A\boldsymbol{u}_k^{\mathrm{stat}}$ and $\boldsymbol{r}_k^{\mathrm{kry}} := M^{-1}\boldsymbol{f} - M^{-1}A\boldsymbol{u}_k^{\mathrm{kry}}$. Then we have that $\|\boldsymbol{r}_k^{\mathrm{kry}}\|_2 \leq \|\boldsymbol{r}_k^{\mathrm{stat}}\|_2$ for any $k = 0, 1, 2, \ldots$. In other words, a stationary iterative method* (4.5) *based on M can never perform fewer iterations than a Krylov method minimizing the residual applied to* (4.1)*.*

Proof. First, notice that $\boldsymbol{r}_0^{\mathrm{stat}} = \boldsymbol{r}_0^{\mathrm{kry}} = \boldsymbol{r}_0^{\mathrm{p}} := M^{-1}\boldsymbol{r}_0$ with $\boldsymbol{r}_0 = \boldsymbol{f} - A\boldsymbol{u}_0$. A stationary iterative method based on the splitting $A = M - N$ computes at the iteration k the approximation

$$\boldsymbol{u}_k = (I - M^{-1}A)\boldsymbol{u}_{k-1} + M^{-1}\boldsymbol{f} = \boldsymbol{u}_{k-1} + \boldsymbol{r}_{k-1}^{\mathrm{stat}},$$

where the *preconditioned residual* $\boldsymbol{r}_k^{\mathrm{stat}}$ satisfies

$$\begin{aligned}\boldsymbol{r}_k^{\mathrm{stat}} &= M^{-1}\boldsymbol{f} - M^{-1}A\boldsymbol{u}_k \\ &= M^{-1}\boldsymbol{f} - M^{-1}A(\boldsymbol{u}_{k-1} + \boldsymbol{r}_{k-1}^{\mathrm{stat}}) \\ &= \boldsymbol{r}_{k-1}^{\mathrm{stat}} - M^{-1}A\boldsymbol{r}_{k-1}^{\mathrm{stat}} = (I - M^{-1}A)\boldsymbol{r}_{k-1}^{\mathrm{stat}}.\end{aligned}$$

Using this recursively we get

$$\boldsymbol{r}_k^{\mathrm{stat}} = (I - M^{-1}A)\boldsymbol{r}_{k-1}^{\mathrm{stat}} = (I - M^{-1}A)^2\boldsymbol{r}_{k-2}^{\mathrm{stat}} = \cdots = (I - M^{-1}A)^k\boldsymbol{r}_0^{\mathrm{p}}.$$

Therefore, we have with the residual polynomial $p_k^{\mathrm{stat}}(x) = (1 - x)^k$

$$\boldsymbol{r}_k^{\mathrm{stat}} = p_k^{\mathrm{stat}}(M^{-1}A)\boldsymbol{r}_0^{\mathrm{p}} \text{ with } p_k^{\mathrm{stat}}(0) = 1.$$

A Krylov method, on the other hand, uses the Krylov space

$$\mathcal{K}_k(M^{-1}A, \boldsymbol{r}_0^{\mathrm{p}}) := \left\{\boldsymbol{r}_0^{\mathrm{p}}, M^{-1}A\boldsymbol{r}_0^{\mathrm{p}}, \ldots, (M^{-1}A)^{k-1}\boldsymbol{r}_0^{\mathrm{p}}\right\}$$

to find an approximation $\boldsymbol{u}_k \in \boldsymbol{u}_0 + \mathcal{K}_k(M^{-1}A, \boldsymbol{r}_0^{\mathrm{p}})$, that is,

$$\boldsymbol{u}_k = \boldsymbol{u}_0 + \sum_{j=1}^{k} \gamma_j (M^{-1}A)^{j-1}\boldsymbol{r}_0^{\mathrm{p}}$$

for some coefficients γ_j. The *preconditioned residual* $\boldsymbol{r}_k^{\mathrm{kry}}$ of the Krylov method thus satisfies

$$\boldsymbol{r}_k^{\mathrm{kry}} = M^{-1}\boldsymbol{f} - M^{-1}A\boldsymbol{u}_k = M^{-1}\boldsymbol{f} - M^{-1}A\boldsymbol{u}_0 - M^{-1}A\sum_{j=1}^{k} \gamma_j (M^{-1}A)^{j-1}\boldsymbol{r}_0^{\mathrm{p}},$$

and hence

$$\boldsymbol{r}_k^{\mathrm{kry}} = p_k^{\mathrm{kry}}(M^{-1}A)\boldsymbol{r}_0^{\mathrm{p}} \text{ with } p_k^{\mathrm{kry}}(0) = 1,$$

where p_k^{kry} is a polynomial of degree lower than or equal to k. Now a Krylov method minimizing the residual will find the polynomial p_k^{kry} such that $\|\boldsymbol{r}_k^{\mathrm{kry}}\|_2$ is as small as possible, and thus at least as small as $\|\boldsymbol{r}_k^{\mathrm{stat}}\|_2$, which used the simple polynomial $p_k^{\mathrm{stat}}(x) = (1-x)^k$ of the associated stationary method. □

The previous result shows that one should never use a stationary iterative method in practice. Even though the Krylov method might have a small overhead, needing a few more scalar products and to store a few more vectors, the benefit of the optimized polynomial far outweighs this additional cost. Hence all the iterative methods studied in Chapter 2, like Jacobi, Gauss–Seidel, and SOR, should be used as preconditioners for a Krylov method. The Krylov method serves as an accelerator of convergence, and Krylov methods can be developed from this point of view; see [86, Chapter 11]. The importance of studying stationary iterative methods lies in the development of preconditioners.

4.2 ▪ Left and right preconditioning

> *The above transformation of the linear system $A \to M^{-1}A$ is often not what is used in practice.*
>
> R. Barrett et al., *Templates for the Solution of Linear Systems: Building Blocks for Iterative Methods*, 1994.

This section is motivated by the following questions: What is the difference between left and right preconditioning? Is there any relation between these two techniques? Do they lead to similar convergence behavior of Krylov methods?

A first simple remark is that $M^{-1}A$ and AM^{-1} share the same spectrum, since

$$M^{-1}A\boldsymbol{v} = \lambda\boldsymbol{v} \quad \Longleftrightarrow \quad M^{-1}AM^{-1}M\boldsymbol{v} = \lambda\boldsymbol{v} \quad \Longleftrightarrow \quad AM^{-1}(M\boldsymbol{v}) = \lambda(M\boldsymbol{v}).$$

Hence, one can expect that a Krylov method applied to the systems

$$M^{-1}A\boldsymbol{u} = M^{-1}\boldsymbol{f} \quad \text{and} \quad AM^{-1}(M\boldsymbol{u}) = \boldsymbol{f} \tag{4.6}$$

would show similar convergence behavior. However, as we have seen in Section 3.5, the spectrum does not necessarily govern the convergence of certain Krylov methods. For this reason, we compare here the optimality properties of GMRES applied to the left- and right-preconditioned systems (4.6).

In case of left preconditioning, GMRES minimizes the residual norm

$$\|M^{-1}\boldsymbol{f} - M^{-1}A\boldsymbol{u}_k\|_2$$

over the affine Krylov space

$$\boldsymbol{u}_0 + \mathcal{K}_k(M^{-1}A, \boldsymbol{r}_0^{\mathrm{p}}), \tag{4.7}$$

where $\boldsymbol{r}_0^{\mathrm{p}}$ is the *preconditioned residual*, that is, $\boldsymbol{r}_0^{\mathrm{p}} = M^{-1}\boldsymbol{r}_0$, with $\boldsymbol{r}_0 = \boldsymbol{f} - A\boldsymbol{u}_0$. Hence, we have that

$$\begin{aligned}\|M^{-1}\boldsymbol{f} - M^{-1}A\boldsymbol{u}_k\|_2 &= \|M^{-1}\boldsymbol{f} - M^{-1}A\boldsymbol{u}_0 - M^{-1}Ap_{k-1}(M^{-1}A)\boldsymbol{r}_0^{\mathrm{p}}\|_2 \\ &= \|\boldsymbol{r}_0^{\mathrm{p}} - M^{-1}Ap_{k-1}(M^{-1}A)\boldsymbol{r}_0^{\mathrm{p}}\|_2,\end{aligned}$$

where p_{k-1} is a polynomial that minimizes the residual norm over all the space of polynomials of degree lower than or equal to $k-1$. We now perform the following simple calculation:

$$\begin{aligned}\boldsymbol{r}_0^{\mathrm{p}} - M^{-1}Ap_{k-1}(M^{-1}A)\boldsymbol{r}_0^{\mathrm{p}} &= M^{-1}\big(\boldsymbol{r}_0 - Ap_{k-1}(M^{-1}A)M^{-1}\boldsymbol{r}_0\big) \\ &= M^{-1}\big(\boldsymbol{r}_0 - AM^{-1}p_{k-1}(AM^{-1})\boldsymbol{r}_0\big).\end{aligned} \tag{4.8}$$

Therefore, GMRES applied to a left-preconditioned system minimizes the norm

$$\|M^{-1}\big(\boldsymbol{r}_0 - AM^{-1}p_{k-1}(M^{-1}A)\boldsymbol{r}_0\big)\|_2$$

over the space of polynomials of degree lower than or equal to $k-1$.

Consider now GMRES applied to the right-preconditioned system in (4.6). In this case GMRES minimizes the residual norm

$$\|\boldsymbol{f} - AM^{-1}\boldsymbol{v}_k\|_2$$

over the affine Krylov space space

$$\boldsymbol{v}_0 + \mathcal{K}_k(AM^{-1}, \boldsymbol{r}_0), \tag{4.9}$$

where $\boldsymbol{r}_0 = \boldsymbol{f} - AM^{-1}\boldsymbol{v}_0 = \boldsymbol{f} - A\boldsymbol{u}_0$. If we express (4.9) in terms of the variable $\boldsymbol{u}$ (rather than $\boldsymbol{v}$), we obtain

$$\begin{aligned} M^{-1}\boldsymbol{v}_0 + M^{-1}\mathcal{K}_k(AM^{-1}, \boldsymbol{r}_0) &= \boldsymbol{u}_0 + \mathcal{K}_k(M^{-1}A, M^{-1}\boldsymbol{r}_0) \\ &= \boldsymbol{u}_0 + \mathcal{K}_k(M^{-1}A, \boldsymbol{r}_0^{\mathrm{p}}), \end{aligned}$$

which is exactly the Krylov space (4.7). In other words, GMRES applied to a right-preconditioned system computes an approximation

$$\boldsymbol{u}_k = \boldsymbol{u}_0 + p_{k-1}(M^{-1}A)M^{-1}\boldsymbol{r}_0,$$

where p_{k-1} is a polynomial obtained by minimizing the residual norm

$$\|\boldsymbol{f} - AM^{-1}\boldsymbol{v}_k\|_2 = \|\boldsymbol{f} - A\boldsymbol{u}_k\|_2 = \|\boldsymbol{r}_0 - AM^{-1}p_{k-1}(AM^{-1})\boldsymbol{r}_0\|_2$$

over the space of polynomials of degree lower than or equal to $k-1$.

Summarizing our findings, we have that GMRES applied to the left-preconditioned system performs the minimization of the preconditioned residual,

$$\min_{\widetilde{\boldsymbol{u}} \in \boldsymbol{u}_0 + \mathcal{K}_k(M^{-1}A, \boldsymbol{r}_0^{\mathrm{p}})} \|M^{-1}(\boldsymbol{f} - A\widetilde{\boldsymbol{u}})\|_2 \quad \Leftrightarrow \quad \min_{p_{k-1}} \|M^{-1}\big(\boldsymbol{r}_0 - AM^{-1}p_{k-1}(M^{-1}A)\boldsymbol{r}_0\big)\|_2,$$

while GMRES applied to the right-preconditioned system performs the minimization of the unpreconditioned residual,

$$\min_{\widetilde{\boldsymbol{u}} \in \boldsymbol{u}_0 + \mathcal{K}_k(M^{-1}A, \boldsymbol{r}_0^{\mathrm{p}})} \|\boldsymbol{f} - A\widetilde{\boldsymbol{u}}\|_2 \quad \Leftrightarrow \quad \min_{p_{k-1}} \|\boldsymbol{r}_0 - AM^{-1}p_{k-1}(M^{-1}A)\boldsymbol{r}_0\|_2,$$

but in both cases the minimization problem is posed on the same (Krylov or polynomial) space. This indicates that significant differences in the convergence behaviors are possible, and this is especially the case when M is ill-conditioned; see, e.g., [160, Section 9.3.4].

4.3 ▪ Preconditioning in practice

> *Remarkably, the splitting of M is in practice not needed.*
>
> R. Barrett et al., *Templates for the Solution of Linear Systems: Building Blocks for Iterative Methods*, 1994.

In many cases (e.g., multigrid methods and domain decomposition methods; see Sections 4.6, 4.7, 4.8, and 4.10) the structure of M is unknown or M is expensive to compute. Moreover, one would certainly not first compute the preconditioned system $M^{-1}A\boldsymbol{u} = M^{-1}\boldsymbol{f}$ and then

use a Krylov method, because assembling the matrix $M^{-1}A$ could be too expensive! At each iteration of the Krylov method, we would like to solve a linear system $M\boldsymbol{v} = \boldsymbol{w}$ at most. This leads to a common question: how does a preconditioner have to be used in practice? Moreover, assuming that one wishes to use CG with a symmetric preconditioner M, how should one handle the symmetric preconditioning (4.3), where the expensive decomposition $M = LL^\top$ is required? These questions are answered in this section; see also the quote above, which is promising. Let us begin with the first one.

A Krylov method applied to the system $A\boldsymbol{u} = \boldsymbol{f}$ constructs the Krylov subspaces $\mathcal{K}_k(A, \boldsymbol{p})$. This is in general obtained by a matrix-vector multiplication of the type $A\boldsymbol{p}$; see, e.g., the CG and GMRES algorithms given in Sections 3.2 and 3.5. Now, a Krylov method applied to the preconditioned system $M^{-1}A\boldsymbol{u} = M^{-1}\boldsymbol{f}$ will construct a Krylov space $\mathcal{K}_k(M^{-1}A, \boldsymbol{p})$ by computing at each step the vector $M^{-1}A\boldsymbol{p}$. Therefore, one can easily modify the Krylov algorithm by adding an extra step at each iteration: once the vector $\boldsymbol{v} = A\boldsymbol{p}$ is computed, one can then compute $\boldsymbol{w} = M^{-1}\boldsymbol{v}$ by solving the linear system $M\boldsymbol{w} = \boldsymbol{v}$. As an example, we modified the GMRES implementation given in Section 3.5 in order to add the possibility of preconditioning:

```
function [u,uk,res]=PGMRES(A,f,u0,M,tol,m)
% PGMRES: Preconditioned Generalized Minimal Residual
%   [u,uk,res]=PGMRES(A,f,u0,M,tol,m) solves M^-1Au=M^-1f using the GMRES
%   method starting at the initial guess u0 up to a tolerance tol using
%   at most m iterations. It computes u in the (affine) preconditioned
%   Krylov space by minimizing the norm ||M^-1f-M^-1A*u||_2 where k is
%   the smallest integer such that ||M^-1f-M^-1A*u||_2<tol.
%   PGMRES returns in the matrix uk the iterates, in u the solution
%   computed, and in res the history of the norm of the residuals.

if nargin<6, m=100; end            % default values
if nargin<5, tol=1e-6; end
if nargin<4, M=speye(length(f)); end
k=1;                               % Initialize the iteration index
uk(:,k)=u0;
r0=f-A*u0;                         % Compute the initial residual
r0=M\r0;                           % Apply the preconditioner to r0
res=norm(r0);                      % Initialize the vercor of residuals
rhs=res;                           % Initialize the right-hand side
Q(:,1)=r0/res;                     % First column of Q
while res(end)/norm(f)>tol && k<=m % GMRES iterations
  Q(:,k+1)=A*Q(:,k);               % PART 1: Arnoldi: (M\A*Q_k=Q_{k+1}*H_k)
  Q(:,k+1)=M\Q(:,k+1);             % Apply the preconditioner
  for j=1:k                        % modified Gram-Schmidt on v=M\A*Q(:,k)
    H(j,k)=Q(:,k+1)'*Q(:,j);
    Q(:,k+1)=Q(:,k+1)-H(j,k)*Q(:,j);
  end
  H(k+1,k)=norm(Q(:,k+1));         % Lower-diagonal element
  Q(:,k+1)=Q(:,k+1)/H(k+1,k);      % Compute the vector Q(:,k+1)
  R(k+1,k)=0;                      % PART 2: QR by Givens rotations
  R(:,k)=H(:,k);                   % New column of R
  for j=1:k-1                      % Former Givens rotations on last column
    Rk=c(j)*R(j,k)+s(j)*R(j+1,k);
    R(j+1,k)=-s(j)*R(j,k)+c(j)*R(j+1,k);
    R(j,k)=Rk;
  end                              % Apply the new Givens rotation
  c(k)=R(k,k)/sqrt(R(k,k)^2+R(k+1,k)^2);
```

```
  s(k)=R(k+1,k)/sqrt(R(k,k)^2+R(k+1,k)^2);
  R(k,k)=c(k)*R(k,k)+s(k)*R(k+1,k);
  R(k+1,k)=0;                          % PART 3: Update rhs and residuals
  rhs(k+1)=-s(k)*rhs(k);               % New Givens rotation on rhs
  rhs(k)=c(k)*rhs(k);
  res(k+1)=abs(rhs(k+1));              % Compute the new norm of the residual
  k=k+1;                               % Update iteration index
  if nargout>1
    y=R\rhs';                          % Compute the coefficients y_j
    uk(:,k)=u0+Q(:,1:end-1)*y;         % Compute u as sum_j y_j q_j
  end
end
y=R\rhs';                              % Compute the coefficients y_j
u=u0+Q(:,1:end-1)*y;                   % Compute u as u0+sum_j y_j q_j
```

Comparing the MATLAB functions `GMRES` and `PGMRES` the reader can easily see the difference: the (inverse) preconditioner M^{-1} is applied to the vector $\boldsymbol{r}_0$ before the GMRES loop and to the vector $\boldsymbol{q}_{k+1}$ only once per iteration.

Consider now a case where we would like to use a stationary method

$$\boldsymbol{u}_{k+1} = M^{-1}N\boldsymbol{u}_k + M^{-1}\boldsymbol{f}$$

as a preconditioner, but we do not know explicitly M.[33] Using a stationary method, however, means that one knows at least (in form of a program) the function

$$(A, \boldsymbol{f}, \boldsymbol{u}_0, k) \mapsto \boldsymbol{u}_k = stationary(A, \boldsymbol{f}, \boldsymbol{u}_0, k)$$

that for a given matrix A, right-hand-side $\boldsymbol{f}$, and initial guess $\boldsymbol{u}_0$ allows us to compute the approximation $\boldsymbol{u}_k$ at iteration k of $A^{-1}\boldsymbol{f}$. In MATLAB, this means that a function of the form

```
function uk=stationary(A,f,u0,k)
```

is available. Notice that `stationary` can represent any stationary method, e.g., Jacobi or Gauss–Seidel. Now, one can easily define the function $\boldsymbol{w} \mapsto g(\boldsymbol{w})$ as

```
g(w)=@(w) stationary(A,w,0,1),
```

which means that

$$g(\boldsymbol{w}) = stationary(A, \boldsymbol{w}, 0, 1) = M^{-1}\boldsymbol{w},$$

exactly the action of M^{-1} on $\boldsymbol{w}$! This means that providing the function g to the Krylov method is enough for the preconditioning, and the explicit matrix M is not needed! The same can also be done for the matrix A: it is sufficient to have a function $\boldsymbol{w} \mapsto g_A(\boldsymbol{w}) = A\boldsymbol{w}$. In other words, we can use the Krylov method in a *matrix-free* way. A matrix-free implementation of GMRES can be easily obtained by modifying a few lines in the previous `PGMRES` function:

```
function [u,uk,res]=PGMRESMFREE(gA,f,u0,g,tol,m)
% PGMRESMFREE: Matrix-free Preconditioned Generalized Minimal Residual
%   [u,uk,res]=PGMRESMFREE(gA,f,u0,g,tol,m) solves g(gA(u))=g(f) using the
%   GMRES method starting at the initial guess u0 up to a tolerance tol
%   using at most m iterations.
```

[33] This arises, e.g., in domain decomposition methods and multigrid methods, where we have a code that computes $\boldsymbol{u}_{k+1}$ from $\boldsymbol{u}_k$, but no direct access to the matrix components involved in these computations; see Sections 4.6, 4.7, 4.8, and 4.10.

```
%   gA and g are two functions that correspond to the actions of the
%   matrices A and M^-1 on a vector v: gA(v)=A*v and g(v)=M^-1*v.
%   PGMRESMFREE computes u in the (affine) preconditioned
%   Krylov space by minimizing the norm ||M^-1f-M^-1A*u||_2 where k is
%   the smallest integer such that ||M^-1f-M^-1A*u||_2<tol.
%   PGMRESMFREE returns in the matrix uk the iterates, in u the solution
%   computed, and in res the history of the norm of the residuals.

if nargin<6, m=100; end            % default values
if nargin<5, tol=1e-6; end
if nargin<4, g=@(v) v; end
k=1;                               % Initialize the iteration index
uk(:,k)=u0;
r0=f-gA(u0);                       % Compute the initial residual
r0=g(r0);                          % Apply the preconditioner to r0
res=norm(r0);                      % Initialize the vercor of residuals
rhs=res;                           % Initialize the right-hand side
Q(:,1)=r0/res;                     % First column of Q
while res(end)/norm(f)>tol && k<=m % GMRES iterations
  Q(:,k+1)=gA(Q(:,k));             % PART 1: Arnoldi (M\A*Q_k=Q_{k+1}*H_k)
  Q(:,k+1)=g(Q(:,k+1));            % Apply the preconditioner
  for j=1:k                        % Gram-Schmidt on v=M\A*Q(:,k)
    H(j,k)=Q(:,k+1)'*Q(:,j);
    Q(:,k+1)=Q(:,k+1)-H(j,k)*Q(:,j);
  end
  H(k+1,k)=norm(Q(:,k+1));         % Lower-diagonal element
  Q(:,k+1)=Q(:,k+1)/H(k+1,k);      % Compute the vector Q(:,k+1)
  R(k+1,k)=0;                      % PART 2: QR by Givens rotations
  R(:,k)=H(:,k);                   % New column of R
  for j = 1:k-1                    % Former Givens rotations on last column
    Rk=c(j)*R(j,k)+s(j)*R(j+1,k);
    R(j+1,k)=-s(j)*R(j,k)+c(j)*R(j+1,k);
    R(j,k)=Rk;
  end                              % Apply the new Givens rotation
  c(k)=R(k,k)/sqrt(R(k,k)^2+R(k+1,k)^2);
  s(k)=R(k+1,k)/sqrt(R(k,k)^2+R(k+1,k)^2);
  R(k,k)=c(k)*R(k,k)+s(k)*R(k+1,k);
  R(k+1,k)=0;                      % PART 3: Update rhs and residuals
  rhs(k+1)=-s(k)*rhs(k);           % New Givens rotation on rhs
  rhs(k)=c(k)*rhs(k);
  res(k+1)=abs(rhs(k+1));          % Compute the new norm of the residual
  k=k+1;                           % Update iteration index
  if nargout>1
    y=R\rhs';                      % Compute the coefficients y_j
    uk(:,k)=u0+Q(:,1:end-1)*y;     % Compute u as sum_j y_j q_j
  end
end
y=R\rhs';                          % Compute the coefficients y_j
u=u0+Q(:,1:end-1)*y;               % Compute u as sum_j y_j q_j
```

One can also use GMRES to solve directly the preconditioned system. To see this, we recall that

$$stationary(A, 0, \boldsymbol{w}, 1) = M^{-1}N\boldsymbol{w},$$

and $M^{-1}A = M^{-1}(M - N) = I - M^{-1}N$, and we can easily obtain the action of the

preconditioned matrix as

$$g_{M^{-1}A}(\boldsymbol{w}) = \boldsymbol{w} - stationary(A, 0, \boldsymbol{w}, 1) = M^{-1}A\boldsymbol{w}.$$

Therefore, we can feed GMRES with $g_{M^{-1}A}$ (instead of g_A) and without any explicit preconditioning function. This trick allows us to apply GMRES "directly" to the preconditioned system.

Let us now answer the second question posed at the beginning of this section. Assume that the matrix A and the preconditioner M are symmetric and positive definite. The following theorem shows that the explicit computation of the decomposition $M = LL^\top$ is not necessary in practice. The CG method can be easily modified in a way that only the solution of a system $M\boldsymbol{v} = \boldsymbol{w}$ (hence the action of M^{-1} over a vector $\boldsymbol{w}$) is required.

Theorem 4.2 (Preconditioned conjugate gradient). *Let A and M be symmetric and positive definite and assume that M is decomposed as $M = LL^\top$. Denote by $\{\widetilde{\boldsymbol{u}}_k\}_k$, $\{\widetilde{\boldsymbol{r}}_k\}_k$, and $\{\widetilde{\boldsymbol{p}}_k\}_k$ the sequences of approximations, residuals, and directions generated by CG applied to the system $\widetilde{A}\widetilde{\boldsymbol{u}} = \widetilde{\boldsymbol{f}}$, where $\widetilde{A} = L^{-1}AL^{-\top}$, $\widetilde{\boldsymbol{u}} = L^\top\boldsymbol{u}$, and $\widetilde{\boldsymbol{f}} = L^{-1}\boldsymbol{f}$. Consider the sequences $\{\boldsymbol{u}_k\}_k$, $\{\boldsymbol{r}_k\}_k$, and $\{\boldsymbol{p}_k\}_k$ defined as $\boldsymbol{u}_k := L^{-\top}\widetilde{\boldsymbol{u}}_k$, $\boldsymbol{r}_k := L\widetilde{\boldsymbol{r}}_k$, and $\boldsymbol{p}_k := L^{-\top}\widetilde{\boldsymbol{p}}_k$ for $k = 0, 1, \ldots$. These sequences satisfy the relations*

$$\boldsymbol{p}_0 = M^{-1}\boldsymbol{r}_0, \tag{4.10}$$

$$\boldsymbol{u}_{k+1} = \boldsymbol{u}_k + \alpha_k\boldsymbol{p}_k, \tag{4.11}$$

$$\boldsymbol{r}_{k+1} = \boldsymbol{r}_k - \alpha_k A\boldsymbol{p}_k, \tag{4.12}$$

$$\boldsymbol{p}_{k+1} = M^{-1}\boldsymbol{r}_{k+1} + \beta_{k+1}\boldsymbol{p}_k, \tag{4.13}$$

$$\alpha_{k+1} = \frac{(M^{-1}\boldsymbol{r}_{k+1})^\top\boldsymbol{r}_{k+1}}{\|\boldsymbol{p}_{k+1}\|_A^2}, \tag{4.14}$$

$$\beta_{k+1} = \frac{(M^{-1}\boldsymbol{r}_{k+1})^\top\boldsymbol{r}_{k+1}}{(M^{-1}\boldsymbol{r}_k)^\top\boldsymbol{r}_k} \tag{4.15}$$

for $k = 0, 1, \ldots$. The method obtained by (4.10)–(4.15) *is called the preconditioned CG method.*

Proof. CG applied to the system $\widetilde{A}\widetilde{\boldsymbol{u}} = \widetilde{\boldsymbol{f}}$ produces the iterates (see Theorem 3.3)

$$\widetilde{\boldsymbol{p}}_0 = \widetilde{\boldsymbol{r}}_0, \tag{4.16}$$

$$\widetilde{\boldsymbol{u}}_{k+1} = \widetilde{\boldsymbol{u}}_k + \alpha_k\widetilde{\boldsymbol{p}}_k, \tag{4.17}$$

$$\widetilde{\boldsymbol{r}}_{k+1} = \widetilde{\boldsymbol{r}}_k - \alpha_k A\widetilde{\boldsymbol{p}}_k, \tag{4.18}$$

$$\widetilde{\boldsymbol{p}}_{k+1} = \widetilde{\boldsymbol{r}}_{k+1} + \beta_{k+1}\widetilde{\boldsymbol{p}}_k, \tag{4.19}$$

$$\alpha_{k+1} = \frac{(\widetilde{\boldsymbol{r}}_{k+1})^\top\widetilde{\boldsymbol{r}}_{k+1}}{\|\widetilde{\boldsymbol{p}}_{k+1}\|_A^2}, \tag{4.20}$$

$$\beta_{k+1} = \frac{(\widetilde{\boldsymbol{r}}_{k+1})^\top\widetilde{\boldsymbol{r}}_{k+1}}{(\widetilde{\boldsymbol{r}}_k)^\top\widetilde{\boldsymbol{r}}_k}. \tag{4.21}$$

To get (4.10) we use the definitions of $\boldsymbol{r}_k$ and $\boldsymbol{p}_k$ together with (4.16),

$$\boldsymbol{p}_0 = L^{-\top}\widetilde{\boldsymbol{p}}_0 = L^{-\top}\widetilde{\boldsymbol{r}}_0 = L^{-\top}L^{-1}\boldsymbol{r}_0 = M^{-1}\boldsymbol{r}_0.$$

Using the definitions of $\boldsymbol{u}_k$ and $\boldsymbol{p}_k$ together with (4.17), we get

$$\boldsymbol{u}_{k+1} = L^{-\top}\widetilde{\boldsymbol{u}}_{k+1} = L^{-\top}\widetilde{\boldsymbol{u}}_k + \alpha_k L^{-\top}\widetilde{\boldsymbol{p}}_k = \boldsymbol{u}_k + \alpha_k\boldsymbol{p}_k,$$

which is (4.11). The relations (4.12), (4.13), (4.14), and (4.15) are obtained by similar calculations. □

For an implementation of preconditioned CG see Problem 51.

4.4 ▪ Flexible GMRES: FGMRES

In order to be able to enhance robustness of iterative solvers, we should be able to determine, e.g., by means of heuristics, whether or not a given preconditioner is suitable for the problem at hand. If not one can attempt another possible iterative method/preconditioner and switch periodically if necessary. It is desirable to be able to switch within the outer iteration instead of restarting.

Yousef Saad, *A Flexible Inner-Outer Preconditioned GMRES Algorithm*, 1993.

Yousef Saad, the inventor of GMRES, proposed in [161] a generalization of GMRES which permits the change of the preconditioner in each iteration; see also the quote above. Different preconditioners can have very different properties, which could all be desirable when attempting to solve efficiently a large linear system. The idea of Saad opened the path for a new field of research called *multipreconditioning*, which is still an active area of investigation.

To allow the change of the preconditioner in the course of the iterations, Saad proposed in [161] a very interesting strategy, which is a simple modification of GMRES. To explain the *flexible GMRES* method (FGMRES), let us consider the right-preconditioned system

$$AM^{-1}(M\boldsymbol{u}) = \boldsymbol{f},$$

where both the matrices A and M are assumed to be invertible. GMRES applied to this system is given by the following algorithm:

1. Input $\boldsymbol{u}_0$ (initial guess), ϵ (tolerance).
2. Compute $\boldsymbol{r}_0 = \boldsymbol{f} - A\boldsymbol{u}_0$ and $\boldsymbol{q}_1 = \boldsymbol{r}_0/\|\boldsymbol{r}_0\|_2$ and set $k = 1$.
3. Compute $\boldsymbol{z}_k = M^{-1}\boldsymbol{q}_k$.
4. Compute $\boldsymbol{w} = A\boldsymbol{z}_k$.
5. For $j = 1, \ldots, k$ do (modified Gram–Schmidt)
   - Compute $h_{j,k} = \boldsymbol{w}^\top \boldsymbol{q}_j$.
   - Update $\boldsymbol{w} = \boldsymbol{w} - h_{j,k}\boldsymbol{q}_j$.
6. Compute $h_{k+1,k} = \|\boldsymbol{w}\|_2$ and $\boldsymbol{q}_{k+1} = \boldsymbol{w}/h_{k+1,k}$.
7. Define $Q_k = [\boldsymbol{q}_1, \ldots, \boldsymbol{q}_k]$.
8. Compute $\boldsymbol{y}_k = \arg\min_{\boldsymbol{y}\in\mathbb{R}^k} \|\|\boldsymbol{r}_0\|_2\boldsymbol{e}_1 - H_k\boldsymbol{y}\|_2$.
9. Compute $\boldsymbol{u}_k = \boldsymbol{u}_0 + M^{-1}Q_k\boldsymbol{y}_k$ and $\boldsymbol{r}_k = \boldsymbol{f} - A\boldsymbol{u}_k$.
10. If $\|\boldsymbol{r}_k\|_2 > \epsilon$, update $k = k + 1$ and go to step 3.

Since the idea of FMGRES is to change the preconditioner in the course of the iterations, step 3 in the algorithm above is replaced by

$$\boldsymbol{z}_k = M_k^{-1}\boldsymbol{q}_k,$$

where now the preconditioner is indexed by k. This simple modification allows one to change the preconditioner at each GMRES iteration. Moreover, together with storing the vectors $\boldsymbol{q}_j$, FGMRES stores also the vectors $\boldsymbol{z}_j$. Hence, we need to modify step 7 by defining $Z_k = [\boldsymbol{z}_1, \ldots, \boldsymbol{z}_k]$, and step 9 by computing $\boldsymbol{u}_k = \boldsymbol{u}_0 + Z_k\boldsymbol{y}_k$. This leads to the FGMRES algorithm, where the three modifications are underlined:

1. Input $\boldsymbol{u}_0$ (initial guess), ϵ (tolerance).
2. Compute $\boldsymbol{r}_0 = \boldsymbol{f} - A\boldsymbol{u}_0$ and $\boldsymbol{q}_1 = \boldsymbol{r}_0/\|\boldsymbol{r}_0\|_2$ and set $k = 1$.
3. Compute $\underline{\boldsymbol{z}_k = M_k^{-1}\boldsymbol{q}_k}$.

4. Compute $\boldsymbol{w} = A\boldsymbol{z}_k$.
5. For $j = 1, \ldots, k$ do (modified Gram–Schmidt)
   - Compute $h_{j,k} = \boldsymbol{w}^\top \boldsymbol{q}_j$.
   - Update $\boldsymbol{w} = \boldsymbol{w} - h_{j,k}\boldsymbol{q}_j$.
6. Compute $h_{k+1,k} = \|\boldsymbol{w}\|_2$ and $\boldsymbol{q}_{k+1} = \boldsymbol{w}/h_{k+1,k}$.
7. Define $\underline{Z_k = [\boldsymbol{z}_1, \ldots, \boldsymbol{z}_k]}$.
8. Compute $\boldsymbol{y}_k = \arg\min_{\boldsymbol{y}\in\mathbb{R}^k} \|\|\boldsymbol{r}_0\|_2\boldsymbol{e}_1 - H_k\boldsymbol{y}\|_2$.
9. Compute $\underline{\boldsymbol{u}_k = \boldsymbol{u}_0 + Z_k\boldsymbol{y}_k}$ and $\boldsymbol{r}_k = \boldsymbol{f} - A\boldsymbol{u}_k$.
10. If $\|\boldsymbol{r}_k\|_2 > \epsilon$, update $k = k + 1$ and go to step 3.

An implementation of FGMRES is given by the MATLAB function

```
function [u,uk,res]=FGMRES(A,f,u0,M,tol,m)
% FGMRES: Flexible Generalized Minimal Residual
%   [u,uk,res]=FGMRES(A,f,u0,M,tol,m) solves Au=f using the FGMRES
%   method starting at the initial guess u0 up to a tolerance tol using
%   at most m iterations. It computes u by changing cyclically the
%   (right) preconditioner at each iteration. The preconditioners are
%   contained in a cell M. For example given a matrix A, one can have
%   M=cell(3,1);
%   M{1}=@(v) diag(diag(A))\v  (Jacobi preconditioner)
%   M{2}=@(v) tril(A)\v        (Gauss-Seidel preconditioner)
%   M{3}=@(v) eye(size(A,1))\v (no preconditioner)
%   FGMRES returns in the matrix uk the iterates, in u the solution
%   computed, and in res the history of the norm of the residuals.

if nargin<6, m=100; end            % default values
if nargin<5, tol=1e-6; end
num_p=length(M);                   % Compute the number of preconditioners
k=1;                               % Initialize the iteration index
uk(:,k)=u0;
r0=f-A*u0;                         % Compute the initial residual
res=norm(r0);                      % Initialize the vercor of residuals
rhs=res;                           % Initialize the right-hand side
Q(:,1)=r0/res;                     % First column of Q
Z=[];                              % Initialize matrix Z
ind=0;                             % Set preconditioner index ind=0
while res(end)/norm(f)>tol && k<=m % FGMRES iterations
  if ind>=num_p || ind==0          % Reset/increase the preconditioner index
      ind=1;
  else
      ind=ind+1;
  end
  Z(:,k)=M{ind}(Q(:,k));           % PART 1: Arnoldi-apply ind-th preconditioner
  Q(:,k+1)=A*Z(:,k);               % Apply the matrix A
  for j = 1:k                      % modified Gram-Schmidt
    H(j,k)=Q(:,k+1)'*Q(:,j);
    Q(:,k+1)=Q(:,k+1)-H(j,k)*Q(:,j);
  end
  H(k+1,k)=norm(Q(:,k+1));         % Lower-diagonal element
  Q(:,k+1)=Q(:,k+1)/H(k+1,k);      % Compute the vector Q(:,k+1)
  R(k+1,k)=0;                      % PART 2: QR by Givens rotations
```

```
  R(:,k)=H(:,k);                    % New column of R
  for j=1:k-1                       % Former Givens rotations on last column
    Rk=c(j)*R(j,k)+s(j)*R(j+1,k);
    R(j+1,k)=-s(j)*R(j,k)+c(j)*R(j+1,k);
    R(j,k)=Rk;
  end                               % Next apply the new Givens rotation
  c(k)=R(k,k)/sqrt(R(k,k)^2+R(k+1,k)^2);
  s(k)=R(k+1,k)/sqrt(R(k,k)^2+R(k+1,k)^2);
  R(k,k)=c(k)*R(k,k)+s(k)*R(k+1,k);
  R(k+1,k)=0;
  rhs(k+1)=-s(k)*rhs(k);            % PART 3: Update rhs and residuals
  rhs(k)=c(k)*rhs(k);               % New Givens rotation on rhs
  res(k+1)=abs(rhs(k+1));           % Compute the new norm of the residual
  k=k+1;                            % Update iteration index
  if nargout>1
    y=R\rhs';                       % Compute the coefficients y_j
    uk(:,k)=u0+Z*y;                 % Compute u as u0+sum_j y_j z_j
  end
end
y=R\rhs';                           % Compute the coefficients y_j
u=u0+Z*y;                           % Compute u as u0+sum_j y_j z_j
end
```

The main important difference between the standard GMRES and FGMRES is that the classical Arnoldi-type relation

$$(AM^{-1})Q_k = Q_{k+1}H_k \tag{4.22}$$

is replaced by the more general equality

$$AZ_k = Q_{k+1}H_k. \tag{4.23}$$

Clearly, H_k is a $k+1 \times k$ upper Hessenberg matrix and the two above relations coincide if $M_k = M$ for all k. Similarly to (3.46) for (4.22), an alternative to (4.23) is

$$AZ_k = Q_k\widehat{H}_k + h_{k+1,k}\boldsymbol{q}_{k+1}\boldsymbol{e}_k^\top, \tag{4.24}$$

where $\widehat{H}_k$ is the $k \times k$ matrix obtained from H_k by deleting the last row.

FGMRES satisfies an optimality property similar to the one proved for GMRES in Theorem 3.21.

Theorem 4.3 (Optimality of FGMRES, Saad, 1993). *The approximation $\boldsymbol{u}_k$ computed by FGMRES at step k is the solution to the residual minimization problem*

$$\min_{\widetilde{\boldsymbol{u}} \in \boldsymbol{u}_0 + \operatorname{span}\{\boldsymbol{z}_1,\ldots,\boldsymbol{z}_k\}} \|\boldsymbol{f} - A\widetilde{\boldsymbol{u}}\|_2.$$

Proof. For any $\boldsymbol{w} \in \boldsymbol{u}_0 + \operatorname{span}\{\boldsymbol{z}_1,\ldots,\boldsymbol{z}_k\}$ we write

$$\begin{aligned} \boldsymbol{f} - A\boldsymbol{w} &= \boldsymbol{f} - A(\boldsymbol{u}_0 + Z_k\boldsymbol{y}) \\ &= \boldsymbol{r}_0 - AZ_k\boldsymbol{y} \\ &= \|\boldsymbol{r}_0\|_2\boldsymbol{q}_1 - Q_{k+1}H_k\boldsymbol{y} \\ &= Q_{k+1}\big(\|\boldsymbol{r}_0\|_2\boldsymbol{e}_1 - H_k\boldsymbol{y}\big), \end{aligned} \tag{4.25}$$

where we used (4.23) to get the third equality. The result follows by recalling that $\boldsymbol{y}_k = \arg\min_{\boldsymbol{y}\in\mathbb{R}^k} \|\|\boldsymbol{r}_0\|_2\boldsymbol{e}_1 - H_k\boldsymbol{y}\|_2$ in step 8 of FGMRES. ∎

We now study the possible breakdown of FGMRES, which occurs if $h_{k+1,k} = 0$. This situation is not a problem for the classical GMRES method, because a breakdown occurs only if GMRES converges to the exact solution; see Remark 6. This is not in general the case for FGMRES, where the invertibility of A does not necessarily imply that $\widehat{H}_k$ has full rank, since the matrix Z_k is not necessarily full rank.[34]

Theorem 4.4 (Breakdown of FGMRES, Saad, 1993). *Assume that $\|\boldsymbol{r}_0\|_2 \neq 0$ and that FGMRES performed successfully the first $k-1$ iterations with $h_{j+1,j} \neq 0$ for $j < k$. In addition, assume that $\widehat{H}_k$ has full rank. Then $\boldsymbol{u}_k$ is the exact solution if and only if $h_{k+1,k} = 0$.*

Proof. Assume first that $h_{k+1,k} = 0$. Using the relation (4.24), we obtain that $AZ_k = Q_k \widehat{H}_k$. This and equality (4.25) allow us to write

$$\begin{aligned} \|\boldsymbol{f} - A\boldsymbol{u}_k\|_2 &= \|\|\boldsymbol{r}_0\|_2 \boldsymbol{q}_1 - AZ_k \boldsymbol{y}_k\|_2 \\ &= \|\|\boldsymbol{r}_0\|_2 \boldsymbol{q}_1 - Q_k \widehat{H}_k \boldsymbol{y}_k\|_2 \\ &= \|\|\boldsymbol{r}_0\|_2 \boldsymbol{e}_1 - \widehat{H}_k \boldsymbol{y}_k\|_2. \end{aligned}$$

Since $\widehat{H}_k$ is invertible, the residual norm is minimized by $\boldsymbol{y}_k = \|\boldsymbol{r}_0\|_2 \widehat{H}_k^{-1} \boldsymbol{e}_1$, which gives $\|\boldsymbol{f} - A\boldsymbol{u}_k\|_2 = 0$.

Assume now that $\boldsymbol{u}_k$ coincides with the exact solution $\boldsymbol{u}$; then

$$\begin{aligned} 0 &= \boldsymbol{f} - A\boldsymbol{u}_k \\ &= Q_k \big[\|\boldsymbol{r}_0\|_2 \boldsymbol{e}_1 - \widehat{H}_k \boldsymbol{y}_k\big] + h_{k+1,k} \boldsymbol{q}_{k+1} \boldsymbol{e}_k^\top \boldsymbol{y}_k, \end{aligned} \tag{4.26}$$

where $\boldsymbol{e}_k$ is the kth canonical vector in $\mathbb{R}^k$. If the last entry of $\boldsymbol{y}_k$ is zero, then $\boldsymbol{e}_k^\top \boldsymbol{y}_k = 0$. This implies that $\widehat{H}_k \boldsymbol{y}_k = \|\boldsymbol{r}_0\|_2 \boldsymbol{e}_1$. Since $h_{j+1,j} \neq 0$ for $j < k$, then a simple back substitution starting from the last equation of $\widehat{H}_k \boldsymbol{y}_k = \|\boldsymbol{r}_0\|_2 \boldsymbol{e}_1$ would show that $\boldsymbol{y}_k = 0$, which would then imply $\|\boldsymbol{r}_0\|_2 = 0$, contradicting the assumption. Hence $\boldsymbol{e}_k^\top \boldsymbol{y}_k \neq 0$. Therefore, since $\boldsymbol{q}_{k+1}$ is orthogonal to $\boldsymbol{q}_1, \ldots, \boldsymbol{q}_k$, the only way in which (4.26) can be satisfied is that

$$\widehat{H}_k \boldsymbol{y}_k = \|\boldsymbol{r}_0\|_2 \boldsymbol{e}_1 \quad \text{and} \quad \boldsymbol{q}_{k+1} = 0,$$

which implies that $h_{k+1,k} = 0$. □

4.5 ▪ Algebraic preconditioning methods

> *A particular class of regular splittings of not necessarily symmetric M-matrices is proposed. If the matrix is symmetric, this splitting is combined with the conjugate-gradient method to provide a fast iterative solution algorithm.*
>
> J. A. Meijerink and Henk A. van der Vorst, *An Iterative Solution Method for Linear Systems of Which the Coefficient Matrix is a Symmetric M-Matrix*, 1977.

In Section 2.6 we have studied the classical version of the Gauss–Seidel method, also known as *forward Gauss–Seidel*, which is based on the splitting matrices $M = (D + L)$ and $N = -U$. It is also possible to consider a *backward Gauss–Seidel* method obtained by $M = (D + U)$ and $N = -L$. Combining these two steps, we obtain the *symmetric Gauss–Seidel* method,

$$(D + L)\boldsymbol{u}_{k+\frac{1}{2}} = -U\boldsymbol{u}_k + \boldsymbol{f}, \tag{4.27}$$

$$(D + U)\boldsymbol{u}_{k+1} = -L\boldsymbol{u}_{k+\frac{1}{2}} + \boldsymbol{f}, \tag{4.28}$$

[34] Consider a matrix $Q = [\boldsymbol{q}_1, \boldsymbol{q}_2] = \frac{1}{\sqrt{2}}\begin{bmatrix} 1 & -1 \\ 1 & 1 \end{bmatrix}$ and two preconditioners $M_1 = \begin{bmatrix} 1 & 0 \\ 0 & 1 \end{bmatrix}$ and $M_2 = \begin{bmatrix} \frac{1}{2} & -\frac{1}{2} \\ 0 & 1 \end{bmatrix}$. A simple calculation reveals that $Z = [M_1^{-1}\boldsymbol{q}_1, M_2^{-1}\boldsymbol{q}_2] = \frac{1}{\sqrt{2}}\begin{bmatrix} 1 & 1 \\ 1 & 1 \end{bmatrix}$.

which will lead us naturally to the so-called incomplete LU (ILU) preconditioner [160]. Using the first equation (4.27), we have $\boldsymbol{u}_{k+\frac{1}{2}} = -(D+L)^{-1}U\boldsymbol{u}_k + (D+L)^{-1}\boldsymbol{f}$. Replacing this in the second equation (4.28), we obtain

$$\boldsymbol{u}_{k+1} = (D+U)^{-1}L(D+L)^{-1}U\boldsymbol{u}_k - (D+U)^{-1}L(D+L)^{-1}\boldsymbol{f} + (D+U)^{-1}\boldsymbol{f}.$$

Defining $M := ((D+U)^{-1} - (D+U)^{-1}L(D+L)^{-1})^{-1}$, we obtain the usual stationary iteration relation

$$\boldsymbol{u}_{k+1} = (I - M^{-1}A)\boldsymbol{u}_k + M^{-1}\boldsymbol{f},$$

and we have found the symmetric Gauss–Seidel preconditioner M, whose inverse can be rewritten in the form

$$\begin{aligned} M^{-1} &= (D+U)^{-1} - (D+U)^{-1}L(D+L)^{-1} \\ &= (D+U)^{-1} - (D+U)^{-1}(L+D-D)(D+L)^{-1} \\ &= (D+U)^{-1} - (D+U)^{-1}\big(I - D(D+L)^{-1}\big) \\ &= (D+U)^{-1}D(D+L)^{-1} = \widetilde{U}^{-1}\widetilde{L}^{-1}, \end{aligned}$$

where $\widetilde{U} := D^{-1}(D+U)$ is upper triangular, and $\widetilde{L} := D + L$ is lower triangular. We see that the entries $\widetilde{U}_{ij}$ and $\widetilde{L}_{ij}$ are zero if the corresponding entries A_{ij} of the original matrix are zero. We thus obtained a preconditioner $M = \widetilde{L}\widetilde{U}$ given by its LU factorization. To be a good preconditioner, $M = \widetilde{L}\widetilde{U}$ should be a good approximation of A, and naturally the question arises whether it is possible to replace the entries in $\widetilde{L}$ and $\widetilde{U}$ chosen by symmetric Gauss–Seidel by entries which make $M = \widetilde{L}\widetilde{U}$ an even better approximation of A. This is the idea behind the very popular ILU preconditioner developed and studied independently by Varga [180] and Buleev [28] in 1960 and by Meijerink and van der Vorst in 1977; see [134].

In the original version of ILU, one allowed only nonzero entries in $\widetilde{L}$ and $\widetilde{U}$ where A had a nonzero entry, the structure that was indicated by symmetric Gauss–Seidel. These nonzero entries in $\widetilde{L}$ and $\widetilde{U}$ are then computed using Gaussian elimination:

```
function [L,U]=ILU0(A)
% ILU0 incomplete ILU factorization with zero fill-in
%   [L,U]=ILU0(A); computes an ILU factorization of the matrix
%   A with zero fill-in.

n=size(A,1);
for k=1:n-1
  for i=k+1:n
    if A(i,k)~=0
      A(i,k)=A(i,k)/A(k,k);
      for j=k+1:n
        if A(i,j)~=0
          A(i,j)=A(i,j)-A(i,k)*A(k,j);
        end
      end
    end
  end
end
L=speye(size(A))+tril(A,-1);
U=triu(A,0);
```

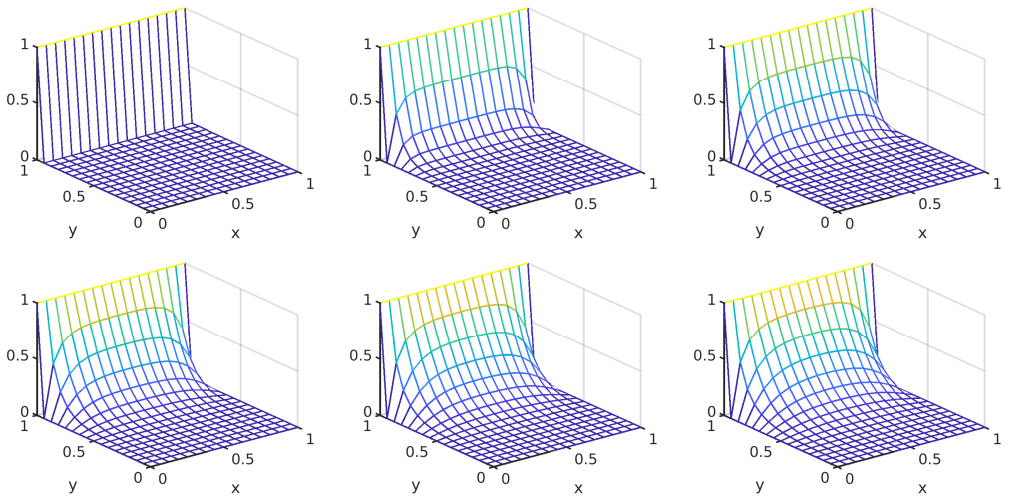

Figure 4.1. *Initial guess and first iterations of ILU as a stationary iteration applied to our Laplace model problem from Section 1.3.*

If we apply ILU as a preconditioner in the stationary iteration to our Laplace model problem from Section 1.3,[35] using the MATLAB statements

```
m=15;                                   % number of gridpoints
A=Laplacian(m,2);                       % five point Laplacian
f=zeros(m*m,1); f(m:m:end)=1;           % put bc into the rhs
u=A\f;                                  % solve by sparse Gaussian elimination
h=1/(m+1); x=0:h:1; y=x;                % mesh point vectors
un=zeros(size(f));                      % initial guess
UU=zeros(m+2); UU(end,1:m+2)=1;         % for plotting
[L,U]=ILU0(A);
for n=0:10
  err(n+1)=max(max(abs(u-un)));         % compute error
  UU(2:m+1,2:m+1)=reshape(un,m,m);
  mesh(x,y,UU)
  xlabel('x');ylabel('y');
  pause
  un=un+U\(L\(f-A*un));
end
```

we get for the first few iterates the approximations shown in Figure 4.1. We see that ILU leads to a more rapidly converging stationary iterative method, substantially better than the other stationary methods we have seen so far, and even better than the CG method in this example. Note that we only show the first five iterates for ILU, as we will do for the other preconditioners in this chapter, in contrast to the earlier chapters where we showed the first 11 iterates. The reason for this superior performance of ILU is that all the earlier methods we studied are based

[35] We use a stationary iterative method here so we can compare to the other stationary iterative methods we tested earlier, even though originally ILU was suggested to be used as a preconditioner for a Krylov method. Theorem 4.1 shows that this would work even better, but then the properties of ILU are mixed with the properties of the Krylov method, and it becomes harder to precisely understand the convergence mechanisms. We thus advocate the principle to always investigate preconditioners first as stationary methods, before accelerating them by a Krylov method.

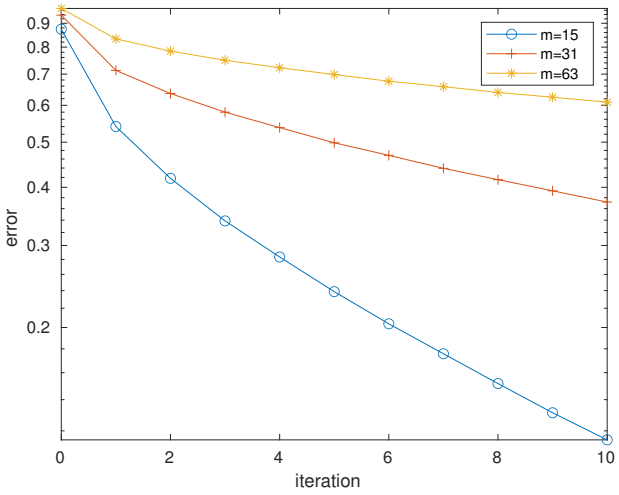

Figure 4.2. *Convergence of the ILU stationary iteration for different mesh sizes* $h = \frac{1}{m+1}$.

on local operations: Jacobi, Gauss–Seidel, SOR, and Richardson only use operations between neighboring gridpoints, and similarly the Krylov methods only use matrix vector multiplications, again with interaction between neighboring gridpoints due to the sparsity of the finite-difference Laplacian. This is why none of these methods could converge rapidly for the unknowns in the corresponding plots of the iterates for small y coordinates in Figures 2.3, 2.5, 2.8, 2.18, 3.3, and 3.7. ILU contains a true attempt to solve the problem by factorization, i.e., nonlocal information, and this is a key ingredient for a good preconditioner; all more sophisticated preconditioners like domain decomposition and multigrid in this chapter contain such components.

Nevertheless, also ILU leads to mesh-dependent convergence, as we can see in Figure 4.2, where we see how the error decreases as the iterations progress when ILU is used as a stationary iteration to solve our Laplace model problem from Section 1.3 for the mesh we used for Figure 4.1 with $m = 15$ interior mesh points, and two refined meshes with $m = 31$ and $m = 63$ interior mesh points.

To improve ILU, one does not have to use the sparsity pattern of the underlying matrix to determine which positions to fill in: one can more generally first decide which entries of the matrices $\widetilde{L}$ and $\widetilde{U}$ can be nonzero, by means of the set

$$\mathcal{Z} := \{(i,j) \,:\, \widetilde{L}_{ij} \neq 0 \quad \text{or} \quad \widetilde{U}_{ij} \neq 0\},$$

and then replace the corresponding condition on A in the algorithm by a condition using the set $\mathcal{Z}$. Meijerink and van der Vorst showed in [134] that if $\mathcal{Z}$ contains the diagonal, and the matrix A is an M-matrix, then the ILU algorithm produces the incomplete factorization

$$A = \widetilde{L}\widetilde{U} - R,$$

which is a regular splitting of A, i.e., the splitting satisfies Definition 2.15. Therefore, the corresponding stationary iterative method converges according to Theorem 2.16.

In order to obtain an even better approximation of A, one can determine the elements of $\widetilde{L}$ and $\widetilde{U}$ to fill in during the factorization process using a tolerance. This is the idea behind ILUT(ϵ), which was introduced by Saad in 1994; see [162]. In this variant of ILU, Gaussian elimination is used, and elements are stored in $\widetilde{L}$ and $\widetilde{U}$ only if they are larger than the specified tolerance. There is no proof that ILUT(ϵ) terminates and leads to an approximate factorization, but it works

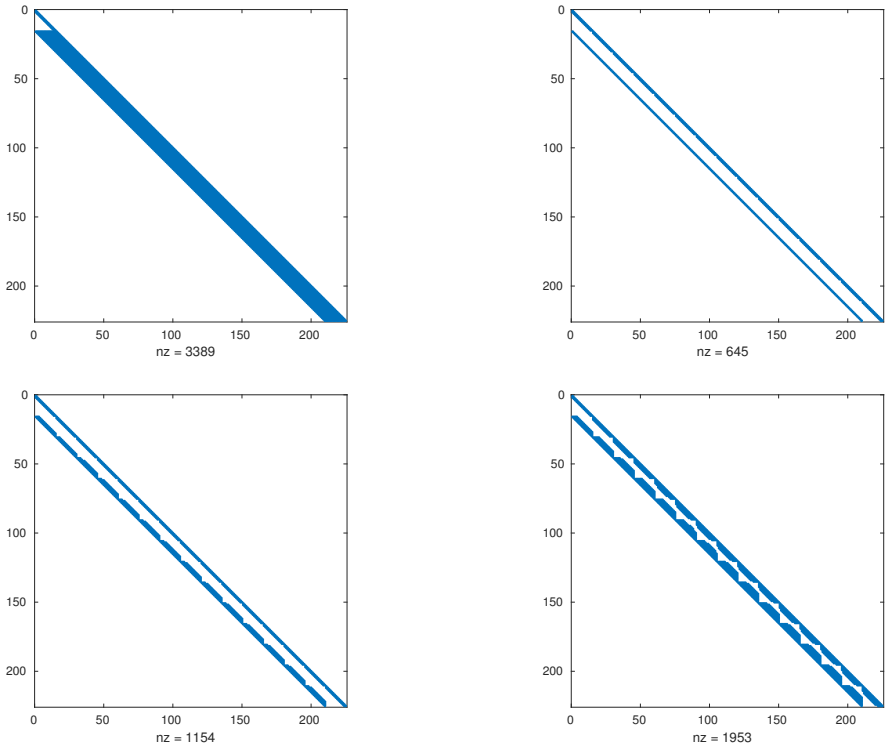

Figure 4.3. *Fill-in in the L factor created by the exact LU factorization (top left), ILU0 (top right), ILUT(0.01) (bottom left), and ILUT(0.002) (bottom right) for the five-point finite-difference Laplacian.*

very well in practice. All these variants of ILU are available in the MATLAB function `ilu`, and we test them using the MATLAB commands

```
m=15;                                % Laplace problem size
A=Laplacian(m,2);
[L,U]=lu(A); spy(L)                  % LU for the Laplace problem
[Lt0,Ut0]=ilu(A); figure(); spy(Lt0)   % ILU0 for the Laplace problem
setup.type='ilutp';
setup.droptol=0.01;                  % ILU(0.01) for the Laplace problem
[Lt001,Ut001]=ilu(A,setup); figure(); spy(Lt001)
setup.droptol=0.002;                 % ILU(0.002) for the Laplace problem
[Lt002,Ut002]=ilu(A,setup); figure(); spy(Lt002)
```

We get the plots we show in Figure 4.3, where we see for our Laplace model problem from Section 1.3 how much fill-in is created in the L factor by the exact LU factorization, compared to ILU0 and ILUT(ϵ) with two values of ϵ. We can see that the exact LU factorization completely fills in the band between the tridiagonal blocks on the diagonal and the off-diagonal blocks of the discrete Laplacian, leading to 3389 nonzero entries in L, while ILU0 preserves the structure of the discrete Laplacian with only 645 nonzero elements in $\widetilde{L}$. With the tolerance 0.01, the band starts to fill in a little, leading to 1154 nonzero elements in $\widetilde{L}$, and with the lower tolerance 0.002 the fill-in becomes more pronounced, with 1953 nonzero elements in $\widetilde{L}$, about two-thirds of the exact L. This fill-in has an important impact on the performance of the preconditioner as

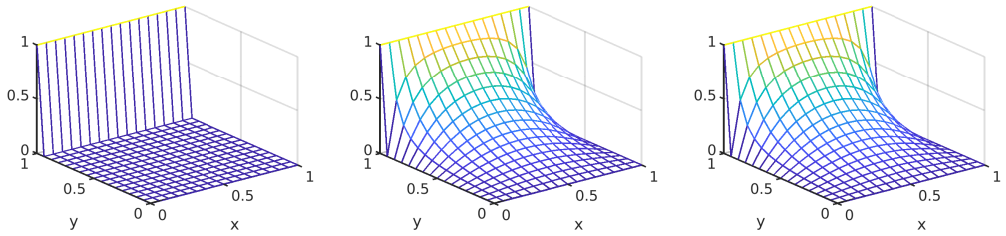

Figure 4.4. *Initial guess and first iterations of the exact LU preconditioner converging after one iteration.*

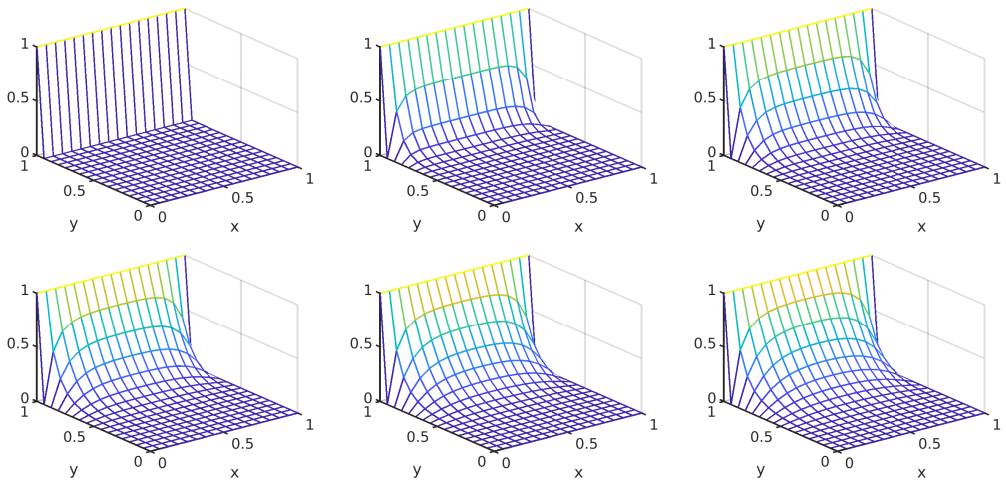

Figure 4.5. *Initial guess and first iterations of the ILU0 preconditioner.*

illustrated in Figures 4.4, 4.5, 4.6, and 4.7, which we obtained continuing the previous MATLAB commands with

```
f=zeros(m*m,1);                          % setup rhs of our model problem
f(m:m:end)=1;
u=A\f;                                   % exact solution
ud=zeros(size(f));                       % initial guess for ILU iterations
u0=ud;u001=ud;u002=ud;
errd=[]; err0=[]; err001=[]; err002=[]; % to store errors
uu=zeros(m+2); uu(m+2,1:m+2)=1;          % for the visualization
x=0:1/(m+1):1;
for n=0:10
  errd(n+1)=max(max(abs(u-ud)));         % compute errors
  err0(n+1)=max(max(abs(u-u0)));
  err001(n+1)=max(max(abs(u-u001)));
  err002(n+1)=max(max(abs(u-u002)));
  uu(2:m+1,2:m+1)=reshape(ud,m,m);       % visualize iterates
  mesh(x,x,uu,'LineWidth',2);
  xlabel('x');ylabel('y');
  set(gca,'FontSize',18,'LineWidth',2)
  print('-depsc',['Laplacem=' num2str(m) 'LUIter=' num2str(n) '.eps'])
```

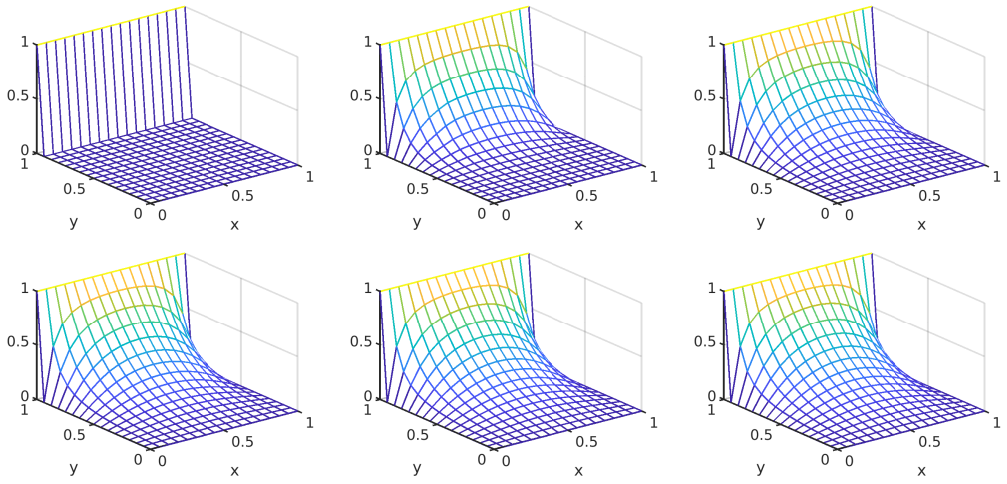

Figure 4.6. *Initial guess and first iterations of the ILUT(0.01) preconditioner.*

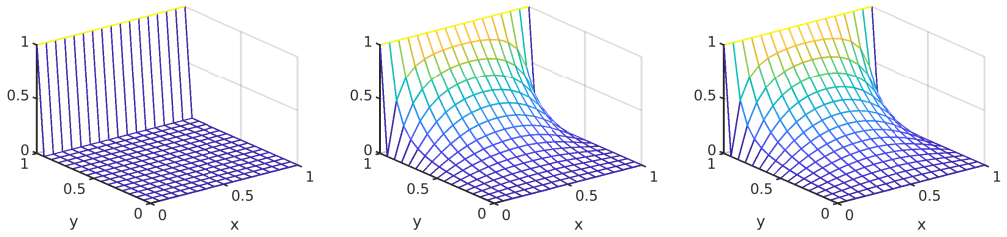

Figure 4.7. *Initial guess and first iterations of the ILUT(0.002) preconditioner, converging visually also after one iteration.*

```
uu(2:m+1,2:m+1)=reshape(u0,m,m);
mesh(x,x,uu,'LineWidth',2);
xlabel('x');ylabel('y');
set(gca,'FontSize',18,'LineWidth',2)
print('-depsc',['Laplacem=' num2str(m) 'ILU0Iter=' num2str(n) '.eps'])
uu(2:m+1,2:m+1)=reshape(u001,m,m);
mesh(x,x,uu,'LineWidth',2);
xlabel('x');ylabel('y');
set(gca,'FontSize',18,'LineWidth',2)
print('-depsc',['Laplacem=' num2str(m) 'ILU0.01Iter=' num2str(n) '.eps'])
uu(2:m+1,2:m+1)=reshape(u002,m,m);
mesh(x,x,uu,'LineWidth',2);
xlabel('x');ylabel('y');
set(gca,'FontSize',18,'LineWidth',2)
print('-depsc',['Laplacem=' num2str(m) 'ILU0.002Iter=' num2str(n) '.eps'])
ud=ud+U\(L\(f-A*ud));                    % compute next iterate
u0=u0+Ut0\(Lt0\(f-A*u0));
u001=u001+Ut001\(Lt001\(f-A*u001));
u002=u002+Ut002\(Lt002\(f-A*u002));
pause
```

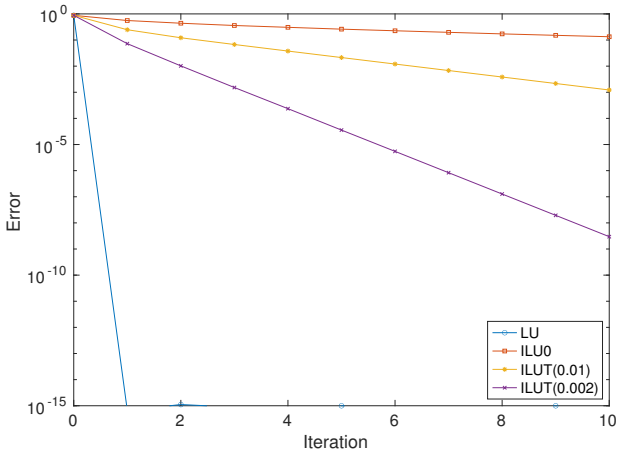

Figure 4.8. *Performance of the different ILU preconditioners when used as stationary iterative solvers for our Laplace model problem.*

```
end
clf                                     % plot error curves
semilogy(0:10,errd,'-o',0:10,err0,'-s',0:10,err001,'-*',0:10,err002,'-x')
xlabel('Iteration'); ylabel('Error')
legend('LU','ILU0','ILUT(0.01)','ILUT(0.002)','Location','SouthEast')
set(gca,'FontSize',20)
axis([0 10 1e-15 1])
```

In Figure 4.8, we show the corresponding convergence curves. As expected, the exact LU factorization leads to a preconditioner such that the stationary iterative method converges in one iteration, but it is as expensive as solving the system directly using the LU factorization. ILU0 leads already to reasonably fast convergence, but with ILUT(ϵ) one can reach any convergence speed, if one is willing to pay enough with the fill-in. This is one of the great strengths of ILUT: it is possible to obtain a preconditioner as close as one wants to the direct solver.

A slightly different but related idea is to directly construct an approximate LU factorization of the inverse of the system matrix $A \in \mathbb{R}^{n\times n}$, which leads to the *sparse approximate inverse (AINV) preconditioner* for symmetric positive definite matrices introduced by Benzi, Meyer, and Tůma in 1996; see [17]. AINV is based on the fact that one can readily obtain a factorization of A^{-1} from a set of conjugate (A-orthogonal) search directions $\boldsymbol{z}_j$, $j = 1, 2, \ldots, n$: if one collects these search directions in the matrix $Z := [\boldsymbol{z}_1, \boldsymbol{z}_2, \ldots, \boldsymbol{z}_n]$, then we get, because of A-orthogonality,

$$Z^\top AZ = D, \quad p_i = \boldsymbol{z}_i^\top A\boldsymbol{z}_i,$$

where $D := \operatorname{diag}(p_1, \ldots, p_n)$, and hence for the inverse

$$A^{-1} = ZD^{-1}Z^\top.$$

If one constructs the conjugate directions using the conjugate Gram–Schmidt process and starts with the canonical basis vectors $\boldsymbol{e}_i$, it turns out that the resulting Z matrix is upper triangular, $Z = L^{-\top}$ with $A = LDL^\top$ being the Cholesky factorization of A; see [17]. AINV is then obtained by only computing a sparse approximation of Z by specifying either a fill-in pattern or a drop tolerance like in ILU.

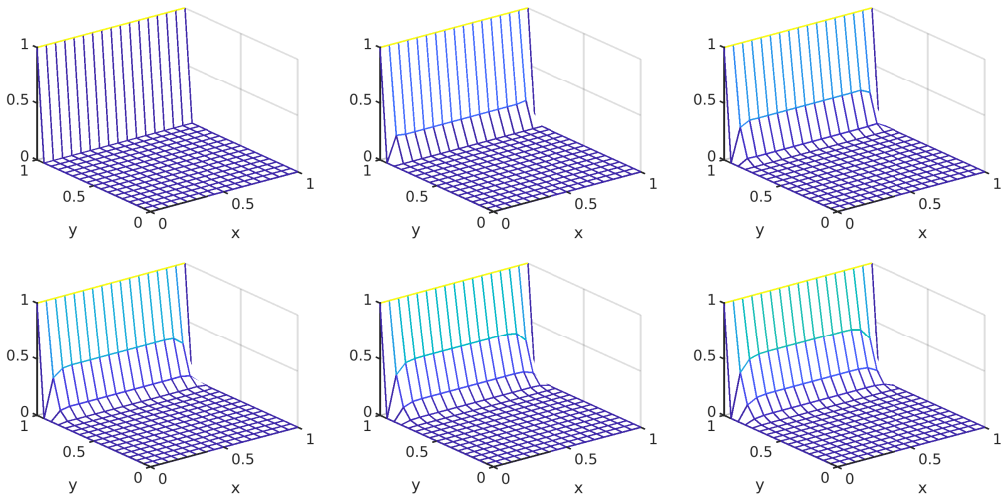

Figure 4.9. *Initial guess and first iterations of the SPAI preconditioner with a diagonal sparsity pattern only, applied to our Laplace model problem from Section 1.3.*

A different idea to obtain a preconditioner at the algebraic level is to construct directly a matrix M^{-1} which is a good approximation of A^{-1}. A well-known preconditioner is the *sparse approximate inverse preconditioner (SPAI)*, which was introduced by Grote and Huckle in 1997;[36] see [98]. Here, a sparse matrix M^{-1} is directly constructed by minimizing the Frobenius norm

$$\|I - AM^{-1}\|_F^2 := \sum_{i=1}^{n} \|(I - AM^{-1})\boldsymbol{e}_i\|_2^2,$$

which can be naturally done in parallel for each column, and leads to n independent least squares problems when a sparsity pattern is imposed on M^{-1}. Here is an implementation in MATLAB:

```
function M=SPAI(A,Z)
% SPAI computes a sparse approximate inverse
%   M=SPAI(A,Z); computes a sparse approximate inverse M of A with the
%   sparsity pattern in the matrix Z using the SPAI technique.

n=size(A,2);
I=speye(n);
M=Z;
for i=1:n
  id=find(Z(:,i)~=0);                  % find nonzero entries in Z
  M(id,i)=A(:,id)\I(:,i);              % fill them with least squares
end
```

If one puts as sparsity pattern `Z` a dense matrix, for example `M=SPAI(A,ones(size(A)))`, then SPAI computes actually the inverse of A, $M = A^{-1}$. If we give only a diagonal matrix, `M=SPAI(A,speye(size(A)))`, we obtain for our Laplace model problem when SPAI is used in a stationary iteration the first iterates in Figure 4.9. We see that even though this is the best

[36] The second author was sitting as a fresh graduate student with Marcus Grote and Thomas Huckle on the lawn at Stanford when SPAI was invented.

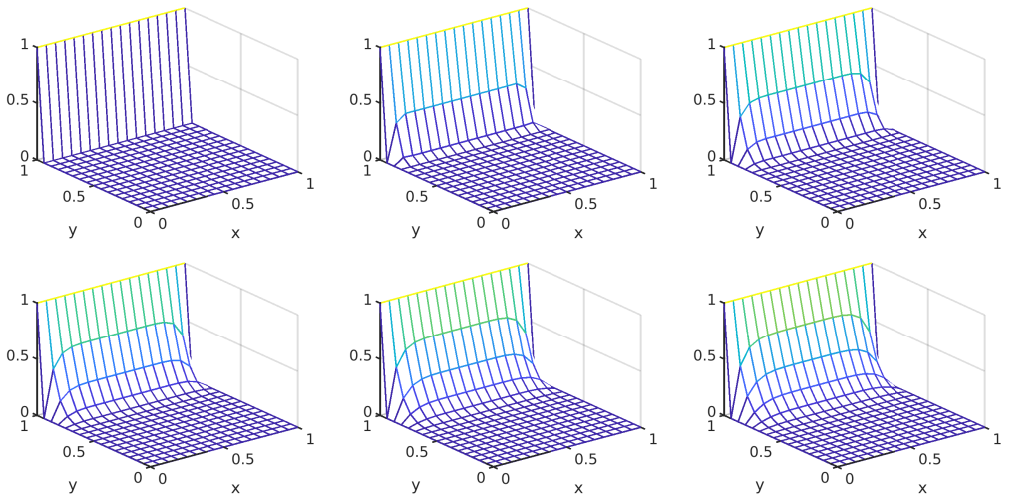

Figure 4.10. *Initial guess and first iterations of the SPAI preconditioner with sparsity pattern corresponding to the sparsity pattern of the matrix A from our Laplace model problem in Section 1.3.*

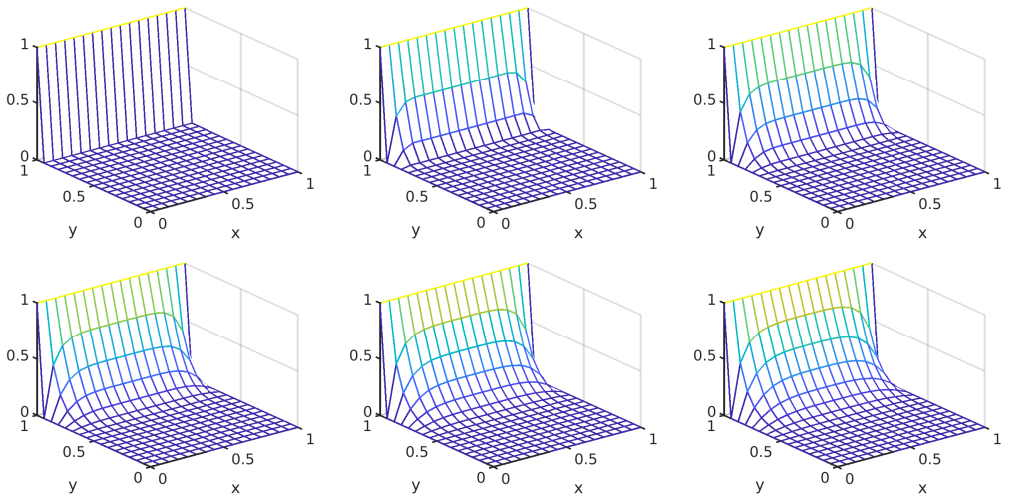

Figure 4.11. *Initial guess and first iterations of the SPAI preconditioner with sparsity pattern corresponding to the sparsity pattern of the matrix A^2 from our Laplace model problem in Section 1.3.*

possible diagonal approximation of the inverse in the SPAI sense, convergence is rather slow. To improve it, we give as sparsity pattern `Z` the matrix A, `M=SPAI(A,A)`. This leads to the iterates in Figure 4.10. We see that convergence is already better, and we can further improve it by giving a sparsity pattern which connects further neighbors, e.g., `M=SPAI(A,A^2)` with the results in Figure 4.11, and `M=SPAI(A,A^3)` with the results in Figure 4.12. We see that convergence is improving further and further, which is due to more and more fill-in created in the sparsity pattern by taking powers, as illustrated in Figure 4.13. Similar to ILU, one can thus obtain an arbitrarily good preconditioner if one is willing to pay with more and more fill in. We illustrate

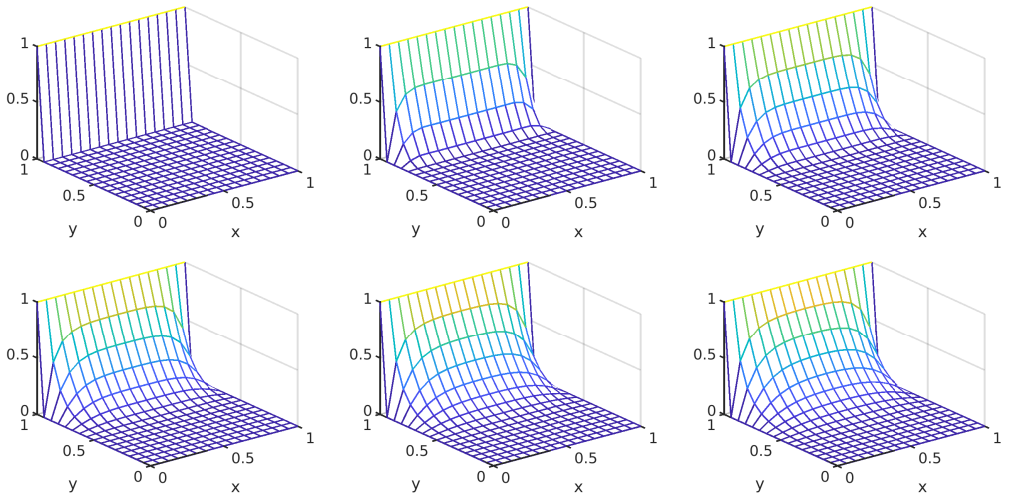

Figure 4.12. *Initial guess and first iterations of the SPAI preconditioner with sparsity pattern corresponding to the sparsity pattern of the matrix A^3 from our Laplace model problem in Section 1.3.*

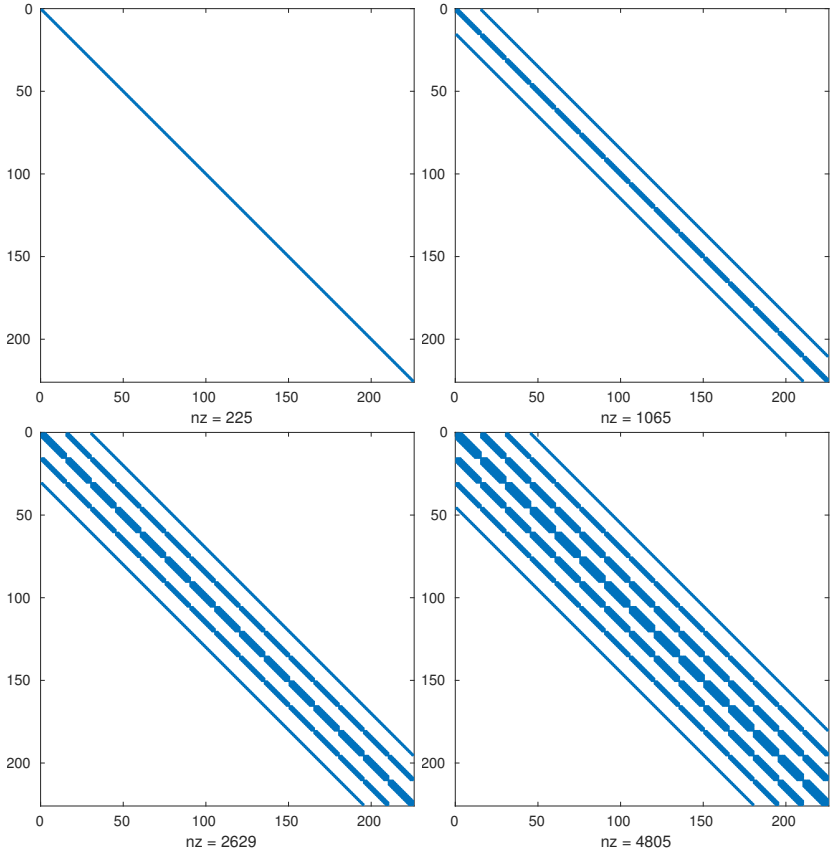

Figure 4.13. *SPAI fill-in patterns created by A^0, A^1, A^2, and A^3, where A is the five-point finite-difference stencil from our Laplace model problem in Section 1.3.*

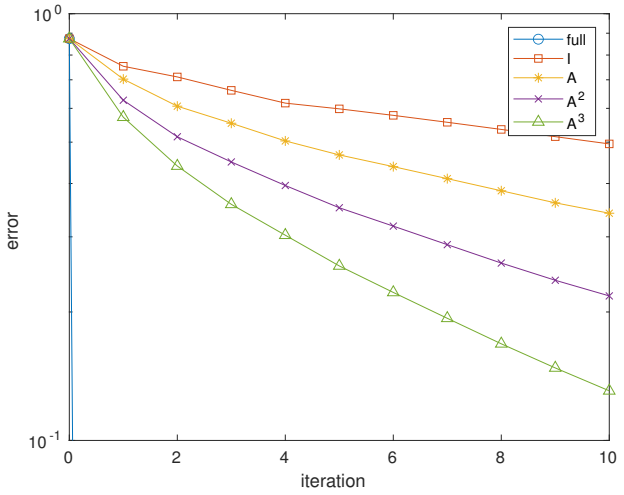

Figure 4.14. *Performance of the different SPAI preconditioners when used as stationary iterative solvers for our Laplace model problem.*

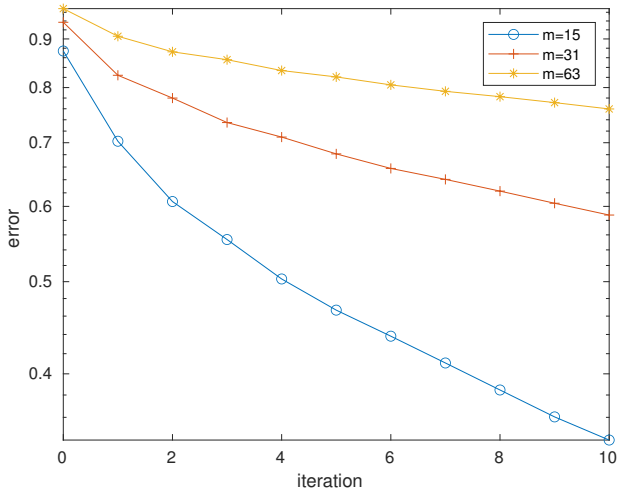

Figure 4.15. *Convergence of the SPAI stationary iteration for different mesh sizes* $h = \frac{1}{m+1}$.

this in Figure 4.14. As expected, using the completely dense pattern indicated by "full" leads to a preconditioner such that the stationary iterative method converges in one iteration. Increasing the fill-in starting from the diagonal approximation with powers of the matrix improves the convergence, but comparing to the ILU approach in Figure 4.8 we see that convergence for a comparable fill-in in SPAI is much slower than for ILU (note the difference in scale). This is because the exact inverse is fully dense, while the exact LU factorization only fills in the band width in our Laplace example, and so a much better approximation can be obtained in ILU when a similar number of fill-in elements is used compared to SPAI. SPAI convergence is also mesh dependent, as we can see in Figure 4.15, where we used as the fill-in pattern the sparsity pattern of A^3 when solving our Laplace model problem from Section 1.3 for the mesh we used for

Figure 4.12 with $m = 15$ interior mesh points, and two refined meshes with $m = 31$ and $m = 63$ interior mesh points.

There is also an adaptive version of SPAI, where one starts with a given sparsity pattern, for example diagonal, and then one adds adaptively nonzero entries in M^{-1} in such a way that the residual is reduced as much as possible; see [98] and, e.g., [15].

4.6 ▪ Schwarz domain decomposition methods

Durch Fortsetzung einiger Untersuchungen, welche gewisse Arten von Abbildungsaufgaben betreffen, und von denen ein Theil im 70. Bande von Borchardt's Journal und in dem das Programm der eidgenössischen poytechnischen Schule für das Wintersemester 1869-70 begleitenden Aufsatze: "Zur Theorie der Abbildung" veröffentlicht ist, bin ich auf ein Beweisverfahren geführt worden, durch welches, wie ich mich überzeugt zu haben glaube, alle Sätze, deren Beweis Riemann in seinen veröffentlichten Abhandlungen mittelst des Dirichletschen Princips zu führen gesucht hat, mit Strenge bewiesen werden können.

Hermann Amandus Schwarz, *Über einen Grenzübergang durch alternierendes Verfahren*, 1869.

We have seen in Chapter 1 that the linear system $A\boldsymbol{u} = \boldsymbol{f}$ often represents a discretization of a PDE, e.g.,

$$\begin{aligned} -\Delta u &= f \text{ in } \Omega := (0,1) \times (0,L), \\ u &= g \text{ on } \partial\Omega. \end{aligned} \tag{4.29}$$

This suggests that the continuous problem corresponding to $A\boldsymbol{u} = \boldsymbol{f}$ can be used to derive good preconditioners. In particular, if we can define a good stationary iterative method at the continuous level, we can construct a preconditioner by the corresponding discretization, and since the method already works at the continuous level, it is very likely that the discretized method then converges independently of the mesh size, i.e., the number of iterations for a certain accuracy does not depend on the size of the problem. Domain decomposition methods follow exactly this idea.

Schwarz domain decomposition methods are the oldest domain decomposition methods, and in their classical variant they need overlapping subdomain decompositions to converge. Schwarz methods were first defined at the continuous level directly for the PDE, and the goal of Schwarz was to close a gap in the proof of the Riemann mapping theorem; see the quote above, and see [84] for more details on the historical context. This led to the *alternating Schwarz method*, which a century later was generalized by *Pierre-Louis Lions* to the *parallel Schwarz method*. These methods can be discretized and used as iterative solvers, but there are also discrete Schwarz methods, namely the *multiplicative Schwarz method*, the *additive Schwarz method*, and the *restricted additive Schwarz method*, and we will see why there are three discrete methods and only two classical continuous ones.

The classical Schwarz methods are overlapping domain decomposition methods, but there are also *nonoverlapping domain decomposition* methods. Their roots lie in the substructuring methods of *Janusz S. Przemieniecki* [150], but they evolved rapidly into the Dirichlet–Neumann, Neumann–Neumann, and finite element tearing and interconnecting (FETI) algorithms, and we will directly introduce and study the latter later in this section.

There are also domain decomposition methods for time-dependent problems, which have their roots in the work of *Emile Picard* [148] and *Ernest Lindelöf* [125] and became numerical solvers with the invention of *waveform relaxation methods* in the group of *Albert E. Ruehli* at IBM [123], but since we do not treat time-dependent problems in this book, we will not explain these methods further.

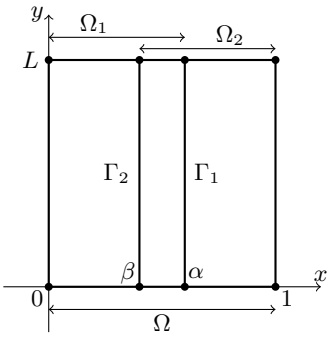

Figure 4.16. *Decomposition of the domain* $\Omega = (0,1) \times (0,L)$ *into* $\Omega = \Omega_1 \cup \Omega_2$*, where* $\Omega_1 := (0,\alpha) \times (0,L)$ *and* $\Omega_2 := (\beta,1) \times (0,L)$*. The interfaces are denoted by* Γ_1 *and* Γ_2*.*

Classical alternating and parallel Schwarz methods

The first domain decomposition method in history is the alternating Schwarz method, which was proposed by *Hermann Amandus Schwarz* in 1869; see [168]. To define the alternating Schwarz method for the solution to (4.29), we consider the simple domain decomposition $\Omega = \Omega_1 \cup \Omega_2$, where the two subdomains are $\Omega_1 := (0,\alpha) \times (0,L)$ and $\Omega_2 := (\beta,1) \times (0,L)$ with $\alpha > \beta$; see Figure 4.16. The two subdomains Ω_1 and Ω_2 have boundaries $\partial\Omega_1$ and $\partial\Omega_2$, and $\Gamma_1 := \partial\Omega_1 \setminus (\partial\Omega \cap \partial\Omega_1)$ and $\Gamma_2 := \partial\Omega_2 \setminus (\partial\Omega \cap \partial\Omega_2)$ are called interfaces. The *alternating Schwarz method* is defined by iteratively solving the two subproblems[37]

$$\begin{aligned} -\Delta u_1^n &= f && \text{in } \Omega_1, & -\Delta u_2^n &= f && \text{in } \Omega_2, \\ u_1^n &= u_2^{n-1} && \text{on } \Gamma_1, & u_2^n &= u_1^n && \text{on } \Gamma_2, \\ u_1^n &= g && \text{on } \partial\Omega \cap \partial\Omega_1, & u_2^n &= g && \text{on } \partial\Omega \cap \partial\Omega_2. \end{aligned} \tag{4.30}$$

In particular, the Schwarz iterative procedure starts with an initial guess u_2^0 on Γ_1, which is used to solve the first subproblem to get u_1^1. The function u_1^1 is then traced on Γ_2 to solve the second subproblem that gives u_2^1. Again, the function u_2^1 is traced on Γ_1 to solve the first subproblem and compute u_1^2. One can then trace u_1^2 on Γ_2, and solve the second subproblem to get u_2^2. Continuing in this way, it is possible to obtain two sequences $\{u_1^n\}_n$ and $\{u_2^n\}_n$ that approximate the solution u on Ω_1 and Ω_2. A small modification which leads to the *parallel Schwarz method* was introduced by Lions in [127]: instead of using the transmission condition $u_2^n = u_1^n$ for the second subdomain problem (4.30) he proposed to use

$$u_2^n = u_1^{n-1} \qquad \text{on } \Gamma_2, \tag{4.31}$$

which then allows the two subdomain solves to be done in parallel, before exchanging information with the neighboring subdomain. In the case of many subdomains, this leads to a large-scale parallel method which is of great interest. In the two-subdomain case, however, this modification just leads to a method which computes the original alternating Schwarz sequence $\{u_2^0, u_1^1, u_2^2, u_1^3, u_2^4, \dots\}$ and the analogous one starting on the other subdomain $\{u_1^0, u_2^1, u_1^2, u_2^3, u_1^4, \dots\}$, so not much is gained then with this parallelism, and the convergence behavior is the same. We thus study only the convergence of the alternating Schwarz method (4.30) in what follows; for the well-posedness of the Schwarz algorithm, see the appendix, Section 6.1.

The convergence of classical alternating and parallel Schwarz methods can be proved by different techniques: an analysis based on variational arguments and orthogonal projection

[37] In contrast to the earlier chapters, it is more common to use n as the iteration index here and to put it as superscript, a convention we follow throughout this chapter.

[127, 39], which provides convergence in the H^1-norm, an analysis based on maximum principle estimates, which allows one to obtain convergence in the maximum norm [128, 38, 40, 42, 43], and Fourier analysis [68, 37, 32, 46]. The following theorem is based on Fourier analysis, and we suppose for the rest of this section that the assumptions in Theorem 6.2 (respectively, Theorem 6.3) hold for the Schwarz algorithm to be well posed.

Theorem 4.5 (Convergence of the classical Schwarz method). *Assume that the domain $\Omega = (0,1)\times(0,L)$ is decomposed as in Figure 4.16. For any sufficiently regular initialization u^0 such that $u^0 = g$ on $\partial\Omega$, the alternating Schwarz method* (4.30) *converges to the solution u of* (4.29) *and satisfies the convergence estimate*

$$\|u - u_j^n\|_{L^2(\Omega_j)} \leq \rho_s^n \|u - u^0\|_{L^2(\Omega)}, \tag{4.32}$$

where $\|\cdot\|_{L^2}$ is the classical L^2-norm, and

$$\rho_s(\alpha,\beta,L) = \frac{\sinh(\frac{\pi}{L}\beta)}{\sinh(\frac{\pi}{L}\alpha)} \frac{\sinh(\frac{\pi}{L}(1-\alpha))}{\sinh(\frac{\pi}{L}(1-\beta))} < 1. \tag{4.33}$$

Proof. Define the errors $e_j^n := u - u_j^n$ for $j = 1, 2$. Since the Schwarz subproblems are linear, the errors e_j^n satisfy the so-called error equations

$$\begin{aligned} -\Delta e_1^n &= 0 \quad \text{in } \Omega_1, & -\Delta e_2^n &= 0 \quad \text{in } \Omega_2, \\ e_1^n &= e_2^{n-1} \quad \text{on } \Gamma_1, & e_2^n &= e_1^n \quad \text{on } \Gamma_2, \\ e_1^n &= 0 \quad \text{on } \partial\Omega \cap \partial\Omega_1, & e_2^n &= 0 \quad \text{on } \partial\Omega \cap \partial\Omega_2. \end{aligned} \tag{4.34}$$

Hence, by Weyl's theorem [88] they are harmonic functions. It is well known that a separation of variables ansatz permits us to show that the solutions e_j^n to (4.34) have the form of the Fourier sine series [139, Section 4.3]

$$e_j^n(x,y) = \sum_{k\in K} \widehat{e}_j^n(x,k)\sin(ky), \tag{4.35}$$

with $K := \{\frac{\pi}{L}, \frac{2\pi}{L}, \frac{3\pi}{L}, \ldots\}$ and where $\widehat{e}_j^n(x,k)$ are the Fourier coefficients that solve the second-order ordinary differential equations

$$\begin{aligned} \partial_{xx}\widehat{e}_1^n(x,k) - k^2\widehat{e}_1^n(x,k) &= 0 \quad \text{for } x \in (0,\alpha), \\ \widehat{e}_1^n(0,k) &= 0, \\ \widehat{e}_1^n(\alpha,k) &= \widehat{e}_2^{n-1}(\alpha,k) \end{aligned}$$

and

$$\begin{aligned} \partial_{xx}\widehat{e}_2^n(x,k) - k^2\widehat{e}_2^n(x,k) &= 0 \quad \text{for } x \in (\beta,1), \\ \widehat{e}_2^n(\beta,k) &= \widehat{e}_1^n(\beta,k), \\ \widehat{e}_2^n(1,k) &= 0. \end{aligned}$$

The solutions to these two ordinary differential equations have the form

$$\widehat{e}_j^n(x,k) = A_j^n(k)e^{kx} + B_j^n(k)e^{-kx}$$

for $j = 1, 2$, where $A_j^n(k)$ and $B_j^n(k)$ are determined by imposing the boundary conditions. Using first the outer boundary conditions posed in the original problem, we obtain

$$\begin{aligned} \widehat{e}_1^n(0,k) = 0 \quad &\Longrightarrow \quad B_1^n(k) = -A_1^n(k), \\ \widehat{e}_2^n(1,k) = 0 \quad &\Longrightarrow \quad B_2^n(k) = -A_2^n(k)e^{2k}, \end{aligned} \tag{4.36}$$

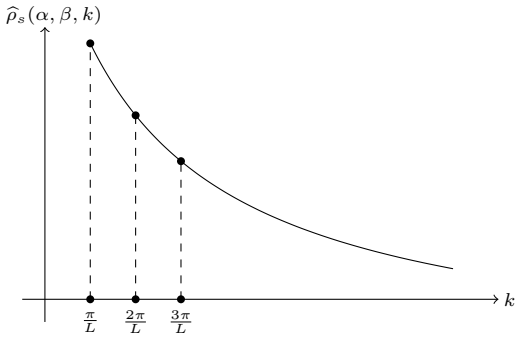

Figure 4.17. *Qualitative behavior of the convergence factor $\widehat{\rho}_s(\alpha,\beta,k)$ as a function of k. Notice that we are interested in the values $k = \frac{\pi}{L}, \frac{2\pi}{L}, \frac{3\pi}{L}, \ldots$.*

which implies that

$$\begin{aligned}\widehat{e}_1^n(x,k) &= A_1^n(k)(e^{kx} - e^{-kx}) = 2A_1^n(k)\sinh(kx),\\ \widehat{e}_2^n(x,k) &= A_2^n(k)(e^{kx} - e^{2k}e^{-kx}) = -2A_2^n(k)e^k\sinh(k(1-x)).\end{aligned} \tag{4.37}$$

Now, from the transmission condition in (4.34) we have that $\widehat{e}_1^n(\alpha,k) = \widehat{e}_2^{n-1}(\alpha,k)$, which implies

$$A_1^n(k)2\sinh(k\alpha) = A_2^{n-1}(k)\big(-2e^k\sinh(k(1-\alpha))\big), \tag{4.38}$$

and $\widehat{e}_2^n(\beta,k) = \widehat{e}_1^n(\beta,k)$ gives

$$A_1^n(k)2\sinh(k\beta) = A_2^n(k)\big(-2e^k\sinh(k(1-\beta))\big). \tag{4.39}$$

By combining (4.38) and (4.39), we obtain that

$$A_2^n(k) = \frac{\sinh(k\beta)}{\sinh(k(1-\beta))}\frac{\sinh(k(1-\alpha))}{\sinh(k\alpha)}A_2^{n-1}(k).$$

The convergence factor of this iteration is thus

$$\widehat{\rho}_s(\alpha,\beta,k) := \frac{\sinh(k\beta)}{\sinh(k(1-\beta))}\frac{\sinh(k(1-\alpha))}{\sinh(k\alpha)}, \tag{4.40}$$

and repeating a similar argument also for A_1^n, we obtain by induction

$$A_2^n(k) = \big(\widehat{\rho}_s(\alpha,\beta,k)\big)^n A_2^0(k) \quad \text{and} \quad A_1^n(k) = \big(\widehat{\rho}_s(\alpha,\beta,k)\big)^n A_1^0(k). \tag{4.41}$$

The qualitative behavior of the convergence factor $\widehat{\rho}_s(\alpha,\beta,k)$ as a function of k is shown in Figure 4.17. A direct calculation shows that the maximum of $\widehat{\rho}_s(\alpha,\beta,k)$ is attained for the lowest frequency $k = \frac{\pi}{L}$, $\max_{k\in K}\widehat{\rho}_s(\alpha,\beta,k) = \widehat{\rho}_s(\alpha,\beta,\frac{\pi}{L})$. Equation (4.41) implies that

$$\begin{aligned}e_1^n(x,y) &= \sum_{k\in K}\widehat{e}_1^n(x,k)\sin(ky)\\ &= \sum_{k\in K}A_1^n(k)2\sinh(kx)\sin(ky)\\ &= \sum_{k\in K}\big(\widehat{\rho}_s(\alpha,\beta,k)\big)^n A_1^0(k)2\sinh(kx)\sin(ky).\end{aligned}$$

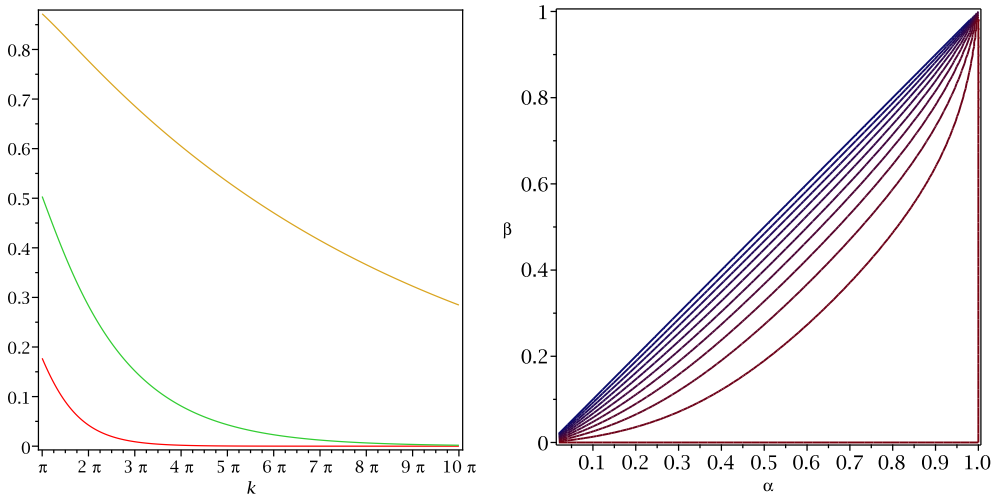

Figure 4.18. *Left: Dependence of the convergence factor $\widehat{\rho}_s(\alpha,\beta,k)$ of the alternating Schwarz method as a function of the frequency parameter k, from top to bottom for $\alpha \in \{0.51, 0.55, 0.625\}$ and $\beta \in \{0.49, 0.45, 0.375\}$. Right: Level sets corresponding to $\{0, 0.1, \ldots, 1\}$ of the overall convergence factor $\rho_s(\alpha,\beta,L)$ from Theorem 4.5.*

We can now use the Parseval–Plancherel formula [48, Theorems 4.9-1 and 4.9-2] to estimate

$$\begin{aligned}\|e_1^n(x,\cdot)\|^2_{L^2(0,1)} &= \sum_{k\in K}\Big[\big(\widehat{\rho}_s(\alpha,\beta,k)\big)^n A_1^0(k)2\sinh(kx)\Big]^2\\ &\le \big(\widehat{\rho}_s(\alpha,\beta,\tfrac{\pi}{L})\big)^{2n}\sum_{k\in K}\Big[A_1^0(k)2\sinh(kx)\Big]^2\\ &= \big(\widehat{\rho}_s(\alpha,\beta,\tfrac{\pi}{L})\big)^{2n}\|e_1^0(x,\cdot)\|^2_{L^2(0,1)},\end{aligned}$$

that is,

$$\|e_1^n(x,\cdot)\|_{L^2(0,1)} \le \big(\widehat{\rho}_s(\alpha,\beta,\tfrac{\pi}{L})\big)^n\|e_1^0(x,\cdot)\|_{L^2(0,1)},$$

and hence

$$\|e_1^n\|_{L^2(\Omega_1)} \le \big(\widehat{\rho}_s(\alpha,\beta,\tfrac{\pi}{L})\big)^n\|u-u^0\|_{L^2(\Omega)}.$$

The result for e_2^n is obtained using the same arguments, and we obtain (4.33) with $\rho_s(\alpha,\beta,L) = \widehat{\rho}_s(\alpha,\beta,\frac{\pi}{L})$. This quantity is smaller than one, since the hyperbolic sine is a growing function, and the subdomains overlap, $\beta < \alpha$, and thus also $1-\alpha < 1-\beta$, which makes the two rearranged fractions in $\rho_s(\alpha,\beta,L)$ both smaller than one. □

The analysis above is typical for the analysis of iterative methods based on the underlying physics of the problem: it is performed whenever possible at the continuous level, without discretization. The convergence result we obtained in Theorem 4.5 shows that the convergence speed of the method depends on the overlap parameters α and β. In Figure 4.18, we show the convergence factor $\widehat{\rho}_s(\alpha,\beta,k)$ from (4.40) as a function of each Fourier frequency k, and also $\rho_s(\alpha,\beta,L)$ from (4.33) as a function of α and β for $L = 1$. The plots were obtained with the Maple commands

```
rho:=sinh(k*beta)/sinh(k*(1-beta))*sinh(k*(1-alpha))/sinh(k*alpha);
alpha:=0.625; beta:=0.375; rho1:=rho;
alpha:=0.55; beta:=0.45; rho2:=rho;
alpha:=0.51; beta:=0.49; rho3:=rho;
plot([rho1,rho2,rho3],k=Pi..10*Pi,axes=boxed);
alpha:='alpha';beta:='beta';k:=Pi;
plots[contourplot](rho,alpha=0..1,beta=0..alpha,contours=
  [seq(i/10,i=0..10)],axes=boxed);
```

We see on the left in Figure 4.18 that the convergence of the alternating Schwarz method is greatly influenced by the overlap size $\alpha - \beta$: if the overlap is large, convergence is fast, and if the overlap is small, convergence is slower. We also see that high frequencies, k large, converge much faster than low frequencies, k small, so the classical Schwarz method is a smoother. On the right in Figure 4.18 we also see that the position of the interfaces defined by α and β, i.e., the subdomain geometry, has an influence on the convergence of the alternating Schwarz method: if one subdomain is small and the other one is big, the method also converges faster for the same overlap size than when both subdomains are of the same size. From the formula for $\rho_s(\alpha, \beta, L)$ from (4.33), we also see that the domain height or interface length L influences the convergence: for L large, the convergence is slow, and for L small, the convergence is fast. This influence of the geometry of the decomposition on the performance of the Schwarz method has been investigated only very recently; see, for example, [70, 7, 44].

Classical Schwarz preconditioners

To use the alternating Schwarz method as a computational tool and then as a preconditioner, we have to discretize the algorithm (4.30). We have seen in Chapter 1 that Laplace's equation (4.29) at the discrete level gives the linear system

$$A\boldsymbol{u} = \boldsymbol{f},$$

where $\boldsymbol{u}, \boldsymbol{f} \in \mathbb{R}^{m^2}$, $A \in \mathbb{R}^{m^2 \times m^2}$ is the discrete Laplacian matrix, and the domain $\overline{\Omega} = [0,1] \times [0,1]$[38] is discretized with a uniform grid of $(m+2) \times (m+2)$ points, including the boundary points.

The matrix A can be decomposed according to the two-subdomain decomposition of the alternating Schwarz method in two different ways,

$$A = \begin{bmatrix} A_1 & B_{12} \\ \times & \times \end{bmatrix} = \begin{bmatrix} \times & \times \\ B_{21} & A_2 \end{bmatrix}, \tag{4.42}$$

where $A_j = R_j A R_j^\top$, and R_1 and R_2 are rectangular restriction matrices given by

$$R_1 = \begin{bmatrix} I_{m_1 m} & 0 \end{bmatrix} \in \mathbb{R}^{m_1 m \times m^2} \quad \text{and} \quad R_2 = \begin{bmatrix} 0 & I_{m_2 m} \end{bmatrix} \in \mathbb{R}^{m_2 m \times m^2},$$

with $I_{m_1 m}$ and $I_{m_2 m}$ the identities of size $m_1 m$ and $m_2 m$, and the discretization points corresponding to m_1 and m_2 are shown in Figure 4.19. To write the alternating Schwarz method at the discrete level, we need to introduce in addition the matrices

$$\widetilde{B}_{12} = \begin{bmatrix} 0 & B_{12} \end{bmatrix} \in \mathbb{R}^{m_1 m \times m_2 m} \quad \text{and} \quad \widetilde{B}_{21} = \begin{bmatrix} B_{21} & 0 \end{bmatrix} \in \mathbb{R}^{m_2 m \times m_1 m}$$

and the vectors $\boldsymbol{f}_j = R_j \boldsymbol{f}$ for $j = 1, 2$. The discrete version of the alternating Schwarz method

[38] We chose for simplicity a square domain here, $L = 1$.

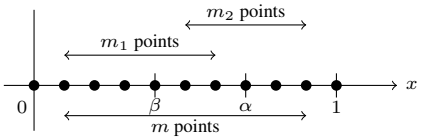

Figure 4.19. *Discretization grid and discrete domain decomposition.*

(4.30) can then be expressed using these matrices by

$$\begin{aligned} A_1 \boldsymbol{u}_1^n &= \boldsymbol{f}_1 - \widetilde{B}_{12} \boldsymbol{u}_2^{n-1}, \\ A_2 \boldsymbol{u}_2^n &= \boldsymbol{f}_2 - \widetilde{B}_{21} \boldsymbol{u}_1^n, \end{aligned} \tag{4.43}$$

where $\boldsymbol{u}_1 \in \mathbb{R}^{m_1 m}$ and $\boldsymbol{u}_2 \in \mathbb{R}^{m_2 m}$. We see that in the first line of (4.43) there is a subdomain solve using the matrix A_1 corresponding to the discretized Laplacian on subdomain Ω_1, and at the interface, this subdomain solve uses data from the previous iteration on subdomain Ω_2 represented by the term $\widetilde{B}_{12} \boldsymbol{u}_2^{n-1}$. Similarly, in the second line of (4.43) there is a subdomain solve using the matrix A_2 corresponding to the discretized Laplacian on subdomain Ω_2, and at the interface, this subdomain solve uses data from the just completed solve on subdomain Ω_1 represented by the term $\widetilde{B}_{21} \boldsymbol{u}_1^n$. An example of matrices A_1, A_2, $\widetilde{B}_{12}$, and $\widetilde{B}_{21}$ for a one-dimensional Laplace problem is the following (see also Problem 56).

Example 4.6. Consider the one-dimensional Laplace problem

$$-u_{xx} = f \quad \text{in } (0,1) \text{ with } u(0) = u(1) = 0$$

and the alternating Schwarz method

$$\begin{aligned} -(u_1^n)_{xx} &= f \quad \text{in } (0,\alpha) \text{ with } u_1^n(0) = 0,\ u_1^n(\alpha) = u_2^{n-1}(\alpha), \\ -(u_2^n)_{xx} &= f \quad \text{in } (\beta,1) \text{ with } u_2^n(\beta) = u_1^n(\beta),\ u_2^n(1) = 0. \end{aligned} \tag{4.44}$$

We use a discretization mesh of $m = 9$ interior points with a mesh size $h = \frac{1}{m+1}$. The two subdomains are $\Omega_1 = (0,\alpha)$ and $\Omega_2 = (\beta,1)$ with $\alpha = 7h$, $\beta = 4h$, and an overlap of $m_{\text{over}} h$ with $m_{\text{over}} = 3$; see Figure 4.19. In Ω_1 and Ω_2 we consider $m_1 = 6$ and $m_2 = 5$ interior mesh points. The discretization of (4.44) is then given by

$$A_1 \boldsymbol{u}_1^n = f_1 + \widetilde{B}_{12} \boldsymbol{u}_2^{n-1}, \quad A_2 \boldsymbol{u}_2^n = f_2 + \widetilde{B}_{21} \boldsymbol{u}_1^n,$$

where $\boldsymbol{u}_1 \in \mathbb{R}^{m_1}$, $\boldsymbol{u}_2 \in \mathbb{R}^{m_2}$,

$$A_1 = \frac{1}{h^2} \begin{bmatrix} 2 & -1 & & & & \\ -1 & 2 & -1 & & & \\ & -1 & 2 & -1 & & \\ & & -1 & 2 & -1 & \\ & & & -1 & 2 & -1 \\ & & & & -1 & 2 \end{bmatrix} \in \mathbb{R}^{6\times 6}, \quad B_{12} = \frac{1}{h^2} \begin{bmatrix} & & \\ & & \\ & & \\ & & \\ & & \\ -1 & & \end{bmatrix} \in \mathbb{R}^{6\times 3},$$

$$A_2 = \begin{bmatrix} 2 & -1 & & & \\ -1 & 2 & -1 & & \\ & -1 & 2 & -1 & \\ & & -1 & 2 & -1 \\ & & & -1 & 2 \end{bmatrix} \in \mathbb{R}^{5\times 5}, \quad B_{21} = \frac{1}{h^2} \begin{bmatrix} & & & -1 \\ & & & \\ & & & \\ & & & \\ & & & \end{bmatrix} \in \mathbb{R}^{5\times 4},$$

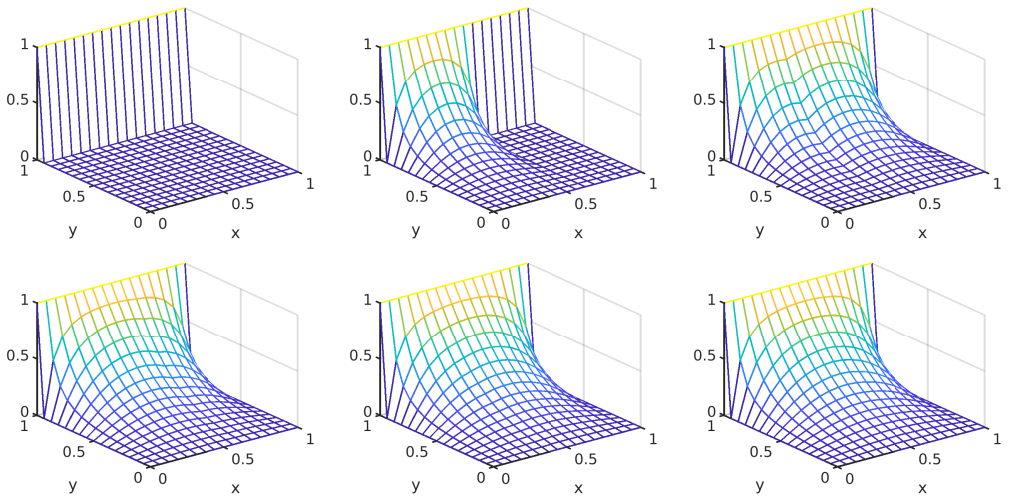

Figure 4.20. *Initial guess and first iterations of the alternating Schwarz method applied to our Laplace model problem.*

and the matrices $\widetilde{B}_{12}$ and $\widetilde{B}_{21}$ are

$$\widetilde{B}_{12} = \frac{1}{h^2}\begin{bmatrix} 0_{m_1 \times m_{\text{over}}-1} & B_{12} \end{bmatrix} \in \mathbb{R}^{6\times 5}, \quad \widetilde{B}_{21} = \frac{1}{h^2}\begin{bmatrix} B_{21} & 0_{m_2 \times m_{\text{over}}-1} \end{bmatrix} \in \mathbb{R}^{5\times 6}.$$

Notice that

$$\widetilde{B}_{12}\boldsymbol{u}_2^{n-1} = \frac{1}{h^2}\begin{bmatrix} 0 \\ 0 \\ 0 \\ 0 \\ 0 \\ -(\boldsymbol{u}_2^{n-1})_3 \end{bmatrix}, \quad \widetilde{B}_{21}\boldsymbol{u}_1^{n} = \frac{1}{h^2}\begin{bmatrix} -(\boldsymbol{u}_1^{n})_4 \\ 0 \\ 0 \\ 0 \\ 0 \end{bmatrix},$$

which clearly shows how the Dirichlet transmission condition is transferred from one subdomain to the other in the discretized alternating Schwarz method. ∎

Getting back to the two-dimensional case, we show in Figure 4.20 the first few iterations of the alternating Schwarz method applied to our Laplace model problem (see also Problem 59). We used $m = 15$ interior mesh points, an overlap of $4h$, $h = \frac{1}{m+1}$, and subdomains of the same size, which means that $\alpha = \frac{1}{2} + 2h = 0.625$ and $\beta = \frac{1}{2} - 2h = 0.375$. One can clearly see how effective subdomain solves are in rapidly giving a very good approximate solution: only after solving on the left and right twice, we arrive basically at the solution.

For fixed positions of the interfaces α and β in physical space, this discretized alternating Schwarz method will converge as predicted by the continuous analysis when the mesh is refined, and the contraction factor will thus not depend on the mesh parameter h when h goes to zero. This is a first iterative solver for the linear system corresponding to the discretized Laplacian whose convergence does not depend on the mesh size! We illustrate this in Figure 4.21, where we show how the error decays in the discretized alternating Schwarz iteration for the mesh we used for Figure 4.20 with $m = 15$, and also on two refined meshes with $m = 31$ and $m = 63$ interior mesh points, keeping the subdomains and hence the interfaces fixed at $\alpha = 0.625$ and $\beta = 0.375$. We clearly see that convergence is independent of the mesh parameter h and is very well predicted by the continuous analysis in Theorem 4.5.

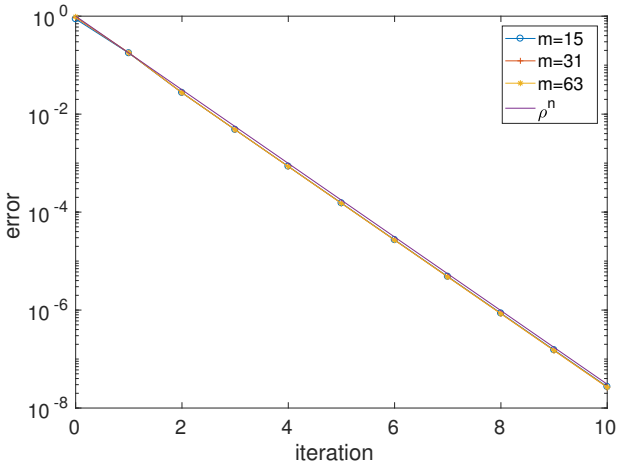

Figure 4.21. *Convergence of the alternating Schwarz method for different mesh sizes* $h = \frac{1}{m+1}$. *For comparison the theoretical convergence estimate based on the continuous analysis from Theorem 4.5 is also shown.*

Multiplicative Schwarz

There is an even more convenient way to implement the alternating Schwarz method than the discretized iteration (4.43), and which one can also more easily generalize to many subdomains. It is based on formulating the iteration for all the unknowns at once and became known under the name *multiplicative Schwarz method*. For our two-subdomain case, the method starts with an initial guess $\boldsymbol{u}^0$ for all the unknowns, and then computes for $n = 0, 1, \ldots$

$$\begin{aligned} \boldsymbol{u}^{n+\frac{1}{2}} &= \boldsymbol{u}^n + R_1^\top A_1^{-1} R_1 \big(\boldsymbol{f} - A\boldsymbol{u}^n\big), \\ \boldsymbol{u}^{n+1} &= \boldsymbol{u}^{n+\frac{1}{2}} + R_2^\top A_2^{-1} R_2 \big(\boldsymbol{f} - A\boldsymbol{u}^{n+\frac{1}{2}}\big). \end{aligned} \tag{4.45}$$

It is not immediately clear how the multiplicative Schwarz method (4.45) is related to the discretization of the alternating Schwarz method (4.43), since the subdomain solutions $\boldsymbol{u}_j^n$ do not even appear in the multiplicative Schwarz method (4.45). We show in the following theorem that (4.43) and (4.45) are in fact equivalent (for a proof in the general case of many subdomains, see [69]).

Theorem 4.7 (Alternating Schwarz = multiplicative Schwarz). *Assume that the initialization* $\boldsymbol{u}^0$ *of the multiplicative Schwarz method* (4.45) *and the initializations* $\boldsymbol{u}_1^0$ *and* $\boldsymbol{u}_2^0$ *of the discretized alternating Schwarz method* (4.43) *satisfy the relation*

$$\boldsymbol{u}^0 := (I - R_2^\top R_2) R_1^\top \boldsymbol{u}_1^0 + R_2^\top \boldsymbol{u}_2^0. \tag{4.46}$$

Then for $n \geq 1$ *the iterates* $\boldsymbol{u}^n$ *of the multiplicative Schwarz method* (4.45) *and the iterates* $\boldsymbol{u}_1^0$ *and* $\boldsymbol{u}_2^0$ *of the discretized alternating Schwarz method* (4.43) *remain related by the same relation,*

$$\boldsymbol{u}^n := (I - R_2^\top R_2) R_1^\top \boldsymbol{u}_1^n + R_2^\top \boldsymbol{u}_2^n. \tag{4.47}$$

Proof. We proceed by induction. Notice that for $n = 0$, (4.47) is equal to (4.46). Now, we assume that (4.47) holds for n and we show that it holds for $n + 1$ as well. The first equation in

(4.45) allows us to compute

$$\begin{aligned}
\boldsymbol{u}^{n+\frac{1}{2}} &= \boldsymbol{u}^n + R_1^\top A_1^{-1} R_1\big(\boldsymbol{f} - A\boldsymbol{u}^n\big) \\
&= \boldsymbol{u}^n + R_1^\top A_1^{-1}\big(R_1\boldsymbol{f} - R_1 A\boldsymbol{u}^n\big) \\
&= \boldsymbol{u}^n + R_1^\top A_1^{-1}\big(\boldsymbol{f}_1 - \begin{bmatrix} A_1 & B_{12}\end{bmatrix}\boldsymbol{u}^n\big) \\
&= \boldsymbol{u}^n + R_1^\top A_1^{-1}(\boldsymbol{f}_1 - A_1 R_1\boldsymbol{u}^n - \widetilde{B}_{12}\boldsymbol{u}_2^n) \\
&= (I - R_1^\top A_1^{-1} A_1 R_1)\boldsymbol{u}^n + R_1^\top A_1^{-1}(\boldsymbol{f}_1 - \widetilde{B}_{12}\boldsymbol{u}_2^n) \\
&= (I - R_1^\top R_1)\boldsymbol{u}^n + R_1^\top \boldsymbol{u}_1^{n+1},
\end{aligned} \tag{4.48}$$

where the last equality follows from the first equation in (4.43). Similarly, using the second equation in (4.45), we get

$$\begin{aligned}
\boldsymbol{u}^{n+1} &= \boldsymbol{u}^{n+\frac{1}{2}} + R_2^\top A_2^{-1} R_2\big(\boldsymbol{f} - A\boldsymbol{u}^{n+\frac{1}{2}}\big) \\
&= \boldsymbol{u}^{n+\frac{1}{2}} + R_2^\top A_2^{-1}\big(R_2\boldsymbol{f} - R_2 A\boldsymbol{u}^{n+\frac{1}{2}}\big) \\
&= \boldsymbol{u}^{n+\frac{1}{2}} + R_2^\top A_2^{-1}\big(\boldsymbol{f}_2 - \begin{bmatrix} B_{21} & A_2\end{bmatrix}\boldsymbol{u}^{n+\frac{1}{2}}\big) \\
&= \boldsymbol{u}^{n+\frac{1}{2}} + R_2^\top A_2^{-1}(\boldsymbol{f}_2 - \widetilde{B}_{21}\boldsymbol{u}_2^{n+\frac{1}{2}} - A_2 R_2\boldsymbol{u}^{n+\frac{1}{2}}) \\
&= (I - R_2^\top R_2)\boldsymbol{u}^{n+\frac{1}{2}} + R_2^\top \boldsymbol{u}_2^{n+1},
\end{aligned}$$

and using (4.48), we obtain

$$\begin{aligned}
\boldsymbol{u}^{n+1} &= (I - R_2^\top R_2)(I - R_1^\top R_1)\boldsymbol{u}^n + (I - R_2^\top R_2)R_1^\top \boldsymbol{u}_1^{n+1} + R_2^\top \boldsymbol{u}_2^{n+1} \\
&= (I - R_2^\top R_2)R_1^\top \boldsymbol{u}_1^{n+1} + R_2^\top \boldsymbol{u}_2^{n+1},
\end{aligned} \tag{4.49}$$

where we used that $(I - R_2^\top R_2)(I - R_1^\top R_1) = 0$. We have then obtained that (4.47) holds for $n+1$ and our proof is complete. □

We are now interested in finding the preconditioner M_{MS} that corresponds to the multiplicative Schwarz method. To do so, we replace the first equation of (4.45) in the second one to get[39]

$$\begin{aligned}
\boldsymbol{u}^{n+1} &= \boldsymbol{u}^n + R_1^\top A_1^{-1} R_1\big(\boldsymbol{f} - A\boldsymbol{u}^n\big) + R_2^\top A_2^{-1} R_2\big[\boldsymbol{f} - A\big(\boldsymbol{u}^n + R_1^\top A_1^{-1} R_1\big(\boldsymbol{f} - A\boldsymbol{u}^n\big)\big)\big] \\
&= \big(I - R_1^\top A_1^{-1} R_1 A - R_2^\top A_2^{-1} R_2 A + R_2^\top A_2^{-1} R_2 A R_1^\top A_1^{-1} R_1 A\big)\boldsymbol{u}^n \\
&\quad + \underbrace{\big(R_1^\top A_1^{-1} R_1 + R_2^\top A_2^{-1} R_2 - R_2^\top A_2^{-1} R_2 A R_1^\top A_1^{-1} R_1\big)}_{M_{\mathrm{MS}}^{-1}}\boldsymbol{f},
\end{aligned}$$

where we identified the inverse of the *multiplicative Schwarz preconditioner* M_{MS}. The previous formula can be rewritten as

$$\boldsymbol{u}^{n+1} = \big(I - R_1^\top A_1^{-1} R_1 A\big)\big(I - R_2^\top A_2^{-1} R_2 A\big)\boldsymbol{u}^n + M_{\mathrm{MS}}^{-1}\boldsymbol{f}, \tag{4.50}$$

which is the equivalent preconditioned form of the multiplicative Schwarz method (4.45).

[39] This type of discrete analysis of Schwarz methods involves more and more complicated sequences of the R_j matrices, especially in the many subdomain case [69], and led Stefan Güttel during his postdoc in Geneva to show us the German tongue twister "Rhabarberbarbara"—just search the Internet.

We can now give the program we used to produce the numerical experiments in Figure 4.20:

```
m=15;                                   % number of gridpoints
A=Laplacian(m,2);                       % five-point Laplacian
f=zeros(m*m,1); f(m:m:end)=1;           % put bc into the rhs
u=A\f;                                  % solve by sparse Gaussian elimination
ai=9; bi=7;                             % alpha=(ai+1)*h, beta=(bi-1)*h
R1=[speye(m*ai) sparse(m*ai,m*(m-ai))]; % construct restriction matrices
R2=[sparse(m*(m-bi+1),m*(bi-1)) speye(m*(m-bi+1))];
A1=R1*A*R1';                            % construct subdomain matrices
A2=R2*A*R2';
h=1/(m+1); x=0:h:1; y=x;                % mesh point vectors
udd=zeros(size(f));                     % initial guess
U=zeros(m+2); U(end,1:m+2)=1;           % for plotting
for n=0:10
  err(n+1)=max(max(abs(u-udd)));        % compute error
  U(2:m+1,2:m+1)=reshape(udd,m,m);
  mesh(x,y,U)
  xlabel('x');ylabel('y');
  pause
  udd=udd+R1'*(A1\(R1*(f-A*udd)));      % first subdomain solve
  U(2:m+1,2:m+1)=reshape(udd,m,m);
  mesh(x,y,U)
  xlabel('x');ylabel('y');
  pause
  udd=udd+R2'*(A2\(R2*(f-A*udd)));      % second subdomain solve
end
```

The multiplication of the two terms stemming from the subdomain solve in the multiplicative Schwarz preconditioner (4.50) is not convenient for parallel computing, since the operations need to be performed sequentially.

Additive Schwarz and restricted additive Schwarz

Multiplying out the two terms in (4.50), we obtain

$$\begin{aligned}&\big(I - R_1^\top A_1^{-1} R_1 A\big)\big(I - R_2^\top A_2^{-1} R_2 A\big)\\ &\qquad = I - R_1^\top A_1^{-1} R_1 A - R_2^\top A_2^{-1} R_2 A + R_1^\top A_1^{-1} R_1 A R_2^\top A_2^{-1} R_2 A,\end{aligned}$$

which led Dryja and Widlund to just drop the last term in the preconditioner, which is the only sequential one [184], and led to the well-known so-called additive Schwarz method,

$$\boldsymbol{u}^{n+1} = \big(I - R_1^\top A_1^{-1} R_1 A - R_2^\top A_2^{-1} R_2 A\big)\boldsymbol{u}^n + M_{\mathrm{AS}}^{-1}\boldsymbol{f}, \tag{4.51}$$

where the additive Schwarz preconditioner M_{AS} is

$$M_{\mathrm{AS}}^{-1} = R_1^\top A_1^{-1} R_1 + R_2^\top A_2^{-1} R_2.$$

It is very tempting to think that this modification is equivalent to the modification proposed by Lions in (4.31) to make the alternating Schwarz method parallel, but this is not so! The additive Schwarz method (4.51) only converges in the case of minimal overlap, that is, $\alpha - \beta = h$, where h is the mesh size, which means the subdomains at the algebraic level have no interior unknowns in common; see [69]. However, it is a good preconditioner for Krylov methods even in the case of

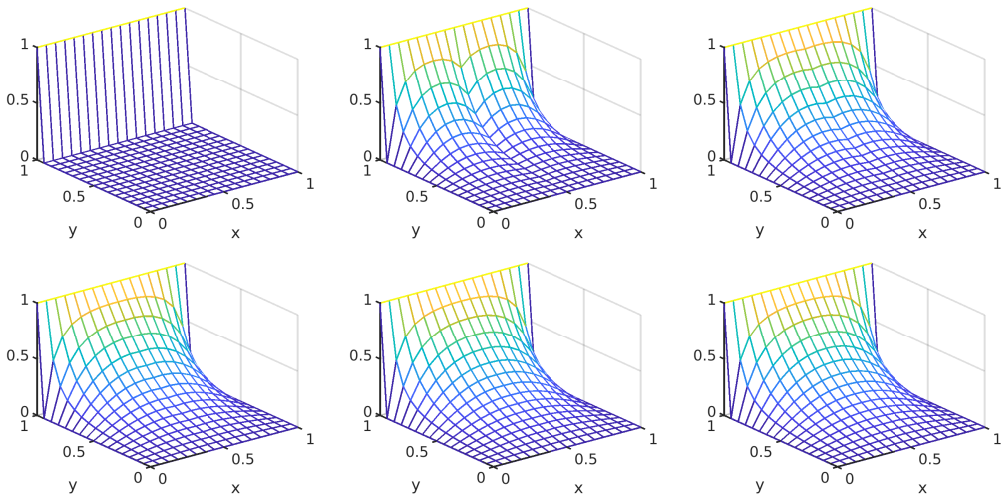

Figure 4.22. *Initial guess and first iterations of the restricted additive Schwarz method, which is equivalent to the discretization of the parallel Schwarz method of Lions, applied to our Laplace model problem.*

larger overlap, and it is symmetric if the underlying problem matrix A is symmetric, which then permits the use of the preconditioned CG method. The *restricted additive Schwarz method (RAS)*, which was discovered due to a programming error in [30], is the correct algebraic formulation of the Lions parallel Schwarz method; for a proof, see [69]. It is obtained by modifying the extension matrices $R_j^\top$ in M_{AS}^{-1} to new extension matrices $\widetilde{R}_j^\top$,

$$M_{\text{RAS}}^{-1} = \widetilde{R}_1^\top A_1^{-1} R_1 + \widetilde{R}_2^\top A_2^{-1} R_2,$$

where the structure of the $\widetilde{R}_j$ is like the structure of the R_j, but the values in $\widetilde{R}_j$ constitute a partition of unity, so that they sum to the identity,

$$\sum_j \widetilde{R}_j^\top R_j = I.$$

Unfortunately RAS is a nonsymmetric preconditioner, even for symmetric matrices A, except in the case of minimal overlap, where RAS and additive Schwarz become the same method; see Problem 58.

We show in Figure 4.22 the initial guess and the first few iterates when using RAS for solving our Laplace model problem. We clearly see that this corresponds to a faithful implementation of the parallel Schwarz method: compared with the alternating Schwarz method in Figure 4.20, now both subdomains solve simultaneously and produce a new approximation, which is combined in the overlap using the partition of unity function in the $\widetilde{R}_j$. These results were obtained with the short MATLAB code

```
m=15;                                   % number of gridpoints
A=Laplacian(m,2);                       % five-point Laplacian
f=zeros(m*m,1); f(m:m:end)=1;           % put bc into the rhs
u=A\f;                                  % solve by sparse Gaussian elimination
ai=9; bi=7;                             % alpha=(ai+1)*h, beta=(bi-1)*h
R1=[speye(m*ai) sparse(m*ai,m*(m-ai))]; % construct restriction matrices
```

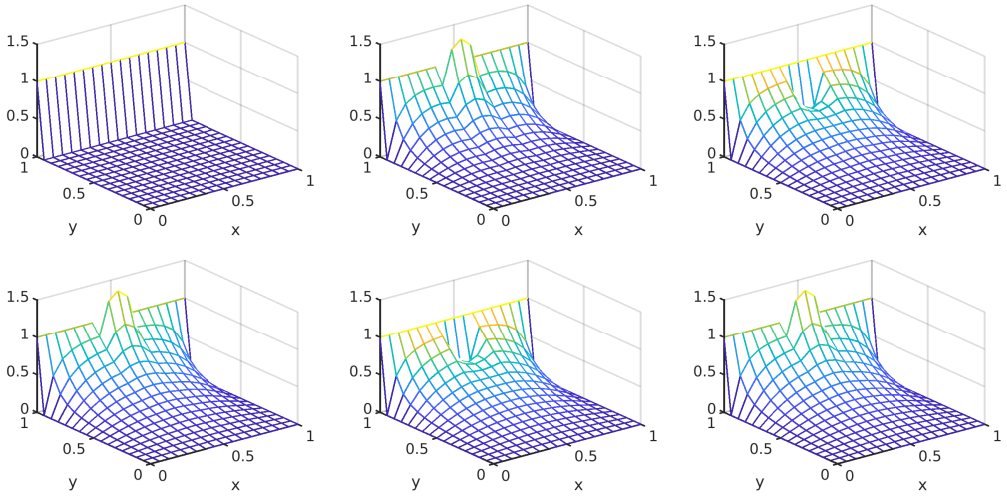

Figure 4.23. *Initial guess and first iterations of the additive Schwarz method applied as stationary iteration to our Laplace model problem.*

```
R2=[sparse(m*(m-bi+1),m*(bi-1)) speye(m*(m-bi+1))];
mi=floor((ai+bi)/2);
R1t=R1;R1t(m*mi+1:end,:)=0;              % up to the middle included
R2t=R2;R2t(1:(mi-bi+1)*m,:)=0;
A1=R1*A*R1';                             % construct subdomain matrices
A2=R2*A*R2';
h=1/(m+1); x=0:h:1; y=x;                 % mesh point vectors
udd=zeros(size(f));                      % initial guess
U=zeros(m+2); U(end,1:m+2)=1;            % for plotting
for n=0:10
  err(n+1)=max(max(abs(u-udd)));         % compute error
  U(2:m+1,2:m+1)=reshape(udd,m,m);
  mesh(x,y,U)
  xlabel('x');ylabel('y');
  pause
  udd=udd+R1t'*(A1\(R1*(f-A*udd)))+R2t'*(A2\(R2*(f-A*udd)));
end
```

If we replace the $\widetilde{R}_j$ by R_j in the sum in the last line of the loop to obtain the additive Schwarz method, we get the results shown in Figure 4.23. We clearly see that the method does not converge in the overlap and can thus not be used as a stationary iterative solver, except when a suitable damping parameter is employed. When additive Schwarz is used as a preconditioner for a Krylov method, however, the Krylov method takes care of the convergence problem. This corresponds in the classical abstract Schwarz theory to the number of colors appearing, which describes how many subdomains contain the same physical point; see, for example, [175].

Optimized Schwarz methods

The classical alternating and parallel Schwarz methods discussed so far have two major drawbacks. On the one hand, the necessary overlap increases the computational effort needed for the solution of each subproblem, because it makes the subproblems bigger. On the other hand, the

convergence of these methods deteriorates rapidly when the size of the overlap becomes small, and in the extreme case of nonoverlapping subdomains, the convergence to the correct limit is lost: the method simply stagnates with the initial guess at the interface if there is no overlap.

For these reasons, Lions introduced in [129] a new domain decomposition method, by replacing the Dirichlet transmission conditions on the interfaces by Robin transmission conditions, namely

$$\begin{aligned} -\Delta u_1^n &= f && \text{in } \Omega_1, \\ \partial_{n_1} u_1^n + p_1 u_1^n &= \partial_{n_1} u_2^{n-1} + p_1 u_2^{n-1} && \text{on } \Gamma_1, \\ u_1^n &= g && \text{on } \partial\Omega \cap \partial\Omega_1, \\ -\Delta u_2^n &= f && \text{in } \Omega_2, \\ \partial_{n_2} u_2^n + p_2 u_2^n &= \partial_{n_2} u_1^n + p_2 u_1^n && \text{on } \Gamma_2, \\ u_2^n &= g && \text{on } \partial\Omega \cap \partial\Omega_2, \end{aligned} \tag{4.52}$$

where n_j are the outward normal vectors on the interfaces Γ_j, and the p_j are parameters or even operators that can be used to tune the convergence speed of the method. Lions designed this method as a variant of the Schwarz method without overlap, $\Omega_1 \cap \Omega_2 = \emptyset$ and $\Gamma_1 = \Gamma_2$ (see [129]), but it can naturally also be used with overlap, as suggested by Nataf and Rogier [136], and has a convergence rate for overlapping decompositions that is in general much faster than the convergence rate of the classical Schwarz methods, especially if the parameters p_j are well chosen; see, e.g., [68, 32]. The underlying principle of optimized Schwarz methods has led to a wealth of research and new algorithms; for a historical perspective, see [69], and for an overview of new wave propagation solvers, see [85].

To illustrate how much faster optimized Schwarz methods converge, we consider again the Poisson model problem on the rectangle decomposed into two rectangular subdomains, as shown in Figure 4.16. Then the normal derivatives in the optimized Schwarz method (4.52) become $\partial_{n_1} = \partial_x$ and $\partial_{n_2} = -\partial_x$, and like for the classical Schwarz method (4.30), we study its convergence using Fourier series. The errors $e_j^n := u - u_j^n$ expanded in a Fourier series are of the same form (4.35) as for the classical Schwarz method,

$$e_j^n(x,y) = \sum_{k \in K} \widehat{e}_j^n(x,k) \sin(ky), \tag{4.53}$$

with $K := \{\frac{\pi}{L}, \frac{2\pi}{L}, \frac{3\pi}{L}, \ldots\}$ as before, and also the subdomain solutions for the Fourier coefficients are of the same form,

$$\begin{aligned} \widehat{e}_1^n(x,k) &= 2A_1^n(k)\sinh(kx), \\ \widehat{e}_2^n(x,k) &= -2A_2^n(k)e^k \sinh(k(1-x)). \end{aligned} \tag{4.54}$$

Using the *transmission conditions* in (4.52) for the errors, we get for the Fourier coefficients of the error using that $\partial_{n_1} = \partial_x$ and $\partial_{n_2} = -\partial_x$ the relations

$$\begin{aligned} &(\partial_x + p_1)\widehat{e}_1^n(\alpha,k) = 2A_1^n(k\cosh(k\alpha) + p_1\sinh(k\alpha)) \\ &= (\partial_x + p_1)\widehat{e}_2^{n-1}(\alpha,k) = -2A_2^{n-1}e^k(-k\cosh(k(1-\alpha)) + p_1\sinh(k(1-\alpha))) \end{aligned} \tag{4.55}$$

and

$$\begin{aligned} &(-\partial_x + p_2)\widehat{e}_2^n(\beta,k) = -2A_2^n e^k(k\cosh(k(1-\beta)) + p_2\sinh(k(1-\beta))) \\ &= (-\partial_x + p_2)\widehat{e}_1^n(\beta,k) = 2A_1^n e^k(-k\cosh(k\beta) + p_2\sinh(k\beta))). \end{aligned} \tag{4.56}$$

Introducing the second relation at iteration index $n-1$ into the first one, we find

$$A_1^n = \widehat{\rho}_{OSM}(\alpha,\beta,k,p_1,p_2)A_1^{n-1}$$

with the convergence factor of the optimized Schwarz method given by

$$\begin{aligned}&\widehat{\rho}_{OSM}(\alpha,\beta,k,p_1,p_2)\\&=\frac{-k\cosh(k(1-\alpha))+p_1\sinh(k(1-\alpha))}{k\cosh(k\alpha)+p_1\sinh(k\alpha)}\frac{-k\cosh(k\beta)+p_2\sinh(k\beta)}{k\cosh(k(1-\beta))+p_2\sinh(k(1-\beta))},\end{aligned}\tag{4.57}$$

and the same relation also holds for A_2^n. We see from this convergence factor that if the parameters p_1 and p_2 are large, we recover in the limit the convergence factor $\widehat{\rho}_s(\alpha,\beta,k)$ of the classical Schwarz method in (4.40), which is natural since the Robin transmission conditions in this case tend to the Dirichlet transmission conditions of the classical Schwarz method. We also see, however, that if we choose

$$\begin{aligned}p_1=p_1(k)&=\frac{k\cosh(k(1-\alpha))}{\sinh(k(1-\alpha))}=k\coth(k\alpha),\\p_2=p_2(k)&=\frac{k\cosh(k\beta)}{\sinh(k\beta))}=k\coth(k\beta),\end{aligned}\tag{4.58}$$

then the convergence factor vanishes identically, $\widehat{\rho}_{OSM}(\alpha,\beta,k)\equiv 0$, and we obtain a direct solver for the kth error component, with convergence achieved in two iterations![40] In order to obtain the best performance, we want to make the contraction factor as small as possible for all the Fourier frequencies we are solving for, i.e., we should solve the *min-max problem*

$$\min_{p_1,p_2\in\mathbb{R}}\max_{k_{\min}\le k\le k_{\max}}|\widehat{\rho}_{OSM}(\alpha,\beta,k,p_1,p_2)|.\tag{4.59}$$

Here $k_{\min}=\frac{\pi}{L}$ and $k_{\max}$ depends on how many Fourier modes we are computing with. If the optimized Schwarz method is discretized on a grid with m gridpoints in the y direction of the interfaces, the mesh size h of a regular grid would be $h=\frac{L}{m+1}$, and we would have $m=\frac{L}{h}-1$ discrete Fourier modes, which leads to

$$k_{\max}=\frac{m\pi}{L}=\left(\frac{L}{h}-1\right)\frac{\pi}{L}\sim\frac{\pi}{h}\tag{4.60}$$

when the mesh size h becomes small. The min-max problem (4.59) can be easily solved numerically using the following MATLAB statements:

```
k=(1:15)*pi;                        % frequencies to be treated
alpha=0.625; beta=0.375;            % overlap parameters
rhoOSM2=@(p) (-k.*cosh(k*(1-alpha))+p(1)*sinh(k*(1-alpha)))...
  ./(k.*cosh(k*alpha)+p(1)*sinh(k*alpha))...
  .*(-k.*cosh(k*beta)+p(2)*sinh(k*beta))...
  ./(k.*cosh(k*(1-beta))+p(2)*sinh(k*(1-beta)));
rhoOSM=@(p) rhoOSM2([p p]);         % when using only one parameter
R2=@(p) max(abs(rhoOSM2(p)));       % functions giving the maximum
R=@(p) max(abs(rhoOSM(p)));         % to use in the minimization
[p2opt,R2opt]=fminsearch(R2,[1 2]) % minimize with p1 and p2
[popt,Ropt]=fminsearch(R,1)         % minimize with p1=p2=p
rhoS=sinh(k*beta)./sinh(k*(1-beta)).*sinh(k*(1-alpha))...
  ./sinh(k*alpha);                  % classical Schwarz
plot(k,rhoS,'-o',k,rhoOSM(popt),'-+',k,rhoOSM2(p2opt),'-*');
xlabel('k');
legend('Classical Schwarz','Optimized Schwarz','Optimized Schwarz 2p');
```

[40] In the parallel Schwarz variant of Lions, we need two iterations; in the alternating one the second subdomain converges already in the first iteration (see Problem 63).

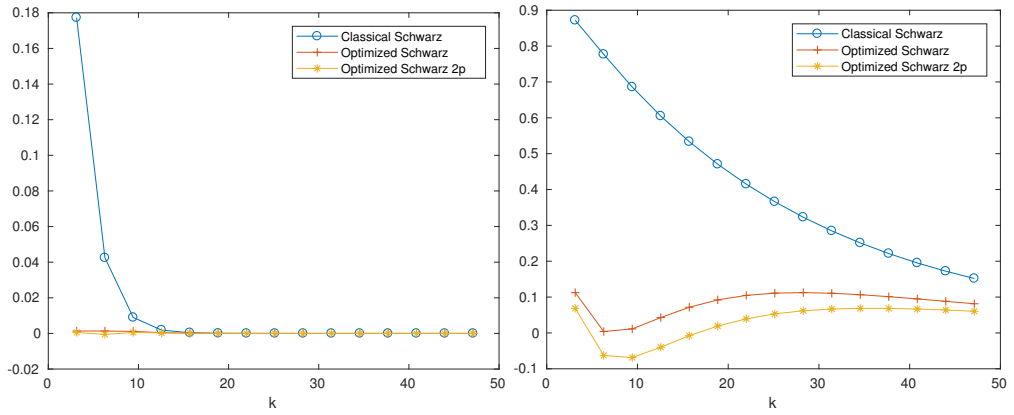

Figure 4.24. *Convergence factors as a function of the frequency parameter k, on the left for a large overlap, and on the right for a small overlap, both for classical and optimized Schwarz methods. Note the different scales in the figures.*

Running the program for the given frequency range `k=(1:15)*pi`, MATLAB finds the best choice is $p_1^* = 3.8679$ and $p_2^* = 7.0775$, with a convergence factor bounded by $5.3847e-04$. If one uses only one parameter, MATLAB finds $p^* = 4.4760$, with a convergence factor bounded by 0.0014. Compared to the classical Schwarz method, which already has quite a good convergence factor of 0.1773, the optimized Schwarz method with two parameters is about five times faster, since $0.1773^5 = 1.7520e-04$. The convergence factors for the three methods is shown in Figure 4.24 on the left for each Fourier mode.

If we make the overlap much smaller, say, $\alpha = 0.51$ and $\beta = 0.49$, we get $p_1^* = 4.3786$ and $p_2^* = 16.5309$, with a convergence factor bounded by 0.0686, and with one parameter $p^* = 7.2842$, with a convergence factor bounded by 0.1125. The classical Schwarz method has in this overlap a convergence factor of 0.8719, which makes it about 20 times slower than the optimized Schwarz method with two parameters. So when the overlap becomes small, which is the case in practice where the overlap is only a few mesh sizes wide, the gap between the performance of the classical Schwarz method and the optimized Schwarz method widens.

To implement the optimized Schwarz method is not more difficult than to implement the classical Schwarz method—it suffices to make only a small change in the RAS implementation replacing the subdomain matrices to become matrices with Robin transmission conditions; see Problem 65 and also [58, 69]. This leads to the so-called *optimized restricted additive Schwarz method (ORAS)*,

```
m=15;                              % number of gridpoints
A=Laplacian(m,2);                  % five-point Laplacian
f=zeros(m*m,1); f(m:m:end)=1;      % put bc into the rhs
u=A\f;                             % solve by sparse Gaussian elimination
ai=10; bi=6;                       % alpha=ai*h, beta=bi*h, 2h less than RAS!
R1=[speye(m*ai) sparse(m*ai,m*(m-ai))];
R2=[sparse(m*(m-bi+1),m*(bi-1)) speye(m*(m-bi+1))];
mi=floor((ai+bi)/2);
R1t=R1;R1t(m*mi+1:end,:)=0;        % up to the middle included
R2t=R2;R2t(1:(mi-bi+1)*m,:)=0;
p1=4.4760; p2=p1;                  % put optimized values
% p1=7.0775; p2=3.8679;              % two-sided optimized values
A1=R1*A*R1';
```

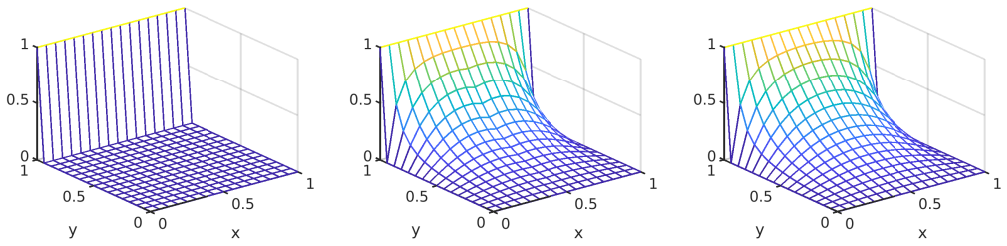

Figure 4.25. *Initial guess and first two iterations of the optimized restricted additive Schwarz method, which is equivalent to the discretization of the optimized parallel Schwarz method, applied to our Laplace model problem.*

```
A2=R2*A*R2';                        % change to Robin transmission conditions
h=1/(m+1);                          % mesh size scaling needed
A1(end-m+1:end,end-m+1:end)=0.5*A1(end-m+1:end,end-m+1:end)+p1*h*speye(m);
A2(1:m,1:m)=0.5*A2(1:m,1:m)+p2*h*speye(m);
x=0:h:1; y=x;                       % mesh point vectors
udd=zeros(size(f));                 % initial guess
U=zeros(m+2); U(end,1:m+2)=1;       % for plotting
for n=0:10
  err(n+1)=max(max(abs(u-udd))); % compute error
  U(2:m+1,2:m+1)=reshape(udd,m,m);
  mesh(x,x,U)
  xlabel('x');ylabel('y');
  pause
  udd=udd+R1t'*(A1\(R1*(f-A*udd)))+R2t'*(A2\(R2*(f-A*udd)));
end
```

Running this code leads to the iterates shown in Figure 4.25. In contrast to the classical Schwarz case, we show only the first two iterates; since the following ones look identical, the method has visually converged already after two iterations! To see the important improvement in convergence more clearly, we show in Figure 4.26 the error reduction over the iterations for RAS and ORAS. We clearly see that ORAS converges much faster than RAS, but why is there a third convergence curve in Figure 4.26 labeled ORASa? This is because of an important difference when one uses the ORAS formulation to implement optimized Schwarz methods compared to RAS: as indicated in the program line defining the interfaces, these lie now exactly on the corresponding gridpoints, not one outside, like in the Dirichlet case, since the Robin matrices also compute the solution along the interfaces. So to have the same *geometric overlap* in the ORAS implementation compared to RAS, one has to include one more grid line on each side. The additional convergence curve in Figure 4.26 corresponds to running the optimized Schwarz method with the same *algebraic overlap* as RAS, `ai=9` and `bi=7`, which means less geometric overlap for ORAS, namely $\alpha = 0.5625$, $\beta = 0.4375$, for which the optimized parameter becomes $p^* = 4.8185$. We see that convergence is still much faster than for classical RAS, so it is always worthwhile to use ORAS. An important consequence of this is that it does not make sense to run the ORAS code without algebraic overlap (just try it), i.e., `bi=ai+1`, since the geometric overlap would then be $-h$! But the ORAS implementation also cannot be used to run a nonoverlapping optimized Schwarz method, i.e., with `bi=ai`. A minimum overlap is needed since the subdomain solutions stored in a truncated way by the $\widetilde{R}_j$ operators in the global vector of unknowns must still retain enough information also to compute the normal derivative; see [170, Assumption 1] for the precise condition, and also Problem 64.

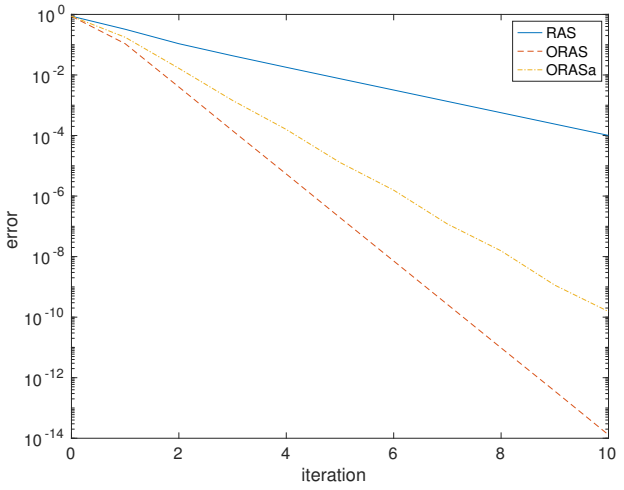

Figure 4.26. *Error reduction as a function of the iteration index n comparing the classical parallel Schwarz method (RAS) and the optimized Schwarz method (ORAS) for our Laplace model problem, corresponding to the iterates shown in Figures 4.22 and 4.25, respectively.*

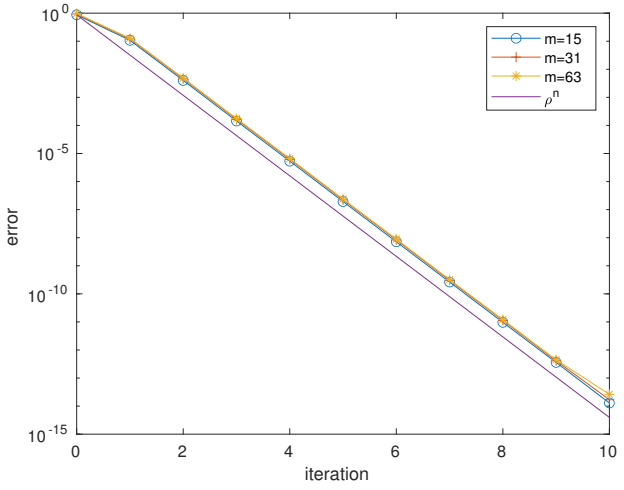

Figure 4.27. *Convergence of the optimized Schwarz method for different mesh sizes $h = \frac{1}{m+1}$. For comparison also the theoretical convergence estimate* (4.57) *based on the continuous analysis is shown for the optimized $p^* = 4.4760$ solving the min-max problem* (4.59)*.*

To illustrate how also the optimized Schwarz method converges independently of the mesh size when the overlap is held constant, independently of the mesh size, we show in Figure 4.27 how the error decays in the discretized optimized Schwarz iteration for the mesh we used in Figure 4.25 with $m = 15$ and $\alpha = 0.625$ and $\beta = 0.375$, and also on two refined meshes with $m = 31$ and $m = 63$ interior mesh points, keeping the interfaces fixed at $\alpha = 0.625$ and $\beta = 0.375$. We see that convergence is independent of the mesh parameter h and very well predicted by the continuous analysis for the optimized parameter p^*.[41]

[41] Convergence flattens out at the roundoff error level for all mesh sizes.

To get a better theoretical understanding of the min-max problem that needs to be solved in optimized Schwarz methods to get this substantially faster convergence, it is convenient to introduce a simplification in our analysis, which is common in the analysis of optimized Schwarz methods, namely to make the subdomain sizes infinitely large on each side. This simplifies the formulas but retains the mathematical essence of the problem for diffusive PDEs.[42] We thus consider now the two subdomains $\Omega_1 = (-\infty, \alpha) \times (0,1)$ and $\Omega_2 = (\beta, \infty) \times (0,1)$. Then the Fourier coefficients of the errors are not given by hyperbolic sines from (4.54) any more, but just exponential functions, namely

$$\begin{aligned} \widehat{e}_1^n(x,k) &= A_1^n(k) e^{kx}, \\ \widehat{e}_2^n(x,k) &= A_2^n(k) e^{-kx}, \end{aligned} \tag{4.61}$$

since they satisfy the error differential equation as well, and now as boundary conditions on the outer boundaries of the subdomains at $-\infty$ and ∞ that the errors must remain bounded there. Using the transmission conditions in (4.52) for these Fourier error coefficients, we get

$$\begin{aligned} &(\partial_x + p_1)\widehat{e}_1^n(\alpha,k) = A_1^n(k+p_1)e^{k\alpha} \\ &= (\partial_x + p_1)\widehat{e}_2^{n-1}(\alpha,k) = A_2^{n-1}(-k+p_1)e^{-k\alpha} \end{aligned} \tag{4.62}$$

and

$$\begin{aligned} &(-\partial_x + p_2)\widehat{e}_2^n(\beta,k) = A_2^n e^k (k+p_2)e^{k\beta} \\ &= (-\partial_x + p_2)\widehat{e}_1^n(\beta,k) = A_1^n e^k(-k+p_2)e^{-k\beta}. \end{aligned} \tag{4.63}$$

Introducing again the second relation at iteration index $n-1$ into the first one, we find

$$A_1^n = \widehat{\rho}_{OSMs}(\alpha,\beta,k,p_1,p_2)A_1^{n-1},$$

with the simplified convergence factor of the optimized Schwarz method given by

$$\widehat{\rho}_{OSMs}(\alpha,\beta,k,p_1,p_2) = \frac{k-p_1}{k+p_1}\frac{k-p_2}{k+p_2}e^{-2k(\alpha-\beta)}, \tag{4.64}$$

and the same relation also holds for A_2^n. If we let p_1 and p_2 go to infinity, we also recover the simplified convergence factor for the classical Schwarz method, namely

$$\widehat{\rho}_s(\alpha,\beta,k) = e^{-2k(\alpha-\beta)}, \tag{4.65}$$

which now explicitly shows the typical exponential decay, depending on the size of the overlap $\delta := \alpha - \beta$, and the Fourier frequency k. We also see that the Robin transmission conditions add an extra factor in front of the classical Schwarz convergence factor, and this factor is smaller than one, provided that $p_1, p_2 > 0$, so the optimized Schwarz method converges even without overlap.

We show now how one can analyze such *min-max problems* in optimized Schwarz methods, for the specific simplified case and one parameter, i.e., $p_1 = p_2 = p$, which leads to the min-max problem

$$\min_{p\in\mathbb{R}} \max_{k_{\min}\le k\le k_{\max}} \left(\frac{k-p}{k+p}\right)^2 e^{-2k\delta}. \tag{4.66}$$

There are three classical steps for solving such min-max problems (see, e.g., [68]). First one finds the range for p in which the solution p^* must lie. Then one identifies the local maxima in

[42] This is not the case for wave propagation type problems, like the Helmholtz equation, where such a modification has an important influence on the min-max problem due to reflections from the boundaries.

k of the convergence factor, and finally one solves the min-max problem using this information. This leads to the following two lemmas and the final convergence theorem.

Lemma 4.8 (Range of p). *If p^* is solution of the min-max problem* (4.66)*, then $p^* \in (k_{\min}, k_{\max})$.*

Proof. First we notice that p^* cannot be negative, since if it were, changing the sign of p^* would make the convergence factor even smaller due to the fraction in the first factor and the fact that $k \geq 0$. Next we compute the partial derivative of $\rho(\delta, k, p) := \left(\frac{k-p}{k+p}\right)^2 e^{-2k\delta}$ with respect to p to find

$$\partial_p \rho(\delta, k, p) = \frac{4(p-k)k}{(p+k)^3} e^{-2k\delta}.$$

Hence, if $p < k_{\min}$, then $\partial_p \rho(\delta, k, p) < 0$, and thus increasing p decreases the convergence factor for all $k \in (k_{\min}, k_{\max})$. Similarly, if $p > k_{\max}$, then $\partial_p \rho(\delta, k, p) > 0$, and thus decreasing p decreases the convergence factor for all $k \in (k_{\min}, k_{\max})$. The optimum p^* must therefore lie in $(k_{\min}, k_{\max})$. ∎

Lemma 4.9 (Local maxima of ρ). *For $p \in (k_{\min}, k_{\max})$, the convergence factor has two local maxima $k_{1,2} \in [k_{\min}, k_{\max}]$: one at $k_1 = k_{\min}$, and the second one at*

$$k_1 = \begin{cases} k_{\max} & \text{if } \delta = 0 \text{ or } k_{\max} < \bar{k} := \sqrt{p^2 + 2p/\delta}, \\ \bar{k} & \text{otherwise}. \end{cases} \tag{4.67}$$

Proof. If the overlap $\delta = 0$, the function $\rho(\delta, k, p)$ is convex in k and thus can only have maxima at the endpoints $k_{\min}$ and $k_{\max}$, since it is nonnegative. If the overlap $\delta > 0$, computing the derivative of $\rho(\delta, k, p)$ with respect to k gives

$$\partial_k \rho(\delta, k, p) = \frac{2(k-p)(\delta p^2 + 2p - \delta k^2) e^{-2*k\delta}}{(k+p)^3}.$$

Therefore $\rho(\delta, k, p)$ has a minimum point at $k = p$ where its value is $\rho(\delta, p, p) = 0$, and one positive maximum point $\bar{k} = \sqrt{p^2 + 2p/\delta}$ (the other one with the minus sign is outside the range of interest $(k_{\min}, k_{\max})$). This maximum $\bar{k}$ is of interest only in the min-max problem if it lies inside $(k_{\min}, k_{\max})$, and by monotonicity otherwise the boundary point $k_{\max}$ is a local maximum. ∎

We can now obtain the best choice of the parameter p in the Robin transmission conditions of the optimized Schwarz method under the simplifying assumption. It is also possible to obtain this result on the bounded domain, but it is technically more involved.

Theorem 4.10 (Convergence of the optimized Schwarz method). *The solution p^* of the min-max problem* (4.66) *is given by* equioscillation *between the maximum points k_1 and k_2 of Lemma 4.9,*

$$\rho(\delta, k_1, p^*) = \rho(\delta, k_2, p^*). \tag{4.68}$$

Without overlap, $\delta = 0$, we have

$$p^* = \sqrt{k_{\min} k_{\max}}, \tag{4.69}$$

and the associated optimized convergence factor is then bounded by

$$\max_{k_{\min} \leq k \leq k_{\max}} \rho(0, k, p^*) = \left(\frac{\sqrt{\frac{k_{\max}}{k_{\min}}} - 1}{\sqrt{\frac{k_{\max}}{k_{\min}}} + 1} \right)^2 \sim 1 - 4\sqrt{\frac{k_{\min}}{k_{\max}}} \tag{4.70}$$

when $k_{\max}$ is large. For positive overlap $\delta > 0$ small, and when $k_{\max} = \infty$, we have

$$p^* \sim \frac{k_{\min}^{\frac{2}{3}}}{2^{\frac{1}{3}}\delta^{\frac{1}{3}}}, \tag{4.71}$$

and the associated optimized convergence factor is then bounded by

$$\max_{k_{\min}\le k\le k_{\max}} \rho(\delta, k, p^*) \sim 1 - 2^{\frac{7}{3}} k_{\min}^{\frac{1}{3}} \delta^{\frac{1}{3}}. \tag{4.72}$$

Proof. Without overlap, $\delta = 0$, and with $p \in (k_{\min}, k_{\max})$, when we increase p, $\rho(0, k_{\min}, p)$ is increasing and $\rho(0, k_{\max}, p)$ is decreasing, and hence by continuity the solution p^* of (4.66) is attained when (4.68) holds, which leads to the solution p^* in (4.69). The asymptotic result for the convergence factor bound is obtained by expanding the expression in a Taylor series for $k_{\max} = \frac{1}{\varepsilon}$ for ε small. For positive overlap $\delta > 0$, the reasoning for equioscillation is analogous, and the asymptotic result is obtained making the ansatz $p^* \sim C_p \delta^{-\frac{1}{3}}$ and expanding (4.68) for δ small, which shows that the equioscillation equation has indeed a solution for this ansatz. Such computations are best performed in Maple, as we explain below. □

We now show how the asymptotic expansions needed for the proof of Theorem 4.10 can easily be done in Maple:

```
rho:=((k-p)/(k+p))^2*exp(-2*k*d):          # simplified convergence factor
solve(factor(diff(rho,k)),k);              # find local maximum
```

$$p, \frac{\sqrt{dp(dp+2)}}{d}, -\frac{\sqrt{dp(dp+2)}}{d}$$

```
k:=kmin;R1:=rho;k:=kb;R2:=rho;k:='k':       # local maxima
kb:=sqrt(d*p*(d*p+2))/d:
p:=Cp/d^(1/3):                             # ansatz based on numerics
se1:=series(R1,d,2);                       # series for d small
```

$$se1 := 1 - 4\,\frac{kmin\,d^{1/3}}{Cp} + 8\,\frac{kmin^2 d^{2/3}}{Cp^2} + \left(-2\,kmin - 12\,\frac{kmin^3}{Cp^3}\right) d + O\left(d^{4/3}\right)$$

```
se2:=series(R2,d,2);
```

$$se2 := 1 - 4\sqrt{2}\sqrt{Cp}d^{1/3} + O\left(d^{2/3}\right)$$

```
Cpsols:=solve(op(2,se1)=op(2,se2),Cp);     # determine constant Cp
Cp:=simplify(Cpsols[1],symbolic);          # choose real root
```

$$Cp := 1/2\,2^{2/3} kmin^{2/3}$$

```
simplify(p,symbolic);
```

$$1/2\,\frac{2^{2/3} kmin^{2/3}}{\sqrt[3]{d}}$$

We show in Table 4.1 a comparison of the optimal choice of the parameter given by the original min-max problem (4.59) and the simplified min-max problem (4.66) when the overlap

Table 4.1. *Comparison of the numerical solution of the min-max problem* (4.59) *and the asymptotic solution of the simplified min-max problem* (4.66) *from Theorem 4.10, and corresponding convergence factor of the optimized Schwarz method (not of the simplified problem).*

		Original min-max (4.59)		Simplified min-max (4.66)	
α	β	p^*	$\rho_s(p^*)$	p^*	$\rho_s(p^*)$
0.625	0.375	4.4760	0.0014	2.7026	0.0072
0.51	0.49	7.2842	0.1125	6.2721	0.1320
0.501	0.499	14.6107	0.3793	13.5128	0.3937

$\delta = \alpha - \beta$ becomes small. We clearly see that the closed form solution from Theorem 4.10 of the simplified min-max problem gives a very good approximation of the best parameter p^* of the original min-max problem, especially when the overlap is becoming small, and the algorithm will perform almost as well as with the numerically optimized parameter. This is the case for many PDEs, and closed form formulas are available in the literature. See [68] for Laplace type problems, [73, 14, 13] for advection reaction diffusion problems, [81, 74] for Helmholtz equations, [75, 72] for the wave equation, and [56, 153, 59] for Maxwell's equations; research is ongoing for further models, especially time harmonic wave propagation [85], and also in the heterogeneous case where different models are used in different subdomains [83]. For further information, it is best to search for optimized Schwarz methods with the corresponding name of the PDE, for example in the proceedings of the international conference series on domain decomposition methods available at www.ddm.org.

All Schwarz methods can be generalized to the case of many subdomains, and their implementation does not present any significant difficulties; see, for example, Problem 66. When the number of subdomains becomes larger, convergence slows down in certain situations, and one needs a coarse correction to fix this, which is well understood in the domain decomposition literature, but goes beyond the introduction to domain decomposition methods here.

4.7 ▪ Dirichlet–Neumann domain decomposition method

> *It is also interesting to note that if a symmetric region is cut in half, and treated fully symmetrically, then $S = 2S^{(1)}$ and the conjugate gradient iteration converges in one step.*
>
> Petter E. Bjørstad and Olof B. Widlund, *Iterative Methods for the Solution of Elliptic Problems on Regions Partitioned into Substructures*, 1986.

The *Dirichlet–Neumann method* is a *nonoverlapping domain decomposition method* going back to the seminal work by Bjorstad and Widlund in 1986 (see [18] and the quote above) and belongs to the class of iterative substructuring methods; for a historical review, see [82]. It uses a different convergence mechanism than the alternating Schwarz method, which used overlap in its classical form, and a combination of overlap and transmission conditions in the optimized form. As its name suggests, it uses on one side of the interface between subdomains a Dirichlet transmission condition, and on the other side a Neumann condition. For the simple two-subdomain configuration indicated in Figure 4.28, the Dirichlet–Neumann algorithm[43] starts with an initial guess λ^0 along the interface Γ, and then computes for our Poisson model problem first a Dirichlet

[43]The Dirichlet–Neumann algorithm was originally introduced directly as a preconditioner for the CG method, but we describe the method here as a stationary iteration like the alternating Schwarz method.

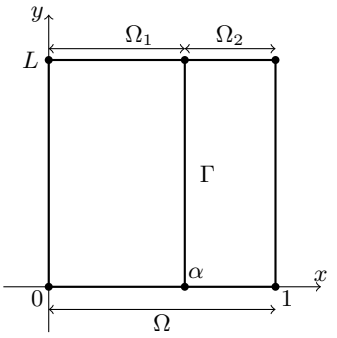

Figure 4.28. *Decomposition of the domain* $\Omega = (0,1) \times (0,L)$ *into* $\overline{\Omega} = \overline{\Omega}_1 \cup \overline{\Omega}_2$*, where* $\Omega_1 := (0,\alpha) \times (0,L)$ *and* $\Omega_2 := (\alpha,1) \times (0,L)$*. The interface is denoted by* Γ*.*

solution on subdomain Ω_1,

$$\begin{array}{rl} -\Delta u_1^n = f & \text{in } \Omega_1, \\ u_1^n = \lambda^{n-1} & \text{on } \Gamma, \\ u_1^n = g & \text{on } \partial\Omega \cap \partial\Omega_1, \end{array} \tag{4.73}$$

followed by computing a Neumann solution on subdomain Ω_2 using as Neumann data the approximation just computed on the subdomain Ω_1,

$$\begin{array}{rl} -\Delta u_2^n = f & \text{in } \Omega_2, \\ \partial_{n_2} u_2^n = \partial_{n_2} u_1^n & \text{on } \Gamma, \\ u_2^n = g & \text{on } \partial\Omega \cap \partial\Omega_2. \end{array} \tag{4.74}$$

Again ∂_{n_2} denotes the unit outer normal derivative of subdomain Ω_2 along the interface Γ, and in our example, we could simply write $\partial_{n_2} = -\partial_x$. The minus sign, however, has no importance since it appears on both sides and can thus be canceled. Finally in the Dirichlet–Neumann algorithm, the interface approximation λ^n is updated using a *relaxation parameter* θ,

$$\lambda^n = \theta\lambda^{n-1} + (1-\theta)u_2^n \quad \text{on } \Gamma. \tag{4.75}$$

In order to understand the convergence properties of the Dirichlet–Neumann method, we proceed like in our analysis of the Schwarz methods: we introduce the equations satisfied by the errors $e_j^n := u - u_j^n$, $d^n := \lambda - \lambda^n$, where $\lambda := u|_\Gamma$, namely

$$\begin{array}{rl} -\Delta e_1^n = 0 & \text{in } \Omega_1, \\ e_1^n = d^{n-1} & \text{on } \Gamma, \\ e_1^n = 0 & \text{on } \partial\Omega \cap \partial\Omega_1, \end{array} \tag{4.76}$$

followed by

$$\begin{array}{rl} -\Delta e_2^n = 0 & \text{in } \Omega_2, \\ \partial_{n_2} e_2^n = \partial_{n_2} e_1^n & \text{on } \Gamma, \\ e_2^n = 0 & \text{on } \partial\Omega \cap \partial\Omega_2, \end{array} \tag{4.77}$$

and with the final update

$$d^n = \theta d^{n-1} + (1-\theta)e_2^n \quad \text{on } \Gamma. \tag{4.78}$$

Using a Fourier sine expansion like in the analysis of the Schwarz method (4.35),

$$e_j^n(x,y) = \sum_{k\in K} \widehat{e}_j^n(x,k)\sin(ky), \tag{4.79}$$

with $K := \{\frac{\pi}{L}, \frac{2\pi}{L}, \frac{3\pi}{L}, \ldots\}$, we find that the Fourier coefficients are of the same form (4.37) as for the Schwarz method,

$$\widehat{e}_1^n(x,k) = 2A_1^n(k)\sinh(kx),$$
$$\widehat{e}_2^n(x,k) = -2A_2^n(k)e^k\sinh(k(1-x)).$$

The Dirichlet transmission condition on subdomain Ω_1 then implies

$$\widehat{e}_1^n(\alpha,k) = \widehat{d}^{n-1}(k) = 2A_1^n(k)\sinh(k\alpha),$$

which gives for the constant

$$A_1^n(k) = \frac{\widehat{d}^{n-1}(k)}{2\sinh(k\alpha)}, \tag{4.80}$$

and hence for the error on Ω_1

$$\widehat{e}_1^n(x,k) = \frac{\sinh(kx)}{\sinh(k\alpha)}\widehat{d}^{n-1}(k). \tag{4.81}$$

Now using the Neumann transmission condition on subdomain Ω_2, we obtain

$$\partial_x\widehat{e}_2^n(x,k)|_{x=\alpha} = 2A_2^n(k)e^k\cosh(k(1-\alpha))k = \partial_x\widehat{e}_1^n(x,k)|_{x=\alpha} = 2A_1^n(k)\cosh(k\alpha)k,$$

which gives for the constant

$$A_2^n(k) = \frac{\cosh(k\alpha)e^{-k}}{\cosh(k(1-\alpha))}A_1^n(k),$$

and inserting (4.80) on the right, we find

$$A_1^n(k) = \frac{1}{2}\frac{\cosh(k\alpha)}{\cosh(k(1-\alpha))}\frac{e^{-k}}{\sinh(k\alpha)}\widehat{d}^{n-1}(k),$$

which finally leads to the error in subdomain Ω_2,

$$\widehat{e}_2^n(x,k) = -\frac{\cosh(k\alpha)}{\cosh(k(1-\alpha))}\frac{\sinh(k(1-x))}{\sinh(k\alpha)}\widehat{d}^{n-1}(k). \tag{4.82}$$

We can now trace this error on the interface Γ and introduce it into the update condition for $\widehat{d}^n$ in (4.78),

$$\widehat{d}^n(k) = \left(\theta - (1-\theta)\frac{\tanh(k(1-\alpha))}{\tanh(k\alpha)}\right)\widehat{d}^{n-1}(k) \quad \text{on } \Gamma.$$

Therefore, the *convergence factor of the Dirichlet–Neumann method* is

$$\widehat{\rho}_{DN}(\alpha,k,\theta) = \left(\theta - (1-\theta)\frac{\tanh(k(1-\alpha))}{\tanh(k\alpha)}\right), \tag{4.83}$$

and by induction the error on the interface satisfies

$$\widehat{d}^n(k) = \left(\widehat{\rho}_{DN}(\alpha,k,\theta)\right)^n\widehat{d}^0(k).$$

In order to understand the convergence behavior of the Dirichlet–Neumann method, we need to study $\widehat{\rho}_{DN}(\alpha,k,\theta)$, for which the following two lemmas are useful.

Lemma 4.11 (Properties of F_{DN}). *For $\alpha \in (0,1)$ and $k > 0$ the function*

$$F_{DN}(\alpha,k) = \frac{\tanh(k(1-\alpha))}{\tanh(k\alpha)} \tag{4.84}$$

has the following properties:

1. $\lim_{k\to\infty} F_{DN}(\alpha,k) = 1$;
2. *for* $\alpha = \frac{1}{2}$, $F_{DN}(\frac{1}{2},k) \equiv 1$;
3. *for* $\alpha > \frac{1}{2}$, $F_{DN}(\alpha,k)$ *is growing in* k, *and* $F_{DN}(\alpha,k) < 1$;
4. *for* $\alpha < \frac{1}{2}$, $F_{DN}(\alpha,k)$ *is decreasing in* k, *and* $F_{DN}(\alpha,k) > 1$.

Proof.

1. We compute directly

$$\lim_{k\to\infty} F_{DN}(\alpha,k) = \lim_{k\to\infty} \frac{e^{k(1-\alpha)} - e^{-k(1-\alpha)}}{e^{k(1-\alpha)} + e^{-k(1-\alpha)}} \frac{e^{k\alpha} + e^{-k\alpha}}{e^{k\alpha} - e^{-k\alpha}}$$
$$= \lim_{k\to\infty} \frac{1 - e^{-2k(1-\alpha)}}{1 + e^{-2k(1-\alpha)}} \frac{1 + e^{-2k\alpha}}{1 - e^{-2k\alpha}} = 1.$$

2. We simply insert $\alpha = \frac{1}{2}$, $F_{DN}(\frac{1}{2},k) = \frac{\tanh(k\frac{1}{2})}{\tanh(k\frac{1}{2})} = 1$.

3. Since $\alpha > 1/2$, we have that $1 - \alpha < \alpha$, which implies that $\tanh(\alpha k) > \tanh((1-\alpha)k)$, where we used the strict monotonicity of the hyperbolic tangent function. Hence $\frac{\tanh((1-\alpha)k)}{\tanh(\alpha k)} < 1$. The fact that $F_{DN}(\alpha,k)$ is growing in k follows by inspection; see also the plot in Figure 4.29, obtained with the Maple commands

```
FDN:=tanh(k*(1-alpha))/tanh(k*alpha);
plot3d(FDN,k=Pi..10*Pi,alpha=0..1,axes=boxed);
```

4. This result follows by similar arguments as in 3. □

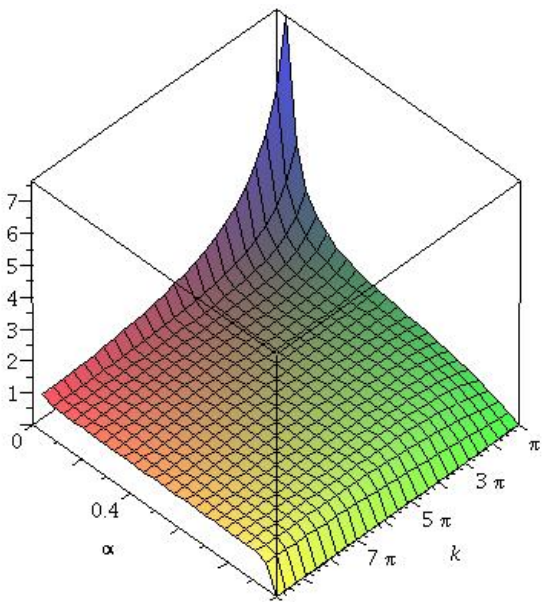

Figure 4.29. *Plot of the function* $F_{DN}(\alpha,k)$ *defined in* (4.84) *from the Dirichlet–Neumann algorithm.*

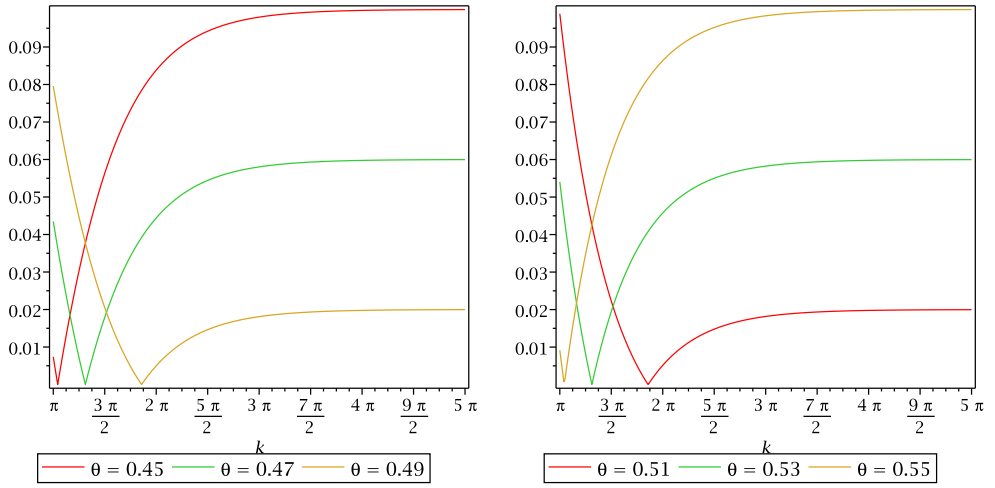

Figure 4.30. *Convergence factor of the Dirichlet–Neumann method in modulus, $|\widehat{\rho}_{DN}(\alpha,k,\theta)|$ for interface position $\alpha = 2/3$ on the left (left subdomain bigger) and $\alpha = 1/3$ on the right (right subdomain bigger).*

In order to get some intuition on how the relaxation parameter θ should be chosen in the Dirichlet–Neumann method, we first look at the plot of the convergence factor in modulus shown in Figure 4.30, which we obtained with the Maple commands

```
rhoDN:=theta-(1-theta)*tanh(k*(-alpha+1))/tanh(k*alpha);
alpha:=2/3;
plot([seq(abs(rhoDN),theta=[0.45,0.47,0.49])],k=Pi..5*Pi,
     axes=boxed,legend=['theta=0.45','theta=0.47','theta=0.49']);
```

We clearly see that there is an optimal choice for the relaxation parameter θ: if the left subdomain is bigger, then if θ is too small, low frequencies k converge faster than high frequencies, and if θ is too large, high frequencies converge faster than low frequencies. If the right subdomain is bigger, it is the opposite. From Lemma 4.11 we also know that if both subdomains have the same size, then the optimal choice is $\theta = \frac{1}{2}$, and the algorithm converges in one iteration, since $\widehat{\rho}_{DN}(\frac{1}{2},k,\frac{1}{2}) \equiv 0$ for all frequencies k, it becomes a direct solver.[44] If the subdomains are of different size, the following lemma gives the optimal choice θ^* of the relaxation parameter.

Lemma 4.12 (Optimal relaxation parameter for Dirichlet–Neumann). *The optimal choice θ^* for the relaxation parameter in the Dirichlet–Neumann method is given by*

$$\theta^* = \frac{F_{DN}(\alpha,k_{\max}) + F_{DN}(\alpha,k_{\min})}{2 + F_{DN}(\alpha,k_{\max}) + F_{DN}(\alpha,k_{\min})} \tag{4.85}$$

with the function $F_{DN}(\alpha,k)$ defined in (4.84)*. The associated convergence factor of the Dirichlet–Neumann method then satisfies*

$$\max_{k_{\min}\le k\le k_{\max}} |\widehat{\rho}_{DN}(\alpha,k,\theta^*)| = \left| \frac{F_{DN}(\alpha,k_{\max}) - F_{DN}(\alpha,k_{\min})}{2 + F_{DN}(\alpha,k_{\max}) + F_{DN}(\alpha,k_{\min})} \right|. \tag{4.86}$$

[44] Note, however, that after one iteration, only the interface trace λ is known, and one has to do a second solve in the subdomains to obtain the correct solution also inside the subdomains.

Proof. If $\alpha > \frac{1}{2}$, then $F_{DN}(\alpha, k)$ is increasing in k according to Lemma 4.11, and hence the maximum of $\widehat{\rho}_{DN}(\alpha, k, \theta) = \theta - (1-\theta)F_{DN}(\alpha, k)$ is attained at $k = k_{\min}$, and the minimum at $k = k_{\max}$, and since $\widehat{\rho}_{DN}(\alpha, k, \theta)$ is a linear function in θ, one can equilibrate the maximum and the minimum to achieve that $\widehat{\rho}_{DN}(\alpha, k, \theta)$ is as close as possible to zero. If $\alpha < \frac{1}{2}$, then $F_{DN}(\alpha, k)$ is decreasing in k according to Lemma 4.11, and thus the maximum of $\widehat{\rho}_{DN}(\alpha, k, \theta)$ is attained at $k = k_{\max}$, and the minimum at $k = k_{\min}$, and one can again equilibrate the maximum and the minimum. Therefore in both cases, the optimal choice θ^* satisfies the *equioscillation* equation

$$\widehat{\rho}_{DN}(\alpha, k_{\min}, \theta^*) = -\widehat{\rho}_{DN}(\alpha, k_{\max}, \theta^*),$$

which is a linear equation for θ^*,

$$\theta^* - (1-\theta^*)F_{DN}(\alpha, k_{\min}) = -(\theta^* - (1-\theta^*)F_{DN}(\alpha, k_{\max}))$$

that leads to the solution given in (4.85). Inserting this choice into $\widehat{\rho}_{DN}(\alpha, k_{\min}, \theta^*)$ (or evaluated at $k_{\max}$ since their modulus is now equal), we get

$$\begin{aligned}
\widehat{\rho}_{DN}(\alpha, k_{\min}, \theta^*) &= \theta^* - (1-\theta^*)F_{DN}(\alpha, k_{\min}) \\
&= \tfrac{F_{DN}(\alpha,k_{\max})+F_{DN}(\alpha,k_{\min})}{2+F_{DN}(\alpha,k_{\max})+F_{DN}(\alpha,k_{\min})} - \left(1 - \tfrac{F_{DN}(\alpha,k_{\max})+F_{DN}(\alpha,k_{\min})}{2+F_{DN}(\alpha,k_{\max})+F_{DN}(\alpha,k_{\min})}\right) F_{DN}(\alpha, k_{\min}) \\
&= \tfrac{F_{DN}(\alpha,k_{\max})-F_{DN}(\alpha,k_{\min})}{2+F_{DN}(\alpha,k_{\max})+F_{DN}(\alpha,k_{\min})},
\end{aligned}$$

which concludes the proof. □

We can now show that with this optimized choice of the relaxation parameter θ, the Dirichlet–Neumann method is convergent.

Theorem 4.13 (Convergence of the Dirichlet–Neumann method). *With the optimized choice of the relaxation parameter*

$$\theta^* = \frac{1 + \tilde{F}_{DN}(\alpha, L)}{3 + \tilde{F}_{DN}(\alpha, L)}, \tag{4.87}$$

where

$$\tilde{F}_{DN}(\alpha, L) := \frac{\tanh(\frac{\pi}{L}(1-\alpha))}{\tanh(\frac{\pi}{L}\alpha)}, \tag{4.88}$$

the Dirichlet–Neumann method (4.73)*,* (4.74)*, and* (4.75) *converges for all initial guesses λ^0 along the interface Γ, and we have the linear convergence estimate*

$$||\lambda - \lambda^n||_2 \leq \rho_{DN}^n ||\lambda - \lambda^0||_2 \tag{4.89}$$

with the convergence factor

$$\rho_{DN} = \left| \frac{1 - \tilde{F}_{DN}(\alpha, L)}{3 + \tilde{F}_{DN}(\alpha, L)} \right| < 1. \tag{4.90}$$

Proof. When $k_{\max}$ goes to infinity, Lemma 4.11 shows that $F_{DN}(\alpha, k_{\max}) \to 1$, and inserting this into (4.86) of Lemma 4.12, we obtain

$$\max_{k_{\min} \leq k \leq \infty} |\widehat{\rho}_{DN}(\alpha, k, \theta^*)| = \left| \frac{1 - F_{DN}(\alpha, \frac{\pi}{L})}{3 + F_{DN}(\alpha, \frac{\pi}{L})} \right|,$$

where we also used that $k_{\min} = \frac{\pi}{L}$. Since $F_{DN}(\alpha, \frac{\pi}{L})$ is positive, this quantity is clearly less than 1, and we can then use the Parseval–Plancherel identity to obtain the L^2-error estimate (4.89). □

We show in Figure 4.31 how the convergence factor $\rho_{DN}(\alpha, L)$ of the Dirichlet–Neumann method from Theorem 4.89 depends on the interface position α and the domain height L. We see that convergence is better for small L than for large L like for the Schwarz methods, and the lateral boundary conditions help convergence. We also see that a small Dirichlet subdomain is worse than a small Neumann subdomain, and comparable size is best for convergence, in contrast to the Schwarz method, which converges better when one subdomain is small compared to the other; see the right plot in Figure 4.18. The convergence result in Theorem 4.89 shows that if the two subdomains are equal, $\alpha = \frac{1}{2}$, the Dirichlet–Neumann method is a direct solver, since $\tilde{F}_{DN}(\frac{1}{2}, L) = 1$, which implies $\theta^* = \frac{1}{2}$ as we have seen earlier, and $\rho_{DN} = 0$, which is clearly visible in Figure 4.31. Note in addition that for the choice $\theta = \frac{1}{2}$, we have

$$\lim_{k\to\infty} \widehat{\rho}_{DN}(\alpha, k, \frac{1}{2}) = \frac{1}{2} - \frac{1}{2} F_{DN}(\alpha, k) = 0$$

because of Lemma 4.11, and thus for high frequencies, the Dirichlet–Neumann method always converges very fast for the choice of relaxation parameter $\theta = \frac{1}{2}$, independently of the interface position α. This is because the damping nature of the Poisson equation does not allow high frequencies to propagate very far, and so they cannot see that the subdomain decomposition is not symmetric. This is the fundamental reason why the Dirichlet–Neumann method converges robustly for all frequencies, even when $k_{\max}$ becomes large, and thus Dirichlet–Neumann converges independently of the mesh size h, which gives $k_{\max} \sim \frac{\pi}{h}$ as we have seen in (4.60). This is also the case for Schwarz methods, if the overlap size does not depend on the mesh size, as we have seen in Figure 4.21, but in practice often the overlap is proportional to the mesh size, since it is only a few mesh cells wide.

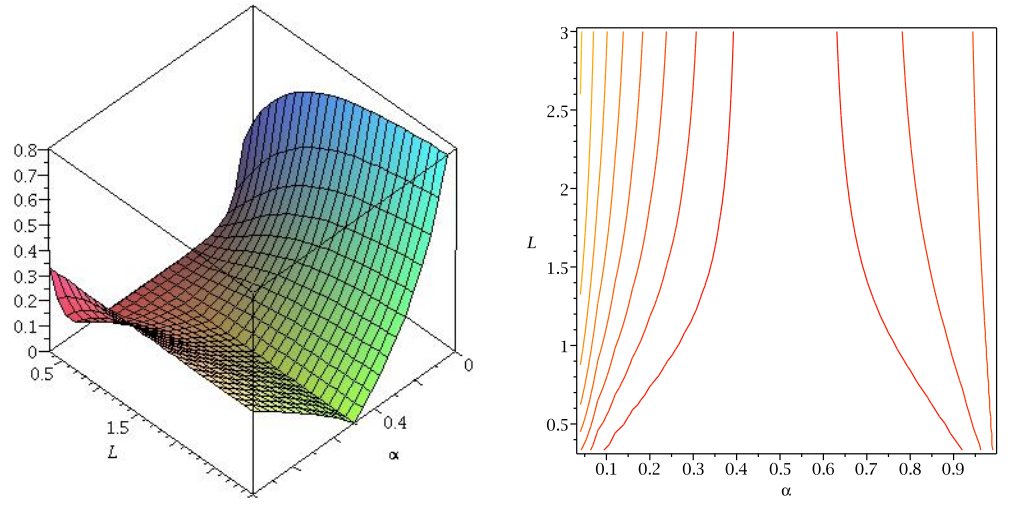

Figure 4.31. *Dependence of the convergence factor $\rho_{DN}(\alpha, L)$ of the Dirichlet–Neumann method from Theorem 4.89 as a function of the interface position α, and the domain height L, with a three-dimensional plot on the left, and the corresponding contour plot on the right, with the level sets corresponding to $\{0, 0.1, \ldots, 1\}$.*

The Dirichlet–Neumann method can also be discretized to be used as a numerical solver. It is convenient for this to first implement a subdomain solver with general Robin boundary conditions on the left and right, as for example the one here in MATLAB:

```
function U=Solve2dR(f,ai,bi,gl,gr,p1,p2)
% SOLVE2DR solves 2d Poisson problem using Robin conditions
%   u=Solve2dR(f,ai,bi,gl,gr,p1,p2) solves the two dimensional
%   Poisson equation Delta u=f on the domain Omega=(ai*h,bi*h)x(0,1) with
%   Robin boundary conditions (dn+p1)u=gl at x=ai*h and (dn+p2)u=gr at
%   x=bi*h and u=0 at y=0 and y=1 using a finite difference
%   approximation with interior gridpoints (bi-ai) times length(gl)
%   using the same mesh size h=1/(length(gl)+1) in both x and y.

nx=bi-ai+1;                                  % number of point in x direction
ny=length(gl);                               % number of point in y direction
h=1/(ny+1);                                  % mesh size
ex=ones(nx,1);                               % construct 1d finite differences
Dxx=spdiags([-ex/h^2 2/h^2*ex -ex/h^2],[-1 0 1],nx,nx);
ey=ones(ny,1);
Dyy=spdiags([-ey/h^2 2/h^2*ey -ey/h^2],[-1 0 1],ny,ny);
A=kron(speye(size(Dxx)),Dyy)+kron(Dxx,speye(size(Dyy)));
A(1:ny,1:ny)=A(1:ny,1:ny)/2+p1/h*speye(ny);  % put Robin conditions
A(end-ny+1:end,end-ny+1:end)=A(end-ny+1:end,end-ny+1:end)/2+p2/h*speye(ny);
f(1:ny,1)=f(1:ny,1)/2+gl/h;                  % add boundary conditions into rhs
f(1:ny,end)=f(1:ny,end)/2+gr/h;
u=A\f(:);                                    % solve by sparse Gaussian el.
U=reshape(u,ny,nx);                          % put solution into matrix
```

We can then use this solver to solve both subdomain problems using Dirichlet conditions and Neumann conditions, as in the following implementation of the Dirichlet–Neumann method:

```
m=15;                                % number of gridpoints
h=1/(m+1);                           % include the h^2 scaling for
A=Laplacian(m,2)/h^2;                % the negative five-point Laplacian
f=zeros(m*m,1); f(m:m:end)=1/h^2;    % include h^2 scaling also in rhs
u=A\f;                               % since true solver Solve2dR is used
a=6;                                 % alpha=(ai+1)*h
F1=zeros(m,a+1); F1(m,:)=1/h^2;      % f for subdomain solves must
F2=zeros(m,m-a+2); F2(m,:)=1/h^2;    % include Robin bc columns
x1=0:h:a*h; x2=a*h:h:1; y=0:h:1;     % finite difference meshes
z1=zeros(1,a+1);z2=zeros(1,m-a+2);   % for plotting purposes
o1=ones(1,a+1);o2=ones(1,m-a+2);     % for plotting purposes
e=ones(m,1);                         % construct normal derivative
Na=[speye(m) -spdiags([-e +4*e -e],[-1 0 1],m,m)]/h;
la=zeros(m,1);                       % zero initial guess
U2=zeros(size(F2));
f1=@(al,L) tanh(pi/L*(1-al))/tanh(pi/L*al);
th=(1+f1(a*h,1))/(3+f1(a*h,1));      % optimized relaxation parameter
pe=1e10;                             % 1e10 to emulate a Dirichlet condition
g=zeros(m,1);                        % left and right Dirichlet condition
for n=1:10
  err(n)=norm(la-u((a-1)*m+1:a*m),'inf');
  U1=Solve2dR(F1,0,a,g*pe,la*pe,pe,pe);
  mesh(x1,y,[z1;U1;o1]); hold on; mesh(x2,y,[z2;U2;o2]); hold off
  xlabel('x'); ylabel('y'); zlabel('Dirichlet Step');
```

```
  axis([0 1 0 1 0 1])
  pause
  ta=Na*[U1(:,end-1);U1(:,end)]+F2(:,1)*h/2;
  U2=Solve2dR(F2,a,m+1,ta,g*pe,0,pe);
  la=th*la+(1-th)*U2(:,1);
  mesh(x1,y,[z1;U1;o1]); hold on; mesh(x2,y,[z2;U2;o2]); hold off
  xlabel('x'); ylabel('y'); zlabel('Neumann Step');
  axis([0 1 0 1 0 1])
  pause
end
```

Note that to obtain Dirichlet conditions, we need to choose a very large Robin parameter in this implementation, which we call `pe`. Running this code, with different positions for the interface indicated by `a`, we get the results in Figure 4.32. We see that the Dirichlet–Neumann method

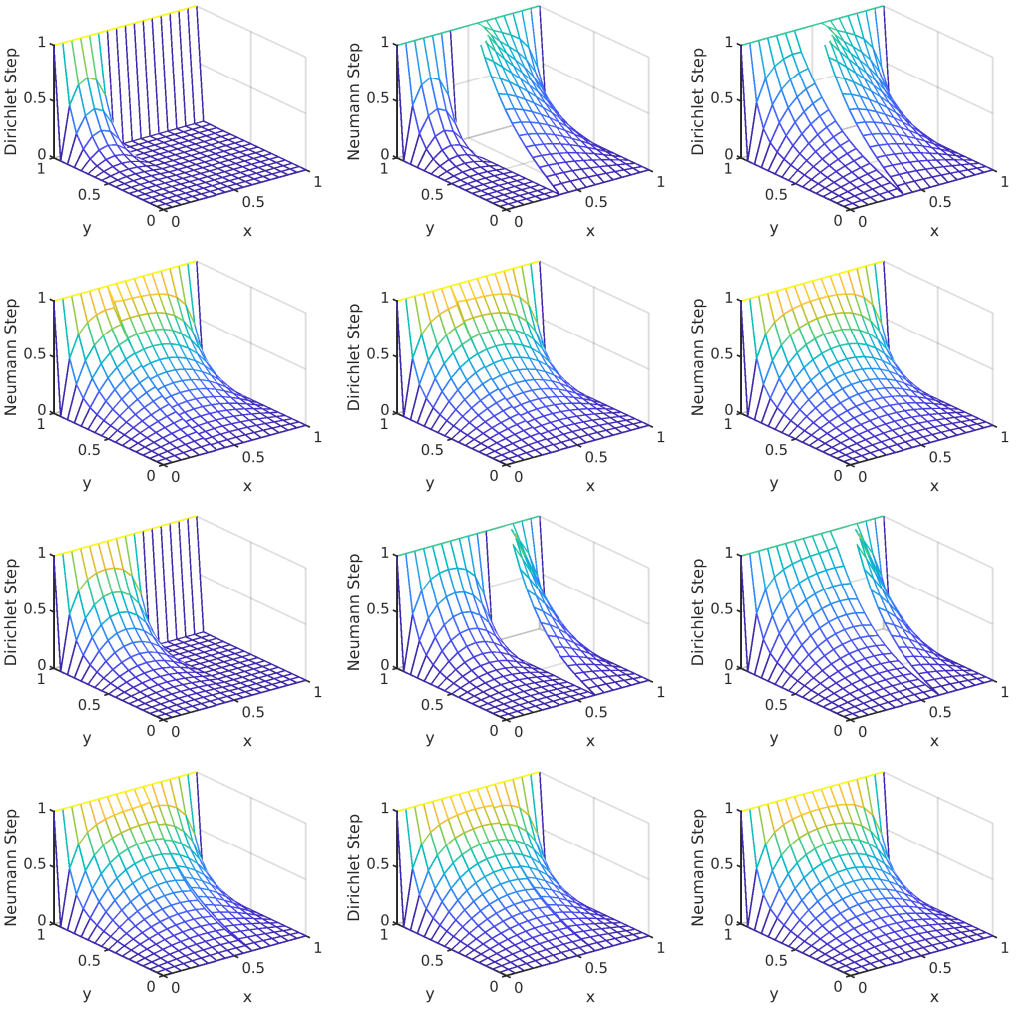

Figure 4.32. *First iterations of the Dirichlet–Neumann method with optimized relaxation parameter θ^* from Theorem 4.13, applied to our Laplace model problem. Top two rows: $\alpha = 0.375$. Bottom two rows: $\alpha = 0.625$.*

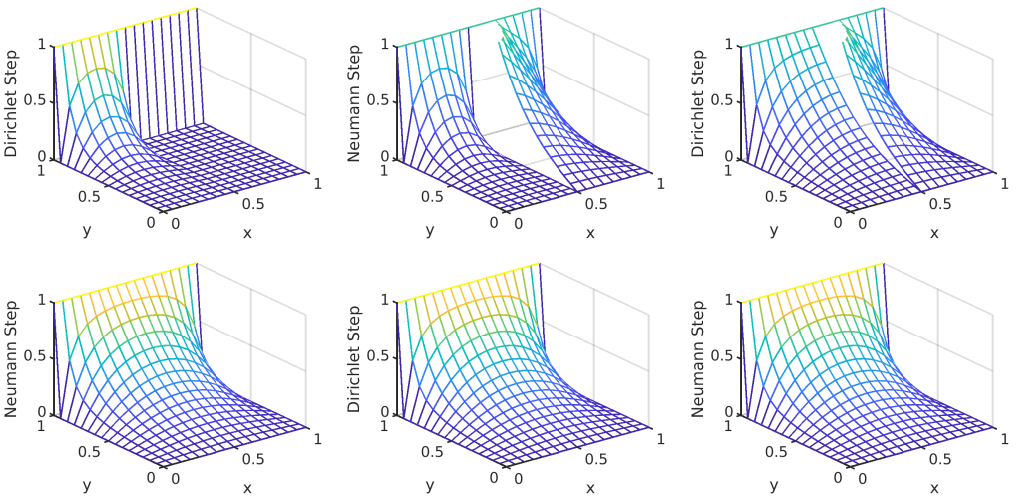

Figure 4.33. *First iterations of the Dirichlet–Neumann method with symmetric subdomains, $\alpha = \frac{1}{2}$, where the optimized relaxation parameter $\theta^* = \frac{1}{2}$ from Theorem 4.13, applied to our Laplace model problem.*

converges for the optimized choice of the relaxation parameter, adapted to the interface position α. Note that for an arbitrary choice of the relaxation parameter, the Dirichlet–Neumann method can also diverge. If we put the interface into the middle, so that the two subdomains are identical in size, we get the results shown in Figure 4.33. We see that indeed, as predicted, the Dirichlet–Neumann method becomes a direct solver: after the first iteration, the predicted interface value λ^1 coincides with the solution of the problem, so that the next subdomain solves deliver the exact solution also in volume, and the algorithm has arrived at its fixed point in the second row of Figure 4.33.

To illustrate how the Dirichlet–Neumann method converges independently of the mesh size, we show in Figure 4.34 how the error decays in the discretized Dirichlet–Neumann iteration for the mesh we used for Figure 4.32 with $m = 15$ and $\alpha = 0.375$, and also on two refined meshes with $m = 31$ and $m = 63$ interior mesh points, keeping the interface fixed at $\alpha = 0.375$. We clearly see that convergence is independent of the mesh parameter h and very well predicted by the continuous analysis in Theorem 4.13 for the optimized parameter θ^*.[45]

There is an important comment here to make about the *relaxation parameter*, which seems so important for the Dirichlet–Neumann method used as a stationary iterative solver. As soon as one uses the method as a preconditioner for a Krylov method, this parameter becomes completely irrelevant! To see this, consider an arbitrary stationary iterative method, to which we add in the end a relaxation parameter,

$$\begin{aligned} \boldsymbol{u}^{n+\frac{1}{2}} &= \boldsymbol{u}^n + M^{-1}(\boldsymbol{f} - A\boldsymbol{u}^n), \\ \boldsymbol{u}^{n+1} &= \theta\boldsymbol{u}^n + (1-\theta)\boldsymbol{u}^{n+\frac{1}{2}} \\ &= \theta\boldsymbol{u}^n + (1-\theta)(\boldsymbol{u}^n + M^{-1}(f - A\boldsymbol{u}^n)). \end{aligned}$$

Using this method as a preconditioner for a Krylov method is equivalent to applying the Krylov method to the equation at the fixed point, where it reads

$$\boldsymbol{u} = \theta\boldsymbol{u} + (1-\theta)(\boldsymbol{u} + M^{-1}(\boldsymbol{f} - A\boldsymbol{u})) \iff (1-\theta)M^{-1}A\boldsymbol{u} = (1-\theta)M^{-1}\boldsymbol{f},$$

[45] Convergence flattens out at the level chosen to emulate the Dirichlet conditions, `1/pe=1e-10`.

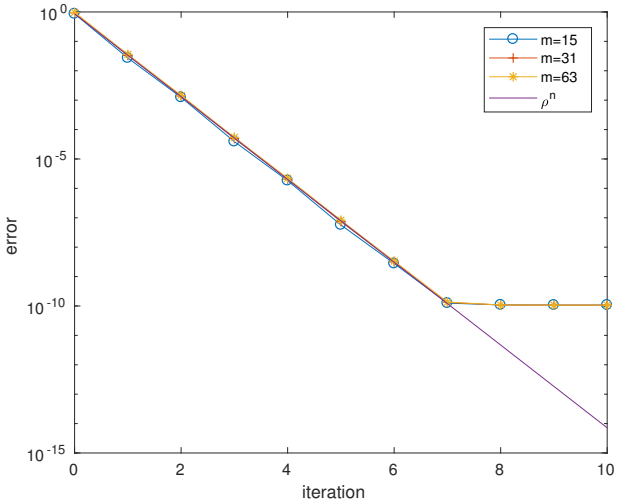

Figure 4.34. *Convergence of the Dirichlet–Neumann method for different mesh sizes* $h = \frac{1}{m+1}$. *For comparison also the theoretical convergence estimate based on the continuous analysis from Theorem 4.13 is shown.*

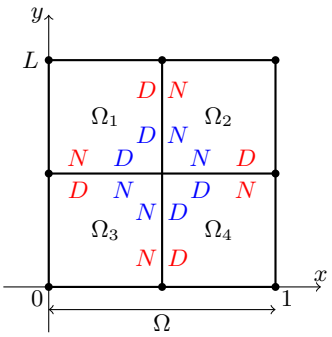

Figure 4.35. *Decomposition of the domain* $\Omega = (0,1) \times (0,L)$ *into four subdomains with a cross point, and possible assignments of Dirichlet and Neumann conditions for the Dirichlet–Neumann algorithm, one in red and one in blue.*

and we see that the multiplication of the preconditioned system by $(1-\theta)$, which comes from the relaxation step, will have no effect whatsoever on the convergence properties of the Krylov method which is used to solve it. So the Krylov method takes care of any possible relaxation at the end of an iteration. This is very different for the optimization in the Robin transmission conditions of the optimized Schwarz method, which truly improves the preconditioner.

As a final remark, the Dirichlet–Neumann method can be generalized to decompositions into more than just two subdomains, otherwise it would not be interesting for parallel computing. One has to take care, however, when assigning which interface side takes Dirichlet data and which takes Neumann data; for an example, see Figure 4.35. There are very few studies in the literature on how such assignments affect the convergence of the Dirichlet–Neumann method, and different assignments then require different schedulings for the order in which subdomain problems are solved; see, for example, [78]. These are precisely the difficulties which make the Dirichlet–Neumann method less popular in practice. The Neumann–Neumann method in the following

section does not have this problem, but it shares a further drawback of these nonoverlapping methods: in the presence of a cross point, the middle point in Figure 4.35 where more than two subdomains meet, the methods are in general not well defined at the continuous level; see, for example, [33].

4.8 ▪ Neumann–Neumann domain decomposition method

> *Ce préconditionneur agit sur l'opérateur de Steklov-Poincaré (représenté après discrétisation par la matrice complément de Schur) par un calcul de moyenne de traces et la résolution d'un problème de Neumann par sous-domaine.*
>
> Jean-François Bourgat, Roland Glowinski, Patrick Le Tallec, and Marina Vidrascu, *Variational Formulation and Algorithm for Trace Operator in Domain Decomposition Calculations*, 1989.

The *Neumann–Neumann method* is also a *nonoverlapping domain decomposition* method, invented by Bourgat et al. in 1989 (see [24] and the quote above); a brief historical review can be found in [82]. Its name can be a bit confusing, since at each iteration, first Dirichlet problems are solved on each subdomain, followed by Neumann correction problems, also on each subdomain, so each iteration is twice as expensive as the iterations of the earlier domain decomposition methods we have seen. If the order is reversed, and one starts with the Neumann problems, followed by Dirichlet correction problems, the algorithm is known under the name *FETI (finite element tearing and interconnect)*, invented by Farhat and Roux in 1991; see [63]. Since the two algorithms are very much related, we will study only the Neumann–Neumann method in detail here. For the simple two subdomain configuration shown in Figure 4.28, the Neumann–Neumann algorithm starts with an initial guess λ^0 along the interface Γ, and then computes for our Poisson model problem first two Dirichlet solutions, one on each subdomain Ω_j, $j = 1, 2$,

$$\begin{aligned} -\Delta u_j^n &= f && \text{in } \Omega_j, \\ u_j^n &= \lambda^{n-1} && \text{on } \Gamma, \\ u_j^n &= g && \text{on } \partial\Omega \cap \partial\Omega_j, \end{aligned} \tag{4.91}$$

followed by computing two Neumann corrections, one on each subdomain, using as Neumann data the jump remaining after the Dirichlet step,[46]

$$\begin{aligned} -\Delta \psi_j^n &= 0 && \text{in } \Omega_j, \\ \partial_{n_j} \psi_j^n &= \partial_{n_1} u_1^n + \partial_{n_2} u_2^n && \text{on } \Gamma, \\ \psi_j^n &= 0 && \text{on } \partial\Omega \cap \partial\Omega_j. \end{aligned} \tag{4.92}$$

Here ∂_{n_j}, $j = 1, 2$, denotes the unit outer normal derivative of subdomain Ω_j along the interface Γ, and in our example, we could simply write $\partial_{n_1} = \partial_x$, $\partial_{n_2} = -\partial_x$. Finally, like in the Dirichlet–Neumann algorithm, the interface approximation λ^n is updated using a *relaxation parameter* θ, traditionally written in the form

$$\lambda^n = \lambda^{n-1} - \theta(\psi_1^n + \psi_2^n) \quad \text{on } \Gamma. \tag{4.93}$$

To understand the convergence properties of the Neumann–Neumann method, we use again Fourier analysis for the *error equations*: with $e_j^n := u - u_j^n$, $d^n := \lambda - \lambda^n$, $\lambda := u|_\Gamma$, and leaving the ψ_j, which are already correction terms, these quantities satisfy for $j = 1, 2$

$$\begin{aligned} -\Delta e_j^n &= 0 && \text{in } \Omega_j, \\ e_j^n &= d^{n-1} && \text{on } \Gamma, \\ e_j^n &= 0 && \text{on } \partial\Omega \cap \partial\Omega_j \end{aligned} \tag{4.94}$$

[46] In the original presentation of the Neumann–Neumann algorithm, there is a factor one-half in front of the sum of the Neumann derivatives, $\frac{1}{2}(\partial_{n_1} u_1^n + \partial_{n_2} u_2^n)$, but this just scales the relaxation parameter θ that follows, so we do not put this factor here.

and

$$\begin{aligned} -\Delta\psi_j^n &= 0 && \text{in } \Omega_j, \\ \partial_{n_j}\psi_2^n &= \partial_{n_1}e_1^n + \partial_{n_2}e_2^n && \text{on } \Gamma, \\ \psi_j^n &= 0 && \text{on } \partial\Omega \cap \partial\Omega_j, \end{aligned} \tag{4.95}$$

followed by the final update

$$d^n = d^{n-1} - \theta(\psi_1^n + \psi_2^n) \quad \text{on } \Gamma. \tag{4.96}$$

Using a Fourier sine expansion,

$$\begin{aligned} e_j^n(x,y) &= \sum_{k\in K} \widehat{e}_j^n(x,k)\sin(ky), \\ \psi_j^n(x,y) &= \sum_{k\in K} \widehat{\psi}_j^n(x,k)\sin(ky), \end{aligned} \tag{4.97}$$

with $K := \{\frac{\pi}{L}, \frac{2\pi}{L}, \frac{3\pi}{L}, \ldots\}$, we find that the Fourier coefficients are of the form

$$\begin{aligned} \widehat{e}_1^n(x,k) &= \frac{\sinh(kx)}{\sinh(k\alpha)}\widehat{d}^{n-1}(k), \quad \widehat{e}_2^n(x,k) = \frac{\sinh(k(1-x))}{\sinh(k(1-\alpha))}\widehat{d}^{n-1}(k), \\ \widehat{\psi}_1^n(x,k) &= B_1^n(k)\frac{\sinh(kx)}{\sinh(k\alpha)}, \qquad \widehat{\psi}_2^n(x,k) = B_2^n(k)\frac{\sinh(k(1-x))}{\sinh(k(1-\alpha))}. \end{aligned} \tag{4.98}$$

To determine the remaining constants $B_j^n(k)$ in the $\widehat{\psi}_j^n$, we need to compute the right-hand side in the Neumann boundary condition (4.95),

$$\begin{aligned} (\partial_{n_1}\widehat{e}_1^n + \partial_{n_2}\widehat{e}_2^n)|_{x=\alpha} &= (\partial_x\widehat{e}_1^n - \partial_x\widehat{e}_2^n)|_{x=\alpha} \\ &= \left(\frac{k\cosh(k\alpha)}{\sinh(k\alpha)} + \frac{k\cosh(k(1-\alpha)}{\sinh(k(1-\alpha))}\right)\widehat{d}^{n-1} \\ &= k\big(\coth(k\alpha) + \coth(k(1-\alpha))\big)\widehat{d}^{n-1}. \end{aligned}$$

Imposing this as Neumann boundary condition on the corrections ψ_j^n leads to

$$\begin{aligned} B_1^n(k)\frac{k\cosh(k\alpha)}{\sinh(k\alpha)} &= k\big(\coth(k\alpha) + \coth(k(1-\alpha))\big)\widehat{d}^{n-1}, \\ B_2^n(k)\frac{k\cosh(k(1-\alpha))}{\sinh(k(1-\alpha))} &= k\big(\coth(k\alpha) + \coth(k(1-\alpha))\big)\widehat{d}^{n-1}. \end{aligned}$$

Solving for the $B_j^n(k)$, we get

$$\begin{aligned} B_1^n(k) &= \tanh(k\alpha)\big(\coth(k\alpha) + \coth(k(1-\alpha))\big)\widehat{d}^{n-1}, \\ B_2^n(k) &= \tanh(k(1-\alpha))\big(\coth(k\alpha) + \coth(k(1-\alpha))\big)\widehat{d}^{n-1}, \end{aligned}$$

and inserting them into the $\widehat{\psi}_j^n$ leads to

$$\begin{aligned} \widehat{\psi}_1^n(x,k) &= \tanh(k\alpha)\big(\coth(k\alpha) + \coth(k(1-\alpha))\big)\frac{\sinh(kx)}{\sinh(k\alpha)}\widehat{d}^{n-1}, \\ \widehat{\psi}_2^n(x,k) &= \tanh(k(1-\alpha))\big(\coth(k\alpha) + \coth(k(1-\alpha))\big)\frac{\sinh(k(1-x))}{\sinh(k(1-\alpha))}\widehat{d}^{n-1}. \end{aligned}$$

We can then evaluate the updating formula (4.96) which contains the sum $\widehat{\psi}_1^n(\alpha,k)+\widehat{\psi}_2^n(\alpha,k)$ to find

$$\widehat{d}^n=\widehat{d}^{n-1}-\theta\big(\tanh(k\alpha)+\tanh(k(1-\alpha))\big)\big(\coth(k\alpha)+\coth(k(1-\alpha))\big)\widehat{d}^{n-1}\quad\text{on }\Gamma,$$

which implies that the *convergence factor of the Neumann–Neumann method* is given by

$$\widehat{\rho}_{NN}(\alpha,k,\theta)=1-\theta\big(\tanh(k\alpha)+\tanh(k(1-\alpha))\big)\big(\coth(k\alpha)+\coth(k(1-\alpha))\big). \quad (4.99)$$

By induction, the error on the interface satisfies

$$\widehat{d}^n(k)=(\widehat{\rho}_{NN}(\alpha,k,\theta))^n\,\widehat{d}^0(k).$$

To understand the convergence behavior of the Neumann–Neumann method, we need to study $\widehat{\rho}_{NN}(\alpha,k,\theta)$, for which we use again two lemmas.

Lemma 4.14 (Properties of F_{NN}). *The function*

$$F_{NN}(\alpha,k)=(\tanh(k\alpha)+\tanh(k(1-\alpha))\,(\coth(k\alpha)+\coth(k(1-\alpha)) \quad (4.100)$$

has the following properties:

1. $\lim_{k=\infty}F_{NN}(\alpha,k)=4$*;*
2. *for* $\alpha=\frac{1}{2}$, $F_{NN}(\frac{1}{2},k)\equiv 4$*;*
3. $F_{NN}(\alpha,k)$ *is decreasing in* k*.*

Proof. These results can be obtained by direct computations, analogously to those in the proof of Lemma 4.11 for the Dirichlet–Neumann method; see also Figure 4.36. □

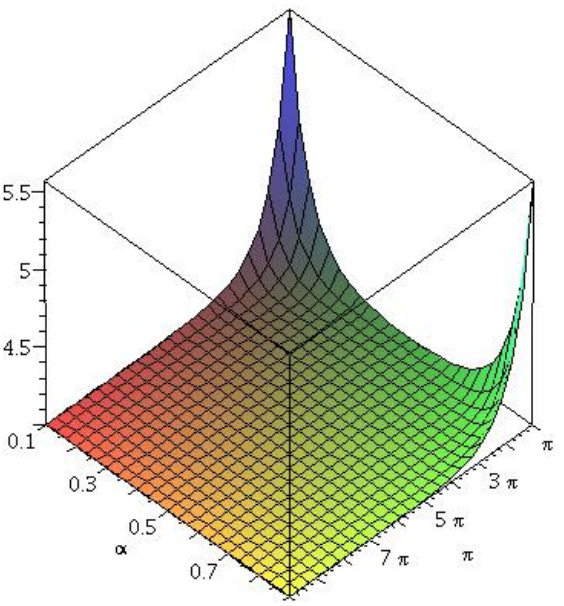

Figure 4.36. *Plot of the function* $F_{NN}(\alpha,k)$ *defined in* (4.100) *from the Neumann–Neumann algorithm.*

Like in the Dirichlet–Neumann method, there is an optimal choice for the relaxation parameter θ.

Lemma 4.15 (Optimal relaxation parameter for Neumann–Neumann). *The optimal choice θ^* for the relaxation parameter in the Neumann–Neumann method is given by*

$$\theta^* = \frac{2}{F_{NN}(\alpha, k_{\max}) + F_{NN}(\alpha, k_{\min})} \tag{4.101}$$

with the function $F_{NN}(\alpha, k)$ defined in (4.100)*. The associated convergence factor of the Neumann–Neumann method then satisfies*

$$\max_{k_{\min} \le k \le k_{\max}} |\widehat{\rho}_{NN}(\alpha, k, \theta^*)| = \left| \frac{F_{NN}(\alpha, k_{\max}) - F_{NN}(\alpha, k_{\min})}{F_{NN}(\alpha, k_{\max}) + F_{NN}(\alpha, k_{\min})} \right|. \tag{4.102}$$

Proof. Since $F_{NN}(\alpha, k)$ is decreasing in k according to Lemma 4.14, the maximum of $\widehat{\rho}_{NN}(\alpha, k, \theta) = 1 - \theta F_{NN}(\alpha, k)$ is attained at $k = k_{\max}$ and the minimum at $k = k_{\min}$, and because $\widehat{\rho}_{NN}(\alpha, k, \theta)$ is a linear function in θ, one can equilibrate the maximum and the minimum to get $\widehat{\rho}_{NN}(\alpha, k, \theta)$ as close as possible to zero. The optimal choice θ^* therefore satisfies the equioscillation equation

$$\widehat{\rho}_{NN}(\alpha, k_{\min}, \theta^*) = -\widehat{\rho}_{NN}(\alpha, k_{\max}, \theta^*),$$

which gives (4.101), and a direct computation leads to (4.102). □

With this optimized choice of the relaxation parameter θ, the Neumann–Neumann method is convergent.

Theorem 4.16 (Convergence of the Neumann–Neumann method). *With the optimized choice of the relaxation parameter*

$$\theta^* = \frac{2}{4 + \tilde{F}_{NN}(\alpha, L)}, \tag{4.103}$$

where

$$\tilde{F}_{NN}(\alpha, L) := \left(\tanh(\tfrac{\pi}{L}\alpha) + \tanh(\tfrac{\pi}{L}(1-\alpha))\right)\left(\coth(\tfrac{\pi}{L}\alpha) + \coth(\tfrac{\pi}{L}(1-\alpha))\right), \tag{4.104}$$

the Neumann–Neumann method (4.91)*,* (4.92)*, and* (4.93) *converges for all initial guesses λ^0 along the interface Γ, and we have the linear convergence estimate*

$$\|\lambda - \lambda^n\|_2 \le \rho_{NN}^n \|\lambda - \lambda^0\|_2 \tag{4.105}$$

with the convergence factor

$$\rho_{NN}(\alpha, L) = \left| \frac{4 - \tilde{F}_{NN}(\alpha, L)}{4 + \tilde{F}_{NN}(\alpha, L)} \right| < 1. \tag{4.106}$$

Proof. When $k_{\max}$ goes to infinity, Lemma 4.14 shows that $F_{NN}(\alpha, k_{\max}) \to 4$, and inserting this into (4.102) of Lemma 4.15, we obtain

$$\max_{k_{\min} \le k \le \infty} |\widehat{\rho}_{NN}(\alpha, k, \theta^*)| = \left| \frac{4 - F_{NN}(\alpha, \frac{\pi}{L})}{4 + F_{NN}(\alpha, \frac{\pi}{L})} \right|,$$

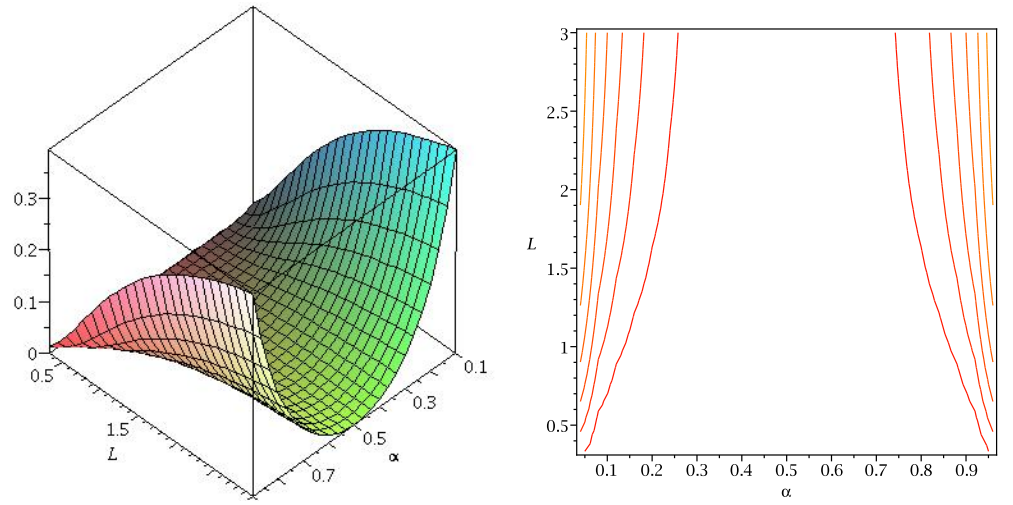

Figure 4.37. *Dependence of the convergence factor $\rho_{NN}(\alpha, L)$ of the Neumann–Neumann method from Theorem 4.16 as a function of the interface position α, and the domain height L, with a three-dimensional plot on the left and the corresponding contour plot on the right, with the level sets corresponding to* $\{0, 0.1, \ldots, 1\}$.

where we also used that $k_{\min} = \frac{\pi}{L}$. Since $F_{NN}(\alpha, \frac{\pi}{L})$ is positive, this quantity is clearly less than 1, and we can then use the Parseval–Plancherel identity to obtain the L^2-error estimate (4.105). □

We show in Figure 4.37 how the convergence factor $\rho_{NN}(\alpha, L)$ in (4.106) of the Neumann–Neumann method from Theorem 4.16 depends on the interface position α and the domain height L. We again see that convergence is better for small L than for large L like for the earlier domain decomposition methods. We also see that the convergence behavior is now symmetric in α, in contrast to the Dirichlet–Neumann method, but again convergence is worse when one subdomain is smaller than the other, in contrast to the Schwarz method; see the right plot in Figure 4.18. The convergence result in Theorem 4.16 also shows that if the two subdomains are equal, $\alpha = \frac{1}{2}$, the Neumann–Neumann method is a direct solver, since $\tilde{F}_{NN}(\frac{1}{2}, L) = 4$, which implies $\theta^* = \frac{1}{4}$ as we have seen earlier, and $\rho_{NN} = 0$, which is clearly visible in Figure 4.37. Like for Dirichlet–Neumann, we also have for the special choice $\theta = \frac{1}{4}$ that

$$\lim_{k\to\infty} \widehat{\rho}_{NN}\left(\alpha, k, \frac{1}{2}\right) = 1 - \frac{1}{4} \lim_{k\to\infty} F_{NN}(\alpha, k) = 0$$

because of Lemma 4.14, and thus for high frequencies, the Neumann–Neumann method always converges very fast for the choice of relaxation parameter $\theta = \frac{1}{4}$, independently of the interface position α. This is again because of the damping nature of the Poisson equation, as in the case of Dirichlet–Neumann.

The Neumann–Neumann method can also be discretized to obtain a preconditioner, and it is again convenient to use the same solver `Solve2dR` with Robin boundary conditions as for Dirichlet–Neumann. We can then use this solver to solve both subdomain problems using Dirichlet conditions followed by both problems using Neumann conditions, as in the following implementation of the Neumann–Neumann method:

```
m=15;                                % number of gridpoints
h=1/(m+1);                           % include the h^2 scaling for
A=Laplacian(m,2)/h^2;                % the true five-point Laplacian
f=zeros(m*m,1); f(m:m:end)=1/h^2;    % include h^2 scaling also in rhs
u=A\f;                               % since true solver Solve2dR is used
a=6;                                 % alpha=ai*h
F1=zeros(m,a+1); F1(m,:)=1/h^2;      % f for subdomain solves must
F2=zeros(m,m-a+2); F2(m,:)=1/h^2;    % include Robin bc columns
x1=0:h:a*h; x2=a*h:h:1; y=0:h:1;     % finite difference meshes
z1=zeros(1,a+1);z2=zeros(1,m-a+2);   % for plotting purposes
o1=ones(1,a+1);o2=ones(1,m-a+2);     % for plotting purposes
e=ones(m,1);                         % construct normal derivative
Na=[speye(m) -spdiags([-e +4*e -e]/2,[-1 0 1],m,m)]/h;
Nb=[-spdiags([-e +4*e -e]/2,[-1 0 1],m,m) speye(m)]/h;
la=zeros(m,1);                       % zero initial guess
U2=zeros(size(F2));
f1=@(al,L) (tanh(pi/L*al)+tanh(pi/L*(1-al)))*(coth(pi/L*al)+coth(pi/L*(1-al)));
th=2/(4+f1(a*h,1));                  % optimized relaxation parameter
pe=1e10;                             % 1e10 to emulate a Dirichlet condition
g=zeros(m,1);                        % left and right Dirichlet condition
for n=0:10
  err(n+1)=norm(la-u((a-1)*m+1:a*m),'inf');
  U1=Solve2dR(F1,0,a,g*pe,la*pe,pe,pe);
  U2=Solve2dR(F2,a,m+1,la*pe,g*pe,pe,pe);
  mesh(x1,y,[z1;U1;o1]); hold on;mesh(x2,y,[z2;U2;o2]);hold off
  xlabel('x'); ylabel('y'); zlabel('Neumann-Neumann Iterate');
  axis([0 1 0 1 0 1])
  pause
  tb=Nb*[U2(:,1);U2(:,2)]+F2(:,1)*h/2;
  ta=Na*[U1(:,end-1);U1(:,end)]+F1(:,end)*h/2;
  psi1=Solve2dR(zeros(size(F1)),0,a,pe*g,ta+tb,pe,0);
  psi2=Solve2dR(zeros(size(F2)),a,m+1,ta+tb,g*pe,0,pe);
  la=la+th*(psi1(:,end)+psi2(:,1));
  mesh(x1,y,[z1;psi1;z1]); hold on;mesh(x2,y,[z2;psi2;z2]);hold off
  xlabel('x'); ylabel('y'); zlabel('Neumann-Neumann Correction');
  pause
end
```

Running this code, with different positions for the interface indicated by a, we get the results in Figure 4.38. We see that the Neumann–Neumann method converges for the optimized choice of the relaxation parameter, adapted to the interface position α, and convergence is very fast, as one can see from the different scales in the plots of the corrections. If we put the interface into the middle, so that the two subdomains are identical in size, we get the results shown in Figure 4.39. We see that indeed as predicted, the Neumann–Neumann method becomes a direct solver: after the first iteration, following the correction, the predicted interface value λ^1 coincides with the solution of the problem, so that the next subdomain Dirichlet solves deliver the solution also in volume, and the algorithm has arrived at its fixed point in the second row of Figure 4.39; the corrections are numerically zero.

To illustrate how the Neumann–Neumann method converges independently of the mesh size, we show in Figure 4.40 how the error decays in the discretized Neumann–Neumann iteration for the mesh we used for Figure 4.38 with $m = 15$ and $\alpha = 0.375$, and also on two refined meshes with $m = 31$ and $m = 63$ interior mesh points, keeping the interface fixed at $\alpha = 0.375$.

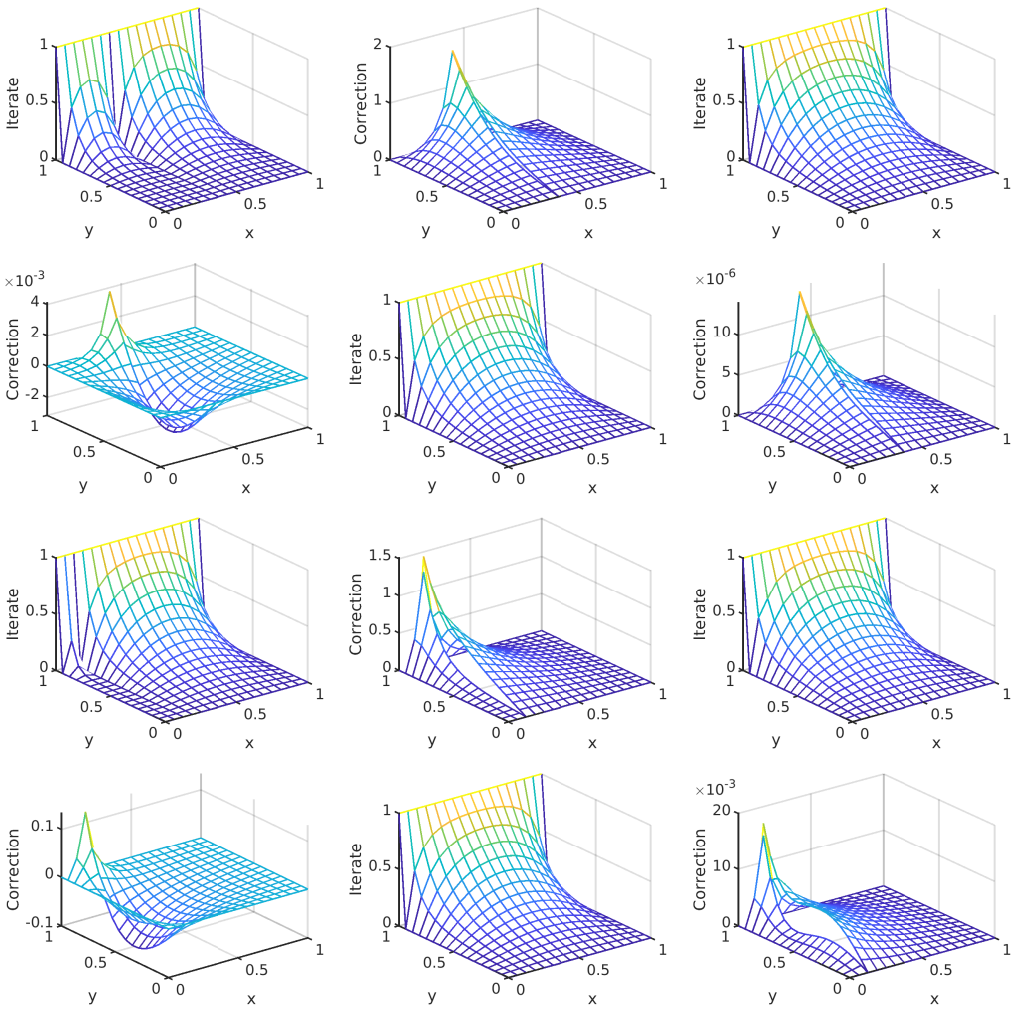

Figure 4.38. *First iterations and corrections of the Neumann–Neumann method with optimized relaxation parameter θ^* from Theorem 4.13, applied to our Laplace model problem. Top 2 rows: $\alpha = 0.375$. Bottom two rows: $\alpha = 0.125$.*

We see that convergence is independent of the mesh parameter h and very well predicted by the continuous analysis in Theorem 4.16 for the optimized parameter θ^*.[47]

As for Dirichlet–Neumann, the relaxation parameter is important only when Neumann–Neumann is used as an iterative solver; as a preconditioner this is not needed, for the same reasons as explained at the end of the Dirichlet–Neumann section.

The generalization to many subdomains is much easier than for Dirichlet–Neumann; since no decisions on the interfaces have to be made, all subdomains must solve a Dirichlet problem followed by a Neumann problem. This Neumann problem can, however, pose difficulties when a subdomain is completely surrounded by other subdomains, so that it only has Neumann boundary conditions. It is then not invertible, and the solution is determined only up to a constant. This was

[47] Convergence flattens out again at the level chosen to emulate the Dirichlet conditions, `1/pe=1e-10`.

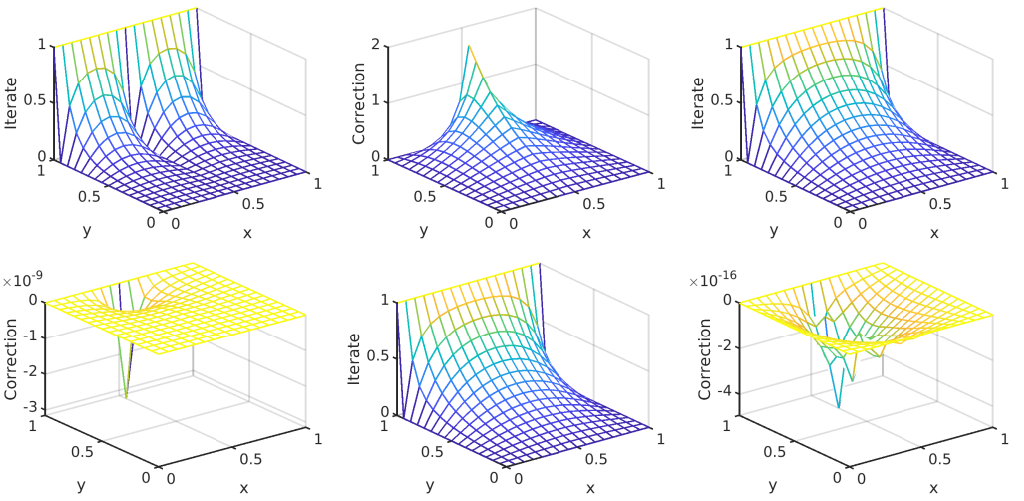

Figure 4.39. *First iterations of the Neumann–Neumann method with symmetric subdomains, $\alpha = \frac{1}{2}$, where the optimized relaxation parameter $\theta^* = \frac{1}{2}$ from Theorem 4.13, applied to our Laplace model problem.*

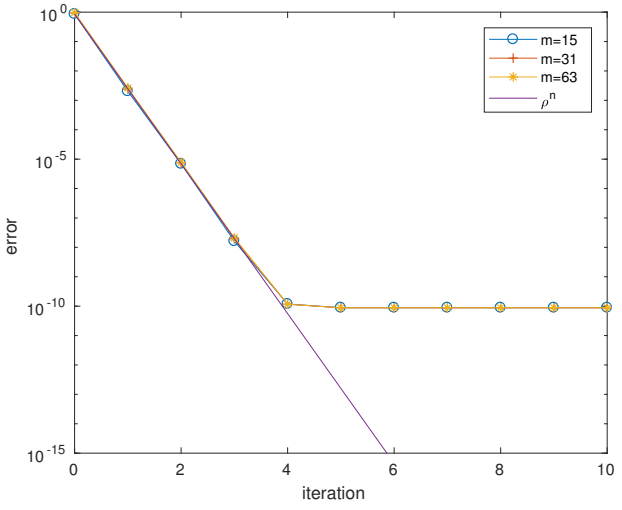

Figure 4.40. *Convergence of the Neumann–Neumann method for different mesh sizes $h = \frac{1}{m+1}$. For comparison also the theoretical convergence estimate based on the continuous analysis from Theorem 4.16 is shown.*

first considered as a disadvantage, but it turned out that one can use this constant to add a coarse correction to the method and make it scalable when many subdomains are used, leading to the balancing Neumann–Neumann method: the bug became a feature, and the same happened for the FETI methods.

But like the Dirichlet–Neumann method, cross points make the Neumann–Neumann method not well posed at the continuous level, and so the analyses were so far performed only at the discrete level in the literature.

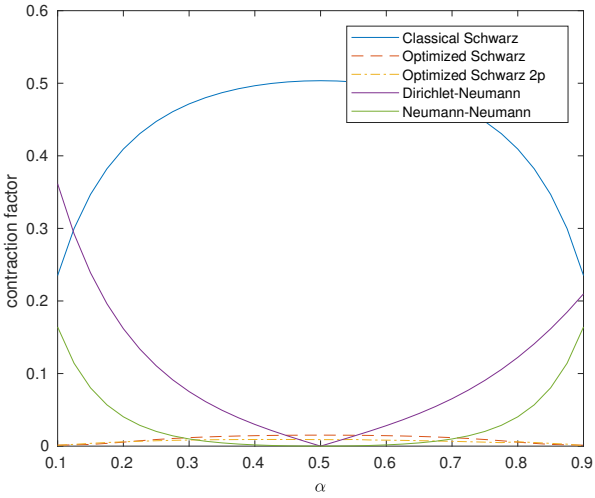

Figure 4.41. *Convergence factors for the various domain decomposition methods and two subdomain decompositions, as a function of the interface position α.*

4.9 ▪ Comparison of Schwarz, Dirichlet–Neumann, and Neumann–Neumann

To conclude this section about domain decomposition preconditioners, we show in Figure 4.41 a comparison of the convergence factors of the classical and optimized Schwarz methods, and the Dirichlet–Neumann and Neumann–Neumann methods, as a function of the interface position α. For the Schwarz methods, we used an overlap $\delta = 0.1$, which we centered around the interface position. We clearly see that if the subdomains are close to the same size, the Dirichlet–Neumann and Neumann–Neumann methods are hard to beat, since their convergence factor tends to zero when the subdomains are exactly symmetric. We also see that the Dirichlet–Neumann method converges in an asymmetric way, as expected from the asymmetric solution process. It also becomes evident that the classical Schwarz method is not competitive; it would need a lot more overlap to beat Dirichlet–Neumann and Neumann–Neumann when the subdomain size becomes quite different. The optimized Schwarz methods are, however, very competitive, and their performance does not deteriorate with the subdomain asymmetry—it becomes better. It is this robustness property of optimized Schwarz methods that makes them so interesting: they can even take advantage of heterogeneities in the PDE and converge faster than without heterogeneity (see, e.g., [71, 83]), whereas classical domain decomposition methods only try to be robust.

4.10 ▪ Multigrid methods

> *The characteristic feature of the multi-grid iteration is its fast convergence. The convergence speed does not deteriorate when the discretization is refined, whereas classical iterative methods slow down for decreasing grid size. As a consequence one obtains an acceptable approximation of the discrete problem at the expense of computational work proportional to the number of unknowns, which is also the number of the equations in the system. It is not only the complexity which is optimal, also the constant of proportionality is so small that other methods can hardly surpass the multi-grid efficiency.*
>
> Wolfgang Hackbusch, *Multi-Grid Methods and Applications*, 1985.

In this section, we present multigrid methods, which are among the most efficient methods to solve linear systems $A\boldsymbol{u} = \boldsymbol{f}$ stemming from discretizations of Laplace-like boundary value

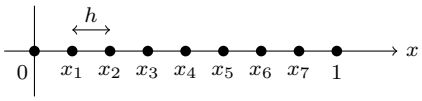

Figure 4.42. *Grid of seven points inside* $(0,1)$.

problems. In contrast to the domain decomposition methods we have seen, which inherit their robust convergence when the mesh is refined from the fact that they were formulated at the continuous level, multigrid methods have mesh-independent convergence for a different reason: they use many levels of approximation, which classical stationary iterative methods like Jacobi and Gauss–Seidel do not; see also the quote above. Early important ideas for multigrid methods can already be found in the work of *Radii Petrovich Fedorenko* [64], but seminal contributions are due to *Achi Brandt* [27] and *Wolfgang Hackbusch* [99] in the 1970s, who both greatly fostered the tremendous development of multigrid methods to come, and there are many variants now of multigrid methods. Further important contributions were also made by *Roy A. Nicolaides* [137], especially also for coarse spaces used in domain decomposition. To make multigrid methods more easily applicable to general matrix problems, algebraic multigrid methods were developed by *John W. Ruge* and *Klaus Stüben* [158], but we will not treat such methods in our simple introduction to multigrid methods here.

To describe the basic multigrid method, we follow the analysis presented by Hackbusch in [101, Chapter 2] and use the simple one-dimensional Laplace equation

$$-u_{xx} = f \quad \text{in } \Omega = (0,1) \text{ with } u(0) = u(1) = 0. \tag{4.107}$$

To motivate this choice of a one-dimensional model, we recall the following excerpt from [101, Chapter 2]:

> A natural model of an elliptic equation is the two-dimensional Poisson equation in a square. Unfortunately, the analysis of the multi-grid algorithm for this problem is still an involved exercise.

A two-dimensional Fourier analysis for the Poisson equation in a square is also possible and given in [101, Chapter 8]. However, the one-dimensional analysis we consider is simpler and then more appropriate to introduce the main ideas of multigrid methods. Notice also that other more general convergence analyses are possible; see, e.g., [101, Chapters 6 and 7]. However, they only lead in general to upper bounds on the contraction factor.

To discretize (4.107), we use a uniform grid of $m = 2^\ell - 1$ gridpoints in $(0,1)$ with $h = \frac{1}{m+1}$, where ℓ is a given integer. For example, if $\ell = 3$ we have a grid of $m = 7$ points inside $(0,1)$; see Figure 4.42. The corresponding linear system $A\boldsymbol{u} = \boldsymbol{f}$ is given by

$$\frac{1}{h^2}\begin{bmatrix} 2 & -1 & & & & & \\ -1 & 2 & -1 & & & & \\ & -1 & 2 & -1 & & & \\ & & -1 & 2 & -1 & & \\ & & & -1 & 2 & -1 & \\ & & & & -1 & 2 & -1 \\ & & & & & -1 & 2 \end{bmatrix}\begin{bmatrix} u_1 \\ u_2 \\ u_3 \\ u_4 \\ u_5 \\ u_6 \\ u_7 \end{bmatrix} = \begin{bmatrix} f_1 \\ f_2 \\ f_3 \\ f_4 \\ f_5 \\ f_6 \\ f_7 \end{bmatrix}, \tag{4.108}$$

where $f_j = f(x_j)$ for $j = 1, \ldots, m$ and $x_j = jh$.

If we use the Jacobi method in the correction form to solve this linear system, we get

$$\boldsymbol{u}^{n+1} = \boldsymbol{u}^n + D^{-1}(\boldsymbol{f} - A\boldsymbol{u}^n),$$

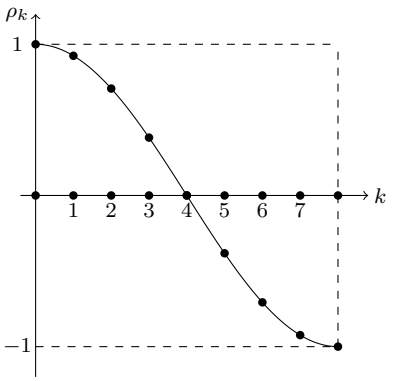

Figure 4.43. *Convergence factor ρ_k: example for $m = 7$, which illustrates that $\rho_k \approx 1$ for $k \approx 1$ and $\rho_k \approx -1$ for $k \approx m = 7$.*

where $D = \frac{2}{h^2} I$. Now, recall that the eigenvectors and eigenvalues of A are given by

$$\varphi_{k,j} = \sin(k\pi x_j) \quad \text{and} \quad \lambda_k = \frac{4}{h^2} \sin^2\Big(k\pi \frac{h}{2}\Big)$$

for $k = 1, \ldots, m$. We call the frequencies k close to 1 low frequencies, the ones close to m high frequencies, and the ones close to $m/2$ medium frequencies, since this corresponds to how the associated eigenfunctions oscillate. If we consider the error at the iteration $n = 0$ to be $\boldsymbol{e}^0 = \boldsymbol{\varphi}_k$, then the Jacobi iteration gives after one iteration the error (recall Theorem 2.1)

$$\begin{aligned} \boldsymbol{e}^1 &= \boldsymbol{e}^0 - D^{-1} A \boldsymbol{e}^0 \\ &= \boldsymbol{\varphi}_k - \frac{h^2}{2} \lambda_k \boldsymbol{\varphi}_k \\ &= \Big[1 - \frac{h^2}{2} \frac{4}{h^2} \sin^2\Big(k\pi \frac{h}{2}\Big)\Big] \boldsymbol{\varphi}_k \\ &= \rho_k \boldsymbol{\varphi}_k, \end{aligned}$$

where the convergence factor is defined as $\rho_k := 1 - 2\sin^2\big(k\pi \frac{h}{2}\big)$. In Figure 4.43, we show a plot of the convergence factor ρ_k as a function of k, which illustrates that ρ_k assumes in modulus values close to 1 for low and high frequencies and is close to 0 for medium frequencies. This means that the Jacobi method for $\boldsymbol{e}^0 = \boldsymbol{\varphi}_k$ converges very fast for a medium frequency k and very slowly for k close to 1 or to m.

This behavior of Jacobi can be controlled with a relaxation[48] (or damping) parameter $\omega \in (0, 1)$,

$$\boldsymbol{u}^{n+1} = \boldsymbol{u}^n + \omega D^{-1}(\boldsymbol{f} - A\boldsymbol{u}^n). \tag{4.109}$$

Computing the *convergence factor for this damped Jacobi iteration* as before, we obtain the convergence factor

$$\rho_{k,\omega} = 1 - 2\omega \sin^2\Big(k\pi \frac{h}{2}\Big).$$

We can now use the parameter ω to tune the convergence of the Jacobi method for different frequencies k. For example, with $\omega = \frac{1}{2}$ Jacobi converges very fast for high-frequency error components $\boldsymbol{e}^0 = \boldsymbol{\varphi}_k$ with k close to m; see Figure 4.44. An optimal choice to damp the upper

[48] The method (4.109) is known as the damped Jacobi method and corresponds to a splitting $A = M - N$ with $M = \frac{1}{\omega} D$ and $N = \frac{1}{\omega}[(1-\omega)D - \omega(L+U)]$.

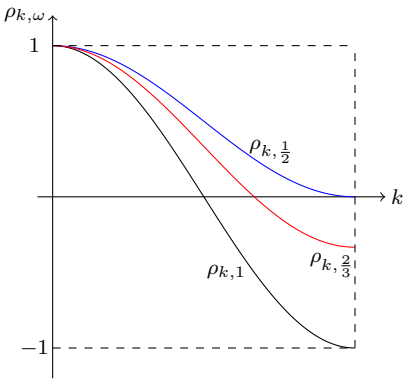

Figure 4.44. *Convergence factor $\rho_{k,\omega}$: example for $\omega = 1$ corresponding to undamped Jacobi (black line), $\omega = \frac{1}{2}$ (blue line), and $\omega = \frac{2}{3}$ (red line).*

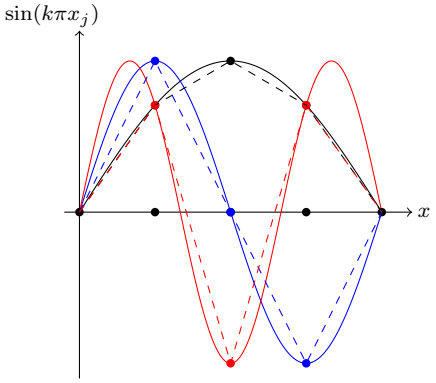

Figure 4.45. *Low frequencies $k = 1$ (black), $k = 2$ (blue), and $k = 3$ (red) and their approximations on a coarse grid (dashed lines).*

half of the frequencies is $\omega = \frac{2}{3}$, which leads to the best overall damping of these frequencies. This value of ω is obtained by setting the convergence factor $\rho_{\frac{m}{2},\omega} = -\rho_{m,\omega}$ following the Chebyshev *equioscillation principle*[49] and solving for ω; see Figure 4.44. However, all the curves shown in Figure 4.44 are very close to 1 for low frequencies. This means that after ν iterations the error $\boldsymbol{e}^\nu$, which satisfies

$$A\boldsymbol{e}^\nu = A(\boldsymbol{u} - \boldsymbol{u}^\nu) = \boldsymbol{f} - A\boldsymbol{u}^\nu = \boldsymbol{r}^\nu, \tag{4.110}$$

contains mostly low frequencies, and we see that ω cannot be used effectively to improve the convergence of the method of Jacobi for low frequencies. The slow convergence of the low frequencies can, however, be addressed by a different mechanism: low frequencies can be well represented on a coarser grid using a smaller number of gridpoints, e.g., $M = 2^{\ell-1} - 1$[50] with coarse mesh size $H = \frac{1}{M+1}$. We show in Figure 4.45 the coarse grid for our initial example,

[49] This principle goes back to the work of Chebyshev [35] and his discovery of the Chebyshev polynomials, which were motivated by minimizing the wear and tear of the force transmission mechanism for steam engines.

[50] This M has no relation to the symbol M we used for the preconditioning matrix.

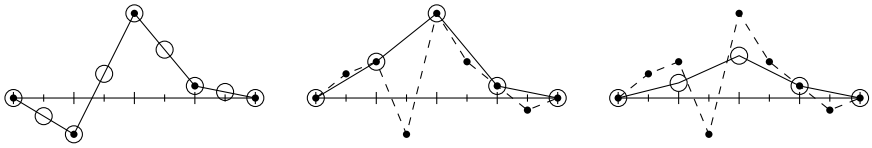

Figure 4.46. *Interpolation and restriction by injection and full weighting.*

where we used only three points instead of the original seven, for the three lowest frequencies. We see that the frequencies $k = 1$ and $k = 2$ are very well approximated with only three gridpoints; the approximation of the frequency $k = 3$ is not quite as good, but it is still oscillating correctly three times when represented by only three gridpoints.

Now, recalling that after ν iterations the error vector $\boldsymbol{e}^\nu$ contains mostly low frequencies, one can solve (4.110) only on a coarse grid:

$$\begin{aligned} A_{\mathrm{H}}\boldsymbol{e}_{\mathrm{H}} &= R(\boldsymbol{f} - A\boldsymbol{u}^\nu) = R\boldsymbol{r}^\nu, \\ \boldsymbol{u}^{new} &= \boldsymbol{u}^\nu + P\boldsymbol{e}_{\mathrm{H}}, \end{aligned} \tag{4.111}$$

where $P \in \mathbb{R}^{m\times M}$ is an *interpolation matrix* (or *prolongation operator*) that interpolates from an approximation on the coarse grid to the fine grid, given for linear interpolation in our example by

$$P = \begin{bmatrix} \frac{1}{2} & & \\ 1 & & \\ \frac{1}{2} & \frac{1}{2} & \\ & 1 & \\ & \frac{1}{2} & \frac{1}{2} \\ & & 1 \\ & & \frac{1}{2} \end{bmatrix}_{7\times 3},$$

and $R \in \mathbb{R}^{M\times m}$ is a *restriction matrix*, which restricts a solution given on the fine grid to the coarse grid nodes. There are two common choices for R: the so-called injection, which simply selects the values on the fine grid where it coincides with the coarse grid, given in our example by

$$R := \begin{bmatrix} 0 & 1 & 0 & & & & \\ & & 0 & 1 & 0 & & \\ & & & & 0 & 1 & 0 \end{bmatrix}_{3\times 7},$$

and the *full weighting restriction matrix* $R := \frac{1}{2}P^\top$, which also takes into account values on the fine grid where there is no coarse grid node by averaging. We show in Figure 4.46 the action of the interpolation P and the restriction R graphically for our example. On the left, we see the action of the interpolation: the black points represent a vector $\boldsymbol{v} \in \mathbb{R}^3$ defined on the coarse grid, not including the boundary points where the function equals zero, and the circles represent the interpolated vector $\boldsymbol{w} = P\boldsymbol{v} \in \mathbb{R}^7$ on the fine grid, again not including the zero boundary points. In the middle of Figure 4.46, we show the action of the restriction operator R by injection: the black points represent a vector $\boldsymbol{w} \in \mathbb{R}^7$ defined on the fine mesh not including the zero boundary points, and the circles are the restricted vector $\boldsymbol{v} = R\boldsymbol{w} \in \mathbb{R}^3$ by injection, again without the zero boundary points. On the right in Figure 4.46, we show the action of the fully weighted restriction R: the black points represent a vector $\boldsymbol{w}$ defined on the fine mesh, and the circles are the fully weighted restricted vector $\boldsymbol{v} = R\boldsymbol{w}$.

Using the damped Jacobi method together with the coarse grid correction leads to one complete step of a two-grid algorithm starting with an initial guess $\boldsymbol{u}_0$, namely

$$\begin{aligned}
\boldsymbol{u}^n &= \boldsymbol{u}^{n-1} + \omega D^{-1}(\boldsymbol{f} - A\boldsymbol{u}^{n-1}) \quad \text{for } n = 1, 2, \ldots, \nu_1, \\
\boldsymbol{u}^0 &= \boldsymbol{u}^{\nu_1} + P A_{\mathrm{H}}^{-1} R(\boldsymbol{f} - A\boldsymbol{u}^{\nu_1}), \\
\boldsymbol{u}^n &= \boldsymbol{u}^{n-1} + \omega D^{-1}(\boldsymbol{f} - A\boldsymbol{u}^{n-1}) \quad \text{for } n = 1, 2, \ldots, \nu_2.
\end{aligned} \tag{4.112}$$

The method first performs ν_1 so-called presmoothing steps using damped Jacobi. Then the residual is computed and restricted to a coarse grid, where a coarse problem is solved, and the correction is prolongated to the fine grid and added to the current approximation. This is called the *coarse correction*. Then again ν_2 steps of damped Jacobi are applied, called *postsmoothing*. This represents one complete step of a stationary iterative method that can be written for the error in the form

$$\boldsymbol{e}^1 = G\boldsymbol{e}^0,$$

where the iteration matrix G is given by

$$G = \Big(I - \omega D^{-1}A\Big)^{\nu_2} \Big[I - P A_{\mathrm{H}}^{-1} RA\Big] \Big(I - \omega D^{-1}A\Big)^{\nu_1}, \tag{4.113}$$

as one can read off from (4.112): the first part of G from the right, i.e., $(I - \omega D^{-1}A)^{\nu_1}$ corresponds to the presmoothing, the second part $[I - P A_{\mathrm{H}}^{-1} RA]$ is the coarse grid correction, and the last part $(I - \omega D^{-1}A)^{\nu_2}$ represents the postsmoothing.

Unfortunately the iteration matrix G of the two-grid method cannot be diagonalized as easily as the Jacobi iteration. It is, however, possible to easily study the effect of G on two modes simultaneously, a low-frequency component and a corresponding high-frequency component, and we thus analyze the convergence of the two-grid method for an initial error given by

$$\boldsymbol{e}^0 = e_k \boldsymbol{\varphi}_k + e_{\widetilde{k}} \boldsymbol{\varphi}_{\widetilde{k}} = \begin{bmatrix} \boldsymbol{\varphi}_k & \boldsymbol{\varphi}_{\widetilde{k}} \end{bmatrix} \begin{bmatrix} e_k \\ e_{\widetilde{k}} \end{bmatrix},$$

where $\widetilde{k} = m + 1 - k$. The following two lemmas show that it is because of the restriction R and prolongation P that one has to use a low-frequency mode and its high-frequency companion together in the analysis.

Lemma 4.17 (Action of the fully weighted restriction operator). *Let the eigenfunction of the coarse discrete Laplacian matrix A_H be denoted by $\phi_{k,j} := \sin(k\pi 2jh)$ for $k = 1, \ldots, m$ with m odd. Then the fully weighted restriction matrix R combines a low-frequency mode $\boldsymbol{\varphi}_k$ together with its high-frequency counterpart $\boldsymbol{\varphi}_{\widetilde{k}}$, with $\widetilde{k} = m + 1 - k$, into a corresponding coarse mode $\boldsymbol{\phi}_k$,*

$$R \begin{bmatrix} \boldsymbol{\varphi}_k & \boldsymbol{\varphi}_{\widetilde{k}} \end{bmatrix} \begin{bmatrix} e_k \\ e_{\widetilde{k}} \end{bmatrix} = R\big(e_k \boldsymbol{\varphi}_k + e_{\widetilde{k}} \boldsymbol{\varphi}_{\widetilde{k}}\big) = (e_k c_k^2 - e_{\widetilde{k}} s_k^2)\boldsymbol{\phi}_k = \boldsymbol{\phi}_k \begin{bmatrix} c_k^2 & -s_k^2 \end{bmatrix} \begin{bmatrix} e_k \\ e_{\widetilde{k}} \end{bmatrix},$$

with the abbreviations $c_k := \cos(k\pi \frac{h}{2})$, $s_k := \sin(k\pi \frac{h}{2})$. The middle mode is mapped to zero by the restriction, $R\boldsymbol{\varphi}_{\frac{m+1}{2}} = 0$.

Proof. The proof is obtained by a direct calculation using trigonometric identities: for $k \leq \frac{m+1}{2}$, we obtain for $j \leq \frac{m+1}{2}$ that

$$\begin{aligned}\big[R\boldsymbol{\varphi}_k\big]_j &= \frac{1}{4}\big(\varphi_{k,2j-1} + 2\varphi_{k,2j} + \varphi_{k,2j+1}\big)\\ &= \frac{1}{4}\big(\sin(k\pi(2j-1)h) + 2\sin(k\pi 2jh) + \sin(k\pi(2j+1)h)\big)\\ &= \frac{1}{4}\big(2\sin(k\pi 2jh) + 2\cos(k\pi h)\sin(k\pi 2jh)\big),\end{aligned}$$

where we used the trigonometric identity $\sin(a-b) + \sin(a+b) = 2\sin a\cos b$. We can then further simplify to obtain

$$\begin{aligned}\big[R\boldsymbol{\varphi}_k\big]_j &= \frac{1}{4}\big(2\sin(k\pi 2jh) + 2\cos(k\pi h)\sin(k\pi 2jh)\big)\\ &= \frac{1}{2}\big(1+\cos(k\pi h)\big)\sin(k\pi 2jh)\\ &= \cos^2\Big(k\pi\frac{h}{2}\Big)\sin(k\pi 2jh)\\ &= c_k^2\phi_{k,j},\end{aligned} \tag{4.114}$$

where we used the identity $\cos^2\big(\frac{a}{2}\big) = \frac{1+\cos a}{2}$ and the definition of c_k and of the coarse mode $\boldsymbol{\phi}_k$.

For the middle mode $k = \frac{m+1}{2}$, one has that $\sin(k\pi 2jh) = \sin\big(\frac{m+1}{2}\pi 2j\frac{1}{m+1}\big) = 0$, which together with (4.114) implies that $R\boldsymbol{\varphi}_{\frac{m+1}{2}} = 0$.

Next, we consider the complementary high-frequency mode $\boldsymbol{\varphi}_{\widetilde{k}}$ and notice that

$$\begin{aligned}\varphi_{\widetilde{k},j} &= \sin(\widetilde{k}\pi jh) = \sin((m+1-k)\pi jh)\\ &= \sin\Big((m+1)\pi j\frac{1}{m+1} - k\pi jh\Big) = -(-1)^j\sin(k\pi jh),\end{aligned} \tag{4.115}$$

where we used the trigonometric identity $\sin(a-b) = \sin a\cos b - \cos a\sin b$. We can now compute similarly the action of the restriction R on the complementary mode, and using (4.115) we obtain

$$\begin{aligned}\big[R\boldsymbol{\varphi}_{\widetilde{k}}\big]_j &= \frac{1}{4}\big(\varphi_{\widetilde{k},2j-1} + 2\varphi_{\widetilde{k},2j} + \varphi_{\widetilde{k},2j+1}\big)\\ &= \frac{1}{4}\big(\sin(\widetilde{k}\pi(2j-1)h) + 2\sin(\widetilde{k}\pi 2jh) + \sin(\widetilde{k}\pi(2j+1)h)\big)\\ &= \frac{1}{4}\Big[-(-1)^{2j-1}\sin(k\pi(2j-1)h) - 2(-1)^{2j}\sin(k\pi 2jh) - (-1)^{2j+1}\sin(k\pi(2j+1)h)\Big]\\ &= -\frac{1}{4}\big(2\sin(k\pi 2jh) - 2\cos(k\pi h)\sin(k\pi 2jh)\big)\\ &= -\frac{1}{2}\big(1-\cos(k\pi h)\big)\sin(k\pi 2jh)\\ &= -\sin^2\Big(k\pi\frac{h}{2}\Big)\sin(k\pi 2jh)\\ &= -s_k^2\phi_{k,j},\end{aligned}$$

where we used the trigonometric identity $\sin^2\big(\frac{a}{2}\big) = \frac{1-\cos a}{2}$. This concludes our proof. ∎

Lemma 4.18 (Action of the prolongation operator). *The prolongation operator P generates from a coarse eigenmode $\boldsymbol{\phi}_k$ of the coarse discretized Laplacian A_H a low-frequency mode $\boldsymbol{\varphi}_k$ and the corresponding high-frequency mode $\boldsymbol{\varphi}_{\widetilde{k}}$ according to*

$$P\boldsymbol{\phi}_k = (c_k^2\boldsymbol{\varphi}_k - s_k^2\boldsymbol{\varphi}_{\widetilde{k}}) = \begin{bmatrix}\boldsymbol{\varphi}_k & \boldsymbol{\varphi}_{\widetilde{k}}\end{bmatrix}\begin{bmatrix}c_k^2\\ -s_k^2\end{bmatrix}.$$

Proof. Recalling the definition of P, we have to distinguish between the cases of j even and odd. For j odd, using that $H = 2h$, we obtain

$$\begin{aligned}[P\boldsymbol{\phi}_k]_j &= \frac{1}{2}\big(\phi_{k,\frac{j-1}{2}} + \phi_{k,\frac{j+1}{2}}\big)\\ &= \frac{1}{2}\left[\sin\left(k\pi\frac{j-1}{2}H\right) + \sin\left(k\pi\frac{j+1}{2}H\right)\right]\\ &= \frac{1}{2}\big[\sin\big(k\pi(j-1)h\big) + \sin\big(k\pi(j+1)h\big)\big]\\ &= \cos(k\pi h)\sin(kj\pi h),\end{aligned} \tag{4.116}$$

where we used the trigonometric identity $\sin(a-b)+\sin(a+b) = 2\sin a\cos b$. Now, we notice that

$$\begin{aligned}&\frac{1}{2}\big(1-\cos(k\pi h)\big) = \sin^2\Big(k\pi\frac{h}{2}\Big)\\ \Longrightarrow\quad &1 - 2\sin^2\Big(k\pi\frac{h}{2}\Big) = \cos(k\pi h)\\ \Longrightarrow\quad &-\sin^2\Big(k\pi\frac{h}{2}\Big) + \cos^2\Big(k\pi\frac{h}{2}\Big) = \cos(k\pi h)\\ \Longrightarrow\quad &\cos(k\pi h) = c_k^2 - s_k^2\end{aligned} \tag{4.117}$$

and

$$\begin{aligned}\sin((m+1-k)j\pi h) &= \sin\Big((m+1)j\pi\frac{1}{m+1} - kj\pi h\Big)\\ &= \sin(j\pi)\cos(kj\pi h) - \cos(j\pi)\sin(kj\pi h)\\ &= \sin(kj\pi h),\end{aligned} \tag{4.118}$$

where we used that j is odd and the trigonometric identity $\sin(a-b) = \sin a\cos b - \cos a\sin b$. Replacing (4.117) in (4.116) and using (4.118), we obtain

$$\begin{aligned}[P\boldsymbol{\phi}_k]_j &= (c_k^2 - s_k^2)\sin(kj\pi h)\\ &= c_k^2\sin(kj\pi h) - s_k^2\sin((m+1-k)j\pi h)\\ &= c_k^2\varphi_{k,j} - s_k^2\varphi_{\widetilde{k},j}.\end{aligned}$$

Now for j even, we first notice similarly as in (4.118) that

$$\begin{aligned}\sin((m+1-k)j\pi h) &= \sin\Big((m+1)j\pi\frac{1}{m+1} - kj\pi h\Big)\\ &= \sin(j\pi)\cos(kj\pi h) - \cos(j\pi)\sin(kj\pi h)\\ &= -\sin(kj\pi h),\end{aligned}$$

and we therefore obtain

$$\begin{aligned}[P\boldsymbol{\phi}_k]_j = \phi_{k,\frac{j}{2}} &= \sin\left(k\pi\frac{j}{2}H\right) = \sin(k\pi jh)\\ &= (c_k^2 + s_k^2)\sin(k\pi jh)\\ &= c_k^2\sin(k\pi jh) - s_k^2\sin((m+1-k)j\pi k)\\ &= c_k^2\varphi_{k,j} - s_k^2\varphi_{\widetilde{k},j},\end{aligned}$$

which concludes our proof. □

Using Lemmas 4.17 and 4.18, we can now precisely describe how the two-grid operator G acts on a low-frequency mode and its complementary high-frequency mode.

Lemma 4.19 (Action of the two-grid operator). *The action of the matrix G of the two-level method on a vector $e_k\boldsymbol{\varphi}_k + e_{\widetilde{k}}\boldsymbol{\varphi}_{\widetilde{k}}$ is given by*

$$G\begin{bmatrix}\boldsymbol{\varphi}_k & \boldsymbol{\varphi}_{\widetilde{k}}\end{bmatrix}\begin{bmatrix}e_k\\ e_{\widetilde{k}}\end{bmatrix} = \begin{bmatrix}\boldsymbol{\varphi}_k & \boldsymbol{\varphi}_{\widetilde{k}}\end{bmatrix} G_k \begin{bmatrix}e_k\\ e_{\widetilde{k}}\end{bmatrix}, \tag{4.119}$$

where

$$G_k := \begin{bmatrix}1-2\omega s_k^2 & 0\\ 0 & 1-2\omega c_k^2\end{bmatrix}^{\nu_2}\begin{bmatrix}s_k^2 & c_k^2\\ s_k^2 & c_k^2\end{bmatrix}\begin{bmatrix}1-2\omega s_k^2 & 0\\ 0 & 1-2\omega c_k^2\end{bmatrix}^{\nu_1}. \tag{4.120}$$

Proof. The proof is obtained in two steps. First, recalling that $D^{-1}A = -\frac{h^2}{2}A$ and the eigenvalues of A, which are $\lambda_k = -\frac{4}{h^2}s_k^2$, we compute for one Jacobi smoothing step

$$\begin{aligned}\left(I-\omega D^{-1}A\right)\begin{bmatrix}\boldsymbol{\varphi}_k & \boldsymbol{\varphi}_{\widetilde{k}}\end{bmatrix}\begin{bmatrix}e_k\\ e_{\widetilde{k}}\end{bmatrix} &= \left(I-\omega D^{-1}A\right)\left(e_k\boldsymbol{\varphi}_k + e_{\widetilde{k}}\boldsymbol{\varphi}_{\widetilde{k}}\right)\\ &= (1-2\omega s_k^2)e_k\boldsymbol{\varphi}_k + (1-2\omega s_{\widetilde{k}}^2)e_{\widetilde{k}}\boldsymbol{\varphi}_{\widetilde{k}}\\ &= (1-2\omega s_k^2)e_k\boldsymbol{\varphi}_k + (1-2\omega c_k^2)e_{\widetilde{k}}\boldsymbol{\varphi}_{\widetilde{k}},\end{aligned}$$

where the last equality is obtained because of

$$\begin{aligned}s_{\widetilde{k}} &= \sin\Big((m+1-k)\pi\frac{h}{2}\Big)\\ &= \sin\Big((m+1)\pi\frac{1}{2(m+1)}\Big)\cos\Big(k\pi\frac{h}{2}\Big) - \cos\Big((m+1)\pi\frac{1}{2(m+1)}\Big)\sin\Big(k\pi\frac{h}{2}\Big)\\ &= \cos\Big(k\pi\frac{h}{2}\Big) = c_k,\end{aligned}$$

since $\sin(a-b) = \sin a\cos b - \cos a\sin b$. We thus have for one Jacobi smoothing step

$$\left(I-\omega D^{-1}A\right)\begin{bmatrix}\boldsymbol{\varphi}_k & \boldsymbol{\varphi}_{\widetilde{k}}\end{bmatrix}\begin{bmatrix}e_k\\ e_{\widetilde{k}}\end{bmatrix} = \begin{bmatrix}\boldsymbol{\varphi}_k & \boldsymbol{\varphi}_{\widetilde{k}}\end{bmatrix}\begin{bmatrix}1-2\omega s_k^2 & 0\\ 0 & 1-2\omega c_k^2\end{bmatrix}\begin{bmatrix}e_k\\ e_{\widetilde{k}}\end{bmatrix}. \tag{4.121}$$

Next, we notice that for the coarse eigenfunction $\boldsymbol{\phi}_k$ we have

$$\begin{aligned}A_H\boldsymbol{\phi}_k &= -\frac{4}{H^2}\sin\Big(k\pi\frac{H}{2}\Big)\boldsymbol{\phi}_k = -\frac{4}{(2h)^2}\sin\Big(k\pi h\Big)\boldsymbol{\phi}_k\\ &= -\frac{2}{h^2}\sin\Big(k\pi\frac{h}{2}\Big)\cos\Big(k\pi\frac{h}{2}\Big)\boldsymbol{\phi}_k = -\frac{2}{h^2}s_kc_k\boldsymbol{\phi}_k,\end{aligned} \tag{4.122}$$

where we used again that $\sin(a+b) = \sin a\cos b + \sin b\cos a$ to obtain that $\sin(k\pi h) = \sin(k\pi h/2 + k\pi h/2) = 2\cos(k\pi h/2)\sin(k\pi h/2)$. Now, we denote by $\lambda_{H,k}$ the eigenvalues of A_H and compute using Lemmas 4.17 and 4.18

$$\begin{aligned}
PA_H^{-1}RA\begin{bmatrix}\boldsymbol{\varphi}_k & \boldsymbol{\varphi}_{\tilde{k}}\end{bmatrix} &= PA_H^{-1}R\begin{bmatrix}\boldsymbol{\varphi}_k & \boldsymbol{\varphi}_{\tilde{k}}\end{bmatrix}\begin{bmatrix}\lambda_k & 0\\ 0 & \lambda_{\tilde{k}}\end{bmatrix}\\
&= PA_H^{-1}\boldsymbol{\phi}_k\begin{bmatrix}c_k^2 & -s_k^2\end{bmatrix}\begin{bmatrix}\lambda_k & 0\\ 0 & \lambda_{\tilde{k}}\end{bmatrix}\\
&= P\boldsymbol{\phi}_k\frac{1}{\lambda_{H,k}}\begin{bmatrix}c_k^2 & -s_k^2\end{bmatrix}\begin{bmatrix}\lambda_k & 0\\ 0 & \lambda_{\tilde{k}}\end{bmatrix}\\
&= P\boldsymbol{\phi}_k\frac{1}{\lambda_{H,k}}\begin{bmatrix}c_k^2\lambda_k & -s_k^2\lambda_{\tilde{k}}\end{bmatrix}\\
&= \begin{bmatrix}\boldsymbol{\varphi}_k & \boldsymbol{\varphi}_{\tilde{k}}\end{bmatrix}\begin{bmatrix}c_k^2\\ -s_k^2\end{bmatrix}\begin{bmatrix}c_k^2\frac{\lambda_k}{\lambda_{H,k}} & -s_k^2\frac{\lambda_{\tilde{k}}}{\lambda_{H,k}}\end{bmatrix}\\
&= \begin{bmatrix}\boldsymbol{\varphi}_k & \boldsymbol{\varphi}_{\tilde{k}}\end{bmatrix}\begin{bmatrix}c_k^4\frac{\lambda_k}{\lambda_{H,k}} & -c_k^2s_k^2\frac{\lambda_{\tilde{k}}}{\lambda_{H,k}}\\ -c_k^2s_k^2\frac{\lambda_k}{\lambda_{H,k}} & s_k^4\frac{\lambda_{\tilde{k}}}{\lambda_{H,k}}\end{bmatrix}.
\end{aligned}$$

We thus obtain for the coarse correction step

$$\left(I - PA_H^{-1}RA\right)\begin{bmatrix}\boldsymbol{\varphi}_k & \boldsymbol{\varphi}_{\tilde{k}}\end{bmatrix} = \begin{bmatrix}\boldsymbol{\varphi}_k & \boldsymbol{\varphi}_{\tilde{k}}\end{bmatrix}\begin{bmatrix}1-c_k^4\frac{\lambda_k}{\lambda_{H,k}} & c_k^2s_k^2\frac{\lambda_{\tilde{k}}}{\lambda_{H,k}}\\ c_k^2s_k^2\frac{\lambda_k}{\lambda_{H,k}} & 1-s_k^4\frac{\lambda_{\tilde{k}}}{\lambda_{H,k}}\end{bmatrix}. \tag{4.123}$$

Using (4.122) and that $H = 2h$, we can simplify the ratios of the fine and coarse eigenvalues appearing in the matrix,

$$\begin{aligned}
\frac{\lambda_k}{\lambda_{H,k}} &= \frac{-\frac{4}{h^2}\sin^2(k\pi h/2)}{-\frac{4}{H^2}\sin^2(k\pi H/2)} = \frac{-\frac{1}{h^2}\sin^2(k\pi h/2)}{-\frac{1}{(2h)^2}\sin^2(k\pi H/2)} = \frac{4s_k^2}{(2s_kc_k)^2} = \frac{1}{c_k^2},\\
\frac{\lambda_{\tilde{k}}}{\lambda_{H,k}} &= \frac{-\frac{4}{h^2}\cos^2(k\pi h/2)}{-\frac{4}{H^2}\sin^2(k\pi H/2)} = \frac{4c_k^2}{(2s_kc_k)^2} = \frac{1}{s_k^2}.
\end{aligned} \tag{4.124}$$

Combining (4.123) and (4.124), we obtain for the coarse correction the simple action

$$\left(I - PA_H^{-1}RA\right)\begin{bmatrix}\boldsymbol{\varphi}_k & \boldsymbol{\varphi}_{\tilde{k}}\end{bmatrix} = \begin{bmatrix}\boldsymbol{\varphi}_k & \boldsymbol{\varphi}_{\tilde{k}}\end{bmatrix}\begin{bmatrix}1-c_k^2 & c_k^2\\ s_k^2 & 1-s_k^2\end{bmatrix} = \begin{bmatrix}\boldsymbol{\varphi}_k & \boldsymbol{\varphi}_{\tilde{k}}\end{bmatrix}\begin{bmatrix}s_k^2 & c_k^2\\ s_k^2 & c_k^2\end{bmatrix}. \tag{4.125}$$

The result in the lemma then follows from (4.125), (4.121) and recalling the structure of G given in (4.113). □

Lemma 4.19 implies that the subspace spanned by a low-frequency mode and its high-frequency companion, $\operatorname{span}\{\boldsymbol{\varphi}_k, \boldsymbol{\varphi}_{\tilde{k}}\}$, is an invariant subspace of the two-grid iteration matrix G. This implies, as the next lemma shows, that G is similar to a block-diagonal matrix.

Lemma 4.20 (Properties of the two-grid operator). *The two-grid matrix G is similar to the block-diagonal matrix*

$$\widetilde{G} = \begin{bmatrix}G_1 & & & \\ & \ddots & & \\ & & G_{\frac{m+1}{2}-1} & \\ & & & g\end{bmatrix}, \tag{4.126}$$

where the matrices G_k are defined in (4.120) *and $g = (1-\omega)^{\nu_1+\nu_2}$.*

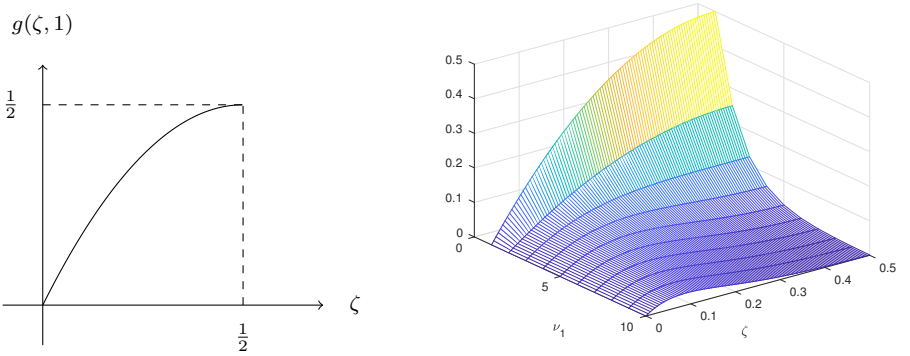

Figure 4.47. *Left: Upper bound of the convergence factor $\rho(G_k)$ as a function of ζ for $\nu_1 = 1$. Right: Spectral radius $\rho(G_k)$ as a function of ζ and ν_1.*

Proof. Consider the eigenvectors $\boldsymbol{\varphi}_k$ of A and define the matrix

$$Q = \begin{bmatrix} \boldsymbol{\varphi}_1 & \boldsymbol{\varphi}_m & \boldsymbol{\varphi}_2 & \boldsymbol{\varphi}_{m-1} & \cdots & \boldsymbol{\varphi}_{\frac{m+1}{2}-1} & \boldsymbol{\varphi}_{\frac{m+1}{2}+1} & \boldsymbol{\varphi}_{\frac{m+1}{2}} \end{bmatrix}.$$

Now, for $k = 1, \ldots, \frac{m+1}{2} - 1$ with $\widetilde{k} = m + 1 - k$ Lemma 4.19 implies that

$$G \begin{bmatrix} \boldsymbol{\varphi}_k & \boldsymbol{\varphi}_{\widetilde{k}} \end{bmatrix} = \begin{bmatrix} \boldsymbol{\varphi}_k & \boldsymbol{\varphi}_{\widetilde{k}} \end{bmatrix} G_k.$$

Moreover, according to Lemma 4.17 it holds that $R\boldsymbol{\varphi}_{\frac{m+1}{2}} = 0$, which allows us to compute that

$$G\boldsymbol{\varphi}_{\frac{m+1}{2}} = \left(1 - 2\omega s^2_{\frac{m+1}{2}}\right)^{\nu_1+\nu-2} = (1-\omega)^{\nu_1+\nu-2},$$

where $s^2_{\frac{m+1}{2}} = \frac{1}{2}$ is used. Therefore, we have obtained that $GQ = Q\widetilde{G}$ and the claim follows. ∎

Lemma 4.20 implies that the convergence factor of the two-grid method is the maximum over all k of the spectral radius of the 2×2 matrix in (4.119). If we consider for simplicity $\nu_2 = 0$, which means no postsmoothing, and $\omega = \frac{1}{2}$, this 2×2 matrix becomes

$$G_k = \begin{bmatrix} s_k^2 & c_k^2 \\ s_k^2 & c_k^2 \end{bmatrix} \begin{bmatrix} 1 - s_k^2 & 0 \\ 0 & 1 - c_k^2 \end{bmatrix}^{\nu_1} = \begin{bmatrix} s_k^2 & c_k^2 \\ s_k^2 & c_k^2 \end{bmatrix} \begin{bmatrix} c_k^2 & 0 \\ 0 & s_k^2 \end{bmatrix}^{\nu_1} = \begin{bmatrix} s_k^2 c_k^{2\nu_1} & c_k^2 s_k^{2\nu_1} \\ s_k^2 c_k^{2\nu_1} & c_k^2 s_k^{2\nu_1} \end{bmatrix}.$$

Notice that G_k is of the form $\begin{bmatrix} \alpha & \beta \\ \alpha & \beta \end{bmatrix}$ with $\alpha = s_k^2 c_k^{2\nu_1}$ and $\beta = c_k^2 s_k^{2\nu_1}$. Therefore, it is possible to compute its eigenvalues and obtain the spectral radius explicitly,

$$\rho(G_k) = s_k^2(1 - s_k^2)^{\nu_1} + (1 - s_k^2)s_k^{2\nu_1}. \tag{4.127}$$

The convergence factor of the multigrid method is then given by $\max_k \rho(G_k)$. The maximum has to be taken over the discrete values s_k, $k = 1, \ldots, \frac{m+1}{2} - 1$, and s_k^2 varies in the interval $[0, \frac{1}{2}]$ with the value $\frac{1}{2}$ attained at $k = \frac{m+1}{2}$. Hence one can bound the convergence factor by the maximum of the function $g(\zeta, \nu_1) := \zeta^2(1 - \zeta^2)^{\nu_1} + (1 - \zeta^2)\zeta^{2\nu_1}$ for $\zeta \in [0, \frac{1}{2}]$. This bound is shown in Figure 4.47 (left) as a function of ζ (and ν_1 fixed) and in Figure 4.47 (right) as a function of ζ and ν_1. These two figures show clearly that $\rho(G_k) \leq \max_{\zeta \in [0, \frac{1}{2}]} g(\zeta, \nu_1) < 1$.

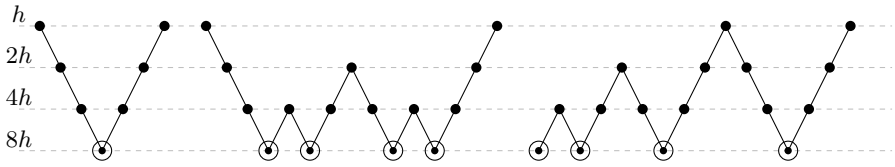

Figure 4.48. *V-cycle (left), W-cycle (middle), and FMG (right). The symbol • represents a smoothing step, while ⊙ represents a direct solution step.*

We thus obtain for the two-grid algorithm the following convergence result.

Theorem 4.21 (Convergence of the two-grid method). *The two-grid method without post-smoothing and relaxation parameter $\omega = \frac{1}{2}$ described by the iteration matrix G given in* (4.113) *converges independently of h, and we have the estimate*

$$\rho(G) \leq \max_{0 \leq \zeta \leq \frac{1}{2}} \left(\zeta(1-\zeta)^{\nu_1} + (1-\zeta)\zeta^{\nu_1} \right) < 1.$$

The theoretical result obtained in Theorem 4.21 is illustrated numerically in Figure 4.50 (left) below, where the decay of the norm of the residual is compared to the theoretical bound of Theorem 4.21 (see Problem 69 to produce this plot). This figure shows that the theoretical bound obtained is quite sharp, since the two curves are essentially parallel.

Now with the two-grid method, we in principle did not gain anything yet, since we still have to solve a problem of the same nature, just half the size, in the coarse correction step. The key idea of multigrid is that in the two-grid operator in (4.113), it is possible to apply the two-level method recursively instead of computing A_H^{-1}. One then does this as long as the coarse problem is still too big to be solved directly, which leads to the so-called multigrid V-cycle; see Figure 4.48 (left).

We now give an implementation of the multigrid V-cycle for our two-dimensional Laplace model problem in MATLAB:

```
function u=VCycle(A,f,u,l)
% VCYCLE performs a V-cycle of multigrid for the Laplace equation
%   u=VCycle(A,f,u,l) computes for the given linear system Au=f
%   representing a discretized Laplacian on a square domain using
%   the five-point finite difference stencil a V-cycle approximation
%   of the solution starting with the guess u using l levels.
%   The resolution size m=sqrt(length(f)) must be such that m+1 can
%   be divided by 2^l. The method uses damped Jacobi, and the number
%   of pre- and postsmoothing steps nu1 and nu2 as well as the damping
%   parameter w can be set in the code.

nu1=1; nu2=1;                          % pre- and postsmoothing steps
w=2/3;                                 % damping parameter for Jacobi
if l==1                                % direct solve on coarsest level
  u=A\f;
else
  for i=1:nu1                          % presmoothing with relaxed Jacobi
    u=u+w*(f-A*u)./diag(A);
  end
  r=f-A*u;                             % compute residual
  m=sqrt(length(f));
```

```
  R=RMatrix(m);                        % compute restriction matrix R
  M=(m+1)/2-1;
  H=1/(M+1);
  AH=Laplacian(M,2)/H^2;               % compute coarse matrix
  % AH=4*R*A*R';                       % can use Galerkin instead
  e=VCycle(AH,R*r,zeros(M^2,1),l-1); % compute coarse correction
  u=u+4*R'*e;                          % use full weighting
  for i=1:nu2                          % postsmoothing with relaxed Jacobi
    u=u+w*(f-A*u)./diag(A);
  end
end
```

Notice that in this V-cycle one reassembles the matrices R and A_H every time. Even though this choice is good for didactical purposes, one would not perform this reassembling in practical implementations (see Problem 68).

We see that to get the V-cycle, one simply calls the program itself when the coarse correction needs to be computed,[51] and the two-grid method is obtained by choosing for the level parameter $l = 2$. The program uses our earlier function `Laplacian.m` to compute the coarser matrices needed in the V-cycle. If the V-cycle is used several times, as is usually the case, it is more economic to compute all these operators at the beginning only once and to store them for later use. We also left a commented line which gives a different option for the coarse matrix, the so-called Galerkin approach which computes the coarse matrix using the restriction matrix R, which is computed in the V-cycle routine using the function `RMatrix`:

```
function R=RMatrix_NEW(m)
% RMATRIX construct restriction matrix of size M^2 x m^2
%   where m must have the form m=2^l-1 and hence M is M=2^(l-1)-1
%   R=RMatrix(m) constructs a restriction matrix of size M^2 x m^2
%   to be used in a multigrid code.

M=(m+1)/2-1;
p=sparse(m+2,1); p(1:3)=[0.5;1;0.5];
P=repmat(p,M,1); P=P(1:m*M); P=reshape(P,m,M);
R1D=1/2*P';
R=kron(R1D,R1D);
```

This is just the two-dimensional analogue of the linear interpolation we have seen. We can now test the V-cycle multigrid method on our model problem:

```
m=15;                                % resolution must be a power of 2 minus 1
l=5;                                 % levels, l not bigger than L in m=2^L-1
h=1/(m+1);
A=Laplacian(m,2)/h^2;                % construct the Laplacian on the fine grid
f=zeros(m*m,1);                      % right-hand side for our model problem
f(m:m:end)=1/h^2;
u=A\f;                               % exact solution
umg=zeros(size(f));                  % multigrid initial guess
U=zeros(m+2); U(end,1:m+2)=1;        % for plotting purposes
x=0:1/(m+1):1; y=x;                  % mesh point vectors
for n=0:10
  err(n+1)=max(max(abs(u-umg)));     % error in the infinity norm
```

[51] We give the coarse correction as initial guess zeros, since the coarse problem has the residual as the right-hand side and computes an approximation to the current error, for which zero is a good initial guess.

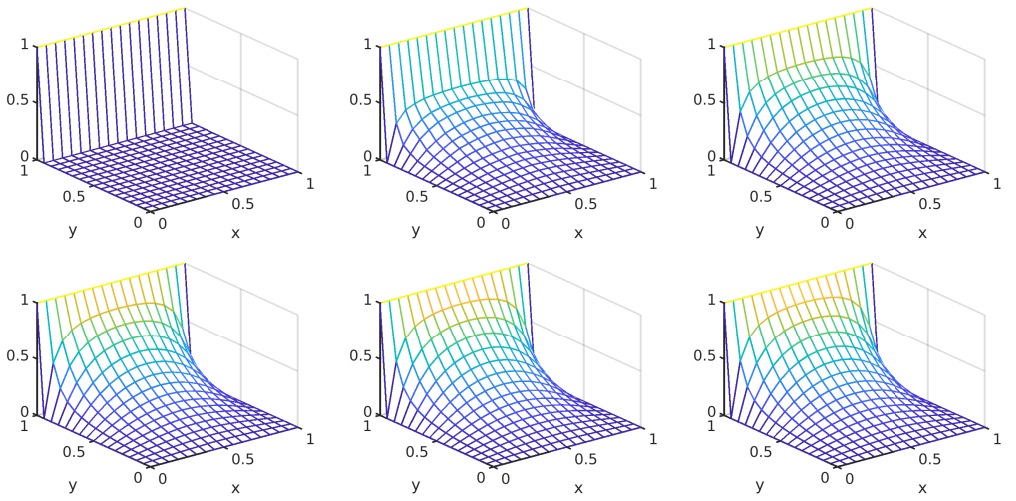

Figure 4.49. *Initial guess and first iterations of the multigrid V-cycle applied to our Laplace model problem.*

```
  U(2:m+1,2:m+1)=reshape(umg,m,m);
  mesh(x,y,U)                          % plot current approximation
  xlabel('x');ylabel('y');
  pause                                % perform a V-cycle
  umg=umg+VCycle(A,f-A*umg,zeros(size(f)),l);
end
```

This leads to the multigrid iterates shown in Figure 4.49. We used again $m = 15$ interior mesh points, and only one pre- and postsmoothing step, $\nu_1 = \nu_2 = 1$, and for the damping parameter in Jacobi $\omega = \frac{1}{2}$. We also used the maximum number of levels possible, $l = 5$, i.e., the coarsest problem we solve by the direct solver backslash in MATLAB is only of size 1×1. One can see how effective the V-cycle is: we arrive sufficiently close to the solution after only five iterations.

To illustrate that the convergence of the multigrid method is also independent of the mesh parameter h, we show in Figure 4.50 how the error decays in the multigrid method for the mesh we used for Figure 4.49 with $m = 15$, and also on two refined meshes with $m = 31$ and $m = 63$ interior mesh points. We clearly see that convergence is independent of the mesh parameter h, and also quite well predicted by the analysis in Theorem 4.21, even though we did not include the postsmoothing step in the analysis.

The performance of the multigrid algorithm is impressive, since it basically gives mesh-independent convergence at a cost per iteration which is bounded by the cost of $1.65(\nu_1 + \nu_2)$ Jacobi iterations on the fine mesh: the main cost in the algorithm are the Jacobi iterations on the finest mesh, where there are $\nu_1 + \nu_2$ of them, and then on the next coarser mesh the matrix is only a quarter of the size, so the Jacobi iterations on that mesh cost only a quarter of $\nu_1 + \nu_2$ on the finest mesh, and on the next coarser one only a sixteenth, and so on, which leads by summing $\sum_{i=1}^{\infty} \frac{1}{i^2} = \frac{1}{6}\pi^2 \approx 1.645$ to the estimate given by the factor 1.65.

The V-cycle is not the only multilevel extension of the two-grid method. Two other common examples are the W-cycle and the full multigrid (FMG), whose schematic representations are given in Figure 4.48 (middle and right). The main idea of the W-cycle is to perform more iterations on the coarse levels which are computationally cheaper and more efficient against low-frequency components of the error. The multigrid setting suggests a natural way of how to get

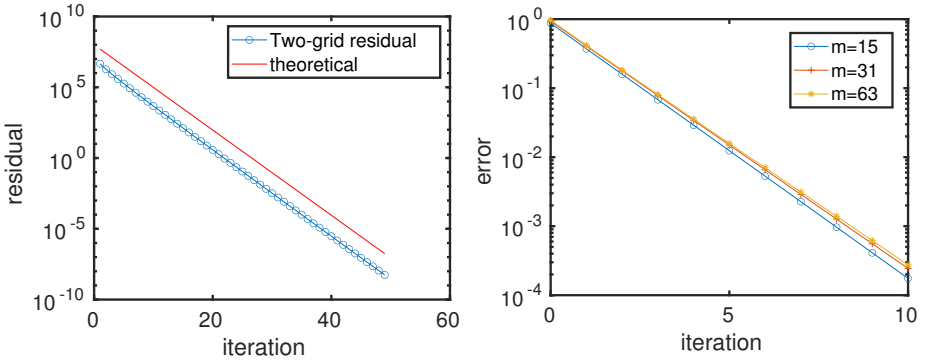

Figure 4.50. *Left: Decay of the residual (blue curve) of a two-grid iteration (with $\nu_1 = 1$ and $\nu_2 = 0$ for the solution of a one-dimensional Laplace problem and theoretical bound (red curve) corresponding to the developed convergence analysis. Right: Convergence of the multigrid method for different mesh sizes $h = \frac{1}{m+1}$.*

a good initial guess cheaply: one can start the multigrid iterations at the coarser level and move iteratively to the upper levels. This idea leads to the FMG depicted in Figure 4.48 (right).

4.11 ▪ Problems

Problem 51. *Implement the preconditioned CG method given in Theorem 4.2.*

Problem 52. *Consider the two-dimensional discrete Laplace problem (characterized by a matrix A and mesh size h). Use the MATLAB function* `ilu` *to obtain the incomplete factorization $A = \widetilde{L}\widetilde{R} - R$ corresponding to a certain tolerance ϵ (see Section 4.5). Write a MATLAB implementation for the stationary method corresponding to the splitting $A = \widetilde{L}\widetilde{R} - R$ and solve the problem for different mesh sizes h. Repeat this experiment changing the ILU parameter ϵ and try to determine how much fill-in of the matrices $\widetilde{L}$ and $\widetilde{R}$ is needed in order to obtain a mesh-independent stationary method.*

Problem 53. *Consider the two-dimensional discrete Laplace problem (characterized by a matrix A and mesh size h). Modify the* `ILU0` *MATLAB algorithm given in Section 4.5 in order to obtain an incomplete factorization using the sparsity pattern of A^k for $k \in \mathbb{N}$.*

Problem 54. *Use the* `SPAI` *function given in Section 4.5 and write a code that produces the plots of Figures 4.9, 4.10, 4.11, and 4.12, representing the first iterates of SPAI (used as a stationary method), the plots of Figures 4.14 and 4.15, showing the convergence of SPAI, and the plots of Figure 4.13, representing the sparsity patterns of the SPAI preconditioners.*

Problem 55. *Consider the two-dimensional advection-reaction-diffusion-problem of Section 1.4 (use, e.g., the data of Problem 4).*

- *Solve the problem using ILU0 and SPAI as stationary methods.*
- *Solve the problem using GMRES preconditioned by ILU0 and SPAI.*
- *Solve the problem using FGMRES preconditioned by both ILU0 and SPAI used in an alternating way.*

In all cases, plot the first few iterations and study the dependence on the mesh size h and on the sparsity pattern (using A^k as in Problem 53).

Problem 56. *Consider the one-dimensional Laplace problem*

$$-\frac{d^2u(x)}{dx^2} = f(x) \quad \text{in } \Omega = (0,1) \text{ with } u(0) = u(1) = 0.$$

Discretize this problem with finite differences on a uniform mesh of size h to obtain $A\boldsymbol{u} = \boldsymbol{f}$, where A is the (negative) discrete Laplacian.

Now, consider a domain decomposition $\Omega = \Omega_1 \cup \Omega_2$ with $\Omega_1 = (0, \alpha)$ and $\Omega_2 = (\beta, 1)$ with $\beta < \alpha$ and $\delta = \alpha - \beta$ being the overlap. The alternating and the parallel Schwarz methods are given by

$$-\frac{d^2u_1^{n+1}(x)}{dx^2} = f(x) \quad \text{in } (0,\alpha) \text{ with } u_1^{n+1}(0) = 0 \text{ and } u_1^{n+1}(\alpha) = u_2^n(\alpha),$$
$$-\frac{d^2u_2^{n+1}(x)}{dx^2} = f(x) \quad \text{in } (\beta,1) \text{ with } u_2^{n+1}(\beta) = u_1^n(\beta) \text{ and } u_2^{n+1}(1) = 0$$

and

$$-\frac{d^2u_1^{n+1}(x)}{dx^2} = f(x) \quad \text{in } (0,\alpha) \text{ with } u_1^{n+1}(0) = 0 \text{ and } u_1^{n+1}(\alpha) = u_2^n(\alpha),$$
$$-\frac{d^2u_2^{n+1}(x)}{dx^2} = f(x) \quad \text{in } (\beta,1) \text{ with } u_2^{n+1}(\beta) = u_1^{n+1}(\beta) \text{ and } u_2^{n+1}(1) = 0,$$

respectively. Discretize these subproblems by means of finite differences on uniform meshes of size h. Show that, at a discrete level, the alternating and parallel Schwarz methods with minimal overlap, that is, $\delta = h$, are equivalent to block-Gauss–Seidel and block-Jacobi methods for the solution to $A\boldsymbol{u} = \boldsymbol{f}$. How fast do these methods converge? (Recall Problem 19 in Chapter 2.)

Problem 57. *Consider the one-dimensional Laplace problem and the two-subdomain decomposition as in Problem 56. Prove that (at a continuous level) the alternating and parallel Schwarz methods converge and study the dependence of the corresponding convergence factors on the overlap $\delta = \alpha - \beta$.*

Problem 58. *Consider for simplicity the one-dimensional Laplace problem and the two-subdomain decomposition as in Problem 56. Show that the discrete parallel Schwarz method, the additive Schwarz method, and the restricted additive Schwarz (RAS) method are equivalent if $\delta = h$ (minimal overlap) holds.*

Problem 59. *Implement the discrete alternating and parallel Schwarz method for the Laplace problem on the unit square with two rectangular subdomains. Experiment with different mesh sizes, overlap parameters, and boundary conditions and describe your findings.*

Problem 60. *Implement the additive Schwarz method and the RAS method for the Poisson problem on the unit square with two rectangular subdomains. Experiment with different mesh sizes, overlap parameters, and boundary conditions and describe your findings.*

Problem 61. *Repeat Problem 59 considering an advection-reaction-diffusion problem.*

Problem 62. *Repeat Problem 60 considering an advection-reaction-diffusion problem.*

Problem 63. *Investigate in detail the value of the first three iterates of the optimized Schwarz method* (4.52) *when using the optimal choice of the parameters* p_1 *and* p_2 *in* (4.58)*. Can you also get the result in a finite number of iterations with a different choice? Investigate the same also for the parallel optimized Schwarz variant introduced by Lions.*

Problem 64. *Implement the alternating optimized Schwarz method for the Poisson problem on the unit square with two rectangular subdomains using two different approaches:*

- *By discretizing the continuous formulation and only computing subdomain solutions. Hint: Make use of the Robin solver from the Dirichlet–Neumann section 4.7.*
- *By using restriction operators* R_j *in the form of the optimized multiplicative and RAS methods.*

For the second part, you need to show what changes in the subdomain matrices are necessary to obtain an equivalent program to the first one, similar to the proof of Theorem 4.7. What is the smallest overlap needed so that the second implementation still faithfully represents the discretization of an optimized Schwarz method?

Problem 65. *Implement the parallel optimized Schwarz method for the Poisson problem on the unit square with two rectangular subdomains using two different approaches:*

- *By discretizing the continuous formulation and computing only subdomain solutions.*
- *By using restriction operators* R_j *and* $\widetilde{R}_j$ *in the form of an ORAS method.*

For the second part, you need to show what changes in the subdomain matrices are necessary to obtain a program equivalent to the first one. Is there a restriction on the overlap size? Could this also be done with additive Schwarz?

Problem 66. *Implement RAS for a square decomposed into an arbitrary number* $J \times J$ *of equally sized small square domains. Test the convergence when* J *is increasing. What do you observe? What happens if your domain is a chain of squares, and you add more and more squares to make the domain longer?*

Problem 67. *Show that the damped Jacobi method* (4.109) *corresponds to the splitting* $A = M - N$ *with* $M = \frac{1}{\omega}D$ *and* $N = \frac{1}{\omega}[(1-\omega)D - \omega(L+U)]$.

Problem 68. *Modify the V-cycle algorithm given in Section 4.10 to avoid that the matrices* R *and* A_H *are reassembled at every iteration.*

Problem 69. *Implement a two-grid method (with a damped Jacobi smoother) for the solution of a discrete one-dimensional Laplace problem. Reproduce the results shown in Figure 4.50 (left).*

Problem 70. *Consider the multigrid method for the solution of the two-dimensional Laplacian. Change the codes provided in Section 4.10 in order to replace the Jacobi smoother with other smoothing operators (Gauss–Seidel, SOR, RAS, etc.). Compare and discuss the observed convergence.*

Problem 71. *Consider the discrete Laplace problem. Implement and test the preconditioners considered in this chapter. Compare the different preconditioned GMRES behaviors for different values of mesh size* h.

Chapter 5

Optimal Control

LET THERE BE LIGHT!
So went the seminal control command that created the physical universe, and gave it impetus for the explosive expansion of the original Big-Bang. From the viewpoint of control theory the primary question is:

> *Was the creation an open-loop command initiating the response at a specified time-say, at $t = 0$?*

or

> *Was this a closed-loop command set to trigger action at a specified state of the universe-say, at a quantum-mechanical negative-vacuum?*

Probably we shall never know the answer since the experiment is too difficult to repeat, and, despite scientific chutzpah, the state space is too intricate to analyze.

Lawrence Markus, *A Brief History of Control*, 1994.

Different theories have been suggested in the mathematical literature about the origin of optimal control theory; see for example the nice historical reviews [146] and [80]. H. J. Sussmann and J. C. Willems, two famous control theorists, claimed in [173] that optimal control theory was born in 1697 in Groningen, a beautiful city in the Netherlands[52] where J. Bernoulli (1667–1748) was professor of mathematics. Bernoulli challenged the mathematical community with the famous brachystochrone problem in 1697. As Sussmann and Willems mention in [173], another hypothesis is that optimal control theory was born with the work on the *Pontryagin maximum principle* by L. S. Pontryagin and his group [149]. Lev Semyonovich Pontryagin (1908–1988) was a Soviet mathematician (a topologist) and presented his famous maximum principle at the International Congress of Mathematics in 1958. The mathematical community did not show particular enthusiasm for Pontryagin's work. This reaction was probably motivated by different reasons. First, some mathematicians of that period believed that Pontryagin's work and optimal control theory was no more than a minor addition to the classical calculus of variations. Second, Pontryagin was notoriously anti-Semitic and his result seemed to be primarily intended for military reasons [173]. A beautiful description of the reaction to the work of Pontryagin at the

[52] Jan C. Willems, the second author of [173], is professor at the University of Groningen. Therefore, it is natural to suspect that the thesis presented in [173] is biased by the scientific affiliation of this author. We prefer to let the reader be the judge.

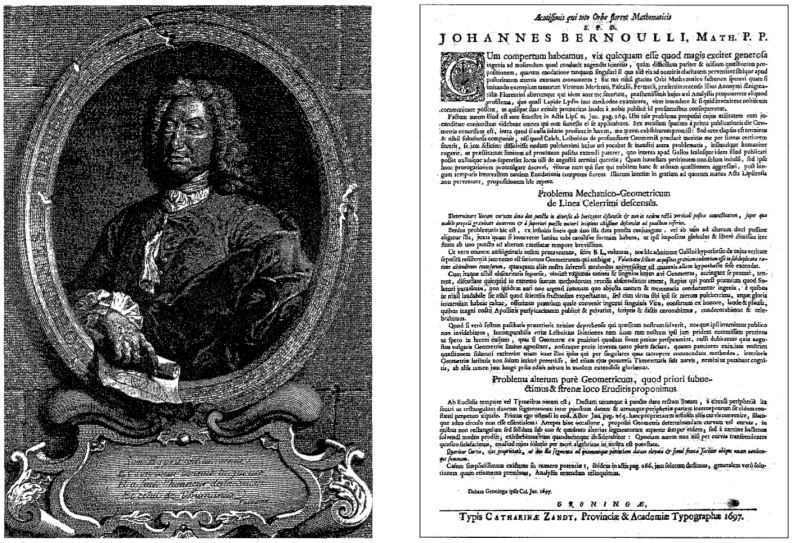

JOHANNES BERNOULLI, MATH. P. P.

Problema Mechanico-Geometricum
de Linea Celerrimi descensus.

Problema alterum parè Geometricum, quod priori subnectimus & ferene loco Eruditis proponimus.

GRONINGÆ,
Typis CATHARINÆ ZANDT, Provinciæ & Academiæ Typographæ 1697.

Figure 5.1. *Johannes Bernoulli (left) and his announcement of the brachystochrone problem (right). © 1997 IEEE. Reprinted, with permission, from [173].*

1958 International Congress of Mathematics is given by Lawrence Markus in his historical work "A Brief History of Control," published in 1994 [60, Section 7]:

> At the International Congress of Mathematicians in Edinburgh in 1958 L. S. Pontryagin presented a major invited address "Optimal Processes of Regulation". At that time Russians in the West were exotic phenomena, and the excitement of the occasion was inflated by the fame and mathematical eminence of Pontryagin—the great topologist who was renowned for his research in cohomology by means of characteristic classes and for the duality theory of topological groups. The lecture hall was overflowing and Lipman Bers[53] had assumed his place for an English simultaneous translation of the lecture. The international mathematical audience, led by a concentration of abstract topologists, were flabbergasted and astonished as the lecture developed. Pontryagin seemed to be talking about some kind of engineering, leaving them feeling ignorant and confused. The Maximum Principle of Pontryagin seemed mysterious and incomprehensible, except to those relatively few who were experts on control theory and who were already familiar with the Bang-Bang principle in the linear case treated previously by Bellman. I recognized this direction of mathematical analysis, and also I had previously met Pontryagin (as Lefschetz' assistant) and knew very well of his long-standing interest in the problems of applied dynamical systems. After a few days of reflection and gossip at the Congress, the mathematical establishment decided that the Maximum Principle wasn't about engineering, after all, but was instead a topic in the classical calculus of variations (similar to earlier results of M. Hestenes). Thus the consensus of the Congress came to the conclusion that control theory might be mathematically respectable, but that it was dull and boring—the position still held by many of the avant-garde of abstract mathematicians.

Lawrence Markus is Professor Emeritus at the University of Minnesota. He is one of the most famous control theorists and is author of the book *Foundations of Optimal Control Theory* [122], a milestone in optimal control theory.

[53] Probably Markus refers to the mathematician Lipman "Lipa" Bers, famous for his theory of pseudoanalytic functions.

Optimal control theory deals with the problem of finding a control law for a given dynamical system such that a certain optimality criterion is achieved. More precisely, consider a dynamical system

$$\dot{\boldsymbol{y}}(t) = \boldsymbol{f}(\boldsymbol{y}(t), \boldsymbol{u}(t), t) \text{ for } t \text{ in } [0, T]. \tag{5.1}$$

The original goal of optimal control theory was to find a control function $\boldsymbol{u} : [0, T] \to \mathbb{R}^m$ such that the state of the system $\boldsymbol{y} : [0, T] \to \mathbb{R}^n$ is steered from a given initial state $\boldsymbol{y}_0 \in \mathbb{R}^n$ to a desired target configuration satisfying certain criteria. The desired optimality criteria are in general incorporated in a cost functional $J(\boldsymbol{y}, \boldsymbol{u})$ that has to be minimized on the space of solutions to (5.1) and such that some constraints on $\boldsymbol{u}$ and $\boldsymbol{y}$ are satisfied, e.g., $\boldsymbol{h}(\boldsymbol{y}(t), \boldsymbol{u}(t)) \leq 0$ for some given function $\boldsymbol{h}$. Optimal control problems have the form

$$\begin{aligned} \min_{\boldsymbol{y},\boldsymbol{u}} \quad & J(\boldsymbol{y}, \boldsymbol{u}) \\ \text{s.t.} \quad & \dot{\boldsymbol{y}}(t) = \boldsymbol{f}(\boldsymbol{y}(t), \boldsymbol{u}(t), t) \text{ for } t \text{ in } [0, T], \boldsymbol{y}(0) = \boldsymbol{y}_0, \\ & \boldsymbol{h}(\boldsymbol{y}(t), \boldsymbol{u}(t)) \leq 0 \text{ for } t \in [0, T]. \end{aligned} \tag{5.2}$$

A typical form of cost functional is

$$J(\boldsymbol{y}, \boldsymbol{u}) = g(\boldsymbol{y}(T)) + \int_0^T L(\boldsymbol{y}(t), \boldsymbol{u}(t), t)\, dt,$$

where the first term is a final-time tracking term, while the second term is used to enforce the trajectory $\boldsymbol{y}(t)$ and the control $\boldsymbol{u}$ to satisfy certain criteria. Typical examples of these terms are

$$g(\boldsymbol{y}(T)) = \frac{\alpha}{2} \|\boldsymbol{y}(T) - \boldsymbol{y}_T\|_2^2,$$

which penalizes the distance between the trajectory at the final time T and a desired target state $\boldsymbol{y}_T \in \mathbb{R}^n$, and

$$\int_0^T L(\boldsymbol{y}(t), \boldsymbol{u}(t), t)\, dt = \frac{\beta}{2} \int_0^T \|\boldsymbol{y}(t) - \boldsymbol{y}_d(t)\|_2^2\, dt + \frac{\nu}{2} \int_0^T \|\boldsymbol{u}(t)\|_2^2\, dt,$$

having the goal of keeping the trajectory $\boldsymbol{y}(t)$ as close as possible to a desired trajectory $\boldsymbol{y}_d(t)$ and to penalize the cost of the control mechanism. The three parameters α, β, and ν are non-negative real numbers and are used to tune the different terms of the cost functional.

Over the course of time, optimal control theory has shown its enormous power and versatility that has allowed scientists, engineers, and many others to use it in a large number of applications. Nowadays, optimal control theory is a very active research area in mathematics, physics, engineering, chemistry, etc.; see, e.g., [20, 23, 114, 126, 178].

Even though optimal control theory was originally developed with the goal of controlling dynamical systems, the control of stationary equations became over the course of time a very important field; see, e.g., [126, 178] and references therein. Since in this book we do not consider time-dependent problems, we will focus on optimal control problems governed by the Laplace equation described in the previous chapters.

5.1 ▪ Optimal control of the Laplace equation

The optimal control of ordinary differential equations is of interest not only for aviation and space technology. In fact, it is also important in fields such as robotics, movement sequences in sports, and the control of chemical processes and power plants, to name just a few of the various applications. In many cases, however, the processes to be optimized can no longer be adequately modeled by ordinary differential equations; instead, partial differential equations have to be employed for their description. For instance, heat conduction, diffusion, electromagnetic waves, fluid flows, freezing processes, and many other physical phenomena can be modeled by partial differential equations.

Fredi Tröltzsch, *Optimal Control of Partial Differential Equations: Theory, Methods, and Applications*, 2010.

Let $\Omega \subset \mathbb{R}^d$ be a bounded Lipschitz domain for $d \in \{1, 2, 3\}$. Consider the optimal control problem governed by the Laplace equation

$$\begin{aligned} \min_{y,u} \quad & J(y,u) := \frac{1}{2}\|y - y_d\|_{L^2}^2 + \frac{\nu}{2}\|u\|_{L^2}^2 \\ \text{s.t.} \quad & -\Delta y = f + u \ \text{ in } \Omega, \\ & y = 0 \qquad \text{on } \partial\Omega, \end{aligned} \tag{5.3}$$

where $f, y_d \in L^2(\Omega)$, $\nu > 0$, and $\|\cdot\|_{L^2}$ is the usual $L^2(\Omega)$-norm. The variable u is called the control function and it is used to influence the physical system (here represented by the Laplace equation) in order to produce a state variable y that is "close" to a given target state configuration y_d.[54] The parameter ν is a regularization parameter used to tune the weight of the control function, that is, $\frac{1}{2}\|u\|_{L^2}^2$, with respect to the weight of the so-called tracking term $\frac{1}{2}\|y - y_d\|_{L^2}^2$. The functional J is called the *cost functional*.

Assume that we discretize the Laplace problem in (5.3) by using, e.g., a finite-difference approximation as done in Chapter 1. In particular, the domain Ω (for example, a d-dimensional cube) is discretized with a uniform grid of m points and mesh size h. Then any vector $\boldsymbol{v} \in \mathbb{R}^m$ can be regarded as a nodal approximation of a function defined in Ω. For any $\boldsymbol{v}, \boldsymbol{w} \in \mathbb{R}^m$ we introduce the inner product $\langle \boldsymbol{v}, \boldsymbol{w} \rangle_h := h^d \boldsymbol{v}^\top \boldsymbol{w}$ and the induced norm $\|\boldsymbol{v}\|_h := \langle \boldsymbol{v}, \boldsymbol{v} \rangle_h^{1/2}$. Notice that $\langle \cdot, \cdot \rangle_h$ and $\|\cdot\|_h$ are approximations of the $L^2(\Omega)$ inner product and the corresponding norm.

A (finite-difference) discretization of (5.3) is then given by

$$\begin{aligned} \min_{\boldsymbol{y},\boldsymbol{u}} \quad & J_h(\boldsymbol{y},\boldsymbol{u}) := \frac{1}{2}\|\boldsymbol{y} - \boldsymbol{y}_d\|_h^2 + \frac{\nu}{2}\|\boldsymbol{u}\|_h^2 \\ \text{s.t.} \quad & A\boldsymbol{y} = \boldsymbol{f} + \boldsymbol{u}, \end{aligned} \tag{5.4}$$

where $A \in \mathbb{R}^{m \times m}$ is the discretization of the negative Laplace operator, and $\boldsymbol{y}$ and $\boldsymbol{u}$ are in $\mathbb{R}^m$ and represent the discrete counterparts of the state y and the control u. The vector $\boldsymbol{y}_d \in \mathbb{R}^m$ is the discrete approximation of the target state y_d, and $\boldsymbol{f} \in \mathbb{R}^m$ represents the approximation of f. Notice also that a finite-element discretization of (5.3) has exactly the form (5.4), assuming that the matrix A and the inner product $\langle \cdot, \cdot \rangle_h$ are appropriately replaced by their finite-element companions.

In this chapter, we discuss iterative methods for the efficient solution of (5.3) and (5.4). However, well-posedness of (5.3) (and hence of (5.4)) is first discussed in Section 5.1.1. Moreover,

[54] Notice that in this chapter y denotes the solution to the Poisson equation, while u is a right-hand-side function for the PDE problem. This is in contrast to the previous chapters of this book, where u denoted the solution to the PDE problem. However, denoting by u the control function and by y the solution to the elliptic PDE is a classical notation in the field of optimal control theory.

iterative methods for the solution of (5.3) and (5.4) are based on the so-called first-order optimality system, which is introduced and discussed in Section 5.1.2.

5.1.1 ▪ Existence and uniqueness of a minimizer

> *We remark generally that if for a given problem existence cannot be shown by standard techniques, this is often due to mistakes made during the process of modeling; such mistakes are also likely to lead to numerical difficulties.*
>
> Fredi Tröltzsch, *Optimal Control of Partial Differential Equations: Theory, Methods, and Applications*, 2010.

In a weak form the Laplace problem in (5.3) is to find a $y \in H_0^1(\Omega)$ such that

$$a(y,v) = \ell(v) + \int_\Omega u(\boldsymbol{x})v(\boldsymbol{x})\,d\boldsymbol{x} \quad \forall v \in H_0^1(\Omega), \tag{5.5}$$

where $a(y,v)$ is a bilinear form defined as

$$a(y,v) := \int_\Omega \nabla y(\boldsymbol{x})\nabla v(\boldsymbol{x})\,d\boldsymbol{x},$$

and $\ell(v)$ is a linear functional given by

$$\ell(v) := \int_\Omega f(\boldsymbol{x})v(\boldsymbol{x})\,d\boldsymbol{x}.$$

The optimal control problem (5.3) becomes

$$\min_{y,u}\ J(y,u) := \frac{1}{2}\|y - y_d\|_{L^2}^2 + \frac{\nu}{2}\|u\|_{L^2}^2 \tag{5.6}$$

subject to

$$\begin{aligned} &a(y,v) = \ell(v) + \int_\Omega u(\boldsymbol{x})v(\boldsymbol{x})\,d\boldsymbol{x} \quad \forall v \in H_0^1(\Omega),\\ &u \in L^2(\Omega). \end{aligned} \tag{5.7}$$

In what follows the space $H_0^1(\Omega)$ is endowed with the usual norm $\|v\|_{H^1}^2 := \|\nabla v\|_{L^2}^2 + \|v\|_{L^2}^2$.[55]

The first step toward existence of a minimizer for (5.6)–(5.7) is to prove existence and uniqueness of a solution to (5.5). To do so, we first show that ℓ is a bounded linear functional and a is a bounded and coercive bilinear form.[56]

Lemma 5.1 (Boundedness of ℓ, boundedness and coercivity of a). *The functional $\ell : H_0^1(\Omega) \to \mathbb{R}$ is linear and bounded. The bilinear form $a : H_0^1(\Omega) \times H_0^1(\Omega) \to \mathbb{R}$ is bounded and coercive.*

Proof. The linearity of ℓ follows from the linearity of the integral. Boundedness of ℓ follows from the Cauchy–Schwarz inequality:

$$|\ell(v)| = \left|\int_\Omega f(\boldsymbol{x})v(\boldsymbol{x})\,d\boldsymbol{x}\right| \le \|f\|_{L^2}\|v\|_{L^2} \le \|f\|_{L^2}\|v\|_{H^1}.$$

[55] Notice that one could equivalently work with the H_0^1-norm defined as $\|v\|_{H_0^1} := \|\nabla u\|_{L^2}$.

[56] The boundedness of the bilinear form $a : H_0^1(\Omega) \times H_0^1(\Omega) \to \mathbb{R}$ must not be confused with the boundedness of the Laplace operator (for which the corresponding domain must be carefully defined).

Using again the Cauchy–Schwarz inequality one obtains boundedness of a:

$$|a(y,v)| \leq \|\nabla y\|_{L^2}\|\nabla v\|_{L^2} \leq \|y\|_{H^1}\|v\|_{H^1}.$$

To show coercivity, we first notice that $a(v,v) = \|\nabla v\|_{L^2}^2$ and then use the Poincaré–Friedrichs inequality [48, Theorem 6.5-2] to write $a(v,v) = \|\nabla v\|_{L^2}^2 \geq \frac{1}{c_\star}\|v\|_{L^2}^2$, where $c_\star$ is a (Poincaré) constant depending on the domain Ω. This implies that

$$a(v,v) \geq \frac{1}{c_\star}\|v\|_{L^2}^2 \geq \min\left\{1, \frac{1}{c_\star}\right\}\|v\|_{L^2}^2$$

and

$$a(v,v) = \|\nabla v\|_{L^2}^2 \geq \min\left\{1, \frac{1}{c_\star}\right\}\|\nabla v\|_{L^2}^2,$$

where we introduced the $\min$ over the constants in order to sum these two estimates to get $a(v,v) \geq \frac{1}{2}\min\{1, \frac{1}{c_\star}\}\|v\|_{H^1}^2$, which is our claim. □

The previous lemma allows us to prove existence and uniqueness of a weak solution to (5.5).

Theorem 5.2 (Existence and uniqueness of a weak solution). *For every $u \in L^2(\Omega)$ there exists a unique weak solution $y \in H_0^1(\Omega)$ to* (5.5)*. Moreover, there exists a positive constant c_0 such that*

$$\|y\|_{H^1} \leq c_0(\|f\|_{L^2} + \|u\|_{L^2}). \tag{5.8}$$

Proof. Note that, similarly as done for ℓ, one can show that the map $v \in H_0^1(\Omega) \mapsto \int_\Omega u(\boldsymbol{x})v(\boldsymbol{x})\,d\mathbf{x} \in \mathbb{R}$ is a bounded linear functional. Hence, using the previous lemma, one can invoke the Lax–Milgram theorem (see Theorem 6.8 in the appendix), which allows us to obtain existence and uniqueness of a weak solution. The bound (5.8) follows by combining coercivity and boundedness of the bilinear form a. □

We now prove the following technical result.

Lemma 5.3 (Control-to-state map). *Let $\{u_k\}_{k\in\mathbb{N}}$ be a weakly convergent sequence in $L^2(\Omega)$, i.e., $u_k \rightharpoonup \widetilde{u}$ in $L^2(\Omega)$ for $k \to \infty$. Consider the sequence $\{y_k\}_{k\in\mathbb{N}} \subset H_0^1(\Omega)$ defined as $y_k := y(u_k)$ (solutions to* (5.5)*). There exists a subsequence $\{y_{\widetilde{k}}\}_{\widetilde{k}\in\mathbb{N}}$ that converges weakly in $H_0^1(\Omega)$ to a (weak) limit $\widetilde{y} = y(\widetilde{u})$, i.e., $y_{\widetilde{k}} \rightharpoonup \widetilde{y} = y(\widetilde{u})$ in $H_0^1(\Omega)$.*

Proof. By Theorem 5.2 the sequence $\{y_k\}_{k\in\mathbb{N}}$ is well defined. Since the sequence of controls $\{u_k\}_{k\in\mathbb{N}}$ converges weakly in $L^2(\Omega)$, it is bounded; see, e.g., [48, Theorem 5.12-2] and Theorem 6.11 in the appendix. Hence, the bound (5.8) implies that the sequence $\{y_k\}_{k\in\mathbb{N}}$ is bounded in $H^1(\Omega)$. Recalling that $H^1(\Omega)$ is a reflexive Hilbert space, boundedness of the sequence $\{y_k\}_{k\in\mathbb{N}}$ implies the existence of a weakly convergent subsequence $\{y_{\widetilde{k}}\}_{\widetilde{k}\in\mathbb{N}}$ (see, e.g., [48, Theorem 5.14-4] and Theorem 6.12 in the appendix): $y_{\widetilde{k}} \rightharpoonup \widetilde{y}$ in $H_0^1(\Omega)$. It remains to show that the weak limit $\widetilde{y}$ solves (5.5) for $u = \widetilde{u}$. To do so, we recall the structure of (5.5) and notice that

$$\int_\Omega u_{\widetilde{k}}(\boldsymbol{x})v(\boldsymbol{x})\,d\boldsymbol{x} \to \int_\Omega \widetilde{u}(\boldsymbol{x})v(\boldsymbol{x})\,d\boldsymbol{x}, \qquad \int_\Omega \nabla y_{\widetilde{k}}(\boldsymbol{x})\nabla v(\boldsymbol{x})\,d\boldsymbol{x} \to \int_\Omega \nabla\widetilde{y}(\boldsymbol{x})\nabla v(\boldsymbol{x})\,d\boldsymbol{x},$$

which then imply that $a(y_k, v) \to a(\widetilde{y}, v)$ and that $\ell(v) + \int_\Omega u_{\widetilde{k}}(\boldsymbol{x})v(\boldsymbol{x})\,d\boldsymbol{x} \to \ell(v) + \int_\Omega \widetilde{u}(\boldsymbol{x})v(\boldsymbol{x})\,d\boldsymbol{x}$ for any $v \in H_0^1(\Omega)$. Hence, the claim follows recalling that $y_{\widetilde{k}}$ solves $a(y_{\widetilde{k}}, v) = \ell(v) + \int_\Omega u_{\widetilde{k}}(\boldsymbol{x})v(\boldsymbol{x})\,d\boldsymbol{x}$ for all $v \in H_0^1(\Omega)$. □

We are now ready to prove existence and uniqueness of a minimizer for (5.6)–(5.7).

Theorem 5.4 (Existence and uniqueness of an optimal control function). *Let $\nu > 0$. There exists a unique minimizer $(\widehat{y}, \widehat{u}) \in H_0^1(\Omega) \times L^2(\Omega)$ to the optimal control problem* (5.6)–(5.7)*.*

Proof. Consider some $u_0 \in L^2(\Omega)$ and denote by $y_0 = y(u_0)$ the corresponding solution to (5.7). Since ν is strictly positive, for all $u \in L^2(\Omega)$ such that $\|u\|_{L^2}^2 > \frac{2}{\nu} J(y_0, u_0)$, we have that

$$J(y, u) \geq \frac{\nu}{2} \|u\|_{L^2}^2 > J(y_0, u_0).$$

Therefore, the search for a minimum can be restricted to the set

$$\widetilde{U} := \{v \in L^2(\Omega) \,:\, \|v\|_{L^2}^2 \leq 2\nu^{-1} J(y_0, u_0)\},$$

which is a nonempty (since $u_0 \in \widetilde{U}$), closed, convex, and bounded subset of the reflexive space $L^2(\Omega)$, and hence $\widetilde{U}$ is weakly compact by Theorem 6.13 (see the appendix). This fact allows us to take a minimizing sequence (notice that $J(y, u)$ is bounded from below, $J(y, u) \geq 0$) $\{y_k, u_k\}_{k \in \mathbb{N}}$ such that $u_k \in \widetilde{U}$, $y_k = y(u_k)$, and $\lim_{k\to\infty} J(y_k, u_k) = \inf_{u \in \widetilde{U}} J(y(u), u) =: \widetilde{J}$. Since the set $\widetilde{U}$ is weakly compact, there exists a weakly convergent subsequence $u_{k_j} \rightharpoonup \widetilde{u} \in \widetilde{U}$ in $L^2(\Omega)$. Consider now the subsequence $\{y_{k_j}\}_j$ given by $y_{k_j} = y(u_{k_j})$. Lemma 5.3 implies that there exists a subsequence $\{y_{\widetilde{k}}\}_{\widetilde{k}}$ that converges weakly in $H_0^1(\Omega)$ to the limit $\widetilde{y} = y(\widetilde{u})$. Moreover, the Rellich–Kondrachov theorem (see Theorem 6.7 in the appendix) allows us to choose the subsequence $\{y_{\widetilde{k}}\}_{\widetilde{k}}$ so that it converges strongly in $L^2(\Omega)$. Now, we notice that the map $v \in L^2(\Omega) \mapsto \|v\|_{L^2} \in \mathbb{R}$ is weakly lower semicontinuous because it is convex and continuous (see Theorem 6.14). Hence, we have

$$\liminf_{\widetilde{k}\to\infty} \frac{\nu}{2} \|u_{\widetilde{k}}\|_{L^2}^2 \geq \frac{\nu}{2} \|\widetilde{u}\|_{L^2}^2.$$

We can therefore write that

$$\widetilde{J} = \lim_{\widetilde{k}\to\infty} J(y_{\widetilde{k}}, u_{\widetilde{k}}) = \liminf_{\widetilde{k}\to\infty} J(y_{\widetilde{k}}, u_{\widetilde{k}}) \geq J(\widetilde{y}, \widetilde{u}) \geq \widetilde{J},$$

which implies that $(\widetilde{y}, \widetilde{u})$ is a minimizer for (5.6)–(5.7).

To show uniqueness of the minimizer, we proceed as follows. Since the Laplace problem (5.7) is uniquely solvable for any $u \in L^2(\Omega)$, the control-to-state map $S : u \mapsto y(u) \in H_0^1(\Omega)$ is well defined and linear-affine in the control variable. Hence, we can then introduce the so-called reduced cost functional $\widehat{J}(u) := J(S(u), u)$. This is a strictly convex function; see, e.g., [178, 147, 20]. Therefore, the uniqueness of a minimizer follows from a standard contradiction argument. ∎

We conclude this section with the following counterexample, where we drop the assumption of the strict positivity of ν.

Example 5.5 (Nonexistence of minimizers). Consider the optimal control problem

$$\min_{y,u} \; J(y, u) := \frac{1}{2} \|y - y_d\|_{L^2}^2$$

subject to

$$\begin{aligned} &y''(x) = -u(x) \quad \text{ a.e. in } \Omega := (-1, 1), \text{ with } y(-1) = y(1) = 0, \\ &u \in U_{\text{ad}} := \{v \in L^1(\Omega) \,:\, \|v\|_{L^1} \leq 1\}, \end{aligned}$$

where $y_d(x) = \frac{1}{2}(1 - |x|)$.

It is clear that $J(y,u) \geq 0$ for all the admissible pairs. Now, we define the sequence $\{u_k\}_{k\in\mathbb{N}}$ as

$$u_k(x) := \begin{cases} k & \text{if } x \in [-\frac{1}{2k}, \frac{1}{2k}], \\ 0 & \text{otherwise.} \end{cases}$$

Notice that $\|u_k\|_{L^1} = 1$, hence $\{u_k\}_{k\in\mathbb{N}} \subset U_{\mathrm{ad}}$, and that $\|u_k\|_{L^2} = k$. This means that the sequence $\{u_k\}_{k\in\mathbb{N}}$ is unbounded in $L^2(\Omega)$ and bounded in $L^1(\Omega)$. However, $L^1(\Omega)$ is not a reflexive space and the existence of a subsequence that converges (in a strong or weak sense) in L^1 is not guaranteed.

Now, using u_k, we can compute that

$$y_k'(x) = a - \begin{cases} 0 & \text{if } x < -\frac{1}{2k}, \\ kx + \frac{1}{2} & \text{if } x \in [-\frac{1}{2k}, \frac{1}{2k}], \\ 1 & \text{otherwise} \end{cases}$$

and

$$y_k(x) = ax + b - \begin{cases} 0 & \text{if } x < -\frac{1}{2k}, \\ \frac{k}{2}\big(x^2 - \frac{1}{4k^2}\big) + \frac{1}{2}\big(x + \frac{1}{2k}\big) & \text{if } x \in [-\frac{1}{2k}, \frac{1}{2k}], \\ x & \text{otherwise.} \end{cases}$$

The boundary conditions $y_k(-1) = y_k(1) = 0$ imply that $a = b = \frac{1}{2}$. We have then obtained that

$$y_k(x) = \begin{cases} \frac{1}{2} - \frac{k}{2}x^2 - \frac{1}{8k} & \text{if } x \in [-\frac{1}{2k}, \frac{1}{2k}], \\ \frac{1}{2}(1 - |x|) & \text{otherwise.} \end{cases}$$

We can now compute

$$\begin{aligned} \|y_k - y_d\|_{L^2}^2 &= \int_{-\frac{1}{2k}}^{\frac{1}{2k}} \Big(\frac{1}{2}|x| - \frac{k}{2}x^2 - \frac{1}{8k}\Big)^2 dx = 2\int_0^{\frac{1}{2k}} \Big(\frac{1}{2}x - \frac{k}{2}x^2 - \frac{1}{8k}\Big)^2 dx \\ &= \frac{k^2}{2}\int_0^{\frac{1}{2k}} \Big(x^2 - \frac{1}{k}x + \frac{1}{4k^2}\Big)^2 dx \leq \frac{k^2}{2}\Big(\frac{1}{4k^2}\Big)^2 \frac{1}{2k}, \end{aligned}$$

where we have used that the polynomial $p(x) := x^2 - \frac{1}{k}x + \frac{1}{4k^2}$ for $x \in [0, \frac{1}{2k}]$ is a convex function which attains its maximum at $x = 0$. It is now clear that

$$0 \leq J(y_k, u_k) = \frac{1}{2}\|y_k - y_d\|_{L^2}^2 \leq \frac{1}{2}\frac{k^2}{2}\Big(\frac{1}{4k^2}\Big)^2 \frac{1}{2k} \to 0 \quad \text{as } k \to \infty.$$

Hence the sequence $\{y_k, u_k\}_{k\in\mathbb{N}} \subset H_0^1(\Omega) \times L^1(\Omega)$ is a minimizing sequence and $J = 0$ is the infimum of our problem.

Assume now that a minimum point for the present problem exists. Then the infimum $J = 0$ must be attained at this minimum point (since the map $u \mapsto J(y(u), u)$ is convex, and hence every minimum point is a global minimum point). If we now assume that the infimum is attained at some $(y, u) \in H_0^1(\Omega) \times L^1(\Omega)$, then it has to satisfy $J(y, u) = 0$, which implies $y = y_d$. However, the function $y(x) = \frac{1}{2}(1 - |x|)$ does not satisfy the differential equation $y'' = -u$ in $L^1(\Omega)$.[57] To see this, consider any given test function $\varphi \in C_0^\infty(\Omega)$ and compute that

$$\int_{-1}^{1} y'(x)\varphi'(x)\,dx = \frac{1}{2}\int_{-1}^{0} \varphi'(x)\,dx - \frac{1}{2}\int_0^1 \varphi'(x)\,dx = \varphi(0).$$

[57] The function $y(x) = \frac{1}{2}(1 - |x|)$ solves the equation $y'' = -u$ in a distributional sense with u equal to the Dirac delta. However, this control functional does not belong to the admissible set U_{ad}.

However, $\varphi(0) \neq \int_{-1}^{1} v(x)\varphi(x)\,dx$ for every $v \in L^1(\Omega)$. To see this, consider the sequence $\varphi_k(x) := \max\{0, 1 - k|x|\}$, denote by $\chi_{[-\frac{1}{k},\frac{1}{k}]}(x)$ the characteristic function corresponding to the interval $[-\frac{1}{k}, \frac{1}{k}]$, and then compute

$$\begin{aligned} 1 = \varphi_k(0) &= \int_{-1}^{1} v(x)\varphi_k(x)\,dx = \int_{-\frac{1}{k}}^{\frac{1}{k}} v(x)\varphi_k(x)\,dx \\ &\leq \int_{-\frac{1}{k}}^{\frac{1}{k}} |v(x)|\,dx = \int_{-1}^{1} |v(x)|\chi_{[-\frac{1}{k},\frac{1}{k}]}(x)\,dx \to 0 \end{aligned}$$

(by the Lebesgue dominated convergence theorem), which yields a contradiction. Hence, there exists no minimizer in $H_0^1(\Omega) \times L^1(\Omega)$ for the present optimal control problem. ∎

5.1.2 ▪ Optimality system and adjoint equation

> *These necessary conditions allow for far-reaching conclusions concerning the form of optimal controls and the verification that numerically determined controls are actually optimal. In addition, they form the theoretical basis for the development of numerical methods.*
>
> Fredi Tröltzsch, *Optimal Control of Partial Differential Equations: Theory, Methods, and Applications*, 2010.

The solution to (5.6)–(5.7) is characterized by the following necessary and sufficient optimality condition: $(y, u) \in H_0^1(\Omega) \times L^2(\Omega)$ is the unique solution to the problem (5.6)–(5.7) if and only if there exists a unique $p \in H_0^1(\Omega)$ such that the triple (y, u, p) solves the optimality system[58]

$$a(y, v) = \ell(v) + \int_\Omega u(\boldsymbol{x})v(\boldsymbol{x})\,d\boldsymbol{x} \qquad \forall v \in H_0^1(\Omega), \tag{5.9}$$

$$a(v, p) = \int_\Omega (y_d(\boldsymbol{x}) - y(\boldsymbol{x}))v(\boldsymbol{x})\,d\boldsymbol{x} \qquad \forall v \in H_0^1(\Omega), \tag{5.10}$$

$$\nu u = p \qquad \text{a.e. in } \Omega. \tag{5.11}$$

Equation (5.9) is called *state equation*. Equation (5.10) is the famous *adjoint equation* and the *adjoint variable* p plays the role of the *Lagrange multiplier* associated to the state equation. Equation (5.11) is often called the *optimality condition* or *gradient condition*. The optimality system (5.9)–(5.11) can be derived by direct differentiation of the *Lagrange function*

$$L(y, u, p) := J(y, u) + a(y, p) - \ell(p) - \int_\Omega u(\boldsymbol{x})p(\boldsymbol{x})d\boldsymbol{x}.$$

See, e.g., [178, 147, 20] for more details or [80] for a historical perspective.

The strong form of the optimality system (5.9)–(5.11) is

$$-\Delta y = f + u \qquad \text{in } \Omega, \tag{5.12}$$

$$y = 0 \qquad \text{on } \partial\Omega,$$

$$-\Delta p = y_d - y \qquad \text{in } \Omega, \tag{5.13}$$

$$p = 0 \qquad \text{on } \partial\Omega,$$

$$\nu u = p \qquad \text{in } \Omega. \tag{5.14}$$

[58] Notice that the optimality system (5.9)–(5.11) corresponds not only to a first-order necessary optimality condition but also to a sufficient optimality condition. This is due to the fact that the reduced map (see Section 5.2) $u \mapsto \widehat{J}(u) = J(y(u), u)$ is strictly convex.

The finite-difference discretization of (5.12)–(5.14) (or (5.9)–(5.11)) is given by the linear system

$$\widehat{A}\widehat{\boldsymbol{u}} = \widehat{\boldsymbol{f}}, \tag{5.15}$$

where

$$\widehat{A} = \begin{bmatrix} 0 & A & -I \\ A & I & 0 \\ -I & 0 & \nu I \end{bmatrix}, \quad \widehat{\boldsymbol{u}} = \begin{bmatrix} \boldsymbol{p} \\ \boldsymbol{y} \\ \boldsymbol{u} \end{bmatrix}, \quad \widehat{\boldsymbol{f}} = \begin{bmatrix} \boldsymbol{f} \\ \boldsymbol{y}_d \\ 0 \end{bmatrix}, \tag{5.16}$$

and $\boldsymbol{y} \in \mathbb{R}^m$, $\boldsymbol{u} \in \mathbb{R}^m$, and $\boldsymbol{p} \in \mathbb{R}^m$ are the discrete approximations corresponding to y, u, and p. The vectors $\mathbf{f} \in \mathbb{R}^m$ and $\boldsymbol{y}_d \in \mathbb{R}^m$ are approximations to f and y_d. The matrix $A \in \mathbb{R}^{m\times m}$ is the discretization of the negative Laplace operator, and I is the $m \times m$ identity matrix. Notice that in our particular example, the discrete system (5.15) coincides with the optimality system of the discrete optimization problem (5.4). Notice also that if the *finite-element method* is used to discretize (5.12)–(5.14), then A represents the finite-element stiffness matrix and the identities appearing in $\widehat{A}$ have to be replaced with a mass matrix.

The discrete optimality system is uniquely solvable, as we show in the next theorem.

Theorem 5.6 (Solvability of discrete optimality systems). *Consider a matrix B with the block structure*

$$B = \begin{bmatrix} 0 & C & -M \\ C & M & 0 \\ -M & 0 & \gamma M \end{bmatrix},$$

where $\gamma \in \mathbb{R}$ is a positive parameter, $C \in \mathbb{R}^{m\times m}$ is a symmetric matrix, and $M \in \mathbb{R}^{m\times m}$ is a symmetric and positive definite matrix. Then the matrix B is invertible and its determinant is

$$\det(B) = (-1)^m \det(M)^2 \det(M + \gamma C M^{-1} C). \tag{5.17}$$

Proof. The proof uses the following well-known formula for the determinant of block matrices (see [108, Section 0.8.5]):

$$\det \begin{bmatrix} A_{11} & A_{12} \\ A_{21} & A_{22} \end{bmatrix} = \det(A_{22}) \det(A_{11} - A_{12} A_{22}^{-1} A_{21}), \tag{5.18}$$

where A_{11} and A_{22} must be square matrices, A_{22} must be invertible, and A_{12} and $A_{21}^\top$ must have the same size.

Applying (5.18) to B with $A_{22} = \gamma M$, we get

$$\det(B) = \det(\gamma M) \det\left(\begin{bmatrix} -\frac{1}{\gamma} M & C \\ C & M \end{bmatrix} \right).$$

Applying again (5.18) to the matrix $\begin{bmatrix} -\frac{1}{\gamma} M & C \\ C & M \end{bmatrix}$ with $A_{22} = M$, we get

$$\begin{aligned} \det(B) &= \det(\gamma M) \det(M) \det\left(-\frac{1}{\gamma} M - C M^{-1} C \right) \\ &= (-1)^m \det(M)^2 \det(M + \gamma C M^{-1} C). \end{aligned}$$

Since C is symmetric and M is symmetric and positive definite, the matrix $M + \gamma C M^{-1} C$ is symmetric and positive definite. Hence, the determinants $\det(M)$ and $\det(M + \gamma C M^{-1} C)$ are both nonzero and B is invertible. □

Notice that if we choose $M = I$, $C = A$, and $\gamma = \nu$, then $B = \widehat{A}$. Hence Theorem 5.6 guarantees that $\widehat{A}$ is invertible and its determinant is given by

$$\det(\widehat{A}) = (-1)^m \prod_{j=1}^{m} \big(1 + \nu(\lambda_j(A))^2\big), \tag{5.19}$$

where $\lambda_j(A)$ are the eigenvalues of the matrix A for $j = 1, \ldots, m$. Moreover, according to Theorem 5.6 and formula (5.19) the invertibility of $\widehat{A}$ does not necessarily require the invertibility of A.

Finally, if the optimality system (5.12)–(5.14) is discretized by a finite-element method, then A is the stiffness matrix and M the mass matrix. These are generally symmetric and positive definite. Hence Theorem 5.6 has a more general applicability than the particular system considered in this chapter.

In the next sections, we study different approaches for the numerical solution of (5.15).

5.2 ▪ Reduced approach

> *All reduced versions require one solution of the nonlinear model per step, whereas no nonlinear model is solved in the all-at-once-versions.*
>
> Barbara Kaltenbacher, *All-at-Once versus Reduced Iterative Methods for Time Dependent Inverse Problems*, 2017.

> *The application of the implicit function theorem leads to so-called black-box-methods. A partial application of the implicit function theorem leads to Schur-complement-type multigrid methods as considered in section 6. These methods are of particular advantage if one wants to implement multigrid optimization approaches within an existing multigrid code for the state equation.*
>
> Alfio Borzì and Volker Schulz, *Multigrid Methods for PDE Optimization*, 2009.

One of the most used and efficient approaches for the numerical solution of (5.15) is based on a classical optimization argument, which allows one to "reduce" the system and define so-called black-box methods (see the quote above). The term "reduce" here refers to the number of optimization variables, which are reduced from two (state and control) to one (the control only).

Since the Laplace problem in (5.6)–(5.7) is uniquely solvable for any right-hand-side function $w \in H^{-1}(\Omega)$, the so-called control-to-state map $S : H^{-1}(\Omega) \to H_0^1(\Omega)$, given as $z = Sw$, where z is the solution to the Poisson problem

$$a(z, v) = \int_\Omega w(\boldsymbol{x}) v(\boldsymbol{x})\, d\boldsymbol{x} \quad \forall v \in H_0^1(\Omega),$$

is well defined. Notice that the operator S is linear. Clearly, the solution to (5.7) is given by $y(u) = Su + Sf$. Therefore, we can formulate the constrained problem (5.6)–(5.7) as an unconstrained problem

$$\min_{u \in L^2(\Omega)} \widehat{J}(u), \tag{5.20}$$

where $\widehat{J}(u) := J(Su + Sf, u)$ is the *reduced cost functional*. This formulation allows one to use any unconstrained-optimization method (sometimes called black-box methods; see the quote

above) to minimize $\widehat{J}$ and obtain the optimal control function. Moreover, a direct calculation allows us to obtain the derivative of $\widehat{J}$ at a point $w \in L^2(\Omega)$ along any direction $v \in L^2(\Omega)$:

$$D\widehat{J}(w; v) = \langle \nu w, v \rangle_{L^2} + \langle S(w + f) - y_d, Sv \rangle_{L^2}.$$

A necessary and sufficient optimality condition for u to be a minimizer is that $D\widehat{J}(u; v) = 0$ for all $v \in L^2(\Omega)$. This is equivalent to

$$g(u, v) := \langle \nu u, v \rangle_{L^2} + \langle Su, Sv \rangle_{L^2} = \langle y_d - Sf, Sv \rangle_{L^2} =: q(v) \quad \forall v \in L^2(\Omega).$$

Notice that $g : L^2(\Omega) \times L^2(\Omega) \to \mathbb{R}$ is a bounded and coercive bilinear form, and $q : L^2(\Omega) \to \mathbb{R}$ is a bounded linear functional. Hence the Lax–Milgram theorem (see Theorem 6.8 in the appendix) guarantees the existence of a unique solution $u \in L^2(\Omega)$ to the problem

$$g(u, v) = q(v) \quad \forall v \in L^2(\Omega).$$

Since g is symmetric and coercive, we expect that its discrete companion must be a symmetric and positive definite matrix. In fact, if we repeat the same arguments for the discrete problem (5.4), we obtain the discrete reduced problem

$$\min_{\boldsymbol{u} \in \mathbb{R}^m} \widehat{J}_h(\boldsymbol{u}),$$

where the discrete reduced cost functional is $\widehat{J}_h(\boldsymbol{u}) := J_h(A^{-1}\boldsymbol{u} + A^{-1}\boldsymbol{f}, \boldsymbol{u})$. A direct calculation reveals that the optimality condition $\nabla \widehat{J}_h(\mathbf{u}) = 0$ becomes

$$(\nu I + A^{-1}A^{-1})\boldsymbol{u} = A^{-1}(\boldsymbol{y}_d - A^{-1}\boldsymbol{f}). \tag{5.21}$$

We wish to remark that the discrete system (5.21) can also be obtained by formally solving the first two equations in (5.15) and substituting their solutions into the third equation.

Since A is symmetric and $\nu > 0$, the matrix $A_{\mathrm{red}} := \nu I + A^{-1}A^{-1}$ is symmetric and positive definite. Therefore, the linear system can be solved using the CG method (see Section 3.2). Clearly, one should not assemble first the matrix $\nu I + A^{-1}A^{-1}$ and then feed it to the CG method. This would be computationally too expensive! To overcome this problem, it is necessary to define a map

$$\boldsymbol{v} \mapsto A_{\mathrm{fun}}(\boldsymbol{v}) := A_{\mathrm{red}}\boldsymbol{v} = (\nu \boldsymbol{v} + (A^{-1}(A^{-1}\boldsymbol{v})) \tag{5.22}$$

that computes the action of A_{red} on a vector $\mathbf{v} \in \mathbb{R}^m$. Notice that the implementation of this map requires three operations. First, one solves the linear system $A\boldsymbol{w} = \boldsymbol{v}$ and computes $\boldsymbol{w}$. Second, one solves the linear system $A\boldsymbol{z} = \boldsymbol{w}$ and computes $\boldsymbol{z}$. Third, one assembles $A_{\mathrm{fun}}(\boldsymbol{v}) := \nu\boldsymbol{v} + \boldsymbol{z}$. Using this map, one can solve (5.21) by the CG algorithm (implemented in a matrix-free way).

Notice also that the reduced approach considered in this section allowed us to reduce the dimension of the overall system from $3m$ to m (a factor of 3) at the cost of solving two m-dimensional systems per CG iteration. However, there are other types of optimal control problems (like boundary control problems), where the reduction in terms of dimension obtained by the reduced approach is much higher; see, e.g., [23, 178] and references therein for more details.

Let us now test the performance of CG and GMRES for the solution of (5.21) by running the MATLAB script[59]

[59]Notice that, in contrast to the previous chapters, we consider here the source term $f = -1$. This source pushes the state y toward negative values and acts against the control u, which instead tries to make y close to the desired state $y_d = 1$.

```
m=15;                              % number of mesh points in each direction
d=2;                               % dimension of the problem
nu=1e-3;                           % regularization parameter
h=1/(m+1);                         % mesh size
A=Laplacian(m,d)/h^2;              % negative 2D discrete Laplacian
Afun=@(v) nu*v+(A\(A\v));          % define function Afun
f=-ones(m^d,1);                    % discrete f=-1
yd=ones(m^d,1);                    % discrete y_d=1
rhs=-A\(A\f-yd);                   % assemble the right-hand-side vector
u0=rand(m^d,1);                    % random initial guess
kmax=min(100,m^d);                 % set max number of iterations
[u1,~,~,~,rv1]=gmres(Afun,rhs,[],1e-6,kmax,[],[],u0);
[u2,~,~,~,rv2]=pcg(Afun,rhs,1e-6,kmax,[],[],u0);
semilogy(0:length(rv1)-1,rv1./rv1(1),'o-b'); hold on;
semilogy(0:length(rv2)-1,rv2./rv2(1),'x-r');
axis([0 50 1e-8 1]); yticks([1e-8 1e-6 1e-4 1e-2 1]);
legend('GMRES','CG','Location','NorthEast');
xlabel('iterations');
ylabel('norms of the residuals');
set(gca,'fontsize',18,'linewidth',2);
```

Using this script for different values of ν and different mesh sizes h, we obtain a figure similar[60] to Figure 5.2. The results shown in Figure 5.2 show clearly two different behaviors. For ν fixed (fixed column in the figure) and decreasing mesh size (moving from the top to the bottom of the fixed column of the figure) both CG and GMRES methods are quite robust. For fixed mesh size (fixed row in the figure) and decreasing ν (moving from left to right on the fixed row) one clearly observes an enormous deterioration of the convergence behavior of CG and GMRES. These two different observations are theoretically explained by the next theorem.

Theorem 5.7 (The reduced matrix A_{red}). *Assume that $\nu > 0$ and denote by h the mesh size. The reduced matrix $A_{\mathrm{red}} = \nu I + A^{-1}A^{-1}$ is symmetric positive definite, its eigenvalues are*

$$\lambda(A_{\mathrm{red}}) = \nu + \frac{1}{(\lambda(A))^2},$$

and the corresponding (spectral) condition number is

$$\kappa(A_{\mathrm{red}}) = \kappa(A)^2 \frac{1 + \nu(\lambda_{\min}(A))^2}{1 + \nu(\lambda_{\max}(A))^2}, \tag{5.23}$$

where $\kappa(A)^2 = O(h^{-4})$. Moreover, for fixed h one has that $\kappa(A_{\mathrm{red}})$ is a monotonically decreasing function of ν and it holds that

$$\kappa(A_{\mathrm{red}}) \leq 1 + \frac{1}{\nu(\lambda_{\min}(A))^2}. \tag{5.24}$$

Proof. It is clear that the eigenvalues of A_{red} are $\lambda(A_{\mathrm{red}}) = \nu + \frac{1}{(\lambda(A))^2}$. Hence, since A is symmetric and positive definite (it is the discrete finite-difference negative Laplace), it holds that

$$\lambda_{\max}(A_{\mathrm{red}}) = \nu + \frac{1}{(\lambda_{\min}(A))^2}, \quad \lambda_{\min}(A_{\mathrm{red}}) = \nu + \frac{1}{(\lambda_{\max}(A))^2}. \tag{5.25}$$

[60] Notice that the results of Figure 5.2 are obtained by using a random initial guess u_0. Hence the reader will observe similar (but not equal) figures.

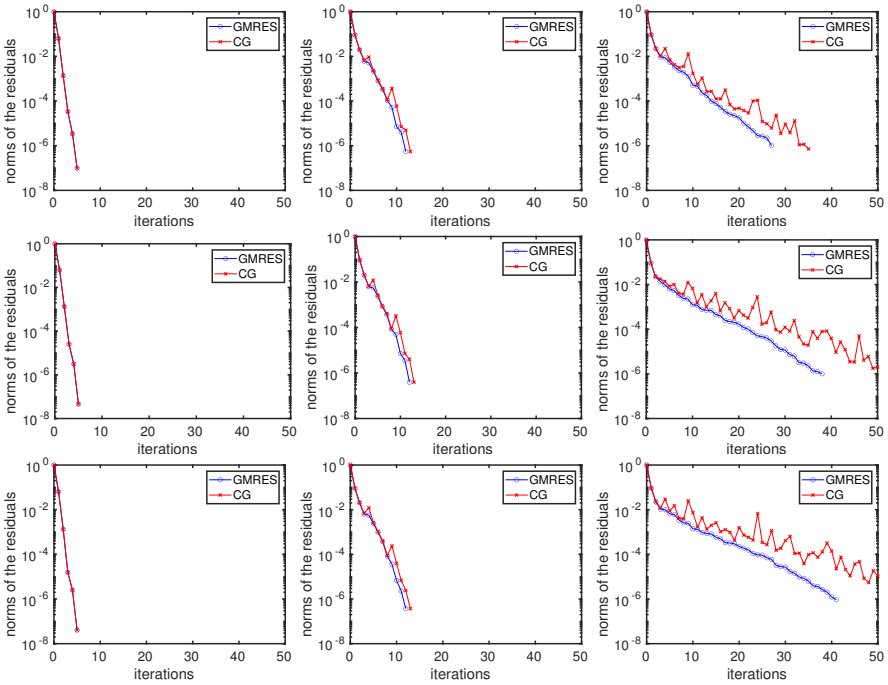

Figure 5.2. *Convergence of CG and GMRES (relative residuals) for the solution of the reduced problem* (5.21) *for a unit square* $\Omega \subset \mathbb{R}^2$. *First row:* $m = 15$, $\nu = 10^{-3}$, $\nu = 10^{-5}$, *and* $\nu = 10^{-7}$. *Second row:* $m = 31$, $\nu = 10^{-3}$, $\nu = 10^{-5}$, *and* $\nu = 10^{-7}$. *Third row:* $m = 63$, $\nu = 10^{-3}$, $\nu = 10^{-5}$, *and* $\nu = 10^{-7}$. *The results of the different figures are obtained with different (randomly chosen) initialization vectors.*

Hence, we use (5.25) and compute

$$\begin{aligned}\kappa(A_{\mathrm{red}}) &= \frac{\lambda_{\max}(A_{\mathrm{red}})}{\lambda_{\min}(A_{\mathrm{red}})} = \Big(\nu + \frac{1}{(\lambda_{\min}(A))^2}\Big)\Big(\nu + \frac{1}{(\lambda_{\max}(A))^2}\Big)^{-1} \\ &= \frac{1+\nu(\lambda_{\min}(A))^2}{(\lambda_{\min}(A))^2}\,\frac{(\lambda_{\max}(A))^2}{1+\nu(\lambda_{\max}(A))^2} = \kappa(A)^2\,\frac{1+\nu(\lambda_{\min}(A))^2}{1+\nu(\lambda_{\max}(A))^2},\end{aligned}$$

which is exactly (5.23). A direct calculation shows that the derivative of the map $\nu \mapsto \frac{1+\nu(\lambda_{\min}(A))^2}{1+\nu(\lambda_{\max}(A))^2}$ is negative. Hence, $\kappa(A_{\mathrm{red}})$ is monotonically decreasing in ν. The upper bound (5.24) follows by noticing that $\lambda_{\min}(A_{\mathrm{red}}) \geq \nu$ and performing a direct estimation. ∎

Recalling that $\lambda_{\min}(A) = 2\pi^2 - O(h^2)$ (see also Problem 11), the upper bound (5.24) shows that the condition number of A_{red} is robust with respect to h. Moreover, from Theorem 5.7 one can also see that the condition number of A_{red} deteriorates fast with ν. In fact, we can use formula (5.23) to obtain the expansion

$$\kappa(A_{\mathrm{red}}) = \kappa(A)^2\big(1 - \nu(\lambda_{\max}(A)^2 - \lambda_{\min}(A)^2) + O(\nu^2)\big).$$

This suggests that for large and moderate values of the regularization parameter ν, GC and GMRES perform quite well, but the situation changes drastically for small values of ν.

Note that the cost per iteration of both CG and GMRES is dominated by the solution of the two subproblems of size m required by the function A_{fun}. If the matrix A is a discretization of

some PDE operator, as in the case here, one could then accelerate the process of solving each of the two subproblems by using the preconditioning techniques described in Chapter 4. In particular, multigrid methods and domain decomposition techniques can be successfully used. Our example is a fortunate one because the (two-dimensional negative finite-difference Laplace) matrix A has a very special sparse and banded structure that permits the use of very efficient sparse direct solvers (performed via the MATLAB "backslash" command);[61] see, e.g., [92, Section 4.3]. However, if the cost of the solutions of the two subproblems is too high (comparable to the cost of solving the entire problem), or the matrix A is very ill-conditioned, or the weight parameter ν is extremely small, then the reduced approach becomes problematic. A possible solution would be the use of a preconditioner combined with a Krylov method to accelerate the solution of the two subproblems required to compute the action of $A_{\rm red}$ on a given vector.

In general, the design of a preconditioner for the matrix $A_{\rm red}$ is not an easy task. For example, the use of an algebraic preconditioner is generally not possible, because it would need the explicit knowledge of the matrix $A_{\rm red}$. However, two possible preconditioners for $A_{\rm red}$ are discussed in the next subsection.

We wish also to remark that a multigrid method for the numerical solution of (5.21) was introduced in [100] by using the stationary iteration

$$\boldsymbol{u}^{n+1} = \frac{1}{\nu} A^{-2} \boldsymbol{u}^n + \frac{1}{\nu} \boldsymbol{b}, \tag{5.26}$$

where $\boldsymbol{b} := A^{-1}(\boldsymbol{y}_d - A^{-1}\boldsymbol{f})$, as a smoother. The iteration (5.26) is clearly not convergent for all values of ν, and a more detailed analysis of this stationary method is a good exercise that we leave to the reader (see Problem 72). However, the multigrid method obtained using (5.26) is convergent if the mesh size (in particular the mesh size of the coarsest level) is sufficiently small; see [100, page 576] and Problem 73.

Finally, the techniques described in this section are based on the reduction of the optimization variables. The optimality system is written only in terms of the control. A completely different approach is the one described in Section 5.3, where all the optimization variables (including the adjoint variable) are solved in a monolithic fashion.

Two Laplace-based preconditioners

> *There are many kind of physical systems, differential equations, and finite element models, and so many methods. We cannot hope to cover all or even most interesting situations, so we will limit ourselves to a model problem, the standard finite difference approximation to Poisson's equation on a square. Poisson's equation and its close relation, Laplace's equation, arise in many applications, including electromagnetics, fluid mechanics, heat flow, diffusion, and quantum mechanics, to name a few.*
>
> James W. Demmel, *Applied Numerical Linear Algebra*, 1997.

The structure of the matrix $A_{\rm red} = \nu I + A^{-1}A^{-1}$ intuitively suggests the use of A or A^2 as preconditioners. Let us analyze these two cases.

If we use A as preconditioner, problem (5.21) becomes

$$(\nu A + A^{-1})\boldsymbol{u} = \boldsymbol{y}_d - A^{-1}\boldsymbol{f}. \tag{5.27}$$

Notice that the computation of the action of $\nu A + A^{-1}$ on a given vector is much cheaper if compared to $A_{\rm red}$, since only one inverse A^{-1} is considered. If we repeat the experiments of

[61] Notice the matrix A can be written in the Kronecker format $A = A_{1D} \otimes I + I \otimes A_{1D}$, where A_{1D} is the one-dimensional Laplace matrix (see Problem 11). This allows one to use very efficient *fast Poisson solvers*, which permit the solution of the system in $O(n \log(n))$ operations; see, e.g., [92, Section 4.8.4]. Moreover, the use of a multigrid method is also possible. This would require only $O(n)$ operations and would perform faster than a fast Poisson solver. These methods are particularly useful when a Poisson problem must be solved repeatedly, as in our example.

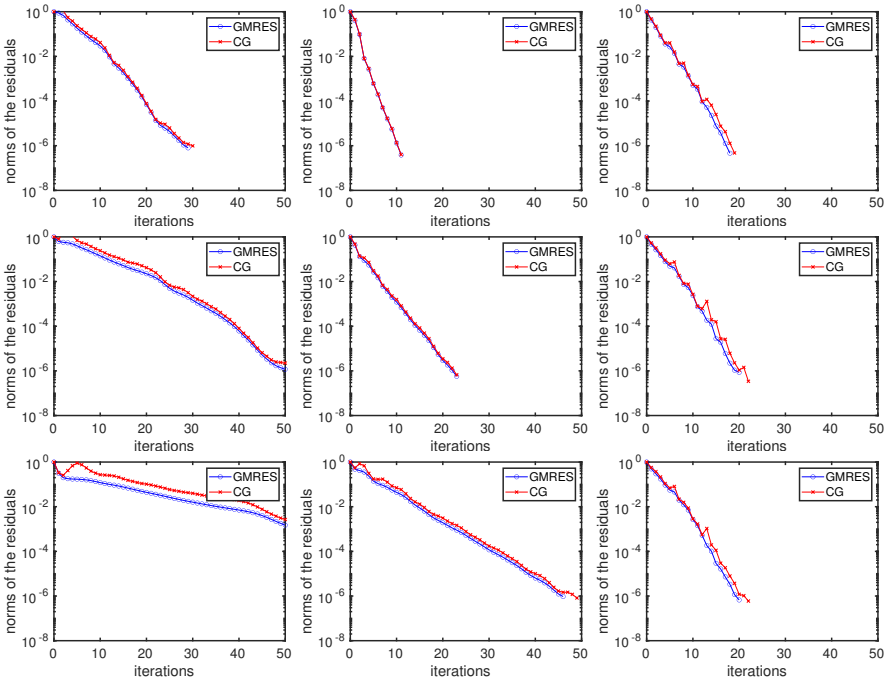

Figure 5.3. *Convergence of CG and GMRES (relative residuals) for the solution of the reduced problem* (5.27) *for a unit square* $\Omega \subset \mathbb{R}^2$. *First row:* $m = 15$, $\nu = 10^{-3}$, $\nu = 10^{-5}$, *and* $\nu = 10^{-7}$. *Second row:* $m = 31$, $\nu = 10^{-3}$, $\nu = 10^{-5}$, *and* $\nu = 10^{-7}$. *Third row:* $m = 63$, $\nu = 10^{-3}$, $\nu = 10^{-5}$, *and* $\nu = 10^{-7}$. *The results of the different figures are obtained with different (randomly chosen) initialization vectors.*

Figure 5.2 for (5.27), we obtain the results shown in Figure 5.3. These show that for ν "large" the convergence of CG and GMRES deteriorates fast for decreasing values of h (first column in the figure). However, when we reduce ν the convergence greatly improves and becomes robust in h (third column in the figure). This seems to suggest that the smaller ν is, the easier the solution of (5.27) is. This is however not true. In fact, if one repeats the same experiments for even smaller values of ν, the results shown in Figure 5.4 are obtained. These show clearly that a further decrease of the regularization parameter ν leads to a deterioration of CG and GMRES convergence (which is no longer robust with respect to the mesh size h).

To explain this behavior, we study the condition number of the preconditioned matrix $AA_{\text{red}} = \nu A + A^{-1}$.

Theorem 5.8 (The preconditioned reduced matrix AA_{red}). *The condition number of the matrix* AA_{red} *is bounded (uniformly in* ν*) as*

$$\kappa(AA_{\text{red}}) \leq \kappa(A). \tag{5.28}$$

Moreover, it satisfies the relation

$$\kappa(AA_{\text{red}}) = \begin{cases} \frac{1}{\kappa(A)} \frac{\nu\lambda_{\max}(A)+1}{\nu\lambda_{\min}(A)+1} & \text{if } \frac{1}{\sqrt{\nu}} \leq \lambda_{\min}(A), \\ \kappa(A) \frac{\nu\lambda_{\min}(A)+1}{\nu\lambda_{\max}(A)+1} & \text{if } \frac{1}{\sqrt{\nu}} \geq \lambda_{\max}(A) \end{cases} \tag{5.29}$$

with $\lim_{\nu\to 0} \kappa(A^{-1}A_{\text{red}}) = \lim_{\nu\to+\infty} \kappa(A^{-1}A_{\text{red}}) = \kappa(A)$.

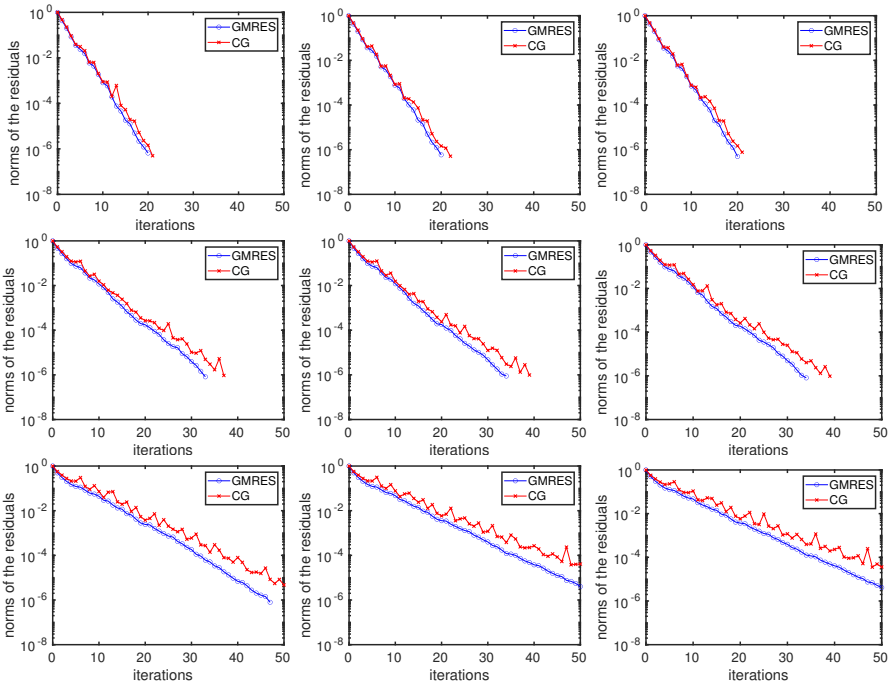

Figure 5.4. *Convergence of CG and GMRES (relative residuals) for the solution of the reduced problem* (5.21) *for a unit square* $\Omega \subset \mathbb{R}^2$. *First row:* $m = 15$, $\nu = 10^{-9}$, $\nu = 10^{-11}$, *and* $\nu = 10^{-13}$. *Second row:* $m = 31$, $\nu = 10^{-9}$, $\nu = 10^{-11}$, *and* $\nu = 10^{-13}$. *Third row:* $m = 63$, $\nu = 10^{-9}$, $\nu = 10^{-11}$, *and* $\nu = 10^{-13}$. *The results of the different figures are obtained with different (randomly chosen) initialization vectors.*

Proof. If $\lambda(A)$ denotes any eigenvalue of A, it is clear that the eigenvalues of $A^{-1}A_{\mathrm{red}}$ have the form $\lambda(A^{-1}A_{\mathrm{red}}) = \nu\lambda(A) + \frac{1}{\lambda(A)}$.

To prove the first upper bound (5.28), it is enough to recall that A is symmetric and positive definite (and hence $A^{-1}A_{\mathrm{red}} = \nu A + A^{-1}$ is symmetric and positive definite as well) and notice that

$$\lambda_{\min}(A^{-1}A_{\mathrm{red}}) \geq \nu\lambda_{\min}(A) + \frac{1}{\lambda_{\max}(A)},$$

$$\lambda_{\max}(A^{-1}A_{\mathrm{red}}) \leq \nu\lambda_{\max}(A) + \frac{1}{\lambda_{\min}(A)}.$$

These estimates allow us to compute

$$\kappa(AA_{\mathrm{red}}) = \frac{\lambda_{\max}(A^{-1}A_{\mathrm{red}})}{\lambda_{\min}(A^{-1}A_{\mathrm{red}})} \leq \frac{\nu\lambda_{\max}(A) + \frac{1}{\lambda_{\min}(A)}}{\nu\lambda_{\min}(A) + \frac{1}{\lambda_{\max}(A)}}$$

$$= \frac{\lambda_{\max}(A)}{\lambda_{\min}(A)} \frac{\nu\lambda_{\max}(A)\lambda_{\min}(A) + 1}{\nu\lambda_{\max}(A)\lambda_{\min}(A) + 1} = \kappa(A),$$

which is (5.28).

To prove (5.29) we first analyze the function $f(x) := \nu x + \frac{1}{x}$ for $x > 0$. We have that $f'(x) = \nu - \frac{1}{x^2}$ and $f''(x) = \frac{2}{x^3}$. Hence, $f''(x) > 0$ for all $x > 0$, which implies that f is strictly convex for all $x > 0$, and $f'(x) = 0$ if and only if $x = \pm\frac{1}{\sqrt{\nu}}$, and we exclude the negative root, since we are interested in $x > 0$. Therefore, f has on the positive real line a unique global minimum point in $\frac{1}{\sqrt{\nu}}$ and it holds that f is strictly monotonically increasing for $x > \frac{1}{\sqrt{\nu}}$ and strictly monotonically decreasing for $x < \frac{1}{\sqrt{\nu}}$.

Let us now consider the constrained minimization problem

$$\min_{x \in [\lambda_{\min}(A), \lambda_{\max}(A)]} f(x).$$

We distinguish three cases: $\frac{1}{\sqrt{\nu}} \leq \lambda_{\min}(A)$, $\frac{1}{\sqrt{\nu}} \in (\lambda_{\min}(A), \lambda_{\max}(A))$, and $\frac{1}{\sqrt{\nu}} \geq \lambda_{\max}(A)$. In the first case, the properties of f imply that its minimum is attained at $\lambda_{\min}(A)$ and its maximum is attained at $\lambda_{\max}(A)$. Hence, it follows that

$$\lambda_{\min}(A^{-1}A_{\text{red}}) = \nu\lambda_{\min}(A) + \frac{1}{\lambda_{\min}(A)},$$

$$\lambda_{\max}(A^{-1}A_{\text{red}}) = \nu\lambda_{\max}(A) + \frac{1}{\lambda_{\max}(A)},$$

which imply

$$\kappa(A^{-1}A_{\text{red}}) = \frac{\nu\lambda_{\min}(A) + \frac{1}{\lambda_{\min}(A)}}{\nu\lambda_{\max}(A) + \frac{1}{\lambda_{\max}(A)}} = \frac{1}{\kappa(A)}\frac{\nu\lambda_{\min}(A)^2 + 1}{\nu\lambda_{\max}(A)^2 + 1}.$$

In the third case, the minimum and maximum of f are, respectively, attained at $\lambda_{\max}(A)$ and $\lambda_{\min}(A)$. Thus

$$\lambda_{\min}(A^{-1}A_{\text{red}}) = \nu\lambda_{\max}(A) + \frac{1}{\lambda_{\max}(A)},$$

$$\lambda_{\max}(A^{-1}A_{\text{red}}) = \nu\lambda_{\min}(A) + \frac{1}{\lambda_{\min}(A)},$$

which gives us

$$\kappa(A^{-1}A_{\text{red}}) = \frac{\nu\lambda_{\max}(A) + \frac{1}{\lambda_{\max}(A)}}{\nu\lambda_{\min}(A) + \frac{1}{\lambda_{\min}(A)}} = \kappa(A)\frac{\nu\lambda_{\max}(A)^2 + 1}{\nu\lambda_{\min}(A)^2 + 1},$$

and (5.29) follows. □

Theorem 5.8 explains clearly the observed numerical results. On the one hand, for ν sufficiently large (with $\frac{1}{\sqrt{\nu}} \leq \lambda_{\min}(A)$) the condition number $\kappa(A^{-1}A_{\text{red}})$ is equal to $\frac{1}{\kappa(A)}\frac{\nu\lambda_{\max}(A)+1}{\nu\lambda_{\min}(A)+1}$, which is an increasing function of ν. Hence, for increasing ν (with $\frac{1}{\sqrt{\nu}}$ smaller than $\lambda_{\min}(A)$), the condition number deteriorates and converges to $\kappa(A)$ for $\nu \to \infty$. This is exactly what one can observe from Figure 5.3. On the other hand, for ν sufficiently small (with $\frac{1}{\sqrt{\nu}} \geq \lambda_{\max}(A)$), the condition number is equal to $\kappa(A)\frac{\nu\lambda_{\min}(A)+1}{\nu\lambda_{\max}(A)+1}$, which is a decreasing function of ν. Hence,

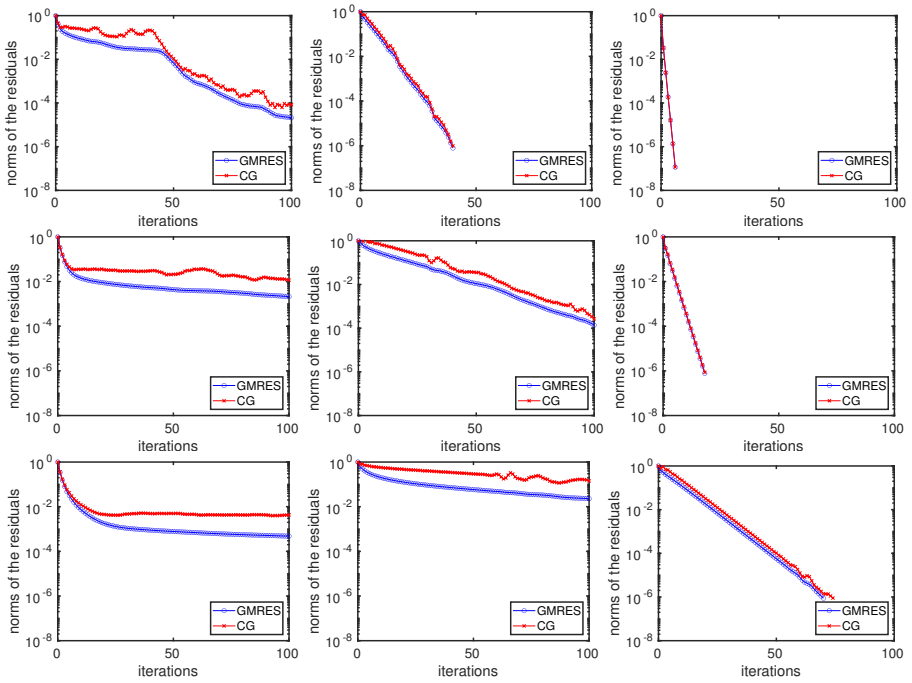

Figure 5.5. *Convergence of CG and GMRES (relative residuals) for the solution of the reduced problem* (5.30) *for a unit square* $\Omega \subset \mathbb{R}^2$. *First row:* $m = 15$, $\nu = 10^{-3}$, $\nu = 10^{-5}$, *and* $\nu = 10^{-7}$. *Second row:* $m = 31$, $\nu = 10^{-3}$, $\nu = 10^{-5}$, *and* $\nu = 10^{-7}$. *Third row:* $m = 63$, $\nu = 10^{-3}$, $\nu = 10^{-5}$, *and* $\nu = 10^{-7}$. *The results of the different figures are obtained with different (randomly chosen) initialization vectors.*

for decreasing ν (with $\frac{1}{\sqrt{\nu}}$ larger than $\lambda_{\max}(A)$) the condition number deteriorates and converges to $\kappa(A)$ for $\nu \to 0$. This is exactly what one can observe from Figure 5.4.

Let us now use A^2 as a preconditioner. In this case problem (5.21) becomes

$$(\nu A^2 + I)\boldsymbol{u} = A\boldsymbol{y}_d - \boldsymbol{f}. \tag{5.30}$$

Notice that this system is similar (up to an appropriate change in the right-hand side) to a system that one would obtain by reducing (5.15)–(5.16) to an equation for the variable $\boldsymbol{y}$ (or for $\boldsymbol{p}$).

The condition number of the preconditioned reduced matrix $A^2 A_{\text{red}} = \nu A^2 + I$ is

$$\kappa(A^2 A_{\text{red}}) = \frac{\nu\lambda_{\max}(A)^2 + 1}{\nu\lambda_{\min}(A)^2 + 1},$$

which is an increasing function of ν with

$$\lim_{\nu\to 0} \frac{\nu\lambda_{\max}(A)^2 + 1}{\nu\lambda_{\min}(A)^2 + 1} = 1 \quad \text{and} \quad \lim_{\nu\to\infty} \frac{\nu\lambda_{\max}(A)^2 + 1}{\nu\lambda_{\min}(A)^2 + 1} = \kappa(A)^2.$$

Therefore, the convergence behavior of CG and GMRES must improve for decreasing values of ν and deteriorates for decreasing values of mesh size (or increasing number of points m), with the latter more evident for large values of ν. This is exactly the behavior observed in Figure 5.5.

5.3 ▪ All-at-once approach

When there is no constraint on the set of controls, the optimality condition can be used to eliminate the control variable from the state equation and we simply deal with a coupled system of elliptic equations.

Jean-David Benamou, *A Domain Decomposition Method with Coupled Transmission Conditions for the Optimal Control of Systems Governed by Elliptic Partial Differential Equations*, 1996.

Potential computational advantages of the all-at once versions are expected to be more pronounced for nonlinear models. However, tests of their numerical performance for several practically relevant examples are yet to be done and will be subject of future work.

Barbara Kaltenbacher, *All-at-Once versus Reduced Iterative Methods for Time Dependent Inverse Problems*, 2017.

The term "one-shot method" is used for solution methods for optimization problems, which solve the optimization problem during the solution of the state equation. [...] Thus the state equation and all other restrictions are never feasible during the optimization iterations besides at the optimal solution.

Alfio Borzì and Volker Schulz, *Computational Optimization of Systems Governed by Partial Differential Equations*, 2012.

A famous alternative to the reduced approach of Section 5.2 is the so-called *all-at-once approach*, which is sometimes referred to as *one-shot method*; see the quotes above and, e.g., [117, 116, 23, 178].

One of the main drawbacks of the reduced approach is that it requires at each iteration of the iterative solver (e.g., CG) the solution of a PDE, whose discretization leads to the matrix A. If the PDE governing the optimal control problem is ill-posed or gives rise to a very ill-conditioned matrix, the reduced approach is in general not the best choice. These issues arise in many inverse problems that deal with ill-conditioned PDEs; see, e.g., [117].

The all-at-once approach tackles directly the full system (5.15). Note that the matrix

$$\widehat{A} = \begin{bmatrix} 0 & A & -I \\ A & I & 0 \\ -I & 0 & \nu I \end{bmatrix}$$

is invertible and symmetric, but not positive definite. Consider for example $\boldsymbol{e}_1^\top \widehat{A} \boldsymbol{e}_1 = 0$, where $\boldsymbol{e}_1 \in \mathbb{R}^{3m}$ is the first canonical vector. Hence, the CG method is in general not suitable for the solution of (5.15), and one has to consider other Krylov methods, like MINRES or GMRES. However, the performance of these methods for the solution of (5.15) can be very poor. To see this, we can run (for different values of ν and m) the MATLAB script

```
m=15;                          % number of mesh points in each direction
d=2;                           % dimension of the problem
nu=1e-3;                       % regularization parameter
h=1/(m+1);                     % mesh size
A=Laplacian(m,d)/h^2;          % negative 2D discrete Laplacian
Ahat=[sparse(m^d,m^d), A, -speye(m^d); ...
      A, speye(m^d), sparse(m^d,m^d); ...
      -speye(m^d), sparse(m^d,m^d), nu*speye(m^d)]; % all-at-once operator
f=-ones(m^d,1);                % discrete f=-1
yd=ones(m^d,1);                % discrete y_d=1
fhat=[f;yd;zeros(m^d,1)];      % assemble the right-hand-side vector
u0=rand(3*m^d,1);              % random initial guess
kmax=min(200,m^d);             % set max number of iterations
[u1,~,~,~,rv]=gmres(Ahat,fhat,[],1e-6,kmax,[],[],u0);
```

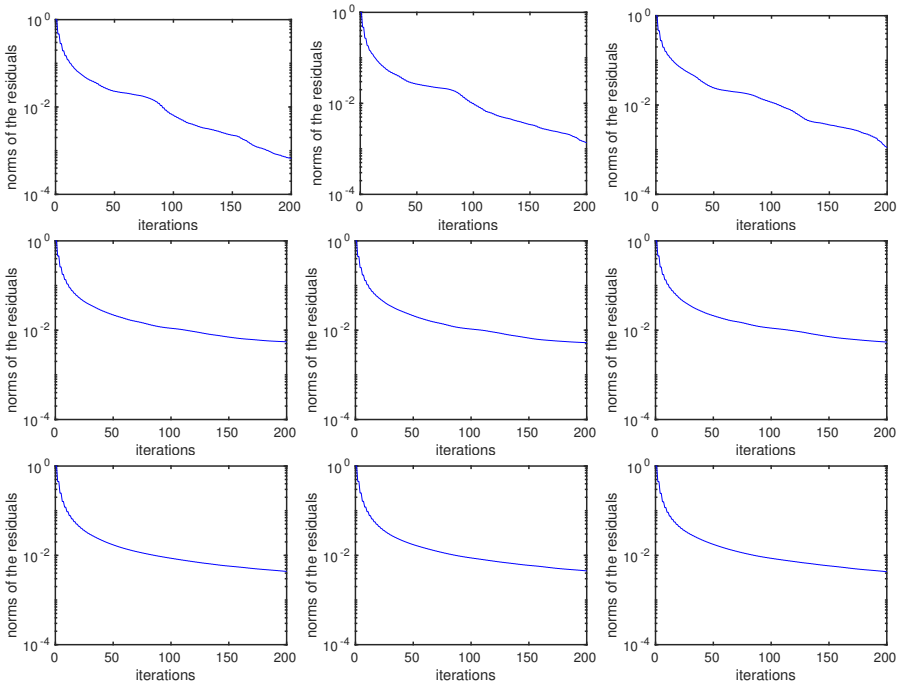

Figure 5.6. *Convergence of GMRES for the solution of the all-at-once problem* (5.15)–(5.31) *for a unit square* $\Omega \subset \mathbb{R}^2$ *and different values of* ν *and* $h = \frac{1}{m+1}$. *First row:* $m = 15$, $\nu = 10^{-3}$, $\nu = 10^{-5}$, *and* $\nu = 10^{-7}$. *Second row:* $m = 31$, $\nu = 10^{-3}$, $\nu = 10^{-5}$, *and* $\nu = 10^{-7}$. *Third row:* $m = 63$, $\nu = 10^{-3}$, $\nu = 10^{-5}$, *and* $\nu = 10^{-7}$. *The results of the different figures are obtained with different (randomly chosen) initialization vectors.*

```
semilogy(0:length(rv)-1,rv./rv(1),'b');
axis([0 200 1e-4 1]); yticks([1e-4 1e-2 1]);
xlabel('iterations');
ylabel('norms of the residuals');
set(gca,'fontsize',18,'linewidth',2);
```

which produces convergence curves that are similar (notice that the initialization vectors are chosen randomly) to the ones given in Figure 5.6.

We can clearly see the poor convergence behavior of GMRES. Notice that the matrix $\widehat{A}$ is symmetric, and hence the convergence bound given in Theorem 3.22 indicates that it is sufficient to study the eigenvalue distribution (the matrix S is orthogonal and hence $\kappa(S) = 1$). A direct numerical inspection of the eigenvalues of $\widehat{A}$ reveals that these are distributed in a uniform-type way on a segment containing the origin and lying on the real line. No clusters of eigenvalues are present. This explains the slow convergence behavior of GMRES and indicates clearly the need of a robust preconditioner.

The extremely bad behavior observed above can be mitigated if one formally solves the last equation in (5.15) to write $\boldsymbol{u} = \frac{1}{\nu}\boldsymbol{p}$ and replaces this in the first equation. If we do so, we obtain a new all-at-once system:

$$\begin{bmatrix} -\frac{1}{\nu}I & A \\ A & I \end{bmatrix} \begin{bmatrix} \boldsymbol{p} \\ \boldsymbol{y} \end{bmatrix} = \begin{bmatrix} \boldsymbol{f} \\ \boldsymbol{y}_d \end{bmatrix}. \tag{5.31}$$

This system is also symmetric but not positive definite. To observe the performance of GMRES for the solution of (5.31), we can run the MATLAB script

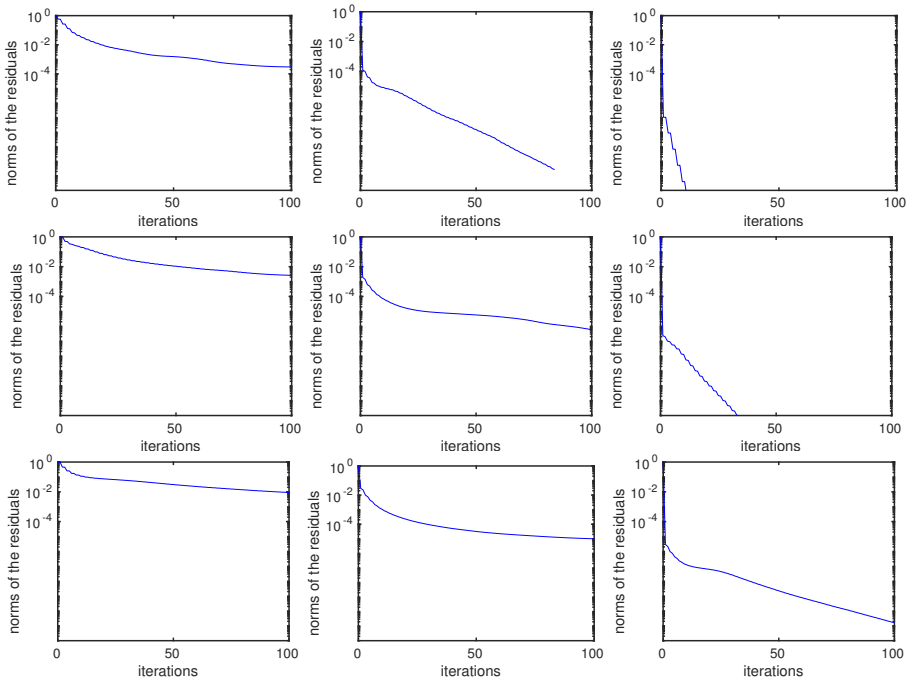

Figure 5.7. *Convergence of GMRES for the solution of problem* (5.31) *for a unit square* $\Omega \subset \mathbb{R}^2$ *and different values of* ν *and* $h = \frac{1}{m+1}$. *First row:* $m = 15$, $\nu = 10^{-3}$, $\nu = 10^{-5}$, *and* $\nu = 10^{-7}$. *Second row:* $m = 31$, $\nu = 10^{-3}$, $\nu = 10^{-5}$, *and* $\nu = 10^{-7}$. *Third row:* $m = 63$, $\nu = 10^{-3}$, $\nu = 10^{-5}$, *and* $\nu = 10^{-7}$. *The results of the different figures are obtained with different (randomly chosen) initialization vectors.*

```
m=15;                          % number of mesh points in each direction
d=2;                           % dimension of the problem
nu=1e-3;                       % regularization parameter
h=1/(m+1);                     % mesh size
A=Laplacian(m,d)/h^2;          % negative 2D discrete Laplacian
At=[-(1/nu)*speye(m^d), A; ...
    A, speye(m^d)];            % all-at-once operator
f=-ones(m^d,1);                % discrete f=-1
yd=ones(m^d,1);                % discrete y_d=1
ft=[f;yd];                     % assemble the right-hand-side vector
u0=rand(2*m^d,1);              % random initial guess
kmax=min(200,m^d);             % set max number of iterations
[u,~,~,~,rv]=gmres(At,ft,[],1e-6,kmax,[],[],u0);
semilogy(0:length(rv)-1,rv./rv(1),'b');
axis([0 100 1e-12 1]); yticks([1e-4 1e-2 1]);
xlabel('iterations');
ylabel('norms of the residuals');
set(gca,'fontsize',18,'linewidth',2);
```

which produces convergence curves similar to the ones given in Figure 5.7.

We can clearly see that the behavior of GMRES improved. Moreover, GMRES seems to converge faster when the regularization parameter ν becomes smaller! To explain this surprising behavior, we compute the eigenvalues of the all-at-once matrix $A_t := \begin{bmatrix} -\frac{1}{\nu} I & A \\ A & I \end{bmatrix}$.

Theorem 5.9 (Eigenvalues of the all-at-once matrix A_t). *Consider the matrix* $A_t := \begin{bmatrix} -\frac{1}{\nu}I & A \\ A & I \end{bmatrix}$ *with* $\nu > 0$*. The eigenvalues of* A_t *are*

$$\lambda_{j,\pm}(A_t) = \frac{\nu - 1}{2\nu} \pm \sqrt{\left(\frac{\nu - 1}{2\nu}\right)^2 + \frac{1}{\nu} + \lambda_j(A)^2} \quad \text{for } j = 1, \ldots, m, \tag{5.32}$$

where $\lambda_j(A)$*,* $j = 1, \ldots, m$*, are the eigenvalues of* A*.*

Proof. The proof can be carried out by noticing that $A = U^\top DU$, where D is diagonal and U orthogonal (since A is symmetric) and

$$A_t = \begin{bmatrix} U & 0 \\ 0 & U \end{bmatrix}^\top \begin{bmatrix} -\frac{1}{\nu}I & D \\ D & I \end{bmatrix} \begin{bmatrix} U & 0 \\ 0 & U \end{bmatrix}.$$

The result follows by computing explicitly the eigenvalues of $\begin{bmatrix} -\frac{1}{\nu}I & D \\ D & I \end{bmatrix}$ by means of formula (5.18) (as already done in the proof of Theorem 5.6). The detailed calculations are left to the reader as an exercise; see Problem 74. □

If we consider now the eigenvalues (5.32) as a function of ν and compute an expansion around zero, we get

$$\lambda_{j,+}(A_t) = 1 + O(\nu),$$
$$\lambda_{j,-}(A_t) = -\frac{1}{\nu} + O(\nu).$$

This means that when ν decreases toward zero, the eigenvalues of A_t tend to be split into two clusters: one cluster of eigenvalues that accumulate around 1 and another cluster of eigenvalues that indefinitely move to the left (away from zero) and accumulate around $-\frac{1}{\nu}$. This clustering behavior explains the improvement in the convergence of GMRES for decreasing ν. The GMRES residual decays very fast after two iterations (this is particularly evident in the pictures in the second and third columns in Figure 5.7) and then the convergence becomes slower again. Recalling Theorem 3.22, this behavior is due to the fact that GMRES can easily find a polynomial that passes through the two clusters of eigenvalues, but then it gets more complicated to obtain a polynomial approximating well all the single eigenvalues in the two clusters.

The all-at-once formulation represents the basis for the use of the optimized Schwarz method for optimal control problems introduced and analyzed in Section 5.3.1.

Finally, we wish to remark that rather than reducing the all-at-once system to the variables $(\boldsymbol{y}, \boldsymbol{p})$, one could also reduce it to the variables $(\boldsymbol{y}, \boldsymbol{u})$ or to $(\boldsymbol{p}, \boldsymbol{u})$; see Problem 75.

5.3.1 ▪ Optimized Schwarz methods

> *This domain decomposition strategy defines a sequence of local problems which themselves can be reformulated as optimal control problems.*
>
> Jean-David Benamou, *A Domain Decomposition Method with Coupled Transmission Conditions for the Optimal Control of Systems Governed by Elliptic Partial Differential Equations*, 1996.

In this section, we introduce a very efficient preconditioner for optimal control problems. It is based on the optimized Schwarz method (OSM) discussed in Section 4.6. Notice that similar OSMs were introduced by Benamou in [10, 12, 11]; see also [53]. However, while Benamou considers transmission conditions where state and adjoint variables are combined, we extend

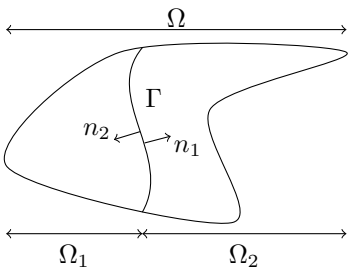

Figure 5.8. *Example of a nonoverlapping decomposition of a domain Ω.*

here the OSM described in Section 4.6 to optimal control problems. Nevertheless, we will prove convergence of the OSM using energy estimates similarly as in [10].

In Section 5.3, we have introduced the all-at-once system (5.31), namely

$$\begin{bmatrix} -\frac{1}{\nu}I & A \\ A & I \end{bmatrix} \begin{bmatrix} \boldsymbol{p} \\ \boldsymbol{y} \end{bmatrix} = \begin{bmatrix} \boldsymbol{f} \\ \boldsymbol{y}_d \end{bmatrix}. \tag{5.33}$$

At the continuous level, the system (5.33) corresponds to

$$\begin{aligned} -\Delta y &= f + \frac{1}{\nu}p && \text{in } \Omega, && (5.34)\\ y &= 0 && \text{on } \partial\Omega, \\ -\Delta p &= y_d - y && \text{in } \Omega, && (5.35)\\ p &= 0 && \text{on } \partial\Omega, \end{aligned}$$

which is obtained by solving (5.14) in u and replacing it in (5.12).

Consider a nonoverlapping domain decomposition $\overline{\Omega} = \overline{\Omega}_1 \cup \overline{\Omega}_2$, where Ω_1 and Ω_2 are two Lipschitz domains with $\Omega_1 \cap \Omega_2 = \emptyset$. Moreover, we define the interface between the two subdomains as $\Gamma := \partial\Omega_1 \setminus \Omega = \partial\Omega_2 \setminus \Omega$. An example of this decomposition is given in Figure 5.8. Given a positive real parameter q, the parallel OSM for the solution of the optimality system (5.34)–(5.35) is

$$\begin{aligned} -\Delta y_j^n &= f + \frac{1}{\nu}p_j^n && \text{in } \Omega_j, && (5.36)\\ \partial_{n_j} y_j^n + q y_j^n &= \partial_{n_j} y_{3-j}^{n-1} + q y_{3-j}^{n-1} && \text{on } \Gamma, && (5.37)\\ y_j^n &= 0 && \text{on } \partial\Omega \cap \partial\Omega_j, && (5.38)\\ -\Delta p_j^n &= y_d - y_j^n && \text{in } \Omega_j, && (5.39)\\ \partial_{n_j} p_j^n + q p_j^n &= \partial_{n_j} p_{3-j}^{n-1} + q p_{3-j}^{n-1} && \text{on } \Gamma, && (5.40)\\ p_j^n &= 0 && \text{on } \partial\Omega \cap \partial\Omega_j && (5.41) \end{aligned}$$

for $j = 1, 2$ and $n \in \mathbb{N}^+$. We assume that the OSM is initialized by some functions $g_j^y, g_j^p \in L^2(\Gamma)$ for $j = 1, 2$ by setting $\partial_{n_j} y_j^1 + q y_j^1 = g_j^y$ and $\partial_{n_j} p_j^1 + q p_j^1 = g_j^p$ for $j = 1, 2$. Using this assumption we can prove that the OSM is well posed.

Lemma 5.10. *Let $g_j^y, g_j^p \in L^2(\Gamma)$ for $j = 1, 2$ be initialization functions, that is, $\partial_{n_j} y_j^1 + q y_j^1 = g_j^y$ and $\partial_{n_j} p_j^1 + q p_j^1 = g_j^p$ for $j = 1, 2$. The sequences $\{y_j^n\}_{n\in\mathbb{N}^+} \subset H^1(\Omega_j)$ and $\{p_j^n\}_{n\in\mathbb{N}^+} \subset H^1(\Omega_j)$ for $j = 1, 2$ are well posed.*

Proof. Consider the problem

$$
\begin{aligned}
-\Delta y_j &= f + \frac{1}{\nu} p_j && \text{in } \Omega_j, && (5.42)\\
\partial_{n_j} y_j + q y_j &= g_j^y && \text{on } \Gamma, && (5.43)\\
y_j &= 0 && \text{on } \partial\Omega \cap \partial\Omega_j, && (5.44)\\
-\Delta p_j &= y_d - y_j && \text{in } \Omega_j, && (5.45)\\
\partial_{n_j} p_j + q p_j &= g_j^p && \text{on } \Gamma, && (5.46)\\
p_j &= 0 && \text{on } \partial\Omega \cap \partial\Omega_j, && (5.47)
\end{aligned}
$$

where $g_j^y, g_j^p \in L^2(\Gamma)$. By introducing the variable $u_j = \frac{1}{\nu} p_j$, the system (5.42)–(5.47) is the optimality system of the auxiliary problem

$$
\begin{aligned}
\min_{y_j, u_j} \quad & J_{\text{aux}}(y_j, u_j) := \frac{1}{2}\|y_j - y_d\|^2_{L^2(\Omega_j)} + \frac{\nu}{2}\|u_j\|^2_{L^2(\Omega_j)} + \int_\Gamma g_j^p y_j \, ds \\
\text{s.t.} \quad & -\Delta y_j = f + u_j \ \text{ in } \Omega_j, \\
& \partial_{n_j} y_j + q y_j = g_j^y \qquad \text{on } \Gamma, \\
& y_j = 0 \qquad \text{on } \partial\Omega_j \setminus \Gamma.
\end{aligned} \tag{5.48}
$$

Since (5.48) is strictly convex and uniquely solvable by $(y_j, u_j) \in H^1(\Omega_j) \times L^2(\Omega_j)$, there exists a unique solution $(y_j, p_j) \in H^1(\Omega_j) \times H^1(\Omega_j)$ to the optimality system (5.42)–(5.47). Therefore, since $\partial_{n_j} y_j^1 + q y_j^1 = g_j^y \in L^2(\Gamma)$ and $\partial_{n_j} p_j^1 + q p_j^1 = g_j^p \in L^2(\Gamma)$ for $j = 1, 2$, the OSM (5.36)–(5.41) is well posed for $n = 1$. Moreover, we get $\partial_{n_j} y_j^2 + q y_j^2 = \partial_{n_j} y_{3-j}^1 + q y_{3-j}^1 \in L^2(\Gamma)$ and $\partial_{n_j} p_j^2 + q p_j^2 = \partial_{n_j} p_{3-j}^2 + q p_{3-j}^2 \in L^2(\Gamma)$ for $j = 1, 2$. Hence (5.36)–(5.41) is well posed for $n = 2$. The result follows by repeating this argument for $n \geq 2$. ∎

Next, we wish to prove convergence of the OSM (5.36)–(5.41) by using an *energy estimate* technique in the same spirit as [10]. To do so, we write the weak forms of (5.36)–(5.41),

$$
\begin{aligned}
&\int_{\Omega_j} \nu \nabla y_j^n \cdot \nabla v - p_j^n v \, d\boldsymbol{x} - \int_\Gamma \nu \partial_{n_j} y_j^n v \, ds = \int_{\Omega_j} \nu f v \, d\boldsymbol{x} \\
&\forall v \in H^1(\Omega_j) \text{ s.t. } v = 0 \text{ on } \partial\Omega_j \setminus \Gamma \text{ and } \partial_{n_j} y_j^n + q y_j^n = \partial_{n_j} y_{3-j}^{n-1} + q y_{3-j}^{n-1} \text{ on } \Gamma,
\end{aligned} \tag{5.49}
$$

$$
\begin{aligned}
&\int_{\Omega_j} \nabla p_j^n \cdot \nabla v + y_j^n v \, d\boldsymbol{x} - \int_\Gamma \partial_{n_j} p_j^n v \, ds = \int_{\Omega_j} y_d v \, d\boldsymbol{x} \\
&\forall v \in H^1(\Omega_j) \text{ s.t. } v = 0 \text{ on } \partial\Omega_j \setminus \Gamma \text{ and } \partial_{n_j} p_j^n + q p_j^n = \partial_{n_j} p_{3-j}^{n-1} + q p_{3-j}^{n-1} \text{ on } \Gamma.
\end{aligned} \tag{5.50}
$$

The weak forms of (5.34) and (5.35) are

$$
\int_\Omega \nu \nabla y \cdot \nabla v - p v \, d\boldsymbol{x} = \int_\Omega \nu f v \, d\boldsymbol{x} \quad \forall v \in H_0^1(\Omega),
$$

$$
\int_\Omega \nabla p \cdot \nabla v + y v \, d\boldsymbol{x} = \int_\Omega y_d v \, d\boldsymbol{x} \quad \forall v \in H_0^1(\Omega),
$$

which are equivalent to

$$\begin{aligned}&\int_{\Omega_j} \nu\nabla y_j\cdot\nabla v - p_j v\,d\boldsymbol{x} - \int_\Gamma \nu\partial_{n_j} y_j v\,ds = \int_{\Omega_j} \nu f v\,d\boldsymbol{x}\\ &\forall v\in H^1(\Omega_j) \text{ s.t. } v=0 \text{ on } \partial\Omega_j\setminus\Gamma \text{ and } \partial_{n_j}y_j + qy_j = \partial_{n_j}y_{3-j} + qy_{3-j} \text{ on } \Gamma,\end{aligned} \tag{5.51}$$

$$\begin{aligned}&\int_{\Omega_j} \nabla p_j\cdot\nabla v + y_j v\,d\boldsymbol{x} - \int_\Gamma \partial_{n_j} p_j v\,ds = \int_{\Omega_j} y_d v\,d\boldsymbol{x}\\ &\forall v\in H^1(\Omega_j) \text{ s.t. } v=0 \text{ on } \partial\Omega_j\setminus\Gamma \text{ and } \partial_{n_j}p_j + qp_j = \partial_{n_j}p_{3-j} + qp_{3-j} \text{ on } \Gamma\end{aligned} \tag{5.52}$$

for $j=1,2$.

Next, we introduce the errors $\widehat{y}_j^n := y_j - y_j^n$ and $\widehat{p}_j^n := p_j - p_j^n$ for $j=1,2$, which satisfy the system

$$\begin{aligned}&\int_{\Omega_j} \nu\nabla\widehat{y}_j^n\cdot\nabla v - \widehat{p}_j^n v\,d\boldsymbol{x} = \int_\Gamma \nu\partial_{n_j}\widehat{y}_j^n v\,ds \quad \forall v\in H^1(\Omega_j) \text{ s.t. } v=0 \text{ on } \partial\Omega_j\setminus\Gamma\\ &\text{and } \partial_{n_j}\widehat{y}_j^n + q\widehat{y}_j^n = \partial_{n_j}\widehat{y}_{3-j}^{n-1} + q\widehat{y}_{3-j}^{n-1} \text{ on } \Gamma,\end{aligned} \tag{5.53}$$

$$\begin{aligned}&\int_{\Omega_j} \nabla\widehat{p}_j^n\cdot\nabla v + \widehat{y}_j^n v\,d\boldsymbol{x} = \int_\Gamma \partial_{n_j}\widehat{p}_j^n v\,ds \quad \forall v\in H^1(\Omega_j) \text{ s.t. } v=0 \text{ on } \partial\Omega_j\setminus\Gamma\\ &\text{and } \partial_{n_j}\widehat{p}_j^n + q\widehat{p}_j^n = \partial_{n_j}\widehat{p}_{3-j}^{n-1} + q\widehat{p}_{3-j}^{n-1} \text{ on } \Gamma\end{aligned} \tag{5.54}$$

for $j=1,2$. We are now ready to prove the following convergence result.

Theorem 5.11 (Convergence of the OSM by energy estimates). *Let $g_j^y, g_j^p \in L^2(\Gamma)$ for $j=1,2$ be initialization functions as in Lemma 5.10. The OSM converges in the sense that*

$$\|\widehat{y}_j^n\|_{H^1(\Omega_j)} \to 0, \quad \|\widehat{p}_j^n\|_{H^1(\Omega_j)} \to 0$$

for $j=1,2$ as $n\to\infty$.

Proof. Let us define the energy

$$E_n := \sum_{j=1}^2 \nu\|\partial_{n_j}\widehat{y}_j^n\|_{L^2(\Gamma)}^2 + \nu q^2\|\widehat{y}_j^n\|_{L^2(\Gamma)}^2 + \|\partial_{n_j}\widehat{p}_j^n\|_{L^2(\Gamma)}^2 + q^2\|\widehat{p}_j^n\|_{L^2(\Gamma)}^2$$

for $n\in\mathbb{N}$ and use it to write

$$\begin{aligned}E_n &= \sum_{j=1}^2 \Big[\nu\|\partial_{n_j}\widehat{y}_j^n + q\widehat{y}_j^n\|_{L^2(\Gamma)}^2 - 2q\nu\langle\partial_{n_j}\widehat{y}_j^n, \widehat{y}_j^n\rangle_{L^2(\Gamma)}\\ &\quad + \|\partial_{n_j}\widehat{p}_j^n + q\widehat{p}_j^n\|_{L^2(\Gamma)}^2 - 2q\langle\partial_{n_j}\widehat{p}_j^n, \widehat{p}_j^n\rangle_{L^2(\Gamma)}\Big]\\ &= \sum_{j=1}^2 \Big[\nu\|\partial_{n_j}\widehat{y}_{3-j}^{n-1} + q\widehat{y}_{3-j}^{n-1}\|_{L^2(\Gamma)}^2 - 2q\nu\langle\partial_{n_j}\widehat{y}_j^n, \widehat{y}_j^n\rangle_{L^2(\Gamma)}\\ &\quad + \|\partial_{n_j}\widehat{p}_{3-j}^{n-1} + q\widehat{p}_{3-j}^{n-1}\|_{L^2(\Gamma)}^2 - 2q\langle\partial_{n_j}\widehat{p}_j^n, \widehat{p}_j^n\rangle_{L^2(\Gamma)}\Big]\end{aligned}$$

$$= \sum_{j=1}^{2}\Big[\nu\|\partial_{n_j}\widehat{y}_{3-j}^{n-1}\|_{L^2(\Gamma)}^2 + \nu q^2\|\widehat{y}_{3-j}^{n-1}\|_{L^2(\Gamma)}^2 + \|\partial_{n_j}\widehat{p}_{3-j}^{n-1}\|_{L^2(\Gamma)}^2 + q^2\|\widehat{p}_{3-j}^{n-1}\|_{L^2(\Gamma)}^2\Big]$$

$$- 2q\sum_{j=1}^{2}\sum_{m=n-1}^{n}\Big[\nu\langle\partial_{n_j}\widehat{y}_j^m,\widehat{y}_j^m\rangle_{L^2(\Gamma)} + \langle\partial_{n_j}\widehat{p}_j^m,\widehat{p}_j^m\rangle_{L^2(\Gamma)}\Big]$$

$$= E_{n-1} - 2q\sum_{j=1}^{2}\sum_{m=n-1}^{n}\Big[\nu\langle\partial_{n_j}\widehat{y}_j^m,\widehat{y}_j^m\rangle_{L^2(\Gamma)} + \langle\partial_{n_j}\widehat{p}_j^m,\widehat{p}_j^m\rangle_{L^2(\Gamma)}\Big],$$

where we used the Robin transmission conditions of (5.53) and (5.54) and that $n_1 = -n_2$.

Now, we test (5.53) with $v = \widehat{y}_j^n$ and (5.54) with $v = \widehat{p}_j^n$ to obtain

$$\nu\langle\partial_{n_j}\widehat{y}_j^n,\widehat{y}_j^n\rangle_{L^2(\Gamma)} = \nu\|\nabla\widehat{y}_j^n\|_{L^2(\Omega_j)}^2 - \langle\widehat{p}_j^n,\widehat{y}_j^n\rangle_{L^2(\Omega_j)}$$

and

$$\langle\partial_{n_j}\widehat{p}_j^n,\widehat{p}_j^n\rangle_{L^2(\Gamma)} = \|\nabla\widehat{p}_j^n\|_{L^2(\Omega_j)}^2 + \langle\widehat{y}_j^n,\widehat{p}_j^n\rangle_{L^2(\Omega_j)}.$$

If we insert these into the above energy relation, we obtain

$$E_n = E_{n-1} - 2q\sum_{j=1}^{2}\sum_{m=n-1}^{n}\Big[\nu\|\nabla\widehat{y}_j^m\|_{L^2(\Omega_j)}^2 + \|\nabla\widehat{p}_j^m\|_{L^2(\Omega_j)}^2\Big], \tag{5.55}$$

where the second term on the right-hand side is nonnegative. This yields $0 \le E_n \le E_{n-1}$ for any $n \in \mathbb{N}$ and hence $E_n \to \ell$ as $n \to \infty$ for some real value $\ell < \infty$. Now, using (5.55) we write

$$\sum_{j=1}^{2}\Big[\nu\|\nabla\widehat{y}_j^n\|_{L^2(\Omega_j)}^2 + \|\nabla\widehat{p}_j^n\|_{L^2(\Omega_j)}^2\Big] \le \frac{1}{2q}(E_{n-1} - E_n).$$

Summing left- and right-hand sides over n, we get

$$\sum_{n=1}^{\infty}\sum_{j=1}^{2}\Big[\nu\|\nabla\widehat{y}_j^n\|_{L^2(\Omega_j)}^2 + \|\nabla\widehat{p}_j^n\|_{L^2(\Omega_j)}^2\Big] \le \frac{1}{2q}(E_0 - \ell).$$

Since this series converges, we obtain that $\|\nabla\widehat{y}_j^n\|_{L^2(\Omega_j)} \to 0$ and $\|\nabla\widehat{p}_j^n\|_{L^2(\Omega_j)} \to 0$ for $j = 1, 2$, as $n \to \infty$. Recalling that $\widehat{y}_j^n$ and $\widehat{p}_j^n$ vanish on $\partial\Omega_j \setminus \Gamma$ (a set of positive measure) for $j = 1, 2$, we can invoke the generalized Friedrich–Poincaré inequality [48, Theorem 6.6-6] to obtain that there exist two constants $C_y > 0$ and $C_p > 0$ such that $\|\widehat{y}_j^n\|_{L^2(\Omega_j)} \le C_y\|\nabla\widehat{y}_j^n\|_{L^2(\Omega_j)}$ and $\|\widehat{p}_j^n\|_{L^2(\Omega_j)} \le C_p\|\nabla\widehat{p}_j^n\|_{L^2(\Omega_j)}$. The claim follows. ∎

Let us now study the numerical convergence of the OSM (5.36)–(5.36) as a stationary method and as a preconditioner for GMRES. To do so, we consider the optimal control system (5.34)–(5.35) on a domain $\Omega = (-1, 1) \times (0, 1)$ and the nonoverlapping decomposition $\overline{\Omega} = \overline{\Omega}_1 \cup \overline{\Omega}_2$ with $\overline{\Omega}_1 = (-1, 0) \times (0, 1)$ and $\overline{\Omega}_2 = (0, 1) \times (0, 1)$. Each of these subdomains is discretized by a grid of m interior points for each edge. If we run the OSM (see Problem 76) for different values of grid sizes h and parameter ν, we obtain the results shown in Figure 5.9. We can clearly observe that GMRES preconditioned by the OSM is quite robust with respect to the regularization parameter ν and the grid size $h = \frac{1}{m+1}$.

We wish to remark that, on the one hand, it is certainly possible to include an overlap in the OSM implementation and, on the other hand, to optimize the Robin parameter q. These two modifications will certainly (and greatly) improve the convergence of the method (as discussed in Section 4.6); see Problem 77. Notice also that a multiple-domain implementation must be considered for a suitable parallel implementation.

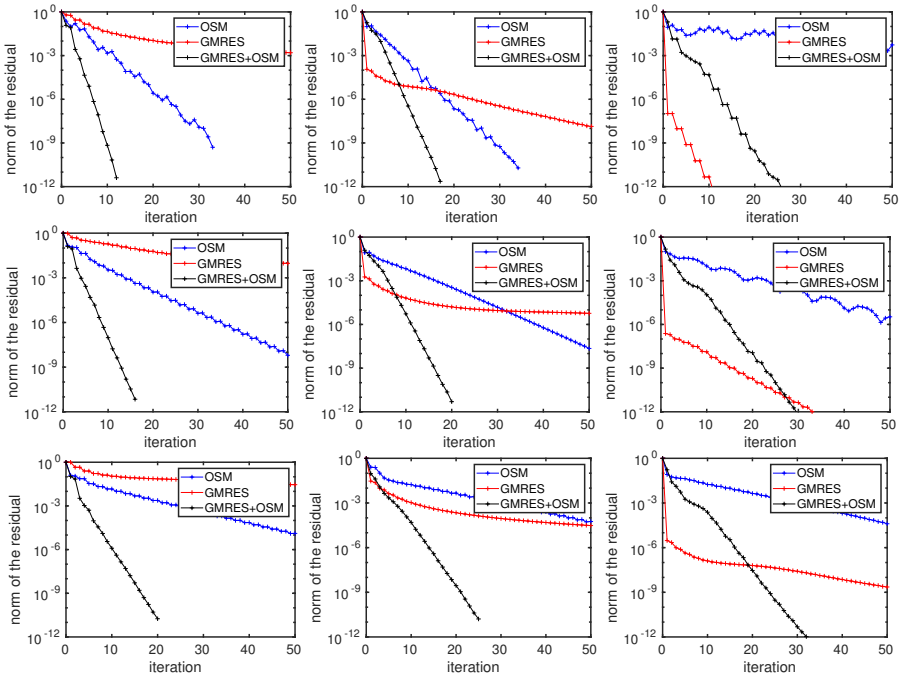

Figure 5.9. *Convergence of GMRES and OSM (as a stationary method and as a preconditioner) for the solution of problem* (5.31) *for a rectangle* $\Omega = (-1, 1) \times (0, 1)$ *and different values of* ν *and* $h = \frac{1}{m+1}$ *and Robin parameter* $q = 15$. *First row:* $m = 15$, $\nu = 10^{-3}$, $\nu = 10^{-5}$, *and* $\nu = 10^{-7}$. *Second row:* $m = 31$, $\nu = 10^{-3}$, $\nu = 10^{-5}$, *and* $\nu = 10^{-7}$. *Third row:* $m = 63$, $\nu = 10^{-3}$, $\nu = 10^{-5}$, *and* $\nu = 10^{-7}$. *The results of the different figures are obtained with different (randomly chosen) initialization vectors.*

5.3.2 ▪ Block-diagonal preconditioners

The systems under consideration exhibit a specific structure that should be exploited in order to develop an efficient algorithm. [...] we are interested in preconditioners for such matrices K that maintain the block structure of the system and that are composed of subblocks themselves.

Astrid Battermann and Ekkehard Sachs, *Block Preconditioners for KKT Systems in PDE-Governed Optimal Control Problems*, 2001.

Preconditioners are often conceived as approximate inverses. For nonsingular indefinite matrices of saddle-point (or KKT) form, we show how preconditioners incorporating an exact Schur complement lead to preconditioned matrices with exactly two or exactly three distinct eigenvalues. Thus approximations of the Schur complement lead to preconditioners which can be very effective even though they are in no sense approximate inverses.

Malcolm F. Murphy, Gene H. Golub, and Andrew J. Wathen, *A Note on Preconditioning for Indefinite Linear Systems*, 2000.

The goal of this section is to construct block-diagonal preconditioners by using the structure of the all-at-once matrix $\widehat{A}$, which is invertible, symmetric, but indefinite. Thus, the optimality system (5.15)–(5.31) represents a saddle-point problem, for which very efficient block-diagonal preconditioners can be constructed following the work of Murphy, Golub, and Wathen [135].

Consider an invertible and indefinite matrix W having the block form

$$W = \begin{bmatrix} 0 & W_{12} \\ W_{21} & W_{22} \end{bmatrix},$$

where the block W_{22} is assumed to be invertible as well. A direct calculation using the well-known formula (5.18) for the determinant of block matrices (see [108, Section 0.8.5]) allows us to obtain that the matrix $W_{12}W_{22}^{-1}W_{21}$, called the *Schur complement of* W, is invertible. Murphy, Golub, and Wathen proposed the use of the block-diagonal preconditioner

$$M = \begin{bmatrix} W_{12}W_{22}^{-1}W_{21} & 0 \\ 0 & W_{22} \end{bmatrix}, \tag{5.56}$$

which leads to the preconditioned matrix

$$T := M^{-1}W = \begin{bmatrix} 0 & (W_{12}W_{22}^{-1}W_{21})^{-1}W_{12} \\ W_{22}^{-1}W_{21} & I \end{bmatrix}, \tag{5.57}$$

and they proved the following key result.

Theorem 5.12 (Murphy, Golub, and Wathen, 2000). *The preconditioned matrix T defined in* (5.57) *satisfies*

$$T(T-I)(T^2-T-I) = 0. \tag{5.58}$$

Proof. A direct calculation allows us to obtain that

$$\Big(T - \frac{1}{2}I\Big)^2 = \begin{bmatrix} \frac{5}{4}I & 0 \\ 0 & \frac{1}{4}I + \widehat{W} \end{bmatrix},$$

where $\widehat{W} := W_{22}^{-1}W_{21}(W_{12}W_{22}^{-1}W_{21})^{-1}W_{12}$. Since the matrix $\widehat{W}$ is a projection, that is, $\widehat{W}^2 = \widehat{W}$, it is possible to show that

$$\Big[\Big(T - \frac{1}{2}I\Big)^2 - \frac{1}{4}I\Big]^2 = \Big[\Big(T - \frac{1}{2}I\Big)^2 - \frac{1}{4}I\Big],$$

which simplifies to $T(T-I)(T^2-T-I) = 0$. □

Theorem 5.12 has an important consequence. Since, the matrix T is invertible, it follows from (5.58) that $(T-I)(T^2-T-I) = 0$. Thus, we have constructed the third-order monic polynomial $q(z) = (z-1)(z^2-z-1)$ that satisfies $q(T) = 0$. Hence, the minimal polynomial $p_{\min}$ of T must have degree lower than or equal to three. On the other hand, using the structure of T (and its invertibility), it is possible to show that $\deg p_{\min} \geq 3$. By the uniqueness of the minimal polynomial (Lemma 3.6, point (a)), it follows that $q = p_{\min}$. Hence, Lemma 3.6, point (d), guarantees that T has three distinct eigenvalues:

$$1, \quad \frac{1}{2} + \frac{\sqrt{5}}{2}, \quad \frac{1}{2} - \frac{\sqrt{5}}{2}.$$

This surprising result shows very nicely how an appropriately chosen preconditioner can cluster the eigenvalues of the system matrix. Moreover, since the degree of the minimal polynomial is

equal to three, Theorem 3.8 guarantees that the Krylov space

$$\mathcal{K}_k(T, \boldsymbol{v}) := \operatorname{span}\{\boldsymbol{v}, T\boldsymbol{v}, \dots, T^{k-1}\boldsymbol{v}\}$$

has at most dimension equal to three. In this case, Theorem 3.32 guarantees that GMRES (or other Krylov methods like, e.g., MINRES) converges in at most three iterations! Recalling Section 4.1, for M to be an efficient preconditioner, it is necessary that the action of M^{-1} on a given vector must be cheap to compute. From the structure of M given in (5.56), it is clear that this requirement is met if W_{22} and the Schur complement $W_{12}W_{22}^{-1}W_{21}$ are cheap to invert. Unfortunately, this condition is not satisfied in general, and one needs to approximate either W_{22} or $W_{12}W_{22}^{-1}W_{21}$ or both matrices; see, e.g., [9, 154].

Notice that a result similar to Theorem 5.12 can be proved if one uses a block-triangular preconditioner. See [135, Remark 4] and Problems 78, 79, and 80.

To apply the beautiful theory of Murphy, Golub, and Wathen to our optimal control problem, we recall the system matrix $\widehat{A}$ and set

$$W_{12} = \begin{bmatrix} A & -I \end{bmatrix}, \quad W_{21} = \begin{bmatrix} A \\ -I \end{bmatrix}, \quad W_{22} = \begin{bmatrix} I & 0 \\ 0 & \nu I \end{bmatrix}.$$

This means that the Schur complement is

$$S := W_{12}W_{22}^{-1}W_{21} = \frac{1}{\nu}I + AA,$$

which coincides (after multiplication by ν) with the matrix of the (reduced) system (5.30). Thus, the preconditioner M and the preconditioned matrix T are

$$M = \begin{bmatrix} S & 0 & 0 \\ 0 & I & 0 \\ 0 & 0 & \nu I \end{bmatrix} \quad \text{and} \quad T := M^{-1}\widehat{A} = \begin{bmatrix} 0 & S^{-1}A & -S^{-1} \\ A & I & 0 \\ -\frac{1}{\nu}I & 0 & I \end{bmatrix}. \tag{5.59}$$

In this case, the inverse of $W_{22} = \begin{bmatrix} I & 0 \\ 0 & \nu I \end{bmatrix}$ is very cheap to compute, but the action of $S^{-1} = (W_{12}W_{22}^{-1}W_{21})^{-1}$ can be rather expensive (see, e.g., Figure 5.5). Hence, we look for an approximation of the Schur complement $W_{12}W_{22}^{-1}W_{21}$ with an inverse that is cheap to compute. A typical strategy consists in dropping the term $\frac{1}{\nu}I$ to obtain

$$S \approx AA. \tag{5.60}$$

This is exactly the approach considered in [9] and [154] and leads to the preconditioner and preconditioned matrix given by

$$\widetilde{M} = \begin{bmatrix} A^2 & 0 & 0 \\ 0 & I & 0 \\ 0 & 0 & \nu I \end{bmatrix} \quad \text{and} \quad \widetilde{T} := \widetilde{M}^{-1}\widehat{A} = \begin{bmatrix} 0 & A^{-1} & -A^{-2} \\ A & I & 0 \\ -\frac{1}{\nu}I & 0 & I \end{bmatrix}. \tag{5.61}$$

The approximation (5.60) has a tremendous impact on the spectrum of the preconditioned matrix, as the next theorem shows; see also [154, Proposition 3.2] and [3] for similar results.

Theorem 5.13 (Spectra of the preconditioned matrices $\boldsymbol{M^{-1}\widehat{A}}$ and $\boldsymbol{\widetilde{M}^{-1}\widehat{A}}$). *The spectra of the matrices $T := M^{-1}\widehat{A}$ and $\widetilde{T} := \widetilde{M}^{-1}\widehat{A}$ are*

$$\sigma(T) = \left\{1, \frac{1+\sqrt{5}}{2}, \frac{1-\sqrt{5}}{2}\right\}$$

and

$$\sigma(\widetilde{T}) = \{1\} \cup \left(\bigcup_{j=1}^{n} \left\{ \frac{1+\sqrt{1+4\widehat{\lambda}_j}}{2}, \frac{1-\sqrt{1+4\widehat{\lambda}_j}}{2} \right\} \right),$$

where $\widehat{\lambda}_j = 1 + \frac{1}{\nu(\lambda_j(A))^2}$, $j = 1, \ldots, n$, *and* $\lambda_j(A)$ *denote the eigenvalues of* A.

Proof. The spectrum $\sigma(T)$ can be obtained using Theorem 5.12 or as done below for $\sigma(\widetilde{T})$. To obtain $\sigma(\widetilde{T})$, we apply the formula (5.18) for the determinant of block matrices (see [108, Section 0.8.5]) to compute

$$\begin{aligned}
\det(\lambda I - \widetilde{T}) &= \det \begin{bmatrix} (1-\lambda)I & 0 \\ 0 & (1-\lambda)I \end{bmatrix} \det \left(-\lambda I - \frac{1}{(1-\lambda)} \begin{bmatrix} A^{-1} & A^{-2} \end{bmatrix} \begin{bmatrix} A \\ -\frac{1}{\nu} I \end{bmatrix} \right) \\
&= (1-\lambda)^{2n} \det \left(-\lambda I - \frac{1}{(1-\lambda)} \left(I + \frac{1}{\nu} A^{-2} \right) \right) \\
&= (1-\lambda)^{n} \det \left(-\lambda(1-\lambda) I - \left(I + \frac{1}{\nu} A^{-2} \right) \right) \\
&= (1-\lambda)^{n} \det \left(-\widehat{\lambda} I - \left(I + \frac{1}{\nu} A^{-2} \right) \right),
\end{aligned}$$

where we defined $\widehat{\lambda} := \lambda(1-\lambda)$. Hence, the condition $\det(\lambda I - \widetilde{T}) = 0$ implies that $\widehat{\lambda}$ must be an eigenvalue of $I + \frac{1}{\nu} A^{-2}$. Thus, the matrix $\widetilde{T}$ has n eigenvalues equal to 1, n eigenvalues of the type $\frac{1+\sqrt{1+4\widehat{\lambda}_j}}{2}$, and n eigenvalues of type $\frac{1-\sqrt{1+4\widehat{\lambda}_j}}{2}$. ∎

Theorem 5.13 is a beautiful example of the clustering effect that preconditioners can generate. The preconditioned matrix T has exactly three eigenvalues. These do not depend on the mesh size $h = \frac{1}{m+1}$ (hence on the dimension of the discrete problem) and on the regularization parameter ν. Thus, the block-diagonal preconditioner M defined in (5.59) is optimal in terms of spectral properties of the preconditioned optimality system. However, every iteration of a Krylov method applied to the preconditioned system requires the evaluation of the action of S^{-1}, but this corresponds to solving the optimal control problem in a reduced form (as we have seen in Section 5.2). For this reason, an approximation of S is sought. By dropping the term $\frac{1}{\nu} I$, one gets $S \approx A^2$, whose inverse is simply $A^{-1}A^{-1}$. The action of this matrix on a vector corresponds to two Laplace solves, which can be performed efficiently using, e.g., sparse solvers (if A is a pentadiagonal matrix) or a few multigrid V-cycles, as suggested in [154]. However, Theorem 5.13 shows that dropping the simple term $\frac{1}{\nu} I$ has a tremendous effect on the spectrum of the preconditioned matrix $\widetilde{T}$: the eigenvalues depend on both the regularization parameter ν and the mesh size h. A closer inspection of the formulas of the eigenvalues of $\widetilde{T}$ reveals that as ν grows the eigenvalues cluster around the three eigenvalues of T, but as ν decreases the eigenvalues spread along the real line and move toward $+\infty$ and $-\infty$. This behavior can be clearly observed if we compute numerically the spectra of T and $\widetilde{T}$ for different values of ν. The obtained results are shown in Figure 5.10, where we can see that the eigenvalues are real (up to errors due to floating point arithmetic), the matrix T has clearly the three eigenvalues $\lambda = 1$, $\lambda = \frac{1+\sqrt{5}}{2} \approx 1.6180$, and $\lambda = \frac{1-\sqrt{5}}{2} \approx -0.6180$, and the matrix $\widetilde{T}$ has multiple eigenvalues distributed on the real line and depending on the value of ν. In particular, the smaller ν is, the larger the distribution of eigenvalues on the real axis becomes.

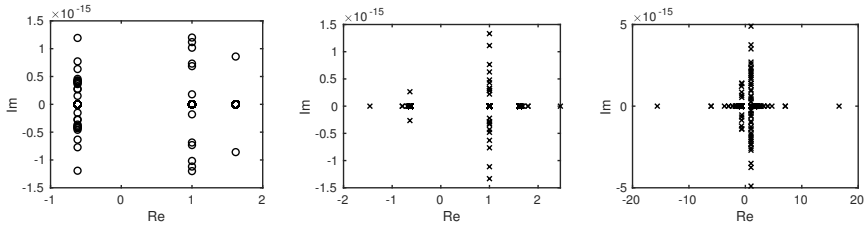

Figure 5.10. *Spectrum of the preconditioned matrix T (left) and of the matrix $\widetilde{T}$ for $\nu = 10^{-3}$ (middle) and $\nu = 10^{-5}$ (right). The figures correspond to $m = 15$.*

Now, we wish to test the behavior of GMRES[62] for the solution of the preconditioned system $\widetilde{M}^{-1}\widehat{A}\widehat{\boldsymbol{u}} = \widetilde{M}^{-1}\widehat{\boldsymbol{f}}$. To do so, one can run the MATLAB script

```
m=15;                          % number of mesh points in each direction
d=2;                           % dimension of the problem
nu=1e-3;                       % regularization parameter
h=1/(m+1);                     % mesh size
A=Laplacian(m,d)/h^2;          % negative 2D discrete Laplacian
Ahat=[sparse(m^d,m^d), A, -speye(m^d); ...
      A, speye(m^d), sparse(m^d,m^d); ...
      -speye(m^d), sparse(m^d,m^d), nu*speye(m^d)]; % all-at-once operator
Mt = blkdiag(A*A,speye(m^d),nu*speye(m^d)); % block-diag precond Mtilde
f=-ones(m^d,1);                % discrete f=-1
yd=ones(m^d,1);                % discrete y_d=1
fhat=[f;yd;zeros(m^d,1)];      % assemble the right-hand-side vector
u0=rand(3*m^d,1);              % random initial guess
kmax=min(200,m^d);             % set max number of iterations
[u,~,~,~,rv]=gmres(Ahat,fhat,[],1e-6,kmax,Mt,[],u0);
semilogy(0:length(rv)-1,rv./rv(1),'b-');
axis([0 50 1e-10 1]); yticks([1e-10 1e-8 1e-6 1e-4 1e-2 1]);
xlabel('iterations');
ylabel('norms of the residuals');
set(gca,'fontsize',18,'linewidth',2);
```

which permits us to obtain the results shown in Figure 5.11. These confirm the theoretical result of Theorem 5.13: as ν gets smaller, the eigenvalues are less clustered and GMRES converges more slowly. Moreover, we can also observe that the convergence of GMRES is robust against the mesh size h. Recalling the explicit formula for the eigenvalues of A (see also (2.26) and Problem 11), that is,

$$\lambda_{j,k}(A) = \frac{1}{h^2}\Big(4 + 2\cos\Big(\frac{k\pi}{m+1}\Big) + 2\cos\Big(\frac{j\pi}{m+1}\Big)\Big),$$

a direct expansion allows us to get

$$\lambda_{j,k}(A) \geq \lambda_{\min}(A) = 2\pi^2 - \frac{\pi^2 h^2}{6} + O(h^6).$$

This means that

$$\widehat{\lambda} = 1 + \frac{1}{\nu(\lambda(A))^2} \leq 1 + \frac{1}{\nu(\lambda_{\min}(A))^2},$$

[62]Notice that since both $\widetilde{M}$ and $\widehat{A}$ are symmetric, it is numerically more efficient to use MINRES. See, e.g., Section 3.6.

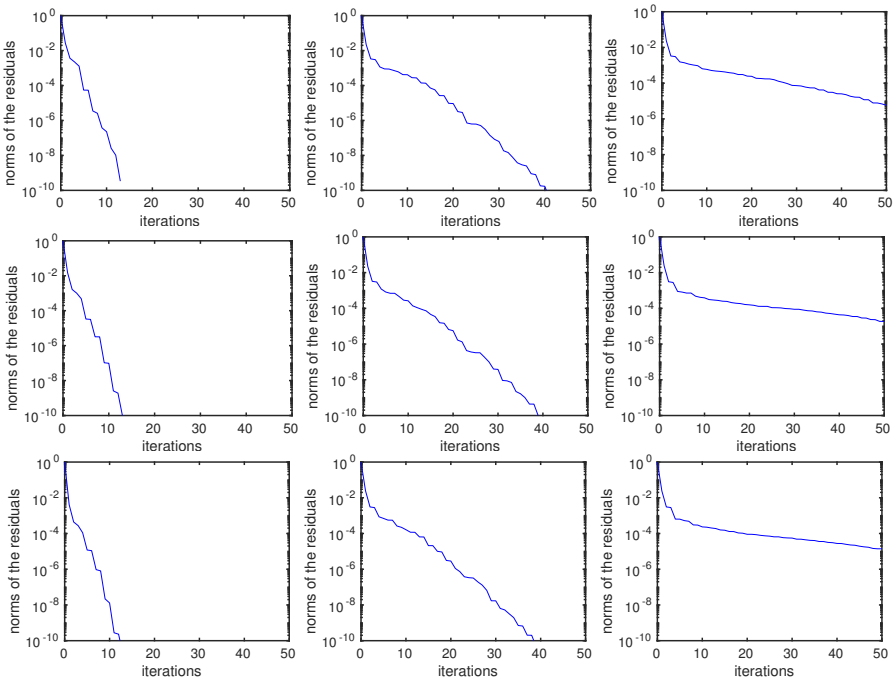

Figure 5.11. *Convergence of GMRES (preconditioned by the block-diagonal preconditioner $\widetilde{M}$ defined in* (5.61)*) for the solution of problem* (5.15) *for a unit square $\Omega \subset \mathbb{R}^2$ and different values of ν and $h = \frac{1}{m+1}$. First row: $m = 15$, $\nu = 10^{-3}$, $\nu = 10^{-5}$, and $\nu = 10^{-7}$. Second row: $m = 31$, $\nu = 10^{-3}$, $\nu = 10^{-5}$, and $\nu = 10^{-7}$. Third row: $m = 63$, $\nu = 10^{-3}$, $\nu = 10^{-5}$, and $\nu = 10^{-7}$. The results of the different figures are obtained with different (randomly chosen) initialization vectors.*

and the upper bound approaches $1 + \frac{1}{\nu 4\pi^4}$ as $h \to 0$. Moreover, as $\lambda(A)$ gets larger, $\widehat{\lambda}$ gets closer to 1. Therefore, the eigenvalues of $\widetilde{T}$ remain clustered for $h \to 0$ and ν fixed.

5.3.3 ▪ Schur-complement-based preconditioners

> *Schur complement methods are pervasive in numerical linear algebra where they represent a canonical way of implementing divide-and-conquer principles.*
>
> Yousef Saad, *Schur Complement Preconditioners for Distributed General Sparse Linear Systems*, 2007.

Schur-complement-based preconditioners are in general formulated for linear systems with a block structure. Consider for example a block matrix

$$K = \begin{bmatrix} K_{11} & K_{12} \\ K_{12}^\top & K_{22} \end{bmatrix}$$

and the corresponding linear system $K\boldsymbol{w} = \boldsymbol{f}$. A direct calculation allows one to verify the relation

$$K \begin{bmatrix} I & -K_{11}^{-1}K_{12} \\ 0 & I \end{bmatrix} = \begin{bmatrix} K_{11} & 0 \\ K_{12}^\top & S \end{bmatrix},$$

where $S = K_{22} - K_{12}^\top K_{11}^{-1} K_{12}$ is called the *Schur complement* of K. This relation gives us the

decomposition

$$K = \begin{bmatrix} K_{11} & 0 \\ K_{12}^\top & S \end{bmatrix} \begin{bmatrix} I & -K_{11}^{-1}K_{12} \\ 0 & I \end{bmatrix}^{-1} \Leftrightarrow K^{-1} = \begin{bmatrix} I & -K_{11}^{-1}K_{12} \\ 0 & I \end{bmatrix} \begin{bmatrix} K_{11} & 0 \\ K_{12}^\top & S \end{bmatrix}^{-1}.$$

Notice that the computational effort needed to obtain K^{-1} (or to apply it to a vector) is dominated by the inversion of the elements K_{11} and S. Seeking a good preconditioner M^{-1} for K, and recalling that M^{-1} has to be a good approximation to K^{-1} (see Section 4.1), we can replace the elements K_{11} and S by two approximations that are cheaper to invert. If we denote these approximations by $\widetilde{K}_{11}$ and $\widetilde{S}$, the Schur-complement-based preconditioner is then given by

$$M^{-1} = \begin{bmatrix} I & -\widetilde{K}_{11}^{-1}K_{12} \\ 0 & I \end{bmatrix} \begin{bmatrix} \widetilde{K}_{11} & 0 \\ K_{12}^\top & \widetilde{S} \end{bmatrix}^{-1}.$$

This preconditioner leads to the stationary method in correction form (see Section 2.1)

$$\boldsymbol{w}_{k+1} = \boldsymbol{w}_k + \begin{bmatrix} I & -\widetilde{K}_{11}^{-1}K_{12} \\ 0 & I \end{bmatrix} \begin{bmatrix} \widetilde{K}_{11} & 0 \\ K_{12}^\top & \widetilde{S} \end{bmatrix}^{-1} \Big(\boldsymbol{f} - K\boldsymbol{w}_k \Big), \tag{5.62}$$

which (assuming convergence) converges for $k \to \infty$ to the solution of the preconditioned system $M^{-1}K\boldsymbol{w} = M^{-1}\boldsymbol{f}$. The iteration (5.62) is sometimes called a *Schur-complement-based smoother* and it has been studied and applied in several practical (optimization) applications; see, e.g., [167, 130, 166, 57, 22]. However, in this book we will not use it as a stationary method, but only as a preconditioner.

Let us now look at the all-at-once matrix

$$\widehat{A} = \begin{bmatrix} 0 & A & -I \\ A & I & 0 \\ -I & 0 & \nu I \end{bmatrix}.$$

We identify $\widehat{A}$ with K by posing

$$K_{11} = \begin{bmatrix} 0 & A \\ A & I \end{bmatrix}, \quad K_{22} = \nu I, \quad K_{12}^\top = \begin{bmatrix} -I & 0 \end{bmatrix}, \text{ and } S = \nu I + A^{-1}A^{-1}.$$

Notice that the Schur-complement matrix S corresponds exactly to the matrix of the reduced approach described in Section 5.2. Now, we construct two preconditioners by choosing two different approximations,

$$K_{11} \approx \widetilde{K}_{11} = \begin{bmatrix} 0 & A \\ A & 0 \end{bmatrix} \quad \text{and} \quad S \approx \widetilde{S} = \nu I \tag{5.63}$$

and

$$K_{11} \approx \widetilde{K}_{11} = \begin{bmatrix} 0 & \widetilde{A} \\ \widetilde{A} & I \end{bmatrix} \quad \text{and} \quad S \approx \widetilde{S} = \nu I, \tag{5.64}$$

where $\widetilde{A}$ is an approximation to A, e.g., the diagonal of A, which we consider in our experiments. Another possible and efficient choice is to use a few multigrid V-cycles to approximate directly the inverse of A. These are two typical choices to construct optimal control preconditioners; see, e.g., [22]. Let us consider the first choice (5.63). Since the inverses of $\widetilde{K}_{11}$ and $\widetilde{S}$ are given by

$$\widetilde{K}_{11}^{-1} = \begin{bmatrix} 0 & A^{-1} \\ A^{-1} & 0 \end{bmatrix} \quad \text{and} \quad \widetilde{S}^{-1} = \frac{1}{\nu} I,$$

we obtain for M^{-1} the form

$$\begin{aligned} M_1^{-1} &= \begin{bmatrix} I & 0 & 0 \\ 0 & I & A^{-1} \\ 0 & 0 & I \end{bmatrix} \begin{bmatrix} 0 & A & 0 \\ A & 0 & 0 \\ -I & 0 & \nu I \end{bmatrix}^{-1} \\ &= \begin{bmatrix} I & 0 & 0 \\ 0 & I & A^{-1} \\ 0 & 0 & I \end{bmatrix} \begin{bmatrix} 0 & A^{-1} & 0 \\ A^{-1} & 0 & 0 \\ 0 & \frac{1}{\nu}A^{-1} & \frac{1}{\nu}I \end{bmatrix} \\ &= \begin{bmatrix} 0 & A^{-1} & 0 \\ A^{-1} & \frac{1}{\nu}A^{-1}A^{-1} & \frac{1}{\nu}A^{-1} \\ 0 & \frac{1}{\nu}A^{-1} & \frac{1}{\nu}I \end{bmatrix}. \end{aligned} \tag{5.65}$$

Notice that this preconditioner is symmetric. To implement it in an efficient way, we define the action of the operator M_1^{-1} on a vector $\boldsymbol{v} = \begin{bmatrix} \mathbf{v}_1^\top & \boldsymbol{v}_2^\top & \boldsymbol{v}_2^\top \end{bmatrix}^\top$ by

$$M_{1,\text{fun}}^{\text{inv}}(\boldsymbol{v}) = \begin{bmatrix} \boldsymbol{w} \\ A^{-1}(\boldsymbol{v}_1 + \frac{1}{\nu}\boldsymbol{w} + \frac{1}{\nu}\boldsymbol{v}_3) \\ \frac{1}{\nu}(\boldsymbol{w} + \boldsymbol{v}_3) \end{bmatrix},$$

where $\boldsymbol{w} = A^{-1}\boldsymbol{v}_2$. This action requires the solution of only two subsystems, $A\boldsymbol{w} = \boldsymbol{v}_2$ and $A\boldsymbol{z} = \boldsymbol{v}_1 - \frac{1}{\nu}\boldsymbol{w} - \frac{1}{\nu}\boldsymbol{v}_3$, and it can be computed using the MATLAB function

```
function Mv=Mfun1(v,A,nu)
  n=length(v)/3;
  w=A\v(n+1:2*n);
  z=(w+v(2*n+1:3*n))./nu;
  Mv=[w;A\(v(1:n)+z);z];
end
```

Notice that the computational cost required by $M_{1,\text{fun}}^{\text{inv}}$ is the same required by the reduced matrix A_{fun} defined in (5.22).

We next consider the second choice (5.64). As before, we can compute that

$$M_2^{-1} = \begin{bmatrix} I & 0 & -\widetilde{A}^{-2} \\ 0 & I & \widetilde{A}^{-1} \\ 0 & 0 & I \end{bmatrix} \begin{bmatrix} -\widetilde{A}^{-2} & \widetilde{A}^{-1} & 0 \\ \widetilde{A}^{-1} & 0 & 0 \\ -\frac{1}{\nu}\widetilde{A}^{-2} & \frac{1}{\nu}\widetilde{A}^{-1} & \frac{1}{\nu}I \end{bmatrix},$$

which can be easily verified to be symmetric. The action of M_2^{-1} can be computed by the MATLAB function

```
function Mv=Mfun2(v,At,nu)
  n=length(v)/3;
  w1=At\v(1:n);
  w2=At\w1;
  w3=At\v(n+1:2*n);
  z1=-w2+w3;
  z3=-(w2+w3+v(2*n+1:3*n))./nu;
  z2=At\z3;
  Mv=[z1-At\z2;w1+z2;z3];
end
```

which corresponds to the map

$$M_{2,\mathrm{fun}}^{\mathrm{inv}}(\boldsymbol{v}) = \begin{bmatrix} \boldsymbol{z}_1 - \widetilde{A}^{-1}\boldsymbol{z}_2 \\ \boldsymbol{w}_1 + \boldsymbol{z}_2 \\ \boldsymbol{z}_3 \end{bmatrix},$$

where $\boldsymbol{z}_1 = -\boldsymbol{w}_2 + \boldsymbol{w}_3$, $\boldsymbol{z}_2 = \widetilde{A}^{-1}\boldsymbol{z}_3$, $\boldsymbol{z}_3 = -\frac{1}{\nu}(\boldsymbol{w}_2 + \boldsymbol{w}_3 + \boldsymbol{v}_2)$, $\boldsymbol{w}_1 = \widetilde{A}^{-1}\boldsymbol{v}_1$, $\boldsymbol{w}_2 = \widetilde{A}^{-1}\boldsymbol{w}_1$, and $\boldsymbol{w}_3 = \widetilde{A}^{-1}\boldsymbol{v}_2$.

To test the two Schur-complement-based preconditioners, we can run the MATLAB script (for different values of ν and m).

```
m=15;                              % number of mesh points in each direction
d=2;                               % dimension of the problem
nu=1e-3;                           % regularization parameter
h=1/(m+1);                         % mesh size
A=Laplacian(m,d)/h^2;              % negative 2D discrete Laplacian
Ahat=[sparse(m^d,m^d), A, -speye(m^d); ...
      A, speye(m^d), sparse(m^d,m^d); ...
      -speye(m^d), sparse(m^d,m^d), nu*speye(m^d)]; % all-at-once operator
f=-ones(m^d,1);                    % discrete f=-1
yd=ones(m^d,1);                    % discrete y_d=1
fhat=[f;yd;zeros(m^d,1)];          % assemble the right-hand-side vector
Afun1=@(v) Mfun1(Ahat*v,A,nu);     % action of the preconditioned matrix 1
Mfhat1=Mfun1(fhat,A,nu);           % rhs of the preconditioned system 1
u0=rand(3*m^d,1);                  % random initial guess
kmax=min(200,m^d);                 % set max number of iterations
[u1,~,~,~,rv1]=gmres(Afun1,Mfhat1,[],1e-6,kmax,[],[],u0);
At=spdiags(diag(A),0,m^d,m^d);
Afun2=@(v) Mfun2(Ahat*v,At,nu);    % action of the preconditioned matrix 2
Mfhat2=Mfun2(fhat,At,nu);          % rhs of the preconditioned system 2
[u2,~,~,~,rv2]=gmres(Afun2,Mfhat2,[],1e-6,kmax,[],[],u0);
semilogy(0:length(rv1)-1,rv1./rv1(1),'b'); hold on;
semilogy(0:length(rv2)-1,rv2./rv2(1),'r');
axis([0 40 1e-6 1]); yticks([1e-6 1e-4 1e-2 1]);
legend('Schur1','Schur2','location','NorthEast');
xlabel('iterations');
ylabel('norm of the residual');
set(gca,'fontsize',18,'linewidth',2);
```

This script produced the results given in Figure 5.12. We can now see that GMRES applied to the all-at-once system preconditioned by the Schur-complement-based preconditioners performs much better if compared to the unpreconditioned case studied in Figure 5.6. In particular, the first preconditioner performs better for larger values of ν, while the second preconditioner performs better for smaller values of ν. To explain this behavior, let us first compute explicitly the preconditioned matrix $M_1^{-1}\widehat{A}$,

$$M_1^{-1}\widehat{A} = \begin{bmatrix} I & A^{-1} & 0 \\ 0 & I + \frac{1}{\nu}A^{-2} & 0 \\ 0 & \frac{1}{\nu}A^{-1} & 0 \end{bmatrix}.$$

Hence, the preconditioned system $M_1^{-1}\widehat{A} = M_1^{-1}\widehat{\boldsymbol{f}}$ is essentially a triangular system, where most of the computational effort is required for the solution of the second system of equations characterized by the matrix $I + \frac{1}{\nu}A^{-2}$. After multiplication by ν, this matrix is equal to the reduced matrix A_{red} of the reduced approach discussed in Section 5.2. Therefore, the deterioration

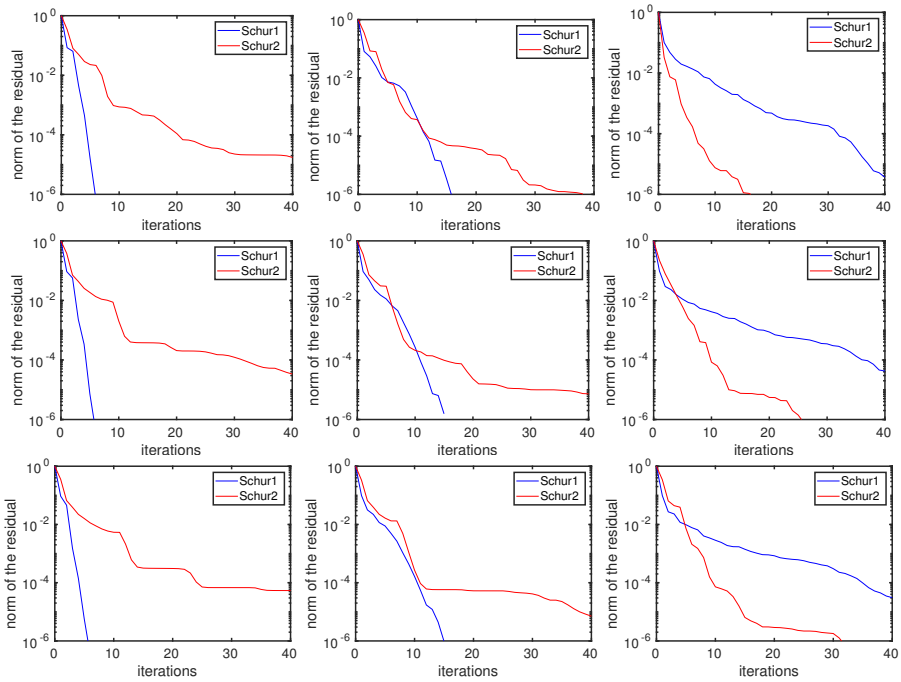

Figure 5.12. *Convergence of GMRES (preconditioned by the Schur-complement preconditioners M_1 (blue lines) and M_2 (red lines)) for the solution of problem* (5.15) *for a unit square $\Omega \subset \mathbb{R}^2$ and different values of ν and $h = \frac{1}{m+1}$. First row: $m = 15$, $\nu = 10^{-3}$, $\nu = 10^{-5}$, and $\nu = 10^{-7}$. Second row: $m = 31$, $\nu = 10^{-3}$, $\nu = 10^{-5}$, and $\nu = 10^{-7}$. Third row: $m = 63$, $\nu = 10^{-3}$, $\nu = 10^{-5}$, and $\nu = 10^{-7}$. The results of the different figures are obtained with different (randomly chosen) initialization vectors.*

of the GMRES behavior for the solution of $M_1^{-1}\widehat{A} = M_1^{-1}\widehat{\boldsymbol{f}}$ is explained as for A_{red} by Theorem 5.7. Regarding the second preconditioned system $M_2^{-1}\widehat{A} = M_2^{-1}\widehat{\boldsymbol{f}}$, a direct numerical calculation of the eigenvalues of $M_2^{-1}\widehat{A}$ reveals that they form two clusters for small values of ν, while it is not possible to identify clusters for large values of ν. This explains (as for the case discussed in Theorem 5.9) the reason GMRES performs better for smaller values of ν.

5.3.4 ▪ Collective smoothing

> *A collective smoothing multigrid (CSMG) approach means solving the optimality system for the state, adjoint, and control variables simultaneously in the multigrid process by using collective smoothers for the optimization variables. The CSMG approach is in contrast to the sequential solving of the state, adjoint, and control equations.*
>
> *A CSMG-based scheme aims at realizing the tight coupling in the optimality system along the hierarchy of grids. By employing collective smoothing, that is, by realizing the coupling in the optimality system at the smoothing step level, robustness and typical multigrid efficiency are achieved.*
>
> Alfio Borzì and Volker Schulz, *Multigrid Methods for PDE Optimization*, 2009.

The goal of this section is to introduce a class of iterative methods that are among the most used smoothers in the context of multigrid methods for optimal control problems: the so-called *collective smoothers*. We will discuss multigrid methods for elliptic optimal control problems in

the next section and focus here on the collective smoothing approach. As explained in the quote above, a collective smoothing approach consists in an iterative procedure that performs at each step local "nodal solves" of the optimality system. With the term "nodal solve" we mean that the optimization variables, namely state $\boldsymbol{y}$, control $\boldsymbol{u}$, and adjoint $\boldsymbol{p}$, are simultaneously updated on a node of the grid, while their values on the other nodes are frozen. To explain this in detail, let us consider the discrete optimality system (5.15)–(5.16) obtained by the finite-difference method with a uniform grid which discretizes the unit square Ω with m interior points on each edge. The grid size is then $h = \frac{1}{m+1}$. In this setting, if we denote by $y_{i,j}$, $u_{i,j}$, and $p_{i,j}$ the components of $\boldsymbol{y}$, $\boldsymbol{u}$, and $\boldsymbol{p}$ at the gridpoint (jh, ih) (see Section 1.3), for $i, j = 0, \dots, m+1$ (we included the homogeneous boundary condition values), the optimality system (5.15)–(5.16) can be written in the componentwise form

$$4y_{i,j} - (y_{i-1,j} + y_{i+1,j} + y_{i,j-1} + y_{i,j+1}) - h^2 u_{i,j} = h^2 f_{i,j}, \tag{5.66}$$

$$4p_{i,j} - (p_{i-1,j} + p_{i+1,j} + p_{i,j-1} + p_{i,j+1}) + h^2 y_{i,j} = h^2 (y_d)_{i,j}, \tag{5.67}$$

$$\nu u_{i,j} - p_{i,j} = 0 \tag{5.68}$$

for $i, j = 1, \dots, m$, where $f_{i,j}$ and $(y_d)_{i,j}$ are the components of $\boldsymbol{f}$ and $\boldsymbol{y}_d$ at the gridpoint (jh, ih). If now we introduce the variables

$$c_y := (y_{i-1,j} + y_{i+1,j} + y_{i,j-1} + y_{i,j+1}) + h^2 f_{i,j},$$
$$c_p := (p_{i-1,j} + p_{i+1,j} + p_{i,j-1} + p_{i,j+1}) + h^2 (y_d)_{i,j},$$

the system (5.66)–(5.68) can be written as

$$\begin{bmatrix} 0 & 4 & -h^2 \\ 4 & h^2 & 0 \\ -1 & 0 & \nu \end{bmatrix} \begin{bmatrix} p_{i,j} \\ y_{i,j} \\ u_{i,j} \end{bmatrix} = \begin{bmatrix} c_y \\ c_p \\ 0 \end{bmatrix}, \tag{5.69}$$

where the matrix

$$A_s := \begin{bmatrix} 0 & 4 & -h^2 \\ 4 & h^2 & 0 \\ -1 & 0 & \nu \end{bmatrix}$$

is clearly invertible since its determinant is $\det(A_s) = -(16\nu + h^4) < 0$. Notice that the structure of this matrix resembles the one of the optimality system matrix $\widehat{A}$. A "local solve" consists in solving (5.69) where the variables y, p, and u on the right-hand side (namely on the nodes different from (jh, ih)) are considered constant, while $y_{i,j}$, $p_{i,j}$, and $u_{i,j}$ are the variables to be updated.

In an iterative fashion, given the variables $y_{i,j}$, $p_{i,j}$, and $u_{i,j}$, for all j, i, each iteration of a collective smoother consists in a lexicographic sweep over the indices (i, j), where for each pair (i, j) one performs three steps:

1. Assemble

$$c_y = (y_{i-1,j} + y_{i+1,j} + y_{i,j-1} + y_{i,j+1}) + h^2 f_{i,j},$$
$$c_p = (p_{i-1,j} + p_{i+1,j} + p_{i,j-1} + p_{i,j+1}) + h^2 (y_d)_{i,j}.$$

2. Compute
$$\begin{bmatrix} p_{\text{aux}} \\ y_{\text{aux}} \\ u_{\text{aux}} \end{bmatrix} = A_s^{-1} \begin{bmatrix} c_y \\ c_p \\ 0 \end{bmatrix}.$$

3. Update the three variables $y_{i,j}$, $p_{i,j}$, and $u_{i,j}$ as
$$\begin{bmatrix} p_{i,j} \\ y_{i,j} \\ u_{i,j} \end{bmatrix} = \begin{bmatrix} p_{\text{aux}} \\ y_{\text{aux}} \\ u_{\text{aux}} \end{bmatrix}.$$

It is then clear that the optimality system is solved "locally" at each step.

A MATLAB implementation of the described collective smoothing procedure is given by the following function.

```
function [w,res]=GS_CollectiveS(w0,rhs,Ahat,nu,tol,kmax)
% GS_CollectiveS: Gauss-Seidel Collective Smoothing Iteration
%   [w,res]=GS_CollectiveS(v,rhs,Ahat,nu,tol,kmax) solves the optimality
%   system Ahat w=fhat  using the Gauss-Seidel Collective Smoothing
%   method starting at the initial guess w0 up to a tolerance tol using
%   at most kmax iterations.
%   GS_CollectiveS returns in w the solution computed and in res the
%   history of the norm of the residuals.

n=length(w0)/3; m=sqrt(n); h=1/(m+1);
w=w0;
y=zeros(m+2,m+2); p=y; u=y; f=y; yd=y;
f(2:end-1,2:end-1)=reshape(rhs(1:n),m,m);
yd(2:end-1,2:end-1)=reshape(rhs(n+1:2*n),m,m);
p(2:end-1,2:end-1)=reshape(w(1:n),m,m);
y(2:end-1,2:end-1)=reshape(w(n+1:2*n),m,m);
u(2:end-1,2:end-1)=reshape(w(2*n+1:3*n),m,m);
res(1)=norm(rhs-Ahat*w);
k=1;
vv=(4+h^4/(4*nu));
while k<=kmax && res(end)/res(1)>tol
  k=k+1;
  for i=2:m+1
    for j=2:m+1
      cy=(y(i-1,j)+y(i+1,j)+y(i,j-1)+y(i,j+1))+h^2*f(i,j);
      cp=(p(i-1,j)+p(i+1,j)+p(i,j-1)+p(i,j+1))+h^2*yd(i,j);
      p(i,j)=(cp-h^2*cy/4)/vv;
      y(i,j)=(h^2*p(i,j)/nu+cy)/4;
      u(i,j)=p(i,j)/nu;
    end
  end
  w=[p(2:end-1,2:end-1),y(2:end-1,2:end-1),u(2:end-1,2:end-1)];
  w=w(:);
  res(k)=norm(rhs-Ahat*w);
end
```

This process is clearly a stationary method. If one wishes to write it in a compact standard form (see Section 2.1), it is first convenient to rearrange the order of the components of the vector

$\widehat{\boldsymbol{u}} = \begin{bmatrix}\boldsymbol{p}^\top & \boldsymbol{y}^\top & \boldsymbol{u}^\top\end{bmatrix}^\top$ as

$$\boldsymbol{w} := \begin{bmatrix}p_{1,1} & y_{1,1} & u_{1,1} & p_{2,1} & y_{2,1} & u_{2,1} & \cdots & p_{m,m} & y_{m,m} & u_{m,m}\end{bmatrix}^\top.$$

Notice that this corresponds to applying a permutation matrix P to $\boldsymbol{v}$, that is, $\boldsymbol{w} = P\widehat{\boldsymbol{u}}$. Now notice that the right-hand-side vector of (5.69) can be written as

$$\begin{bmatrix}c_y\\ c_p\\ 0\end{bmatrix} = -N_1\begin{bmatrix}p_{i,j-1}\\ y_{i,j-1}\\ u_{i,j-1}\end{bmatrix} - N_2\begin{bmatrix}p_{i,j+1}\\ y_{i,j+1}\\ u_{i,j+1}\end{bmatrix} - N_3\begin{bmatrix}p_{i-1,j}\\ y_{i-1,j}\\ u_{i-1,j}\end{bmatrix} - N_4\begin{bmatrix}p_{i+1,j}\\ y_{i+1,j}\\ u_{i+1,j}\end{bmatrix} + \begin{bmatrix}h^2 f_{i,j}\\ h^2(y_d)_{i,j}\\ 0\end{bmatrix}$$

for some matrices N_1, N_2, N_3, and N_4. Therefore, the optimality system (5.66)–(5.68) (namely (5.15)–(5.16)) becomes

$$P^\top \widehat{A} P \boldsymbol{w} = P\widehat{\boldsymbol{f}}, \tag{5.70}$$

where the matrix $P^\top \widehat{A} P$ has the block pentadiagonal structure

$$P^\top \widehat{A} P = \begin{bmatrix}
\ddots & & & \ddots & \ddots & \ddots & & & \ddots & & \\
 & N_1 & & & N_3 & A_s & N_4 & & & N_2 & \\
 & & \ddots & & & \ddots & \ddots & \ddots & & & \ddots
\end{bmatrix}.$$

It is then clear that the iterative process given by steps 1, 2, and 3 above is a block-Gauss–Seidel method for the system (5.70). Once we have clarified the precise structure of the procedure as a stationary method, it is not difficult to introduce also a block-Jacobi collective smoothing method; see Problem 81. For convergence analyses of collective smoothing procedures see, e.g., [22, 19, 21] and references therein.

Let us now test the convergence behavior of the Gauss–Seidel collective smoothing algorithm numerically. To do so, one can run (for several ν and m) the MATLAB script

```
m=15;                          % number of mesh points in each direction
d=2;                           % dimension of the problem
nu=1e-3;                       % regularization parameter
h=1/(m+1);                     % mesh size
A=Laplacian(m,d)/h^2;          % negative 2D discrete Laplacian
Ahat=[sparse(m^d,m^d), A, -speye(m^d); ...
      A, speye(m^d), sparse(m^d,m^d); ...
      -speye(m^d), sparse(m^d,m^d), nu*speye(m^d)]; % all-at-once operator
f=-ones(m^d,1);                % discrete f=-1
yd=ones(m^d,1);                % discrete y_d=1
fhat=[f;yd;zeros(m^d,1)];      % assemble the right-hand-side vector
u0=rand(3*m^d,1);              % random initial guess
kmax=min(200,m^d);             % set max number of iterations
[u1,~,~,~,RESVEC]=gmres(@(v)(v-GS_CollectiveS(v,0*fhat,Ahat,nu,eps,1)),...
                        GS_CollectiveS(0*fhat,fhat,Ahat,nu,eps,1),...
                        [],1e-6,kmax,[],[],u0);
[u2,res]=GS_CollectiveS(u0,fhat,Ahat,nu,1e-14,kmax);
semilogy(0:length(RESVEC)-1,RESVEC./RESVEC(1),'b'); hold on;
semilogy(0:length(res)-1,res./res(1),'r');
axis([0 50 1e-10 1e2]); yticks([1e-10 1e-6 1e-2 1e2]);
xlabel('iterations');
ylabel('norm of the residual');
legend('GMRES+CS','CS Stat','location','NorthEast');
set(gca,'fontsize',18,'linewidth',2);
```

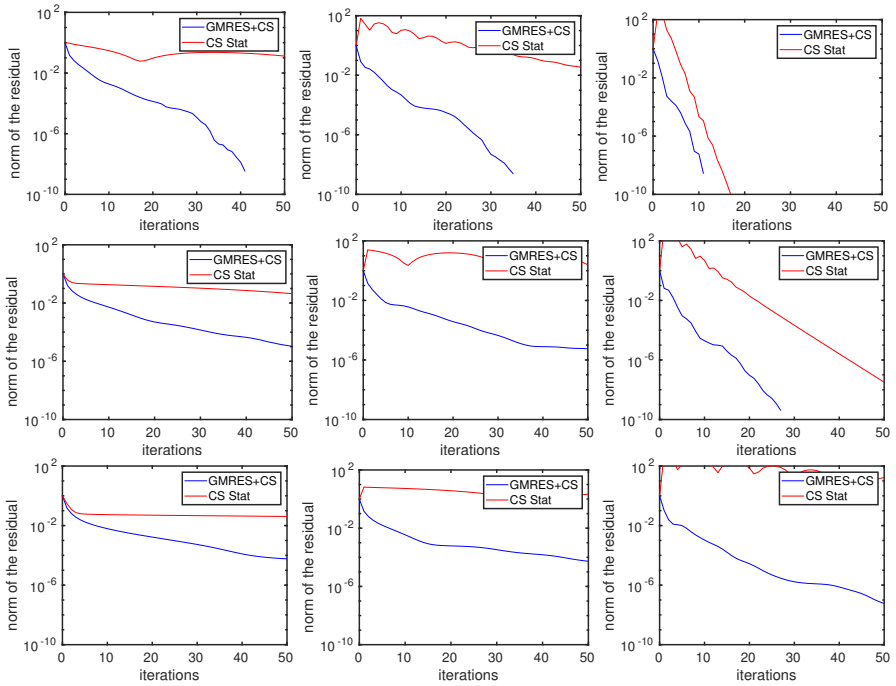

Figure 5.13. *Convergence of the Gauss–Seidel collective smoothing method (as a stationary iteration and as a preconditioner for GMRES) for the solution of* (5.15) *for a unit square* $\Omega \subset \mathbb{R}^2$ *and different values of* ν *and* $h = \frac{1}{m+1}$. *First row:* $m = 15$, $\nu = 10^{-3}$, $\nu = 10^{-5}$, *and* $\nu = 10^{-7}$. *Second row:* $m = 31$, $\nu = 10^{-3}$, $\nu = 10^{-5}$, *and* $\nu = 10^{-7}$. *Third row:* $m = 63$, $\nu = 10^{-3}$, $\nu = 10^{-5}$, *and* $\nu = 10^{-7}$. *The results of the different figures are obtained with different (randomly chosen) initialization vectors.*

which allows us to obtain the results shown in Figure 5.13. We can clearly see that as a stationary method the Gauss–Seidel collective smoother always converges, even though very slowly in most of the cases. As a preconditioner, it also works quite nicely, since GMRES converges much faster compared to the nonpreconditioned case corresponding to Figure 5.6. However, the Gauss–Seidel collective smoothing method is best used as a component of the multigrid method described in the next section.

5.3.5 ▪ Multigrid methods

> *While research on multigrid methods has been motivated by the need to efficiently solve large application problems, the purpose of optimization has been to define ways of how to optimally change, influence, or estimate features of real world systems. This requires the development of optimization strategies for current practical applications of increasing complexity, and so the need to solve large-scale optimization problems in an accurate and computationally efficient way. For this reason, the idea of using multigrid strategies for optimization purposes has received increasing attention, encouraged by results obtained in the last few years.*
>
> Alfio Borzì and Volker Schulz, *Multigrid Methods for PDE Optimization*, 2009.

Multigrid methods for optimal control problems represent an active research field of the last decade (see the quote above). A single subsection is clearly not sufficient to give a complete overview about this topic, especially if one wants to consider control- or state-constrained

optimal control problems, optimal control problems governed by nonlinear elliptic equations, and time-dependent optimal control problems. We refer the reader to, e.g., [22, 23] for extensive reviews; see also [19, 21] and references therein.

In this last section of the book, we limit ourselves to extending the multigrid framework introduced in Section 4.10 to elliptic optimal control problems of the form (5.3)–(5.4). In particular, we describe a V-cycle for the solution of the discrete optimality system (5.15)–(5.16) obtained by the finite-difference method and a uniform grid of $m = 2^\ell - 1$, $\ell \in \mathbb{N}$, interior points on each edge to discretize a unit square.

To form a V-cycle we need the following components: a smoother, prolongation and restriction operators, and a systematic way to obtain a coarse optimality system matrix. As a smoother, we consider the collective smoothing method described in Section 5.3.4. To construct restriction and prolongation operators, we first consider the two-dimensional restriction operator R (full weighting restriction matrix) obtained by the MATLAB function `RMatrix` given in Section 4.10 and the corresponding prolongation operator $P = 2R^\top$. We can then introduce the block-diagonal matrices

$$\widehat{R} = \mathrm{diag}(R, R, R) \quad \text{and} \quad \widehat{P} = \mathrm{diag}(P, P, P),$$

which are restriction and prolongation operators of the triple $(\boldsymbol{p}, \boldsymbol{y}, \boldsymbol{u})$ between the ℓ-grid and the $\ell - 1$-grid. Using these operators, we can define the coarse matrix in a Galerkin fashion, that is, $\widehat{A}_c = \widehat{R}\widehat{A}\widehat{P}$. Once these components are fixed, a multigrid V-cycle for our optimal control problem is obtained exactly as in Section 4.10. A corresponding MATLAB implementation is

```
function u=VCycleOC(A,f,nu,u,l)
% VCYCLEOC performs a V-cycle of multigrid for the Laplace equation
%   u=VCycleOC(A,f,nu,u,l) computes for the given linear system Au=f
%   representing a an optimality system of a linear quadratic elliptic
%   optimal control problem (with an l2 regularization parameter nu)
%   defined on a square domain a V-cycle approximation of the solution
%   starting with the guess u using l levels.
%   The resolution size m=sqrt(length(f)/2) must be such that m+1 can
%   be divided by 2^l. The method uses a Gauss-Seidel collective smoothing
%   method, and the number of pre- and postsmoothing steps nu1 and nu2
%   can be set in the code.

nu1=1; nu2=1;                          % pre- and postsmoothing steps
if l==1                                % direct solve on coarsest level
  u=A\f;
else
  u=GS_CollectiveS(u,f,A,nu,eps,nu1);% presmoothing
  r=f-A*u;                             % compute residual
  m=sqrt(length(f)/3);
  R=RMatrix(m);                        % compute restriction matrix R
  Rt=blkdiag(R,R,R);
  M=(m+1)/2-1;
  AH=4*Rt*A*Rt';                       % compute (Galerkin) coarse matrix
  e=VCycleOC(AH,Rt*r,nu,zeros(3*M^2,1),l-1);% compute coarse correction
  u=u+4*Rt'*e;                         % use full weighting
  u=GS_CollectiveS(u,f,A,nu,eps,nu2);% postsmoothing
end
```

Hence a multigrid method can be easily obtained by repeating iteratively V-cycles:

```
function [u,res]=MG_OC(A,f,nu,u,ell,tol,m)
% MG_OC: Multigrid for Laplace-type optimal control problems
%   [u,res]=MG_OC(A,f,nu,u,ell,tol,m) solves the first-order
%   optimality system written in the form Au=f of an l2-regularized
%   (with regularization parameter nu) optimal control problems. It
%   performs at most m V-cycles of a multigrid methods with ell levels
%   until the norm of the residual smaller than the tolerance tol.
%   The output variables are the computed solution u and the vector
%   res, containing the history of the residual norms.

res(1)=norm(f-A*u);
k=0;
while k<=m && res(end)>tol
  k=k+1;
  u=VCycleOC(A,f,nu,u,ell);
  res(k)=norm(f-A*u);
end
```

To test the convergence of the described multigrid algorithm, we consider three levels (hence `l=3` in `MG_OC`) and run (for different ν and m) the MATLAB script

```
m=15;                          % number of mesh points in each direction
d=2;                           % dimension of the problem
nu=1e-3;                       % regularization parameter
h=1/(m+1);                     % mesh size
A=Laplacian(m,d)/h^2;          % negative 2D discrete Laplacian
Ahat=[sparse(m^d,m^d), A, -speye(m^d); ...
      A, speye(m^d), sparse(m^d,m^d); ...
      -speye(m^d), sparse(m^d,m^d), nu*speye(m^d)]; % all-at-once operator
f=-ones(m^d,1);                % discrete f=-1
yd=ones(m^d,1);                % discrete y_d=1
fhat=[f;yd;zeros(m^d,1)];      % assemble the right-hand-side vector
u0=rand(3*m^d,1);              % random initial guess
[u,res] = MG_OC(Ahat,fhat,nu,u0,3,1e-16,21);
semilogy(0:20,res(1:21)./res(1),'o-b');
axis([0 20 1e-10 1]); yticks([1e-10 1e-8 1e-6 1e-4 1e-2 1]);
xlabel('iterations');
ylabel('norm of the residual');
set(gca,'fontsize',18,'linewidth',2);
```

which produces the results given in Figure 5.14. The convergence curves shown in this figure show the incredible convergence behavior of the multigrid methods, which is the fastest among the methods discussed in this chapter and the most robust against ν and h.

5.4 ▪ Further preconditioners for optimal control problems

The literature on preconditioning techniques for optimal control problems is rather rich. In this section, we provide a very brief summary of the existing literature in this research area that is not covered in the present chapter. Surveys, overviews, and comparisons of different preconditioners for optimal control problems can be found in the standard textbook [23] and in the review papers [2, 23]. In addition to these references, it is worth mentioning the approach based on the famous *preconditioned projected CG method* (see, e.g., [138]) presented in [154, Section 4]. In this work, the authors propose a block preconditioner embedded in the projected CG method and used in

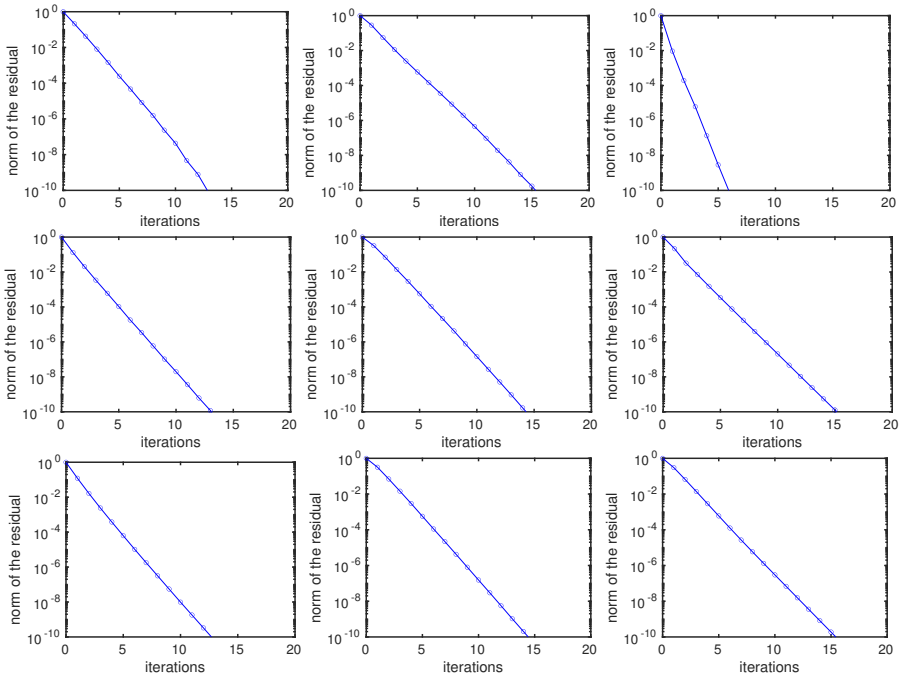

Figure 5.14. *Convergence of the multigrid method (with three levels) for the solution of the reduced problem* (5.15) *for a unit square* $\Omega \subset \mathbb{R}^2$ *and different values of* ν *and* $h = \frac{1}{m+1}$. *First row:* $m = 15$, $\nu = 10^{-3}$, $\nu = 10^{-5}$, *and* $\nu = 10^{-7}$. *Second row:* $m = 31$, $\nu = 10^{-3}$, $\nu = 10^{-5}$, *and* $\nu = 10^{-7}$. *Third row:* $m = 63$, $\nu = 10^{-3}$, $\nu = 10^{-5}$, *and* $\nu = 10^{-7}$. *The results of the different figures are obtained with different (randomly chosen) initialization vectors.*

combination with an algebraic multigrid strategy. The computational framework obtained is shown to be quite efficient for elliptic optimal control problems.

Four block preconditioners, used to accelerate the solution of Newton-type linear systems (in the context of sequential quadratic programming methods [138]) have been developed in [9]; see also [8, 144] for preconditioners of KKT systems used in the context of *interior-point* and *sequential quadratic programming* methods. The four preconditioners in [9] are a block-diagonal preconditioner, which can be considered an approximation of the one proposed by Golub and collaborators in [135] and presented in Section 5.3.2, a block-triangular preconditioner, a preconditioner based on the Schur complement corresponding to the reduced form of the optimization problem, and an indefinite preconditioner. A precise eigenvalue characterization is obtained in all cases. Related to the indefinite preconditioner presented in [9] is the recent work [4], where block-counterdiagonal and block-countertriangular preconditioners have been designed and analyzed. Further block-diagonal preconditioners have been developed in [145].

An interesting approach based on the *Bramble–Pasciak CG method* has been presented in [155]. In their seminal work [26], Bramble and Pasciak showed that a symmetric and indefinite problem with a saddle-point structure can be transformed, by an appropriately chosen block-triangular preconditioning, into a symmetric and positive definite system. The symmetry is obtained with respect to a scalar product depending on an approximation of the Schur complement of the original saddle-point system. This scalar product was used by Bramble and Pasciak to replace the classical Euclidean scalar product in the CG procedure. The authors of [155] developed this idea for indefinite optimality systems characterizing the solution of optimal control problems

governed by elliptic PDEs, and they showed how an appropriate block-triangular preconditioner can be constructed in this case.

Domain decomposition methods for PDE-constrained optimal control problems already have been developed in the literature. For elliptic optimal control problems classical Schwarz methods were considered in [103] as preconditioners, and in [10, 12, 54, 6, 53], OSMs have been introduced and analyzed. Neumann–Neumann methods are studied in [104, 105, 77]. Moreover, for nonlinear preconditioning of optimal control problem, we refer the reader to [45, 47].

Other interesting preconditioning techniques have been developed in the context of time-dependent PDE-constrained optimization problems, which are, however, beyond the scope of this book. We refer the interested reader to, e.g., [2, 11, 23, 41, 79, 107, 131, 133, 182] and references therein.

5.5 ▪ Problems

Problem 72. *Study the convergence of the stationary iteration* (5.26) *with respect to* ν *and the mesh size* h*.*

Problem 73. *Implement a multigrid method for the solution of the reduced problem* (5.21)*. Consider in particular a V-cycle, use the full weighting restriction matrices, and assemble the coarse matrix as* $R\widehat{A}P$ *(as described in Section 4.10).*

Problem 74. *Prove Theorem 5.9.*

Problem 75. *Consider the all-at-once system* (5.15)–(5.31)*. Rewrite/reduce it in terms of the variables* $(\boldsymbol{y}, \boldsymbol{u})$ *and* $(\boldsymbol{p}, \boldsymbol{u})$ *and test the convergence behavior of GMRES for the two linear systems obtained. Discuss the numerical results you obtain.*

Problem 76. *Implement the OSM described in Section 5.3.1 for the solution of the optimal control problem considered in this chapter. Test the OSM algorithm as a stationary method and as a preconditioner for GMRES. Discuss the obtained results.*

Problem 77. *Implement an overlapping OSM for the solution of the optimal control problem considered in this chapter. Test the convergence of the implemented algorithm as a stationary method and as a preconditioner for GMRES. Investigate the dependence of the convergence on the Robin parameter* q*: In both cases of a stationary method and preconditioning find numerically the best Robin parameter. Discuss the results you obtain.*

Problem 78. *Recall the matrix* $W = \begin{bmatrix} 0 & W_{12} \\ W_{21} & W_{22} \end{bmatrix}$ *from Section 5.3.2 and consider the block-triangular preconditioner*

$$M = \begin{bmatrix} W_{12}W_{22}^{-1}W_{21} & 0 \\ W_{21} & W_{22} \end{bmatrix}.$$

Prove that the spectrum of the preconditioned matrix $M^{-1}W$ *is* $\sigma(M^{-1}W) = \{-1, +1\}$*. Hint: Use the formula for the determinant of block matrices* (5.18) *and the fact that the matrix* $W_{22}^{-1}W_{21}(W_{12}W_{22}^{-1}W_{21})^{-1}W_{12}$ *is a projection.*

Problem 79. *Implement the block-triangular preconditioner of Problem 78 and test the convergence behavior of GMRES for the preconditioned (optimality) system* $M^{-1}\widehat{A}\widehat{\boldsymbol{u}} = M^{-1}\widehat{\boldsymbol{f}}$*. Discuss the results you obtain.*

Problem 80. *Implement the block-triangular preconditioner (approximation of the one of Problem 78)*

$$\widetilde{M} = \begin{bmatrix} A^2 & 0 & 0 \\ A & I & 0 \\ -I & 0 & \nu I \end{bmatrix}$$

and test the convergence behavior of GMRES for the preconditioned (optimality) system $\widetilde{M}^{-1}\widehat{A}\widehat{\boldsymbol{u}} = \widetilde{M}^{-1}\widehat{\boldsymbol{f}}$. *Discuss the results you obtain.*

Problem 81. *Implement a Jacobi collective smoothing procedure and use it for the solution of the optimal control problem governed by the Laplace equation used in this chapter. Test the procedure as a stationary iteration, as a preconditioner for GMRES, and as a smoother in a multigrid V-cycle.*

Chapter 6
Appendix

6.1 ▪ Existence, uniqueness, and well-posedness of Schwarz iterates

To study the well-posedness of the Schwarz iterates, we first recall some existence and regularity results for the Laplace problem (4.29).

Theorem 6.1 (Existence, uniqueness, and regularity of the Laplace solution). *Consider a bounded and convex domain $\Omega \subset \mathbb{R}^2$. We have the following:*

- *For any $f \in L^2(\Omega)$ and $g \in H^{1/2}(\partial\Omega)$ there exists a unique (weak) solution $u \in H^1(\Omega)$ to* (4.29)*.*
- *For any function f bounded and locally Hölder continuous in Ω and $g \in C(\partial\Omega)$ there exists a unique (classical) solution $u \in C(\overline{\Omega}) \cap C^2(\Omega)$ to* (4.29)*.*
- *For any function f bounded and locally Hölder continuous in Ω and any bounded boundary function g there exists a unique (Perron) solution $u \in C^2(\Omega)$ to* (4.29)*. In this case, for any point $\boldsymbol{x}_0$ where g is continuous, the solution u satisfies $\lim_{\boldsymbol{x}\to\boldsymbol{x}_0} u(\boldsymbol{x}) = g(\boldsymbol{x}_0)$.*

Proof. The first statement follows by standard results based, e.g., on the Lax–Milgram theorem [48, Theorem 6.2-1] and on the trace theorem for functions in $H^1(\Omega)$ [118, Corollary 8.16, Theorem 8.17, and Theorem 8.27]; see also [62, Chapter 6]. The second statement follows by classical results based on the Green's function representation [88, Theorem 4.3]; see also [48, pages 342–343]. The last statement follows from the theory of Perron solutions; see [88, Section 2.8]. □

Let us now discuss well-posedness of the Schwarz method (4.30). Consider the Laplace problem (1.5) with a boundary function $g \in H^{1/2}(\partial\Omega)$ and right-hand-side function $f \in L^2(\Omega)$. According to Theorem 6.1, it is uniquely solvable by $u \in H^1(\Omega)$. We have the following result.

Theorem 6.2 (Well-posedness of the Schwarz method—1). *Let $\Omega \subset \mathbb{R}^n$ be a bounded Lipschitz domain, and consider an overlapping domain decomposition $\Omega = \Omega_1 \cup \Omega_2$, where Ω_1 and Ω_2 are both Lipschitz domains. Assume that $f \in L^2(\Omega)$ and $g \in H^{1/2}(\partial\Omega)$, and consider the trace operator $\tau : H^1(\Omega) \to H^{1/2}(\partial\Omega)$. Let $u^0 \in H^1(\Omega)$ be an initial guess such that*

$\tau(u^0) = g$. *The Schwarz sequences* $\{u_1^n\}_n$ *and* $\{u_2^n\}_n$ *are well-defined in the sense that for* $n \geq 1$ *the Schwarz subproblems* (4.30) *are uniquely solvable by weak solutions* $u_1^n \in H^1(\Omega_1)$ *and* $u_2^n \in H^1(\Omega_2)$.

Proof. Consider the trace operators $\tau_j : H^1(\Omega) \to H^{1/2}(\partial\Omega_j)$ for $j = 1, 2$. Since $u^0 \in H^1(\Omega)$, we have that $\tau_1(u^0) \in H^{1/2}(\partial\Omega_1)$. Hence, for $n = 1$, the first-subdomain problem is

$$\begin{aligned} \Delta u_1^1 &= f && \text{in } \Omega_1, \\ u_1^1 &= \tau_1(u^0) && \text{on } \partial\Omega_1, \end{aligned}$$

which is uniquely solved by $u_1^1 \in H^1(\Omega_1)$. Now, we define a function

$$\widetilde{u} := \begin{cases} u_1^1 & \text{in } \Omega_1, \\ u^0 & \text{in } \Omega \setminus \Omega_1. \end{cases}$$

Notice that a direct calculation shows that $\widetilde{u} \in H^1(\Omega)$ (see [39]) and $\tau(\widetilde{u}) = g$. Therefore, the second-subdomain problem is

$$\begin{aligned} \Delta u_2^1 &= f && \text{in } \Omega_1, \\ u_2^1 &= \tau_2(\widetilde{u}) && \text{on } \partial\Omega_2, \end{aligned}$$

which is uniquely solved by $u_2^1 \in H^1(\Omega_2)$. One can now define a function

$$\widehat{u} := \begin{cases} u_2^1 & \text{in } \Omega_2, \\ u_1^1 & \text{in } \Omega \setminus \Omega_2, \end{cases}$$

rewrite the first-subdomain problem, and repeat recursively the above argument to obtain the result. ∎

Consider the example of Laplace problem (1.5), with boundary function g as described in Figure 1.10, that we always consider in this book as a test problem for numerical experiments. According to Theorem 6.1, it is uniquely solvable by $u \in C^2(\Omega)$. Moreover, since the boundary function g has two singularities (jumps) in the two corners $(x, y) = (0, 0)$ and $(x, y) = (0, 1)$ of the square domain, we have that $\lim_{\boldsymbol{x} \to \boldsymbol{x}_0} u(\boldsymbol{x}) = g(\boldsymbol{x}_0)$ for every $\boldsymbol{x}_0 \in \partial\Omega \setminus \{(0, 0), (0, 1)\}$. For this reason, g is neither in $C(\partial\Omega)$ nor in $H^{1/2}(\partial\Omega)$. Therefore, u is neither a classical solution nor a weak solution. In this case, the Schwarz method is still well posed, as the following theorem shows.

Theorem 6.3 (Well-posedness of the Schwarz method—2). *Assume that the domain* $\Omega = (0, 1) \times (0, L)$ *is decomposed as in Figure 4.16. Assume that* f *is bounded and locally Hölder continuous in* Ω *and that* g *is bounded in* $\partial\Omega$ *and continuous at the interface points* $(\beta, 0)$, $(\alpha, 0)$, $(\beta, 1)$, *and* $(\alpha, 1)$. *If* $u_2^0 \in C(\overline{\Omega})$, *then the Schwarz sequences* $\{u_1^n\}_n$ *and* $\{u_2^n\}_n$ *are well defined in the sense that for* $n \geq 1$ *the Schwarz subproblems* (4.30) *are uniquely solvable by Perron solutions* $u_1^n \in C^2(\Omega_1)$ *and* $u_2^n \in C^2(\Omega_2)$. *Moreover, it holds that* $u_1^n|_{\overline{\Gamma}_2} \in C(\overline{\Gamma}_2)$ *and* $u_2^n|_{\overline{\Gamma}_1} \in C(\overline{\Gamma}_1)$ *for* $n \geq 1$.

Proof. Since the initial guess u_2^0 is in $C(\overline{\Omega})$, we can trace it along the interface Γ_1. Since f is bounded and locally Hölder continuous in Ω, g is bounded, and the domain is a convex open set in $\mathbb{R}^2$, Theorem 6.1 guarantees that the Schwarz subproblem (4.30) (left) is uniquely solvable by a (Perron) solution $u_1^1 \in C^2(\Omega_1)$. Notice that u_2^0 is not necessarily equal to g in $(\alpha, 0)$ and

$(\alpha, 1)$ (jumps can occur), and g is not necessarily continuous on $\partial\Omega$. Hence (even in the case that $g \in C(\partial\Omega)$) the solution u_1^1 is in general neither a classical solution nor a weak solution. However, we can trace its value along the interface Γ_2, and since g is continuous at the points $(\beta, 0)$ and $(\beta, 1)$, it holds that $u_1^1|_{\overline{\Gamma}_2} \in C(\overline{\Gamma}_2)$. With this trace, one can solve (4.30) (right). Its solution is a Perron function $u_2^1 \in C^2(\Omega_2)$. Again, one can trace u_2^1 along the interface Γ_1 and, since g is continuous in $(\alpha, 0)$ and $(\alpha, 1)$, it holds that $u_2^1|_{\overline{\Gamma}_1} \in C(\overline{\Gamma}_1)$. This can be used to solve again (4.30) (left) to get $u_1^2 \in C^2(\Omega_1)$, which can be traced on Γ_2 to define a boundary condition for (4.30) (right). By continuing with these arguments we obtain a sequence of Perron solutions $u_1^n \in C^2(\Omega_1)$ and $u_2^n \in C^2(\Omega_2)$, for any $n \geq 1$, such that their traces on the interfaces $\overline{\Gamma}_2$ and $\overline{\Gamma}_1$ are continuous functions. □

6.2 ▪ Some polynomial identities

In this section, we prove the polynomial identities used in Chapter 3. Some of their proofs are adapted from [102].

Theorem 6.4. *For any $z \in \mathbb{C}$, the following polynomial identities hold:*

$$1 - z^m = \prod_{k=1}^{m} (1 - w^k z), \tag{6.1}$$

$$1 = \sum_{k=1}^{m} \frac{1}{m} \prod_{\ell=1, \ell \neq k}^{m} (1 - w^\ell z), \tag{6.2}$$

where $w = \exp(\frac{2\pi i}{m})$, i is the imaginary unit, and m is an arbitrary positive integer.

Proof. To prove the identity (6.1) we first notice that

$$\begin{aligned} \prod_{k=1}^{m} w^k &= \prod_{k=1}^{m} \exp\Big(\frac{2\pi i k}{m}\Big) = \exp\Big(\frac{2\pi i \sum_{k=1}^{m} k}{m}\Big) \\ &= \exp\Big(\frac{2\pi i \frac{m(m+1)}{2}}{m}\Big) = \exp(\pi i (m+1)) = (-1)^{m+1} \end{aligned}$$

and that w^{-k}, $k = 1, 2, \ldots$, are roots of the polynomial $p(z) = z^m - 1$, which implies that $z^m - 1 = \prod_{k=1}^{m} (z - 1/w^k)$. Therefore, we obtain

$$\begin{aligned} 1 - z^m &= -(z^m - 1) = -\prod_{k=1}^{m} \left(z - \frac{1}{w^k}\right) = -\prod_{k=1}^{m} \frac{w^k z - 1}{w^k} \\ &= \frac{(-1)^{m+1} \prod_{k=1}^{m} (1 - w^k z)}{\prod_{k=1}^{m} w^k} = \prod_{k=1}^{m} (1 - w^k z), \end{aligned}$$

which is exactly (6.1).

Let us now prove the identity (6.2). To do so, we first notice that $w^m = \exp(\frac{2\pi i m}{m}) = 1$. Therefore, for any nonnegative integer j, we have that $w^{\ell+j} = w^{m+\widehat{\ell}} = w^{\widehat{\ell}}$ for $\ell + j > m$ and $\widehat{\ell} = \ell + j - m$. Hence the sets $\{w^\ell, w^{\ell+1}, \ldots, w^{\ell+m-1}\}$ are equal for any nonnegative integer ℓ. This fact implies that the polynomial $p(z) := \sum_{k=0}^{m-1} \frac{1 - z^m}{1 - \omega^k z}$ satisfies the relation

$$p(w^\ell z) = \sum_{k=0}^{m-1} \frac{1 - w^{\ell m} z^m}{1 - \omega^{k+\ell} z} = \sum_{k=0}^{m-1} \frac{1 - z^m}{1 - \omega^k z} = p(z), \tag{6.3}$$

which means that $p(z)$ is invariant under any transformation $z \mapsto w^\ell z$, $\ell = 1, \dots, m$. Let us now write $p(z)$ as $p(z) = \gamma_0 + \sum_{j=1}^{m-1} \gamma_j z^j$. Using the relation $p(z) = p(w^\ell z)$ for any ℓ, we can compute

$$0 = p(z) - p(w^\ell z) = \sum_{j=1}^{m-1} \gamma_j (1 - w^{j\ell}) z^j \quad \forall z \in \mathbb{C} \text{ and for } \ell = 1, \dots, m.$$

This implies that $\gamma_j = 0$, $j = 1, \dots, m-1$, which means that the polynomial p is constant: $p(z) = \gamma_0$. The constant coefficient γ_0 can be computed by evaluating p in $z = 0$: $\gamma_0 = p(0) = m$. We have then obtained $m = p(z) = \sum_{k=0}^{m-1} \frac{1-z^m}{1-\omega^k z}$. The identity (6.2) follows by using (6.1) and dividing by m. ∎

6.3 ▪ Sobolev embedding theorems

In this section, we briefly recall the famous *Sobolev embedding theorems* and *Rellich–Kondrachov compact embedding theorems*. We refer the reader to [48].

Definition 6.5. *Let X and Y be two normed vector spaces. The space X is said to be continuously embedded in Y, $X \hookrightarrow Y$ if $X \subset Y$ and there exists a constant c such that $\|x\|_Y \le c\|x\|_X$ for all $x \in X$. Furthermore, X is said to be compactly embedded in Y, $X \Subset Y$ if $X \hookrightarrow Y$ and every bounded sequence $(x_k)_{k\in\mathbb{N}}$ in X contains a subsequence converging in Y.*

Theorem 6.6 (Sobolev embedding theorems). *Let Ω be a Lipschitz domain in $\mathbb{R}^N$, let $m \ge 1$ be an integer, and let $1 \le p < \infty$. Then the following continuous embeddings hold:*

(a)	$W^{m,p}(\Omega) \hookrightarrow L^{p^*}(\Omega)$	with $\frac{1}{p^*} = \frac{1}{p} - \frac{m}{N}$ if $m < \frac{N}{p}$,
(b)	$W^{m,p}(\Omega) \hookrightarrow L^{q}(\Omega)$	$\forall q$ with $1 \le q < \infty$ if $m = \frac{N}{p}$,
(c)	$W^{m,p}(\Omega) \hookrightarrow C^{0,m-N/p}(\bar\Omega)$	if $\frac{N}{p} < m < \frac{N}{p} + 1$,
(d)	$W^{m,p}(\Omega) \hookrightarrow C^{0,\lambda}(\bar\Omega)$	$\forall \lambda$ with $0 < \lambda < 1$ if $m = \frac{N}{p} + 1$,
(e)	$W^{m,p}(\Omega) \hookrightarrow C^{0,1}(\bar\Omega)$	if $m > \frac{N}{p} + 1$.

Theorem 6.7 (Rellich–Kondrachov compact embedding theorems). *Let $\Omega \subset \mathbb{R}^N$ be a bounded domain that satisfies the cone condition, let $m \ge 1$ be an integer, and let $1 \le p < \infty$. Then the following compact embeddings hold:*

(a)	$W^{m,p}(\Omega) \Subset L^{q}(\Omega)$	$\forall q$ with $1 \le q < p^* = \frac{pN}{N-mp}$ if $m < \frac{N}{p}$,
(b)	$W^{m,p}(\Omega) \Subset L^{q}(\Omega)$	$\forall q$ with $1 \le q < \infty$ if $m = \frac{N}{p}$,
(c)	$W^{m,p}(\Omega) \Subset C(\bar\Omega)$	if $m > \frac{N}{p}$.

6.4 ▪ Lax–Milgram theorem

Theorem 6.8 (Lax–Milgram theorem). *Let V be a real Hilbert space endowed with the norm $\|\cdot\|$. Let $a : V \times V \to \mathbb{R}$ be a bilinear form and $\ell : V \to \mathbb{R}$ be a bounded linear functional. If*

(a) *a is coercive, that is, there exists a positive constant c such that for all $v \in V$ it holds that $a(v, v) \ge c\|v\|^2$, and*

(b) *a is bounded, that is, there exists a positive constant $\widetilde{c}$ such that for all $v, w \in V$ it holds that $|a(v, w)| \le \widetilde{c}\|v\|\|w\|$,*

then there exists a unique $y \in V$ such that $a(y, v) = \ell(v)$ for all $v \in V$.

6.5 ▪ Weak compactness

Definition 6.9 (Weakly convergent sequence and weakly compact set). *Let X be a normed vector space. A sequence $(x_n)_{n\in\mathbb{N}}$ is said to converge weakly to a (weak) limit $x \in X$ (denoted by $x_n \rightharpoonup x$) if and only if*

$$\lim_{n\to\infty} g(x_n) = g(x) \quad \forall g \in X^*,$$

where X^* is the dual space of X. A set $C \subset X$ is said to be weakly (sequentially) compact if every sequence $(x_n)_{n\in\mathbb{N}} \subset C$ has a weakly convergent subsequence to some (weak) limit $x \in C$.

Definition 6.10 (Weakly lower semicontinuous functional). *A functional $f : C \to \mathbb{R}$ is called weakly lower semicontinuous at $x \in C$ if for every sequence $(x_n)_{n\in\mathbb{N}}$ with $x_n \rightharpoonup x$ as $n \to \infty$ it holds that*

$$\liminf_{n\to\infty} f(x_n) \geq f(x).$$

If f is weakly lower semicontinuous at any $x \in C$, we say that f is weakly lower semicontinuous.

Theorem 6.11 (Weakly convergent sequences). *Let X be a normed vector space. Then*

- *the limit of a weakly convergent sequence in X is unique, and*
- *a weakly convergent sequence is bounded in X.*

Proof. See, e.g., [48, Theorem 5.12-2]. □

Theorem 6.12 (Weakly convergent sequences in a reflexive Banach space). *Let X be a reflexive Banach space. Any bounded sequence in X contains a weakly convergent subsequence.*

Proof. See, e.g., [48, Theorem 5.14-4]. □

Theorem 6.13 (Weakly compact subsets). *Let X be a reflexive Banach space. Any closed, convex, and bounded subset of X is weakly sequentially compact.*

Proof. See, e.g., [48, 147]. □

Theorem 6.14 (Weakly lower semicontinuous functions). *Let C be a convex subset of a normed vector space X. If $f : C \to \mathbb{R}$ is convex and continuous, then it is weakly lower semicontinuous.*

Proof. See, e.g., [48, 147]. □

Translation of Quotes

Section 1.2, p. 3

> You will in the future hardly ever eliminate directly anymore, at least not when you have more than two unknowns. The indirect procedure can be done while one is half asleep, or one can think about other things while doing it.
>
> Carl F. Gauss, in a letter to his friend Christian L. Gerling, 1823.

> The difficulty of the strict resolution of a larger number of linear equations, to which in many cases the method of least squares leads, led me to think about the application of approximation methods.
>
> Carl G. J. Jacobi, *On a new way of resolving the linear equations occurring in the method of least squares*, 1845.

Section 2.5, p. 37

> Such a [method of approximation] comes very naturally, if in the different equations always a different variable is multiplied with a preferably large coefficient.
>
> Carl G. J. Jacobi, *On a new way of resolving the linear equations occurring in the method of least squares*, 1845.

Section 2.6, p. 42

> If, therefore, starting from any system of initial values, and in any succession of the unknowns (whereby it is not necessary to go through the whole cycle of them before coming back to an already improved one), one applies successive corrections to the unknowns, taking care to determine the improvement of each one always in such a way that the corresponding normal equation holds in which the unknown takes the specific position on the diagonal, then one reduces step by step the sum of the error squares, as long as something is still to be reduced in it.
>
> Ludwig von Seidel, *On a method to solve the equations to which the method of least squares leads, as well as linear equations in general, by successive approximation*, 1874.

Section 3.1, p. 68

Given a system of simultaneous equations to be solved, one usually begins by reducing them to a single one, by means of successive eliminations, except for solving the resulting equation definitively, if possible. But it is important to observe: 1. that in a large number of cases the elimination cannot be carried out in any way; 2. that the resulting equation is usually very complicated, even when the given equations are quite simple. For these two reasons, we realize that it would be very useful to know a general method which could be used to solve directly a system of simultaneous equations. This is the one I have obtained, and of which I will say a few words here.

Augustin-Luis Cauchy, *General method for solving systems of simultaneous equations*, 1847.

This is in principle an application of Ritz's idea of approximating a minimum by restricting the competition to an easily manageable linear set.

Eduard Stiefel, *About some methods of relaxation calculations*, 1952.

Section 3.2, p. 74

Following the well-known method of steepest descent and the iteration in complete steps, an "n-step method" is given in Section 5, which provides both a successive approximation to the solution, and its exact determination in a finite number of steps.

Eduard Stiefel, *About some methods of relaxation calculations*, 1952.

Chapter 4, p. 123

In general, several of the coefficients outside the diagonal will assume such significant values that the success of the approximation method just given is ruined. However, as I will show in the following, by repeating an easy calculation, the equations can be transformed into other equations, in which the deficiency mentioned becomes less and less pronounced, so that finally the equations obtain a form, which allows the successful application of the approximation method above.

Carl G. J. Jacobi, *On a new way of resolving the linear equations occurring in the method of least squares*, 1845.

Section 4.6, p. 147

By continuing some investigations, which concern certain types of mapping problems, and of which a part is published in the 70th volume of Borchardt's Journal and in the essay accompanying the program of the Federal Polytechnical School for the winter semester 1869–70: "On the Theory of Mapping," I have been led to a proof technique, by which, as I believe to have convinced myself, all the theorems, whose proof Riemann has tried to do in his published works by means of the Dirichlet Principle, can be proved rigorously.

Hermann Amandus Schwarz, *On a limiting process by an alternating procedure*, 1869.

Section 4.8, p. 179

> This preconditioner acts on the Steklov-Poincaré operator (represented after discretization by the Schur complement matrix) by trace averaging and solving a Neumann problem per subdomain.
>
> Jean-François Bourgat, Roland Glowinski, Patrick Le Tallec, and Marina Vidrascu, *Variational Formulation and Algorithm for Trace Operator in Domain Decomposition Calculations*, 1989.

Bibliography

[1] W. E. Arnoldi. The principle of minimized iterations in the solution of the matrix eigenvalue problem. *Quarterly of Applied Mathematics*, 9(1):17–29, 1951. (Cited on p. 94)

[2] O. Axelsson, S. Farouq, and M. Neytcheva. Comparison of preconditioned Krylov subspace iteration methods for PDE-constrained optimization problems. *Numerical Algorithms*, 73(3):631–663, 2016. (Cited on pp. 247, 249)

[3] O. Axelsson and M. Neytcheva. Eigenvalue estimates for preconditioned saddle point matrices. *Numerical Linear Algebra with Applications*, 13(4):339–360, 2006. (Cited on p. 234)

[4] Z.-Z. Bai. Block preconditioners for elliptic PDE-constrained optimization problems. *Computing*, 91(4):379–395, 2011. (Cited on p. 248)

[5] R. Barrett, M. Berry, T. F. Chan, J. Demmel, J. Donato, J. Dongarra, V. Eijkhout, R. Pozo, C. Romine, and H. van der Vorst. *Templates for the Solution of Linear Systems: Building Blocks for Iterative Methods*. SIAM, 1994. (Cited on p. 1)

[6] R. Bartlett, M. Heinkenschloss, D. Ridzal, and B. van Bloemen Waanders. Domain decomposition methods for advection dominated linear quadratic elliptic optimal control problem. *Computer Methods in Applied Mechanics and Engineering*, 195:44–47, 2006. (Cited on p. 249)

[7] H. Barucq, M. J. Gander, and Y. Xu. On the influence of curvature on transmission conditions. In *Domain Decomposition Methods in Science and Engineering XXI*, pages 323–331. Springer, 2014. (Cited on p. 152)

[8] A. Battermann and M. Heinkenschloss. Preconditioners for Karush-Kuhn-Tucker matrices arising in the optimal control of distributed systems. In W. Desch, F. Kappel, and K. Kunisch, editors, *Control and Estimation of Distributed Parameter Systems*, pages 15–32. Birkhäuser Basel, 1998. (Cited on p. 248)

[9] A. Battermann and E. W. Sachs. Block preconditioners for KKT systems in PDE-governed optimal control problems. In Karl-Heinz Hoffmann, Ronald H. W. Hoppe, and Volker Schulz, editors, *Fast Solution of Discretized Optimization Problems*, pages 1–18. Birkhäuser Basel, 2001. (Cited on pp. 234, 248)

[10] J.-D. Benamou. A domain decomposition method with coupled transmission conditions for the optimal control of systems governed by elliptic partial differential equations. *SIAM Journal on Numerical Analysis*, 33(6):2401–2416, 1996. (Cited on pp. 227, 228, 229, 249)

[11] J.-D. Benamou. A domain decomposition method for control problems. In *Proceedings of the 9th International Conference on Domain Decomposition Methods*, pages 266–273. DDM.org, 1998. (Cited on pp. 227, 249)

[12] J.-D. Benamou and B. Desprès. *A Domain Decomposition Method for the Helmholtz Equation and Related Optimal Control Problems*. Research Report RR-2791, INRIA, 1996. (Cited on pp. 227, 249)

[13] D. Bennequin, M. J. Gander, L. Gouarin, and L. Halpern. Optimized Schwarz waveform relaxation for advection reaction diffusion equations in two dimensions. *Numerische Mathematik*, 134(3):513–567, 2016. (Cited on p. 168)

[14] D. Bennequin, M. J. Gander, and L. Halpern. A homographic best approximation problem with application to optimized Schwarz waveform relaxation. *Mathematics of Computation*, 78(265):185–223, 2009. (Cited on p. 168)

[15] M. Benzi. Preconditioning techniques for large linear systems: A survey. *Journal of Computational Physics*, 182(2):418–477, 2002. (Cited on p. 147)

[16] M. Benzi. Splittings of symmetric matrices and a question of Ortega. *Linear Algebra and Its Applications*, 429:2340–2343, 2008. (Cited on p. 35)

[17] M. Benzi, C. D. Meyer, and M. Tůma. A sparse approximate inverse preconditioner for the conjugate gradient method. *SIAM Journal on Scientific Computing*, 17(5):1135–1149, 1996. (Cited on p. 142)

[18] P. E. Bjørstad and O. B. Widlund. Iterative methods for the solution of elliptic problems on regions partitioned into substructures. *SIAM Journal on Numerical Analysis*, 23(6):1097–1120, 1986. (Cited on p. 168)

[19] A. Borzì. High-order discretization and multigrid solution of elliptic nonlinear constrained optimal control problems. *Journal of Computational and Applied Mathematics*, 200(1):67–85, 2007. (Cited on pp. 244, 246)

[20] A. Borzì, G. Ciaramella, and M. Sprengel. *Formulation and Numerical Solution of Quantum Control Problems*. SIAM, Philadelphia, PA, 2017. (Cited on pp. 207, 211, 213)

[21] A. Borzì, K. Kunisch, and D. Y. Kwak. Accuracy and convergence properties of the finite difference multigrid solution of an optimal control optimality system. *SIAM Journal on Control and Optimization*, 41(5):1477–1497, 2002. (Cited on pp. 244, 246)

[22] A. Borzì and V. Schulz. Multigrid methods for PDE optimization. *SIAM Review*, 51(2):361–395, 2009. (Cited on pp. 238, 244, 246)

[23] A. Borzì and V. Schulz. *Computational Optimization of Systems Governed by Partial Differential Equations*. SIAM, Philadelphia, PA, 2012. (Cited on pp. 207, 216, 224, 246, 247, 249)

[24] J.-F. Bourgat, R. Glowinski, P. Le Tallec, and M. Vidrascu. Variational formulation and algorithm for trace operator in domain decomposition calculations. In Tony Chan, Roland Glowinski, Jacques Périaux, and Olof Widlund, editors, *Domain Decomposition Methods. Second International Symposium on Domain Decomposition Methods*, pages 3–16. SIAM, Philadelphia, PA, 1989. (Cited on p. 179)

[25] S. Boyd and L. Vandenberghe. *Convex Optimization*. Cambridge University Press, New York, 2004. (Cited on p. 68)

[26] J. H. Bramble and J. E. Pasciak. A preconditioning technique for indefinite systems resulting from mixed approximations of elliptic problems. *Mathematics of Computation*, 50(181):1–17, 1988. (Cited on p. 248)

[27] A. Brandt. Multi-level adaptive technique (MLAT) for fast numerical solution to boundary value problems. In *Proceedings of the Third International Conference on Numerical Methods in Fluid Mechanics 1972*, pages 82–89. Springer, 1973. (Cited on p. 188)

[28] N. I. Buleev. Numerical method for solving two- and three-dimensional diffusion equations. *Matematicheskiĭ Sbornik*, 51(93)(2):227–238, 1960. (Cited on p. 136)

[29] A. L. Cauchy, Translated by R. J. Pulskamp. *Méthode générale pour la résolution des systemes d'équations simultanées*. Department of Mathematics and Computer Science, Xavier University, Cincinnati, 2010. (Cited on p. 68)

[30] X.-C. Cai and M. Sarkis. A restricted additive Schwarz preconditioner for general sparse linear systems. *SIAM Journal on Scientific Computing*, 21(2):792–797, 1999. (Cited on p. 158)

[31] A. L. Cauchy. Méthode générale pour la résolution des systemes d'équations simultanées. *Comptes Rendus*, 25(2):536–538, 1847. (Cited on p. 68)

[32] F. Chaouqui, G. Ciaramella, M. J. Gander, and T. Vanzan. On the scalability of classical one-level domain-decomposition methods. *Vietnam Journal of Mathematics*, 46(4):1053–1088, 2018. (Cited on pp. 149, 160)

[33] F. Chaouqui, M. J. Gander, and K. Santugini-Repiquet. A local coarse space correction leading to a well-posed continuous Neumann-Neumann method in the presence of cross points. In *Proceedings of the 25th International Conference on Domain Decomposition Methods*. Springer, 2020. (Cited on p. 179)

[34] P. L. Chebychev. Théorie des mécanismes connus sous le nom de parallélogrammes. *Mémoires des Savants étrangers présentés à l'Académie de Saint-Pétersbourg*, 7:539–586, 1854. (Cited on p. 87)

[35] P. L. Chebyshev. Theory of the mechanisms known as parallelograms. *Uspekhi Matematicheskikh Nauk*, 1(2):12–37, 1946. (Cited on p. 190)

[36] D. Choi. A proof of Crouzeix's conjecture for a class of matrices. *Linear Algebra and Its Applications*, 438(8):3247–3257, 2013. (Cited on p. 109)

[37] G. Ciaramella and M. J. Gander. Analysis of the parallel Schwarz method for growing chains of fixed-sized subdomains: Part I. *SIAM Journal on Numerical Analysis*, 55(3):1330–1356, 2017. (Cited on p. 149)

[38] G. Ciaramella and M. J. Gander. Analysis of the parallel Schwarz method for growing chains of fixed-sized subdomains: Part II. *SIAM Journal on Numerical Analysis*, 56(3):1498–1524, 2018. (Cited on p. 149)

[39] G. Ciaramella and M. J. Gander. Analysis of the parallel Schwarz method for growing chains of fixed-sized subdomains: Part III. *Electronic Transactions on Numerical Analysis*, 49:201–243, 2018. (Cited on pp. 149, 252)

[40] G. Ciaramella and M. J. Gander. Happy 25th anniversary DDM!... but how fast can the Schwarz method solve your logo? In *Domain Decomposition Methods in Science and Engineering XXV*, pages 83–91. Lecture Notes in Computational Science and Engineering 138. Springer, 2020. (Cited on p. 149)

[41] G. Ciaramella, L. Halpern, L. Mechelli, and R. Racke. On the convergence analysis of optimized waveform-relaxation methods for parabolic optimal control problems. In preparation, 2021. (Cited on p. 249)

[42] G. Ciaramella, M. Hassan, and B. Stamm. On the scalability of the parallel Schwarz method in one-dimension. In *Domain Decomposition Methods in Science and Engineering XXV*, pages 151–158. Lecture Notes in Computational Science and Engineering 138. Springer, 2020. (Cited on p. 149)

[43] G. Ciaramella, M. Hassan, and B. Stamm. On the scalability of the Schwarz method. *SMAI Journal of Computational Mathematics*, 6:33–68, 2020. (Cited on p. 149)

[44] G. Ciaramella and R. Höfer. Non-geometric convergence of the classical alternating Schwarz method. In *Domain Decomposition Methods in Science and Engineering XXV*, pages 193–201. Lecture Notes in Computational Science and Engineering 138. Springer, 2020. (Cited on p. 152)

[45] G. Ciaramella, F. Kwok, and G. Müller. Nonlinear optimized Schwarz preconditioner for elliptic optimal control problems. In *Domain Decomposition Methods in Science and Engineering XXVI*, Lecture Notes in Computational Science and Engineering. Springer, 2021. (Cited on p. 249)

[46] G. Ciaramella and L. Mechelli. On the effect of boundary conditions on the scalability of Schwarz methods. In *Domain Decomposition Methods in Science and Engineering XXVI*, Lecture Notes in Computational Science and Engineering. Springer, 2021. (Cited on p. 149)

[47] G. Ciaramella and L. Mechelli. An overlapping waveform-relaxation preconditioner for economic optimal control problems with state constraints. In *Domain Decomposition Methods in Science and Engineering XXVI*, Lecture Notes in Computational Science and Engineering. Springer, 2021. (Cited on p. 249)

[48] P. G. Ciarlet. *Linear and Nonlinear Functional Analysis with Applications*. SIAM, Philadelphia, PA, 2013. (Cited on pp. 151, 210, 231, 251, 254, 255)

[49] M. Crouzeix. Bounds for analytical functions of matrices. *Integral Equations and Operator Theory*, 48:461–477, 2004. (Cited on p. 109)

[50] M. Crouzeix. Numerical range and functional calculus in Hilbert space. *Journal of Functional Analysis*, 244(2):668–690, 2007. (Cited on p. 109)

[51] M. Crouzeix and A. Greenbaum. Spectral sets: Numerical range and beyond. *SIAM Journal on Matrix Analysis and Applications*, 40(3):1087–1101, 2019. (Cited on p. 109)

[52] M. Crouzeix and C. Palencia. The numerical range is a $(1 + \sqrt{2})$-spectral set. *SIAM Journal on Matrix Analysis and Applications*, 38(2):649–655, 2017. (Cited on p. 109)

[53] B. Delourme and L. Halpern. A complex homographic best approximation problem. Application to optimized Robin–Schwarz algorithms, and optimal control problems. *SIAM Journal on Numerical Analysis*, 59(3):1769–1810, 2021. (Cited on pp. 227, 249)

[54] B. Delourme, L. Halpern, and B. T. Nguyen. Optimized Schwarz methods for elliptic optimal control problems. In Petter E. Bjørstad, Susanne C. Brenner, Lawrence Halpern, Hyea Hyun Kim, Ralf Kornhuber, Talal Rahman, and Olof B. Widlund, editors, *Domain Decomposition Methods in Science and Engineering XXIV*. Springer, 2018. (Cited on p. 249)

[55] B. Delyon and F. Delyon. Generalization of von Neumann's spectral sets and integral representation of operators. *Bulletin de la Societe Mathematique de France*, 127:25–41, 1999. (Cited on pp. 108, 109)

[56] V. Dolean, M. J. Gander, and L. Gerardo-Giorda. Optimized Schwarz methods for Maxwell's equations. *SIAM Journal on Scientific Computing*, 31(3):2193–2213, 2009. (Cited on pp. 11, 168)

[57] T. Dreyer, B. Maar, and V. Schulz. Multigrid optimization in applications. *Journal of Computational and Applied Mathematics*, 120(1–2):67–84, 2000. (Cited on p. 238)

[58] E. Efstathiou and M. J. Gander. Why restricted additive Schwarz converges faster than additive Schwarz. *BIT Numerical Mathematics*, 43(5):945–959, 2003. (Cited on p. 162)

[59] M. El Bouajaji, V. Dolean, M. J. Gander, and S. Lanteri. Optimized Schwarz methods for the time-harmonic Maxwell equations with damping. *SIAM Journal on Scientific Computing*, 34(4):A2048–A2071, 2012. (Cited on p. 168)

[60] K. D. Elworthy, W. N. Everitt, and E. B. Lee. *Differential Equations, Dynamical Systems, and Control Science: A Festschrift in Honor of Lawrence Markus*. Marcel Dekker, New York, 1994. (Cited on p. 206)

[61] M. Embree. *How Descriptive Are GMRES Convergence Bounds?* Technical report, Oxford University Computing Laboratory, 1999. (Cited on pp. 100, 109, 110)

[62] L. C. Evans. *Partial Differential Equations*. Graduate Studies in Mathematics 19. American Mathematical Society, Providence, 2002. (Cited on p. 251)

[63] C. Farhat and F.-X. Roux. A method of finite element tearing and interconnecting and its parallel solution algorithm. *International Journal for Numerical Methods in Engineering*, 32(6):1205–1227, 1991. (Cited on p. 179)

[64] R. P. Fedorenko. A relaxation method for solving elliptic difference equations. *Zhurnal Vychislitel'noi Matematiki i Matematicheskoi Fiziki*, 1(5):922–927, 1961. (Cited on p. 188)

[65] G. E. Forsythe. Notes. *Mathematical Tables and Other Aids to Computation*, 5(36):255–258, 1951. (Cited on pp. 4, 6)

[66] G. E. Forsythe, M. R. Hestenes, and J. B. Rosser. Iterative methods for solving linear equations. *Bulletin of the American Mathematical Society*, 57(6):480–480, 1951. (Cited on p. 77)

[67] R. W. Freund and N. M. Nachtigal. QMR: A quasi-minimal residual method for non-Hermitian linear systems. *Numerische Mathematik*, 60(1):315–339, 1991. (Cited on p. 118)

[68] M. J. Gander. Optimized Schwarz methods. *SIAM Journal on Numerical Analysis*, 44(2):699–731, 2006. (Cited on pp. 11, 149, 160, 165, 168)

[69] M. J. Gander. Schwarz methods over the course of time. *Electronic Transactions on Numerical Analysis*, 31(5):228–255, 2008. (Cited on pp. 155, 156, 157, 158, 160, 162)

[70] M. J. Gander. On the influence of geometry on optimized Schwarz methods. *SeMA Journal*, 53(1):71–78, 2011. (Cited on p. 152)

[71] M. J. Gander and O. Dubois. Optimized Schwarz methods for a diffusion problem with discontinuous coefficient. *Numerical Algorithms*, 69(1):109–144, 2015. (Cited on p. 187)

[72] M. J. Gander and L. Halpern. Absorbing boundary conditions for the wave equation and parallel computing. *Mathematics of Computation*, 74(249):153–176, 2005. (Cited on p. 168)

[73] M. J. Gander and L. Halpern. Optimized Schwarz waveform relaxation methods for advection reaction diffusion problems. *SIAM Journal on Numerical Analysis*, 45(2):666–697, 2007. (Cited on p. 168)

[74] M. J. Gander, L. Halpern, and F. Magoules. An optimized Schwarz method with two-sided Robin transmission conditions for the Helmholtz equation. *International Journal for Numerical Methods in Fluids*, 55(2):163–175, 2007. (Cited on p. 168)

[75] M. J. Gander, L. Halpern, and F. Nataf. Optimal Schwarz waveform relaxation for the one dimensional wave equation. *SIAM Journal on Numerical Analysis*, 41(5):1643–1681, 2003. (Cited on p. 168)

[76] M. J. Gander and F. Kwok. *Numerical Analysis of Partial Differential Equations Using Maple and MATLAB*. SIAM, Philadelphia, PA, 2018. (Cited on pp. 11, 20)

[77] M. J. Gander, F. Kwok, and B. C. Mandal. Convergence of substructuring methods for elliptic optimal control problems. In *Domain Decomposition Methods in Science and Engineering XXIV*, pages 291–300. Springer, 2018. (Cited on p. 249)

[78] M. J. Gander, F. Kwok, and B. C. Mandal. Dirichlet-Neumann waveform relaxation methods for parabolic and hyperbolic problems in multiple subdomains. *BIT Numerical Mathematics*, 61(1):173–207, 2021. (Cited on p. 178)

[79] M. J. Gander, F. Kwok, and J. Salomon. ParaOpt: A parareal algorithm for optimality systems. *SIAM Journal on Scientific Computing*, 42(5):A2773–A2802, 2020. (Cited on p. 249)

[80] M. J. Gander, F. Kwok, and G. Wanner. Constrained optimization: From Lagrangian mechanics to optimal control and PDE constraints. In *Optimization with PDE Constraints*, pages 151–202. Springer, 2014. (Cited on pp. 205, 213)

[81] M. J. Gander, F. Magoulés, and F. Nataf. Optimized Schwarz methods without overlap for the Helmholtz equation. *SIAM Journal on Scientific Computing*, 24(1):38–60, 2002. (Cited on p. 168)

[82] M. J. Gander and X. Tu. On the origins of iterative substructuring methods. In *Domain Decomposition Methods in Science and Engineering XXI*, pages 597–605. Springer, 2014. (Cited on pp. 168, 179)

[83] M. J Gander and T. Vanzan. Heterogeneous optimized Schwarz methods for second order elliptic PDEs. *SIAM Journal on Scientific Computing*, 41(4):A2329–A2354, 2019. (Cited on pp. 168, 187)

[84] M. J. Gander and G. Wanner. The origins of the alternating Schwarz method. In *Domain Decomposition Methods in Science and Engineering XXI*, pages 487–495. Springer, 2014. (Cited on p. 147)

[85] M. J. Gander and H. Zhang. A class of iterative solvers for the Helmholtz equation: Factorizations, sweeping preconditioners, source transfer, single layer potentials, polarized traces, and optimized Schwarz methods. *SIAM Review*, 61(1):3–76, 2019. (Cited on pp. 160, 168)

[86] W. Gander, M. J. Gander, and F. Kwok. *Scientific Computing—An Introduction Using Maple and MATLAB*. Texts in Computational Science and Engineering 11. Springer, 2014. (Cited on pp. 2, 67, 94, 118, 126)

[87] C. F. Gauss. Letter to Gerling, December 26, 1823. In *Werke*, Volume 9, pages 278–281. Göttingen, 1903. (Cited on p. 4)

[88] D. Gilbarg and N. S. Trudinger. *Elliptic Partial Differential Equations of Second Order*. Grundlehren der Mathematischen Wissenschaften 224. Springer, 1983. (Cited on pp. 149, 251)

[89] C. Glader, M. Kurula, and M. Lindström. Crouzeix's conjecture holds for tridiagonal 3×3 matrices with elliptic numerical range centered at an eigenvalue. *SIAM Journal on Matrix Analysis and Applications*, 39(1):346–364, 2018. (Cited on p. 109)

[90] G. H. Golub. *The Use of Chebyshev Matrix Polynomials in the Iterative Solution of Linear Equations Compared to the Method of Successive Overrelaxation*. Ph.D. thesis, University of Illinois at Urbana-Champaign, 1959. (Cited on pp. 67, 89)

[91] G. H. Golub and C. F. Van Loan. *Matrix Computations*. Johns Hopkins Studies in the Mathematical Sciences. Johns Hopkins University Press, Baltimore, MD, 1996. (Cited on p. 27)

[92] G. H. Golub and C. F. Van Loan. *Matrix Computations (Fourth Edition)*. Johns Hopkins Studies in the Mathematical Sciences. Johns Hopkins University Press, Baltimore, MD, 2013. (Cited on p. 219)

[93] M. Gonzalez. *Classical Complex Analysis*. Chapman & Hall Pure and Applied Mathematics. Taylor & Francis, 1991. (Cited on p. 103)

[94] A. Greenbaum. *Iterative Methods for Solving Linear Systems*. Frontiers in Applied Mathematics 17. SIAM, Philadelphia, PA, 1997. (Cited on pp. 1, 33, 55, 56, 100, 105, 106, 109, 110)

[95] A. Greenbaum and M. L. Overton. Numerical investigation of Crouzeix's conjecture. *Linear Algebra and Its Applications*, 542:225–245, 2018. (Cited on p. 109)

[96] A. Greenbaum, V. Pták, and Z. Strakoš. Any nonincreasing convergence curve is possible for GMRES. *SIAM Journal on Matrix Analysis and Applications*, 17(3):465–469, 1996. (Cited on p. 110)

[97] A. Greenbaum and Z. Strakoš. Matrices that generate the same krylov residual spaces. In Gene Golub, Mitchell Luskin, and Anne Greenbaum, editors, *Recent Advances in Iterative Methods*, pages 95–118, Springer, 1994. (Cited on p. 110)

[98] M. J. Grote and T. Huckle. Parallel preconditioning with sparse approximate inverses. *SIAM Journal on Scientific Computing*, 18(3):838–853, 1997. (Cited on pp. 143, 147)

[99] W. Hackbusch. *Ein iteratives Verfahren zur schnellen Auflösung elliptischer randwertprobleme*. Technical report 76-12, Institute for Applied Mathematics, University of Cologne, 1976. (Cited on p. 188)

[100] W. Hackbusch. Fast solution of elliptic control problems. *Journal on Optimization Theory and Apllications*, 31(4):565–581, 1980. (Cited on p. 219)

[101] W. Hackbusch. *Multi-Grid Methods and Applications*. Springer, 2003. (Cited on p. 188)

[102] P. R. Halmos. *A Hilbert Space Problem Book*. Graduate Texts in Mathematics 19. Springer, 1982. (Cited on pp. 105, 253)

[103] M. Heinkenschloss and H. Nguyen. *Domain Decomposition Preconditioners for Linear-Quadratic Elliptic Optimal Control Problems*. CAAM Technical Reports. https://hdl.handle.net/1911/102032, 2004. (Cited on p. 249)

[104] M. Heinkenschloss and H. Nguyen. Balancing Neumann-Neumann methods for elliptic optimal control problems. In *Domain Decomposition Methods in Science and Engineering*, pages 589–596, Springer, 2005. (Cited on p. 249)

[105] M. Heinkenschloss and H. Nguyen. Neumann–Neumann domain decomposition preconditioners for linear-quadratic elliptic optimal control problems. *SIAM Journal on Scientific Computing*, 28(3):1001–1028, 2006. (Cited on p. 249)

[106] M. R. Hestenes and E. Stiefel. *Methods of Conjugate Gradients for Solving Linear Systems*, *Journal of Research of the National Bureau of Standards*, 49(6):409–436, 1952. (Cited on pp. 77, 117)

[107] M. Hintermüller, I. Kopacka, and S. Volkwein. Mesh-independence and preconditioning for solving parabolic control problems with mixed control-state constraints. *ESAIM: Control, Optimisation and Calculus of Variations*, 15(3):626–652, 2009. (Cited on p. 249)

[108] R. A. Horn and C. R. Johnson. *Matrix Analysis*. Cambridge University Press, 1990. (Cited on pp. 82, 118, 214, 233, 235)

[109] R. A. Horn and C. R. Johnson. *Topics in Matrix Analysis*. Cambridge University Press, 1994. (Cited on p. 105)

[110] A.S. Householder. *On the Convergence of Matrix Iterations*. Technical Report 1883, Oak Ridge National Laboratory, 1955. (Cited on p. 35)

[111] A. Iserles. *A First Course in the Numerical Analysis of Differential Equations*. Cambridge Texts in Applied Mathematics. Cambridge University Press, 2nd edition, 2008. (Cited on pp. 55, 56)

[112] C. G. J. Jacobi. Ueber eine neue Auflösungsart der bei der Methode der kleinsten Quadrate vorkommenden lineären Gleichungen. *Astronomische Nachrichten*, 22(20):297–306, 1845. (Cited on pp. 9, 123)

[113] F. John. *Advanced Numerical Methods*. Lecture Notes, Department of Mathematics, New York University, 1956. (Cited on p. 35)

[114] V. Jurdjevic. *Geometric Control Theory*. Cambridge Studies in Advanced Mathematics. Cambridge University Press, 1996. (Cited on p. 207)

[115] W. Kahan. *Gauss-Seidel Methods of Solving Large Systems of Linear Equations*. Ph.D. thesis, University of Toronto, 1958. (Cited on p. 46)

[116] B. Kaltenbacher. All-at-once versus reduced iterative methods for time dependent inverse problems. *Inverse Problems*, 33(6):064002, 2017. (Cited on p. 224)

[117] B. Kaltenbacher, A. Neubauer, and O. Scherzer. *Iterative Regularization Methods for Nonlinear Ill-Posed Problems*. Radon Series on Computational and Applied Mathematics. De Gruyter, Berlin, 2008. (Cited on p. 224)

[118] R. Kress. *Linear Integral Equations*. Applied Mathematical Sciences 82. Springer, 2013. (Cited on p. 251)

[119] E. Kreyszig. *Introductory Functional Analysis with Applications*. Wiley Classics Library. John Wiley & Sons, 1978. (Cited on p. 32)

[120] A. N. Krylov. On the numerical solution of the equation by which in technical questions frequencies of small oscillations of material systems are determined. *Izvestija AN SSSR (News of Academy of Sciences of the USSR)*, 7(4):491–539, 1931. (Cited on pp. 67, 80)

[121] C. Lanczos. An iteration method for the solution of the eigenvalue problem of linear differential and integral operators. *Journal of Research of the National Bureau of Standards*, 45(4):255–282, 1950. (Cited on p. 94)

[122] E. B. Lee and L. Markus. *Foundations of Optimal Control Theory*. Wiley, 1967. (Cited on p. 206)

[123] E. Lelarasmee, A. E. Ruehli, and A. L. Sangiovanni-Vincentelli. The waveform relaxation method for time-domain analysis of large scale integrated circuits. *IEEE Transactions on Computer-Aided Design of Integrated Circuits and Systems*, 1(3):131–145, 1982. (Cited on p. 147)

[124] J. Liesen and Z. Strakoš. *Krylov Subspace Methods: Principles and Analysis*. Oxford University Press, 2013. (Cited on pp. 1, 80, 105, 117, 118, 123)

[125] E. Lindelöf. Sur l'Application de la méthode des approximations successives aux équations différentielles ordinaires du premier ordre. *Comptes Rendus Hebdomadaires Des Séances de l'Académie des Sciences*, 116(3):454–457, 1894. (Cited on p. 147)

[126] J. L. Lions. *Optimal Control of Systems Governed by Partial Differential Equations*. Grundlehren der Mathematischen Wissenschaften 170. Springer, 1971. (Cited on p. 207)

[127] P.-L. Lions. On the Schwarz alternating method. I. In *First International Symposium on Domain Decomposition Methods for Partial Differential Equations*, pages 1–42. Paris, France, 1988. (Cited on pp. 148, 149)

[128] P.-L. Lions. On the Schwarz alternating method. II. In *Domain Decomposition Methods*, pages 47–70. SIAM, Philadelphia, PA, 1989. (Cited on p. 149)

[129] P.-L. Lions. On the Schwarz alternating method. III: A variant for nonoverlapping subdomains. In *Third International Symposium on Domain Decomposition Methods for Partial Differential Equations*, Volume 6, pages 202–223. SIAM Philadelphia, PA, 1990. (Cited on p. 160)

[130] B. Maar and V. Schulz. Interior point multigrid methods for topology optimization. *Structural and Multidisciplinary Optimization*, 19(3):214–224, 2000. (Cited on p. 238)

[131] Y. Maday, J. Salomon, and G. Turinici. Monotonic parareal control for quantum systems. *SIAM Journal on Numerical Analysis*, 45(6):2468–2482, 2007. (Cited on p. 249)

[132] L. Markus. A brief history of control. In *Differential Equations, Dynamical Systems, and Control Science*. Dekker, New York, 1994. (Not cited)

[133] T. P. Mathew, M. Sarkis, and C. E. Schaerer. Analysis of block parareal preconditioners for parabolic optimal control problems. *SIAM Journal on Scientific Computing*, 32(3):1180–1200, 2010. (Cited on p. 249)

[134] J. A. Meijerink and H. A. van der Vorst. An iterative solution method for linear systems of which the coefficient matrix is a symmetric M-matrix. *Mathematics of Computation*, 31(137):148–162, 1977. (Cited on pp. 124, 136, 138)

[135] M. F. Murphy, G. H. Golub, and A. J. Wathen. A note on preconditioning for indefinite linear systems. *SIAM Journal on Scientific Computing*, 21(6):1969–1972, 2000. (Cited on pp. 232, 234, 248)

[136] F. Nataf and F. Rogier. Factorization of the convection-diffusion operator and the Schwarz algorithm. *Mathematical Models and Methods in Applied Sciences*, 5(1):67–93, 1995. (Cited on p. 160)

[137] R. A. Nicolaides. On multiple grid and related techniques for solving discrete elliptic systems. *Journal of Computational Physics*, 19(4):418–431, 1975. (Cited on p. 188)

[138] J. Nocedal and S. Wright. *Numerical Optimization*. Springer Series in Operations Research and Financial Engineering. Springer, 2006. (Cited on pp. 85, 247, 248)

[139] P. J. Olver. *Introduction to Partial Differential Equations*. Undergraduate Texts in Mathematics. Springer, 2013. (Cited on p. 149)

[140] A. M. Ostrowski. On the linear iteration procedures for symmetric matrices. *Rendiconti di Matematica e delle sue Applicazioní*, 14:140–163, 1954. (Cited on p. 48)

[141] C. C. Paige. *The Computation of Eigenvalues and Eigenvectors of Very Large Sparse Matrices*. Ph.D. thesis, University of London, 1971. (Cited on p. 80)

[142] C. C. Paige and M. A. Saunders. Solution of sparse indefinite systems of linear equations. *SIAM Journal on Numerical Analysis*, 12(4):617–629, 1975. (Cited on p. 117)

[143] C. Pearcy. An elementary proof of the power inequality for the numerical radius. *Michigan Mathematics Journal*, 13(3):289–291, 1966. (Cited on p. 106)

[144] J. W. Pearson and J. Gondzio. Fast interior point solution of quadratic programming problems arising from PDE-constrained optimization. *Numerische Mathematik*, 137:959–999, 2017. (Cited on p. 248)

[145] J. W. Pearson and A. J. Wathen. A new approximation of the Schur complement in preconditioners for PDE-constrained optimization. *Numerical Linear Algebra with Applications*, 19(5):816–829, 2012. (Cited on p. 248)

[146] H. Pesch and M. Plail. The maximum principle of optimal control: A history of ingenious ideas and missed opportunities. *Control and Cybernetics*, 38:973–995, 2009. (Cited on p. 205)

[147] P. Philip. *Optimal Control of Partial Differential Equations (Lecture Notes)*. HU Berlin, LMU Munich, 2013. (Cited on pp. 211, 213, 255)

[148] E. Picard. Sur l'application des méthodes d'approximations successives à l'étude de certaines équations différentielles ordinaires. *Journal de Mathématiques Pures et Appliquées*, 9:217–272, 1893. (Cited on p. 147)

[149] L. S. Pontryagin, V. G. Boltyanskii, R. V. Gamkrelidze, and E. F. Mishechenko. *The Mathematical Theory of Optimal Processes*. Wiley, 1962. (Cited on p. 205)

[150] J. S. Przemieniecki. Matrix structural analysis of substructures. *AIAA Journal*, 1(1):138–147, 1963. (Cited on p. 147)

[151] P. J. Psarrakos and M. J. Tsatsomeros. *Numerical Range: (In) a Matrix Nutshell*. Vol. 1. Mathematics Notes from Washington State University. Department of Mathematics, Washington State University, 2002. (Cited on pp. 105, 106)

[152] A. Quarteroni. *Numerical Models for Differential Problems.* Modeling, Simulation and Applications. Springer, 2009. (Cited on p. 20)

[153] V. Rawat and J.-F. Lee. Nonoverlapping domain decomposition with second order transmission condition for the time-harmonic Maxwell's equations. *SIAM Journal on Scientific Computing*, 32(6):3584–3603, 2010. (Cited on p. 168)

[154] T. Rees, H. S. Dollar, and A. J. Wathen. Optimal solvers for PDE-constrained optimization. *SIAM Journal on Scientific Computing*, 32(1):271–298, 2010. (Cited on pp. 234, 235, 247)

[155] T. Rees and M. Stoll. Block-triangular preconditioners for PDE-constrained optimization. *Numerical Linear Algebra with Applications*, 17(6):977–996, 2010. (Cited on p. 248)

[156] E. Reich. On the convergence of the classical iterative procedures for symmetric matrices. *Annals of Mathematical Statistics*, 20:448–451, 1949. (Cited on p. 48)

[157] L. F. Richardson. The approximate arithmetical solution by finite differences of physical problems involving differential equations, with an application to the stresses in a masonry dam. *Philosophical Transactions of the Royal Society of London. Series A, Containing Papers of a Mathematical or Physical Character*, 210:307–357, 1911. (Cited on p. 58)

[158] J. W. Ruge and K. Stüben. Algebraic multigrid. In *Multigrid Methods*, pages 73–130. SIAM, Philadelphia, PA, 1987. (Cited on p. 188)

[159] Y. Saad. Krylov subspace methods for solving large unsymmetric linear systems. *Mathematics of Computation*, 37(155):105–126, 1981. (Cited on p. 117)

[160] Y. Saad. *Numerical Methods for Large Eigenvalue Problems*. Manchester University Press, Manchester, UK, 1992. (Cited on pp. 80, 82, 88, 95, 96, 116, 127, 136)

[161] Y. Saad. A flexible inner-outer preconditioned GMRES algorithm. *SIAM Journal on Scientific Computing*, 14(2):461–469, 1993. (Cited on p. 132)

[162] Y. Saad. ILUT: A dual threshold incomplete LU factorization. *Numerical Linear Algebra with Applications*, 1(4):387–402, 1994. (Cited on p. 138)

[163] Y. Saad. *Iterative Methods for Sparse Linear Systems*. SIAM, Philadelphia, PA, 2003. (Cited on p. 1)

[164] Y. Saad. Schur complement preconditioners for distributed general sparse linear systems. In *Domain Decomposition Methods in Science and Engineering XVI*, pages 127–138. Springer, Berlin, 2007. (Not cited)

[165] Y. Saad and M. H. Schultz. GMRES: A generalized minimal residual algorithm for solving nonsymmetric linear systems. *SIAM Journal on Scientific and Statistical Computing*, 7(3):856–869, 1986. (Cited on pp. 67, 98, 118)

[166] V. Schulz and G. Wittum. Multigrid optimization methods for stationary parameter identification problems in groundwater flow. In *Multigrid Methods V*, pages 276–288. Springer, 1998. (Cited on p. 238)

[167] V. Schulz and G. Wittum. Transforming smoothers for PDE-constrained optimization problems. *Computing and Visualization in Science*, 11(4):207–219, 2008. (Cited on p. 238)

[168] H. A. Schwarz. Über einen Grenzübergang durch alternierendes Verfahren. *Vierteljahrsschrift der Naturforschenden Gesellschaft in Zürich*, 15:272–286, May 1870. (Cited on p. 148)

[169] L. Seidel. Über ein Verfahren, die Gleichungen, auf welche die Methode der kleinsten Quadrate führt, sowie lineäre Gleichungen überhaupt, durch successive Annäherung aufzulösen. In *Abhandlungen der Mathematisch-Physikalischen Klasse der Königlich Bayerischen Akademie der Wissenschaften, Band 11, III. Abtheilung*, pages 81–108, 1874. (Cited on p. 9)

[170] A. St-Cyr, M. J. Gander, and S. J. Thomas. Optimized multiplicative, additive, and restricted additive Schwarz preconditioning. *SIAM Journal on Scientific Computing*, 29(6):2402–2425, 2007. (Cited on p. 163)

[171] E. M. Stein and R. Shakarchi. *Complex Analysis*. Princeton Lectures in Analysis. Princeton University Press, 2010. (Cited on p. 101)

[172] E. Stiefel. Über einige Methoden der Relaxationsrechnung. *Zeitschrift für angewandte Mathematik und Physik ZAMP*, 3(1):1–33, 1952. (Cited on pp. 67, 73, 76)

[173] H. J. Sussmann and J. C. Willems. 300 years of optimal control: From the brachystochrone to the maximum principle. *IEEE Control Systems Magazine*, 17:32–44, 1997. (Cited on pp. 205, 206)

[174] E. C. Titchmarsh. *The Theory of Functions*. Oxford Science Publications. Oxford University Press, 2nd edition, 1939. (Cited on pp. 101, 103)

[175] A. Toselli and O. Widlund. *Domain Decomposition Methods—Algorithms and Theory*. Springer Series in Computational Mathematics 34. Springer, 2006. (Cited on p. 159)

[176] L. N. Trefethen and D. Bau, III. *Numerical Linear Algebra*. SIAM, Philadelphia, PA, 1997. (Cited on p. 96)

[177] N. Trefethen. Approximation theory and numerical linear algebra. In J. C. Mason and M. G. Cox, eds., *Algorithms for Approximation II*. Chapman and Hall, 1990. (Cited on pp. 100, 109)

[178] F. Tröltzsch. *Optimal Control of Partial Differential Equations: Theory, Methods, and Applications*. Graduate Studies in Mathematics 112. American Mathematical Society, 2010. (Cited on pp. 207, 211, 213, 216, 224)

[179] H. A. van der Vorst. Bi-CGSTAB: A fast and smoothly converging variant of Bi-CG for the solution of nonsymmetric linear systems. *SIAM Journal on Scientific and Statistical Computing*, 13(2):631–644, 1992. (Cited on p. 117)

[180] R. S. Varga. Factorization and normalized iterative methods. In *Proceedings of the Symposium on Boundary Problems in Differential Equations*, 1960. (Cited on p. 136)

[181] R. S. Varga. *Matrix Iterative Analysis*. Prentice-Hall, 1962. (Cited on pp. 11, 32, 33)

[182] S. Volkwein. Lagrange-SQP techniques for the control constrained optimal boundary control for the Burgers equation. *Computational Optimization and Applications*, 26:253–284, 2003. (Cited on p. 249)

[183] S. Warner. *Modern Algebra*. Dover Books on Mathematics. Dover, 1990. (Cited on p. 28)

[184] O. Widlund and M. Dryja. *An Additive Variant of the Schwarz Alternating Method for the Case of Many Subregions*. Technical report, Department of Computer Science, Courant Institute, 1987. (Cited on pp. 124, 157)

[185] S. Yang and M. K. Gobbert. The optimal relaxation parameter for the SOR method applied to the Poisson equation in any space dimensions. *Applied Mathematics Letters*, 22:325–331, 03 2009. (Cited on pp. 55, 57)

[186] D. M. Young. *Iterative Methods for Solving Partial Difference Equations of Elliptic Type*. Ph.D. thesis, Harvard University, 1950. (Cited on pp. 45, 48, 51)

Index

Fundamentals *of* Algorithms

Iterative methods use successive approximations to obtain more accurate solutions. This book gives an introduction to iterative methods and preconditioning for solving discretized elliptic partial differential equations and optimal control problems governed by the Laplace equation, for which the use of matrix-free procedures is crucial. All methods are explained and analyzed starting from the historical ideas of the inventors, which are often quoted from their seminal works.

Iterative Methods and Preconditioners for Systems of Linear Equations grew out of a set of lecture notes that were improved and enriched over time, resulting in a clear focus for the teaching methodology, which

- presents historical background,
- derives complete convergence estimates for all methods,
- illustrates and provides MATLAB codes for all methods, and
- studies and tests all preconditioners first as stationary iterative solvers.

This textbook is appropriate for undergraduate and graduate students who want an overview or deeper understanding of iterative methods. Its focus on both analysis and numerical experiments allows the material to be taught with very little preparation, since all the arguments are self-contained, and makes it appropriate for self-study as well. It can be used in courses on iterative methods, Krylov methods and preconditioners, and numerical optimal control. Scientists and engineers interested in new topics and applications will also find the text useful.

Gabriele Ciaramella is an assistant professor with tenure at the Politecnico di Milano (MOX Lab). His main research interests are in numerical analysis, specifically parallel iterative methods, and in numerical optimization with applications to quantum systems.

Martin J. Gander is a professor of mathematics at the University of Geneva. Together with Felix Kwok he won the SIAM 100-Dollar 100-Digit Challenge, and with Albert Ruehli the best paper award at the 19th IEEE EPEPS conference. Professor Gander became a SIAM Fellow in 2020 and was nominated for the Jean-Morlet Chair of the CIRM for 2022. His main research interest is numerical analysis, specifically parallel iterative methods for space-time problems.

For more information about SIAM books, journals, conferences, memberships, or activities, contact:

siam

Society for Industrial and Applied Mathematics
3600 Market Street, 6th Floor
Philadelphia, PA 19104-2688 USA
+1-215-382-9800
siam@siam.org • *www.siam.org*

ISBN: 978-1-611976-89-2

FA19

SIAM Textbooks